E A R T H S C I E N C E S
S I M O N F R A S E R U N I V E R S I T Y

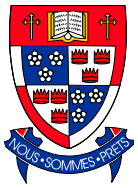

Climate Change and Groundwater: A Modelling Approach for Identifying Impacts and Resource Sustainability in the Central Interior of British Columbia

Summary Report Prepared by:

Diana M. Allen and Jacek Scibek
Department of Earth Sciences
Simon Fraser University
Burnaby, B.C.

In Collaboration with:

Mike Wei
Climate Change Branch
BC Ministry of Water, Land and Air Protection
Victoria, BC

Paul Whitfield
Branch Science Division, Meteorological Service of Canada
Pacific and Yukon Region, Environment Canada
Vancouver, British Columbia

Prepared for:

Climate Change Action Fund, Natural Resources Canada

March 2004

EXECUTIVE SUMMARY

A case study of an unconfined aquifer in the Grand Forks valley in south-central BC was used to develop methodology for linking climate models, hydrologic models, and groundwater models to investigate future impacts of climate change on groundwater resources. The aquifer is 34 km^2, located in a semi-arid climate, and comprised of heterogeneous glaciofluvial / glaciolacustrine sediments that partially infill steep and variable bedrock topography in a mountainous valley. The bedrock surface of the Grand Forks valley was eroded by glacial processes during the Wisconsin glaciation, and by pre-glacial fluvial erosion. The valley shape was modelled using profile extrapolation, constrained by well lithologs, and geostatistical interpolation. Total sediment thickness was estimated. The hydrostratigraphic units were modelled in three-diemensions from standardized, reclassified, and interpreted well borehole lithologs. Solid models were constructed. A stochastic hydrostratigraphic model was also generated and compared to the layered hydrostratigraphic model.

A three dimensional groundwater flow model of variable spatial resolution (constrained by borehole spacing) was implemented in MODFLOW, and calibrated to observation well data. Two model types were constructed: a "homogeneous" layered model, and a "heterogeneous" layered model in which the hydraulic conductivity and specific yield properties are spatially-distributed in the aquifer layers. A new methodology was developed for generating spatially-distributed and temporally-varying recharge zonation for the surficial aquifer, using GIS linked to the one-dimensional HELP (USEPA) hydrologic model, which estimates aquifer recharge. The recharge model accounts for soil distribution, vadose zone depth and hydraulic conductivity, the extent of impermeable areas, and surficial geology. Production well pumping and irrigation return flow during the summer season were included in recharge computations. Although recharge was computed as monthly averages per climate scenario, it is driven by physically-based daily weather inputs generated by a stochastic weather generator and calibrated to local observed climate.

Four year long climate scenarios were run, each representing one typical year in the present and future (2020s, 2050s, and 2080s), by perturbing the historical weather according to the downscaled CGCM1 general circulation model results (Environment Canada). CGCM1 model outputs were calibrated for local conditions during the downscaling procedure. These include absolute and relative changes in precipitation; including indirect measures of precipitation intensity, dry and wet spell lengths, temperature, and solar radiation for the evapotranspiration model. The downscaling of CGCM1 results was accomplished using 2 independently calculated methods: 1) using SDSM software (at Simon Fraser University by authors of this report), and 2) using a different method (undertakne by Environment Canada). Large uncertainties exist in the actual precipitation forecasting ability of GCMs, and the ability to downscale to local conditions (“model bias”), thus relative and absolute changes in precipitation were quantifed. Summer precipitation is predicted to increase in July and August, but in other months there are either no changes or decreases. The % of wet days in the summer months is predicted to increase in future climate. For temperature, the results are simple and consistent; temperatures are predicted to increase in all months from present to future. The two downscaling methods used agree that summer temperatures will increase at a relatively constant rate of 1ºC per 30 years.

The use of spatial analysis tools in a GIS environment allowed for spatial and temporal data integration. Therefore, the following results have both temporal and spatial components. This has not been done for any aquifer in BC, especially regional aquifers. To the best of our knowledge, this type of comprehensive climate change modelling and recharge estimation for groundwater flow modelling has not been done yet in Canada. The temporal variation of precipitation was accounted for by calculating monthly recharge values (as opposed to annual only), which give relatively good temporal distribution of recharge and capture the main inter-

annual variation. Most aerial recharge probably occurs either during snowmelt or during large rainstorms. The LARS-WG weather generator, as opposed to WGEN, which is the weather generator used directly by the HELP program in UnSat Suite, allows for better representation of dry and wet spells and provides a better fit to observed data. Higher resolution CRCM1 results and stochastic weather from LARS-WG were used for climate scenarios. Overall, the recharge model in HELP accounted for soil properties, hydraulic conductivity, and depth of the unsaturated zone.

According to HELP model results, in this climatic region there isn't enough precipitation to recharge the aquifer where there are thick sand and gravel terraces – most of the precipitation changes moisture content in these areas of thick gravels above water table, but little of it recharges the groundwater aquifer. This situation would be different if this was a wet climatic zone – most recharge would occur in most permeable areas with less influence on depth of sediment to water table. The HELP modelled-recharge is similar in magnitude but smaller than previously estimated, and results indicate that Grand Forks receives between 10% and 80% of recharge from precipitation.

CGCM1 downscaling was also used to predict basin-scale runoff for the Kettle River upstream of Grand Forks. The streamflow hydrographs were analysed and compared. The streamflow hydrographs were dominated by a spring snow melt event, followed by low flow until early winter. In future climate scenarios the hydrograph peak is shifted to earlier date, although the peak flow remains the same. Large changes to the river hydrograph are predicted for the 2040-2069 period and the 2010-2039 years, compared to historical 1961-1999 time period. The hydrograph derived for the downstream section of Kettle River was the sum of Kettle and Granby Rivers. Kettle River discharge is much greater than the inflow of tributaries in the valley watershed, but many of the water balance components in the valley aquifer are not quantified. This river exerts strong control on the groundwater levels in the aquifer and physically-based discharge predictions were used in the transient groundwater flow model. Modelled discharge hydrographs were converted to river stage hydrographs at each of 123 river segments, and interpolated between known river channel cross-sections. Stage-discharge curves were estimated using the BRANCH model and calibrated to observed historical data. River channels were represented in three-dimensions using a high grid density (14 to 25 m) in MODFLOW, which were mapped onto river segments. River stage schedules along the 26 km long meandering channel were imported at varying, but high, temporal resolution (1 to 5 days) for every cell location independently. Head differences were computed at each time step for historical and future, mapped in GIS and linked to the MODFLOW model.

The final calibrated transient model was used for all climate scenarios, and all sensitivity scenarios (to aquifer heterogeneity and recharge distribution assumptions). Model scenarios were based on: 1) recharge for one selected climate, either historical or predicted future climate, 2) river hydrograph, either historical or predicted for future conditions, 3) pumping or no-pumping, 4) type of recharge distribution over the aquifer area, 5) type of aquifer representation (homogeneous or heterogeneous K distribution). Groundwater flow components were computed with Zone Budget (ZBUD) in MODFLOW. The zones represent irrigation districts within the unconfined aquifer, the river floodplain, and deeper model layers. Temporal changes in mass balance components show relations between pumping, storage, recharge, and flow. Within an annual cycle and between climate scenarios the results show different spatial and temporal distributions in groundwater conditions. At present day, the flow patterns are influenced by river channel profile, and generally follow valley floor topography. The heterogeneous model has smaller drawdowns near productions wells than in the homogeneous layered model. Flow patterns and gradients are characterized in cross-sections and maps. River reaches with net inflow and outflow to and from the aquifer were mapped, showing a complete pattern.

Recharge follows precipitation patterns. The largest predicted increase due to climate change is in late spring, which suggests a factor of 3 or more increase from present levels. Predictions suggest 50% increase in recharge in summer months, and 10 to 25% increase in autumn, but in some areas there are no changes from present. Irrigation return flow contributed 10 to 20% of recharge. In this aquifer, the effect of changing recharge on groundwater levels is very small compared to changes in the timing of basin-scale snowmelt events in the Kettle River and the subsequent shift in the hydrograph. During spring freshet on the Kettle River, the rise in river stage causes an inflow of water to the aquifer, where it is stored. As river stage drops, the hydraulic gradient is reversed and water is released from storage in this zone and leaves mostly to the floodplain zone as it returns to river as baseflow. In the floodplain zone, the rate of inflow of groundwater from the river and into the aquifer along the floodplain zone follows the river hydrograph very closely during the rise in river stage. As the river stage levels off and begins to decrease, the flow direction is reversed within 10 days. During this time, the rate of inflow from the river to the aquifer begins to rise, and then dominates for the rest of the year, as water previously stored in the aquifer drains back to the river as baseflow seepage. Storage rates are less than 50% of inter-zonal groundwater flux, and 15 to 20% of river-aquifer flux. The river-aquifer interaction has a maximum flow rate of 41 m3/s, which translates to between 11 and 20% of river flow during spring freshet - the river puts about 15% of its spring freshet flow into storage in Grand Forks valley aquifers alone, and within 30 to 60 days most of that water is released back to the river as baseflow. As the climate impacts are mainly driven by river stage, and in particular, its shift to an earlier date, parts of valley aquifer that are strongly connected to the river have the largest climate-driven changes. As the river peak flow shifts to an earlier date in the year, the "hydrographs" for flow rates also shift by the same interval. The various zones have different sensitivity to aquifer heterogeneity representation in the model, in terms of flow to storage and inter-zonal flow. In the floodplain, storage was not affected significantly by heterogeneity of aquifer, but inter-zonal flow was very different and very much larger than in the homogeneous model by 50-75%. In other zones, heterogeneity of the aquifer created higher flow rates, less drawdown due to pumping, and caused larger responses to river hydrograph changes as a result of predicted climate changes. Impacts of climate change on water levels were represented by head difference maps for different model time steps. The differences were calculated between the output from each future climate scenario model and output from the present climate scenario model, separately for pumping and non-pumping models. In the 2010-2039 scenario, water levels rise and fall with the river hydrograph at different times because of a shift in river hydrograph peak flow to an earlier date. Elevated water levels up to 30 to 40 cm persist along the channel and drain within a month. From late summer to the end of the year, water levels are similar to present conditions, with small increases observed due to the increase in recharge in areas away from the river channel. In the 2040-2069 climate scenario, the hydrograph shift is larger than in the 2010-2039 climate scenario. In the heterogeneous aquifer model, the climate change effects are no longer limited to floodplain, but extent over most parts of the valley, and the effect of heterogeneity on water levels is arguably as strong as the shift of the river hydrograph due to climate change. In profile views or as water table elevation maps, the climate change effects (river + recharge) are much smaller in magnitude than typical seasonal variation, but are significant. Sensitivity analysis also showed that the control of spatial distribution of recharge on water levels is much larger than that of temporal variation in recharge. In Grand Forks aquifer, the model is sensitive to recharge only away from the river floodplain and the maximum change expected in water table elevation is between 10 and 50 cm, but typically about 20 cm.

TABLE OF CONTENTS

LIST OF FIGURES

LIST OF MAPS

LIST OF TABLES

1. INTRODUCTION

1.1. BACKGROUND

In 1996, Environment Canada initiated a countrywide study to evaluate the impacts of climate change and the variability on Canada as a whole, and to consider existing and potential adaptive responses (Environment Canada, 1997). Impacts on hydrologic systems are expected to be significant in most parts of Canada, and specifically, in British Columbia. While not pervasive in all regions of the province, evidence of limited water availability exists, especially in the interior of the province. For instance, over 17% of surface water sources are at or nearing their capacity to reliably supply water for extractive uses (BC Ministry of Environment, Lands and Parks, 1999), and groundwater-surface water conflicts have been identified in a few interior aquifers. Thus, groundwater management is among the important water issues facing British Columbia (GCSI and Environment Canada, 2000).

Water resources are central to any study on climate change, however, most research to-date has been directed at forecasting the potential impacts to surface water hydrology in British Columbia (e.g., Whitfield and Taylor, 1998), but relatively little research has been undertaken to determine the sensitivity of groundwater systems to changes in critical input parameters, such as precipitation and runoff, despite the fact that British Columbia is one of the largest users of groundwater in Canada. In the south-central interior of the province, where agriculture is a significant component of the economy, groundwater resources may be particularly impacted by climate change. With increasing concerns surrounding global climate change, there has been growing interest in the potential impacts to aquifers.

The main reason for studying the interactions between aquifers and the atmosphere is to determine how groundwater resources are affected by climate variability and climate change. It is expected that changes in temperature and precipitation will alter groundwater recharge to aquifers, causing shifts in water table levels in unconfined aquifers as a first response to climate trends (Changnon et al, 1988; Zektser and Loaciga, 1993). Although the most notable impacts could be changes in surface water levels in lakes (Winter, 1983), the greatest concern of water managers and government officials is the potential decrease of groundwater supplies for municipal and agricultural uses. These changes may decrease quantity, and perhaps, quality of water, which would also have detrimental environmental effects on fisheries and other wildlife by changing baseflow dynamics in streams (Bredehoeft and Papadopulos, 1982; Gleick, 1986). Aquifer recharge and groundwater levels interact, and depend on climate and groundwater use; each aquifer has different properties and requires detailed characterization and eventually quantification (e.g., numerical modelling) of these processes and linking the recharge model to climate model predictions (York et al., 2002). In practice, any aquifer that has an existing and verified conceptual model, together with a calibrated numerical model, can be assessed for climate change impacts through scenario simulations. The accuracy of predictions depends largely of scale of project and availability of hydrogeologic and climatic datasets.

1.2. PREVIOUS WORK

Simon Fraser University and the Groundwater Section of the former BC Ministry of Environment, Lands and Parks (now BC Ministry of Water, Land and Air Protection) undertook collaborative research in 1999-2000 and 2000-2001, respectively:

1. to develop a numerical groundwater model (using Visual MODFLOW, Waterloo Hydrogeologic Inc.) of the Grand Forks aquifer. The purpose of the model was to generate well capture zones using numerical methods and to study the interaction of surface water (rivers) and groundwater, and
2. to model the sensitivity of the aquifer to climate change variables (e.g., precipitation, evapotranspiration and river stage) under steady-state conditions.

The Grand Forks aquifer, located in south-central British Columbia, roughly 500 km east of Vancouver, was used as a case study area (Map 1) because an excellent database was available to undertake the modeling and the aquifer was one of two pilot study areas under BC's Freshwater Initiative. As well, the Grand Forks region is arid and the community relies on groundwater for domestic and irrigation use.

Estimates of recharge to the unconfined alluvial aquifer were made using the HELP software package in UnSat Suite (Waterloo Hydrogeologic Inc.) for both current climate conditions and for a range of climate change scenarios (as published in the Canada Country Study – BC and Yukon Volume). The results of that work were published as reports (Allen, 2000 and Allen 2001, respectively), and a scientific paper that summarizes the results of the climate change sensitivity analysis is in press (Allen et al., in press).

Results of the modelling confirmed that the hydrogeology of the Grand Forks aquifer is largely controlled by river stage elevation, but that variations in the amount of recharge do cause measurable changes in water table elevation throughout the aquifer. Under various climate change scenarios, including extreme cases of low and high recharge, small but measurable variations in the elevation of the water table and overall flow direction were simulated under steady-state conditions. However, steady-state simulations do not address temporal changes in groundwater storage, which are of critical importance for assessing seasonal variations in the overall water budget of an aquifer. The high temporal dependence on river stage on the water table elevation, coupled with the increased demand for groundwater during the summer months (when crop irrigation is at a maximum) will likely result in significant changes to the monthly water budgets. Transfers of groundwater to and from storage can only be assessed by considering the transient behaviour of the aquifer. We hypothesized that changes in groundwater levels could be compromised during the summer months if either recharge is reduced substantially over the course of the year or, perhaps more importantly, if the timing of recharge events changes.

An analysis of Kettle River flows, (the Kettle River passes through the Grand Forks valley), undertaken in conjunction with the Cascade Heritage hydro project indicate that annual low flows are now taking place in September / October instead of March, and that March flows themselves have been lower in the most recent decade (Whitfield, personal communication). As well, annual flows throughout the Kettle Basin have been persistently lower in the past two decades when compared to earlier periods. Fluctuations in river stage, timing of flood events, and fluctuations in river stage accompanying flood events and reduced baseflow in the summer are also expected to impact the groundwater system under transient (dynamic) conditions. Thus, an examination of temporal changes in groundwater storage will be particularly important for evaluating potential supply shortages during the summer months (Allen, 2001). Changes in water table elevation, associated with modified base flow in the Kettle and Granby Rivers, differences in total amount and timing of precipitation, changes in evaporation, and increased groundwater usage, are important to quantify in order to assess potential impacts to groundwater supply as well as to determine the potential impacts to the environment.

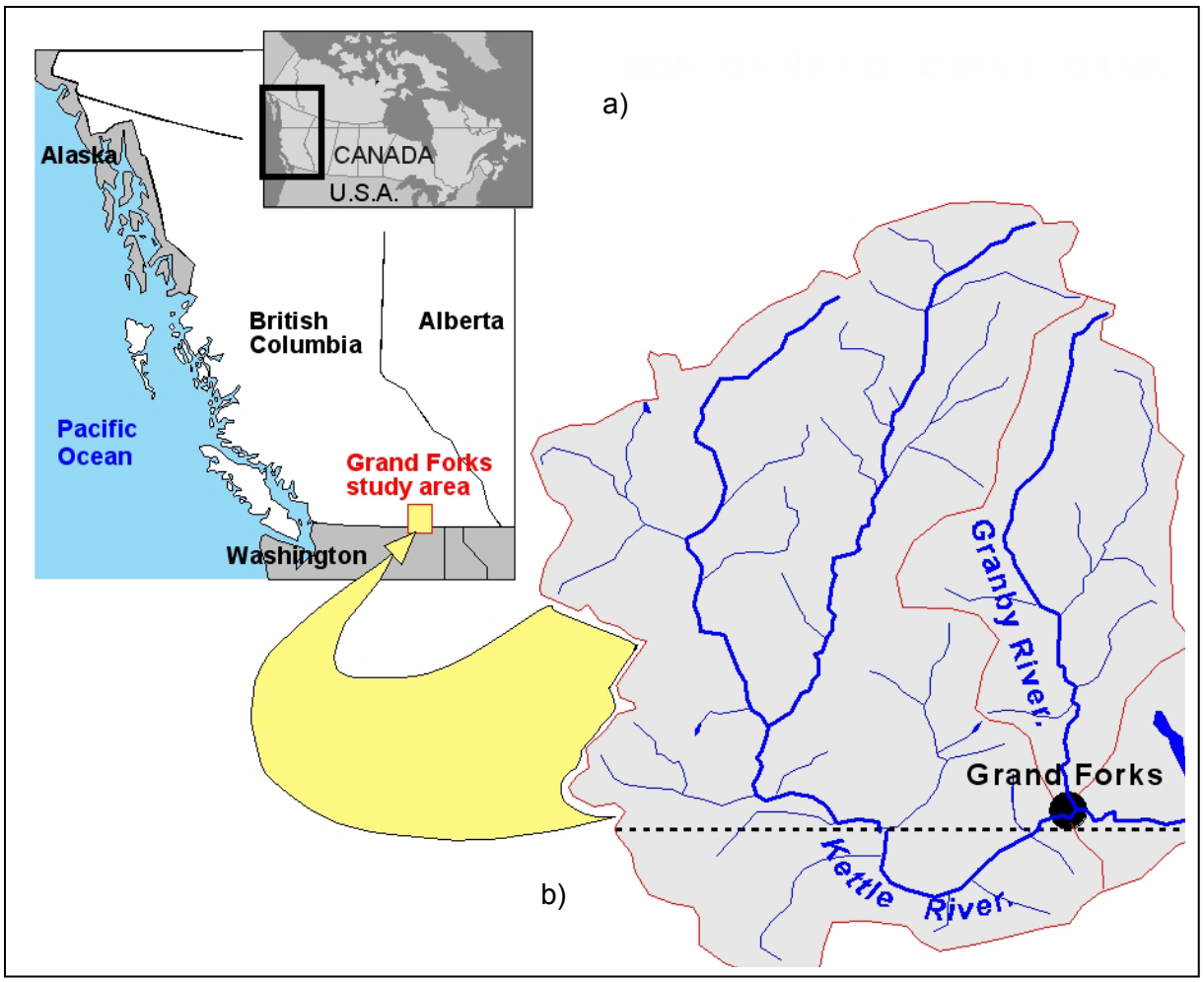

Map 1 (a) Location map of the study area in British Columbia, and (b) map of the Kettle and Granby River drainage areas.

The purpose of this study is to extend the analysis of climate change impact on groundwater by modelling groundwater flow within the Grand Forks aquifer under transient conditions for different climate change scenarios. This will permit a more comprehensive evaluation of water budgets, incorporation of seasonal changes in demand for groundwater, and provide for a better understanding of the direct impact of climate change on alluvial aquifers in the province. The Grand Forks aquifer will join the ranks for heavily-studied aquifers, such as the Waterloo Moraine in Ontario (Martin and Frind, 1998) as the best candidates for climate change scenario modelling. Furthermore, the same aquifers will be most likely studied in the future for other purposes, due to large datasets for hydrostratigraphy, hydraulic and water quality information, and the availability of a calibrated numerical model.

This research aims to address the following knowledge gaps:

1. The vulnerability of water (specifically groundwater) resources to climate change, specifically, by undertaking a quantitative assessment of the direct impact of seasonal variations in recharge and river stage on groundwater levels under different climate change scenarios.

2. The impacts of climate change on socio-economic aspects of water resource management, specifically related to irrigation practices, potential user conflict and resource sustainability.
3. Developing methods for enhancing adaptive capacity of water resource planning and management to the impacts of climate change, specifically, by implementing predictive methodologies (modelling) to identify potential impacts on groundwater resources.
4. Increasing public awareness of groundwater resources, and vulnerability and sustainability of groundwater resources under both current and climate change scenarios.

This research project parallels work undertaken as part of a comprehensive hydrogeological investigation of the Grand Forks aquifer, which was conducted to characterize in more detail than had been done previously (i.e., in Allen, 2000) the three-dimensional architecture of the aquifer (Allen et al., 2003). This report summarizes the methodology and results obtained as part of a CCAF funded (Natural Resources Canada) project aimed at modeling the impacts and resource sustainability of the Grand Forks aquifer under climate change. Partners included Simon Fraser University, Environment Canada, and BC Ministry of Water, Land and Air Protection. Three more extensive reports provide details on each of the three components of the study hydrology (Scibek and Allen, 2003), recharge (Scibek and Allen, 2004) and climate change modeling results (Scibek et al., 2004).

1.3. OBJECTIVES OF RESEARCH

The process of modeling climate change impacts on groundwater aquifers, and more specifically groundwater levels and supplies, involves several steps, and has been applied in various locations around the world (Malcom and Soulsby, 2000; Kruger et al, 2001; York et al, 2002, Yusoff et al, 2002) as well as recent ongoing groundwater assessment initiatives in Canada (Rivera, 2000) and associated aquifer modeling efforts (Allen, 2001):

1) aquifer characterization and creation of conceptual model of aquifer system
2) compilation of representative historical climatic and hydrologic datasets
3) development of a numerical model and calibration to steady state conditions
4) if possible, expansion of the numerical model to transient conditions (seasonal trends) and calibration
5) downscaling of climatic and hydrologic trends and establishing climate change scenarios
6) running climate change scenario simulations and analyzing results to determine impacts on groundwater levels

The first step is, in itself, a multi-step process and takes the longest time since it involves setting up of geological framework based on lithologic and geophysical datasets, definition of hydrostratigraphic units based on hydraulic properties of porous media, and analysis of flow patterns from measured groundwater levels and/or groundwater chemistry (Anderson and Woessner, 1992; Domenico and Schwartz, 1998).

The primary objectives of the research are:

1. To develop and document a methodology that involves the integration time-varying groundwater, surface water and water use data into a comprehensive numerical model of an aquifer system.
2. To provide, using advanced numerical modelling methods, a quantitative measure of the impact of climate change on seasonal groundwater levels, water budgets and overall flow directions within a specific river-dominated alluvial aquifer (i.e., the Grand Forks aquifer).
3. To extend the research findings to other areas within the province of British Columbia (and by inference other aquifer systems in Canada) by undertaking a preliminary comparative examination of similar aquifers in the province.
4. To transfer the scientific knowledge gained from the project to water purveyors and local authorities for use in planning activities that are directly related to assessment of groundwater resource sustainability (e.g., municipal water supply, agriculture).
5. To contribute to the training of highly qualified personnel by providing supervision to students seeking advanced academic training in groundwater science.

1.4. SCOPE OF WORK

This project encompasses three main topics: hydrology and predictions, recharge and predictions, and groundwater flow modeling results. First, the hydrogeology of the Grand Forks aquifer is summarized, based on previous geological work by various researchers as well as detailed aquifer architecture modeling conducted in a parallel project (Allen et al. 2003). The aquifer architecture forms the basis for developing a three-dimensional model of the subsurface stratigraphy and forms the framework for the numerical groundwater flow model. Second, the study evaluates the various sources of recharge to the aquifer and their relative importance to the overall flow regime, and describes the water balance for the watersheds that surround the Grand Forks Valley. A numerical river flow model, which can be used to calculate flow conditions in reaches of the Kettle and Granby Rivers within the Grand Forks Valley for a range of typical flow magnitudes, is also developed. The model prepares river stage data for use in the three-dimensional groundwater flow model that will be used to evaluate transient groundwater flow conditions within the Grand Forks aquifer. Observed climate change effects on hydrology and climate change predictions are presented. Third, a distributed recharge map is developed for the aquifer. This map is derived by modeling recharge using a calibrated weather generator in combination with representative soil columns over the surface of the aquifer. Scenarios for current climate and various climate change scenarios are modeled. The output of the recharge modeling is then input into the groundwater flow model, and forms an upper boundary condition for transient simulations. Fourth, simulations are run in Visual Modflow to evaluate the sensitivity of the aquifer to climate change under both pumping and non-pumping conditions, by comparing the results to current climate conditions for each of these cases. Finally, by way of extension of the project, aquifers in BC are identified that might have similar hydrologic and hydrogeologic conditions as those present in Grand Forks, and by inference, may respond similarly to climate change.

In order to meet the objectives for the research project and in continuation of the previous research on the Grand Forks Aquifer, the following detailed scope of work was undertaken:

Aquifer Architecture (in association with a parallel study)

1. Reviewing existing hydrostratigraphic data for the Grand Forks aquifer and developing a series of geologic cross sections that can be used to represent more accurately than had been done previously (e.g., Allen, 2000) the hydrostratigraphy of the aquifer.
2. Modelling the bedrock surface beneath the valley fill using geostatistical methods in order to better constrain the lower boundary of the aquifer.
3. Developing and implementing a classification and standardization algorithm that can be used to extract, classify and standardize well lithology information from water well logs so that these may be more easily used to construct continuous aquifer layers for model input.
4. Using GMS (version 4.0) to create digital cross sections and aquifer layers, and input of these layers into Visual Modflow. Modification of the aquifer architecture within the existing Modflow model for Grand Forks (Allen, 2000; 2001) required modification of the grid design.

GCM Climate Data

1. Generating scenarios from CGCM1 data for each CGCM1 scenario (4 scenarios, current, 2020s, 2050s, and 2080s) from CICS website for use with SDSM to obtain calibration data and all CGCM1 scenarios.

Hydrology

1. Reviewing river discharge and stage records from selected hydrometric stations on Kettle and Granby Rivers near Grand Forks, BC.
2. Quantifying the water balance components of the Grand Forks Valley watershed, including the aquifer.
3. Describing channel geometry of the Kettle and Granby Rivers, and using it to improve accuracy of river stage predictions and inputs to groundwater model.
4. Using a river flow model to calculate flow conditions in Kettle and Granby River reaches in the Grand Forks Valley for a range of typical flow magnitudes.
5. Using river flow model to calculate stage-discharge rating curves for small segments of the two rivers and develop methodology and software that links the river flow model with the groundwater flow model for the purpose of evaluating groundwater model sensitivity to changes in river hydrographs.
6. Reviewing climate change scenario predictions of coupled hydrologic and meteorologic models for the Kettle and Granby River basins.

Recharge

1. Analyzing continuous time series daily precipitation (P) and temperature (T) data; acquiring evapotranspiration data and solar radiation estimates (monthly means).
2. Undertaking a comparison of downscaling methodologies (SDSM and Environment Canada's k-nn ACS method).
3. Exporting all P and T SDSM downscaled output to separate files for use in LARS-WG; set up scenario files using results from SDSM; calibrate LARS-WG to current data.
4. Generating future weather using the climate change scenarios and comparing LARS output with SDSM output and observed data.
5. Reformatting LARS outputs to be useful for HELP model.

6. Creating HELP projects: 64 different soil / Ksat / depth scenarios, plus sensitivity analysis scenarios. Undertaking sensitivity analysis and evaluating HELP outputs to adjust all parameters and decide on type and number of soil column scenarios.
7. Running all climate change scenarios and evaluating HELP outputs (graphs, stats).
8. Setting up GIS projects to include soils, geology, and depth to water; linking recharge tables (monthly) to polygons of recharge zones and mapping recharge monthly and annually for all climate scenarios.
9. Joinning mid-points of MODFLOW active cells in layer 1 (recharge applied to it) with recharge zone polygons; inputing recharge for every climate scenario to separate transient models
10. Mapping irrigation districts and fields where return flow occurs; for summer months, applying recharge return flow and creating new (combined) recharge zones in MODFLOW.

Groundwater Simulations

1. In association with a related study to model the three dimensional architecture of the aquifer (Allen et al., 2003), refining the layers in the MODFLOW model.
2. Re-designing the numerical model to incorporate changes made to the aquifer architecture, to accept temporal variations in river stage, and distributed recharge.
3. Establishing and testing solver parameters that would enable transient solutions to be obtained.
4. Calibrating the model against mapped historic static water levels and transient water levels in the observation well to establish the base case model for climate change simulations.
5. Running the various climate change scenarios (two future time periods, pumping and non-pumping scenarios).
6. Documenting the water budget components and undertaking a comparison between these components for each scenario.

Other Areas in BC

1. Using existing information on other aquifers in BC to identify other alluvial aquifers within the province that have strong potential interaction with surface water. This exercise will serve to identify those aquifers that should be targeted for long-term monitoring and holding stakeholder meetings to discuss climate change impacts on groundwater resource sustainability.

1.5. OUTLINE OF THE REPORT

This report contains 6 main sections:

- Section 1.0 provides the background information for the project and provides context for the purpose, main objectives and scope of work for the project.
- Section 2.0 provides an overview of the hydrogeology of the Grand Forks aquifer. The lithology database and data standardization methods are described. The aquifer architecture and conceptual models for representing this architecture are presented.
- Section 3.0 discusses General Circulation Models (GCMs) and downscaling.

- Section 4.0 discusses the hydrology of the Grand Forks region. A detailed water balance for the Grand Forks Valley, surrounding catchments, and the aquifer is provided. The physiography of the Kettle and Granby River basins and summary statistics of streamflows and water levels derived from historical flow records are given. The section also includes a discussion of the annual hydrograph and all hydrological flow regimes, describes stage-discharge rating curves fitted to BRANCH model output, and describes the procedures for linking the transient surface water levels to the Grand Forks aquifer groundwater model. Finally, the section summarizes predictions of changes in hydrographs due to climate change.
- Section 5.0 discusses the recharge for the Grand Forks aquifer. It details climate change scenario modelling, identifying the sources of climate data. It provides downscaling results for precipitation, and temperature and solar radiation, respectively. The weather input and methodology for HELP are described. Finally, the recharge results for the Grand Forks aquifer are described.
- Section 6.0 describes model construction and model calibration.
- Section 7.0 gives the results of transient groundwater flow modelling to determine the sensitivity of the aquifer to climate change under both pumping and non pumping conditions. The section also summarizes the modeled water balance for the aquifer under various scenarios.
- Section 8.0 extends in a preliminary fashion the research findings to other similar areas within BC by undertaking comparative examinations of similar aquifers.

1.6. ACKNOWLEDGEMENTS

The authors wish to acknowledge the support of financial support of Natural Resources Canada through the Climate Change Action Fund (CCAF) without which this work would not have been possible. We also with to thank Environment Canada for providing hydrometric records and predictions for to climate change, as well as technical support for climate-change related topics. In particular, Paul Whitfield is recognized for his valuable contribution to technical issues. His expertise in this field was essential for this project. Finally, we wish to acknowledge the financial and technical support of the BC Ministry of Water, Land and Air Protection. A special thanks is given to Mike Wei for providing the Kettle and Granby River survey data, access to electronic maps, and advice on the groundwater issues.

Thanks to Matt Plotnikoff at SFU for helping with intermittent computer problems, and Spatial Info Systems lab administrator Jasper Stoodley at SFU for helping in initial GIS technical problems. Also special thanks to SFU undergraduate students who helped with cross-section drawing of valley sediments (Trevor Bishop). Aparna Desphande and Dr Nadine Shuurman at SFU provided interesting discussions about litholog standardization and GIS as we all tried to use GIS most effectively for this problem.

2. HYDROGEOLOGY OF THE GRAND FORKS AQUIFER

2.1. OVERVIEW OF THE GRAND FORKS VALLEY AND AQUIFER

Grand Forks Valley lies in southern BC along the border with Washington State at the confluence of Kettle and Granby Rivers (see Map 1). The international border runs across the southern portions of the aquifer, subdividing it into ~95% area on the Canadian side, and the remainder on the US side; approximately 30% of the valley watershed lies south of the border. The City of Grand Forks is located on a broad and mostly flat terrace in an elongated valley only 4 km wide near the city, and narrowing to less than 1.5 km to the southwest and east following the Kettle River channel. Map 2 and Map 3 show the shaded relief of the topography surrounding the valley, the extent of the Grand Forks Aquifer, and the approximate boundary of the valley watershed. This local drainage area supplies streamflow to small creeks that flow into the valley and form small tributaries of the Kettle River (Map 3). The Granby River can be considered the largest tributary of the Kettle River in the valley.

The hydraulic connection of the Kettle and Granby Rivers to the shallow aquifer appears to be good as there does not appear to be any till or low permeability silt material overlying the highly permeable sand and gravel in the river beds (Allen, 2000). The upper stratigraphic unit of the aquifer consists of gravel, which appears to be closely linked with the Granby and Kettle Rivers as evidenced by the corresponding rising and falling of water levels in shallow wells situated close to the rivers (Piteau and Associates, 1993). All wells completed in this shallow layer exhibit a static level approximately at river elevation, indicating that the groundwater regime is likely strongly linked to the surface water regime.

2.1.1. CLIMATIC ZONE

The study area lies in the South British Columbia Mountains climate region (Guillet and Skinner, 1992). This region lies between the crest of the Coast Mountains and the Continental Divide of the Rockies, and includes the plateaus, highlands, valleys and mountains south of roughly 56°N latitude. It includes the basins of the Fraser, Thompson, Columbia and Kootenay Rivers as well as the Selkirk, Purcell and Monashee ranges whose heavy winter snows are the source of runoff.

Table 1 shows the Canadian Climate Normals for the Grand Forks area (data from 1941 to 1990). The year average daily maximum temperature is 13.8ºC, the year average daily minimum temperature is 1.3ºC, and the year average daily mean temperature is 7.6ºC. Approximately 352.6 mm of precipitation falls as rain and 118.2 mm falls as snow, with a total yearly average precipitation of 470.9 mm. Roughly 20% of the average annual precipitation of 471 mm was used for the Grand Forks aquifer model (Allen, 2000).

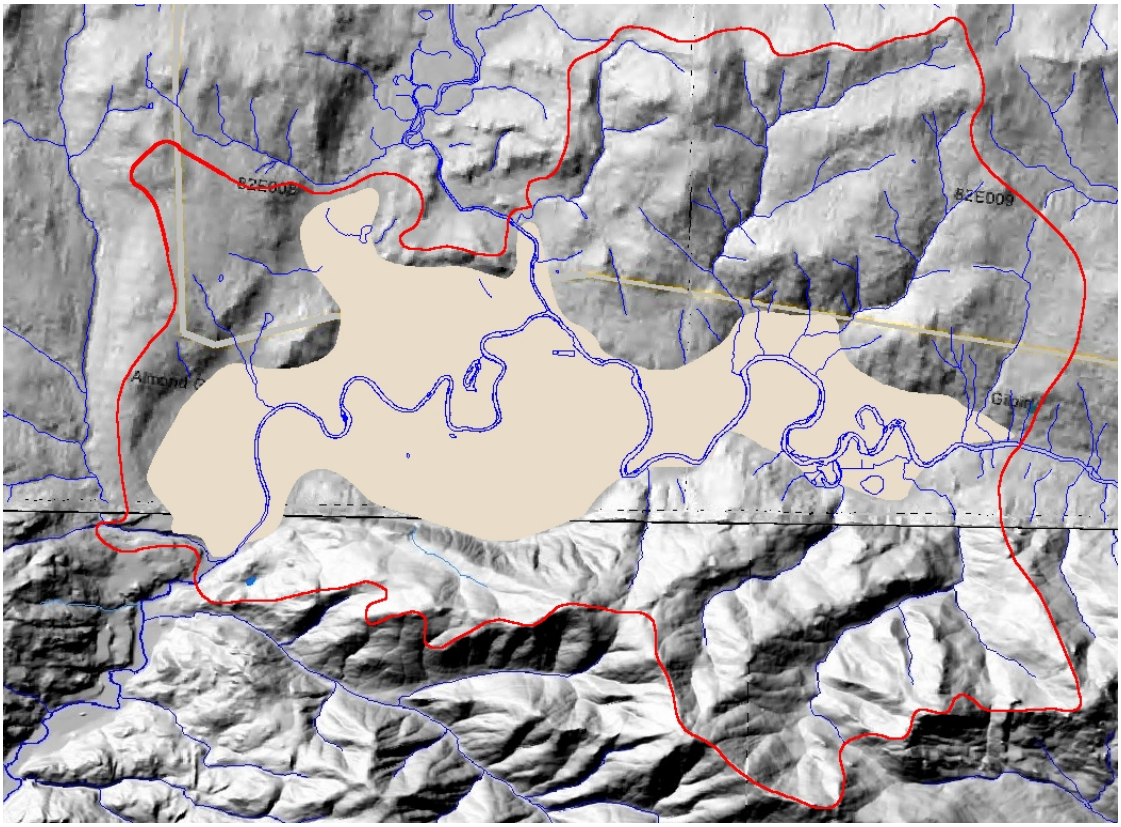

Map 2 Grand Forks Valley shaded relief map, showing the outlines of Grand Forks aquifer (filled beige), drainage (blue) and watershed boundary (red).

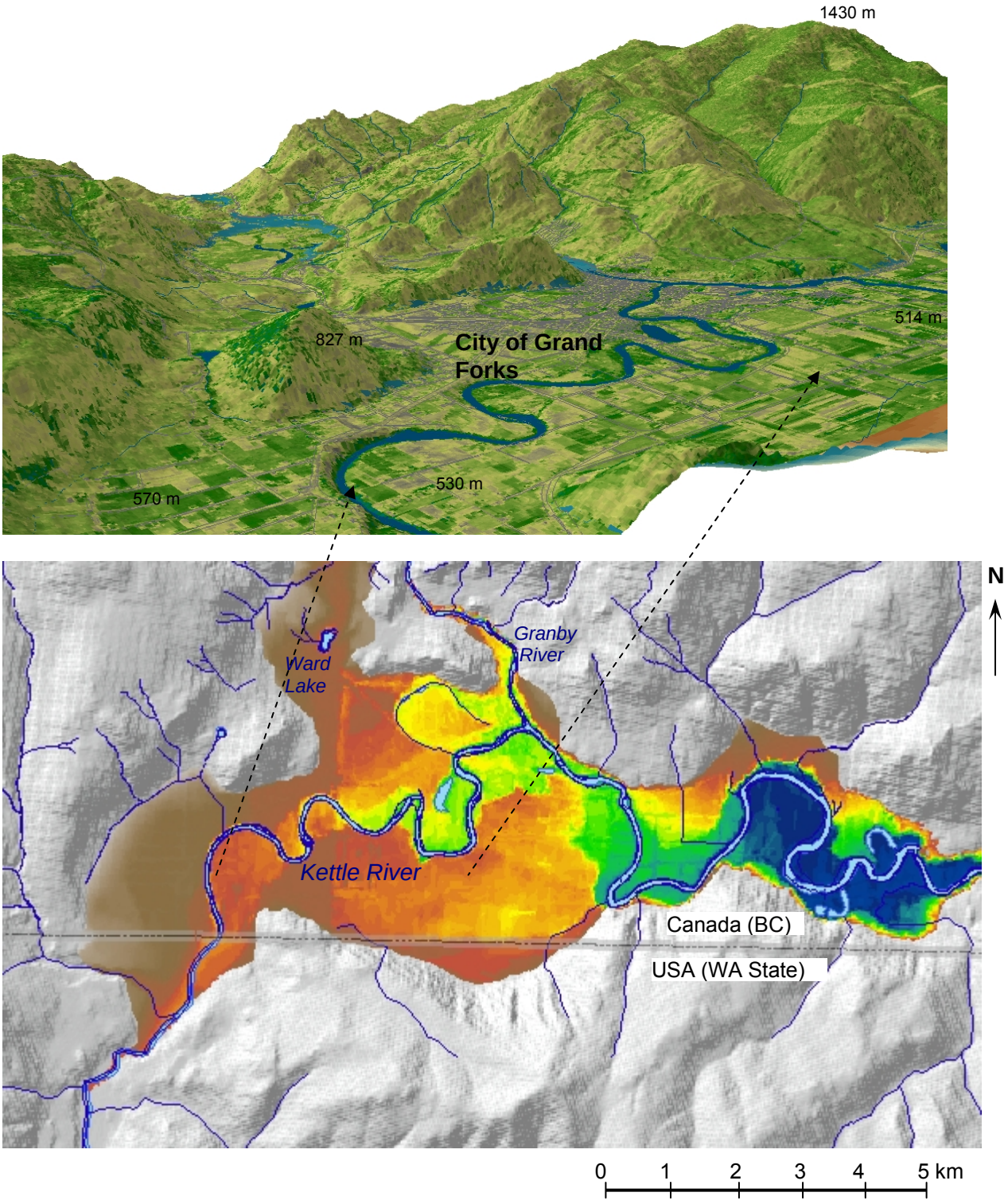

Map 3 Topography of the Grand Forks Valley. International border shown as grey line. Kettle River in blue.

Table 1 Daily Mean Temperature in ºC and Average Monthly Precipitation in mm (as snow and rain) for Grand Forks: 1961-1990 (Environment Canada).

Jan	Feb	Mar	Apr	May	Jun	Jul	Aug	Sept	Oct	Nov	Dec
Daily Mean Temperature (ºC)											
-5.3	-1.4	3.4	8.2	12.7	16.6	19.4	19.1	14.1	7.3	0.9	-4.3
Year Average Mean Daily Temperature: 7.6ºC											
Average Monthly Precipitation (total mm)											
46.4	31.5	29.3	32.5	47.5	51.9	34.2	39.2	28.1	28.8	47.0	54.6
Average Annual Precipitation: 471 mm											

2.2. WELL LITHOLOG DATABASE AND BOREHOLE DISTRIBUTION

There are a number of water well records contained in the BC Ministry Water, Land and Air Protection Water Well Database. A listing of all wells and related information is provided in Scibek et al. (2004). The well locations, relative to valley extent and aquifer bounds, are plotted in Map 4. The aquifer boundary is equivalent to intersection of bedrock valley walls and ground surface at outer extent of the unconsolidated valley sediments. The well distribution is not even, but most of the central areas are represented adequately. The far eastern portion of floodplain has only 2 well records, and the US (WA state) portion has only 2 USGS wells available (noted on map separately). Not all of the wells in BC database have lithology or water level information. Wells that have useful litholog records are shown in Map 5 and classed by total borehole litholog depth below ground surface. Most boreholes are less than 25 m deep and only a few are deeper than 100 m.

Map 4 Locations of groundwater wells in BC database (and two wells from USGS database) in Grand Forks valley.

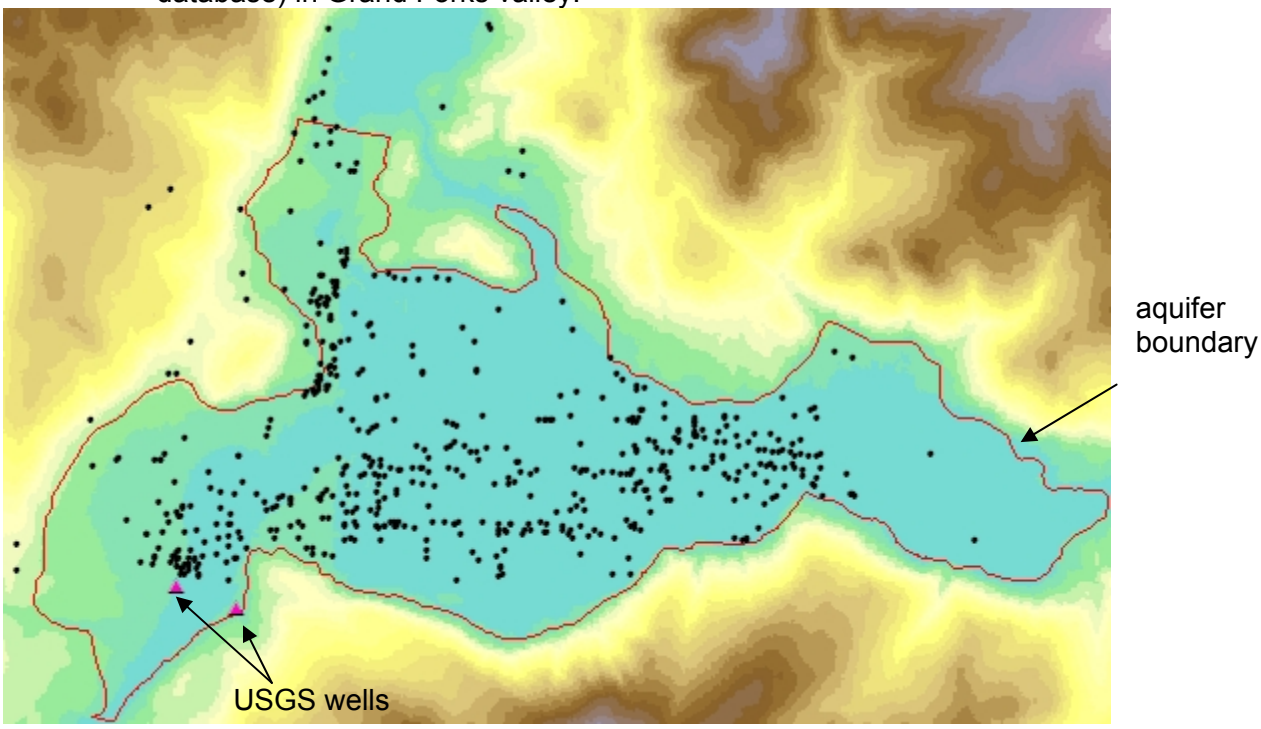

Map 5 Borehole locations and depths in Grand Forks valley. Only boreholes with lithologs in BC Database are shown.

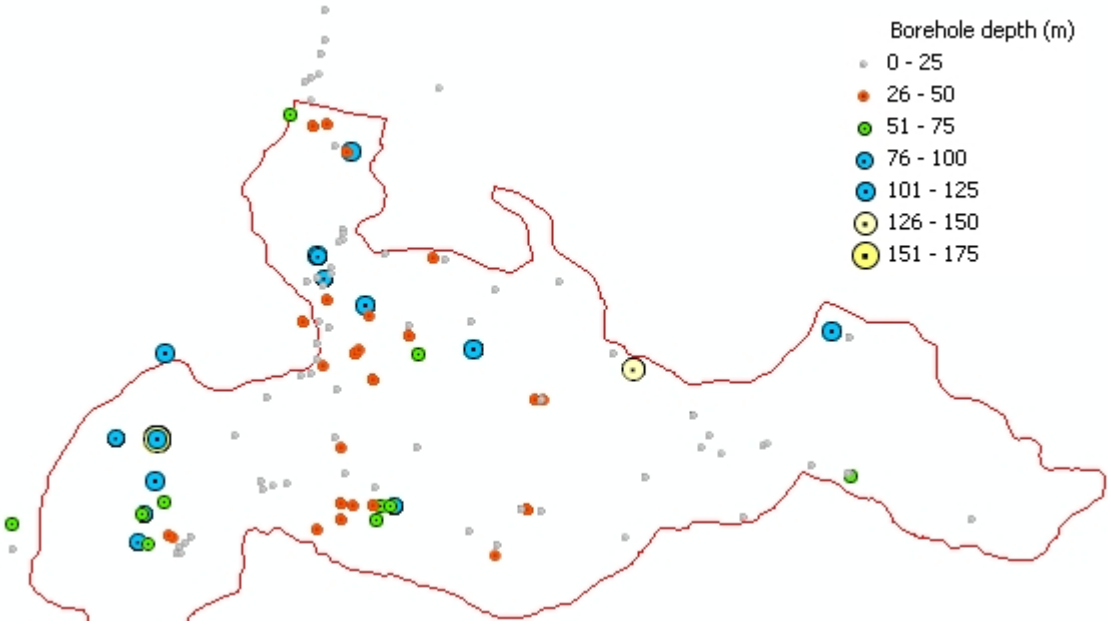

The deepest wells were drilled in W and NW valley sections. The depth distribution is not even. There are clusters of deep wells situated on high terraces above the floodplain, and most productions wells are also deep (except Big Y and Nursery district wells which were shallow). Approximately half of available well lithologs are for shallow wells (< 25 m depth). Little is know about the central and eastern valley areas.

2.3. LITHOLOG DATA STANDARDIZATION

2.3.1. OBJECTIVES OF STANDARDIZATION OF WELL (BOREHOLE) LITHOLOGS

The primary objectives for standardizing well lithologs are:

1. to present litholog data in a standard format to enhance data value (allow queries, inter-comparisons, and spatial analysis)
2. to retain all the information from existing lithology database
3. too correct spelling mistakes, and translate all geologic descriptions into standard descriptors

A borehole litholog is a record of geologic materials encountered at different depths during the drilling process. The level of precision in such records varies between wells, and probably within each well. Numerous contractors and hydrogeologists have worked on groundwater wells in BC. The variables are quality of expertise, field conditions, drilling purpose, cost of drilling, well depth and size, litholog translation into the database, and database management. All lithologs follow a format that identifies the top and bottom depth of each layer, and give a description of

lithology encountered at each depth interval. The choice of words varies slightly to significantly between different lithologs, even those that describe the same material type.

For example, consider a layer of unconsolidated deposits consisting of sand (60% by volume) and gravel (30% by volume) with properties of fine to medium grain size in each, brown in colour, and containing some silt (5% by volume). This lithology description could be worded according to i = 1 to n different sentences as shown in Table 2.

Table 2 Varieties of descriptions for potentially the same lithology

1	*brown fine to medium sand and gravel, and some silt*
2	*silty sand & gravel, fine-medium, brown*
3	*sand, fine to medium, brown & silty, gravel, fine to medium*
4	*brn. fn./med. sand & gravel with silt*
5	*silty sand and gravel*
6	*sand with gravel*
7	*sand*
...	
n	

Each of these descriptions is unique, ambiguous to some extent, and typical of lithologs in the BC database. Some authors describe more lithological details than others, and the degree of generalization varies as well. Furthermore, the complexity is increased by frequent non-standard abbreviations and word misspellings, grammatical ambiguities, and variable delimiters (comma, slash, space).

When using these data some assumptions apply:

1) The descriptions can be taken literally and describe the actual lithology of the site where the borehole was drilled. Wells can be assigned litholog quality designations that can be used for weighing the data in further analysis. These are subjective criteria and may be based on the amount of detail written in a litholog; date of drilling, well size, depth, and purpose, noting that larger hydrogeologic studies usually involve professional hydrogeologists.

2) Each litholog can be successfully interpreted as the authors meant it to be. Therefore, lithologs that are too ambiguous cannot be used.

3) The data are output correctly from the database. In each litholog, the data have to be matched to the right well identifier, the sequence of layers has to be correct, and the depths of layers must be in the correct order.

2.3.2. PRE-PROCESSING OF TEXT FILES

Lithology data are stored in BC government's database, which is publicly accessible via a website. Well lithologs can be downloaded one well at a time, or for whole BCGS mapsheets. A typical text file output for one mapsheet from that database is provided in Table 3 (2 lines shown):

Table 3 Portion of a typical text file output for a mapsheet in the BC Water Well Database

```
BCGS 082E008421 # 1 wtn 000000076552 UTM Zone 11 Easting Northing UTM Code From 6 To 7 Ft. BROKEN
ROCK MOIST CLAY Seq# 2 Water Depth 3.4 Yield 30 Gallons per Hour (U.S./Imperial) Screen from to
PT
BCGS 082E008421 # 1 wtn 000000076552 UTM Zone 11 Easting Northing UTM Code From 0 To 6 Ft. BROWN
SAND & GRAVEL COBBLES Seq# 1 Water Depth 3.4 Yield 30 Gallons per Hour (U.S./Imperial) Screen
from to PT
```

This information can be parsed by a computer program or manually on a spreadsheet to separate the data fields. An in house code was developed as part of this study to undertake these manipulations. Details concerning processing of well litholog data are provided elsewhere (Scibek et al., 2004). A complex word recognition process was then undertaken.

For each litholog layer, in each well, in each mapsheet, the text is broken up into word groups as delineated by word separators in the original text (e.g., commas or spaces); the word groups preserve the grammatical structure of the source text. In the word recognition process, each word is read separately (words are considered to be space delimited within a word group) and compared to a custom dictionary of geological terms. For each word in the dictionary there may be many also alternative spellings, abbreviations, and synonyms. Word recognition reaches practical limits where words are badly misspelled, joined together (missing separator), or totally ambiguous. The program also outputs a list of unrecognized words, which are checked by the user who then updates the appropriate word lists. In the text there are descriptions of different materials (rock or unconsolidated deposit) and their properties. The materials are also arranged in order of importance, where usually the most abundant material is specified first, and all other subsequent materials are present in smaller amounts. The goal is to extract all the materials and all separate properties, in standard form, from all lines in all lithologs. This task involves an iterative process of test-and-run to verify the results and modify the program.

2.3.3. STANDARDIZED LITHOLOGS

The output of standardized lithologs is a text file with special fields for well tag number, layer number, layer class, depth to top of layer, depth to bottom of layer, thickness, material 1, modifier word, grain size, color, structure, material 2 ... (all the properties) ... material n ... (all the properties), hydrogeology terms, drilling terms, and original source text. The original source text must be retained until the database is completely standardized, but should be kept for process verification indefinitely. The number of materials is unlimited in each layer, but it is most practical to have less than 4 materials for unconsolidated sediments. Bedrock wells usually identify a single rock type for each depth interval unless a more detailed mineralogy analysis has been done.

Table 4 shows an example of a non-standardized litholog for one well. The standardized litholog for the same well is shown in Table 5. T he standard forms can also be formatted to show the relative thickness of each unit to improve depth perception and litholog interpretation. Standard forms can be queried in a database environment using SQL statements or other methods, and layers can be generalized for spatial and structural analysis.

Table 4 Example of a non-standardized litholog

```
coarse gravel and silt
 clean coarse sand and small w b  gravel
 very coarse sand/ coarse gravel and fine silt
 coarse sand and med  sand
 med  sand/ thin clay layers and some boulders
 med  and coarse sand/ fine sand and silt
 coarse gravel with clay layers
 coarse sand and some gravel
 medium sand with pebbles
 gravel/ some sand
 very coarse gravel/ very little sand
```

Table 5 Standardized litholog output from in house standardization code

[WTN]	[layer num]	[layer class]	[depth (top of layer)]	[depth (bottom of layer)]	[thickness]	**[material(1)]**	[modifier]	[size]	[color]	[structure]	**[material(2)]**	[modifier]	[size]	[color]	[structure]
22427	1		0	24	24	gravel		coarse			silt				
22427	2		24	50	26	sand	clean	coarse			gravel		fine		
22427	3		50	57	7	sand		very-coarse			gravel		coarse		
22427	4		57	69	12	sand		coarse			sand		medium		
22427	5		69	75	6	sand		medium			clay	thin			layered
22427	6		75	86	11	sand		fine-coarse			silt				
22427	7		86	87	1	gravel		coarse			clay				layered
22427	8		87	90	3	sand		coarse			gravel	some			
22427	9		90	95	5	sand		medium			pebbles				
22427	10		95	102	7	gravel					sand	some			
22427	11		102	116	14	gravel		very-coarse			sand	some			

2.4. LITHOLOG DATA CLASSIFICATION AND INTERPRETATION

Rules were developed for litholog classification, which were used as guides for constructing the cross-sections for the conceptual model. The rules employed are discussed in detail by Scibek et al. (2004). Computer code was written to apply the rules and produce representative (interpreted) material types for all intervals in all lithologs. Not all borehole lithologs have the same quality (Map 5). Quality here refers to the amount of detail recorded and accuracy of descriptions.

The actual implementation of rules was done in VB code and run on an Excel spreadsheet with the litholog database. This method provided a quick and visual environment for data manipulation. Figure 1 shows lithologs that were classified based mainly on primary material (first encountered in litholog) in Grand Forks valley. These lithologs are arranged west to east (projected onto a W-E cross section). W-E sediment trends are shown.

Figure 1 Classified lithologs based mainly on primary material (first encountered in litholog) in Grand Forks valley, arranged West to East (projected onto a W-E cross-section). W-E sediment trends are shown.

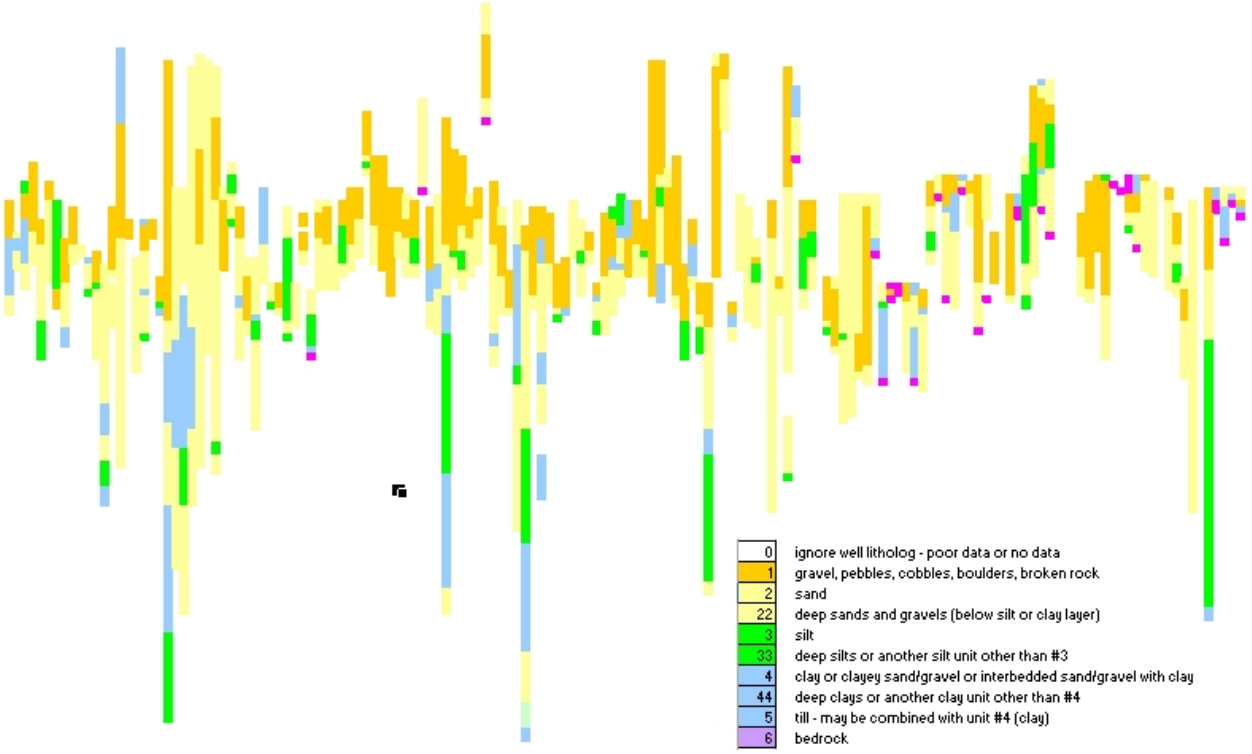

Map 6 Litholog reliability (inferred) classes.

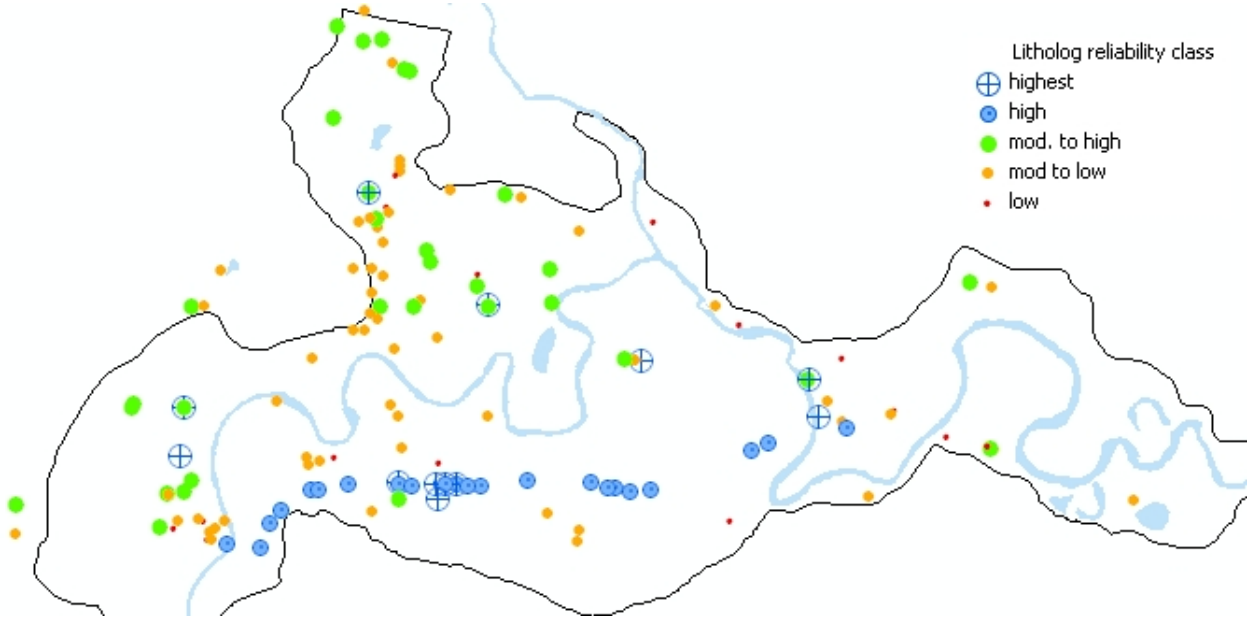

2.5. BEDROCK SURFACE MODEL

The bedrock surface of Grand Forks valley has been eroded by glacial processes during the Wisconsin glaciation, and pre-glacial fluvial erosion. The valley shape is described by nearly-parabolic curves (Graf, 1970; Wheeler, 1984; Hirano and Aruya, 1988) fitted to 67 valley profiles constructed to model the bedrock topography in this project (Map 7). The bedrock surface and representation of sediments in cross section are shown on Map 8 and Map 9, respectively.

Map 7 Bedrock geology of Grand Forks valley, with valley walls, bedrock profile lines, and bedrock elevation points.

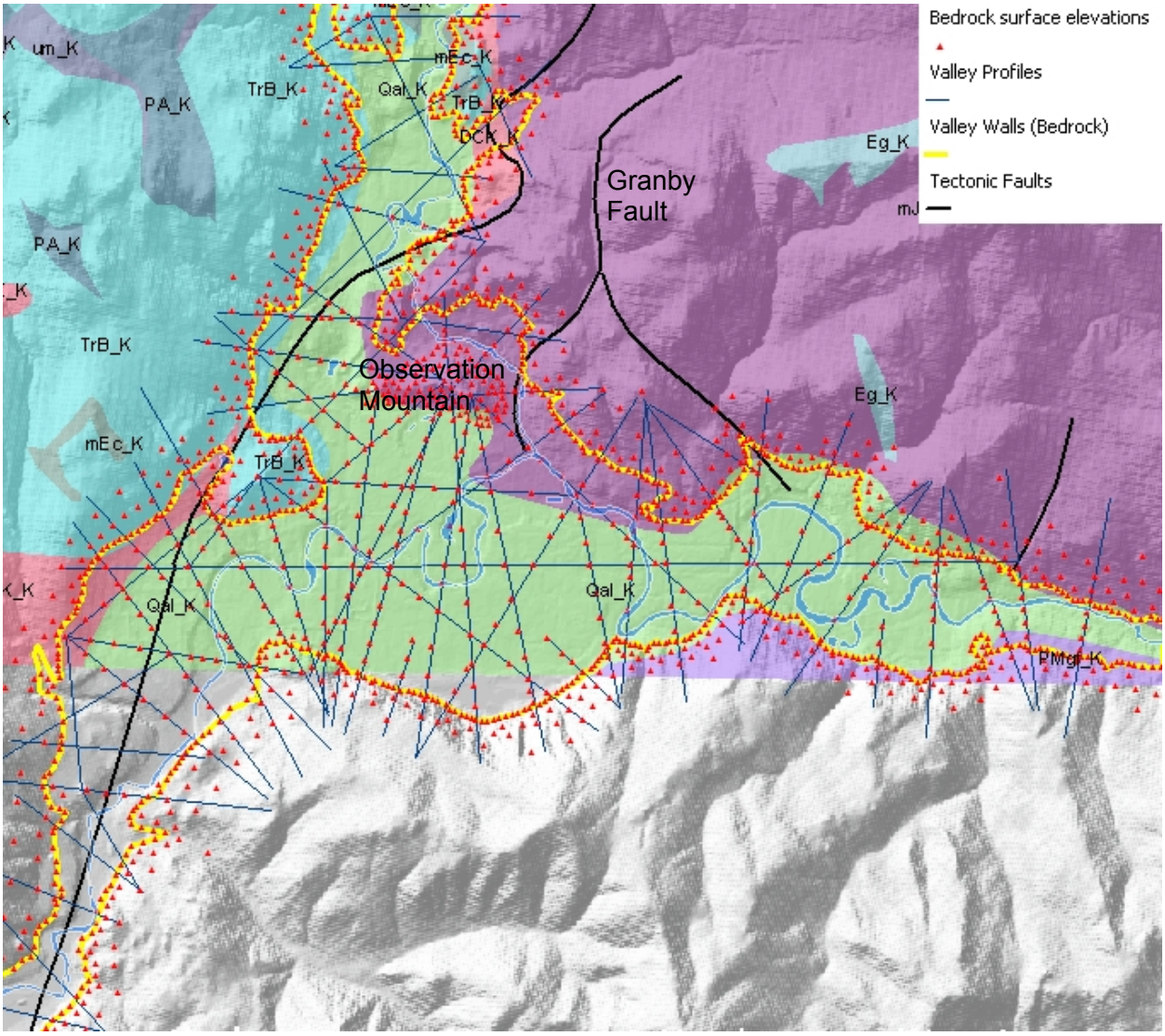

Map 8 Bedrock surface of the Grand Forks valley generated from a geostatistical model.

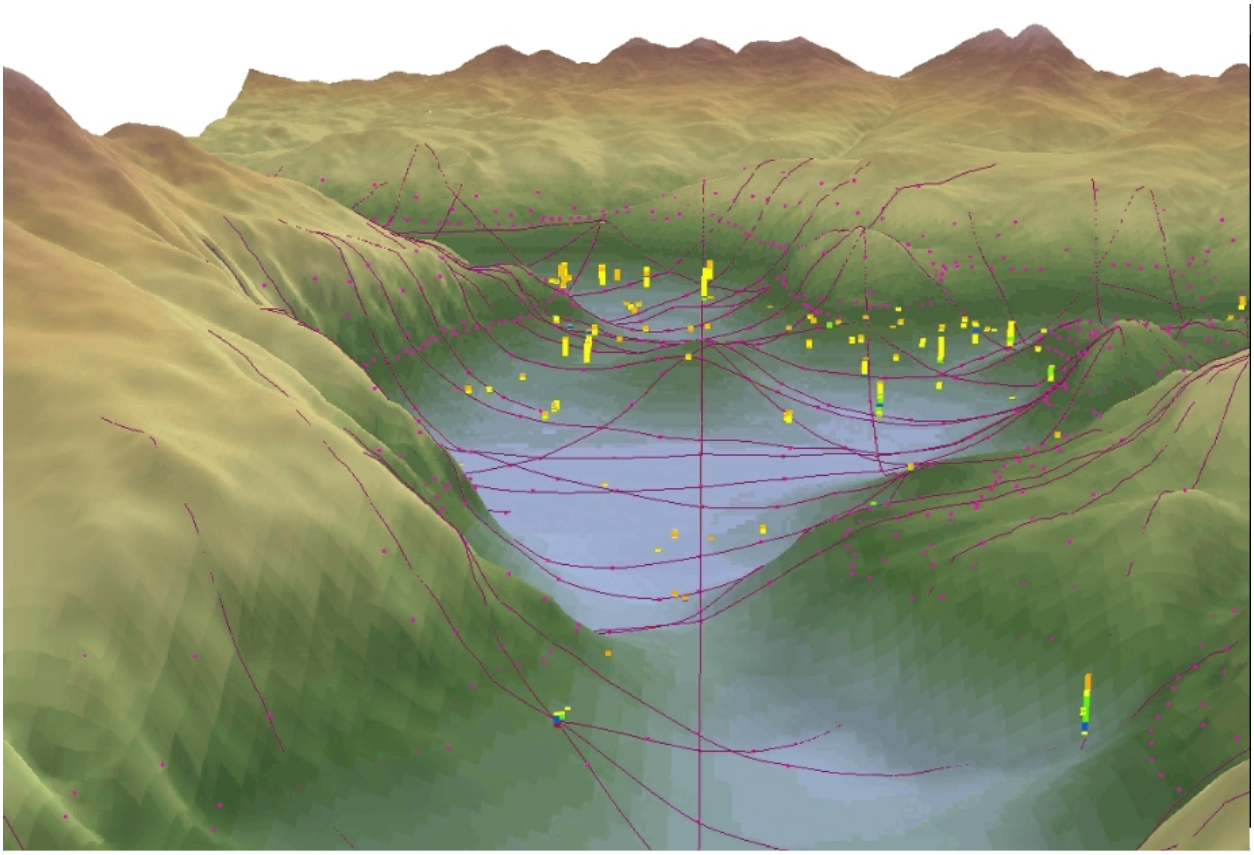

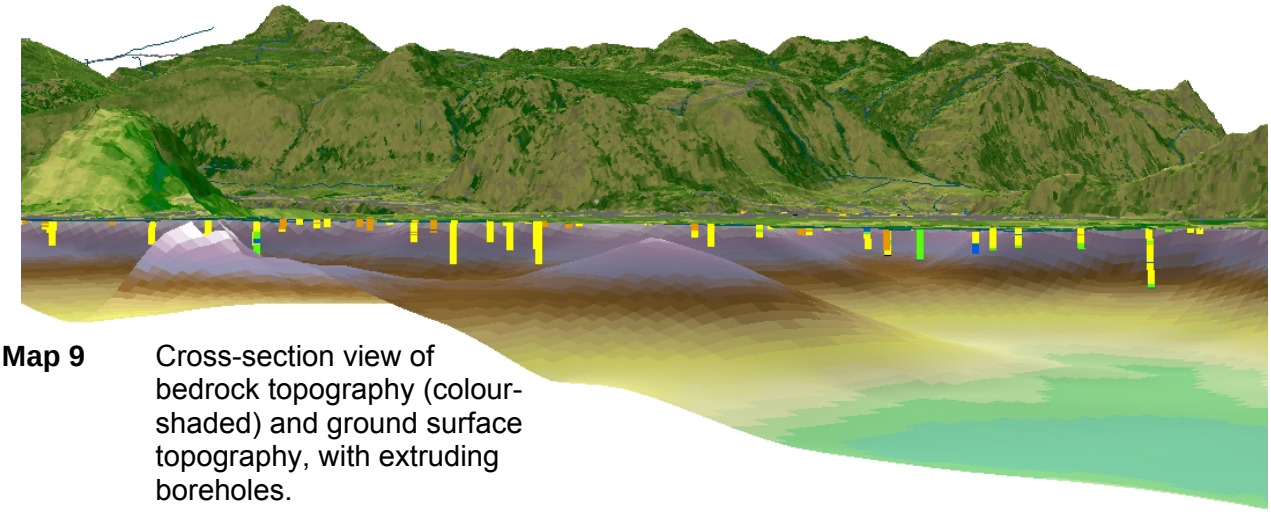

Map 9 Cross-section view of bedrock topography (colour-shaded) and ground surface topography, with extruding boreholes.

2.6. QUATERNARY SEDIMENTS

The Grand Forks valley floodplain is underlain by alluvial and glacial drift units, consisting predominantly of sand, gravel, silt and clay (Wei et al., 1994). Pleistocene sediment fill thickness is up to 300 m (Mullins et al, 1990) in smaller valleys and up to 800 m (Eyles et al, 1991; Eyles and Mullins, 1997) in large tectonic valleys, as obtained from seismic surveys. However, the valley does not appear to be primarily tectonically-controlled compared to other north-south trending troughs, such as the Okanagan valley, Shuswap Lake valley, and other deeply in filled valleys in the southern-interior of British Columbia (Map 7). Most in-filled valleys in BC have very steep valley walls, have deep sediment fill deposited in glaciofluvial and glaciolacustrine environments during the last glaciation (Clague, 1981; Fulton, 1984; Ryder et al., 1991), and have been modified by glacial erosion.

Map 10 Total sediment thickness above bedrock surface in Grand Forks valley.

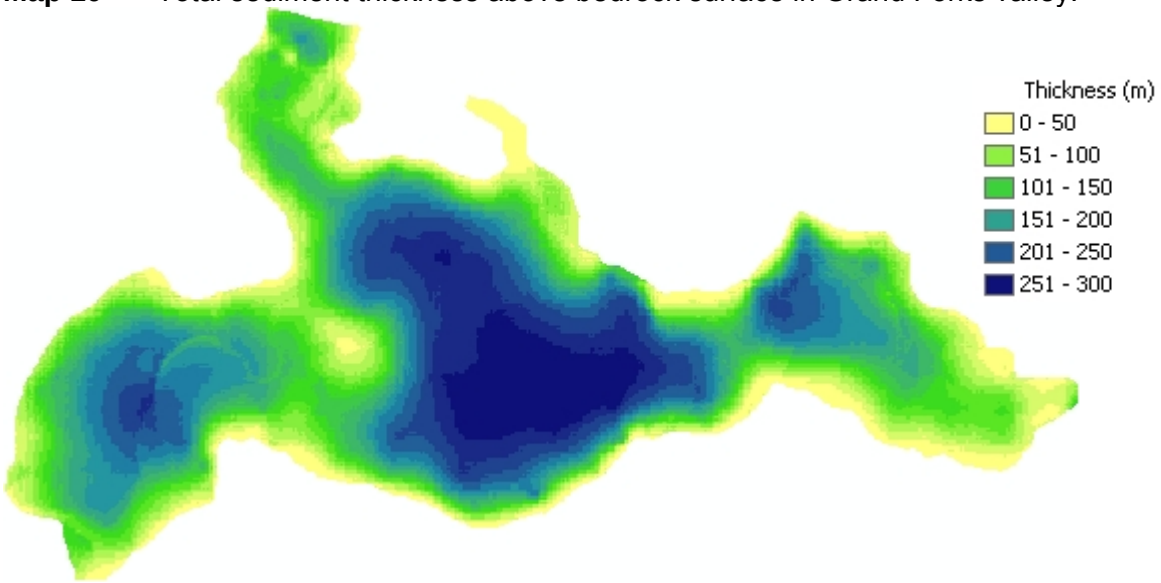

In many locations, large post-glacial lakes were created by ice dams, causing deposition of large volumes of glaciolacustrine sediments, which are now exposed as terraces (Fulton, 1984; Ryder et al., 1991), and are different in origin than Holocene fluvial terraces (Ryder and Church, 1986) that abound in valleys in British Columbia.

The stratigraphic sequences in Grand Forks valley are poorly understood, although approximately 150 well lithologs are available for mostly shallow groundwater wells. Previous investigators have attempted to create a layered conceptual model of the aquifer (Campbell, 1971; Piteau Associates, 1988, 1993; Allen, 2000). In other valleys in southern BC, the basal units are commonly silt, clay and gravel, overlain by thick glaciolacustrine silts (Fulton and Smith, 1978; Vanderburth and Roberts, 1996), and capped by Holocene sandy and gravelly outwash and floodplain deposits; paraglacial alluvial fans are also common (Ryder, 1971).

Literature consulted included a groundwater modelling report prepared for the Ministry of the Environment (now the Ministry of Water, Land and Air Protection) by Allen (2000) and several MELP / MWLAP reports, including a 1992 report on the results of the 1989/90 nitrate sampling programs (Wei, 1994), a 2002 follow-up to that report based on 2001 nitrate sampling data (by Jennifer Maxwell, Kevin Ronneseth and Mike Wei), and a 1999 report outlining preliminary capture zones for community wells in Grand Forks (Wei, 1999). A working hydrostratigraphic

model was created (to be the basis for classifying the subsequently obtained well lithology data). The hydrostratigraphy for Grand Forks, as stated by this model, is (from top to bottom):

(1) Gravel (with or without sand)
(2) Sand
(3) Silt
(4) Clay
(5) Sandy and gravel
(6) Bedrock

These units were created with the caveats: (a) the presence of discrete silt and clay layers and the relative stratigraphic orientation of those layers is somewhat conjectural, and (b) the lower sand and gravel unit is likely not present throughout the basin, and its exact distribution is unknown. It was also determined that the upper gravel and sand units are thickest in the southwest part of the basin, while the underlying silt / clay units approach the surface in the southeast part of the basin. Additionally, the aquifer boundary to the north was inferred to consist of a groundwater divide; the sediments, however, are continuous in this direction (Wei, pers. comm.). Finally, given the Quaternary history of much of British Columbia, it is likely that the sediments in this basin are largely of glaciofluvial and/or glaciolacustrine origin; this genetic model helps to constrain the morphology of these units.

In the Grand Forks valley, the upper gravel (layer 1) and sand (layer 2) deposits are interpreted to be almost all glacial outwash, interspersed on the surface with deposits formed by infilled oxbow lakes, with occasional unsorted and compacted glacial till (diamicton – mostly silt and clay and some sand and gravel). The river meanders and reworks these materials, so the deposits are channel and bar deposits, and very heterogeneous over the valley (sand versus gravel content varies). Clays and silts are laid down on lake bottoms and in slack water deposits at meandering river bends. Cutoff channels and oxbow lakes are also common in this valley. Most of the references interpret the thin clay and silt deposits as localized lenses of such material. A larger lake may have been present in the valley when dammed by retreating and melting glaciers. Thick layers of clay and silt may have been deposited.

The silt layer (layer 3) refers most likely to glaciolacustrine silt which may have been deposited in a ponded glacial lake as the Cordilleran Ice Sheet melted. The clay layer 4 could represent glacial till or combination of till and glaciolacustrine and other sediments, but clay is abundant. It is probably not continuous as suggested by the layered model here.

The unconsolidated sediments thicken toward the middle of the valley, have presumed horizontal stratigraphy, and the topmost coarse grained sediments form the Grand Forks Aquifer (Allen, 2000). The surficial geology of the valley is dominated by outwash gravels, the soils (Sprout and Kelly, 1964) and shallow well lithologs show high degree of heterogeneity of materials in the unconfined aquifer.

2.7. AQUIFER GEOMETRY

2.7.1. DRAFTING OF CROSS-SECTIONS FOR THE CONCEPTUAL MODEL

The first step in drafting the cross-sections was collecting the necessary lithology data. All such data were downloaded from the MWLAP online water well database and integrated into the previously established spreadsheet. Unknown or anomalous ground surface elevations were estimated using the MWLAP supplied UTM coordinates and a digital contour map also supplied by MWLAP. The wells were initially sorted and ranked by depth (deeper wells obviously providing better control on the subsurface lithology), and secondly, ranked based on data quality. Hydrostratigraphic interpretations were made for the lithology data for each well. The interpretations were made for each well individually, but with some consideration given to interpreted hydrostratigraphy for adjacent wells depending on the proximity of those wells to the well being interpreted (closer wells were given greater consideration). Hydrostratigraphic delineation was based on the working model outlined previously, with thought given to the two caveats mentioned. It was observed that a significant number of wells logs did, in fact, describe discrete silt and clay layers with the silt overlying the clay. Also, the lower sand / gravel layer was visible at the base of several wells to the north of the basin. These interpretations were performed within a Microsoft Excel spreadsheet created for the purpose, and which included scaling calculations for subsequent plotting.

With the section lines and interpreted hydrostratigraphy established (and scale distances calculated), cross-section construction using Corel Draw was relatively straightforward (Map 11). Initially, cross sections were constructed as pure, straight line sections with linear interfaces connecting interpreted hydrostratigraphic boundaries at the respective wells. These interfaces were subsequently revised to reflect the inferred morphology of the individual units and to make the interpretations within the east-west cross-sections consistent with the interpretations within the north-south cross-sections. Of note is the lower sand / gravel layer visible in the north of the basin. This layer may have formed early during the infill of the basin, likely soon after the retreat of an ice sheet, and probably represents a delta into a nascent glacial lake (Clague, personal communication). Based on this hypothesis, the lower sand / gravel layer was drafted with the cross-sectional morphology of a typical Gilbert-style delta.

The bedrock surface was created after the initial cross-sections were drawn. Consequently the cross-section drawings were modified to include newly modeled bedrock surface. Figure 2 is one cross-section across the valley. Several difficulties were encountered in the construction of the cross-sections. Firstly, as the lithology data available were from existing water wells, the resulting data distribution was dependant on the subaerial positioning and depths of these wells. This has resulted in undesirable but unavoidable data gaps over certain segments of the cross-sections. Secondly, the lithology information for most of these wells was originally collected by the various drilling contractors during well installation. While such individuals are no doubt familiar with geologic materials, it is likely that a lack of geologic training has resulted in less than accurate well lithology records.

Map 11 Fence diagram constructed from interpreted cross-sections of Grand Forks valley: (a) graphical representation, (b) location of cross-sections in valley (bedrock surface)

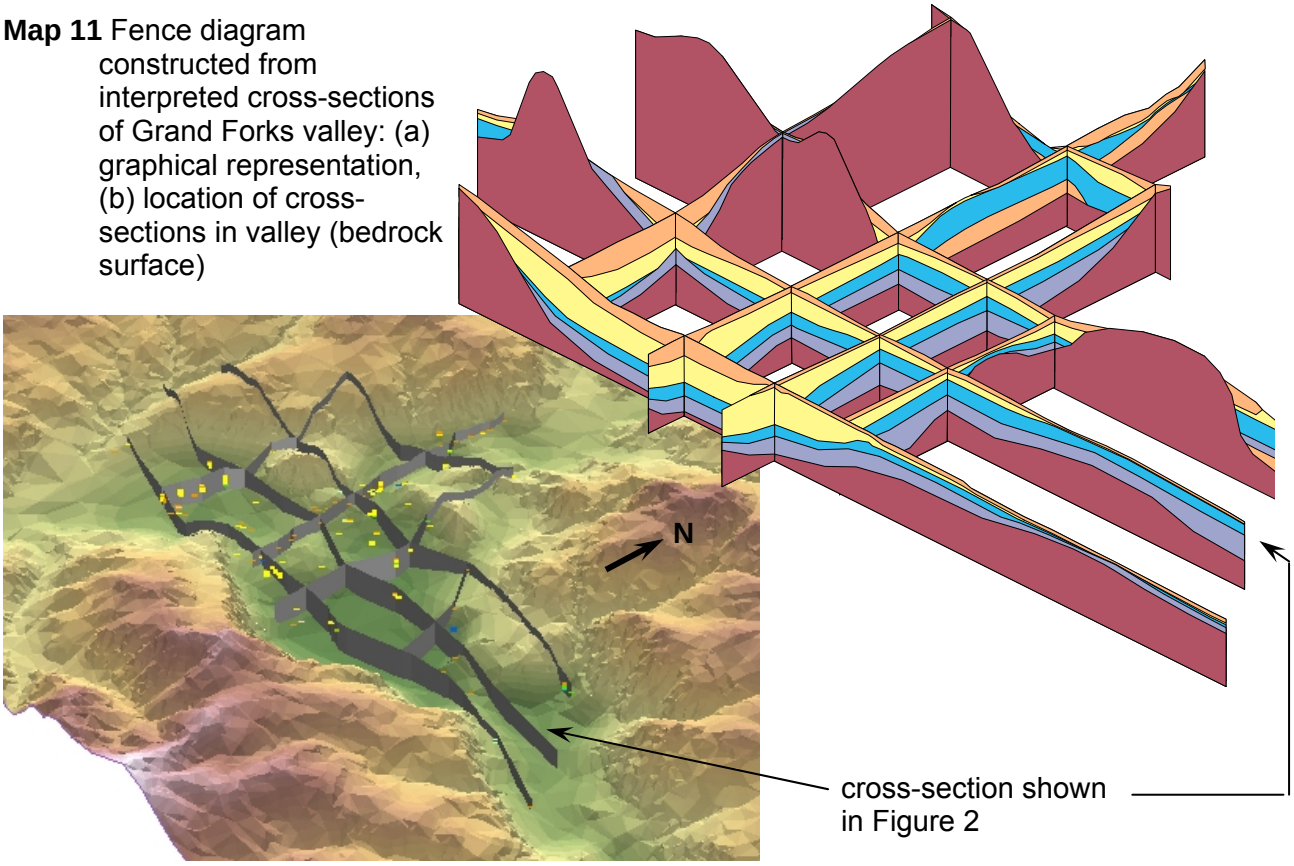

Figure 2 Cross section of sediments in Grand Forks valley (Xsec3)

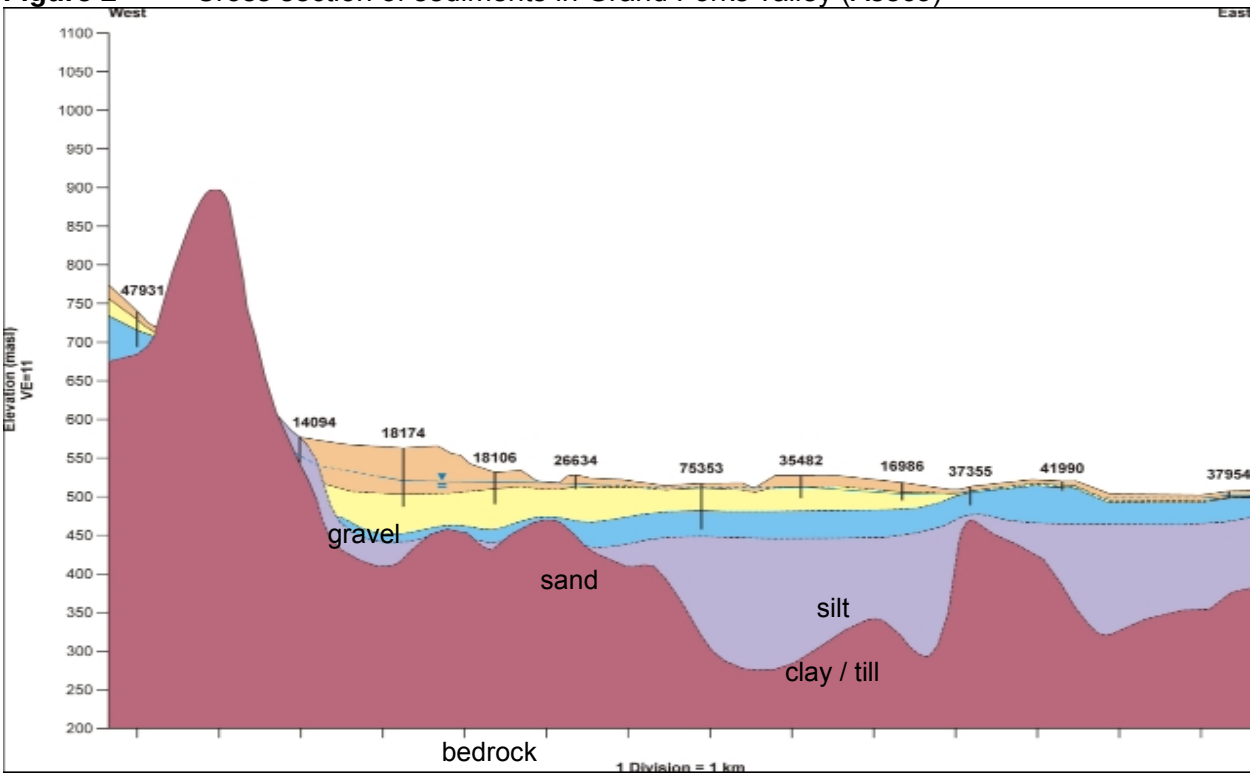

2.7.2. 3D HYDROSTRATIGRAPHIC MODEL IN GMS

The classified lithologs were imported to GMS system, together with ground and bedrock surfaces. The top and bottom elevations of each layer were determined by constructing cross-sections within GMS (version 4.0) and interpolating between points to generate a solid model. The litholog database is visualized as extruded litholog classes (by colours) from ground surface down to appropriate depths for each litholog interval, and superimposed on coloured bedrock surface and shaded-out ground surface in Map 12 (note that valley floor ground surface is turned off to show the lithologs, but the Kettle River is shown as it flows in its channel in the floodplain to help visualized the location of valley ground surface). In Map 13 the hydrostratigraphic model of Grand Forks valley fill is represented as a fence diagram created from solid model in GMS. Layer elevations were then imported into the existing Grand Forks aquifer model that was generated in Visual MODFLOW. The lower discontinuous sand unit is not represented in the model. Additional boreholes were added to "guide" the solid model generation (Map 14b). Ideally the solid model of layers should show thinning and draping onto valley walls. These added control boreholes did not change the stratigraphy of the valley, but helped the solid model algorithm to deal with edge effects and the very complex bedrock topography. The solid model of sediments is contained between two surfaces: ground surface and bedrock surface (represented by TIN model in GMS). Finished solid model, without the surficial gravel layer (to show underlying sands and silts) is displayed in Map 14.

Map 12 Perspective view of borehole lithologs above bedrock surface in Grand Forks valley. (hills above floodplain surface are shown in grey and bedrock in colours; Kettle River is shown)

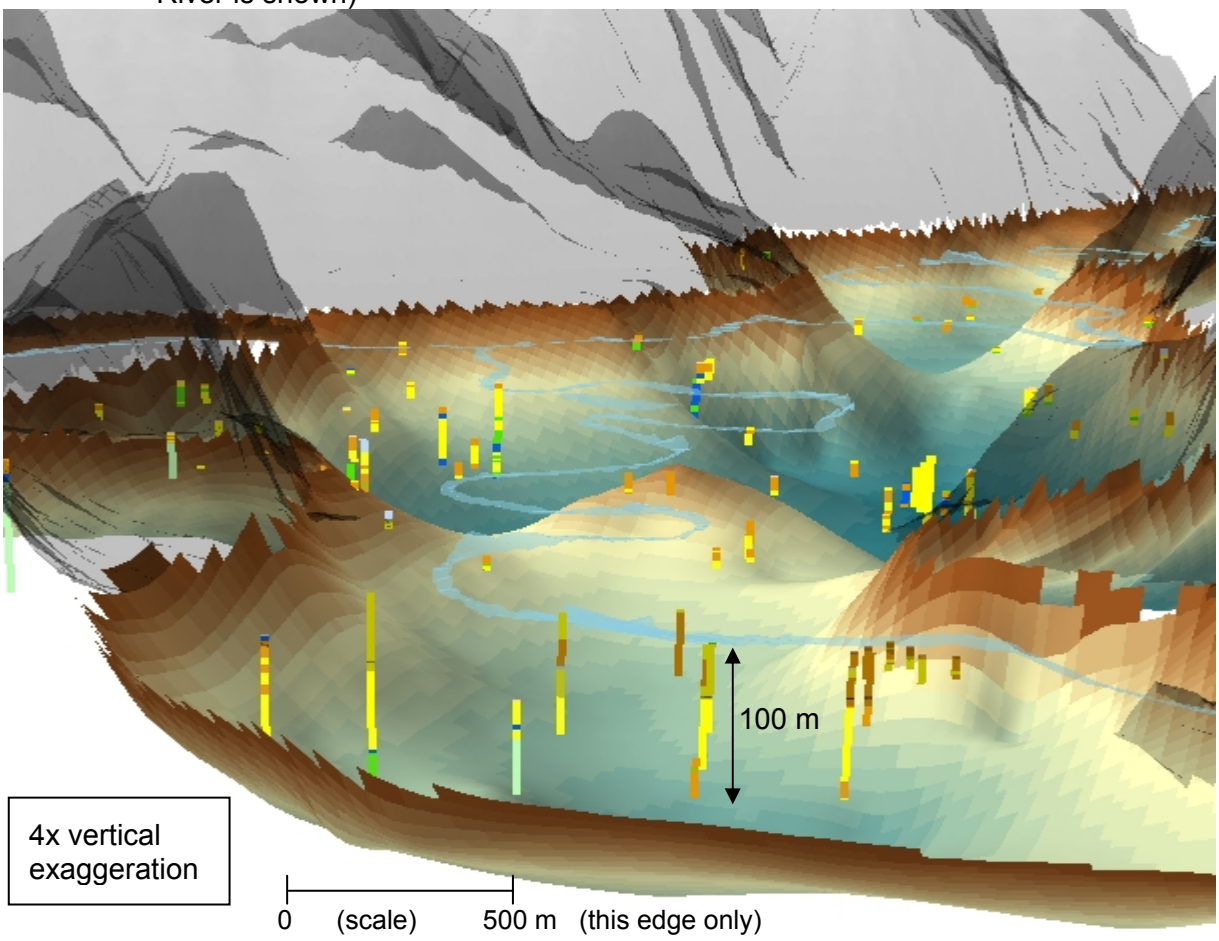

Map 13 Hydrostratigraphic model of Grand Forks valley fill. Fence diagram created from solid model in GMS.

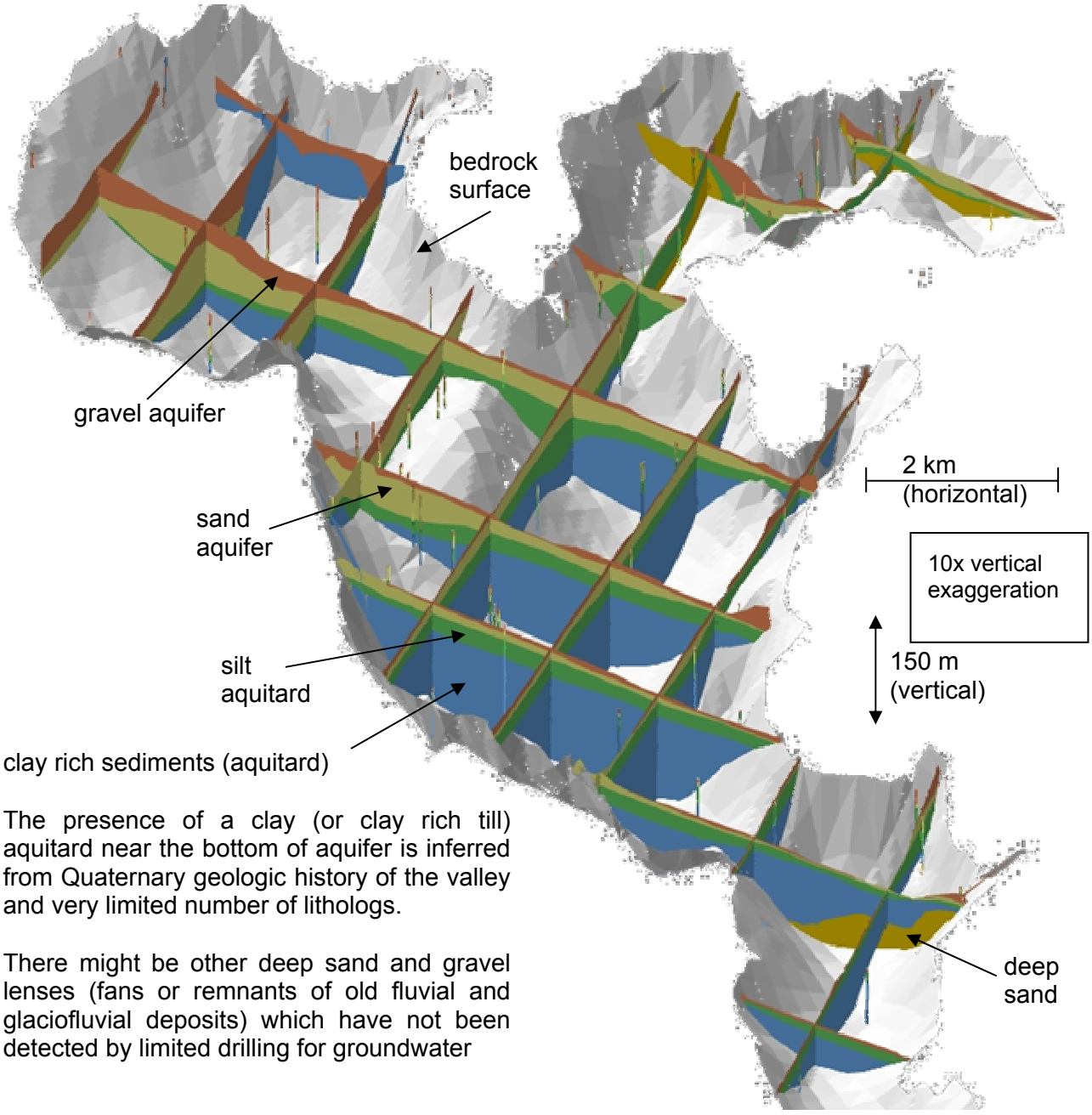

The presence of a clay (or clay rich till) aquitard near the bottom of aquifer is inferred from Quaternary geologic history of the valley and very limited number of lithologs.

There might be other deep sand and gravel lenses (fans or remnants of old fluvial and glaciofluvial deposits) which have not been detected by limited drilling for groundwater

Map 14 Solid model of valley sediments constructed in GMS from all available standardized borehole lithologs: (a) solid model and 3D mesh showing ground surface, (b) solid model of sediments with all boreholes and control points for bedrock representation (long lines around the solid model).

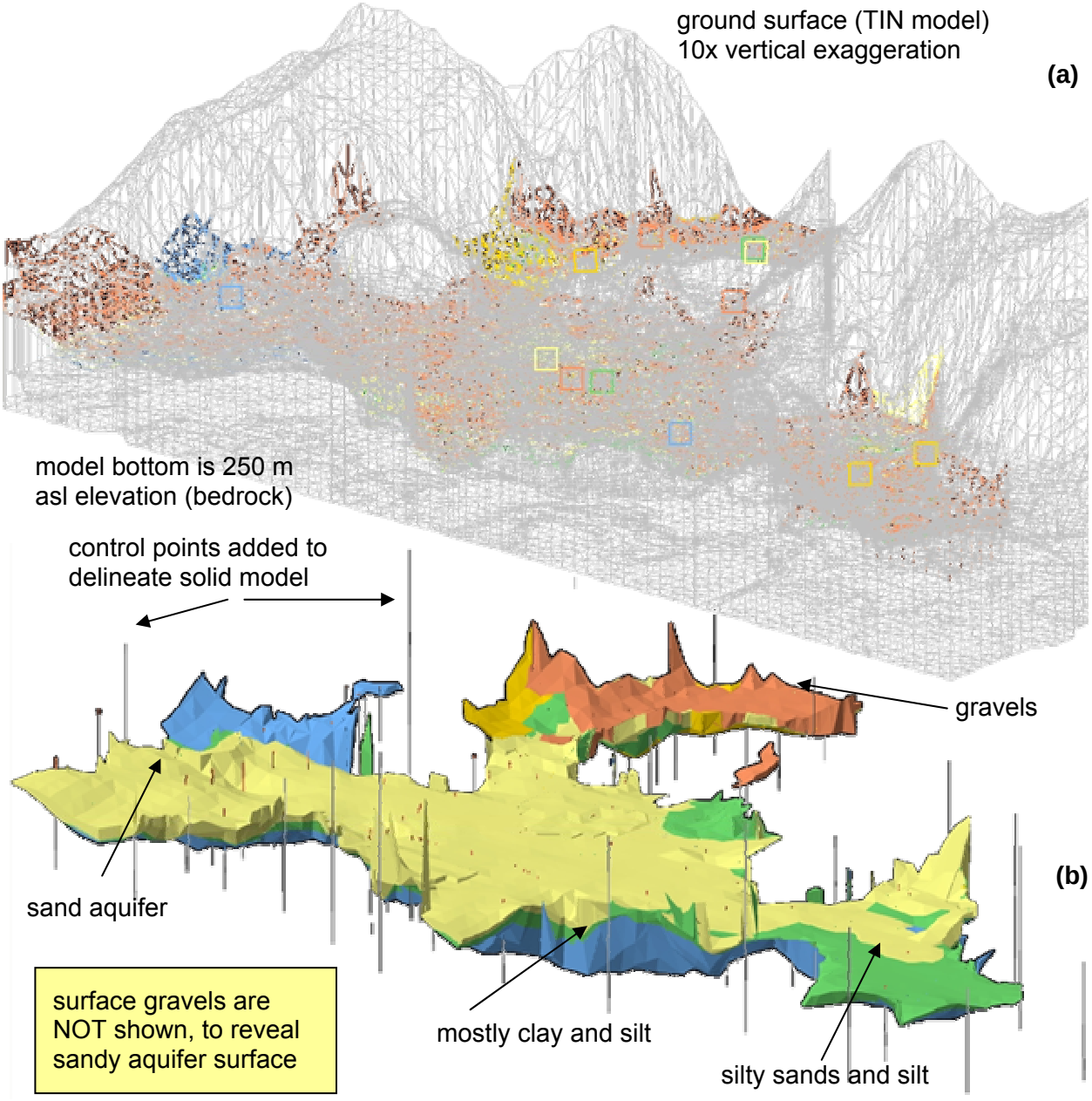

3. GENERAL CIRCULATION MODELS

3.1. INTRODUCTION

Climate simulation models and physically-based numerical models are used for climate prediction, the study of climate change and variability, and to better understand the various processes which govern our climate system. The global climate is modeled by various General Circulation Models (GCMs). One of these is the Canadian Global Coupled Model (CGCM1).

In this report, the climate scenarios and subsequent analyses and models of impacts on groundwater resources are derived from CGCM1 predictions. Therefore, a short introduction to CGCM1 workings and model results is necessary. The Canadian Climate Centre for modelling and Analysis (CCCma) describes the CGCM1 general circulation model as follows. The first version of the CGCM1, and its control climate are described by Flato et al. (2000). The details of the model and discussion of primary results may also be found in Climate Change Digest (as a .PDF) published by Environment Canada. The atmospheric component of the model is essentially AGCM2 described by McFarlane et al. (1992). CGCM1 has a surface grid resolution of roughly 3.7° x 3.7°. An ensemble of four transient climate change simulations has been performed and is described in Boer et al. (2000a and b). Three of these simulations use an effective greenhouse gas forcing change, corresponding to that observed from 1850 to 1990, and a forcing change corresponding to an increase of CO_2 at a rate of 1% per year (compounded) thereafter until year 2100 (the IPCC "IS92a" forcing scenario). The fourth simulation considers the effect of greenhouse gas forcing only. The change in climate predicted by a model clearly depends directly on this specification of greenhouse gas (and aerosol) forcing and, of course, these are not well known. The prescription described above is similar to the IPCC "business as usual" scenario, and using a standard scenario allows the results of this model to be compared to those of other modelling groups around the world. The ability of a climate model to reproduce the present-day mean climate and its historical variation adds confidence to projections of future climate change.

For the globe, between years 1980 and 2050 the prescribed CO_2 concentration doubles, and over this time the greenhouse gas only run (the upper curve) exhibits an increase in temperature of 2.7°C. The increase over the same period in the greenhouse gas plus aerosol run is 1.9°C; the difference of 0.8°C is the cooling effect of the aerosols. One can contrast these results with the equilibrium calculation of Boer et al. (1992), who used the same atmospheric model without the aerosol effect. They obtained a global average warming of 3.5°C upon doubling CO2 concentration. These CGCM1 predictions correspond to observed temperature of the globe for historical and current periods (Jones, 1994).

3.2. SUMMARY OF CGCM1 PREDICITONS FOR BRITISH COLUMBIA

In British Columbia, climate change has been detected from detailed examination of meteorological, hydrologic, sea level, and ecological records and investigations. Analysis of historical data indicates that many properties of climate have changed during the 20th century (Ministry of Water, Land and Air Protection of BC, 2002). Some of the changes were:

- Average annual temperature warmed by 0.6ºC on the coast, 1.1ºC in the interior, and 1.7ºC in northern BC.

- Night-time temperatures increased across most of BC in spring and summer.
- Precipitation increased in southern BC by 2 to 4 percent per decade.
- Lakes and rivers become free of ice earlier in the spring.
- Water temperature increased in rivers and streams.

Climate models and scenarios suggest that the climate in British Columbia will continue to change during the 21st century, according to summary report by Ministry of Water, Land and Air Protection of BC (2002). Future predictions may include:

- Average annual temperature in BC may increase by 1ºC to 4ºC.
- Average annual precipitation may increase by 10 to 20 percent.
- Many small glaciers in southern BC may disappear.
- Some interior rivers may dry up during the summer and early fall.

Climate change scenarios suggest that warmer winter temperatures will result in a greater proportion of precipitation falling as rain. Coulson (1997) computed stream runoff for several stations in BC using the Thornthwaite model. GCM results showed that a CO_2 doubling in the atmosphere (using a GCM model) would result in an increase in the mean annual precipitation and the mean annual temperature for each of the stations examined throughout the province of BC. Based on the projected changes in climate variables for each month, the Thornthwaite model was used to compute monthly runoff. Annual winter and spring runoff are expected to increase, although the additional precipitation would be offset somewhat by greater evapotranspiration associated with rising temperatures and longer growing seasons (Coulson, 1997). Computed runoff, calculated under doubled CO_2 temperature and precipitation conditions, resulted in an 86% change for the climate station at Princeton, BC and a 71% change for Cranbrook, BC. For the South BC region, earlier snowmelt will be especially significant where the spring freshet may occur up to one full month earlier, and there will be a potential for increased peak flows in coastal and southern BC (Coulson, 1997). As well, the summer low flow period will be characterized by even lower streamflows.

3.3. SCALING APPROACH

GCM's do not accurately estimate local statistics of regional climate variables, but the internal consistency of these physically-based climate models provides the most likely estimates of ratios and differences (scaling factors) of climatic variables, such as precipitation and temperature from historical (base case) to predicted scenarios (Loaiciga et al., 1996). Thus, scaling factors are used to generate climate-change scenarios from historical time series. For example, Loaciga et al. (2000) modeled recharge to extensive Edwards Aquifer in Texas using scaled historical precipitation and temperature records to GCM scenarios for doubling of CO_2 (denoted as $2xCO_2$) and present conditions ($1xCO_2$):

$$P\ 2xCO_2\ \text{scenario} = (P\ 2xCO_2 / P\ 1xCO_2) + P\ \text{historical}$$
$$T\ 2xCO_2\ \text{scenario} = (T\ 2xCO_2 - T\ 1xCO_2) + T\ \text{historical}$$

The scaled time series of P and T are used to model recharge, and are input to aquifer numerical models for estimating the impacts on groundwater resources under various climate change scenarios. It is also possible to choose historical time series as a low, medium, and

high P or T base case scenarios. Also, a range of pumping scenarios can be added to further complicate the range of predictions and increase the number of models generated.

The question is then, what is the most reasonable base case? If the historical record is chosen only for drought years, then the base case represents the dry extreme of climatic range for that area, and climate change scenarios will show impacts to groundwater levels that would occur if climate change followed dry conditions, without any future wet years. This is unlikely. The most common approach is to take the entire historical period and average it to derive the base case, assuming that it is representative of pre-climate change conditions. Then, climate change scenario is generated by modifying the base case climatic time series. This approach tends to smooth out climatic variability and assumes average conditions before climate change occurs.

3.4. STATISTICAL APPROACHES

For many climate change studies, scenarios of climate change derived directly from General Circulation Model (GCM) output are of insufficient spatial and temporal resolution. Spatial downscaling techniques are used to derive finer resolution climate information from coarser resolution GCM output, which have been designed to bridge the gap between the information that the climate modelling community can currently provide and that required by the impacts research community (Wilby and Wigley, 1997). The fundamental assumption behind all these methods is that the statistical relationships, which are calculated using observed data, will remain valid under future climate conditions.

A study by Cannon and Whitfield (2000) assessed whether the recent observed changes in streamflow conditions in British Columbia can be accurately predicted using an empirical downscaling approach. The results of that study suggested that neural network empirical downscaling models are capable of predicting changes in streamflow observed during recent decades using only large-scale atmospheric conditions as model inputs.

Beersma (2000) showed climate scenarios useful for hydrologic impacts assessment studies. Climate downscaling techniques are treated in more detail by Hewitson and Crane (1996). A review of applications of downscaling from GCM to hydrologic modelling can be found in Xu (1999). Similar methods apply to temperature and precipitation predictions.

The National Center for Environmental Prediction (NCEP) maintains a Reanalysis Project database (Kalnay et al., 1996), which provides large-scale climate variables that can be used to define analogs with GCM for climate modelling purposes. In the first step, the statistical characteristics of the observed time series at each station are computed. The time series for the relevant parameters are generated using the observed statistical properties. The long time oscillations are combined with shorter seasonal trends (standard deviations), while mean values are modified using an imposed linear trend (climate change). Short oscillations are superimposed randomly to make the time series more realistic. At least one climate change study involving aquifer modelling used this approach recently (Kruger et al., 2001).

In this project, the NCEP datasets will be used to calibrate the downscaling models, which model site-specific precipitation and temperature based on CGCM1 model outputs.

3.5. REGIONAL CLIMATE MODEL OF WESTERN CANADA

An alternative to downscaling using statistical techniques is the use of a regional climate model (RCM). These numerical models are similar to global climate models, but are of higher resolution, and therefore, contain a better representation of, for example, the underlying topography within the model domain and, depending on the model resolution, may also be able to resolve some of the atmospheric processes which are parameterized in a global climate model (CCIS, 2002).

A Canadian RCM (CRCM) has been developed through the collaboration of a modelling team at the Université du Québec à Montréal and the CCCma global climate modelling team in Victoria. CRCM has been used in the simulation of current and future climate for western Canada (Laprise et al., 1998; Cava and Laprise, 1999) at a spatial resolution of 45km. The data available are currently for western Canada only. The time periods for which data are available do not correspond to those recommended by the Intergovernmental Panel on Climate Change (IPCC) and are of shorter duration. This means that scenarios constructed from CRCM would not be consistent with those constructed from the global climate models. Very few simulations have been undertaken with CRCM, due mainly to computing costs, and this means that there is only a very small set of data available for use. Therefore, this limits the number of scenarios that can be constructed using CRCM data, and has implications for the exploration of scenario uncertainty (CCIS, 2002).

3.6. THE APPLICATIONS OF THE CRCM

The CRCMs spatial resolution is fine enough to correctly represent climatic processes of small dimensions, such as the formation of clouds or thunderstorms, precipitation, evaporation and soil moisture. A regional climate model is a sub-model embedded within a world-wide model or a GCM. Once the studied area is determined, it must be isolated on the GCM so that the conditions at the boundaries of the region can be determined. These conditions are then introduced in the regional model, which will simulate the climate of the selected domain. Therefore, the regional simulation can take place over any region of the globe.

As an intelligent interpolator, the CRCM can be used to alleviate the lack of climatological observations in foreign regions, to generate chronological climatic series, or to simulate a future climate.

The CRCMs spatial resolution is adequate to evaluate the regional repercussions of climatic changes. As such, the CRCM is a performant previsional tool offered to the numerous ministries, public and private organisms concerned by climate change. With more and more sophisticated and realist simulations, these first line users can develop strategies to prevent (e.g., the Protocol of Kyoto, 1997, aiming to reduce greenhouse gas emission and signed by 84 countries) climate change or to better adapt themselves.

The process of downscaling GCM climate for use in regional models, then in more localized studies of watersheds, is shown as a schematic diagram in Figure 3. In the conceptual model, a change in global climate causes changes in regional climate, which affect basin-scale hydrology. The Grand Forks valley is one example of local impacts of climate change, where the aquifer is hydraulically connected to the Kettle and Granby Rivers. Impacts of changed climate cascade into the water balance of this area, and consequently into water management, land use, economy, and ecology.

In 1999, a second climate change experiment was completed with the CRCM over western Canada, also at a resolution of 45 km. A different convection was used than during the first experiment. The experiment consisted in three 10-year long integrations, 1975-1984, 2040-2049 and 2080-2089, with transient concentrations of current CO_2, $2xCO_2$ and $3xCO_2$, respectively.

3.7. LIMITATIONS

The main limitation of the CRCM, as seen by the authors of this report, is the lack of daily data availability from model runs. Only monthly summaries and climatologies are given to registered members over the internet. To properly evaluate precipitation variability and its changes in the future, daily precipitation is required. Monthly summaries are useful in comparing absolute and relative changes in parameters such as temperature and precipitation, but not their variability. This would be true only if the CRCM output was representative of local weather at Grand Forks, or in other words, if the modeled time series was downscaled to the local conditions. That is not the case with CRCM because the CRCM is only a higher resolution version of CGCM, and as will be demonstrated in this report, CRCM output must still be downscaled to be useful.

In this report the CRCM monthly summaries will be used to compare to downscaled results. Precipitation, temperature, and solar radiation will be compared for temporal changes in seasonal values between current and predicted climate scenarios. The lack of access to daily CRCM output prevented any downscaling of CRCM results, which would be the preferred choice over the CGCM1, because of higher resolution. These should be attempted to be used in future climate scenario modelling of groundwater if possible.

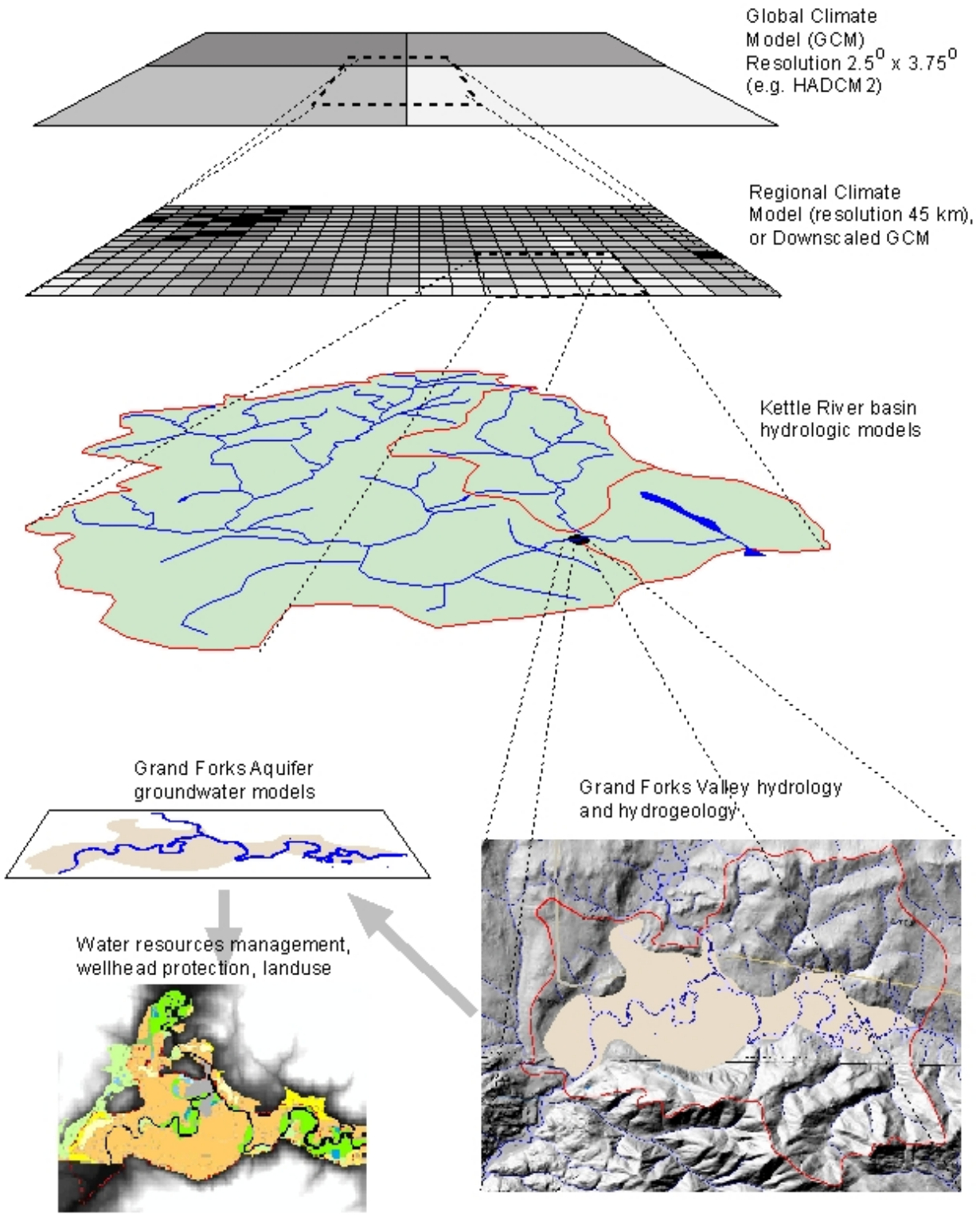

Figure 3 A conceptual diagram showing the range of scales involved in climate change scenario construction, and links to hydrologic models, groundwater models, and impacts assessment for the Grand Forks valley.

4. HYDROLOGY OF THE GRAND FORKS BASIN

4.1. STREAMFLOW IN KETTLE AND GRANBY RIVERS

4.1.1. PHYSIOGRAPHY

The drainage area of the Kettle River lies east of Okanagan Valley and west of the Columbia River Valley (refer to Map 1). The designated portion of the Kettle River is the mainstem of the West Kettle River. Stretching 290 km from its headwaters in the Monashee Mountains to its confluence with the Columbia River, the Kettle River system drains a total of 9,800 square km. Of this area, 8,300 square km are within BC, while the remaining 1,500 square km lie across the international border in Washington State. The Kettle River drops 190 m in elevation within its first 60 km, before assuming a more gradual gradient and meandering across a wide valley for the remainder of its course. The valley widens near town of Grand Forks, where the Granby River flows into the Kettle River. The Kettle River flows east through a narrow valley for about 10 km, turns south near Cristina Lake, and crosses the US border at Laurier. Eventually, it discharges into the Columbia River.

The Granby River has a drainage area of 2,050 km^2 at its confluence with Kettle River (Piteau Associates, 1988), with an average annual basin yield of 493 mm. This river flows north-south and enters the Grand Forks Valley through a narrow gap only few hundred metres wide between Observation Mountain and the valley slopes.

The most significant land uses within the Kettle River and Granby River valleys are agriculture, rural homesteading, and ranching. However, forestry, transportation, mining and quarrying interests are also present along the river. The rivers support numerous water licenses for domestic use, irrigation and power generation.

4.1.2. RUNOFF IN KETTLE AND GRANBY BASINS

On the basin scale of the Kettle River, the surface water balance is controlled by precipitation. Runoff volume is controlled largely by precipitation and snowmelt over the drainage area. In the Kettle River drainage area, the snowpack increases over the winter until early April. Most of the accumulated snow melts from April to end of June, but the end date of the snowmelt season varies from mid-May to mid-July. Hydrological response is extremely sensitive to seasonal patterns. During years with unusually warm winters the system shifts from a snowmelt-dominated regime to a bi-modal regime, where there is an increasing number of days of high flow due to rain, but a decreasing number of days of high flow due to snowmelt. All stations in southern BC are currently snowmelt-dominated, and all will become increasingly bi-modal as a result of climate change that results in winter warming (Environment Canada, 2001).

There are no large glaciers in the Kettle River basin, and no glaciers in the watershed of the Grand Forks valley. A small part of the baseflow is likely supplied by melting of small glaciers, but the Kettle River does not respond significantly to glacier runoff. Glacier-fed creeks maintain relatively large baseflow during the summer, and show strong diurnal variation in discharge.

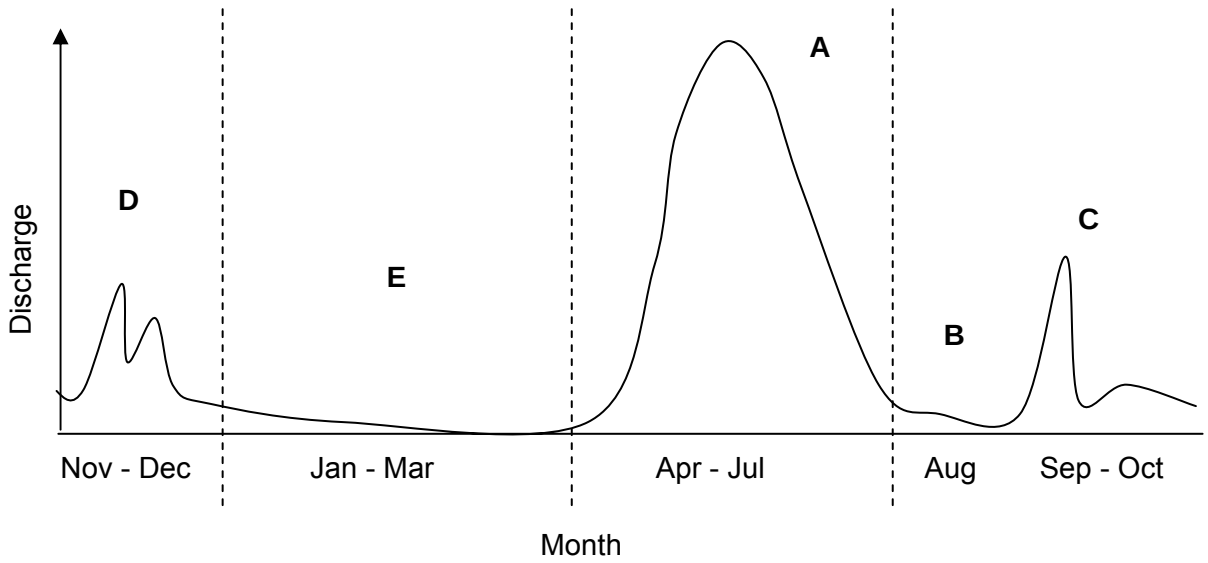

Figure 4 Schematic diagram of Type ***c*** annual hydrograph of Kettle River.

Figure 4 sh ows a schematic hydrograph for the Kettle River. The snowmelt (freshet) season is the largest and longest of high flow events (A). The discharge undergoes recession of flow following the snowmelt (B), but can rebound after rain storms (C). Intense rain events can occur at any time of the year, but are stronger and more frequent in late fall from November to December (D) and early summer seasons May to June. On the Kettle River there are two periods of prolonged low flow conditions, one in late summer, from middle of July to end of September (B) during typical dry weather, and the longest low-flow period after freeze-up during the winter months (E). Both rivers have caused extreme flooding in the Grand Forks area and extensive dyking schemes have been required to minimize the resultant damage (Piteau Associates, 1988).

4.1.3. STAGE AND DISCHARGE RECORDS (HYDROGRAPHS)

Water Survey of Canada has measured discharge and water levels on the Kettle and Granby Rivers at several locations near Grand Forks (Map 15). All hydrometric stations measure water level using either manual, or more recently, automated gauges. However, the published records are most often reported as discharge. Discharges are calculated from stage-discharge rating curves, calculated from the relation between measured stage and measured discharge. Typically, streamflow (discharge) measurements are taken 4 to 10 times during a year period. Discharge is calculated from the river velocity profile, measured using current meters at regular intervals along river cross-section, and the depth profile. The rating curves may change over time as channel geometry changes as a result of geomorphic processes, such as bank erosion, bedform change, shifts of gravel bars, or channel engineering. The rating curve is used for one year or several years, and then recalibrated. Records grade the perceived curve “fit” and thus accuracy, which vary over the years.

The history of river gauging in the vicinity of Grand Forks begins in 1913 when Water Survey of Canada measured streamflow at Carson, BC (08NN005). Gauging stopped soon after in 1922. In 1916 another streamflow gauge was established about 10 km downstream from Grand Forks,

at Cascade, near the village of Billings, BC (08NN006), but, this station was only operational until 1934. The most recent effort of gauging the Kettle River was a single gauge (08NN024) installed 2 km downstream of the Granby-Kettle confluence, which operated from 1974 to 1991.

On the Granby River, water levels were measured as early as 1914 (measured for only one year), but the record was discontinuous between the years 1926-1931, 1966-1996. The gauge (08NN002) on Granby River is located just north of the Grand Forks and has been recording river stage since 1966.

There are longer and more complete stage records on the Kettle River outside the Grand Forks Valley. About 25 km west of Grand Forks and upstream on the river is the community of Ferry, WA, where the river water level has been sampled by the United States Geological Survey (USGS) since 1928. There is also a hydrometric station at Laurier, WA (08NN012), east and downstream of Grand Forks and south of Cristina Lake, which has continuous stage records dating back to 1929. This gauge is the closest location to Grand Forks where streamflow on the Kettle River has been sampled continuously since the 1930's.

Two small creeks were also gauged in the Grand Forks Valley: July Creek (08NN018) and Dan O'Rea Creek (08NN009). The gauges operated intermittently for a few years, but the data are not available in electronic format. These two creeks were not included in the hydrograph analysis in this report, although such records may be useful in characterizing stormflow hydrographs of the small tributaries of Kettle River in the valley.

Station information lists the station number, beginning with 08NN for this geographic area, the station name, location, period of record (POR), basin area upstream of the gauge, mean annual runoff and discharge, and other information. All data tables and graphs for this study are contained in Scibek and Allen (2003). Table 6 provides data for three hydrometric stations (two on the Kettle River and one on Granby River) in the Grand Forks Valley. Table 7 provides station information for Kettle and West Kettle Rivers away from Grand Forks. Table 8 provides station information for two creeks in Grand Forks Valley. A detailed description of six hydrographs (08NN013; 08NN005; 08NNN006; 08NN002; 08NN024; and 08NN012) is provided by Scibek and Allen (2003). The source of data for these tables is Environment Canada. In addition, hydrometric information about creeks in BC was obtained from Environment Canada (2002b) and information about Washington State creeks from USGS (2002a). Appendix A tabulates these data.

A gauge datum correction was determined for each site in order to interface with the groundwater flow model. The station descriptions by Water Survey of Canada include sketched maps of gauge locations, gauge elevation relative to Geological Survey of Canada (GSC) benchmark, and other information.

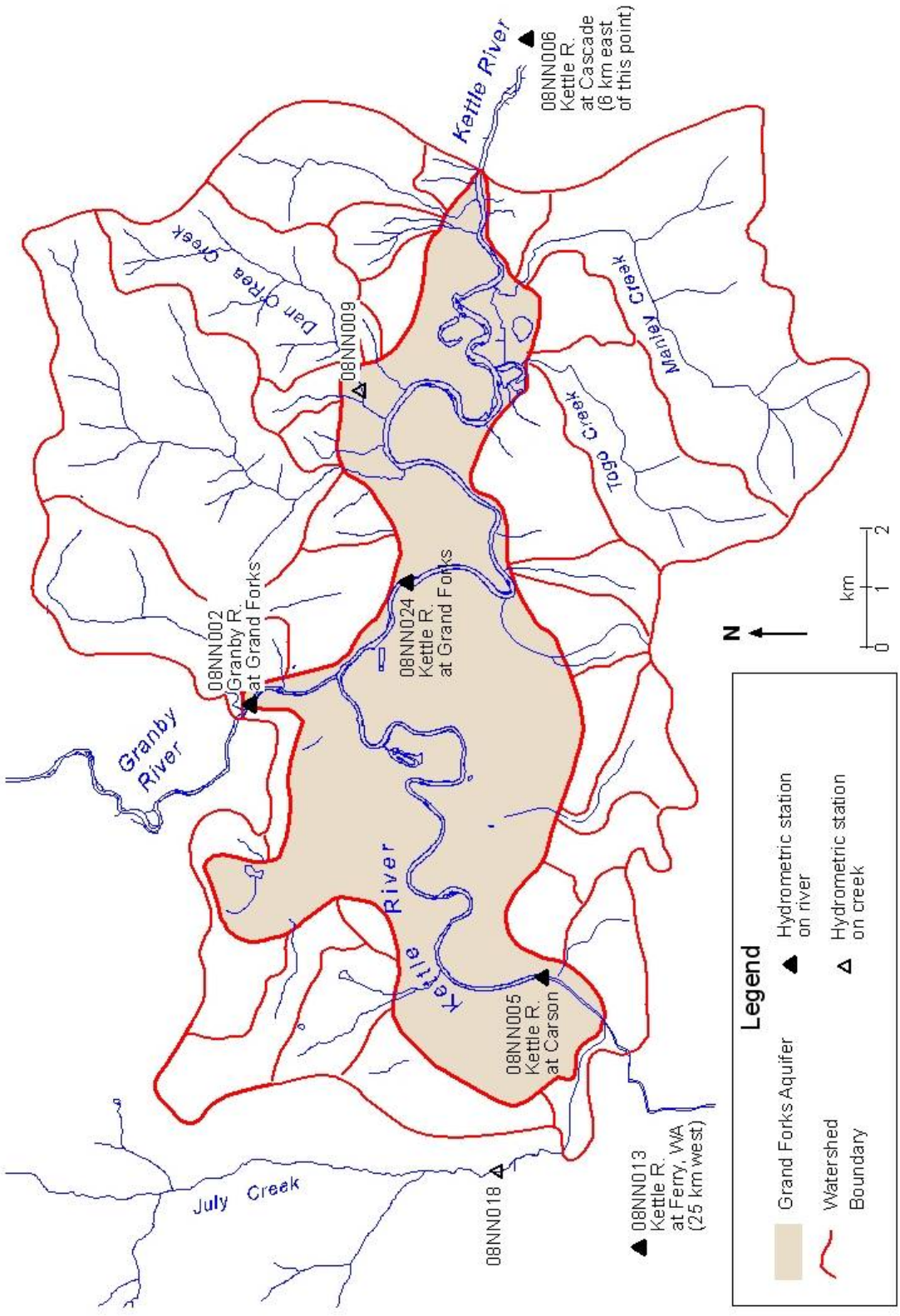

Map 15 Grand Forks valley: tributary catchment boundaries and locations of hydrometric stations.

Table 6 Hydrometric stations on the Kettle and Granby Rivers in Grand Forks valley.

Station ID:	08NN024	08NN005	08NN006	08NN002
Station name:	Kettle River	Kettle River	Kettle River	Granby R.
Location:	Grand Forks, 1 km NE of Airport	at Carson, SW end of GF valley near US border	Cascade near Billings, S of Christina Lake	Grand Forks, 1.5 km N of
Lat.(decimal deg)	49.02167	49	49.02361	49.044167
Long. (decimal deg)	118.4108	118.4958	118.2083	118.43861
Lat (d,m,s)	49o 1' 18" N	49o 0' 0" N	49o 1' 25" N	49°2'39¨N
Long. (d,m,s)	118o 24' 39" W	118o 29' 45" W	118o 12' 30" W	118°26'19¨W
POR start	Jan 1974	Jan 1913	Jan 1916	1914-1931 some years
POR end	Dec 1992	Dec 1922	Dec 1962	1961-present
# Years				42
Station status	Inactive	Inactive	Inactive	Active
Basin Area (km2)	8830	6730	8960	2050
Elevation (m asl)				1496
Data type:	Stage only	Flow	Flow	Flow
Station operation:	Seasonal	Continuous	Continuous	Continuous
Runoff, mean annual (mm)	30	208	256	469
Runoff, max daily rate (mm)	0.0094	1.3	27	7.2
Discharge, max. (m3/s)	10	476	830	385
Discharge , min (m3/s)	6.76	3.82	1.79	0.474
Discharge, mean (m3/s)	8.52	44.3	72.8	30.5
% (below ice)	0	17	19	18
% (estimated)	0	0	0	0

Table 7 Hydrometric stations on Kettle and West Kettle Rivers near Grand Forks.

Station ID:	08NN018	08NN009
Station name:	July Creek	Dan O'Rea Cr.
Location:	10 km W of GF	4 km E of GF
Lat.(decimal deg)	49.01445	49.03
Long. (decimal deg)	118.5411	118.3714
Lat (d,m,s)	49o 0' 52" N	49o 1' 48" N
Long. (d,m,s)	118o 32' 28" W	118o 22' 17" W
POR start	1-Jan-65	1-Jan-21
POR end	31-Dec-74	31-Dec-21
# Years		
Station status	Inactive	Inactive
Basin Area (km2)	45.6	7.77
Elevation (m asl)		
Data type:	Flow	Flow
Station operation:	Seasonal	Seasonal
Runoff, mean annual (mm)	221	36
Runoff, max daily rate (mm)	3.9	0.29
Discharge, max. (m3/s)	6	
Discharge , min (m3/s)	0.00686	0.000571
Discharge, mean (m3/s)	0.32	0.00895
% (below ice)	0	0
% (estimated)	3	0

Table 8 Hydrometric stations on small creeks in Grand Forks Valley.

Station ID:	08NN026	08NN003	08NN015	08NN022	08NN013	08NN012
Station name:	Kettle R.	West Kettle R.	West Kettle R.	West Kettle R.	Kettle River	Kettle R.
Location:	near Westbridge	Westbridge	near McCulloch	below Carmi Creek	near Ferry, WA	near Laurier, WA, S of Christina Lk.
Lat.(deg)	49.23019				48.98139	48.98444
Long. (deg)	118.9275				118.76528	118.2153
Lat (d,m,s)	49°13'48¨N	49°10'12¨N	49°42'15¨N	49°29'3¨N	48o 58' 53"	48°59'4¨N
Long. (d,m,s)	118°55'39¨W	118°58'28¨W	119°5'31¨W	119°6'30¨W	118o 45' 55"	118°12'55¨W
POR start	1975	1914	1949	1973	1928	1929
POR end	present	1999	1999	1996	present	present
# Years with data	25	33	45	24	72	71
Station status	Active	Active	Active	Inactive	Active	Active
Basin Area (km2)	2150				5750	9840
Elevation (m asl)	1563					
Data type:	Flow				Flow	Flow
Station operation:	Seasonal				Continuous	Continuous
Runoff, mean annual (mm)	727			264	239	265
Runoff, max daily rate (mm)	3.5			4	1.9	1.7
Discharge, max. (m3/s)	374			121	575	968
Discharge , min (m3/s)	1.53			0.242	0.425	1.98
Discharge, mean (m3/s)	49.5			9.81	43.7	82.7
% (below ice)	0			39	7.2	14
% (estimated)	2			2	0	2

4.1.4. DERIVATION OF ANNUAL HYDROGRAPH

All available hydrograph data were supplied as files by Environment Canada in Vancouver. The files contained daily mean discharge (streamflow) for most stations, and daily mean river stage (water level) for one station (Kettle River at Grand Forks 08NN024). As most river gauges record only water elevation, the discharge records are calculated from stage-discharge curves (rating curves) fitted to measured stage and discharge graph. Discharges were measured with flow meters at each gauge during freshet increase of river stage in April. The rating curve is used to estimate river discharges for the remainder of the year from gauged stages.

The daily mean discharges for the rivers were graphed as time series to show all the available data for the period of record for each station. A selected two-year hydrograph time series was extracted to show more detail in the time series and to provide an example of a typical day-to-day variation in flow. Using a spreadsheet, summary statistics were calculated for each month for the period of record for each hydrometric station selected. The summary statistics were: average, minimum, maximum, and standard deviation for the period of record for each month. For example, for January statistics, all available data values in January of all years on the record for one station were averaged to determine the mean monthly value (for the period of record). From the monthly summary statistics, representative annual hydrographs were plotted to represent the long term (or at least for period of record) mean discharge and the variation of discharge (Scibek and Allen, 2003). The variation was represented by one standard deviation about the mean, graphed with vertical error bars. The median monthly value (for the POR) was also plotted, and was usually less than the mean monthly value (for the POR), indicating bias toward very large discharge values for the mean.

The spread in values, as shown by standard deviation, may be attributed to differences in timing of snowmelt on basin and local scale, which is a function of air temperature and other meteorological conditions, and rainfall events. A large proportion of the discharge variation can be explained by inter-annual variation of discharge for each month in the POR, which roughly has a decadal cycle (graphs in Scibek and Allen, 2003). The mean annual hydrograph does not show inter-annual variation of streamflow, but it can be inferred from standard deviation bars extending from mean monthly values.

4.1.5. BASIN RUNOFF

Before a representative hydrograph is chosen for the Grand Forks valley sections of Kettle and Granby Rivers, the basin scale effects must be investigated to determine the choice of index hydrometric station. Runoff (R) is the volume of streamflow discharge (Q) over a period of time (t) divided by the drainage area (A_B) of the basin:

$$R = \frac{Q * t}{A_B} \qquad \textbf{[1]}$$

Using runoff as the hydrologic response allows for adjustments for differences in drainage areas. Discharge records from gauges at Ferry, Carson, Cascade, Laurier along the Kettle River, and from the Grand Forks station on the Granby River were converted to 30-day runoff values. The graph in Figure 5 plots all available streamflow data on the Kettle and Granby Rivers near Grand Forks as 30-day runoff depths. It is apparent that records at Carson and Cascade have only short overlapping time periods, whereas data from Ferry and Laurier, and later years for Granby River, have good overlap. The Granby River basin has much larger runoff values than the Kettle River basin, suggesting greater precipitation in that region, which generates greater volumes of flow per unit of basin area.

Runoff was calculated from monthly mean discharge statistics for four stations in the Kettle basin, and one in Granby basin (Figure 6). The Granby River basin has larger runoff, thus, it is wetter than any of the sub-basins catchments of the Kettle River. Among the Kettle River stations, runoff was similar in magnitude at Ferry, Cascade and Laurier, but much less at Carson. The sub-basins of the Kettle River, ending at Cascade and at Laurier, had slightly larger runoff values than the smaller Kettle sub-basin at Ferry for most months. The difference can be attributed to inflow of Granby River into the Kettle River past Carson, but before Cascade, since the Granby River basin was shown previously to have greater runoff than the Kettle River basin. The implication for river modeling is that the hydrographs cannot be simply interpolated between these two stations. The hydrograph shape changes past the confluence of Kettle and Granby Rivers.

The low runoff values at Carson suggest that the short period of record is not representative of the long term mean, and other station records should be scaled to create a representative hydrograph for this location in the valley. Flow records are much longer and more complete at the Ferry and Laurier gauges on Kettle River. The streamflow records at Laurier can be scaled down safely to represent the streamflow hydrographs in the Grand Forks valley downstream of the confluence of the Kettle and Granby Rivers. The upper section of Kettle River in the valley near Grand Forks can be modeled using up-scaled discharge values from the gauge at Ferry.

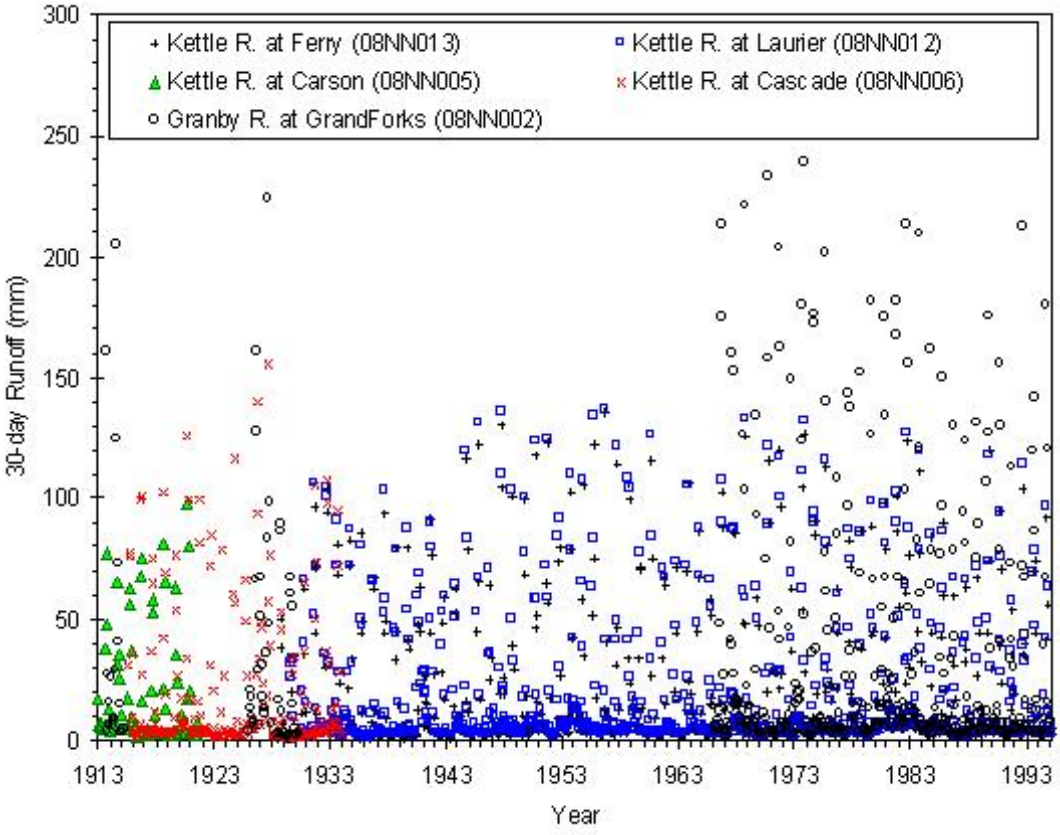

Figure 5 Runoff depths for the Kettle and Granby River basins, calculated for 30-day periods for hydrometric stations near Grand Forks, BC.

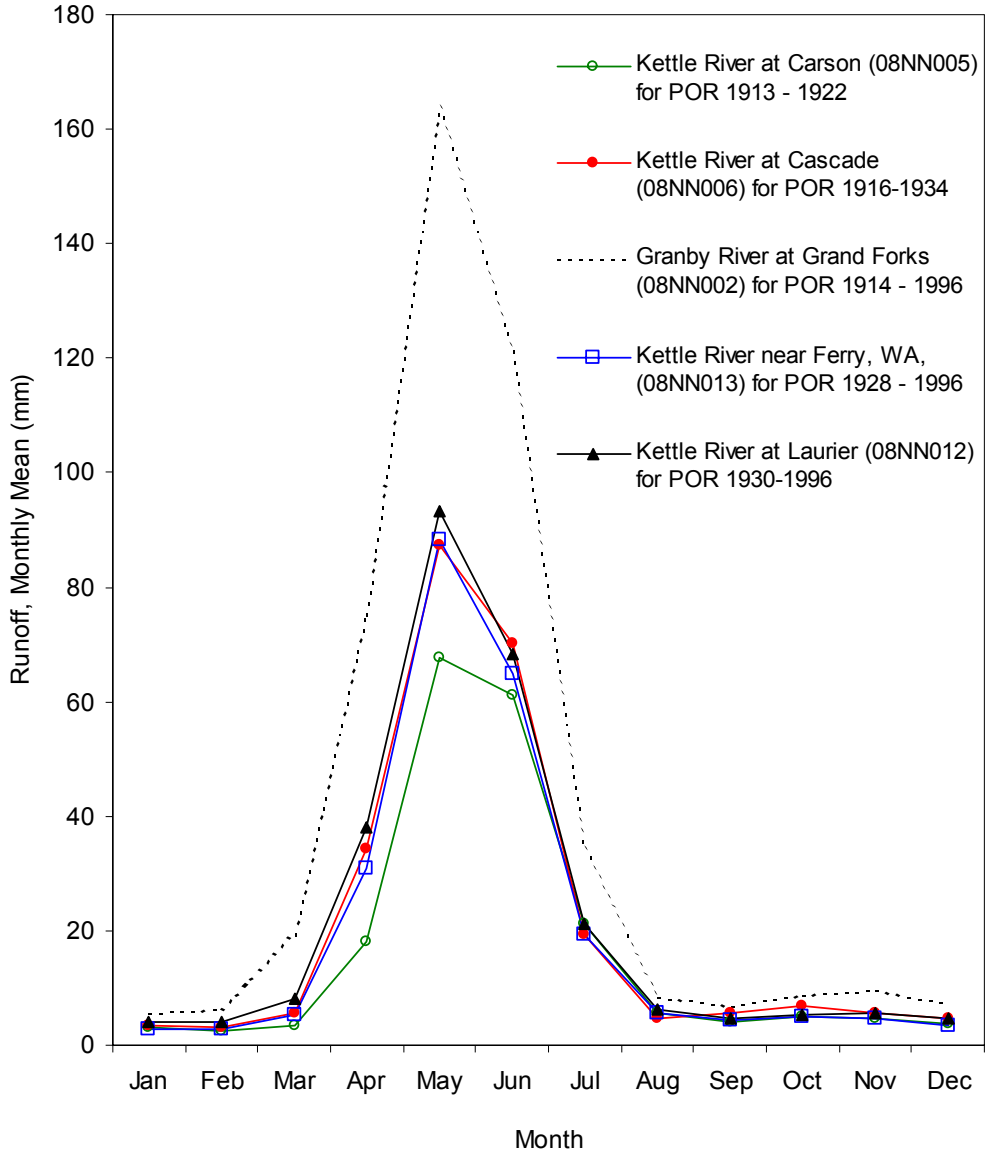

Figure 6 Monthly mean runoff calculated from mean monthly discharges (for available period of record) for selected hydrometric stations on Kettle and Granby Rivers.

4.1.6. HYDROGRAPHS FOR AQUIFER MODELING

The hydraulic connection of the Kettle and Granby Rivers to the shallow aquifer appears to be good, as there does not appear to be any till or low permeability silt material overlying the highly permeable sand and gravel in the river beds. The shallow, more permeable portion of the upper unit (i.e., the gravel layer) appears to be closely linked with the Granby and Kettle Rivers as evidenced by the corresponding rising and falling of water levels in shallow wells situated close to the rivers (Piteau and Associates, 1993). All wells completed in this shallow aquifer layer exhibit a static level approximately at river elevation, indicating that the groundwater regime is likely strongly linked to the surface water regime.

In the Grand Forks valley, an observation well (BC obs. well #217, well tag number 14947) is completed in the shallow unconfined aquifer, several hundred metres north of Kettle River. The well has depth of 8.83 m and the lithology log indicates gravel to this depth. This well belongs to a network of observation wells operated by the BC Ministry of Water, Land, and Air Protection (2002), to provide data on groundwater level fluctuations and groundwater quality information for developed aquifers in British Columbia. Water level data for the entire period of record (POR) are graphed in Figure 7.

To construct the water elevation graph in Figure 8, the recorded water levels in well 217 (m below ground surface) were subtracted from the well casing elevation of 513.5 m a.s.l. The nearest hydrometric gauge on Kettle River was located in Grand Forks, past the confluence with the Granby River (elevation of zero gauge at 500.0 m a.s.l.). The nearest river cross-section is located 400 m west of the observation well, and has number #17 (ID 49). The channel bottom elevation is 509.6 m. Therefore, the river stages were increased by 513.5 – 509.6 = 3.9 m to approximate the location near the well. Since the nearest river channel is that of Kettle River upstream of confluence with the Granby River, the discharge (and presumably water levels) will be lower by about 60% than those recorded past the confluence with Granby River. Accordingly, the water levels were reduced by 60% to compare with observation well water levels.

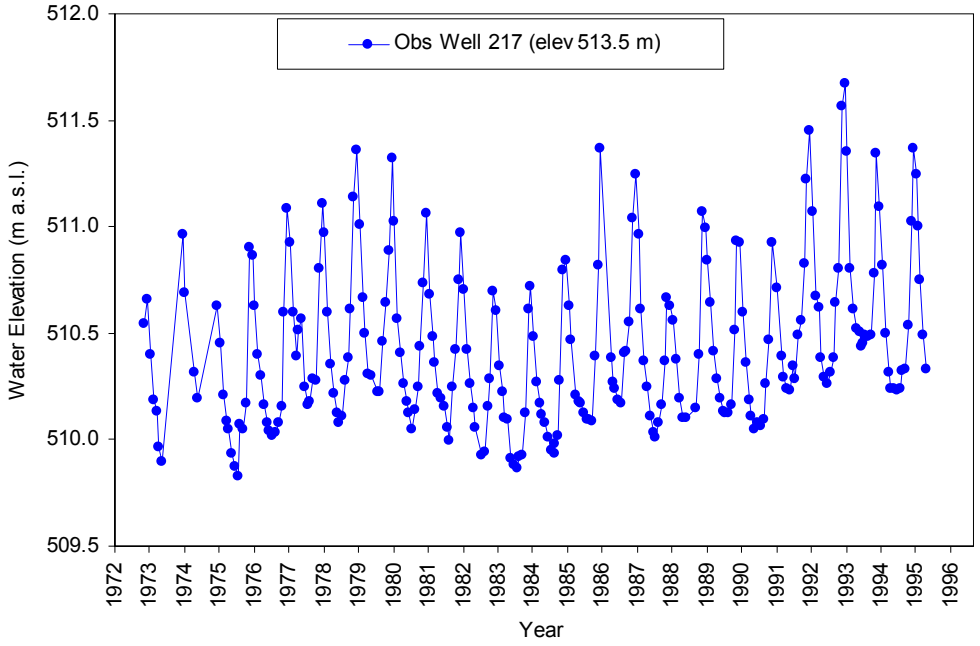

Figure 7 Observation well 217 at Grand Forks monthly water table elevation (total head in unconfined aquifer layer) records for POR of 1974 - 1996. Readings are at the end of the month.

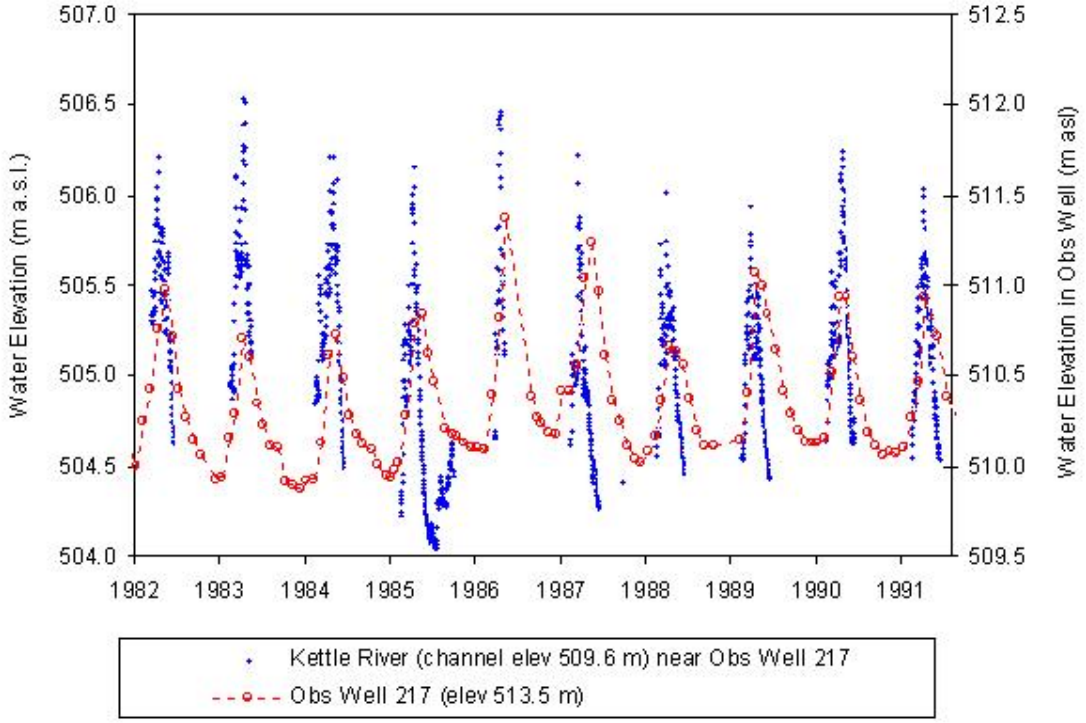

Figure 8 Water Elevations at Observation Well 217 and on the Kettle River (08NN024), for the selected period of record from 1982 to 1991.

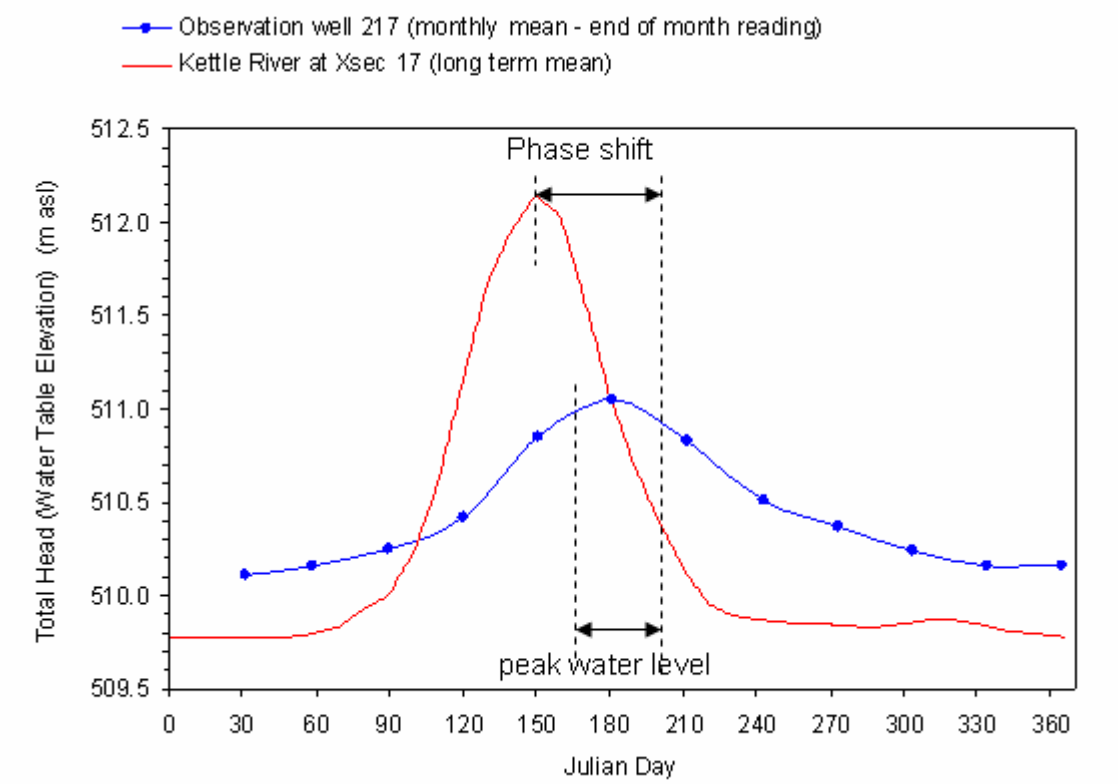

Figure 9 Mean hydrograph of water table elevation (total head) in Observation Well 217 in the Grand Forks aquifer and water surface elevation of Kettle River at cross-section 17 (400 m from well 217).

The mean monthly water table elevation varied only by about 1 meter, with standard deviation of 0.2 m. The shape of well hydrograph was similar to the Kettle River hydrograph (Figure 9), but the peak water level was apparently at end of July, rather than at end of June. However, the actual date of highest water level in well 217 is uncertain to at least 15 days, since the measurements are taken only once each month. For example, if well soundings were taken in the middle of the month, the peak would probably occur in the middle of June. The phase shift of the well hydrograph as induced by river hydrograph is at least 15 days, but could be up to 30 days (Figure 9).

The aquifer water levels appear to be hydraulically connected to the river and the amplitude of seasonal fluctuations show a damping effect, which would be expected to increase with distance away from the river channel. It is one of the goals of groundwater flow model to provide numerical predictions of lag times in aquifer recharge, flow paths, and estimates of storage parameters.

4.1.7. BASE CASE (TYPICAL HYDROGRAPH)

To determine the runoff at a location downstream of a gauge, the observed daily flows at the upstream station were adjusted by the drainage area ratio of downstream/upstream stations, following methodology of Leith and Whitfield (2000). The scaling factor was computed from the product of the ratio of basin areas at upstream station (A_1) and downstream station (A_2)

locations along the river. Then, discharge at downstream station (Q_2) is computed from discharge at the upstream station (Q_1) using the equation:

$$Q_2 = \frac{A_2}{A_1} Q_1 \qquad \textbf{[2]}$$

This calculation was performed on monthly average discharges that were used to construct annual hydrographs, thus the conversion involved time period of 30 days. The scaling ratios are shown in Table 9. Because the groundwater model may require daily stage increments along the rivers, the daily values were interpolated from the annual hydrograph (of monthly average values) using a 30-day moving average function, shifted back by 30 days to fit the annual hydrograph. The moving average function provides more realistic smoothing of the hydrograph than does linear interpolation, and is simpler than fitting complex polynomial curves to the hydrograph.

Table 9 Scaling ratios for annual hydrographs

Station (Kettle River)	Basin Area (km^2)	Conversion	Scaling Ratio
Ferry	5750		
Carson	6730	Ferry --> Carson	1.1704
Gilpin (X-sec 44)	6825	Kettle R. + Granby R.	
Cascade	8960		
Laurier	9840		
(Granby River)			
Grand Forks	2050		

- KETTLE RIVER FROM CARSON TO GRAND FORKS

A base case river hydrograph (Figure 10) for the Kettle River section from Carson to Grand Forks, was derived from up-scaled records at Ferry, WA, since the records at Carson were too short and not representative of long term mean flows.

- KETTLE RIVER FROM GRAND FORKS TO GILPIN

A base case river hydrograph (Figure 10) for the Kettle River section from Grand Forks to Gilpin (at the end of the wide floodplain and aquifer – see cross-section location #44), was derived from the sum of the Kettle and Granby River hydrographs. The Kettle River discharge was taken from the (scaled) Carson hydrograph, and Granby River discharge was taken from Grand Forks station.

- GRANBY RIVER BEFORE GRAND FORKS

A base case river hydrograph (Figure 11) for the Granby River section upstream of Grand Forks (to the end of the wide floodplain and aquifer – see cross-section location #11), was derived from records at Grand Forks. Scaling was not necessary for this gauge record, because it is representative of the Granby River section, and has a relatively long and continuous record.

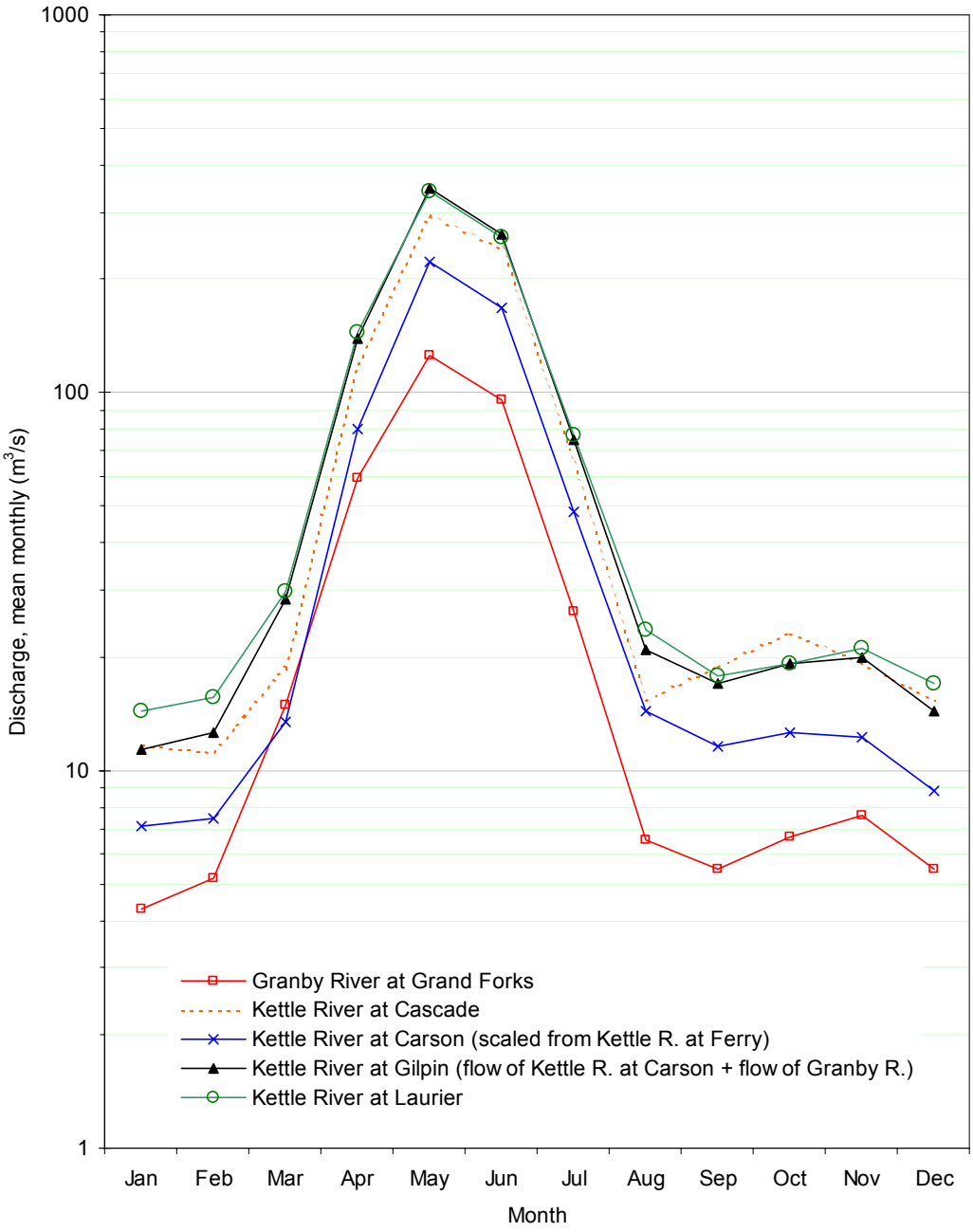

Figure 10 Base case average annual hydrograph of Kettle and Granby Rivers for representative stations in Grand Forks valley, and compared to flow at downstream station at Laurier.

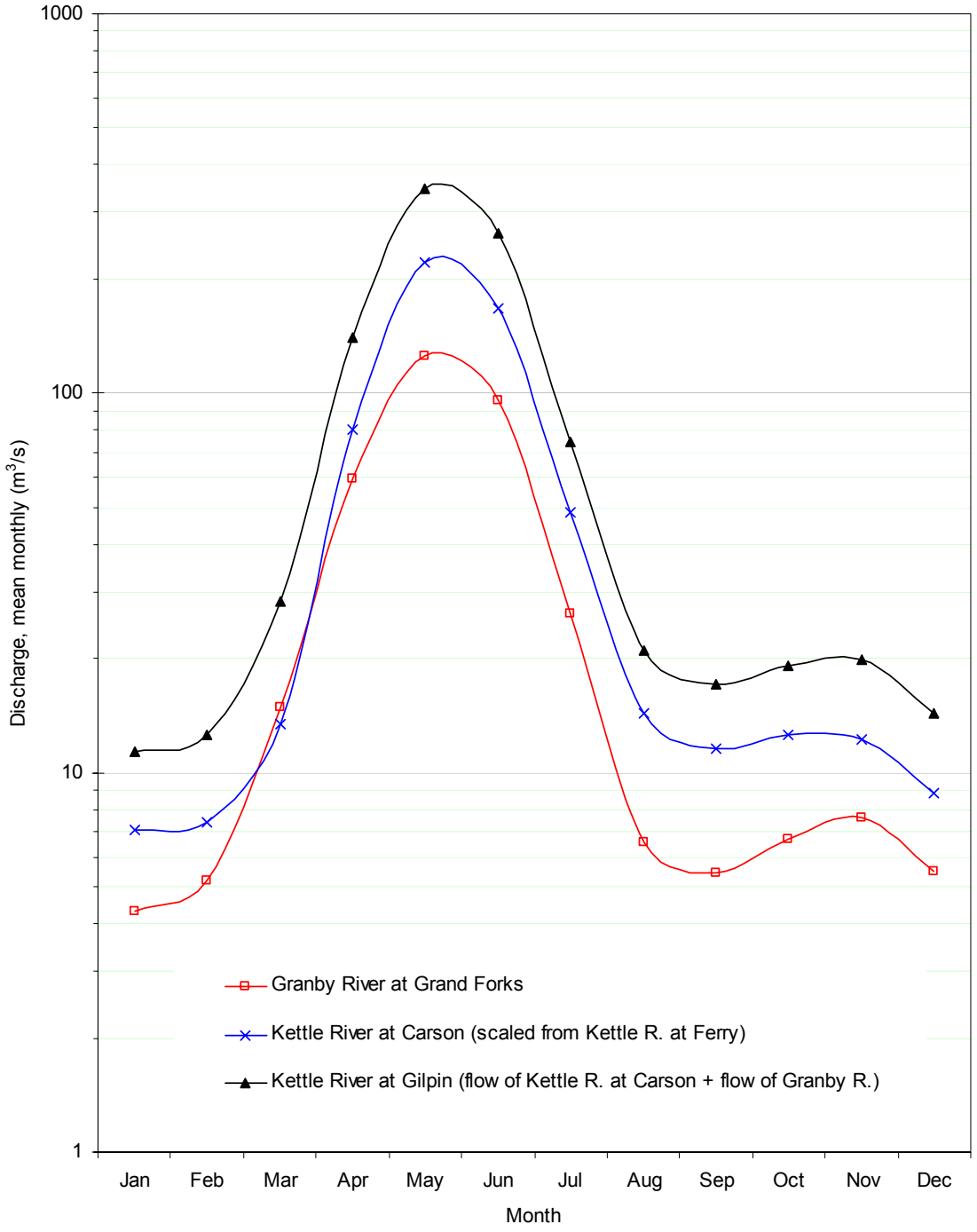

Figure 11 Base case average annual hydrograph of Kettle and Granby Rivers for representative stations in Grand Forks valley, interpolated daily flows using moving average function.

4.2. ANNUAL WATER BALANCE FOR THE GRAND FORKS VALLEY

The following provides the conceptual framework for evaluating the annual water balance for the Grand Forks aquifer. This analysis forms part of the conceptual model. Ultimately, the transient groundwater flow model will compare the computed hydraulic heads for different times of the year and assess the dynamics of the water balance in the aquifer. A water balance approach (Zone Budget in Visual MODFLOW) will be used to estimate change in storage over the course of one year for both current climate and climate change scenarios.

4.2.1. COMPONENTS OF THE WATER BALANCE

The valley floor forms the Grand Forks aquifer. The aquifer is assumed not to discharge groundwater into other aquifers directly (no groundwater flow across groundwater divides). For the valley floor aquifer during a snow/ice free period, the water balance is:

$$(P + Q_{IN}) - (E_T + Q_{OUT}) = (\Delta S_{AQUIFER} + \Delta S_{ARTIFICIAL}) \quad \textbf{[3]}$$

where P is precipitation over the valley area, Q_{IN} is streamflow into the valley floor, E_T is evapotranspiration, Q_{OUT} is streamflow out of the valley floor, $\Delta S_{AQUIFER}$ is the change in aquifer storage of groundwater, which includes surface storage in lakes and ponds as these are directly linked to the aquifer (change in storage also includes artificial discharge by pumping and drainage), and $\Delta S_{ARTIFICIAL}$ is the change in surface water storage in artificial tanks, ponds, crops, or removal of surface water without return-flow for industrial or other purposes. There are no dams or reservoirs in this valley. The aquifer storage is determined from recharge and discharge terms (assuming the entire aquifer as one container unit):

$$\Delta S_{AQUIFER} = \text{Recharge} - \text{Discharge} \quad \textbf{[4]}$$

$$\text{Recharge} = Q_{R(RIVERS)} + Q_{R(CREEKS)} + Q_{R(SLOPES)} + Q_{R(INF)} + Q_{R(IRRIGATION)} \quad \textbf{[5]}$$

$$\text{Discharge} = Q_{D(BASEFLOW)} + Q_{D(DRAINS)} + Q_{D(ET)} + Q_{D(PUMPING)} \quad \textbf{[6]}$$

where $Q_{R(RIVERS)}$ is aquifer recharge from river channels, $Q_{R(CREEKS)}$ is aquifer recharge from creek channels, $Q_{R(SLOPES)}$ is aquifer recharge from seepage from valley slopes (includes springs, waterfalls, and other storm runoff), $Q_{R(INF)}$ is recharge from infiltration of precipitation that replenishes the aquifer, $Q_{R(IRRIGATION)}$ is the return flow from irrigation water applied to crops, and $Q_{D(PUMPING)}$ is discharge into pumping wells.

- RECHARGE OF AQUIFER FROM PRECIPITATION

A detailed analysis of recharge from precipitation to the Grand Forks aquifer is provided in Section 5.0 of this report.

- AQUIFER RECHARGE FROM KETTLE / GRANBY RIVERS

The amount and timing of recharge to aquifers depends largely on the timing, duration, and magnitude of high-flow (freshet) in the rivers. The lag in aquifer response to changes in river stage depends on the distance from the river channel and the aquifer hydraulic properties. Previous steady state modeling using baseflow (low flow river stage) has shown that the Grand Forks aquifer is hydraulically connected with the Kettle River, and receives recharge in the western part of the valley where hydraulic head in the aquifer is the highest (Allen, 2000; 2001).

Aquifer water levels measured at observation well 217 (discussed previously) show good correlation between the water table and the river stage, at least at close to the river. The results are consistent with the observation that the water table elevations in the aquifer range from 518 m a.s.l. in the west to about 503 m a.s.l. in the east (Piteau Associates, 2002). Also, for most of the year, water levels in the aquifer are higher than the Kettle River, which gains water from the aquifer, except in the western part of the valley where the river looses water to aquifer recharge (Piteau Associates, 2002).

Under steady state modeling conditions, recharge occurs in the western, central, and northern portions of the valley (south and southwest of Grand Forks). The river recovers most of the lost water (but not all) in the eastern portion of the valley. Basically, if these low-flow conditions in the river were to last indefinitely as modeled under steady state, the river would slowly flow through the valley, and slowly through the aquifer (recharging it and discharging as baseflow), and it would loose some water to discharge in the aquifer. This interaction is highly variable over the year as river stage changes, recharge to aquifer changes, and locally pumping rates change.

Transient modeling of the aquifer (discussed in Section 7.0) will show how the aquifer responds to changes in river stage over time. Section 4.3 describes the implementation of the BRANCH-network model for the Kettle and Granby Rivers in the Grand Forks Valley. The linking of surface flow (river stages) to groundwater flow is also discussed.

- RECHARGE TO AQUIFER FROM SMALL CREEKS

Small creeks may supply some recharge to the aquifer, especially near boundaries where ground elevation is higher than the elevation of the Kettle River, which controls most of the water levels in this aquifer. There are no data for streamflow in small creeks in the valley. Usually, creeks will be connected to the water table in the aquifer and may act as drains discharging groundwater (baseflow), or as sources of aquifer recharge (water table mounds).

- RECHARGE FROM VALLEY SLOPES

Most of the valley slopes are very steep rock faces or steep forested slopes. Only a few small creeks have been mapped on the valley slopes and most channels are ephemeral and mostly dry during the summer, except during large rain events. Small rain events usually do not produce visible streamflow or overland flow on these slopes, but more observations should be made during large rain storms.

The seepage from slopes is difficult to estimate. In the summer, if no streamflow occurs, the water may infiltrate the soil and remain in storage for a short time until the soils dry up, or it may flow down slope and contribute to aquifer recharge along the valley edges. This amount of recharge may be larger along the valley walls than mean recharge from rainfall in the aquifer area per unit area. However, this is only an assumption. Most of the down slope seepage may eventually channelize into streamflow of small creeks during, and a short time after, a major rain event due to thin soils on the valley slopes. Most of the valley slopes are bedrock outcrops, with some colluvium veneers and thin soils. Thus, any aquifer recharge from the slopes will occur only at small creek outlets into the valley and not along all valley walls. If overland flow (small waterfalls, small creeks, major seepage on slopes) is observed along most of the valley slopes at the valley elevation during large rain event, then the recharge could be assumed evenly distributed. Allen (2000) employed a slightly larger value of recharge to the groundwater model edges to account for added recharge from valley slopes.

-

DISCHARGE BY PUMPING

The current rate of water use in Grand Forks is, on average, 0.32 m^3/s, and will likely increase by 0.16 m^3/s to 0.48 m^3/s (Piteau Associates, 2002). The total consumptive water rights in British Columbia for the Kettle River is currently 1.56 m^3/s + 0.32 m^3/s (water usage in Grand Forks + water usage in Washington State) from this river. A detailed account of groundwater use by major production wells in the valley is provided in Section 7.0.

- RETURN FLOW FROM IRRIGATION

The amount of return flow from infiltration is discussed in Section 7.0.

- DISCHARGE BY EVAPOTRANSPIRATION

Allen (2001) showed that under steady state conditions, the loss of water due to evapotranspiration directly from the aquifer was negligible. However, a transient model will include the seasonal variation in recharge rates to the aquifer, which will account for seasonal variation in evapotranspiration. Evapotranspiration can be expected to be very high in the summer and may prevent significant return flow into the aquifer from water applied for irrigation. In wet areas such as swamps and lakes, evaporation loss may be large in the summer season. Evapotranspiration can be expected to be much lower during the winter months when the aquifer receives increased aerial recharge.

- STORAGE

The overall objective of this research is to model changes in groundwater storage that might arise due to climate change.

4.2.2. GRAND FORKS VALLEY TRIBUTARY WATERSHEDS

The watershed outside the valley consists of smaller catchment areas, each with a separate water balance. The watershed water balance is the sum of water balances for all catchments in that drainage area:

$$P - (E_T + Q_{OUT}) = \Delta S_{WATERSHED} \quad \textbf{[7]}$$

$$Q_{OUT} = P - E_T - \Delta S_{WATERSHED} \quad \textbf{[8]}$$

$$Q_{OUT} = \sum_{i=1}^{n} Q_{OUT(i)} \quad \textbf{[9]}$$

where P is precipitation over the drainage area of watershed, E_T is evapotranspiration from the drainage area, Q_{OUT} is surface runoff from the watershed that enters the Grand Forks valley, and $\Delta S_{WATERSHED}$ is the change in water storage in all the catchments (i to n) that form the watershed. The runoff from catchments was separated because some creeks have flow records, or could be estimated based on catchment characteristics.

Many small creeks drain the valley slopes and upland catchments, and discharge into either the Kettle or Granby Rivers. The watershed for the valley was delineated and subdivided into smaller catchments using topographic maps (see Map 2). Catchment areas (Table A2 in Appendix A) were measured on the British Columbia side of the valley using web-based mapping tools provided by BC Ministry of Water, Land and Air Protection. On the Washington State side of the valley, catchment areas were measured using 1 km x 1 km grid overlay on

topographic maps. The estimated areas have error of up to ± 20% for small areas (less than 3 km^2), and up to ± 5% for large areas, based on repeated measurements of the same catchments and comparing estimated areas. The areas do not account for slope. The total watershed area for the valley is 94.7 km^2, not including the valley area. About 41 km^2 is on the US side and the rest is on BC side. The largest creeks have catchments of up to 25 km^2. The smallest catchments (< 1 km^2) represent steep rocky slopes where often there is lack of defined surface drainage.

4.2.3. ESTIMATES OF MEAN ANNUAL DISCHARGE

Since only one catchment (Dan O'Rea Creek – catchment 5 in Table A2) had available mean annual discharge from previous gauging records, the discharges from other catchments were estimated from a fitted empirical relation between mean annual discharge and catchment (or basin) area. In semiarid regions of large relief the relation of mean flow to drainage area and precipitation may not be usable because of the great range in precipitation with elevation, the lack of good precipitation data, and the strong influence of geology on mean flow (Riggs, 1982). Basin runoff generally increases non-linearly with basin area. In Figure 12, mean annual discharges were plotted against basin area for all available hydrometric stations on small catchments within 1 degree of longitude or latitude from Grand Forks. Data from BC and Washington State were used. The linear model for mean annual discharge ($Q_{m.a.}$) as a function of basin area (A_B) was significant (R^2 = 0.6854 at P = 0.05) and the fitted line was given by:

$$Q_{m.a.} = 0.0052 * A_B \qquad \textbf{[10]}$$

Two very dry catchments were considered as outliers, thus, were excluded from analysis: 08NM082 Big Sheep Creek near Rossland and 12400500 Sheep Creek near Northport. Locations of creek gauges are shown in Figure 12 (Grand Forks is in the centre of the graph). Selected creek gauging points that deviate from the general trend were identified with numbers on the discharge-area graph and location map. There is a trend of increasing runoff with basin area, especially for catchments larger than 100 km^2 (Figure 12), although that trend is poorly defined for small catchments (<100 km^2) where there is much scatter. Points 1 to 5 represent relatively dry watersheds; three of which lie in the very dry Osoyos Lake area, and one is south in the interior of Washington State. All of the relatively wet catchments (numbered 6 to 8), those that fall above the discharge-area trend line, are north of BC/WA border. The creek locations were overlain on the mean annual precipitation in Map 16. Climate data (from various stations shown in Table 10) were contoured and interpolated using PRISM modeling system of Spatial Analysis Center, Oregon State University (OSU, 2002).

Station ID	Name	Lat		Long		Elev (m asl)
1130770	BEAVERDELL	49	25	119	6	780
1130771	BEAVERDELL NORTH	49	29	119	3	838
1130874	BIG WHITE	49	44	118	56	1841
1130975	BRIDESVILLE	49	3	119	10	1187
1133270	GRAND FORKS	49	2	118	28	532
1135126	MIDWAY	49	0	118	46	578
1136813	ROCK CREEK MT BALDY	49	7	119	9	1174

Table 10 Meteorological Stations in the Region

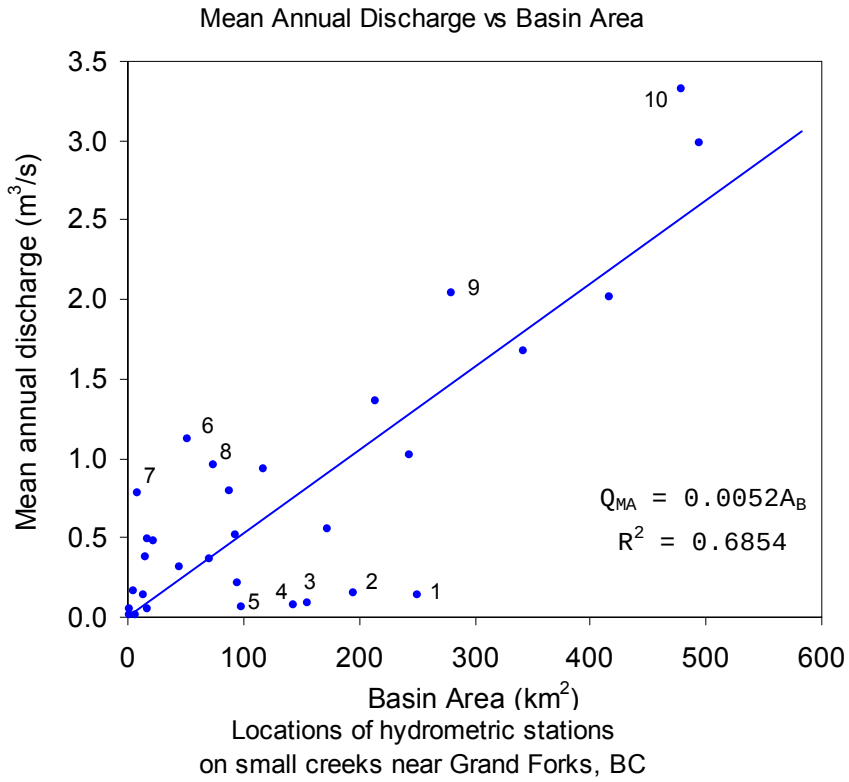

Figure 12 Mean annual discharge graphed against basin area for small to medium size catchments near Grand Forks, BC (Canadian and US data).

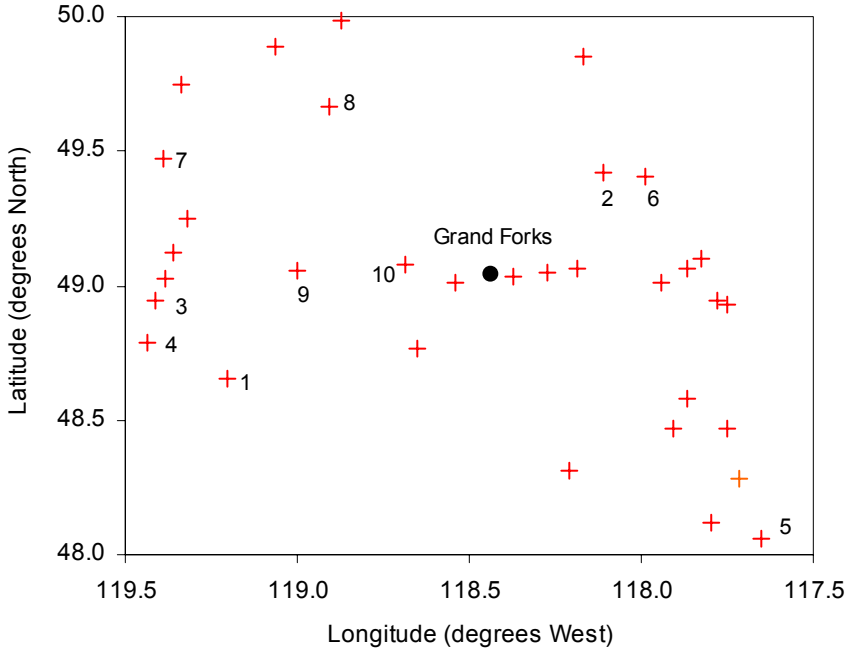

Figure 13 Locations of small to medium sized catchments with available hydrometric data near Grand Forks, BC (Canadian and US data).

Relatively dry areas are along Okanagan Valley (west of Grand Forks), the interior of Washington State (south), and other smaller valleys. Wet areas are over the mountains to the north and east of Grand Forks. However, the locations of hydrometric stations are not representative of each catchment mean annual precipitation, because the gauge positions in valleys are much drier than the uplands. The centroids of catchments are most representative, but were not available (can be inferred upstream of each gauge location – toward wetter areas).

4.2.4. ESTIMATED STREAMFLOWS FOR THE GRAND FORKS VALLEY WATERSHED

It is difficult to derive a regression equation to predict mean annual discharge from basin area because of lack of data, poor correlation between runoff and basin area for small catchments, and the rather arbitrary exclusion of some catchments that do not fit the general trend. The limited period of record, and lack of correspondence between the POR for the different creeks, degraded the relation between basin area and runoff (some stations had records for dry years, and some for more wet years). Nevertheless, a reasonable assumption is that mean annual discharge increases with basin area, and the best fit model currently available for the catchments near Grand Forks is that shown in Figure 12.

The regression equation [10] computed the mean annual discharge for small catchments surrounding Grand Forks Valley. This value should be treated as an order of magnitude estimate. Only actual gauging of streamflow in creeks draining the valley slopes would give more precise number for mean annual discharge, although even that value would be expected to have high inter-annual variability. Flow records for Dan O'Rea Creek (08NN009) and July Creek (08NN018) and other nearby creeks should be extracted from archives (the full time series of records) to examine the annual hydrograph. For the smallest creeks on record, the maximum daily discharge was calculated from maximum daily runoff and catchment area (Table A2 in Appendix A). The calculated mean annual discharges add up to 0.49 m^3/s.

At July Creek east of Grand Forks, just outside the valley, the POR is long enough to reduce the inter-annual variability as for other creeks on record. It has a basin area of 45.6 km^2 and is representative of the topography, land cover, and climate of Grand Forks. The maximum discharge was 2.06 m^3/s, minimum discharge 0.00686 m^3/s, and mean annual discharge 0.32 m^3/s. The entire Grand Forks Valley watershed has catchment area of 95 km^2, which is approximately twice the size of July Creek catchment. Therefore, doubling all discharge values for July Creek would give a good estimate of the discharge regime of the Grand Forks Valley watershed. Using July Creek as a representative catchment area for its given mean annual discharge, the entire Grand Forks valley watershed would have annual discharge statistics calculated in Table 11.

Table 11 Estimated discharge for Grand Forks valley watershed, scaling up from July Creek catchment.

Annual Discharge	July Creek (45.6 km^2) (m^3/s)			GF Watershed (95 km^2) (m^3/s)
minimum	0.00686	x 2	=	0.0137
maximum	2.06	x 2	=	4.12
mean	0.32	x 2	=	0.64

It should be noted that during snowmelt starting in April and ending in June, the discharge will be closer to the estimated maximum annual discharge of 4.12 m^3/s, and during dry season the discharge would be on the order of 0.0137 m^3/s, as calculated above. By combining the two estimates of mean annual discharge, and the minimum and maximum discharge derived from July Creek data, the expected streamflow for the whole watershed of Grand Forks Valley has the following statistics (Table 12).

Table 12 Estimated discharge for Grand Forks valley watershed, using linear regression of mean annual runoff and catchment area (sum of catchments).

	$Q_{OUT} = \Sigma Q_{OUT\ i}$ (m^3/s)
minimum discharge	0.0137
maximum discharge	4.12
mean annual discharge	0.64 to 0.49

The mean annual discharge is between 0.64 and 0.49 m^3/s as estimated from the two methods using July Creek as an index, and from linear regression of mean annual discharge to catchment area for selected small catchments near Grand Forks.

4.2.5. WATER BALANCE FOR KETTLE-GRANBY RIVERS IN THE VALLEY

For the purpose of water balance analysis, the Kettle River was divided into two branches (reaches), and the Granby River formed one reach of the river network in the valley.

Branch 1: Kettle River from south of Carson in Washington State where the Kettle River enters the Grand Forks Valley (about 2 km from the border) to confluence with Granby River at Grand Forks

Branch 2: Granby River from valley walls north of Grand Forks to confluence with Kettle River

Branch 3: Kettle River from confluence with Granby River at Grand Forks, to Gilpin east of Grand Forks where the valley narrows and the aquifer effectively ends.

The period of record varies between the hydrometric gauging stations. In the Grand Forks Valley, only one station (08NN002) is presently active on the Granby River. There is lack of concurrent discharge records at more than one station in the Grand Forks Valley. The gauging locations that do have extensive concurrent records are outside of the valley. The closest upstream station is at Ferry, WA, and the closest downstream stage gauge is at Laurier, WA.

The river system as defined above has a water balance that includes discharge terms and channel storage. Except during ice conditions, channel storage is very transient, only as long as it takes a flood wave to propagate downstream across the valley (time scale of few hours). The water balance is:

$$Q_{IN} - Q_{OUT} = \Delta S_{RIVERS} \qquad \textbf{[1]}$$

where the inflow discharge Q_{IN} can be separated into flow components in the two rivers, tributary creeks, and baseflow from the aquifer in the valley (includes groundwater flow into river channel, flow from drains and ditches and storm sewers, effluent from sewage or other waste discharges (not significant here).
Inflow components:

$$Q_{IN} = Q_{KETTLE(IN)} + Q_{GRANBY(IN)} + Q_{CREEKS} + Q_{BASEFLOW} \qquad \textbf{[2]}$$

There is only one outflow term, since all surface water eventually channels into the Kettle River at the end of the valley:

$$Q_{OUT} = Q_{KETTLE(OUT)} \qquad \textbf{[3]}$$

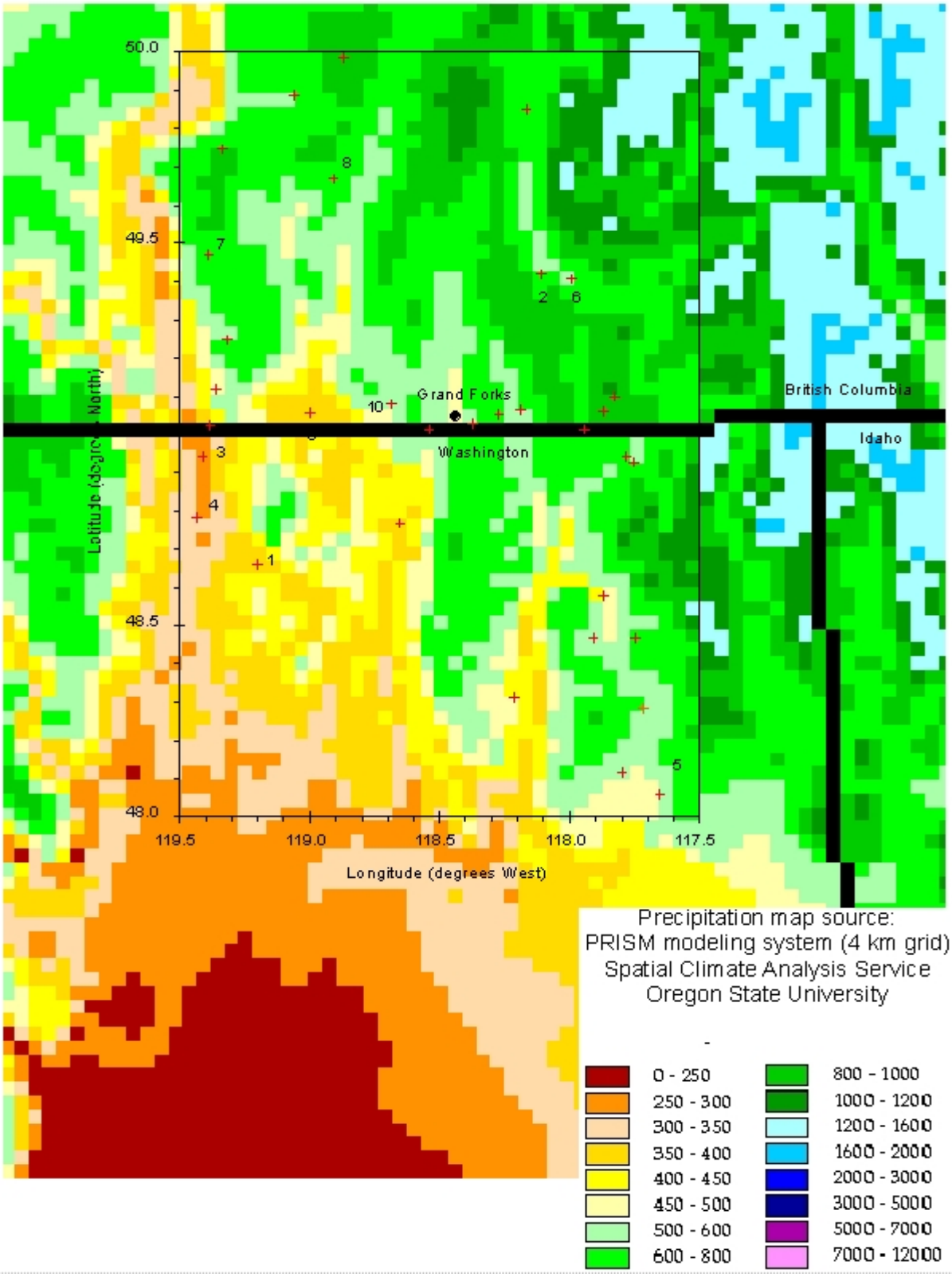

Map 16 Precipitation map and locations of hydrometric stations on creeks near Grand Forks, BC.

ESTIMATED INFLOW FROM KETTLE AND GRANBY RIVERS

The discharge through Branch 1 of Kettle River was based on records from the gauge at Carson (08NN005). The mean annual discharge for the period of record is 165 m^3/s, and one standard deviation about the mean gave flow variability of 100 to 250 m^3/s.

The Granby River (Branch 2 of the network) has records of discharge from a gauge located just north of Grand Forks. The mean annual discharge for the POR was 115 m^3/s. One standard deviation about the mean gave spread of 50 to 185 m^3/s, and the maximum discharge (flood) ever recorded was 385 m^3/s.

Past the confluence with Granby River, the Kettle River has substantially larger flows than upstream of Grand Forks. This downstream Branch 3 can be considered as the sum of Branch 1 and Branch 2. The combined mean discharge was 280 m^3/s (sum of mean discharge for Branches 1 & 2). Flow variability was 150 to 425 m3/s (sum of mean +/- 1σ for Branches 1 & 2). The estimated maximum flow was 450 m^3/s. For reference, the mean discharge at Cascade (08NN006) 10 km downstream was 260 m^3/s, which should be higher by a small amount than mean flow for Branch 3 because more creek tributaries flow into Kettle River along the 10 km stretch. The mean discharge plus/minus one standard deviation was 150 to 450 m^3/s, and the most extreme flow ever recorded was gauged at 830 m^3/s.

The Granby River discharge is smaller than for Kettle River upstream of Grand Forks. The mean annual discharge of the Granby is 30.5 m^3/s, and for Kettle upstream of Grand Forks is 44.3 m^3/s. Past the confluence, the mean annual discharge at Cascade near Billings is 72.8 m^3/s. Therefore, at the confluence of these rivers, the Granby contributes approximately 40% of the flow, and the Kettle contributes 60% of the flow for Kettle River downstream of the confluence. The ratio of discharge from Granby to Kettle of 0.69 varies from year to year.

- ESTIMATED INFLOW FROM KETTLE AND GRANBY RIVERS AT LATE SUMMER LOW FLOW

The low flows of the rivers are of particular importance from a water management and environmental perspectives. In terms of aquifer discharge, the lower the river stage the greater the gradient between stored aquifer water and the river, and the larger the discharge from the aquifer to supply baseflow to the river. When the river baseflow is sensitive to potential climate change in the region, the aquifer water levels will also be increasingly sensitive to such changes.

For Branch 1 of the Kettle River, the low flows during dry summers typically range from 4 to 7 m^3/s (based on records at Carson). In the Granby River (Branch 2) the dry summer low flows were between 2.5 to 4.5 m^3/s, but the river flow could be lower than 2 m^3/s during extremely dry summers (the lowest flow on record is 0.2 m^3/s). The discharge increased during wet summers, typically between 5.5 to 6.5 m^3/s. Branch 3 of Kettle River usually has dry summer discharge of 7 to 12 m^3/s. The flows at Cascade had slightly higher baseflow during dry summers (10 to 12 m^3/s), and as low as 3.4 m^3/s during extremely dry summer weather. Summer rains tended to produce discharge between 10 and 18 m^3/s.

- ESTIMATED INFLOW FROM TRIBUTARIES

The mean annual discharge of Kettle River in the Grand Forks Valley is on the order of 47 m^3/s, and that of Granby River is 30.5 m^3/s. The small tributaries contribute only 0.64 to 0.91 m^3/s mean annual discharge to the larger Kettle River, within the extent of the Grand Forks aquifer. On an annual basis, this flow represents about 2% of the Kettle River flow, or 1% of the combined Kettle and Granby River flow downstream of Grand Forks. During the summer

months, many of the smaller creeks become ephemeral, discharging water only after large rain events, and only a few maintain base flow in dry periods. The Kettle River low flow is about 12 m^3/s and is relatively constant from August to October. The low flows or no flow in the small creeks are expected to occur from June to October; longer than Kettle River because it is assumed that snow melt occurs early in these low altitude small catchments (assumption).

In any case, the river discharge in both the Granby and Kettle Rivers will not be measurably affected by inflows from these small catchments in the Grand Forks Valley from Carson to Gilpin. Thus, water levels in Kettle and Granby will be controlled only by their very large upstream drainage basins (2000 km^2 for Granby and 6000 km^2 for the Kettle). This compares to a total of 95 km^2 for all catchments that provide flow into the valley at Grand Forks.

During high flow periods, the Kettle River carries 200 to 300 m^3/s, while estimated maximum discharge from all creeks into the valley was 4.12 m^3/s. At low flow in August, the Kettle River maintains between 10 and 14 m^3/s in most years compared to minimum discharge of 0.0137 m^3/s for the creeks. In terms of percentages, during the spring high flows, the small creeks contribute 1 to 2 % of Kettle River discharge in the valley. During the late summer low flow, the small creeks contribute about 0.1 % of the river flow in dry conditions, and may contribute more during localized rain storms. The maximum recorded runoff in creeks is during snowmelt in April to May. Although intense rain storms can produce creek discharge as high as one half of maximum recorded runoff from snowmelt, the atmospheric instabilities always affect a wide region. Consequently, the Kettle River stage would already be elevated from increased runoff and the creeks in this watershed would contribute 4.12 / 2 = 2.06 m^3/s to Kettle River conveying flow of 20 to 150 m^3/s. Therefore, at most, the creeks would provide 10% of the river discharge for a short time period, and that contribution would drop to 2% once dry conditions returned. Although the creeks have very little effect on the flow of Kettle River, they may be important for adding storage to the aquifer near valley edges away from the influence of the river on groundwater levels.

- ESTIMATED FLOW BETWEEN KETTLE RIVER AND AQUIFER

The loss of water from the aquifer to the river will be at maximum after a rapid drop in river stage. The amount of baseflow will be related to hydraulic gradient between the aquifer and the river. At the catchment and basin scales, estimates of low-flow characteristics at un-gauged sites are generally quite inaccurate because low flows are highly dependent on the lithology and structure of the rock formations and on the amount of evapotranspiration, neither of which have been adequately described by indices except in a few basins (Riggs, 1972). The gain of water from the river to the aquifer will be at maximum after rapid increase in river stage. The amount of outflow from river will be related to hydraulic gradient between the aquifer and the river.

- WATER BALANCE SUMMARY

Flow from all tributary creeks flowing into Kettle and Granby Rivers in the valley:

- 0.0137 to 4.12 m^3/s range 0.64 to 0.49 m^3/s (about 1% of Kettle River discharge, perhaps up to 10% during localized heavy rain storms)

Flow in the Kettle and Granby Rivers:

1) mean annual flow (1 standard deviation bounds)

- Branch 1 (Kettle R.): 100 to 250 m^3/s or 60 to 50% (typically 60%) of Branch 3 flow
- Branch 2 (Granby R.): 50 to 185 m^3/s or 40 to 50% (typically 40%) of Branch 3 flow
- Branch 3: (Kettle R.): estimated 150 to 425 m^3/s

2) typical monthly mean summer low flow:

- Branch 1 (Kettle R.): 4 to 7 m^3/s (dry weather)
- Branch 2 (Granby R.): 2.5 to 3.0 m^3/s (dry weather), 5.5 to 6.5 m^3/s (with rain storms)
- Branch 3: (Kettle R.): estimated 6.5 to 10 m^3/s (dry weather)

3) lowest summer flow on record:
- Branch 1 (Kettle R.): 5.1 m^3/s on short record (estimated about 2 m^3/s)
- Branch 2 (Granby R.): 0.23 m^3/s
- Branch 3: (Kettle R.): estimated about 2.5 m^3/s

Aquifer recharge and discharge:
- outflow from Kettle River to aquifer recharge: modeled 0.57 m^3/s (summer low flow)
- 28% of total annual precipitation of 409.1 mm/year, or 135 mm/year
- probably significant recharge from small creeks flowing across floodplain
- probably small recharge from valley slopes by seepage, but large in wet weather
- discharge by pumping: maximum near 0.32 m^3/s during summer months
- unknown, but probably small discharge from evapotranspiration by plants
- unknown, but probably small discharge by drainage ditches, especially along escarpments and during wet season when water table is elevated

4.3. SIMULATING RIVER FLOWS OF KETTLE AND GRANBY RIVERS USING BRANCH NETWORK MODEL

4.3.1. BRANCH MODEL DESCRIPTION

The BRANCH model is a publicly available one-dimensional flow model developed and tested by the USGS since early 1980's. The branch-network flow model is a broadly applicable, proven model, intended for operational use to compute unsteady flow and water-surface elevation of either singular or interconnected channels (Schaffranek et al., 1981). The model accommodates tributary inflows and diversions, and includes the effects of wind shear on the water surface.

A typical network is composed of branches (reaches) and segments (sub-reaches) as shown in Map 17. The basic spatial unit is the segment that represents a relatively short and uniform section of the river channel (or Thalweg where the flow occurs). Segments are connected by nodes where cross-sectional channel geometry is defined. The branches group several segments into river reaches, which have similar properties and channel geometries, and are connected to other branches by nodes called internal junctions. External junctions are end points of branches that form boundaries of the network.

The implementation of the one-dimensional river flow model (Regan and Schaffranek, 1985) begin with delineating the channel system and defining the open-channel reaches comprising the system, and selection of suitable cross-section locations at which to represent an open-channel reach. Since the purpose of the river flow model in this study was to provide river stages for input into groundwater flow model as one boundary condition, the branch-network extent was limited to rivers flowing over the Grand Forks aquifer.

The branch-network model for Kettle and Granby Rivers consists of 8 branches. The Kettle River branches are numbered 1, 2, 3, 5, 6, 7 and 8, and the Granby River is represented by one

branch (#4). The external junctions are at cross-sections 66 (Carson, BC, near US border and upstream of Grand Forks), 11 (north of Grand Forks), and 15 (at Gilpin, BC, downstream from Grand Forks). All other junctions are internal. The Granby River can also be represented as a tributary to Kettle River at junction 5, and resulting in only 7-branch network model.

- DATA REQUIREMENTS

The river channel geometry and flow conveyance information that is input to the branch-network model consists of stage-dependent cross-sectional properties at the identified locations. For the branch model, these properties are defined in terms of area, width, wetted perimeter, and hydraulic radius. Boundary conditions must be specified at all external junctions, and consist of sequences of synchronous, precisely timed stage or discharge measurements. A known unique stage-discharge relationship can also be used. Tributary inflows can be designated at any internal junction as a time series of discharges or as constant discharge. Channel conveyance parameters include the flow-resistance coefficient, which is calculated from Manning's formula. Resistance coefficients can be constants or vary with stage or discharge. For wind induced flows, the momentum coefficient, which is a function of water surface drag, must be provided.

- BRANCH MODEL LIMITATIONS

The Branch-network model attempts to model the unsteady flow of water in river channels, and is based on the following assumptions:

1. one-dimensional flow
2. homogeneous density of water
3. flow driven by hydrostatic pressure (elevation difference)
4. slope of channel is mild and constant over segment length to maintain sub-critical flow
5. Manning's n formula provides an accurate estimate of frictional resistance to flow
6. channel geometry is constant at each cross-section

Since this is a one-dimensional flow model, the channel geometry of the network should be relatively simple and one-dimensional flow should dominate. In other words, this model does not simulate turbulent eddies or other flow components except in downstream direction parallel to axis of thalweg. That such a condition is close to reality, where most of the flow is downstream and parallel to the channel, allows for application of a one-dimensional flow model for Kettle and Granby Rivers. The second condition assumes that water flow is homogeneous in density and is driven by hydrostatic pressure (difference in elevation). This condition is also satisfied. The Manning formula is assumed to provide an accurate approximation of the frictional-resistance force for unsteady as well as steady flow, and that uniform velocity profile varies throughout a cross-section but can be represented by a mean velocity.

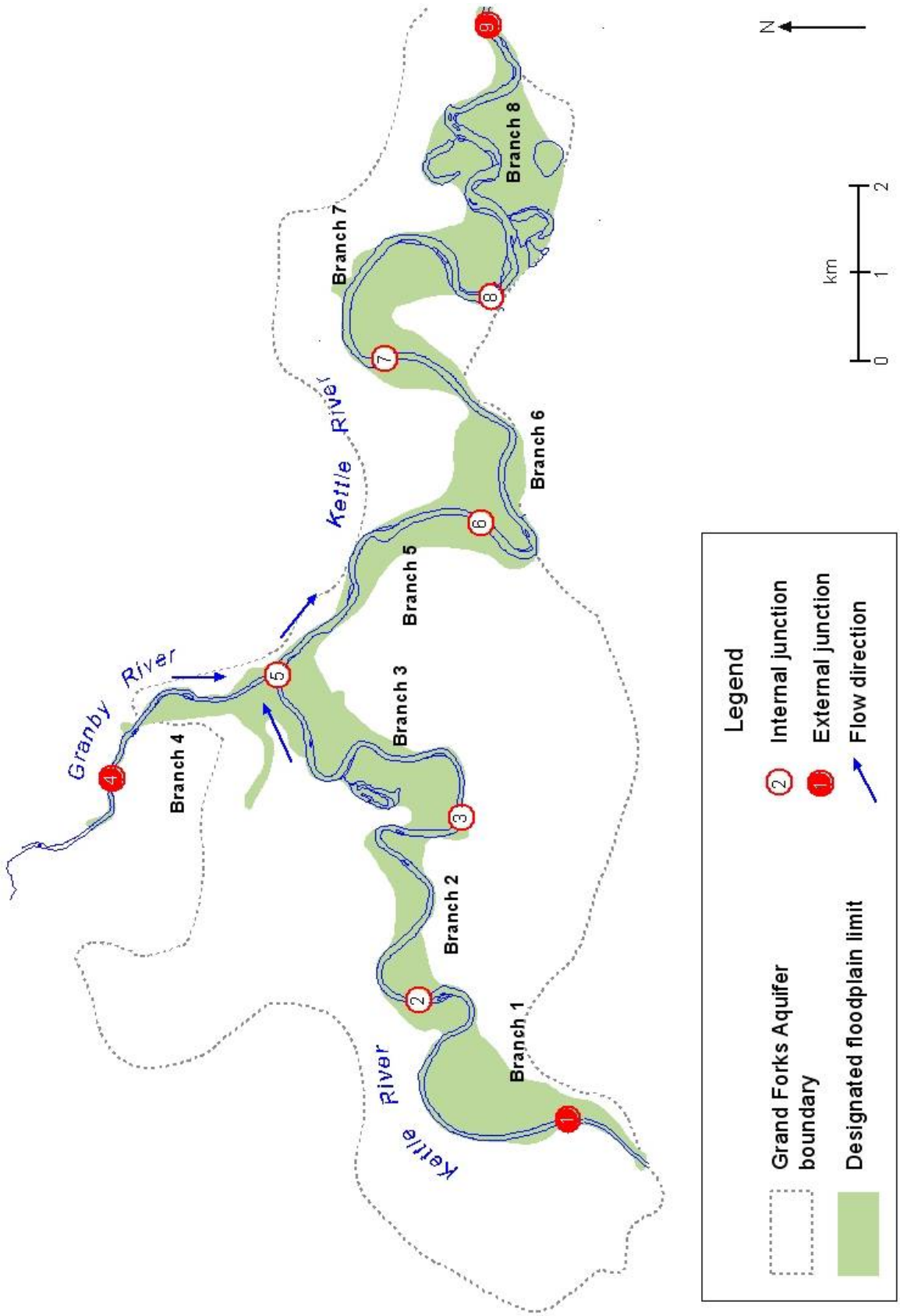

Map 17 Schematic diagram of BRANCH-network model implemented for Kettle and Granby Rivers.

The channels should be straight if the model is used for determination of flow field for particle tracking, but channels with bends of significant curvature may also be treated if determination of the flow field is not required. In the case of the Kettle and Granby Rivers, the meandering channels were subdivided into smaller segments and the curvature was ignored–the longitudinal distance along the channel was measured along the curved channel, but the model assumes that the water flows through a straight channel. The left and right-bank water surface elevations are assumed to be equal at any distance along the channel, which is approximately true in reality. The surveys of cross-sectional geometry show very small variation in water surface elevation from left to right bank of the river, and the water surface was assumed horizontal in a transverse direction to the river channel.

The assumption of constant channel geometry is valid for simulation times shorter than the recurrence of high-flows which cause significant reworking of channel bedforms and channel banks. For this modeling scenario, the required stage accuracy will not be compromised by small changes in channel bed configuration. The river may shift the thalweg from one bank to another, but the water level will probably remain the same. Given that the ultimate purpose of this modeling effort is to provide water elevations for constant head boundary condition in a groundwater flow model, small errors in predicting river stages are inevitable.

- DESCRIPTION OF NEW BRANCH-NETWORK MODEL (VERSION OF CODE WRITTEN FOR GRAND FORKS PROJECT)

A new user interface was developed for the BRANCH model, where all inputs and outputs are included in a single spreadsheet file (Microsoft Excel 97 for Windows). The original Fortran source code was translated to Visual Basic 6.0 code using Microsoft Visual Studio development environment. The inputs and outputs handling was changed, but all mathematical transformations, solver, and data structures were maintained as in original code. The new code was verified using a sample data set supplied by the USGS.The results were identical to all significant figures between output from BRANCH VB version and the original USGS BRANCH (Fortran code) version.

4.3.2. CHANNEL AND CROSS-SECTIONAL GEOMETRY

In 1990, river surveys were done on the Kettle River and Granby River in Grand Forks valley by Surveys Section of Water Management Branch of Environment Canada. Map 18 d isplays the locations of river surveys and shows the floodplain limits. The river cross-sections are numbered 15 to 67, increasing upstream of Kettle River, and starting at Gilpin, 10 km east of Grand Forks. The exception was cross-section 67 which is added between sections 56 and 58. The last cross-section on the Kettle River at the US border, upstream of Grand Forks, is numbered 66. To measure segment lengths, approximate distances between cross-sections were measured from floodplain maps along channel centerline. The cross-sections were spaced (on average) approximately 600 m apart, but segment length varied between 1050 m and 200 m. For the Granby River, the cross-sections were numbered 1 to 12 in the upstream direction starting from confluence of the Granby River with Kettle River at Grand Forks, and ending about 2.3 km north of Grand Forks, with an average distance between cross-sections of 300 m. The available channel surveys on the Kettle and Granby Rivers started at the left bank (looking downstream at cross-section), were variably spaced (average spacing 3 to 4 m) along survey line, and gave average vertical spacing of 0.3 to 0.4 m. One example of a cross-section on the Kettle River is shown in Figure 14.

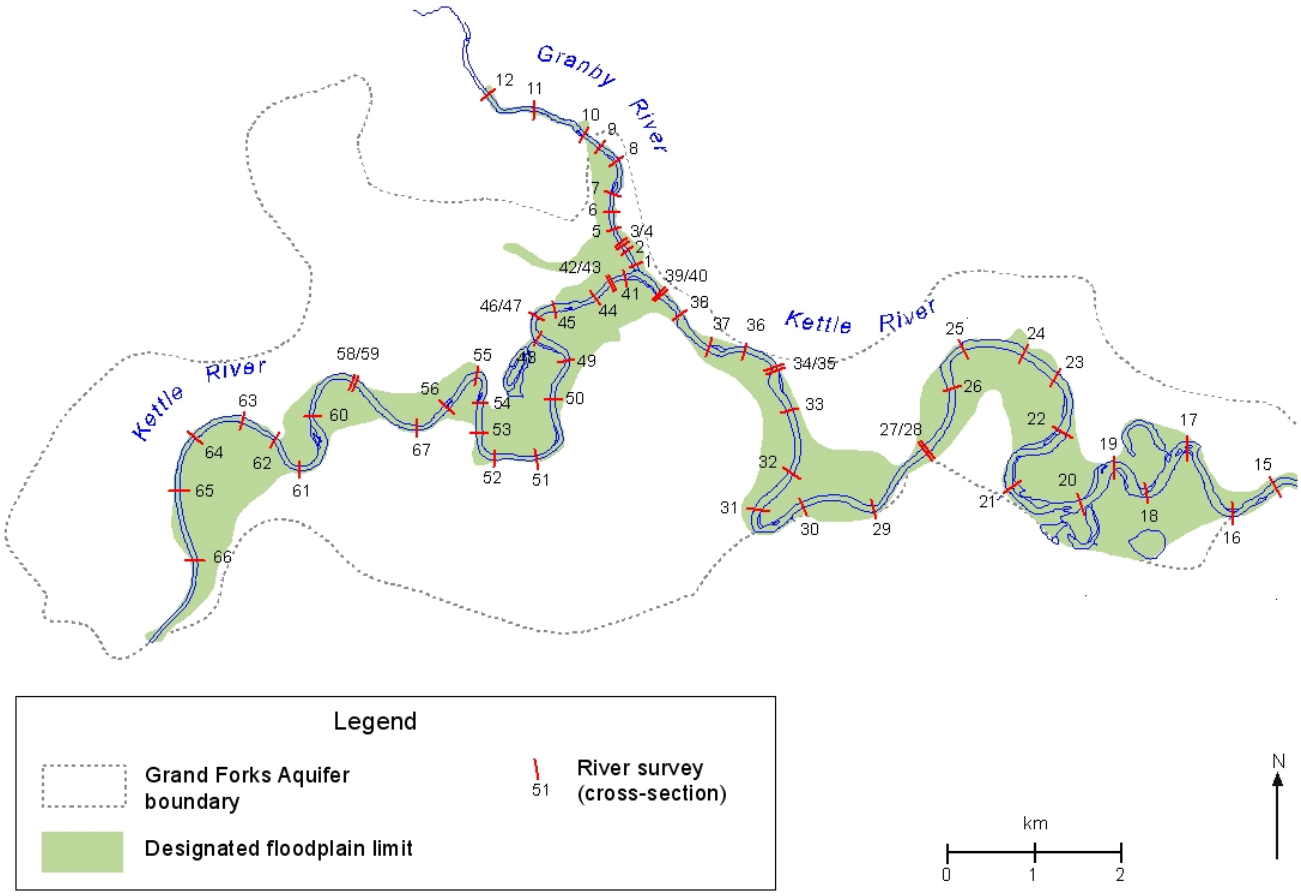

Map 18 River survey stations on Kettle and Granby Rivers, and floodplain limits.

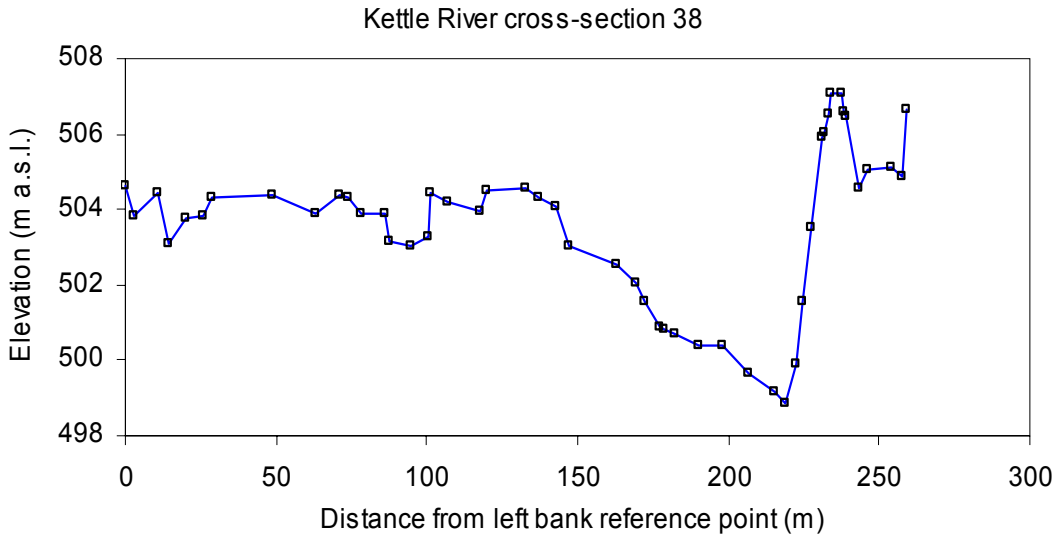

Figure 14 Surveyed cross-section number 38.

The Surveys Section of BC Water Management Branch of Ministry of Environment provided hard copy survey data along each cross-section, and scaled plots of cross-sections. Where bridges were present (4 on Kettle R. and 1 on Granby R.), cross-sections were collected on each side of a bridge, and drawings of bridges and supporting pillars were included in cross-section plots. The surveying work was carried out on different days between September 22, 1990 and October 1, 1990. Stages varied between locations as a result of differences in dates of survey and channel geometries, and water level marks were only recorded for selected locations. The right and left bank stages were within 5 to 20 cm along the survey line for most cross-section locations, but where differences were large, the river probably flowed in multiple channels divided by sand bars. The high water marks were found between 3 and 5.5 m elevation above channel bottom for most channel sections on Kettle River. On the smaller Granby River, the right and left bank stages also showed good correspondence, while the high water level marks were also between 3 and 4 m, but the flood waters did not leave a mark above the 4 m stage. Where two sections were present on each side of a bridge, only the upstream section was used; where sections were spaced too closely, some sections were excluded to increase segment length for the model.

Scibek and Allen (2003) provide data and graphs for each measured cross section. In all cross-sections, a simplified floodplain profile was added to increase the vertical range of stage computation in BRANCH (e.g., Figure 15). During model calibration, overbank flow occurred at several cross-sections until the conveyance parameters were adjusted to reduce stage to in-bank flow.

Figure 15 Surveyed cross-section number 38 and extension of section into floodplain.

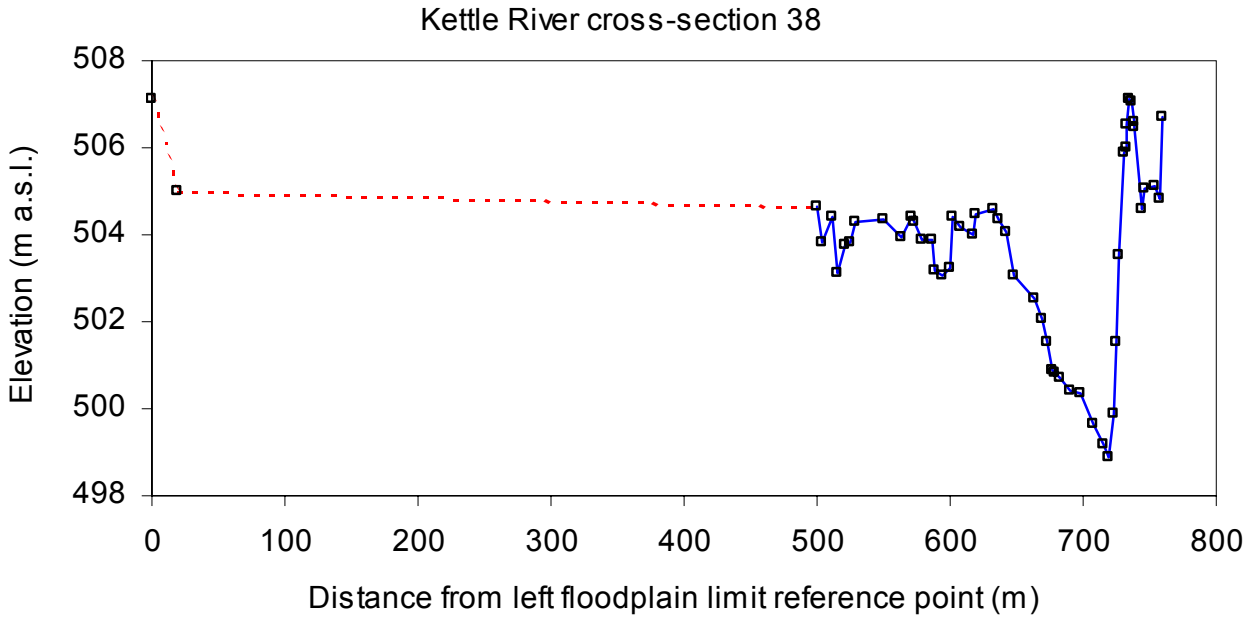

4.3.3. GEOMORPHOLOGY OF THE KETTLE AND GRANBY RIVERS

Within the Grand Forks Valley, the Kettle River is a meandering gravel-bed river incised into glacial outwash sediments. In the eastern portion of the valley, the river slope decreases and the channel widens. There are several oxbow lakes, swampy areas and associated slack-water deposits. The Quaternary geology of this valley is probably similar to other and better studied valleys in southern BC, but as interpreted by Campbell (1971), the valley was infilled by glacial outwash gravels and sands, interlayered silts and clays deposited in lacustrine settings, and some glacial till. All of these sediments have been reworked to some depth by the more recent fluvial processes that shape the present-day floodplain of the Kettle River.

The Granby River enters the valley through a narrow gap between bedrock valley slopes and a bedrock hill called Observation Mountain just north of the city of Grand Forks. Campbell (1971) speculated that the gap lies along faulted zone, which was eroded by draining a lake dammed behind an ice dam, and causing a shift in the flow direction of the Granby River from a previously more straight path along present-day location of Ward Lake, north-west of Grand Forks. The Granby River got entrenched in that gap and it still flows there today.

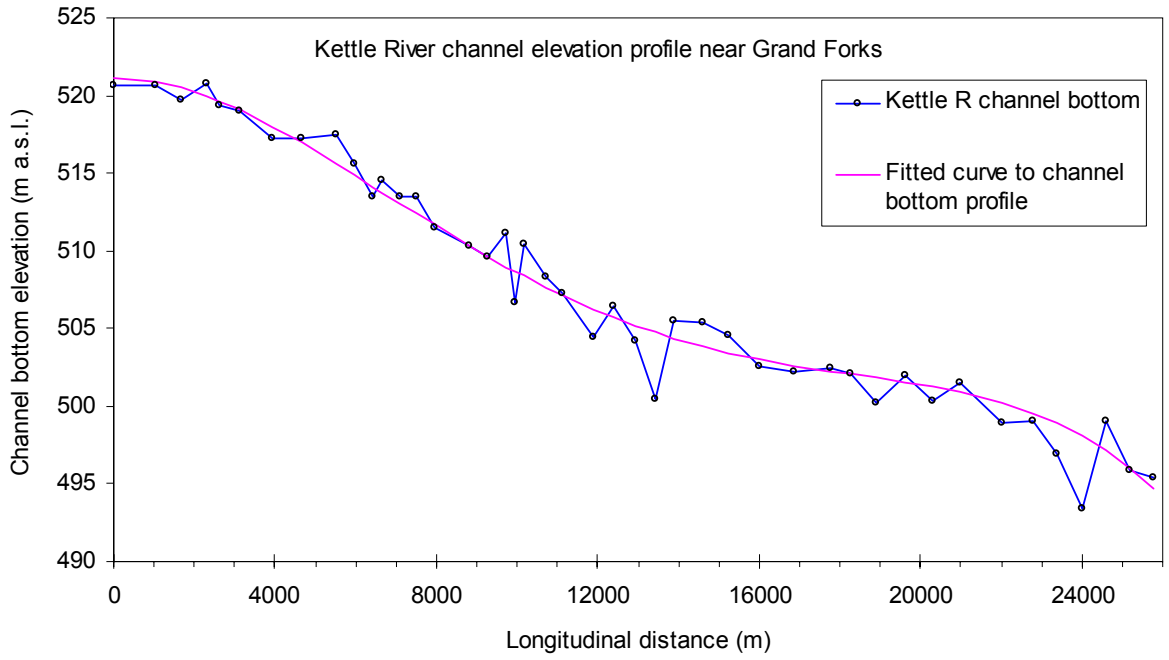

Figure 16 Channel bottom elevation profile for the Kettle River flowing through Grand Forks Valley.

The channel bottom elevation of the Kettle River was graphed against longitudinal distance to show the elevation profile of this river in the Grand Forks Valley (Figure 16). The river drops from 521 m a.s.l. to 495 m a.s.l. over its 25 km length, which gives average slope of 0.0104. Longitudinal distance along channel was measured on floodplain maps (BC Environment, 1992) starting from the US/Canada border at Carson, in the southwest end of the valley, and measured downstream along the river channel. The jagged profile results from errors in

channel cross-section surveys (or errors in benchmark elevations. Confluence with Granby River occurs at 11 km mark. The Kettle River has rapids between sections 24 and 25 (19 km mark) noted on the floodplain map.

The Granby River profile is graphed in Figure 17. The river drops rapidly in elevation between cross-section 12 and 11, but then levels off until the confluence with Kettle River.

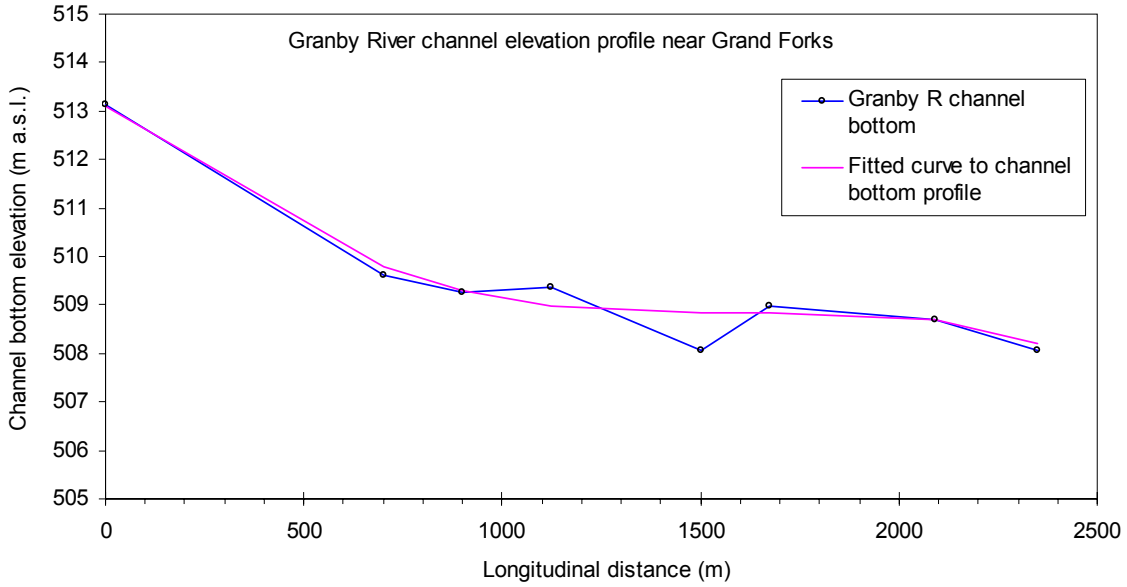

Figure 17 Channel bottom elevation profile the Granby River flowing through Grand Forks Valley.

A smooth profile was obtained by fitting quadratic polynomial curve using least-squares optimization to the Kettle River channel bottom elevation profile. The R^2 was 0.97 for this curve fit and the equation was:

$$Z_{BOTTOM}(x) = 4*10^{-16}x^4 + 2*10^{-11}x^3 - 3*10^{-7}x^2 + 2*10^{-4}x + 520.7 \qquad \textbf{[14]}$$

For the Granby River, the smoothed profile was adjusted by linear interpolation and manual adjustment of two points only, while preserving the remaining points in the profile.

In the BRANCH model, the channel bottom elevation for each cross-section was corrected to the smooth profile using datum correction (DACORR) calculated from the difference between surveyed channel bottom (Z_{MIN}) elevation to the fitted profile ($Z_{BOTTOM}(x)$):

$$DACORR = INT(Z_{BOTTOM}(x) - Z_{MIN}) \qquad \textbf{[15]}$$

During model run, BRANCH adjusts each Z_{MIN} by subtracting DACORR. Figure 18 shows a schematic representation of a channel bottom and the relevant variables.

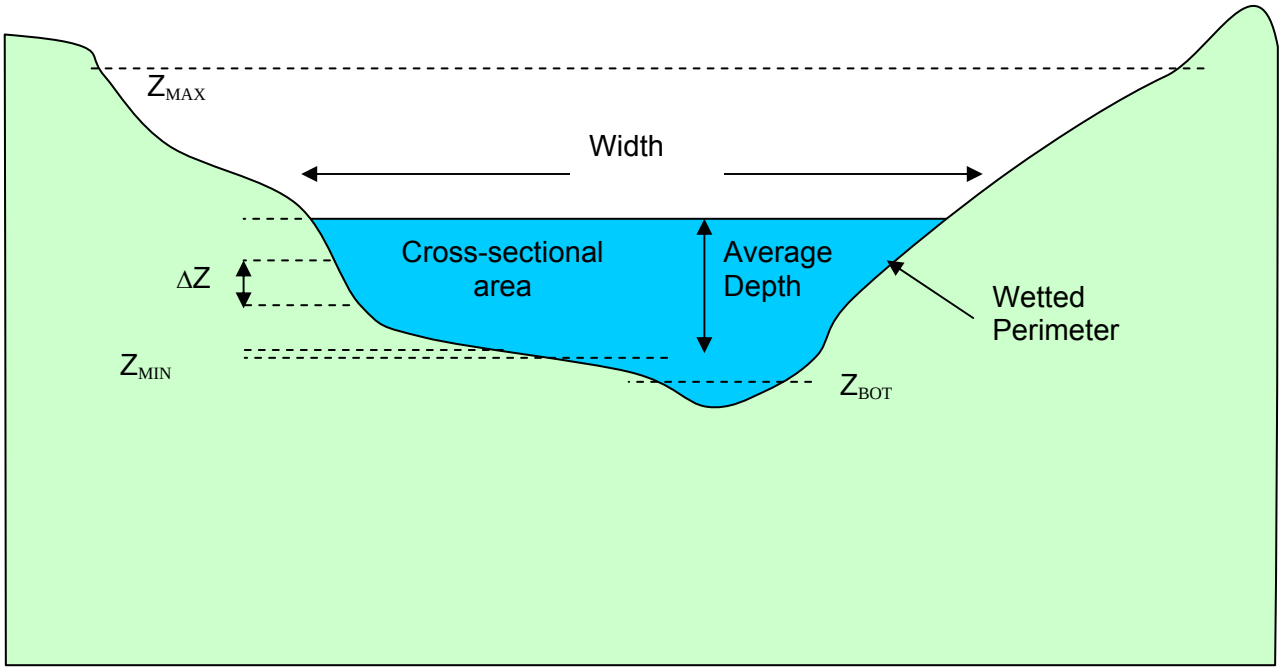

Figure 18 Channel cross-section definition diagram.

- CHANNEL GEOMETRY ANALYSIS WITH CGAP

Regan and Schaffranek (1985) developed the CGAP (Channel Geometry Analysis Program) that permits the analysis, interpretation, and quantification of the physical properties of an open-channel reach as defined by a sequence of cross sections. CGAP requires channel-bottom elevations measured and referenced horizontally to a channel-bank location and referenced vertically to a common datum plane. The use of a left channel bank reference point is the normal convention and is assumed by CGAP.

CGAP was incorporated into the new version of the BRANCH code to provide seamless channel geometry computations for inputs into the flow model. The cross-sections were arranged in spreadsheet columns and referenced by identification numbers. The CGAP program calculates the unadjusted channel bottom elevation (Z_{BOT}) from minimum elevation on each cross-section, the minimum stage to be computed (Z_{MIN} as rounded off value to nearest stage increment), the maximum stage to be computed (Z_{MAX}), and the datum correction (DACORR) to produce smooth river profile. The successive stage to be computed was set at 0.25 m to provide a detailed channel geometry description, following the recommended increment in the BRANCH manual. At each stage increment, CGAP calculates cross-sectional area, channel top width, wetted perimeter, average depth, channel asymmetry, and other parameters. The required values were automatically written into channel geometry input tables used by BRANCH; these included stage, cross-sectional area, and width. Output for cross-section 1 (original #66) at Carson is shown graphed versus stage in Figure 19.

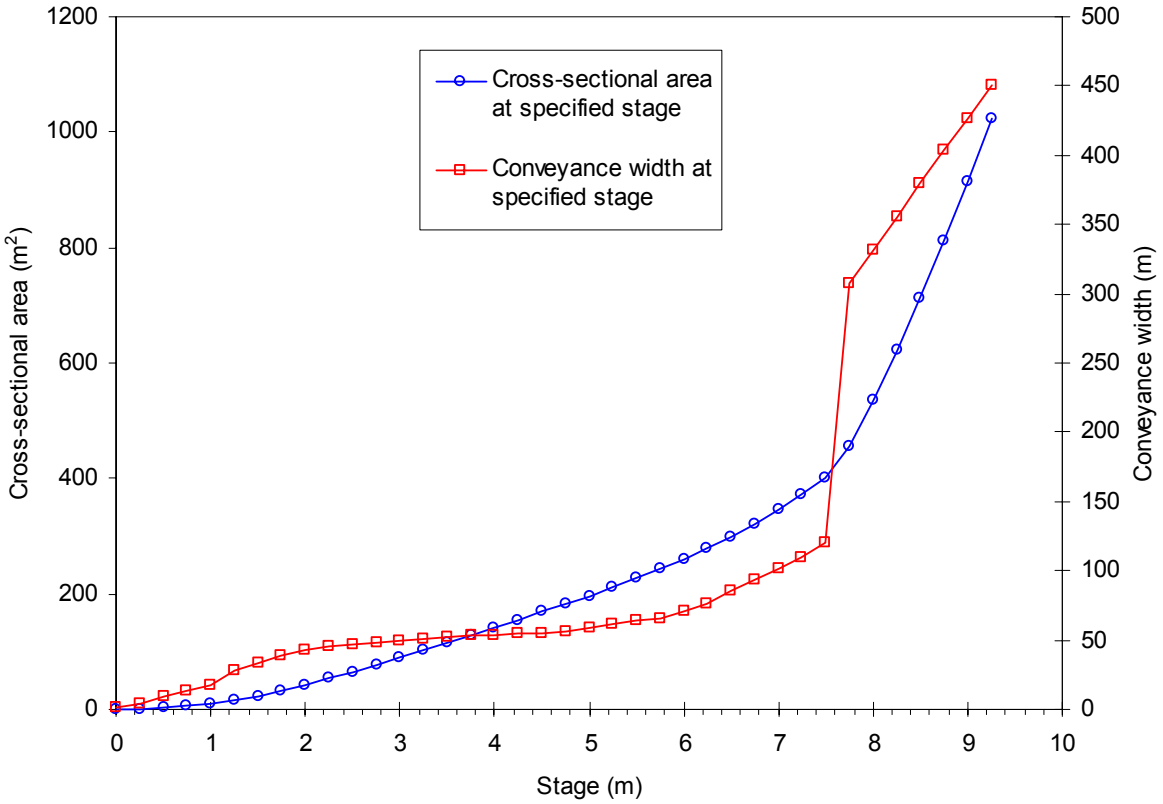

Figure 19 Graph of channel cross-sectional area and conveyance width (channel width at water surface) at specified stages, calculated by CGAP for cross-section 1 on Kettle River at Carson, BC.

4.3.4. MODEL INPUT

Details concerning model input parameters are provided in Scibek and Allen (2003). Two different BRANCH models were set up for simulating the rivers in the Grand Forks Valley. Each simulation run required separate calibration of flow model to initial conditions.

Case 1 involved modeling the Kettle River using only 8 branches, with a total of 40 cross-sections.

Case 2 had a river network consisting of 7 branches (6 of Kettle River, and 1 of Granby River), with a total of 46 cross-sections.

The branch-network model requires initial condition data (stage and discharge) for each node. The discharge initial conditions were equal to first discharge value of input boundary value data, between 4 and 10 m^3/s, which is typical of observed low-flow on Kettle River. The initial stages were unknown, so the values were estimated using iterative-process and feedback from successive model runs using different initial stage values. The model converges to computed stages after several time steps from any initial stage, but model instability is reduced as initial stages are close to computed stages after the first time step. The stages depend on the stage-discharge relationship of each cross-section, which depends on channel conveyance parameters and channel geometry. For case 1, all external and internal nodes began with initial

discharge of 6.00 m^3/s. For case 2, the upstream nodes of Kettle River (above confluence with Granby R.) had 6 m^3/s initial discharge, the upstream node of Granby River had 4 m^3/s initial discharge, and the flow at downstream nodes of Kettle River (below confluence with the Granby R.) received initial value of 10 m^3/s, calculated to balance the flows.

The modeling approach did not attempt to model the actual annual flow hydrograph of the river because the data requirements would be very large and would require changes in code to accommodate larger datasets than typical integer size (>64000). The goal of the simulations was to derive stage-discharge curves for the cross-sections. The input consisted of synthetic (not measured) discharge data created specifically for the modeling purpose. The time series of discharges was at a 1-minute interval, and stretched for a period of 10000 minutes. Results for the two simulations are provided in Scibek and Allen (2003).

An initial time period of constant discharge was applied at external nodes, designed to allow the model to stabilize after the initial oscillations and instabilities commonly seen in such model. The early constant flow period was used to calibrate the initial stage conditions to specified initial stages. Then, the discharge was increased at constant rate of 0.01 m^3/s per minute. The temporal shift (delay) between the two time series was required and it was adjusted during model calibration. The average flow velocity is approximately 0.3 to 0.5 m/s for the Kettle River, thus, it would take a particle about 20 hours to travel through all the branches of the network.

Case 1: Kettle River
The first 300 minutes was a period of constant 6.00 m^3/s discharge. The discharge was increased at constant rate of 0.01 m^3/s per minute until high-flow magnitudes of 400 m^3/s for Kettle River were observed.

Case 2: Kettle and Granby Rivers
The first 1200 minutes was a period of constant discharge applied to external nodes, equal to the initial discharge. The discharge was increased at constant rate of 0.01 m^3/s per minute until high-flow magnitudes of 400 m^3/s for Kettle River were observed.

4.3.5. MODEL CALIBRATION

The BRANCH-network model was calibrated for the Kettle River, and for the combined network of Kettle and Granby Rivers flowing in the Grand Forks Valley. The output consists of plots of stage and discharge at selected cross-sections along the river channel, graphed against elapsed time of model run. Stage-discharge plots were created from scatterplots of computed stage and discharge for each cross-section. Plots of rating curves are provided in Scibek and Allen (2003). Due to model limitations, the simulations did not succeed in reaching very high discharges when overbank flow at a few cross-sections contributed to model instability. As a result, the stage-discharge curves ended at discharge smaller than highest recorded flows during flood conditions. To compensate for this limitation, best fit power-law curves were fitted using spreadsheet solver and manual adjustment of coefficients to the stage-discharge scatterplots. High water marks were added to stage-discharge plots as horizontal lines and the fitted curves were extrapolated to intersect the high-water mark lines at typical flood level discharges.

4.3.6. MODEL LIMITATIONS

Although the cross-section spacing along the Kettle River is dense, the river channel geometry varies greatly with location. There is a lack of consistency in high-water mark surveying along the cross-sections. At the same time, the model did not account for channel storage or variation of channel roughness with stage, or backing up of water along un-surveyed sections of the channel that could impact the surveyed locations. Therefore, neither the surveyed high-water marks nor the modeled stages are without error.

At low flow, there are small rapids in various places along the river channel (both Kettle and Granby Rivers), causing problems with solution of flow equations due to too steep channel slope. The BRANCH-network model was found to be difficult to work with and rather sensitive in its stability to a combination of control parameters, initial conditions, and boundary conditions. River flow through several of the cross-sections gave objectionable results and the curves were adjusted to fit the high-water mark regardless of BRANCH output.

4.4. CLIMATE CHANGE IMPACTS: PREDICTING CHANGES IN STREAMFLOW

In this section, an overview of observed and predicted climate change impacts on hydrologic systems in south-central British Columbia is provided. Also included is the methodology used for generating predicted river discharge hydrographs for Kettle and Granby River basins.

4.4.1. OBSERVED CHANGES

In British Columbia, climate change has been detected from detailed examination of meteorological, hydrologic, sea level, and ecological records and investigations. Analysis of historical data indicates that many properties of climate have changed during the 20th century (Ministry of Water, Land and Air Protection of BC, 2002). Some of the changes were:

- Average annual temperature warmed by 0.6ºC on the coast, 1.1ºC in the interior, and 1.7ºC in northern BC.
- Night-time temperatures increased across most of BC in spring and summer.
- Precipitation increased in southern BC by 2 to 4 percent per decade.
- Lakes and rivers become free of ice earlier in the spring.
- Water temperature increased in rivers and streams.

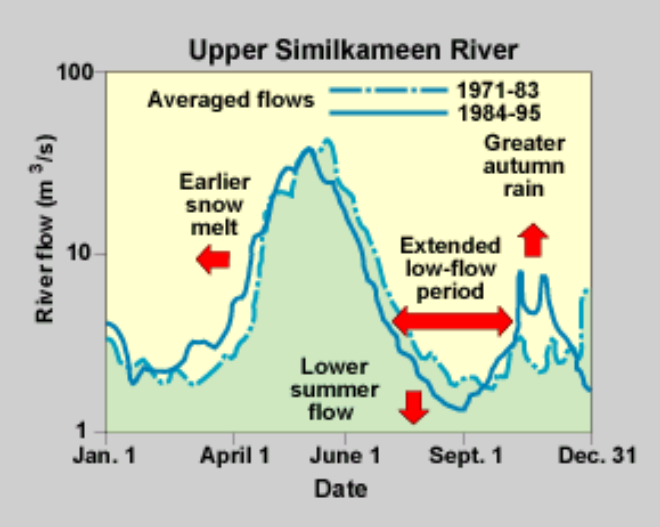

Figure 20 Observed hydrologic changes in BC southern interior rivers: example of Upper Similkameen River (Leith and Whitfield, 1998).

Nival and glacial streams in the southern interior of BC exhibited earlier freshet (peak flow due to snowmelt), an extended summer recession period, and lower flows during late summer and early fall (Leith and Whitfield, 1998). Among the rivers located in the same hydrologic region as the Kettle and Granby (e.g., Similkameen River, West Kettle River at McCulloch, Tulameen River at Princeton), currently the onset of snow-melt freshet (high runoff) occurs around mid April, the peak flow occurs around the end of May (Julian day 150), and the low flow period begins near the end of July, but in some rivers as late as mid-September. The observed hydrologic changes in Upper Similkameen River are shown in Figure 20. For other parts of Canada, the detected climatic and hydrologic changes have been variable for different ecozones. There were variable types of hydrograph shifts as each type of hydrologic system responded to observed variation in climate (Whitfield and Cannon, 2000).

- OBSERVED SHIFTS IN STREAMFLOW IN KETTLE AND GRANBY RIVERS

The observed changes in Kettle and Granby Rivers are presented using a polar plots. Two hydrometric stations on Kettle River were selected with the longest continuous flow records. The first station was at Ferry, WA (Figure 21), and the second was downstream of Grand Forks at Laurier, WA (Figure 22). One station on Granby River at Grand Forks was available (Figure 23). For each location, two consecutive decades of flow records were compared, from 1976-1985 to 1986-1995. The graphed time series represent mean discharge averaged for selected decade. For the purpose of graph clarity, each point represents average for 5 days.

A polar plot is used for visualizing changes in seasonal data, where time is a cyclical variable and the winter year boundary discontinuity is removed (Whitfield and Cannon, 2000). This graph type is read as follows:

- two data series (for different time periods) are plotted such that discharge increases outward from the inner ring toward the outer ring of the graph
- the area between the curves is shaded dark when the second curve (discharge at time period) is larger, light when the second curve is smaller; in other words, discharge increased between the two time periods where the area was shaded, and decreased where not shaded
- arrows indicate statistical significance of change in discharge where present

- added outside arc indicates shift in timing of peak flow
- discharge scale is indicated and applies along any radial line on graph

The Kettle River hydrographs at Ferry and Laurier are very similar in appearance, despite the difference in flow magnitudes. The observed streamflow changed significantly between the two decades, while the pattern and timing of changes were very similar in these two locations, and also on the Granby River, suggesting that the watershed of the Kettle River reacts similarly to climate change at different catchment scales. The most noticeable trend is of lower discharge in the latter decade for hydrograph months May to February. The largest decrease in flow occurred in the early fall months, establishing a new date for lowest river flows in mid-September (from previous lowest flow in January). The arrows on the graphs indicate that the decrease was statistically significant. In the spring from March to April, streamflow increased as a consequence of earlier snow melt under warmer climate. The peak flow date of the spring freshet shifted by approximately 10 days to an earlier date in May. The Granby River hydrographs displayed the same temporal shifts as those detected for the Kettle River, but there were minor differences due to different location and physiography of its catchment area.

Figure 21 Observed changes in streamflow on Kettle River near Ferry, WA. (Environment Canada, 2002).

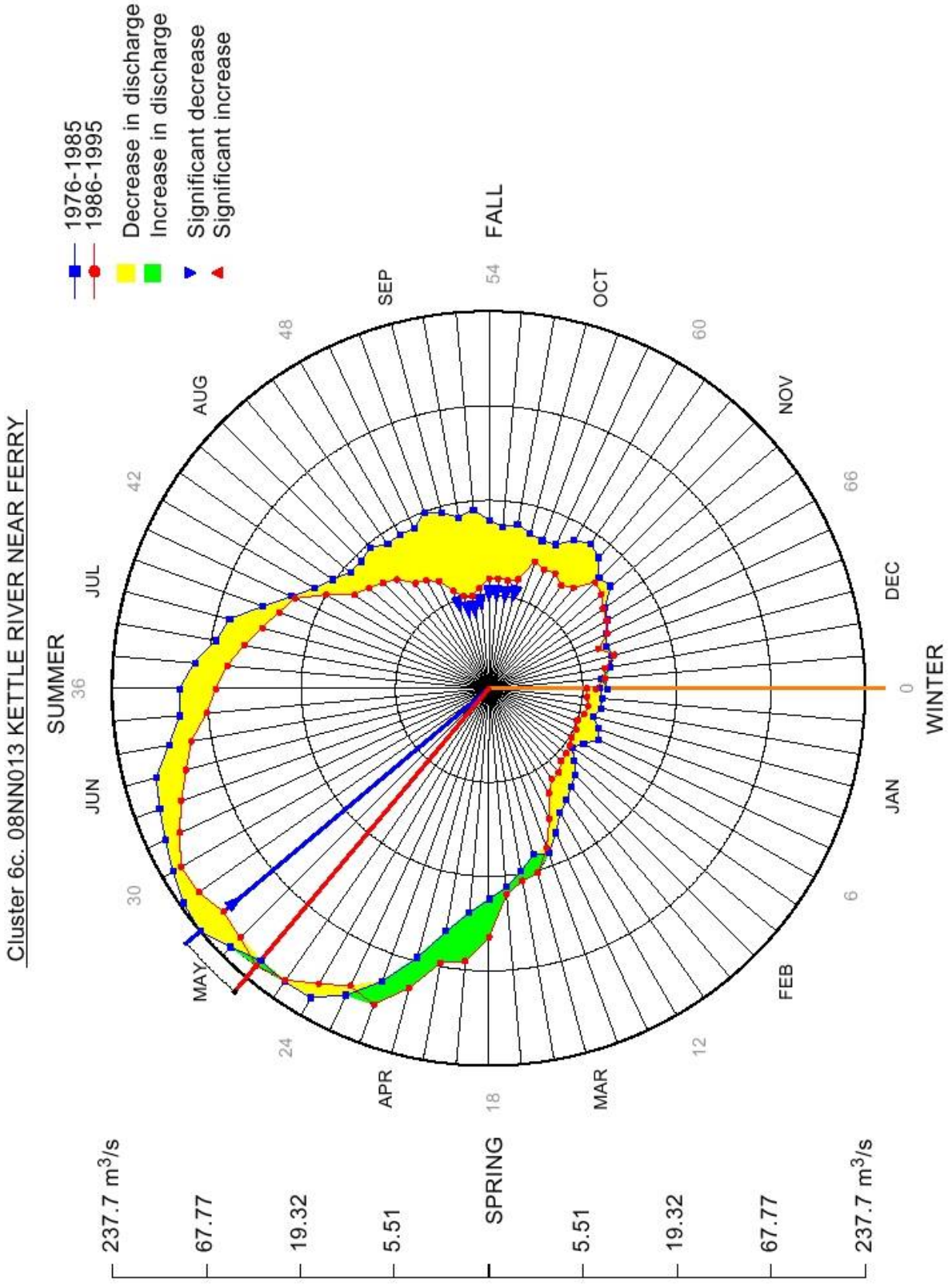

Figure 22 Observed changes in streamflow on Kettle River near Laurier, WA. (Environment Canada, 2002).

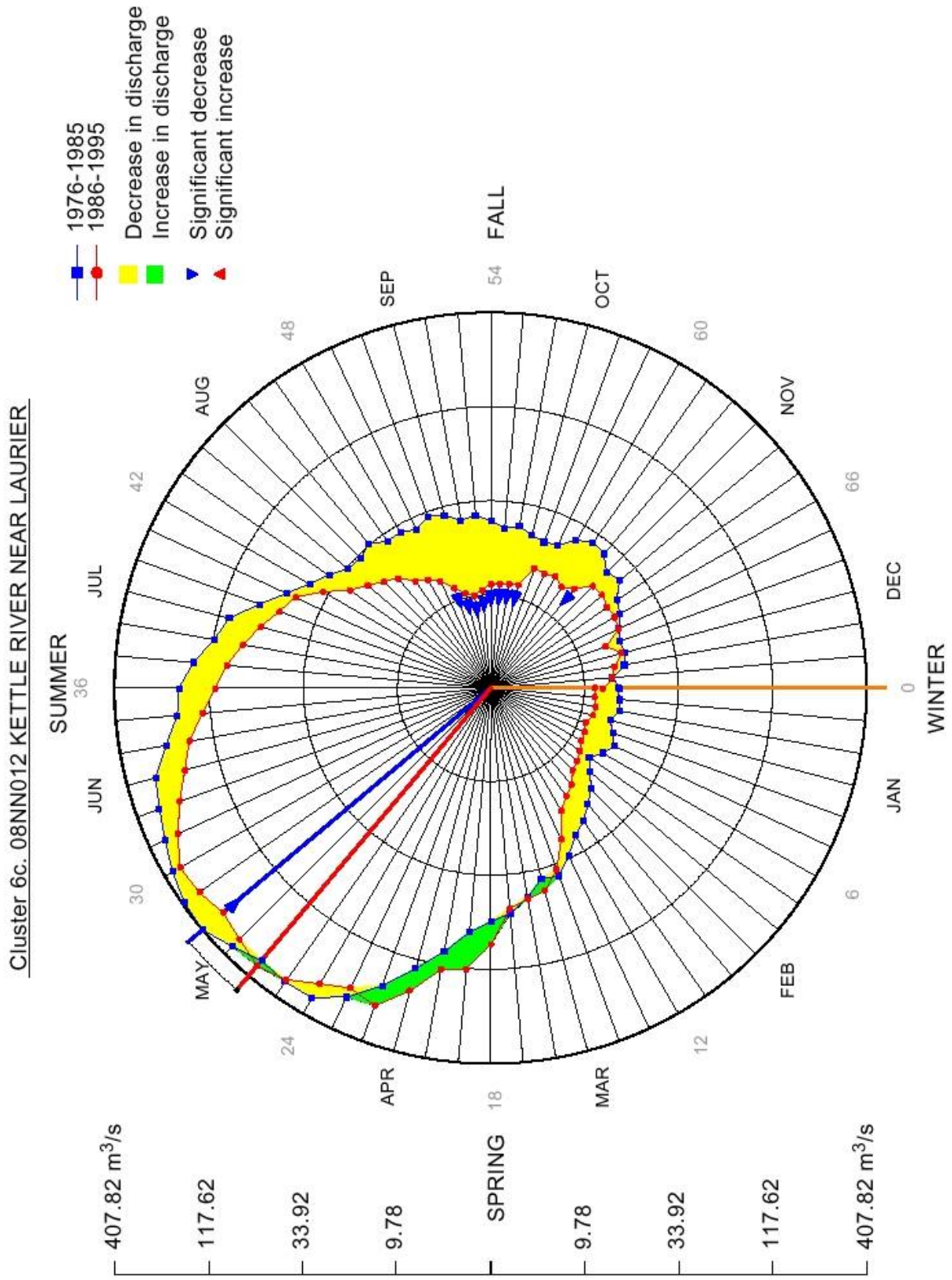

Figure 23 Observed changes in streamflow on Granby River at Grand Forks, BC. (Environment Canada, 2002).

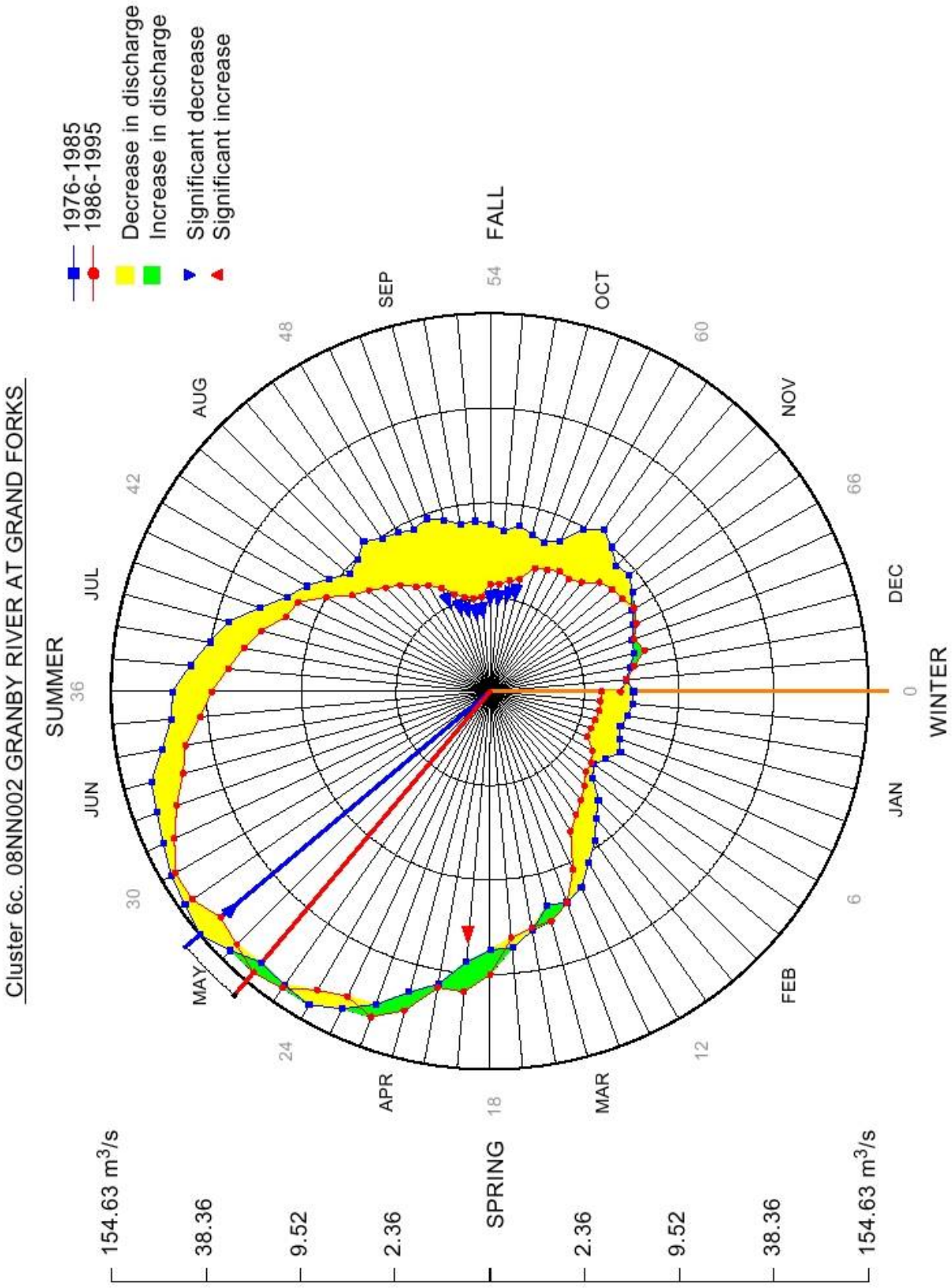

4.4.2. DOWNSCALING OF GLOBAL CLIMATE-CHANGE PREDICTIONS TO THE REGIONAL SCALE

For many climate change studies, scenarios of climate change derived directly from General Circulation Model (GCM) output are of insufficient spatial and temporal resolution. Spatial downscaling techniques are used to derive finer resolution climate information from coarser resolution GCM output, which have been designed to bridge the gap between the information that the climate modelling community can currently provide and that required by the impacts research community (Wilby and Wigley, 1997). The fundamental assumption behind all these methods is that the statistical relationships, which are calculated using observed data, will remain valid under future climate conditions.

Models for streamflow generation from watersheds can be calibrated to present conditions, and extrapolated to predict future conditions. An example of physically-based watershed model used with downscaled GCM output is the modeled streamflow in Georgia Basin study area on south coast of BC (Whitfield et al, 2002). Alternatively, empirical or statistical models relating hydroclimatic variables to streamflow can be developed and applied in a similar manner. The empirical models can be driven by observed climate variables, and impacts due to climate change can be estimated using inputs from GCM predictions. Empirical downscaling models form another approach, where local or regional-scale variables (e.g. streamflow) that are poorly described by coarse-resolution GCMs, are related to synoptic- or global-scale atmospheric fields (Landman et al., 2001).

A study by Cannon and Whitfield (2000) assessed whether the recent observed changes in streamflow conditions in British Columbia can be accurately predicted using an empirical downscaling approach. The results of that study suggest that a neural network empirical downscaling models are capable of predicting changes in streamflow observed during recent decades using only large-scale atmospheric conditions as model inputs. Beersma (2000) showed climate scenarios useful for hydrologic impacts assessment studies. Climate downscaling techniques are treated in more detail by Hewitson and Crane (1996). A review of applications of downscaling from GCM to hydrologic modeling can be found in Xu (1999).

4.4.3. MODEL APPLIED TO KETTLE RIVER BASIN

The National Center for Environmental Prediction (NCEP) maintains a Reanalysis Project database (Kalnay et al, 1996), which provides large-scale climate variables that can be used to define analogs with GCM for climate modeling purposes. Data from the NCEP/NCAR Reanalysis Project were extracted and used as historical analogs to make the climate-hydrology linkage. Climate data from the Canadian Global Coupled Model (CGCM1) (Flato et al., 2000) for the IPCC IS92a greenhouse gas plus aerosol (GHG+A) transient simulation were used to project results into the future.

The climate fields were defined on a 11 x 13 grid (~3.75-deg. x 3.75-deg.) over BC (30N-70N; 200E-250E). The meteorological data included:

1. 7-day sliding average of sea-level pressure, 500-hPa geopotential height, and 850-hPa specific humidity
2. 1-month sliding average of 500-hPa geopotential height and 850-hPa specific humidity
3. 4-month sliding average of 850-hPa specific humidity

The dimension of the large-scale climate dataset was further reduced using principal component analysis (PCA). A k-nearest neighbour analog model was used to link principal component scores (explained variance > 90%) of the climate fields with the maximum temperature, minimum temperature, and precipitation series (of NCEP dataset). The PCA linked the climate fields over BC and the eastern Pacific Ocean with daily discharge values for Kettle and Granby Rivers. The analog modelling approach has the advantage of simplicity and comparable results to other more complex models. It also offers a simple method for controlling model fit and the time structure of the simulated series. The end product is sets of daily discharge data at the three sites for the simulated 1962-2100 period:

- 08NN002 Granby River at Grand Forks, BC
- 08NN012 Kettle River near Laurier, WA, 20 km downstream of Grand Forks, BC
- 08NN013 Kettle River near Ferry, WA, 50 km upstream of Grand Froks, BC

4.4.4. DESCRIPTION OF RESULTS

Output from the model consists of GCM downscaled discharge values for the three analog models with 7, 14, and 24 nearest k neighbours. As the number of nearest k neighbours increases, the day-to-day variability should decrease (unfortunately this also leads to poorer predictions of the peak flows) (Figure 24). There are two sets of results that correspond to different scaling factors being applied to the data:

1) "*variance inflated*" data have been scaled so that the variance of the simulated discharge values for the 1962-2000 period matches the variance of the observed values (i.e. overall variability is preserved)

2) "*mean inflated*" data have been scaled so that the mean values match (i.e. volume is preserved).

There is no unique ideal solution, and the choice of scaling method depends on particular application of climate model results (Whitfield and Cannon, 2003).

Environment Canada (2002) provided statistical comparisons between long-term averages of smoothed discharge values (5-day averages) at each of the stations. All of these are from the mean inflated 24 nearest neighbour model. In the base case scenario, the graphs compare mean and median observed discharge to simulated streamflows for the 1971-2000 time period. Also included are results from a non-parametric Mann-Whitney test for differences in the median value between each 30-year period, following methodology of Leith and Whitfield (1998).

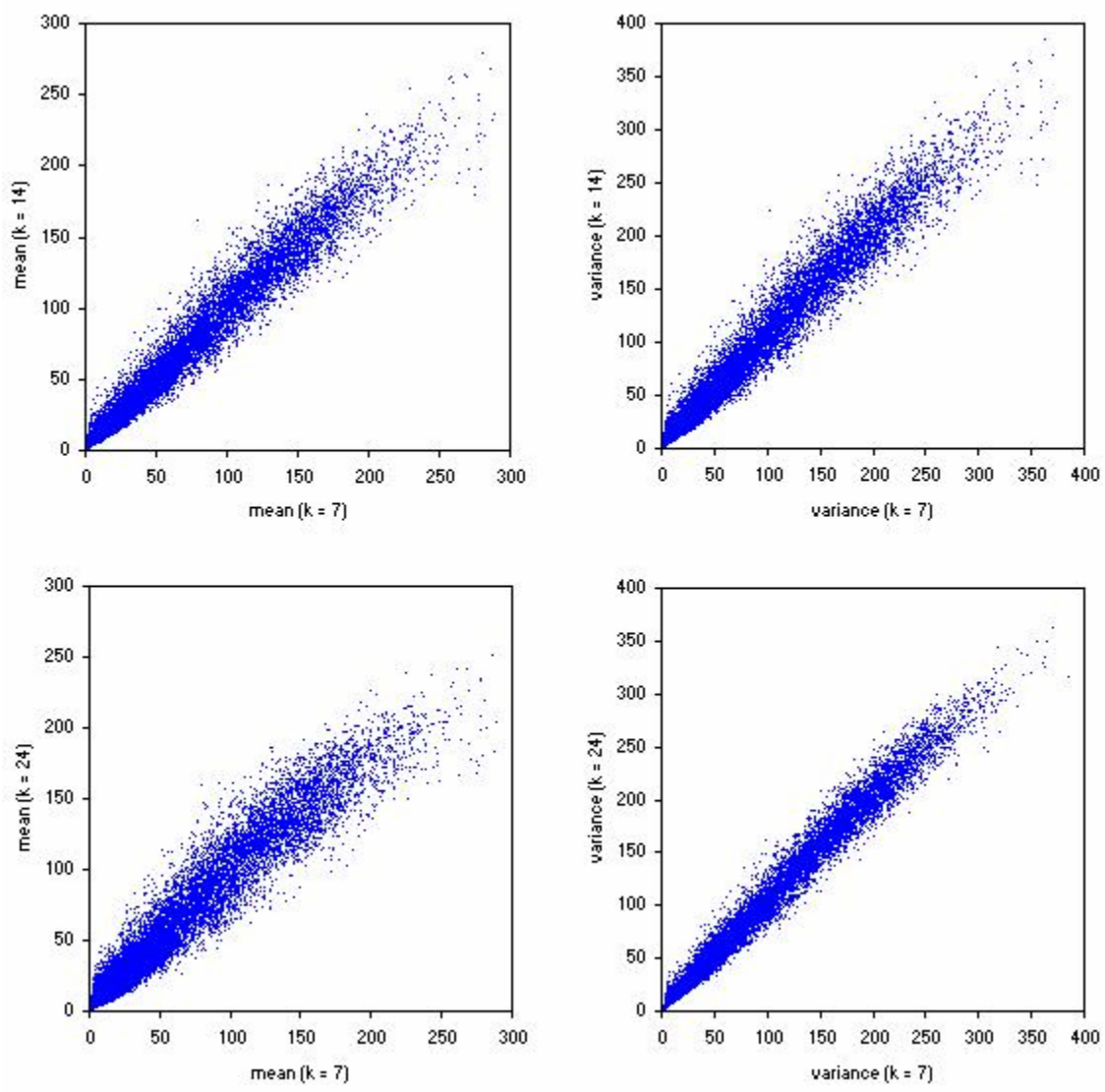

Figure 24 Comparing predicted Kettle River discharge variability between different analog models using k = 7, 14, and 24 nearest neighbours.

4.4.5. MODEL BIAS

The predictive power of hydrologic models depends in part on their ability to model present circumstances. The expected hydrologic changes as a response to higher temperatures were suggested to increase the ratio of rain to snow, accelerate the rate of spring snowmelt, reduce the duration of the snow on ground period, and enhance the spring freshet. To assess the performance of a downscaled GCM results, the modeled hydrographs were compared to observed hydrographs for discharge in Kettle River from 1971 to 2000 time period (Figure 25).

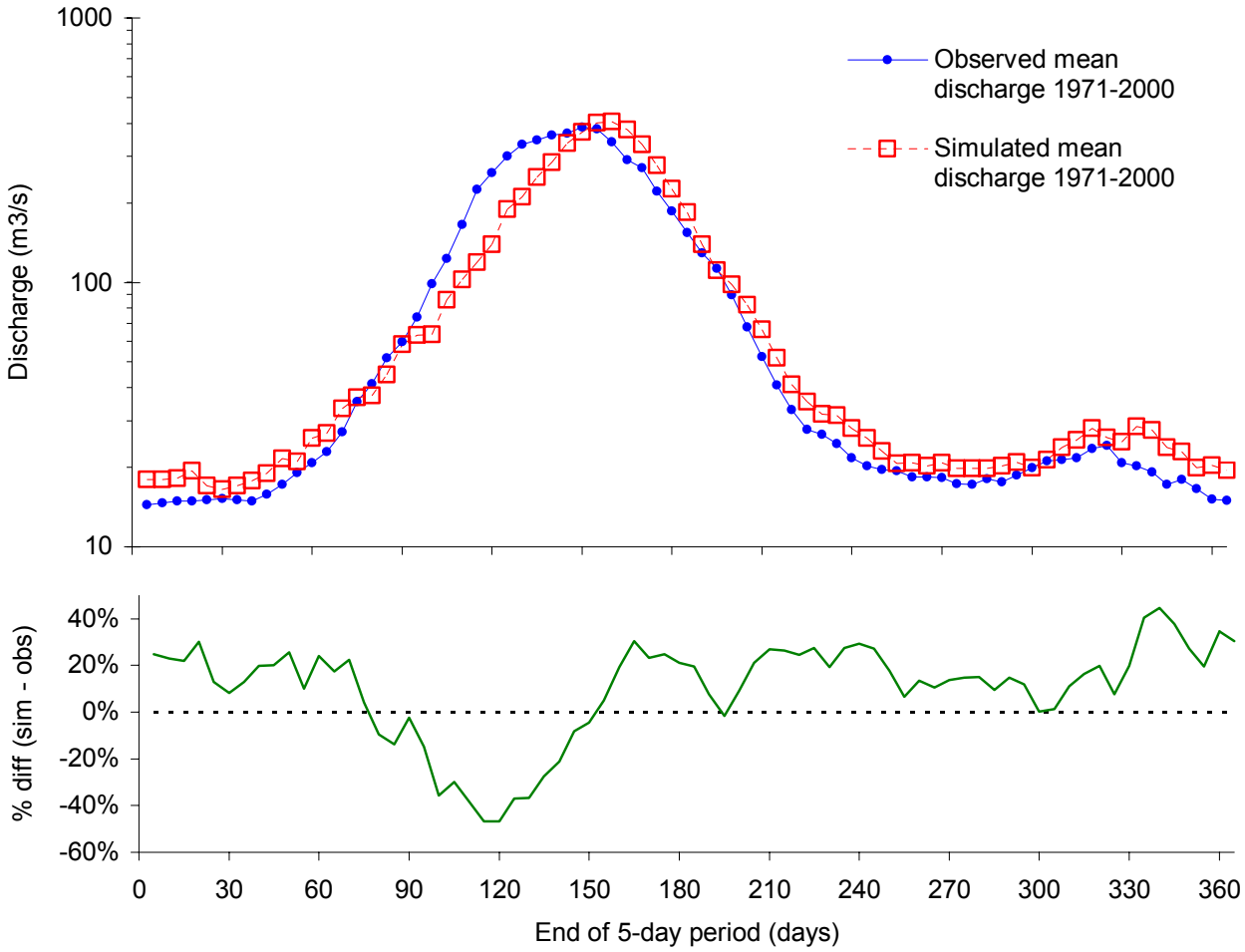

Figure 25 Kettle River near Laurier, WA (08NN012), comparing simulated long-term mean discharge (1971-2000) annual hydrographs generated by downscaled CGCM1 for the IPCC IS92a GHG+A transient simulation, with observed long term mean discharge (1971-2000). Model bias expressed as percent difference between simulated and observed discharge.

The GCM gives one possible realization of simulated climate given historic GHG and SST forcings, thus, the output is not a hindcast for the 1971-2000 period. Still, the poor fit between the downscaled and observed hydrograph for 1971-2000 can mostly be attributed to biases existing between the GCM simulated climate fields and the observed climate fields from the NCEP-NCAR Reanalysis. The downscaled CGCM1 data underestimated temperature in the late winter and early spring periods and overestimated temperature in the late fall and early winter periods. Consequently, the onset of freshet was delayed. A similar problem with delayed spring warming was noted for downscaled temperatures at stations in the Georgia Basin (Whitfield et al, 2002). In particular, Wilby et al. (1999) demonstrated that downscaled climate scenarios are sensitive to many factors, including the choice of predictor variables, downscaling domains, season definitions, mathematical transfer functions, calibration periods, elevation biases and others. Although the output may be adjusted, there is a tradeoff between discharge time series "smoothness" and accuracy of modeled peak flows. This was expected and may be inevitable given the state of GCMs at the moment (Whitfield and Cannon, 2003). The model bias is similar for all three hydrometric stations, but the model bias is greater for median discharges than for

mean discharges (Figure 26). Therefore, only mean hydrographs will be considered in future analyses.

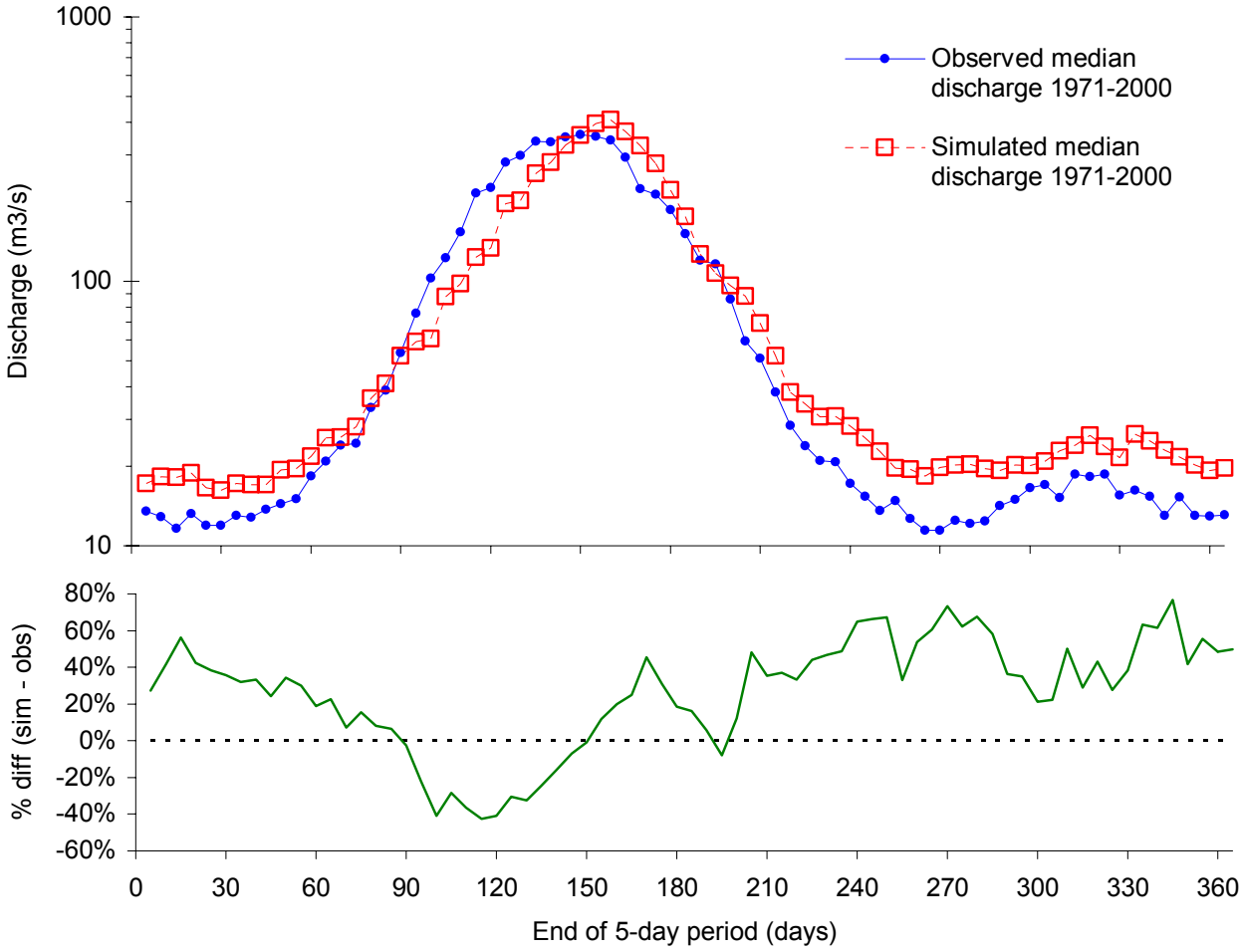

Figure 26 Kettle River near Laurier, WA (08NN012), comparing simulated long-term mean discharge (1971-2000) annual hydrographs generated by downscaled CGCM1 for the IPCC IS92a GHG+A transient simulation, with observed long term mean discharge (1971-2000). Model bias expressed as percent difference between simulated and observed discharge.

4.4.6. PREDICTED CHANGES IN HYDROGRAPHS OF KETTLE AND GRANBY RIVERS

The future-climate scenarios (time periods 2001-2030, 2031-2060, and 2061-2090) were compared to simulated 1971-2000. Scibek and Allen (2003) provide graphic output of each hydrograph (observed and simulated scenarios). Figure 27 and Figure 28 compare the key indicator results for the Kettle River (at Ferry) for observed and simulated scenarios.

Where the model bias is unacceptable, the downscaled results could be used as a basis for adjusting the observed historical hydrograph to match the simulated changes. However, such approach might be hard to justify, especially for the future scenarios. For the Georgia Basin study it was decided that the GCM bias would be explicitly shown, along with the resulting impact on the subsequent hydrologic simulations (Whitfield et al., 2002). The comparisons were then always between the unadjusted GCM-driven hydrologic simulations for future time periods and the unadjusted GCM-driven simulations for the baseline period.

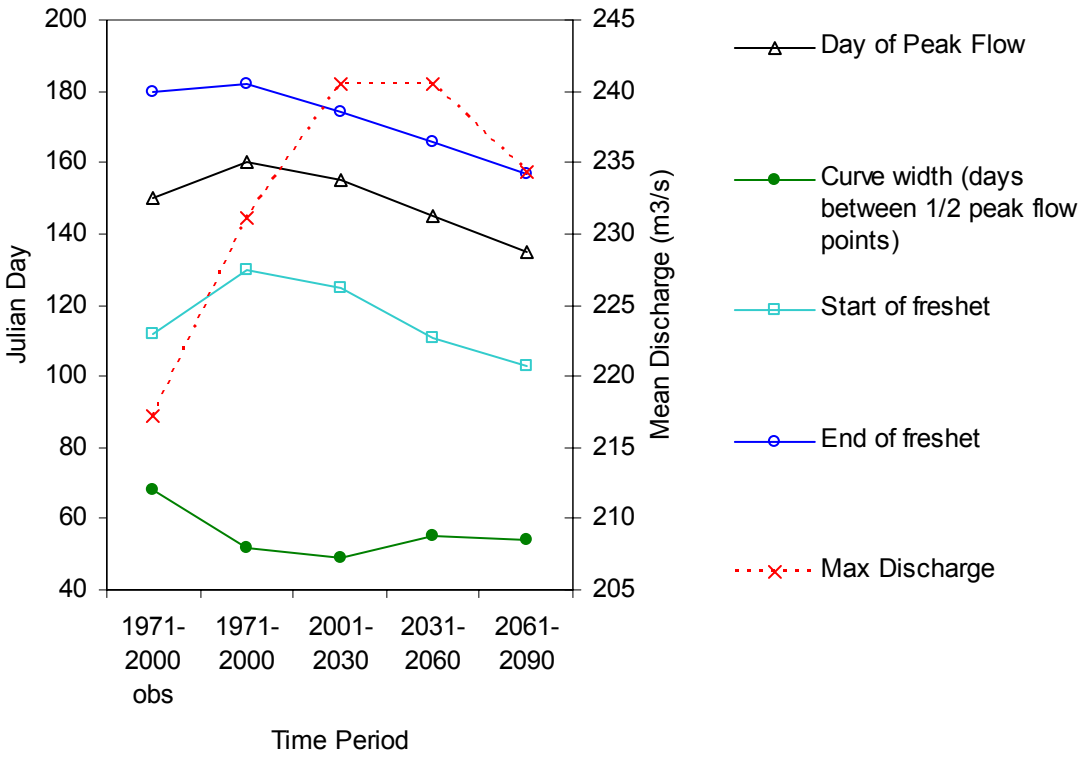

Figure 27 Kettle River near Ferry, WA (08NN013) Peak Flow and Timing of Freshet. Observed and modeled mean discharge from inflated k=24 nearest neighbour analog model for downscaled CGCM1 for the IPCC IS92a GHG+A transient simulation.

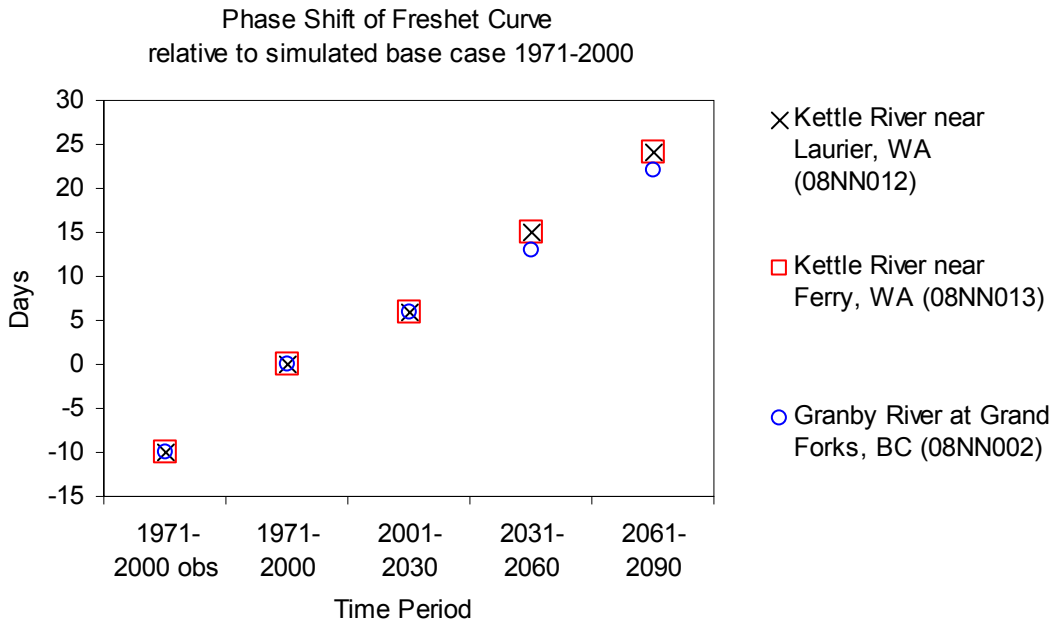

Figure 28 Comparing phase shift of peak flow on Kettle and Granby Rivers. Observed and modeled mean discharge from inflated k=24 nearest neighbour analog model for downscaled CGCM1 for the IPCC IS92a GHG+A transient simulation. The base case is the modeled discharge during time period 1971-2000.

5. RECHARGE MODELLING

5.1. RECHARGE AND NUMERICAL GROUNDWATER MODELS

Groundwater recharge is a very important boundary condition in numerical models, but site-specific recharge data are often not available or are difficult to estimate, thus recharge is used as a fitting parameter during model calibration (Anderson and Woessner, 1994). For example, the Waterloo Moraine model (Martin and Frind, 1998) used such a calibration protocol. Where precipitation records are available and are representative of aquifer area, an assumed fraction of precipitation is often used as an estimate of recharge (Brodie, 1999). The validity of assumptions of recharge rates becomes very important in small-scale transient models, where detailed groundwater flowpaths and levels are required (Jyrkama et al, 2002). For the purposes of climate change impacts modelling, the recharge rates must be as accurate as possible to accurately represent the small shift from present to future climatic conditions.

Groundwater recharge rates depend on climate, land use and cover, soil properties, surficial geology, and depth to water table. Recharge can be measured directly using soil permeameters and lysimeters, or using tracer methods, but the direct measurement methods are too expensive for large regional aquifers, and thus, were not used in the Grand Forks aquifer. An indirect method of estimating recharge is from catchment-scale water balance analysis where stream gauges are available.

The modelling of recharge in this study will consider heterogeneity of soils, surficial geology, depth to water table, and any precipitation and temperature trends over the aquifer area. Full transient behaviour of recharge will be considered. In essence, the approach will follow that of Jyrkama et al. (2002) and will use one-dimensional soil columns within the HELP hydrologic model (U.S. Environmental Protection Agency), before being imported into MODFLOW for groundwater flow modelling. Daily values are used as the basic time-averaged units. However, the groundwater model will receive monthly recharge inputs. The recharge is based on step-like climate scenarios, where in each scenario (“step”), the climate is the same and equivalent to that predicted by General Circulation Models (GCMs) / downscaled / stochastic-generated, and then recharge is averaged for the scenario by month. The GCMs ensure that physical processes are modeled spatially (on very coarse scale) and, more importantly, temporally. The downscaling ensures that processes and resulting values of variables are as close to site-specific as possible, while preserving the GCM predictions. The stochastic weather ensures that daily values of variables are realistic, consistent, site specific, and preserve both values and variability predicted to change from current to future climate scenarios by GCMs.

The recharge model (HELP model in this project) uses daily inputs of weather to calculate daily recharge through soil columns. Thus, appropriate frequency, magnitude and duration of precipitation and other events are modeled. Typically 30 or more years are modeled within each climate scenario, and then monthly averages are computed to represent monthly variations of recharge that are representative of the climate regime being modeled. Because the stochastic weather generator requires more than 100 years of daily weather to be created to begin approaching the statistics specified for climate scenario (and local weather), the recharge model will also receive that long time period of simulated weather, ensuring that the averages are representative. The length of the weather time series is not meant to model actual changing climate year-to-year, but rather to model climate change in a step-wise fashion for each scenario and to generate a long enough weather time series to preserve and properly represent statistical properties for the site and the predicted climate for the scenario.

The groundwater model will be “transient”, but only on monthly time steps due to computational limitations, although 10 day time steps could be modeled with some effort. Since most of the GCM summaries, downscaling tools, and stochastic weather generators are set-up for adjusting monthly statistics for daily weather, it makes sense to model transient groundwater flow also using monthly time steps. The actual groundwater flow model has more time steps, but inputs are modified and outputs generated on monthly time steps. Thus, monthly recharge is required as an input for each climate change scenario.

5.2. OVERVIEW OF RECHARGE MODELLING METHODOLOGY

Allen (2000) undertook a limited sensitivity analysis to determine the impact of changing several model parameters (including recharge and hydraulic properties) on the model calibration. This form of a sensitivity analysis is necessary for determining how sensitive the model is to the various input parameters, so that those model parameters that are poorly constrained by field data can be identified and evaluated as to their relative importance in the overall model calibration. This type of exercise essentially identifies the level of confidence for the model results. Sensitivity analysis can also be used to make predictions related to such factors as climate change, increased water usage, reduction in recharge area due to development, changes in land use, etc.

Allen (2001) used HELP within UNSAT Suite (Waterloo Hydrogeologic Inc.) to model recharge to the Grand Forks aquifer. HELP is typically used for designing landfills, and enables the modeller to generate estimates of recharge using both a weather-generator and the properties of the aquifer column. The weather generator and the model aquifer column provide aquifer recharge (infiltration) values using meteorological records for a 10 year period. A rough estimate of the annual water balance for Grand Forks (excluding pumping and irrigation return flow) was calculated using a sensitivity analysis approach. Results were 60% as evapotranspiration, 10% as runoff, and 28% as aquifer recharge (recharge equaling roughly 135 mm/year). The estimate of recharge from this recharge model was then used for modelling groundwater flow under steady state conditions. A uniform value was applied to the entire aquifer surface, except near the aquifer edge where addition recharge from runoff is anticipated. Allen (2001) also calculated the sensitivity of the water balance to different climate change scenarios. The highest and lowest recharge values were input into the steady-state groundwater flow model to determine the sensitivity of the groundwater regime to climate change.

However, recharge to the aquifer is significantly more complex than captured above. It varies spatially with topography and soil type, and it varies temporally with climate. Following the methodology developed and used for Grand Forks by Allen (2001) and Allen et al. (in press), and similarly used by Jyrkama et al. (2002), recharge to one-dimensional soil columns will be modeled prior to input into the numerical model (MODFLOW). Recharge modelling will consider heterogeneity of soils, surficial geology, depth to water table, and any precipitation and temperature trends over the aquifer area. High-resolution spatially-distributed recharge estimates will be generated using the HELP model (UnSat Suite software), and adjusted for aquifer thickness, material type, soil type, and representative hydraulic properties. These climate simulations will be calibrated to site-specific conditions using Environment Canada climate records, combined with parameters in the HELP model database. Full transient behaviour of recharge will be considered.

Weather generators (WG's) are used to produce synthetic series of given weather variables with desired stochastic structure. As a prerequisite to successful application of a recharge

simulation of one-dimensional soil and sediment columns, the weather generator must adequately reproduce the observed climatic conditions, in particular, rainfall and temperature. These parameters are site-specific, thus, in absence of site-specific data in the HELP model database, the nearest stations can be used as a basis for HELP model calibration, only if the resulting rainfall and temperature trends are very similar to those observed at the weather stations that represent the aquifer location.

Guenni (1994) named three reasons to develop a stochastic weather model: (i) to provide a means to extend historical weather records in time, (ii) to generate weather sequences in locations without historical information in order to evaluate the impact of weather variability on hydrological and water resource planning and ecological management at un-gauged locations, and (iii) to produce climate data that resemble actual and future climate conditions (climate change impact studies). Because the weather generator (WGEN) within HELP was found not to reproduce the observed climate, output from a newer weather generator (LARS-WG) was ultimately imported into HELP. The LARS-WG was calibrated to match the observed records, prior to modelling predicted recharge under climate change scenarios.

Geographic Information Systems (GIS) is increasingly used in spatially-distributed hydrologic and hydrogeologic modelling, especially for data preparation for groundwater flow models (Brodie, 1999). In recharge modelling, the GIS data-handling capabilities allow raster or vector computations that use soil properties from digital soil maps, adjustment of permeabilities using land cover maps, and inputs of spatially-distributed precipitation and evapotranspiration maps into recharge models (Fayer et al., 1996). Coupled hydrologic-hydrogeologic regional models also rely heavily on GIS (Xiao et al., 1996; Zhang et al., 1999). Most recently, York et al. (2002) reviewed existing methods for recharge modelling as inputs for transient groundwater models, and used the HELP model together with GIS-based soil and landuse maps to calculate recharge over regional heterogeneous aquifer in New Jersey.

5.3. SOURCES OF CLIMATE DATA

The historical weather data included average daily observations, monthly summaries, and annual summaries. Initially, station information was explored for sources of long term records at weather stations close to Grand Forks to determine the most useful and representative weather station(s) for the purpose of climate scenario modelling. Canadian data come from Environment Canada (2003), mostly from web-accessed summaries, weather station maps, and even daily data. Most of the daily data were obtained prior to 2003 from Environment Canada (personal communication, Paul Whitfield and Alex Gunn). Daily weather records for the POR 1961-2000 were used for climatic downscaling and weather generation for recharge models. Several US weather stations were also explored (Western Climate Center, 2002), to determine if there is a significant precipitation gradient near that aquifer; none was observed. A summary of weather stations, locations, elevations, available weather records and duration of records are listed in Table 13. The Grand Forks weather station (1133270) was selected.

Data from Environment Canada were contained in a custom database system, which extracts daily listings for precipitation and temperature in CCC (Canadian Climate Centre), fixed width text format. The CCC files were converted using Visual Basic code to continuous time series readable by Access, Excel, and other programs. US data came in text format that was easier to import and read than the CCC files. It was downloaded from web sites of the Western Climate Centre. Solar radiation was estimated from Carlson et al. (2002), NASA remotely sensed values, and from CRCM monthly predictions (CICS, 2003).

For climate change scenarios, the sources of data were primarily the Canadian Institute for Climate Studies (CICS, 2003) for all CRCM and CGCM1 scenarios (note: the acronyms and models were explained in section 3.0). We also had access to daily CGCM1 data for precipitation from Zwiers (2001) and CICS (2003) for calibration of SDSM downscaling tool. Daily outputs of CRCM were not available to this project although these exist. Also from CICS were links for the downscaling software, SDSM, and a stochastic weather generator, LARS-WG (discussed later).

Grand Forks Area (Climate and Weather Stations)

ID	Station	Description	P	T	ET		SR		From	To	Lat	Long	Elev. (m)
1133270	Grand Forks, BC		@	@					1941	present	49° 02'	118° 28'	532
1133275	Grand Forks, BC	Rayfield	@	✔					1987	1990	49° 01'	118° 28'	523
454549	Laurier, WA		✔	✔					1948	1986	49° 00'	118° 14'	500
455946	Northport, WA		✔	✔					1920	present	48° 55'	117° 47'	402
1141455	Castlegar, BC	Airport	✔	✔	✔	E			1973	present	49° 18'	117° 38'	495
1141457	Summerland, BC	CDA	✔	✔	✔	PN	✔	M	1917	present	49° 34'	117° 38'	455
457938	Spokane, WA	WSO Airport	✔	✔	✔	PN	✔	E	1890	present	47° 38'	117° 32'	719

P = precipitation **T** = air temperature **ET** = evapotranspiration **SR** = solar radiation

✔ complete or nearly complete

@ some missing data

E estimated ET from Penman-Monteith formula

PN measured PAN evapotranspiration

M measured solar radiation

E estimated solar radiation

Table 13 Climate and weather stations near Grand Forks, BC: selection of stations with long periods of record, availability of evapotranspiration or solar radiation data, or proximity to aquifer locations.

5.4. DOWNSCALING OF CGCM1 PREDICTIONS

As discussed in Section 3.0, GCMs have coarse spatial resolution, and therefore, these atmospheric models are unable to resolve important small scale effects (smaller than GCM grids), such as clouds and topography, which strongly determine the local weather at a site. For example, precipitation data from GCM output has low variability in output values, and is never zero, because the precipitation averages the whole 50000 km^2 grid cell. In contrast, at local ground sites precipitation occurs in discrete events, separated by periods of dry weather. Furthermore, local topography and land cover also contribute to determining precipitation intensities and amounts. Even the higher resolution RCM models do not account for these effects adequately. Downscaling methods attempt to derive local weather from GCM and regional scale predictor variables.

In this section, two downscaling methods are described: Statistical DownScaling Model (SDSM) and the principal-component k-nearest neighbour method (PCA k-nn), which is used by Environment Canada. A comparison of these two downscaling methods was undertaken to generate observed data.

5.4.1. STATISTICAL DOWNSCALING MODEL (SDSM)

The CICS Statistical DownScaling Model (SDSM), described in Wilby et al. (2002) and the SDSM manual, is a decision support tool for assessing local climate change impacts using a robust statistical downscaling technique for specific sites. The software performs predictor variable pre-screening, model calibration, basic testing, statistical analyses and graphic of climate data. SDSM version 2.3.3. (8 May, 2003) was used in this study. SDSM requires large-scale predictor variable information in order to derive relationships between the large-scale and local climate. These relationships are developed using observed weather data. GCM-derived predictors are then used to drive these relationships, and thus, obtain downscaled information for the site in question for a number of future time periods. Predictor variable information is supplied here for use with SDSM. In order to operate SDSM all that a user is required to supply is the daily predictand, i.e., station, data for the climate variable in question (CICS, 2003). The predicand variable is daily precipitation at Grand Forks. The goal is to generate precipitation time series for future climates and compare to a base case climate, thus enabling the estimate of change in precipitation variability and amounts.

There are several limitations of SDSM. Daily precipitation amounts at individual stations continue to be the most problematic variable to downscale, and research is ongoing. This arises because of low predictability of daily precipitation amounts at local scales by regional forcing factors used in regression-based models such as SDSM for downscaling (SDSM manual). The unexplained behaviour is currently modelled stochastically within SDSM by artificially inflating the variance of the downscaled precipitation series to fit with daily observations. The model must be tested independently with a subset of daily precipitation data not used in model calibration. Also, to evaluate the uncertainties, multiple GCM model runs should be used.

Five data sets were downloaded from CICS website (listed and described in Table 14) for a grid location nearest to Grand Forks (Y=11 Latitude: 50.09°N and X=16 Longitude: 120°W – Grand Forks is at 49.1N and 118.2W). The Calibration data set contains observed daily data for 1961-2000, derived from the NCEP Re-analysis data set (National Centre for Environmental Prediction) (Kalnay et al., 1996) for the period 1961-2000. Most climate modelling experiments in North America use the NCEP datasets for calibration of downscaling models. There were four CGCM1 scenarios, each with data for a number of potential predictor variables. The NCEP dataset includes relative humidity, whereas CGCM1 datasets do not, so specific humidity was used when calibrating the model. The “current climate” scenario was generated by CGCM1 for the period 1961-2000. This was the first greenhouse gas + sulphate aerosol (GHG+A1) experiment undertaken with the CGCM1 global climate model (Boer et al., 2000). The subsequent “future climate” experiments using CGCM1 with GHG+A1 were for 2020s, 2050s, and 2070s.

Table 14 Data sets for SDSM downscaling scenarios (CICS, 2003)

Dataset	Years	Description
Calibration	1961-2000	Observed daily data derived from the NCEP Re-analysis data set (National Centre for Environmental Prediction (Kalnay et al., 1996) for the period 1961-2000.
CGCM1_Current	1961-2000	Daily output from the first greenhouse gas + sulphate aerosol experiment undertaken with the CGCM1 global climate model (Boer et al., 2000) for the period 1961-2000.
CGCM1_2020s	2010-2039	Daily output from the CGCM1 GHG+A1 experiment for the period 2010-2039.
CGCM1_2050s	2040-2069	Daily output from the CGCM1 GHG+A1 experiment for the period 2040-2069.
CGCM1_2080s	2070-2099	Daily output from the CGCM1 GHG+A1 experiment for the period 2070-2099.

Once all input data files were prepared for SDSM, the analysis began. The general steps in the downscaling using SDSM are:

1) Quality Control and data transformation
2) Selection of downscaling predictor variables
3) Model Calibration using selected predictor variables
4) Generation of weather scenario (20 ensemble runs)
5) Analysis of observed and downscaled data
6) Generation of climate change scenarios
7) Analysis of scenario results and comparison to observed

- DATA QUALITY AND TRANSFORMATIONS

During quality control, all file formats are verified, missing data counted and length of time series checked against start and end dates and number of days in a year. Year length and standard start dates were adjusted depending on CGCM1 scenario (as described in CICS, 2002). All predictors, with the exception of wind direction, have been normalized with respect to the 1961-1990 mean and standard deviation (CICS, 2002). The settings shown in Table 15 were used in SDSM (derived through calibration); at higher variance inflations and bias corrections the SDSM gave too high values for December precipitation. Incidentally, the same values were used in SDSM manual for sample model runs. Details concerning quality analysis summaries and types of transformations on daily data are provided in Scibek and Allen (2004).

Table 15 Data quality and transformations in SDSM for precipitation and temperature.

	Precipitation	Temperature
Interval	daily	daily
Transformation	4th root	-
Variance inflation	15	9
Bias correction	0.80	0.95
Event threshold	0	-
Number of days	14236	14233
Missing	375	378

- SELECTION OF PREDICTOR VARIABLES

Selecting the appropriate downscaling predictor variables is the most critical part of this whole process. There are 26 predictor variables for SDSM use provided by CICS; which are meteorological variables generated from CGCM1 model runs for the grid square (listed in Table 16). Multiple regression with the predicant variable (e.g., precipitation at Grand Forks) are run, a correlation matrix produced, and several of the predictor variables that are the most correlated with the predicant (and are statistically significant, low p-value, $p < 0.05$) are selected – this is done by monthly basis. The type of "process" (unconditional for temperature, and conditional for precipitation – where amounts depend on wet-day occurrence) is selected. Different variables were selected for modelling precipitation and temperature, which is expected because of different atmospheric forcings on P and T, and different correlations with synoptic conditions, and thus, CGCM1 variables.

- MODEL CALIBRATION (PRECIPITATION AND TEMPERATURE)

The results of predictor variable screening and selected best predictors for precipitation and temperature are provided in Table 16. The associated partial correlation coefficients and p-values monthly for predictor variables for precipitation and temperature are provided elsewhere (Scibek and Allen, 2004). These are the downscaling calibration results from CGCM1 using SDSM.

It should be noted that at Grand Forks, the local climate and especially valley-mountain-rain-shadow effects have strong influence on local precipitation, which is not modeled very well in regional CGCM1 grid cell. Seasonal precipitation trends were observed to be similar to regional CGCM1 predictions, but this relation breaks down somewhat on monthly time scales. Seasonal values mean more averaging-out of local weather effects and producing less meaningful regional trends.

Temperature was downscaled from CGCM1 using mean temperature predictor variable and few other supporting variables that increased the prediction through their partial correlation with observed temperature. Note that the mean temperature variable in CGCM1 is regional and is an average of the large model grid cell. Nevertheless, this is much an improvement over precipitation because CGCM1 does not model precipitation directly (at least not in the dataset provided by CICS for downscaling).

Table 16 Predictor variables for SDSM downscaling, generated from CGCM1 model runs.

Variable Name	Description	Precipitation	Temperature
Temp	Mean temperature		✔
Mslp	Mean sea level pressure	✔	
p500	500 hPa geopotential height		
p850	850 hPa geopotential height		
Rhum	Near surface relative humidity		
Shum	Near surface specific humidity	✔	
s500	Specific humidity at 500 hPa height	✔	
s850	Specific humidity at 850 hPa height		
**_f	Geostrophic airflow velocity		
p5_z	Vorticity (at 500 hPa height)		
**_z	Vorticity		
p_u	Zonal velocity component (near surface)		✔
p5_u	Zonal velocity component (at 500 hPa height)		
p_v	Meridional velocity component (near surface)		
p5_v	Meridional velocity component (at 500 hPa height)	✔	✔
p8_u	Zonal velocity component (near surface)		
p8_v	Meridional velocity component (near surface)		
**th	Wind direction		
p_zh	Divergence		✔
**zh	Divergence		

** indicates variables p_ = near surface, p5_ = at 500 hPa height, or p8_ = at 850 hPa height

- GENERATION OF WEATHER SCENARIO

Four scenarios were generated using the calibrated model: current climate, 2020's climate, 2050's climate, and 2080's climate. Predictor daily data sets were automatically selected from the corresponding CGCM1 outputs in SDSM, as defined during variable screening process. Daily data sets were generated for each scenario. All results were analyzed in SDSM, and appropriate monthly statistics were generated. For precipitation these were: mean, median, max, variance, dry and wet spell length, and % wet days. Note that minimum precipitation is always zero so it was not analyzed. For temperature the statistics were: mean, median, min, max, variance, and inter-quartile range. After each scenario run, the statistics were compared in SDSM using graphs to observed datasets.

- ANALYSIS OF OBSERVED AND DOWNSCALED DATA

The daily precipitation time series were analyzed using conditional option, thus only WET days were taken into account. For the purpose of graphical displays, and later for inputs to the stochastic weather generator, the mean daily precipitation was converted to mean monthly precipitation, and then converted to mean monthly precipitation for all days in the month by multiplying by % of wet days in a month. Thus, the shown precipitation monthly means are

comparable to observed normals, which are generally calculated based on the entire month (i.e. not only on wet days). For each month:

[Mean Monthly Ppt WET] **=** [Mean Daily Ppt WET] **x** [Number of Days in Month]
[Mean Monthly Ppt ALL] **=** [Mean Monthly Ppt WET] **x** [% Wet Days in Month]

where ALL refers to all days in month, WET refers to only days with Ppt > 0 in a month.

The resulting statistics and daily output were imported to a pre-programmed spreadsheet, which computes monthly total precipitation values (from mean daily values for each month), coverts to WET and DRY precipitation averages for comparing to observed, graphs all results by variable and month (grouped by SDSM outputs and compares to "PCA k-nn outputs" – see next section), computes % error for calibration bias, and model bias to observed. It also includes custom codes for exporting and file formatting of SDSM results to LARS-WG format for subsequent stochastic weather generation.

5.4.2. PCA K-NN METHOD OF DOWNSCALING (FROM ENVIRONMENT CANADA)

An second downscaled data set was provided by Whitfield (personal communication, 2002), based on precipitation and temperature downscaling methodology used for the Georgia Basin Study by Whitfield et al. (2002). The downscaled daily precipitation time series was computed for Grand Forks for the time period 1961 to 2099, from which "scenario" data sets were extracted to compare with other results.

The details and most references for the methodology are provided in Whitfield et al. (2002). In essence, future temperature and precipitation conditions at the stations were estimated using analog downscaling models (Barnett and Preisendorfer, 1978), forced by atmospheric circulation fields from a CGCM. Large-scale climate variables used to define analogs with CGCM variables were taken from the NCAR/NCEP reanalysis model database (Kalnay et al., 1996). To help speed the downscaling process and to remove redundant variables, the dimension of the large-scale climate dataset was further reduced using principal component analysis (PCA). Time-series of variables at each grid-point were first standardized to have zero mean and unit standard deviation over the 1971-1995 period (note: in SDSM, the calibration and scenario data were also standardized). A *k*-nearest neighbour (*k*-nn) model was used to link principal component scores of the climate fields with the maximum temperature, minimum temperature, and precipitation series from Danard and Galbraith's (1997) dataset. In the *k*-nn model, predictions are made by selecting the *k* days from the historical dataset that most closely resemble the current day's climate conditions. Prior to comparison, modelled temperature series were rescaled so that the modelled and observed means and standard deviations were equal (Huth et al., 2001). For precipitation, model outputs were inflated by multiplying by the ratio of the observed and predicted means. This preserves total precipitation amounts, but leads to a slight underestimation of precipitation variance. Hereafter, the Whitfield et al. (2002) method for downscaled precipitation time series is referred to as principal-component k-nearest neighbour method (PCA k-nn).

5.5. DOWNSCALING RESULTS AND CGCM1 PREDICTED CLIMATE SCENARIOS: PRECIPITATON

Precipitation time series were analyzed for the following variables:

1) mean monthly precipitation
2) standard deviation in daily precipitation
3) wet days %
4) dry series length
5) wet series length

Precipitation downscaling output are provided elsewhere (Scibek and Allen, 2004). The following section provides a summary of these results.

5.5.1. ABSOLUTE CHANGE GRAPHS AND MODEL CALIBRATION GRAPHS

The results are arranged by variable, thus giving 5 sets of "grouped" graphs (one set or variable per page). For each variable, there are two figures. One figure has two graphs comparing results for the two downscaling methods (SDSM and PCA k-nn). The second figure, placed lower, compares the observed variable values to those modeled, and presents two smaller graphs of model performance: 1) calibration bias of NCEP dataset to observed, and 2) base case scenario bias of current climate CGCM1 downscaled results to observed, all for the same time period 1961-2000.

The graph sets are colour-coded and are arranged identically for easy inter comparison between different variables. All graphs show monthly statistics (on x-axes). The mean precipitation and other variables are graphed as monthly time series on the y-axes. The observed data are always graphed as background fill (area graph), while the downscaled results are line graphs, superimposed on observed data graph. The styles and colours of line graphs are always the same for each climate scenario (e.g. 2010-2039) on all graphs. The model bias graphs are also colour coded and scaled similarly for easy inter comparison. The graphs should be examined carefully, because the downscaled climate change scenarios are the main reason for this whole endeavor of recharge modelling and groundwater flow modelling in Grand Forks aquifer.

Before looking at predicted changes in precipitation and temperature, it is important to examine the calibration results, and keep in mind the limitations and any model bias. Therefore, these are discussed first.

- MEAN MONTHLY PRECIPITATION

On a first examination of the monthly graphs (Figure 29), the CGCM1-predicted and downscaled with SDSM precipitation series are too low in the late spring to summer months, especially June, but fit the observed normals reasonably well in other months. This is surprising because the SDSM model was well-calibrated for monthly precipitation means, and calibration bias from NCEP dataset to observed was less than a 10% difference for most months (Figure 30). The problem lies in inability of CGCM1 to adequately model precipitation for Grand Forks, especially in the summer months, giving up to 40% underestimate of rainfall compared to observed, even after downscaling with a well-calibrated model (Figure 30). These are fundamental limitations of CGCM1 predictions and will be referred to as "model bias", where model is the general circulation model.

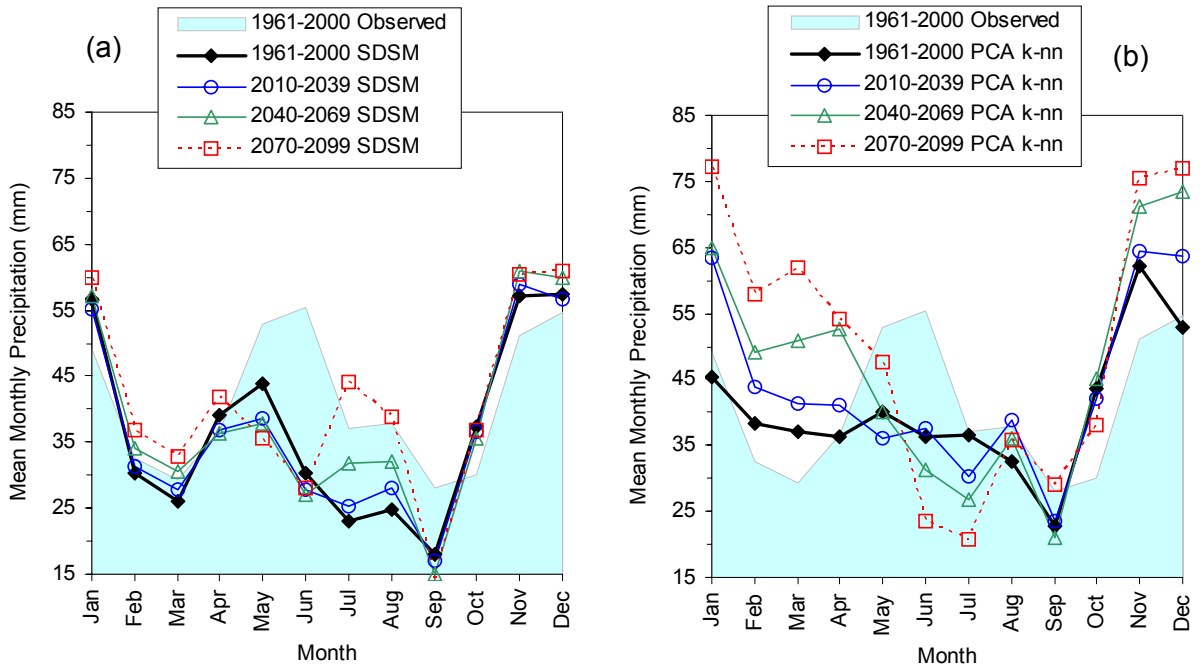

Figure 29 Mean monthly precipitation at Grand Forks, BC: observed and downscaled from CGCM1 model runs for current and future climate scenarios using two downscaling methods: (a) SDSM, (b) PCA k-nn.

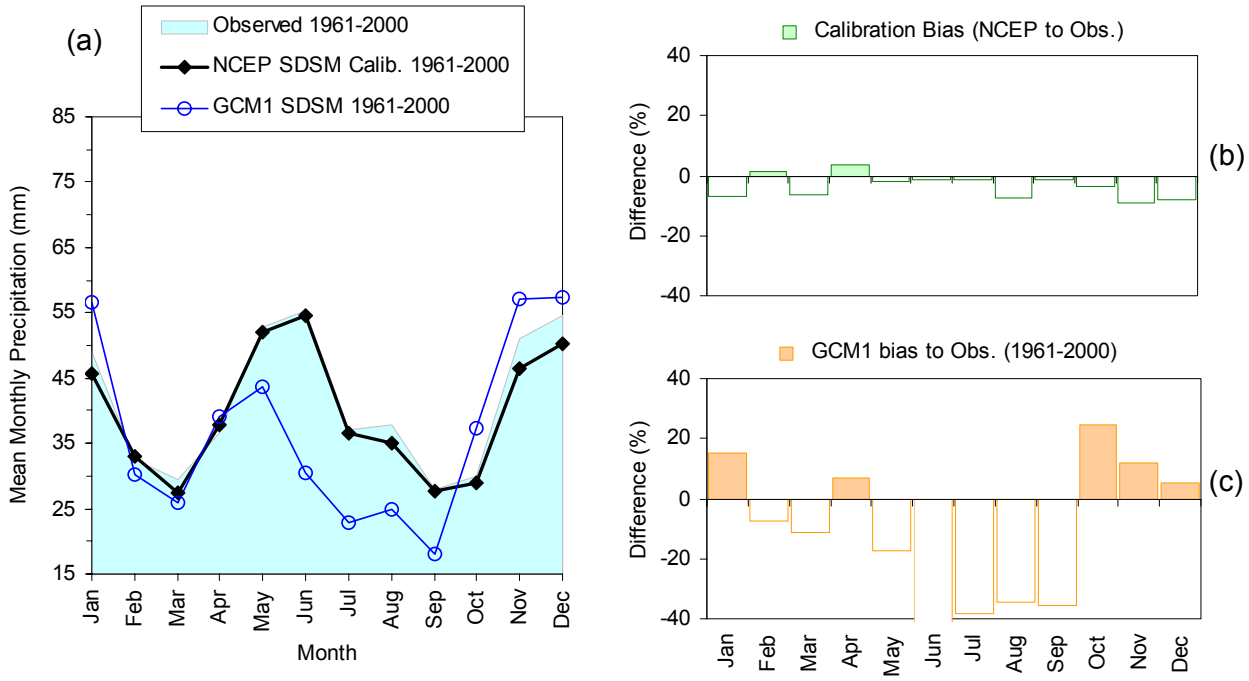

Figure 30 Comparing observed and downscaled precipitation at Grand Forks, BC. SDSM downscaling model performance: (a) monthly precipitation, (b) calibration bias, (c) bias between SDSM downscaled CGCM1 Current precipitation and observed.

The PCA k-nn downscaling (Environment Canada, 2003) of the same dataset for the same location arguably gave worse results than SDSM downscaling, thus the calibration error would be much greater for most months than SDSM. The only exception is late summer when PCA k-nn performed better, in terms of fitting to observed data, than SDSM model. Furthermore, the temporal changes of precipitation are contradictory between the two downscaling methods for some seasons. For example, SDSM model "translated" the CGCM1 results to show that at Grand Forks, from present to 2080s, there will be progressive increase in precipitation in late winter, a decrease in spring, large increase in summer, no change in autumn, and small increase in late autumn to early winter. In contrast, the PCA k-nn results show very large increase in precipitation from autumn through spring and large decrease in early summer, but increase in August (only). Visually, the PCA k-nn results are less calibrated than SDSM and are more chaotic in their predictions.

- PRECIPITATION VARIABILITY

The SDSM model calculated the variance of daily precipitation, which was converted to standard deviation (stdev = sqrt (variance)) because the LARS-WG requires standard deviation of precipitation as input for climate scenario modelling. Precipitation variability refers to distribution of precipitation daily values. The distribution is typically logarithmic and definitely not "normal" in shape. The variance and standard deviation statistics are for such a highly skewed distribution. When variance in precipitation changes, the relative frequencies of small precipitation events and compared to larger ones also change. This is the meaning of precipitation variance in this case.

The figures and results are arranged similarly to monthly precipitation amounts. The monthly precipitation variability, as estimated by standard deviation of daily values in the time series is shown for both models in Figure 31 and Figure 32. The SDSM results again fit better the observed precipitation variability than PCA k-nn results. The predictions are also very different among the two methods of downscaling. SDSM suggests small changes in precipitation variability into the future, while PCA k-nn suggests very large changes. The SDSM model was relatively well calibrated to NCEP data, with slight overestimation of variability in spring and late autumn months. Surprisingly, the downscaled variability if precipitation is very similar to observed, supporting the results of SDSM.

- WET DAYS, DRY SPELLS AND WET SPELLS

Monthly % of wet days suggests how often it rains in that month. It is an indirect measure of both frequency and duration of precipitation events, but does not indicate precipitation amount. As such indicator, it was downscaled and graphed as monthly averages in Figure 33 and 34. Both downscaling methods performed similarly well. The SDSM model was very well calibrated to NCEP data set. Summer months were underestimated in % wet days compared to observed, and other months were usually overestimated.

The dry spell length was a difficult variable to downscale using the available predicant variables. The downscaled model in SDSM had on average -30% difference to NCEP dataset (not terrible, but much worse than for previously discussed variables). The monthly trends of DRY spell length were similar to observed, but usually 30% lower in most months except June and July. The PCA k-nn downscaling gave similar results to SDSM, or even slightly better than SDSM (Figure 35 and 36). WET spell lengths were downscaled to similar results in SDSM and PCA k-nn algorithms. Both underestimate seriously the length of WET spells of actual. SDSM performed well for winter months, better than PCA k-nn, but equally poorly or worse in other months. Calibration bias for SDSM was about -30% for most months (Figure 37 and 38).

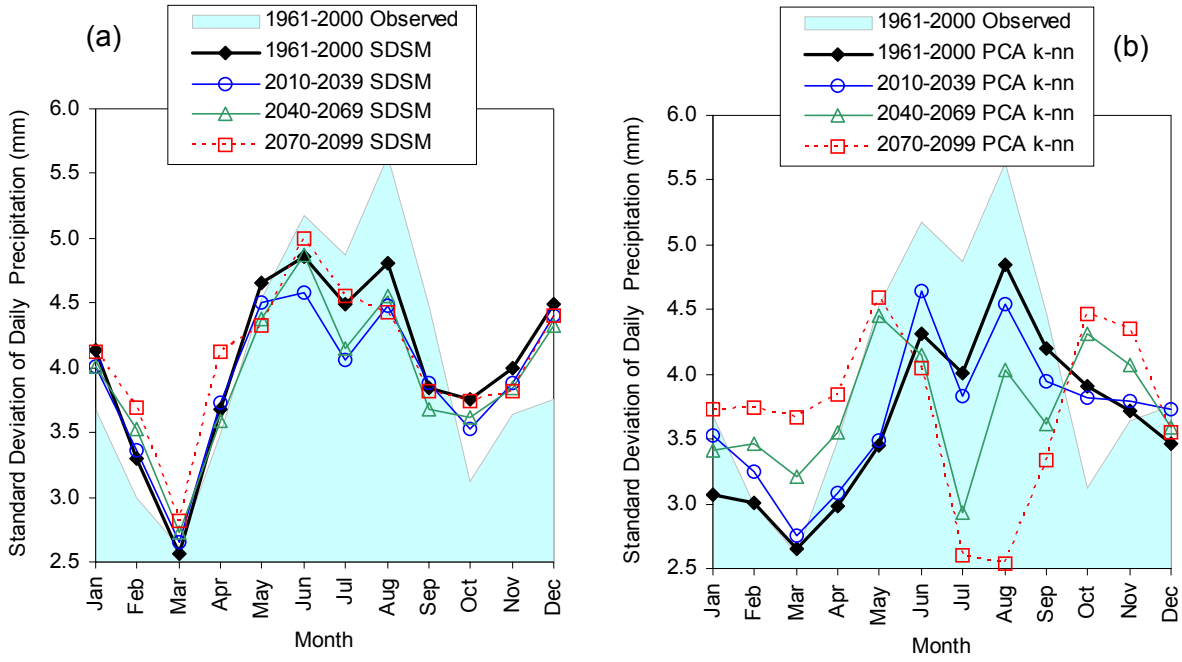

Figure 31 Mean monthly standard deviation of precipitation at Grand Forks, BC: observed and downscaled from CGCM1 model runs for current and future climate scenarios using two downscaling methods: (a) SDSM, (b) PCA k-nn.

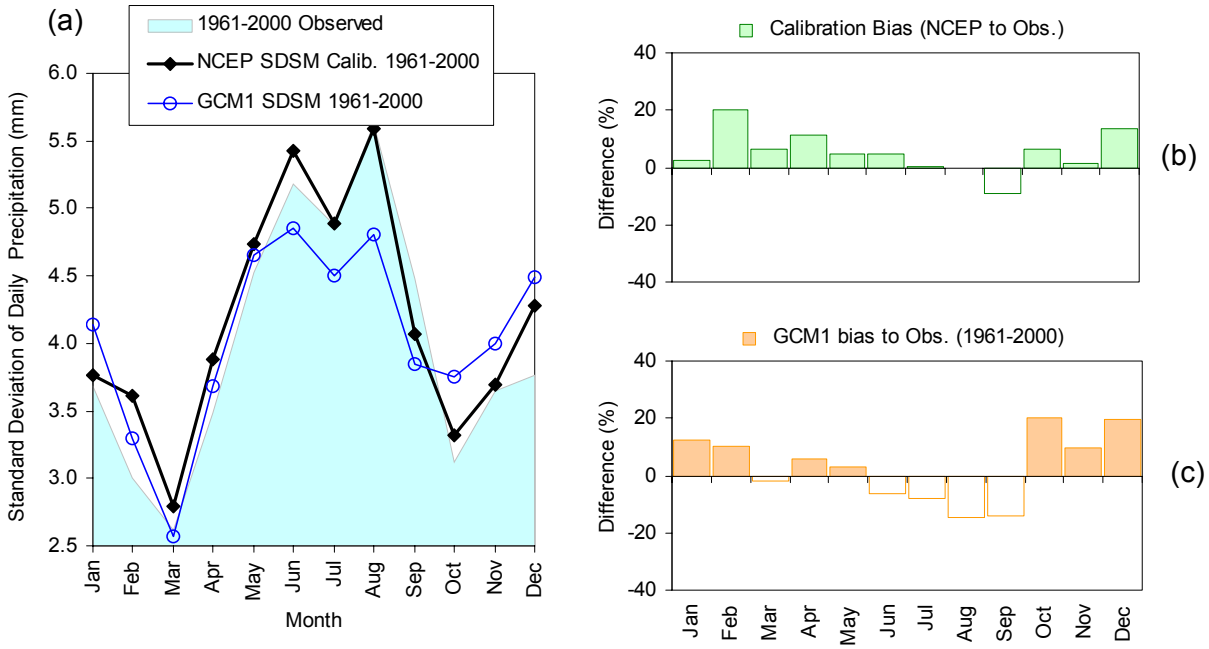

Figure 32 Comparing observed and downscaled standard deviation of precipitation at Grand Forks, BC. SDSM downscaling model performance: (a) monthly variance in precipitation, (b) calibration bias, (c) bias between SDSM downscaled CGCM1 Current variance in precipitation and observed.

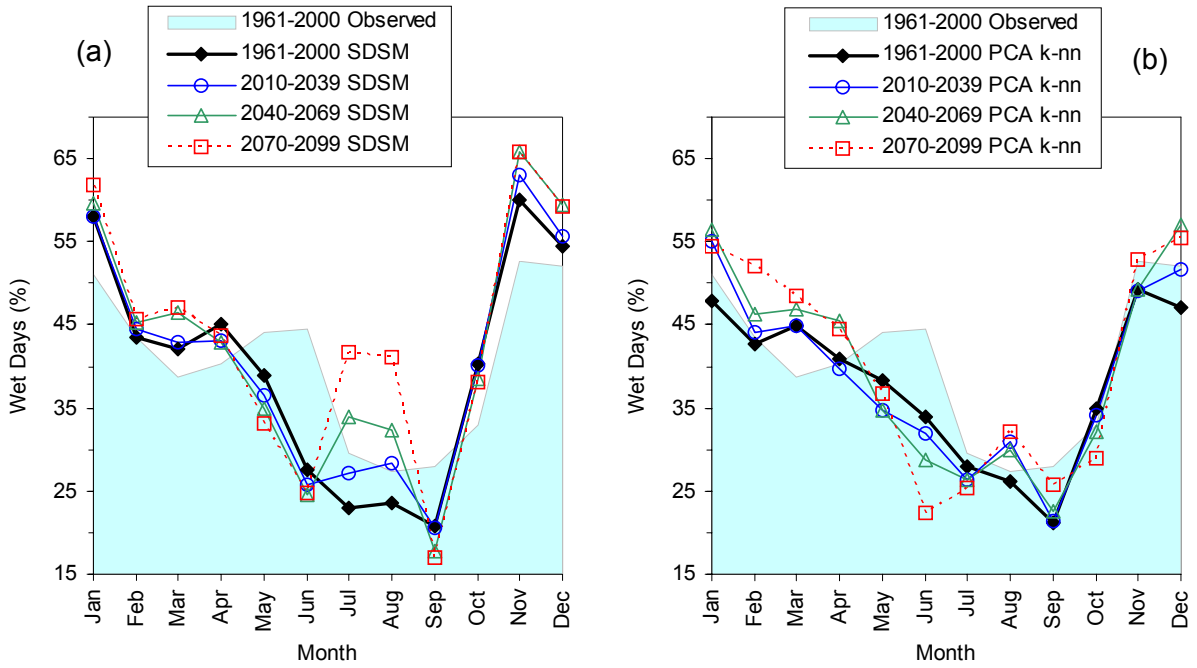

Figure 33 Mean monthly % WET days at Grand Forks, BC: observed and downscaled from CGCM1 model runs for current and future climate scenarios using two downscaling methods: (a) SDSM, (b) PCA k-nn.

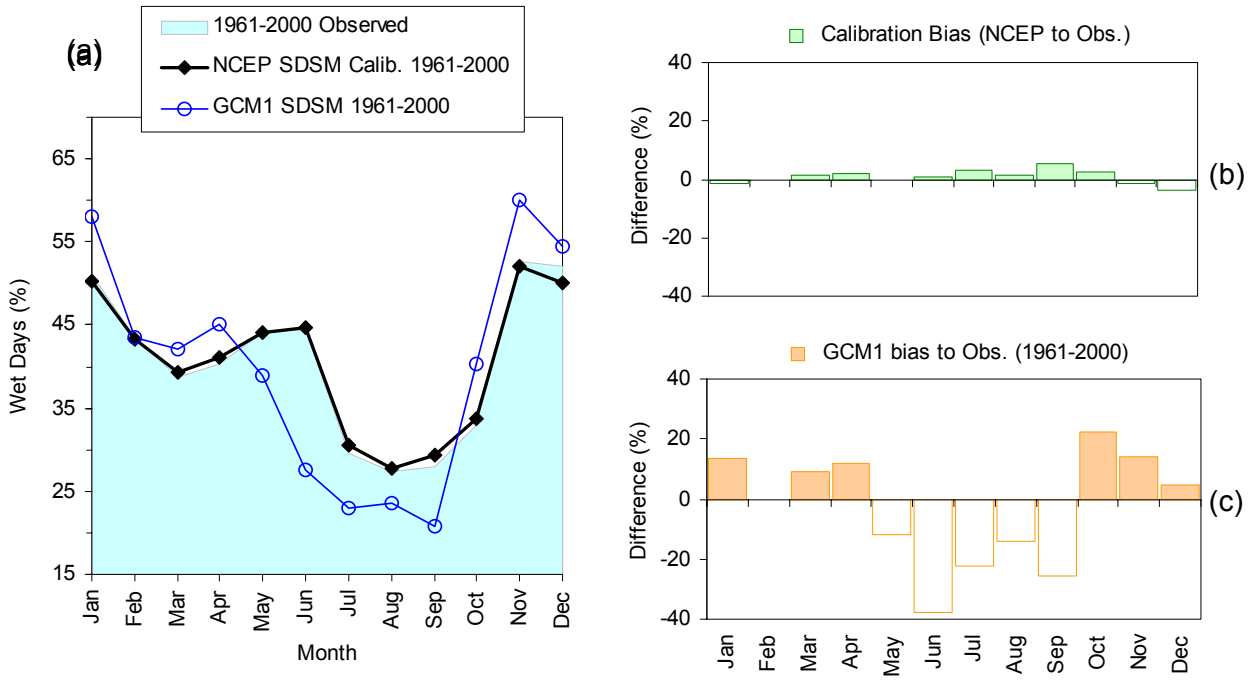

Figure 34 Comparing observed and downscaled % WET days at Grand Forks, BC. SDSM downscaling model performance: (a) monthly % WET days, (b) calibration bias, (c) bias between SDSM downscaled CGCM1 Current % WET days and observed.

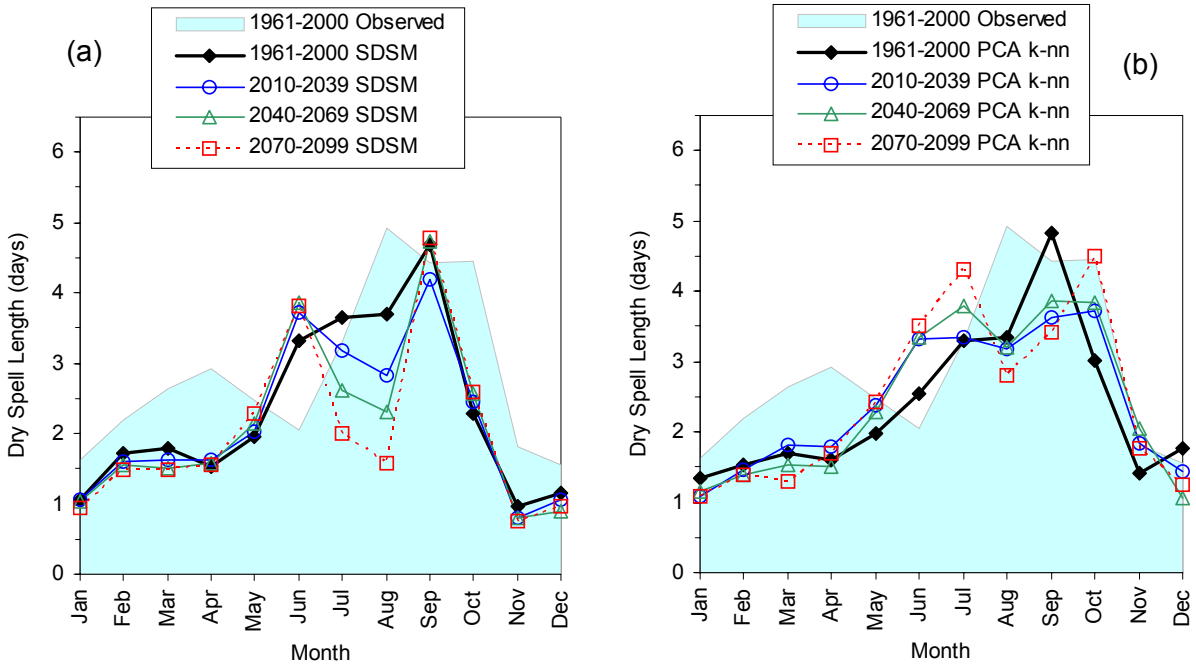

Figure 35 Mean monthly DRY spell length at Grand Forks, BC: observed and downscaled from CGCM1 model runs for current and future climate scenarios using two downscaling methods: (a) SDSM, (b) PCA k-nn.

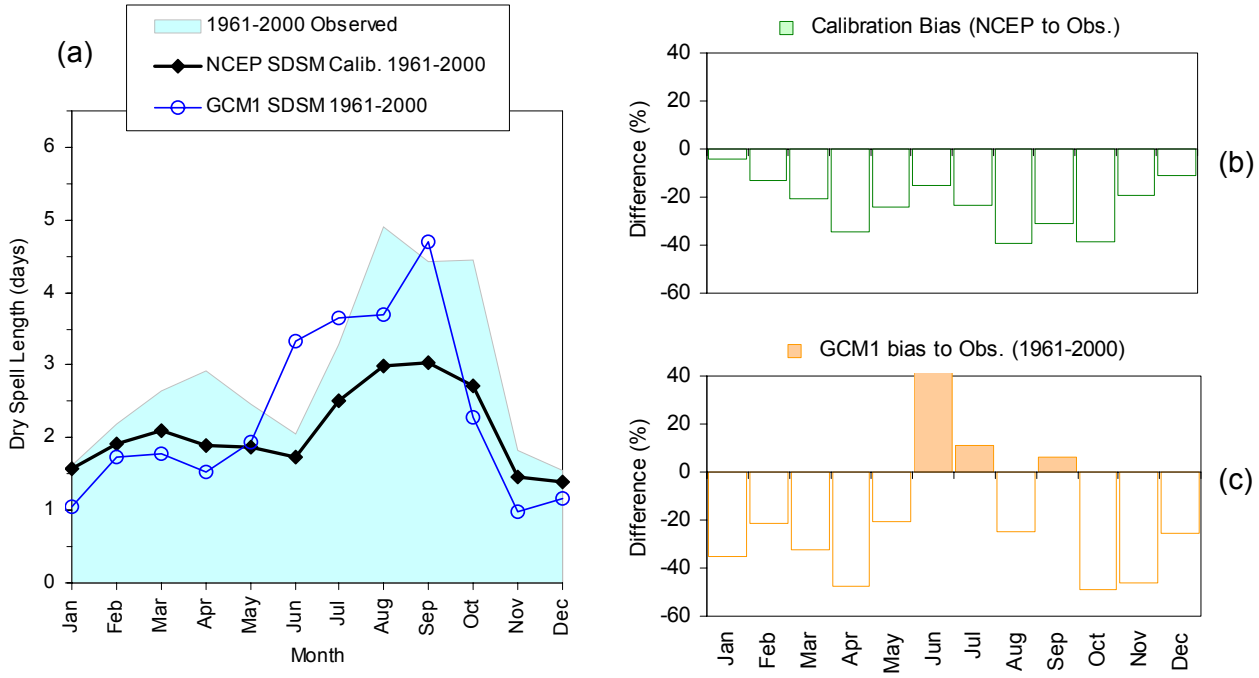

Figure 36 Comparing observed and downscaled DRY spell length at Grand Forks, BC. SDSM downscaling model performance: (a) monthly DRY spell length, (b) calibration bias, (c) bias between SDSM downscaled CGCM1 Current DRY spell length and observed.

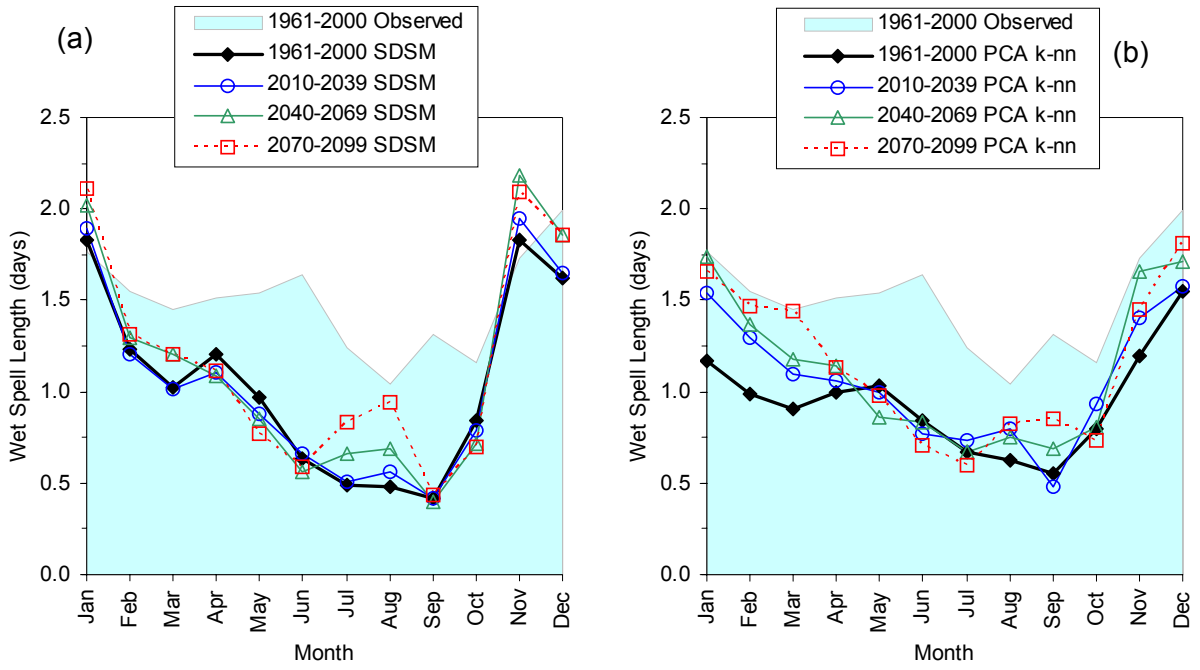

Figure 37 Mean monthly WET spell length at Grand Forks, BC: observed and downscaled from CGCM1 model runs for current and future climate scenarios using two downscaling methods: (a) SDSM, (b) PCA k-nn.

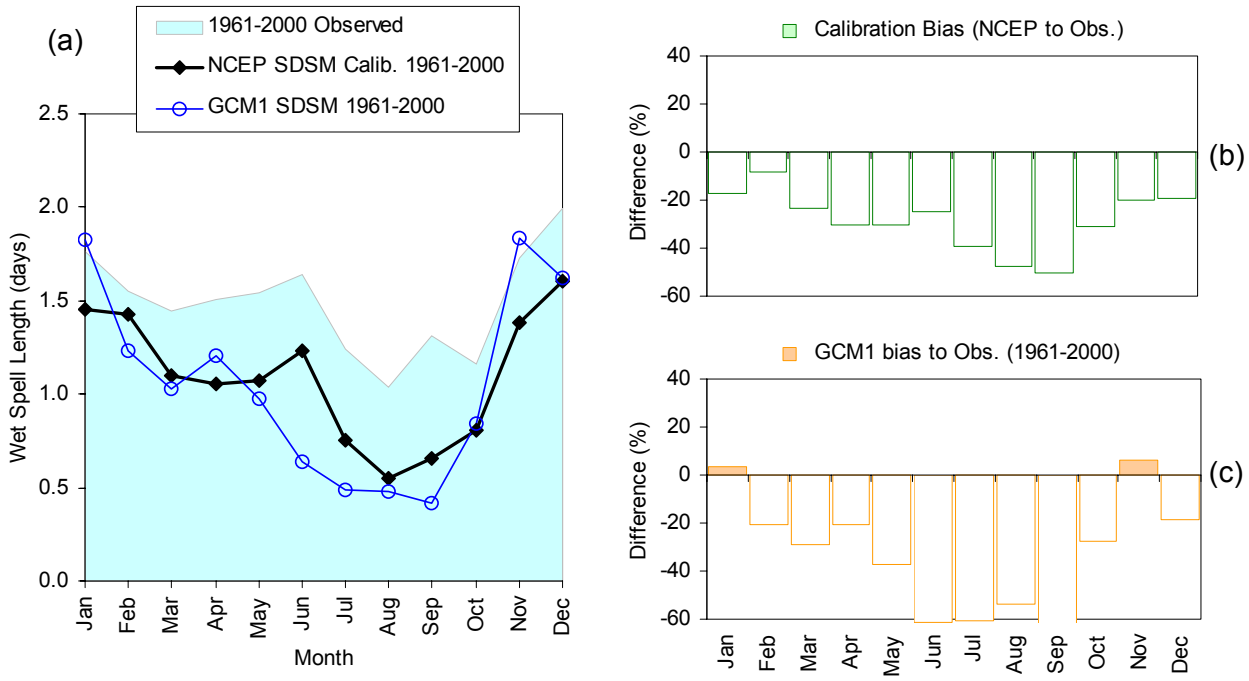

Figure 38 Comparing observed and downscaled WET spell length at Grand Forks, BC. SDSM downscaling model performance: (a) monthly WET spell length, (b) calibration bias, (c) bias between SDSM downscaled CGCM1 Current WET spell length and observed.

5.5.2. RELATIVE CHANGE GRAPHS

Another way of looking at temporal change in precipitation from current to future climate scenarios is to look at relative change, as shown in Figure 39 for downscaled precipitation and Figure 40 for raw CRCM data (not downscaled but better than raw CGCM1 data). Note that relative values for future climates are shown in temporal order but values are not cumulative, or in other words, the precipitation for the future climate scenario is compared to present climate (this is not a cumulative precipitation change graph).

relative change in Ppt **=** current Ppt **/** future Ppt

Similarly, other variables are calculated for relative change graphs, such as standard deviation in precipitation, % WET days and others. All relative precipitation changes are relative to current climate from CGCM1 model run; values less than 1.0 mean a decrease in precipitation, and above 1.0 mean an increase in precipitation relative to current (1961-2000).

The SDSM model calculated the variance of daily precipitation, which was converted to standard deviation (stdev = sqrt (variance)) because the LARS-WG requires standard deviation of precipitation as input for climate scenario modelling. Precipitation variability refers to distribution of precipitation daily values. The distribution is typically logarithmic and definitely not "normal" in shape. The variance and standard deviation statistics are for such highly skewed distribution. When variance in precipitation changes, the relative frequencies of small precipitation events and compared to larger ones also change. This is the meaning of precipitation variance in this case.

Wet and dry spells are required in the serial stochastic weather generator to construct the precipitation time series. Thus, the downscaling results are rather important here. Wet spells model the duration of rain events (where wet spell length refers to number of consecutive days with non-zero precipitation or at least higher than 0, and trace amount is considered as positive rainfall here).

- MEAN MONTHLY PRECIPITATION

The relative change summaries were grouped seasonally (Figure 39) at first. At Grand Forks precipitation is predicted to increase in the summer at increasing rate of change into the future according to SDSM results. However, PCA k-nn analysis showed a different trend (as was noted on monthly graphs previously), where precipitation will be the same in 2020's as present in the summer, but then it will decrease in the future decades. The two downscaling models also disagree on the rates of change of precipitation in other seasons, but generally precipitation will increase in the winter (both agree), remain steady or increase slightly in autumn, and in spring either remain similar to present or increase. Which downscaling method is to be trusted?

One way of analyzing the results is to look at raw CRCM outputs (not downscaled). CRCM predicts that precipitation will increase in the summer (as SDSM method downscaled from CGCM1 suggested, but only for 2050s and then decrease in 2080s), increase slightly in spring and winter, and vary for autumn near present levels. Thus, CRCM output tends to agree with SDSM results that at least until 2050s precipitation will increase in the summer. However, CRCM precipitation has a very large grid cell and does not represent local conditions at Grand Forks, so such comparisons are questionable.

The full story lies with monthly trends in precipitation as shown in Figure 41. Precipitation relative changes were graphed monthly for SDSM results – seasonal average is also plotted. In

the spring months, it is apparent that the seasonal average is just that, an average that hides most of the variability. For example, March rainfall will increase, but April and May rainfall will decrease until 2050s as predicted by CGCM1. In the summer, precipitation will increase in July and August, but remain similar to present in June. In autumn, precipitation will decrease in September, but remain similar to present in October and then increase in November into the future decades. In winter, precipitation will eventually increase into 2050 and continue increasing in all months. One can see how the seasons blend into each other by monthly steps, showing consistent pattern of increase or decrease of precipitation as indicated on monthly graphs of actual precipitation in Figure 41. The monthly trends for PCA k-nn method (Figure 42) also show a range of monthly variation in precipitation predictions, thus this is not unique to SDSM downscaling method. One conclusion can be drawn from looking at monthly variability in precipitation predictions: annual or even seasonal averages are meaningless when modelling precipitation changes into the future from GCMs. There is simply too much inter-monthly variability.

Finally, what is the precipitation change as modeled by CGCM1 for Grand Forks? At this time, the SDSM method looks better than the PCA k-nn method, but large uncertainties exist in actual precipitation forecasting ability of GCMs, and the ability to downscale to local conditions thus quantify relative and absolute changes in precipitation. Both SDSM and PCA k-nn results will be used in stochastic weather generator to create daily precipitation series for Grand Forks as two separate sets of climate scenarios. This is necessary for any climate impacts modelling (e.g., groundwater levels) to encompass the range of relative changes in precipitation predicted by CGCM1 as revealed through both downscaling methods. Note that the ranges of precipitation increase are quantified by the downscaled results to within 40% of current climate, and the differences are in seasonal and monthly details, which cannot be resolved in favour for either method at this time.

- PRECIPITATION VARIABILITY

The relative change in precipitation variability was graphed in Figure 43. As formerly stated, the SDSM predictions show almost no change from present, while PCA k-nn shows large decrease in variability of precipitation in the summer (surprising), and large increase in winter and spring.

- WET DAYS, DRY SPELLS AND WET SPELLS

Figure 44 shows relative changes in % wet days. To be consistent with predicted increase in mean monthly precipitation in the summer months, the SDSM also indicated increase in % wet days in summer months into the future. In other seasons the changes were small and similar to present values. PCA k-nn model showed a larger increase in winter months of % wet days than did SDSM, but for other months the values were similar to SDSM predictions, except that in the summer the % wet days decreased slightly (again consistent with precipitation predictions by that downscaling method).

Magnitudes of temporal changes in DRY spell lengths for future climates were relatively small except in summer months in both method outputs. Figure 44 presents the relative temporal trends. Both downscaled sets of results agree that in spring and autumn the DRY spell length will not change in the future. SDSM predicted decrease in summer (again consistent with its prediction of precipitation increase), and PCA k-nn predicted increase in the summer. Winter dry spells will increase according to SDSM and PCA k-nn, and remembering that precipitation will increase in the winter, this means that WET spell lengths should increase in the winter. In fact, the trends of DRY and WET spell lengths are opposite as would be generally expected.

Both downscaling sets of results (Figure 46) agree that WET spell length will be higher that at present for winter, autumn, and summer (at least from 2020s to 2050s), but differ for spring season. As would be expected at this point of the discussion, the WET spell lengths will increase (SDSM) in the summer to account for decrease in DRY spell length and increase in precipitation for that season.

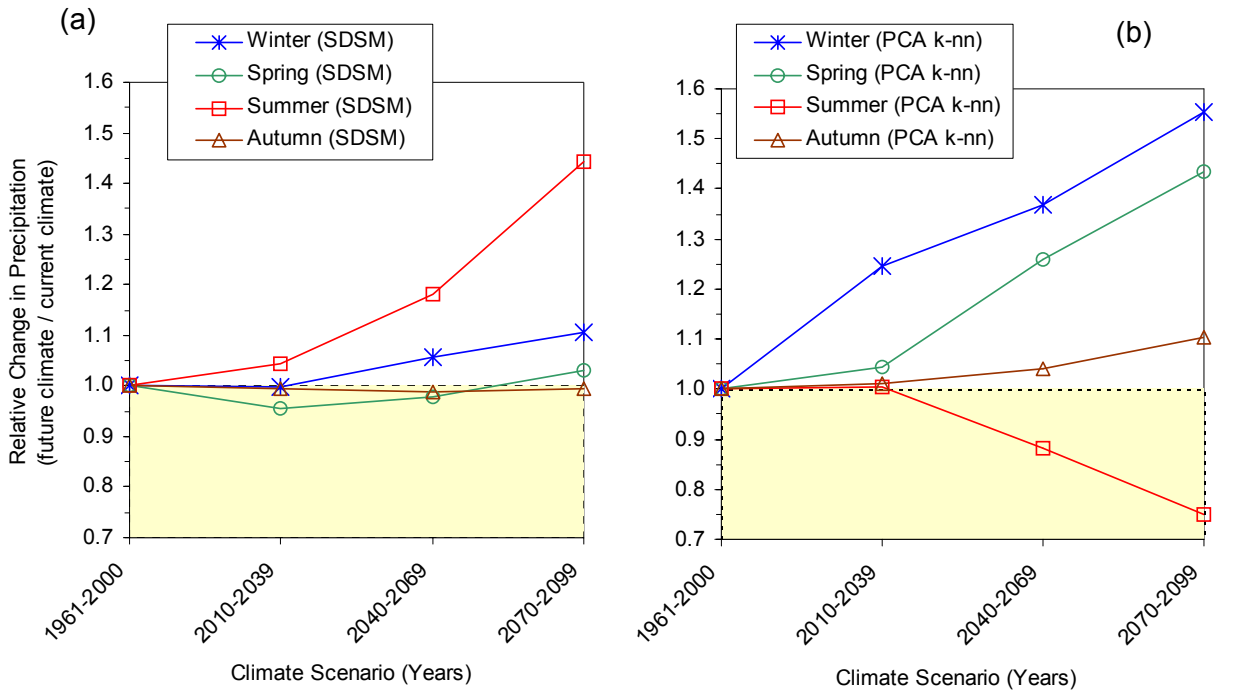

Figure 39 Relative change in precipitation predicted by CGCM1 model runs, after downscaling for Grand Forks, BC. Compared are two different downscaling results: (**a**) SDSM method, (**b**) PCA k-nn method.

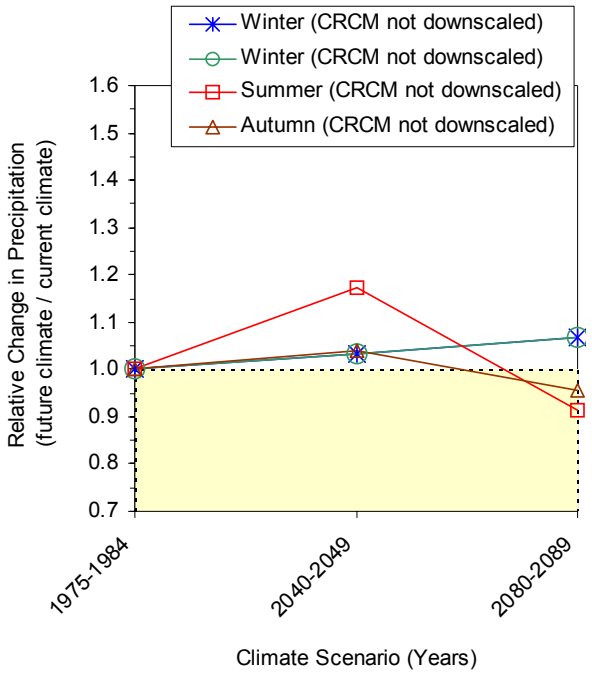

Figure 40 Relative change in precipitation predicted by CRCM model runs, not downscaled, for Grand Forks, BC.

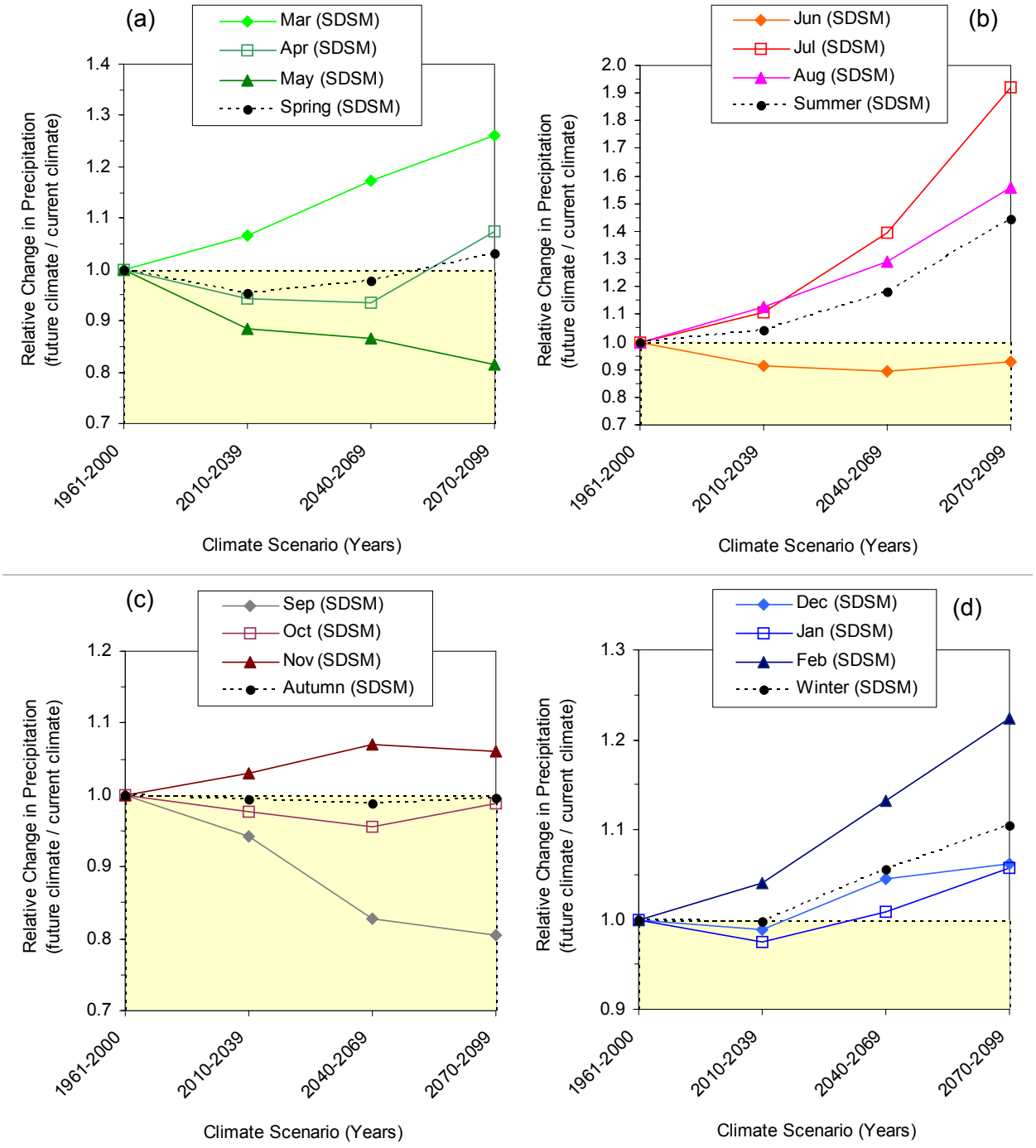

Figure 41 Relative change in monthly and seasonal precipitation predicted by CGCM1 model runs, after downscaling with SDSM for Grand Forks, BC. Comparing four seasons, and months within each season: (**a**) Spring, (**b**) Summer, (**c**) Autumn, (**d**) Winter.

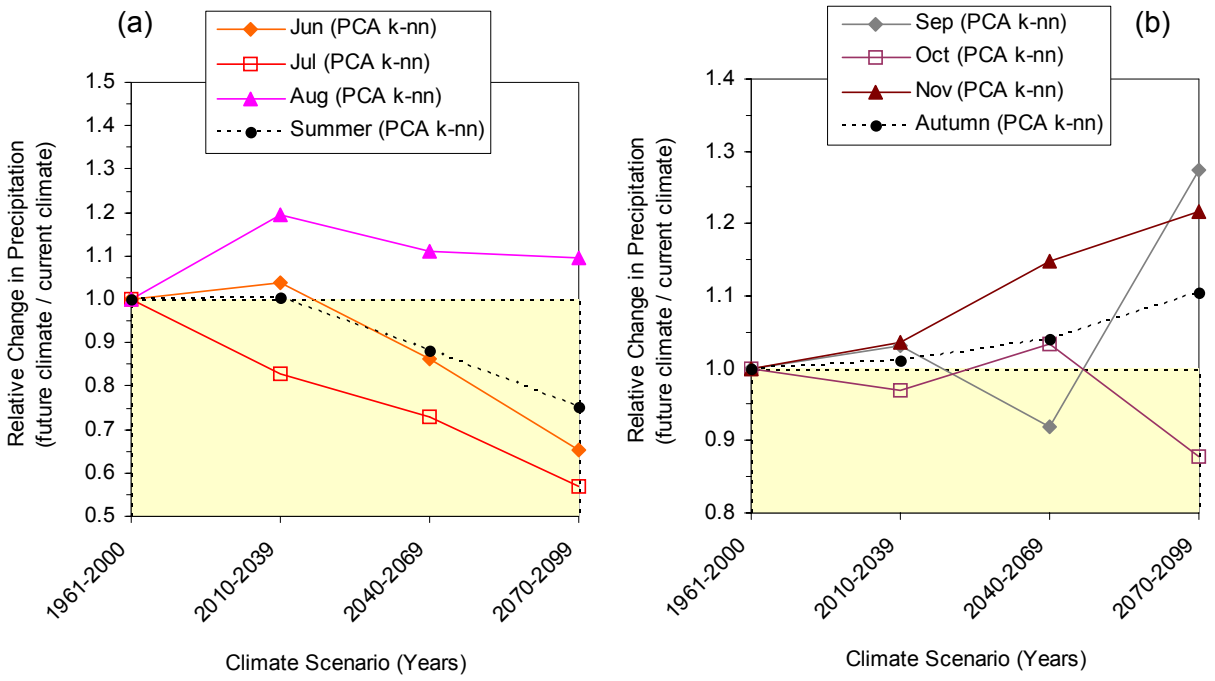

Figure 42 Relative change in monthly precipitation (Summer and Autumn) predicted by CGCM1 model runs, for Grand Forks, BC, after downscaling with (a) SDSM and compared to downscaled with (b) PCA k-nn method. This figure shows different downscaling results for Summer and Autumn, thus different climate change scenario predictions for precipitation, depending on downscaling method.

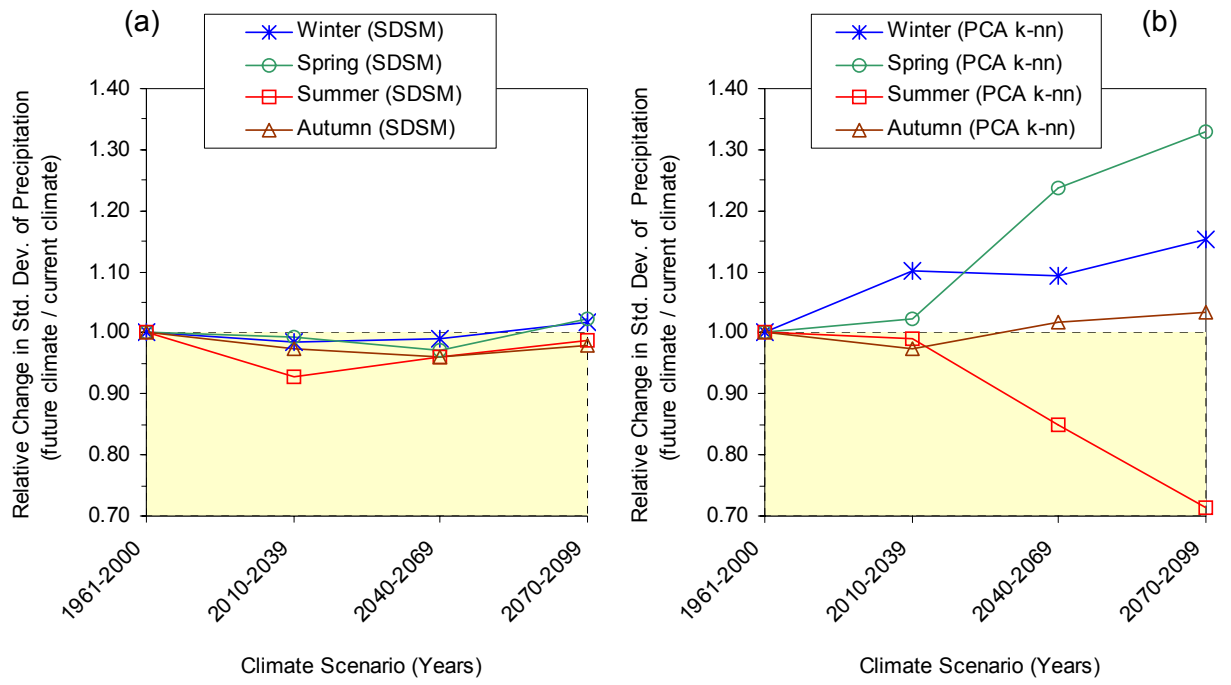

Figure 43 Relative change in standard deviation of precipitation, by season, predicted by CGCM1 model runs, for Grand Forks, BC, after downscaling with (a) SDSM and compared to downscaled with (b) PCA k-nn method.

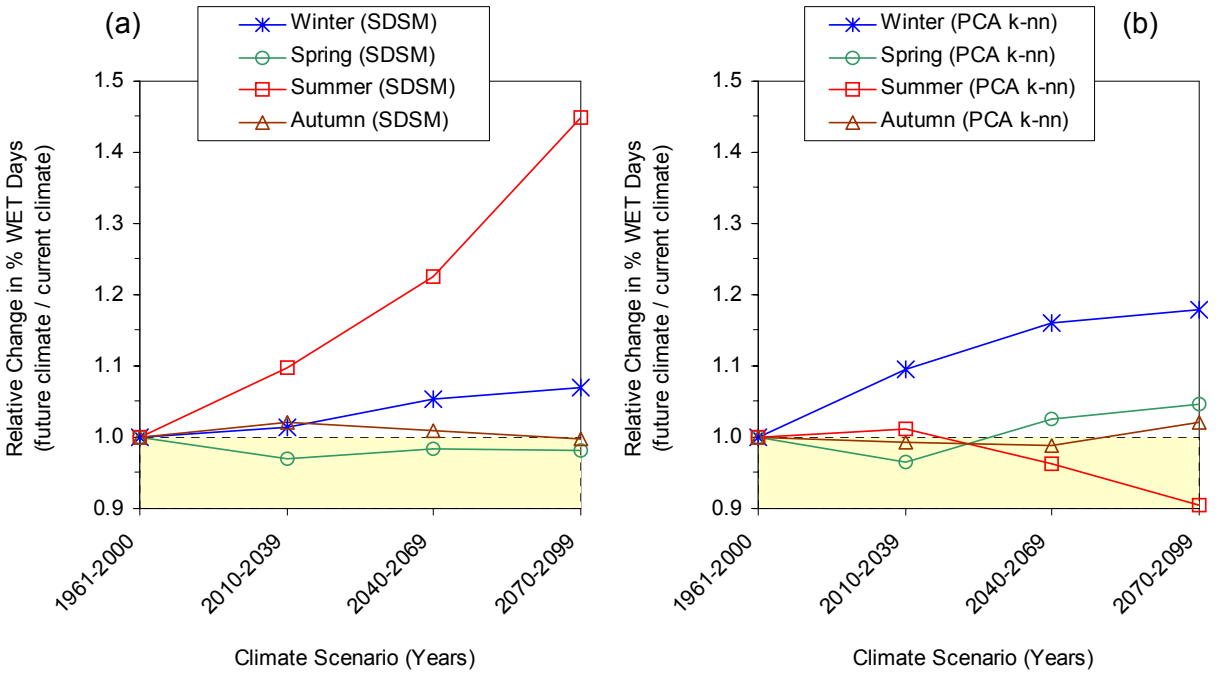

Figure 44 Relative change in % WET days, by season, predicted by CGCM1 model runs, for Grand Forks, BC, after downscaling with (a) SDSM and compared to downscaled with (b) PCA k-nn method.

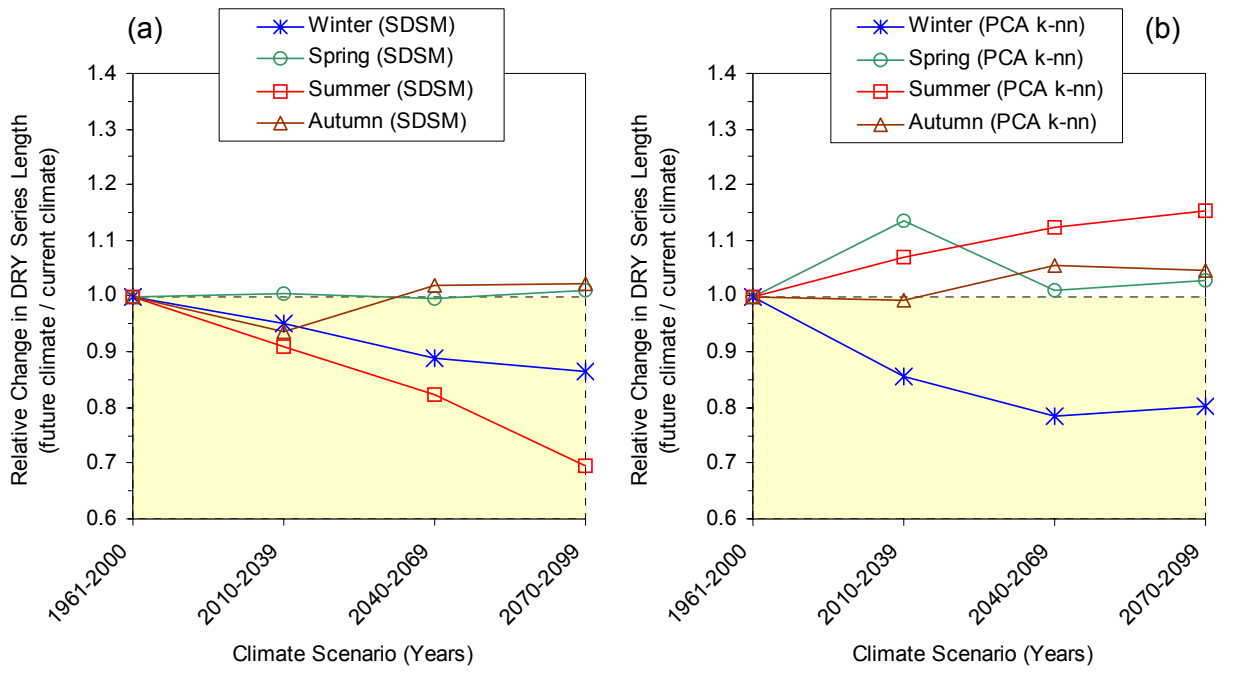

Figure 45 Relative change in DRY spell length, by season, predicted by CGCM1 model runs, for Grand Forks, BC, after downscaling with (a) SDSM and compared to downscaled with (b) PCA k-nn method.

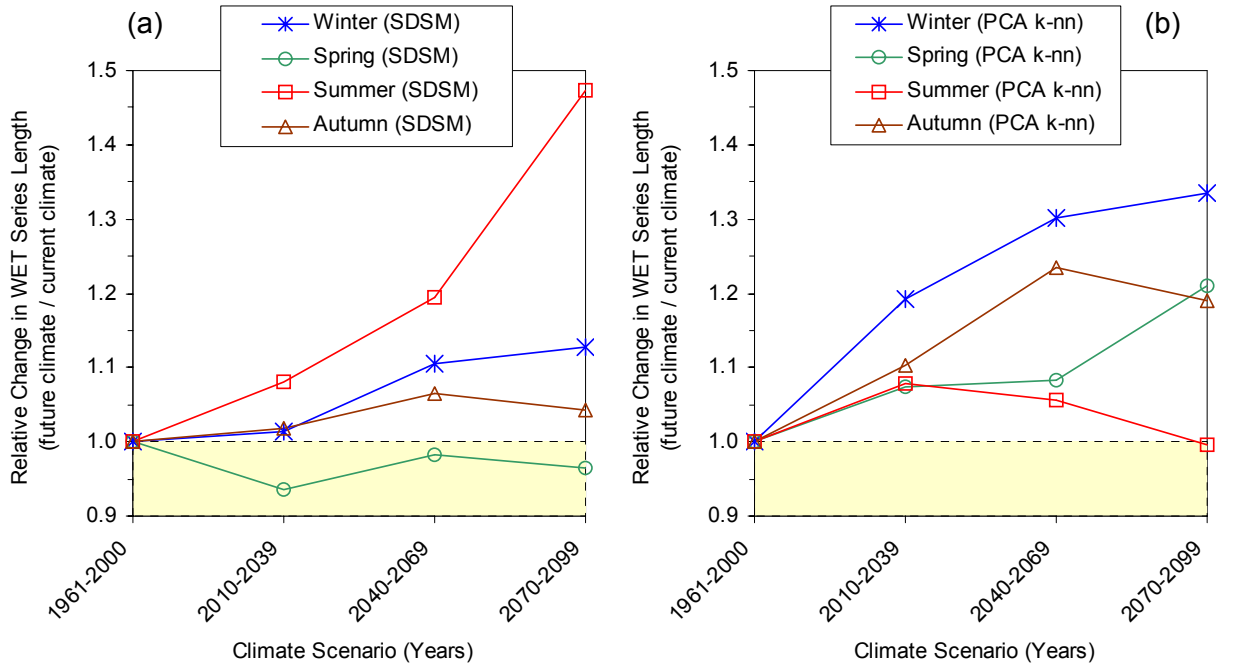

Figure 46 Relative change in WET spell length, by season, predicted by CGCM1 model runs, for Grand Forks, BC, after downscaling with (a) SDSM and compared to downscaled with (b) PCA k-nn method

5.6. DOWNSCALING RESULTS AND CGCM1 PREDICTED CLIMATE SCENARIOS: TEMPERATURE AND SOLAR RADIATION

Temperature time series were analyzed for the following variables:

1) mean daily temperature
2) standard deviation in daily temperature

Mean monthly temperature was calculated from mean daily values, which were downscaled from daily CGCM1 model runs for current and future climate scenarios. Precipitation downscaling output are provided elsewhere (Scibek and Allen, 2004). The following section provides a summary of these results.

Similar to the precipitation results, the results were arranged by variable, thus giving 2 sets of "grouped" graphs (one set or variable per page). For each variable, there are two figures. One figure has two graphs comparing results for the two downscaling methods (SDSM and PCA k-nn). The second figure, placed lower, compares observed variable values to those modeled, and presents two smaller graphs of model performance: 1) calibration bias of NCEP dataset to observed; and 2) base case scenario bias of current climate CGCM1 downscaled results to observed, all for the same time period 1961-2000.

The graph sets are colour-coded and arranged identically for easy inter comparison between different variables. All graphs show monthly statistics (on x-axes). The mean temperature and standard deviation in temperature are graphed as monthly time series on the y-axes. The observed data are always graphed as background fill (area graph), while the downscaled results are line graphs, superimposed on observed data graph. The styles and colours of line graphs are always the same for each climate scenario (e.g., 2010-2039) on all graphs. The model bias graphs are also colour coded and scaled similarly for easy inter comparison.

As was done for precipitation, daily temperature variability was represented by variance in temperature during downscaling, then converted to standard deviation of daily temperatures because LARS-WG requires that input for stochastic weather generation.

In temperature graphs, only absolute changes in temperature are shown (in degrees C) because that is more meaningful, and also to be consistent with inputs to LARS-WG and to published GCM scenarios. These are mean monthly temperatures derived from mean daily temperatures. It can be assumed that minimum and maximum temperatures increase accordingly. However, relative changes in standard deviation of temperature are given in relative amounts (ratios) as were calculated for precipitation.

- MEAN MONTHLY TEMPERATURE

The downscaled temperatures using SDSM were very close to observed (30 years) at Grand Forks in all months (Figure 48). The calibration bias for temperature to NCEP dataset (as graphed in Figure 48) was very small (less than 1%), and the model bias of downscaled CGCM1 to observed was less than 10% for most months and different by only 2ºC in months where % model bias was greater than 40% (due to temperatures close to 0ºC – the % difference is a poor indicator for temperatures close to 0ºC). The alternative downscaling method PCA k-nn produced similar but less calibrated results to observed, thus SDSM performed much better relative to observed temperatures at Grand Forks. This is evident from the monthly graphs in Figure 47.

The temporal trends for future climates, in terms of temperature, are very similar in both downscaled results. Results are simple and consistent: temperatures are predicted to increase in all months from present to future. The differences are in rates of increase, which are explored in temporal change graphs (absolute change in temperature graphs) by season and monthly in Figure 51. Both SDSM and PCA k-nn agree that summer temperatures will increase at relatively constant rate of 1ºC per 30 years, going up 3ºC by end of century compared to present. These are mean monthly temperatures derived from mean daily temperatures. It can be assumed that minimum and maximum temperatures increase accordingly. Rates of change in other seasons will be higher than in summer, with also relatively constant rates of increase, and ending up between 4 and 6ºC higher than present by 2080s. The CRCM results (Figure 52, not downscaled) also show a consistent temperature increase trends for all seasons, similar to those predicted by SDSM downscaled results from CGCM1.

Monthly temperature changes are very consistent within seasons, showing changes similar to mean seasonal temperature (Figure 53). In other words, there is very little inter-monthly variation in predicted changes in temperature, or at least much less than was the case for precipitation. The PCA k-nn downscaled temperatures (Figure 54) show larger monthly differences for summer months than did SDSM results, but PCA k-nn output was not representative of observed temperatures, so the downscaling algorithm did not work as well as SDSM did.

- TEMPERATURE VARIABILITY

Standard deviations of downscaled daily temperatures are graphed in Figure 49. SDSM was able to downscale the temperature variability much better than PCA k-nn method in all months except in autumn. SDSM performed remarkably well from spring to summer months. Both downscaling methods underestimated temperature variability in winter season. The NCEP calibration bias was low and about -10% or less, whereas the % differences between downscaled current temperature from CGCM1 and observed varied over the year, but most were about 20%, except in winter. Relative changes in temperature standard deviation (Figure 55) differ between SDSM and PCA k-nn results. SDSM output shows that in winter T stdev will increase by 20%, have a small increase in spring and autumn, and a small decrease in summer. Overall, except winter, not much change in temperature variability was predicted. The other downscaling method PCA k-nn indicates a decrease in T stdev in summer and autumn, but a small increase in other seasons. In view of the better performance of SDSM, the standard deviation of temperature will be used from SDSM downscaled predictions.

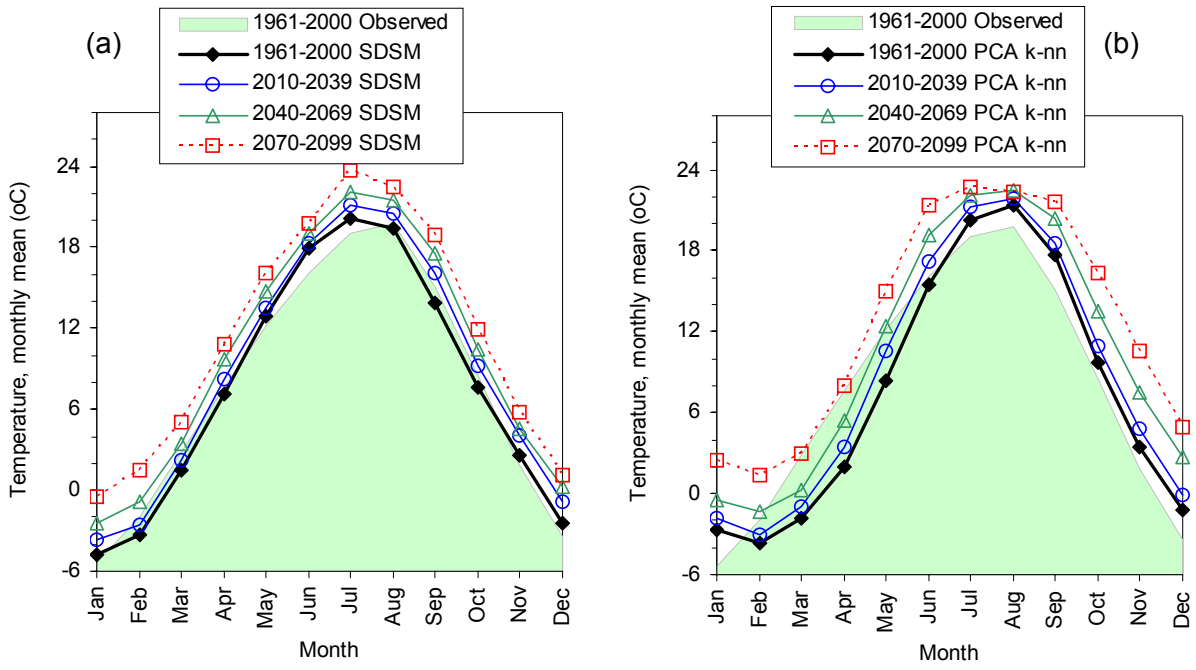

Figure 47 Mean monthly temperature at Grand Forks, BC: observed and downscaled from CGCM1 model runs for current and future climate scenarios using two downscaling methods: (a) SDSM, (b) PCA k-nn.

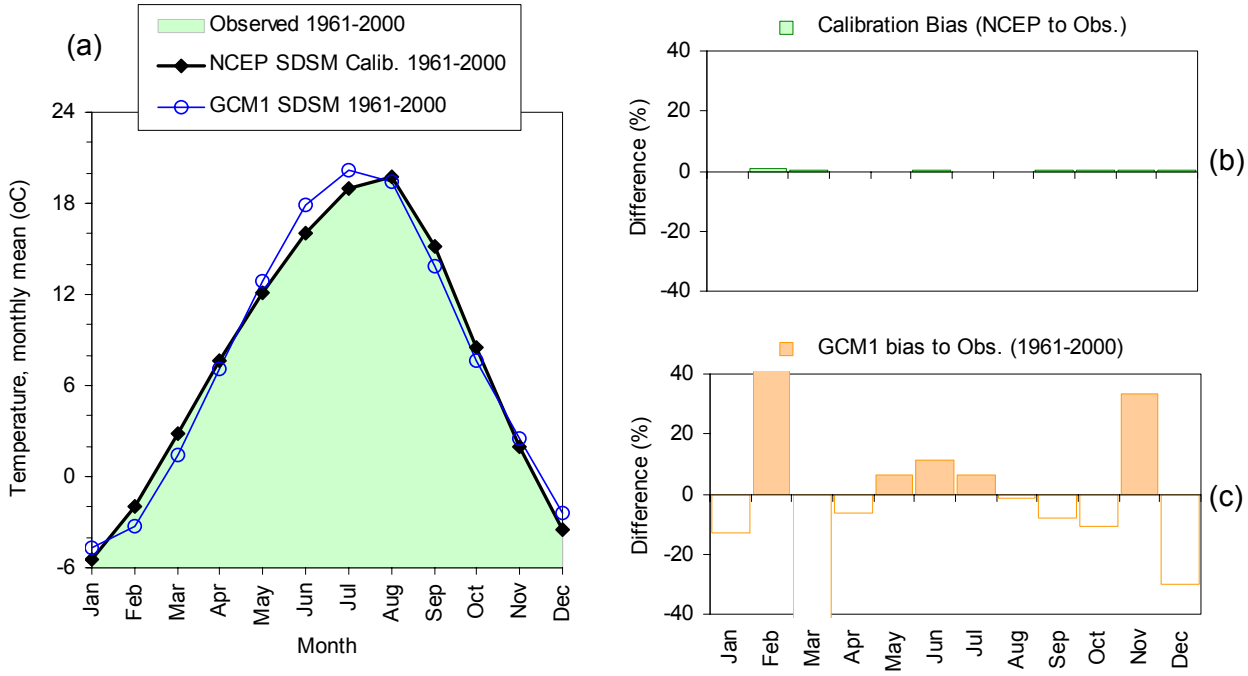

Figure 48 Comparing observed and downscaled temperature at Grand Forks, BC. SDSM downscaling model performance: (a) monthly precipitation, (b) calibration bias, (c) bias between SDSM downscaled CGCM1 Current precipitation and observed.

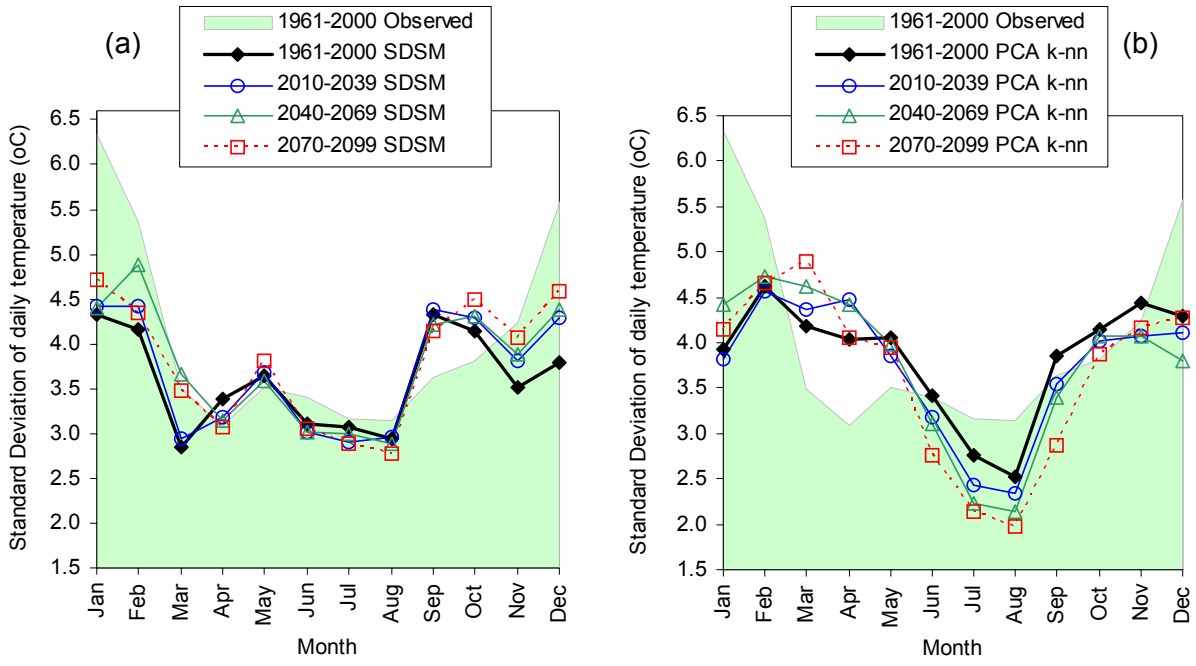

Figure 49 Mean monthly standard deviation of temperature at Grand Forks, BC: observed and downscaled from CGCM1 model runs for current and future climate scenarios using two downscaling methods: (a) SDSM, (b) PCA k-nn.

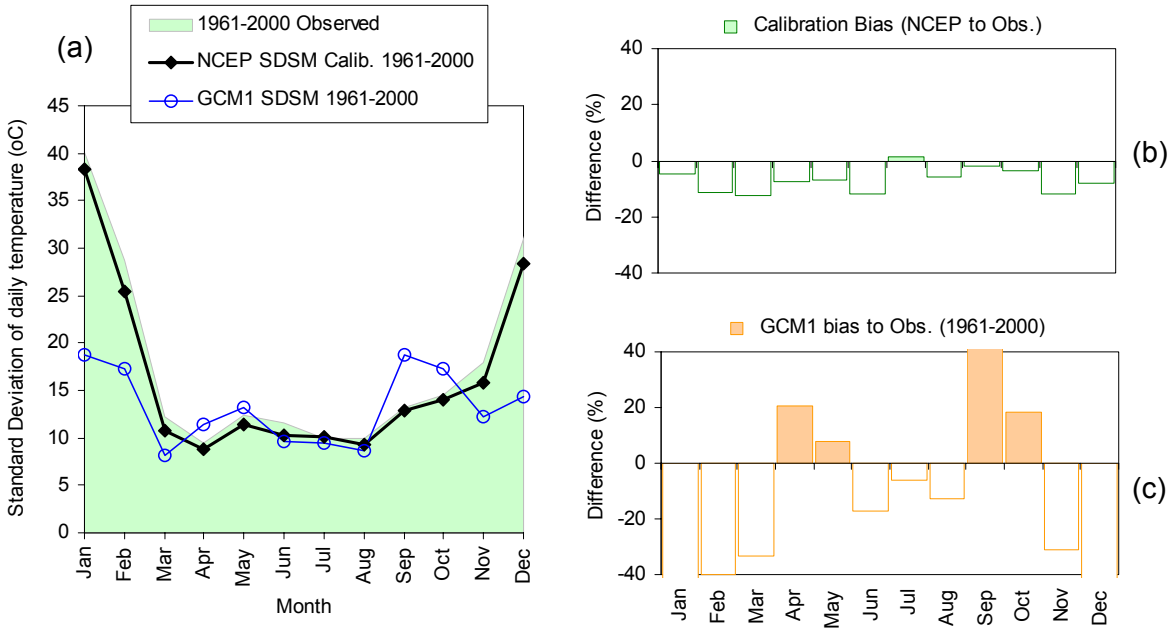

Figure 50 Comparing observed and downscaled standard deviation of temperature at Grand Forks, BC. SDSM downscaling model performance: (a) monthly precipitation, (b) calibration bias, (c) bias between SDSM downscaled CGCM1 Current precipitation and observed.

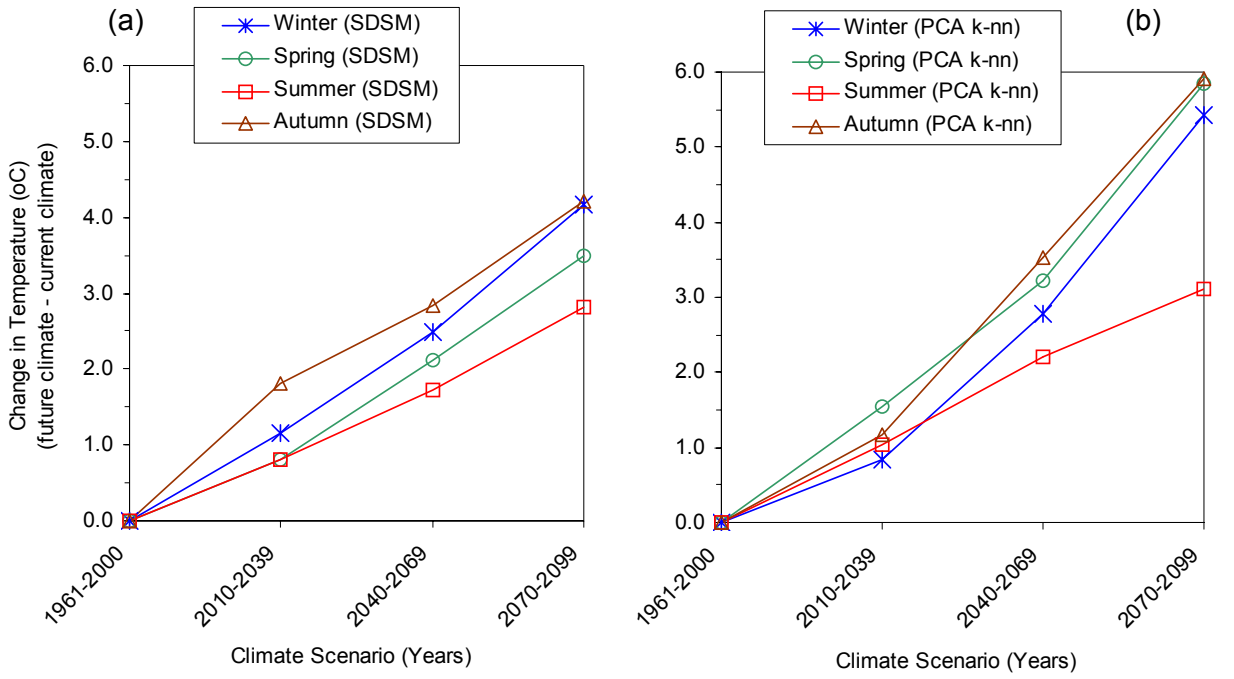

Figure 51 Absolute change in temperature predicted by CGCM1 model runs, after downscaling for Grand Forks, BC. Compared are two different downscaling results: (**a**) SDSM method, (**b**) PCA k-nn method.

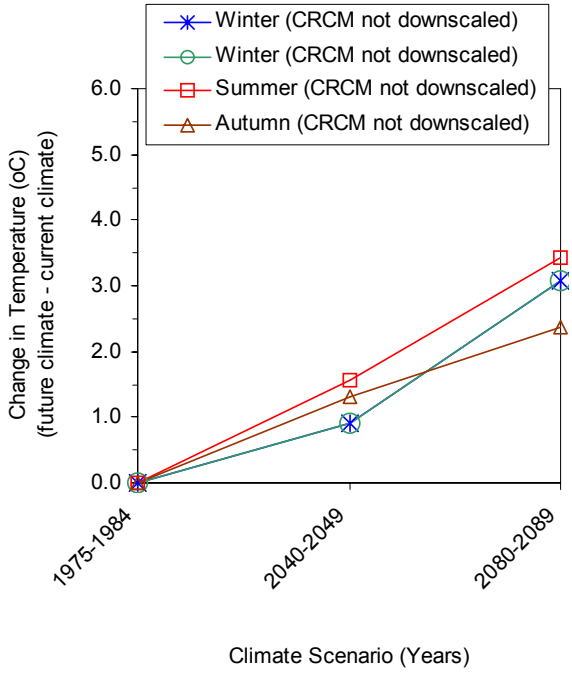

Figure 52 Absolute change in temperature predicted by CRCM model runs, not downscaled, for Grand Forks, BC.

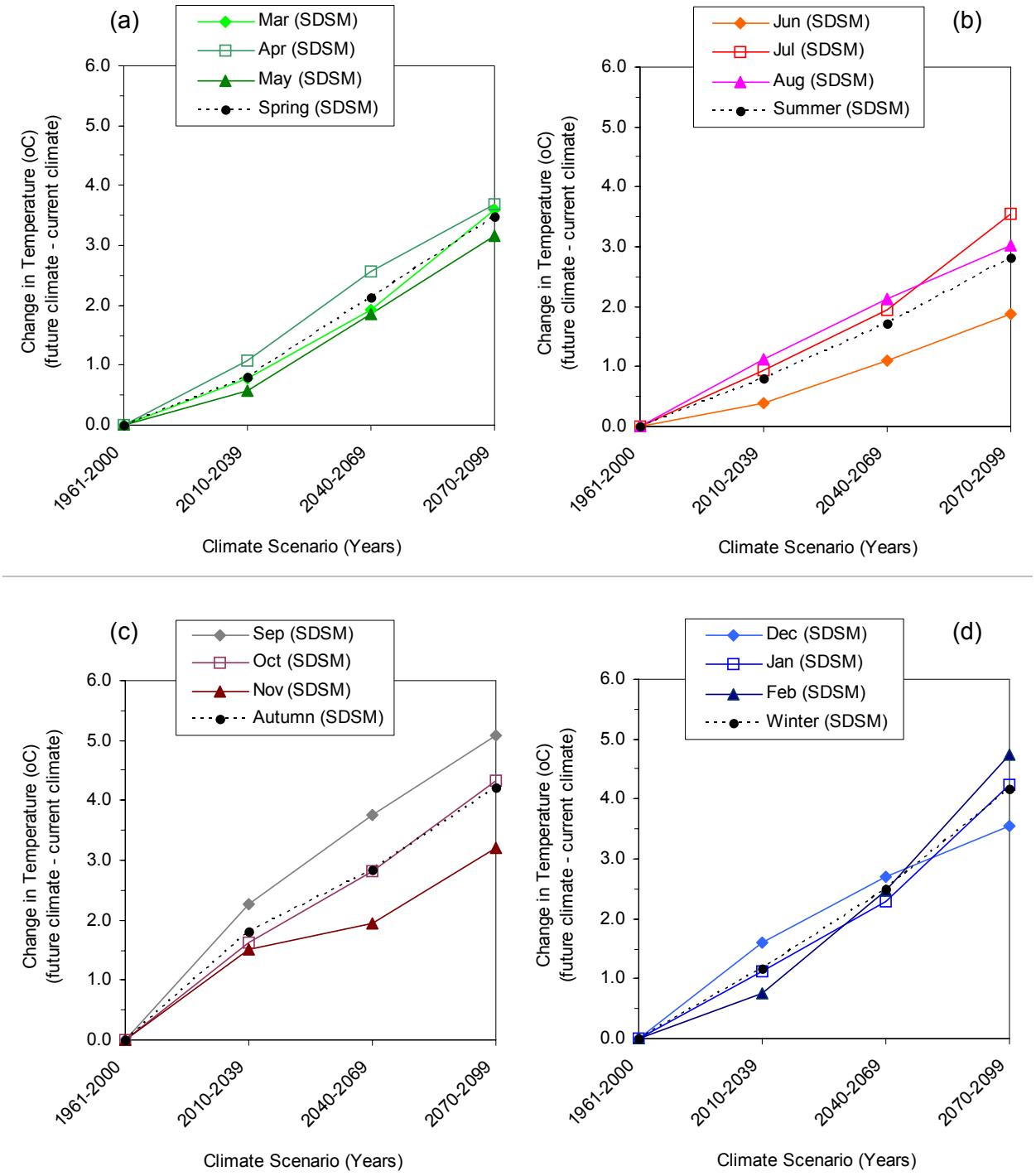

Figure 53 Absolute change in monthly and seasonal temperature predicted by CGCM1 model runs, after downscaling with SDSM for Grand Forks, BC. Comparing four seasons, and months within each season: (**a**) Spring, (**b**) Summer, (**c**) Autumn, (**d**) Winter.

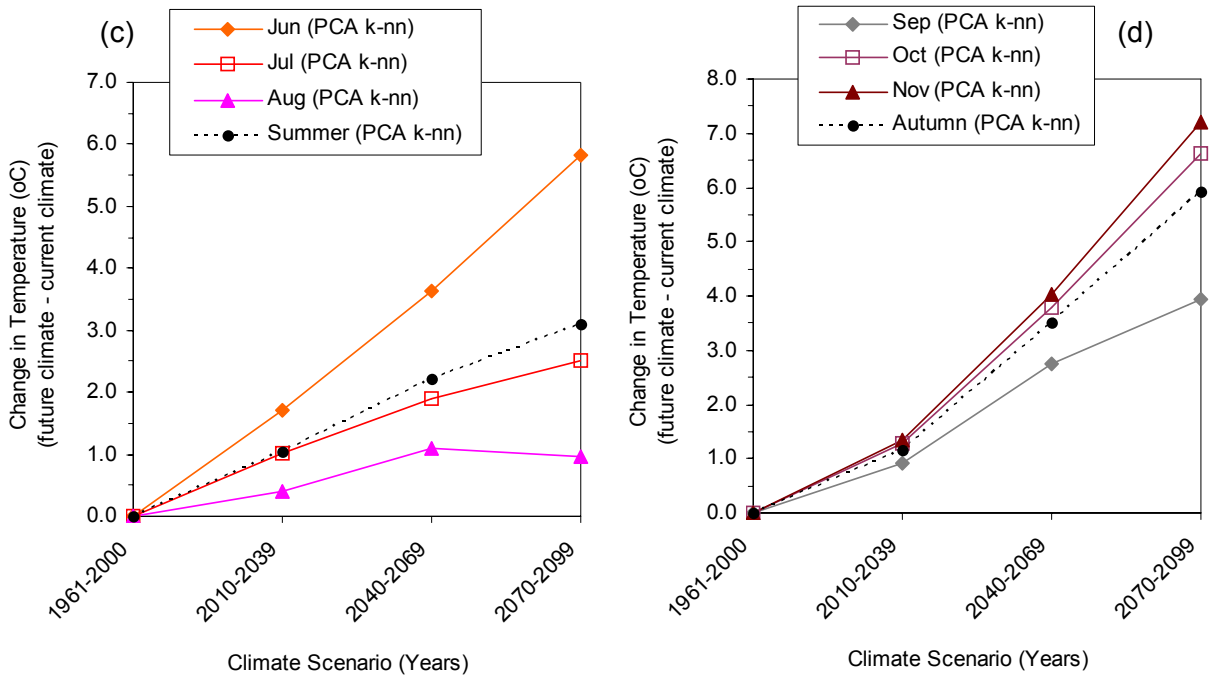

Figure 54 Absolute change in monthly and seasonal temperature predicted by CGCM1 model runs, after downscaling with PCA k-nn method, for Grand Forks, BC. Comparing (a) Summer, and (b) Autumn.

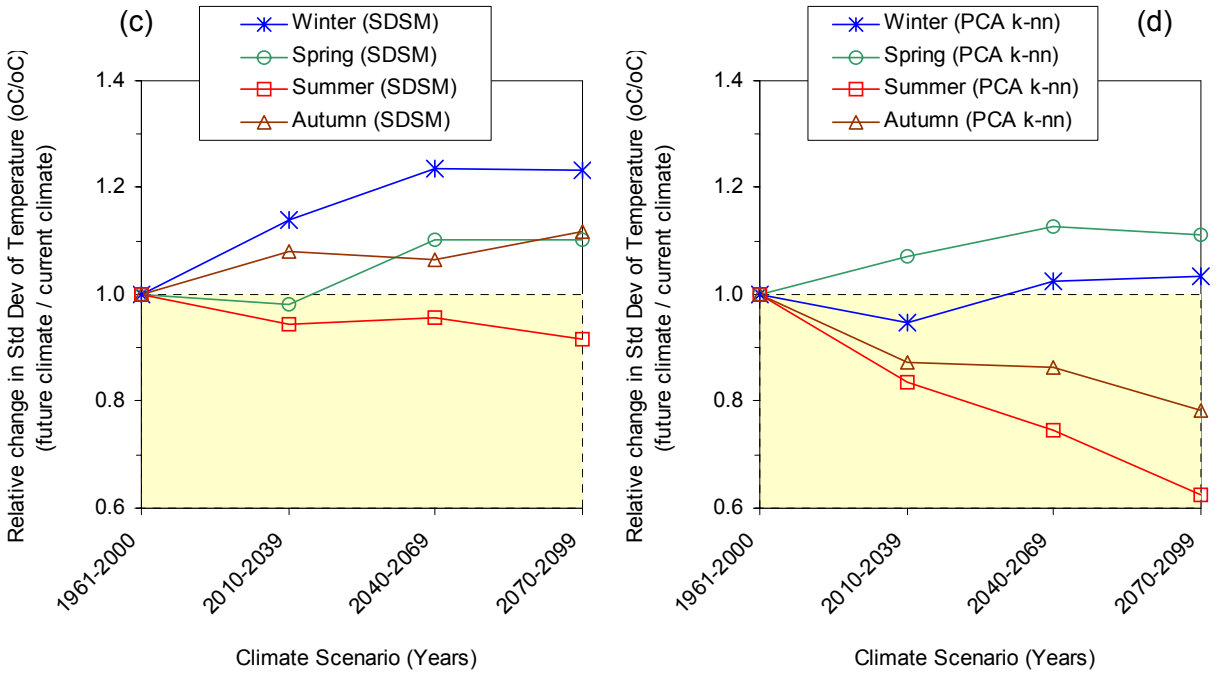

Figure 55 Relative change in standard deviation of temperature, by season, predicted by CGCM1 model runs, for Grand Forks, BC, after downscaling with (a) SDSM and compared to downscaled with (b) PCA k-nn method.

- SOLAR RADIATION FROM CRCM (NOT DOWNSCALED)

It was not possible to downscale solar radiation for Grand Forks due to the lack of observed mean daily incident solar radiation at this location. The LARS-WG weather generator requires an input of absolute changes in solar radiation relative to base case climate in order to generate weather for future climate change scenarios.

Data were extracted from monthly CRCM outputs for grid cells representing Grand Forks and imported from the CICS website (CICS, 2003). Original data are provided elsewhere (Scibek and Allen, 2004) Another solar radiation dataset was obtained from NASA solar energy data set (Carson et al., 2002), but these values differ from CRCM values in spring and summer months (see Figure 56). Thus, these were not explored in this report, but probably are caused by differences in solar radiation data collection and scale effects (CRCM model grid to point location in NASA dataset). For consistency and to calculate relative changes in solar radiation for future climates relative to current, only the CRCM solar radiation monthly values were used and assumed representative. The changes were relatively small, so the downscaled model is assumed to be not sensitive to errors or scale effects in solar radiation values taken from CRCM.

Absolute changes of solar radiation from CRCM, by month, were graphed in Figure 57 for current climate and future climates, corresponding to climate scenarios in CGCM1 and downscaled using SDSM. The CRCM solar radiation values were not downscaled. Changes are relatively small and consistent between the two locations, but there are no clear seasonal patterns.

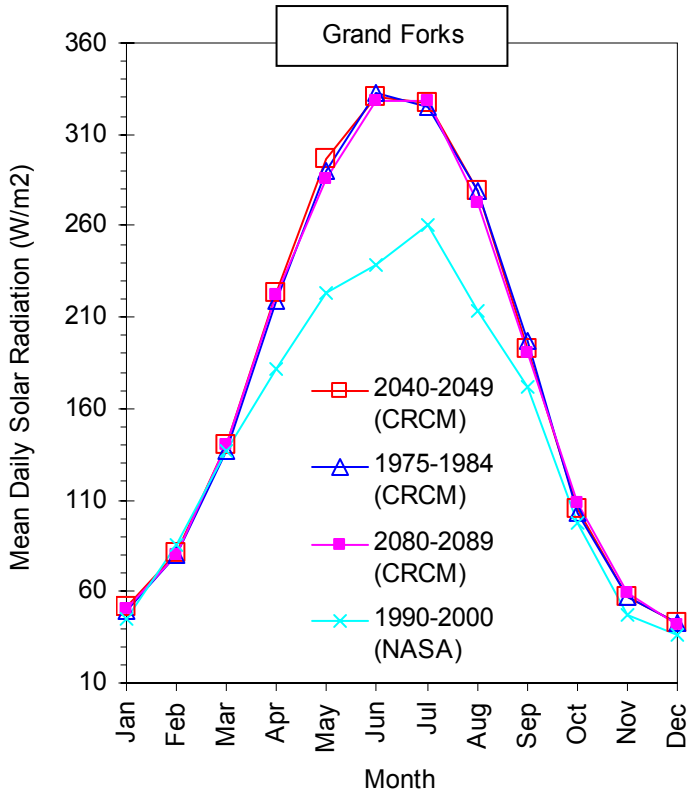

Figure 56 Solar radiation (mean daily averaged per month), modeled by CRCM without downscaling at Grand Forks. Scenarios correspond to CGCM1 climate scenarios.

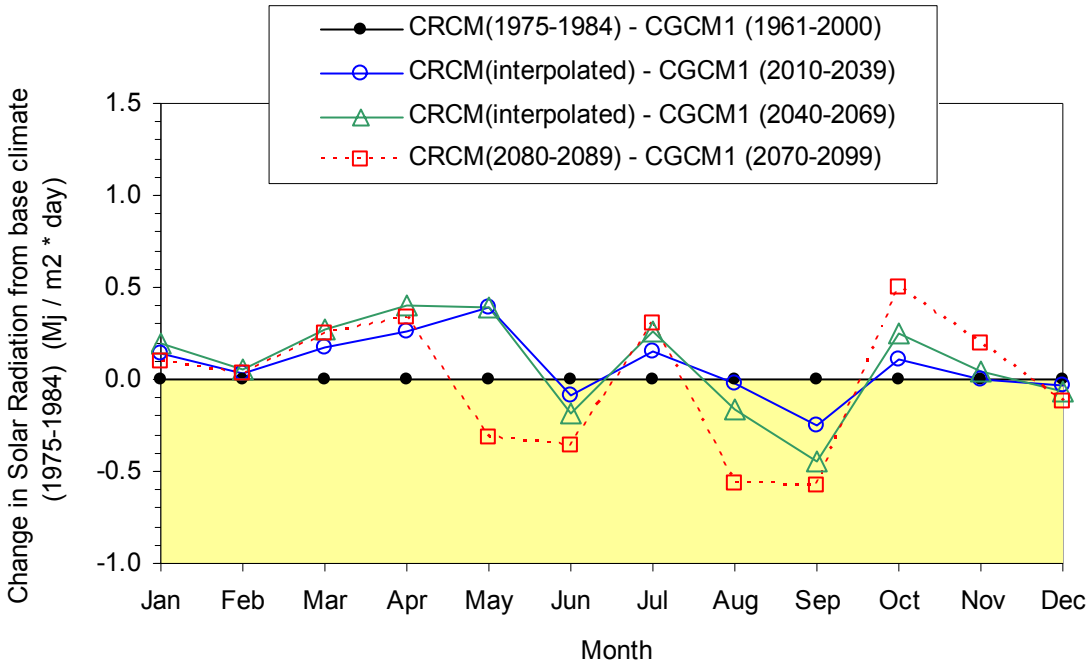

Figure 57 Change in solar radiation (mean daily averaged per month) from current climate, modeled by CRCM without downscaling at Grand Forks, BC. Scenarios correspond to CGCM1 climate scenarios.

5.6.1. MODELLING OF SOLAR RADIATION FROM TEMPERATURE AND PRECIPITATION (WET / DRY DAYS)

There are well-known equations that predict incident solar radiation from cloudless-sky conditions, and these are based on astronomical relationships, time of day, and season. For this project, a simple and yet effective solar radiation model was applied to estimate solar radiation at Grand Forks. The cloudless-sky solar radiation modeling methodology was taken from textbook by Iqbal (1983). The relevant equations are listed as Visual Basic code elsewhere (Scibek and Allen, 2004). The equations specify:

- eccentricity correction factor of the earth's orbit
- solar declination (seasonality)
- equation of time (how solar radiation varies over a day)
- conversion from local apparent time to other time measures, and linking to equation of time
- solar altitude and zenith angles

With the given astronomical parameters for any location and any time, the Grand Forks solar radiation was modeled using the cloudless-sky irradiance formulations as described by Davies and McKay (1982). Although there are many models that predict solar radiation under cloudy conditions, these usually require many measurements to calibrate, and use many parameters that are not known for Grand Forks. Due to lack of data, a simple empirical relation was developed for total cloud opacity effect on solar radiation in this study. There are only few locations in British Columbia where hourly solar radiation and cloud opacity are measured. One of them is the Prince George airport, which represents dry continental climate in central BC. The second locality is Summerland (solar radiation) and nearby Penticton Airport (cloud opacity) in the Okanagan Valley – dry southern-interior climate, somewhat similar to Grand Forks. Port Hardy also has the paired data, and represents wet coastal climate, with frequent fog and cloud cover.

First, the clear-sky solar radiation model was used to generate "ideal" daytime solar radiation data using only astronomical relations as per Iqbal (1983). Then, differences were calculated between clear-sky ideal solar radiation and actual observed solar radiation. Any difference represents decrease in solar radiation due to cloud attenuation, and to a minor extent by dispersion by atmospheric aerosols and dust. Using data for the Prince George weather station, the solar radiation "decreases due to cloud cover" were related to cloud opacity (based on hourly values for all available data – 30 years) via a regression model. The data and fitted quadratic relation is plotted in Figure 58. The correlation coefficient is 0.8377 and the relation is statistically significant. Using this relation, the cloudy-sky solar radiation was modeled at Prince George and then compared to actual observed solar radiation at this location (see Figure 59). This simple model is able to predict solar radiation relatively well just based on cloud opacity alone.

This model was further evaluated by graphing solar radiation time series for two different years at Prince George. The first one in Figure 60 plots three sets of graphs. Modeled and observed solar radiation are compared as daily values and as moving average trends. The modeled values are very close to observed. The cloudless-sky solar radiation curve is also plotted and represents the maximum possible value that could occur at any given time. It also corresponds very well to maximum observed values (forms a maximum envelope). The cloud opacities are graphed and are obviously inversely related to solar radiation (thicker clouds attenuate more solar radiation during daytime). The residuals from modeled / observed differences are small

and randomly distributed, further validating this model. In the second sample year in Figure 61 the model also performs similarly well.

As a further test, the Summerland solar radiation was modeled and compared to observed data. The model performance was similarly good as at Prince George, indicating that such relation is not site-specific and can be applied to other interior locations in British Columbia. The results of that analysis are not shown here.

The next step was a selection of nearest weather station to Grand Forks that recorded cloud opacity, since it was not recorded at Grand Forks. The nearest such station is Castlegar Airport, located about 100 km west of Grand Forks. Although it lies in similar climate zone, the Castlegar Airport weather station has 10 to 20% more monthly rainfall than Grand Forks. The seasonal trends of precipitation are very similar to Grand Forks, and it is assumed here that daily average cloud opacity model will capture major weather events such as frontal passage and regional cloudiness. However, there might be local differences between Castlegar and Grand Forks.

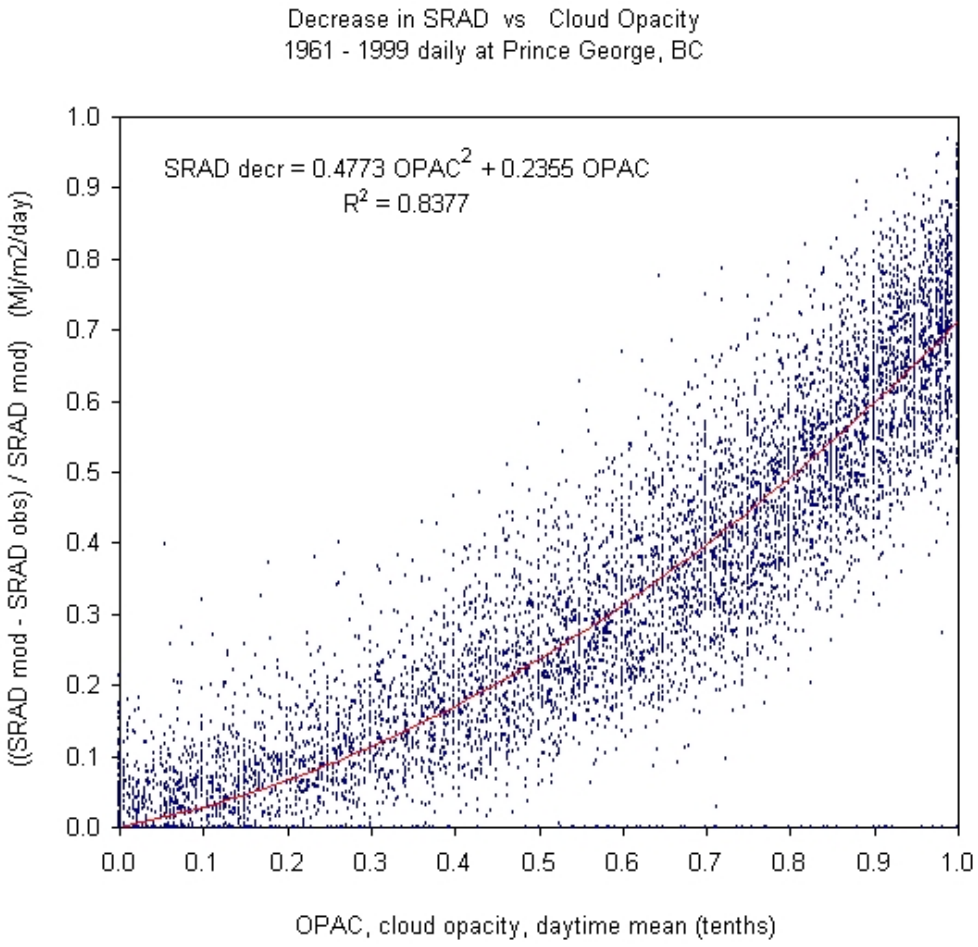

Figure 58 Decrease in solar radiation (clear sky modeled to observed) due to cloud cover (as cloud opacity) at Prince George, BC (1961-1999 daily). Fitted empirical model.

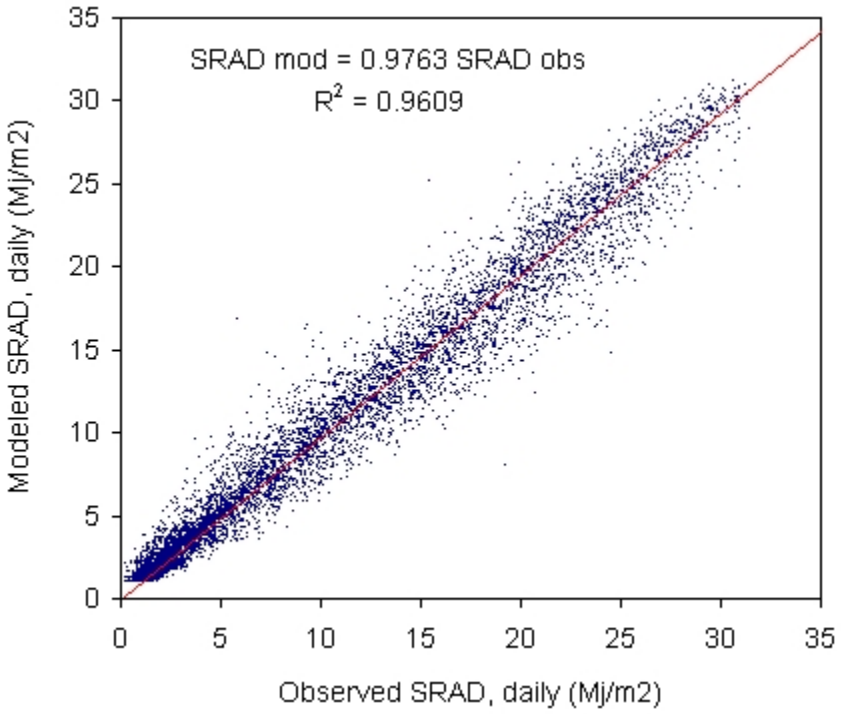

Figure 59 Solar radiation at Prince George, BC: modeled vs observed (1961-1999).

The empirical relation derived at Prince George was applied to Castlegar Airport cloud-opacity dataset and a clear-sky solar radiation model done for Castlegar location. Results are shown for the selected time period in Figure 62 and give reasonable daily solar radiation behaviour over monthly and seasonal time scales. This generated dataset was then assumed to apply also for Grand Forks (again, capturing only regional cloudiness and large weather events that would affect both Grand Forks and Castlegar). The solar radiation daily time series were synchronized by date and joined with Grand Forks precipitation and temperature time series and used as an input to Site Calibration in LARS-WG for Grand Forks.

This modeling approach was suggested to be valid by Environment Canada (pers comm, 2004). Given no other data, it is the only reasonable approach to have somewhat-realistic solar radiation for Grand Forks. Solar radiation is required to estimate evapotranspiration in HELP model. There is error involved in this methodology, but it is the best available at this time given the lack of solar radiation data. However, the air temperatures are known, and these have strong control on evapotranspiration as calculated in the HELP model.

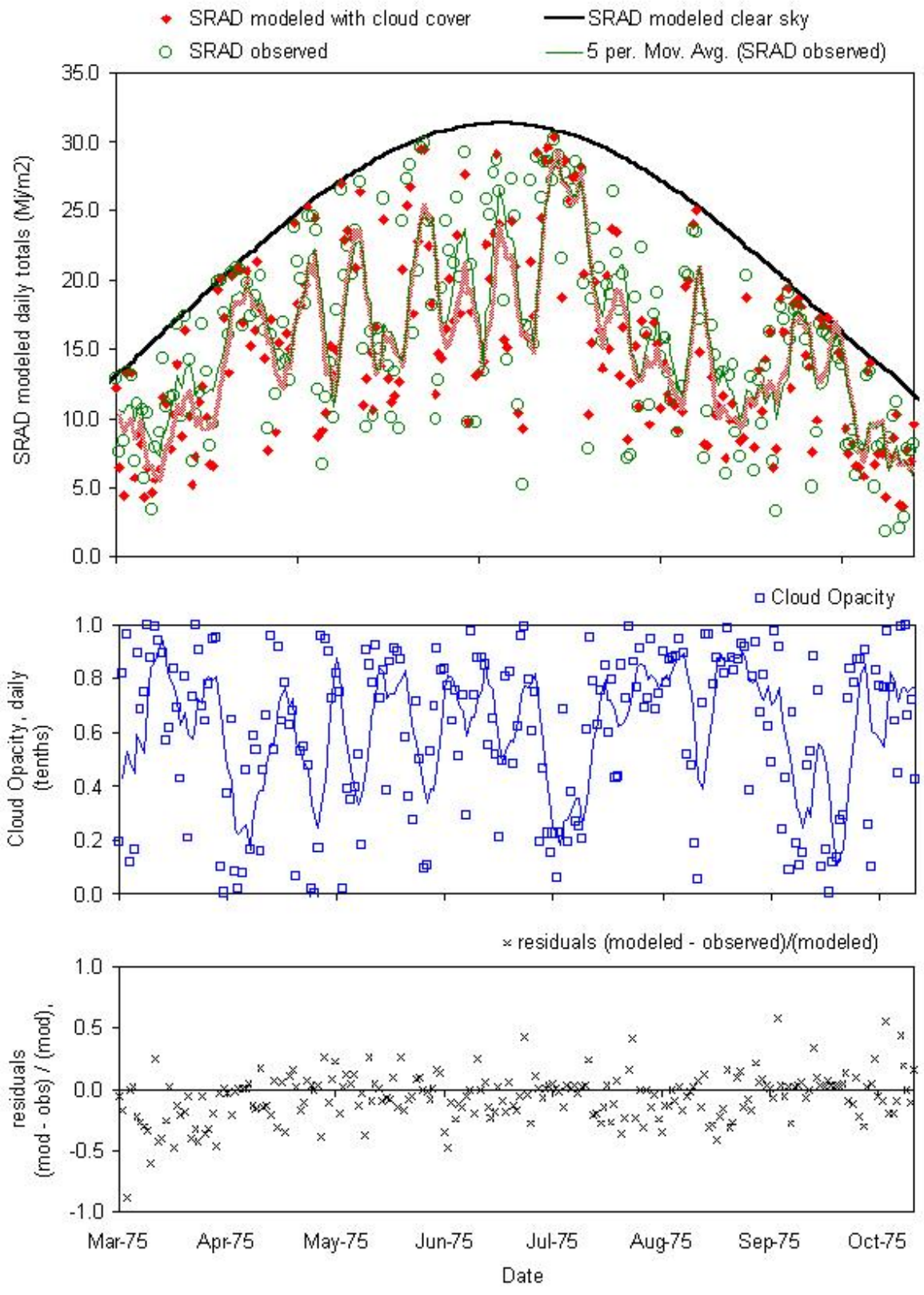

Figure 60 Solar radiation at Prince George, BC, modeled from clear sky incident solar radiation, adjusted by cloud opacity, observed, and residuals (1975).

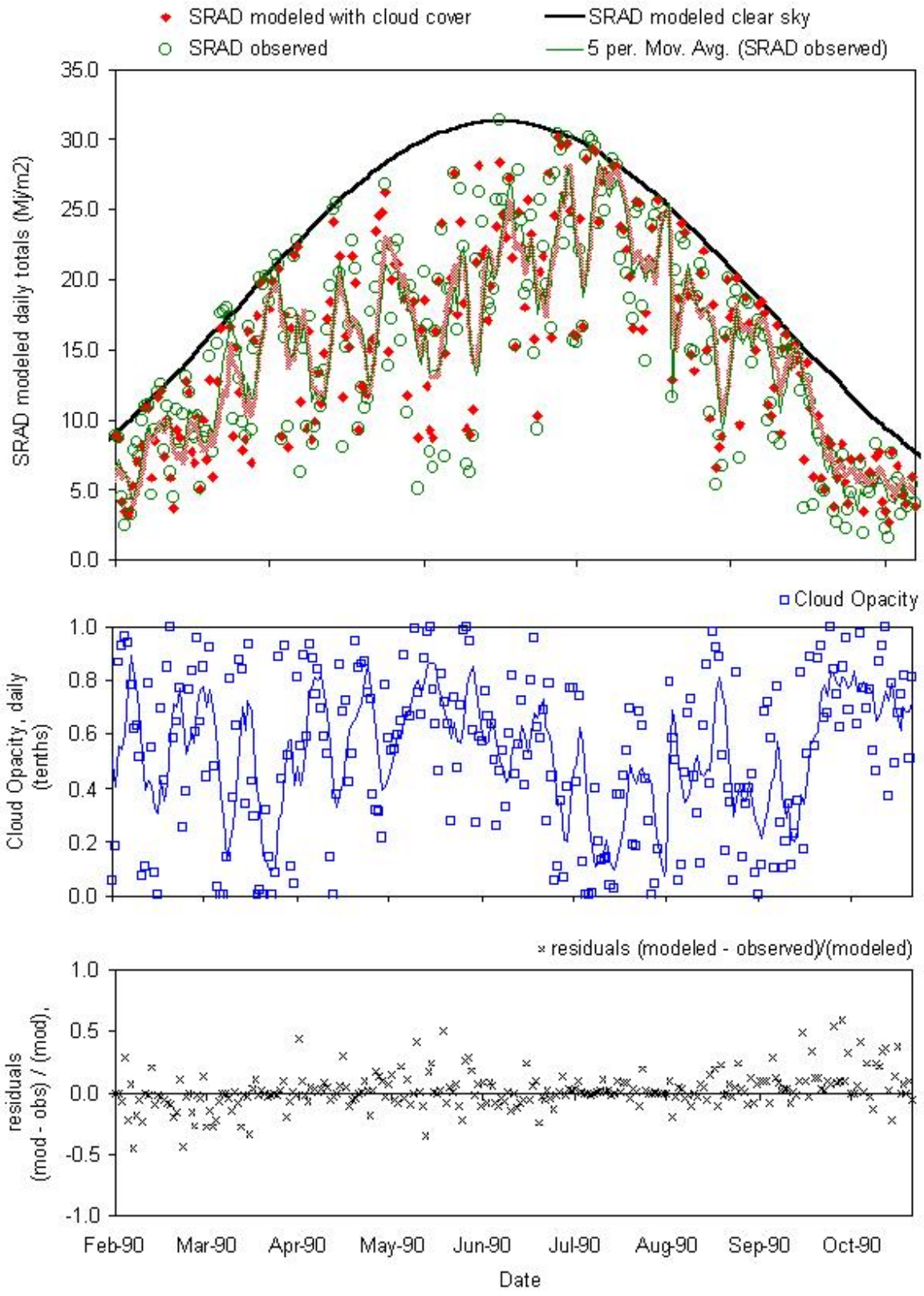

Figure 61 Solar radiation at Prince George, BC, modeled from clear sky incident solar radiation, adjusted by cloud opacity, observed, and residuals (1990).

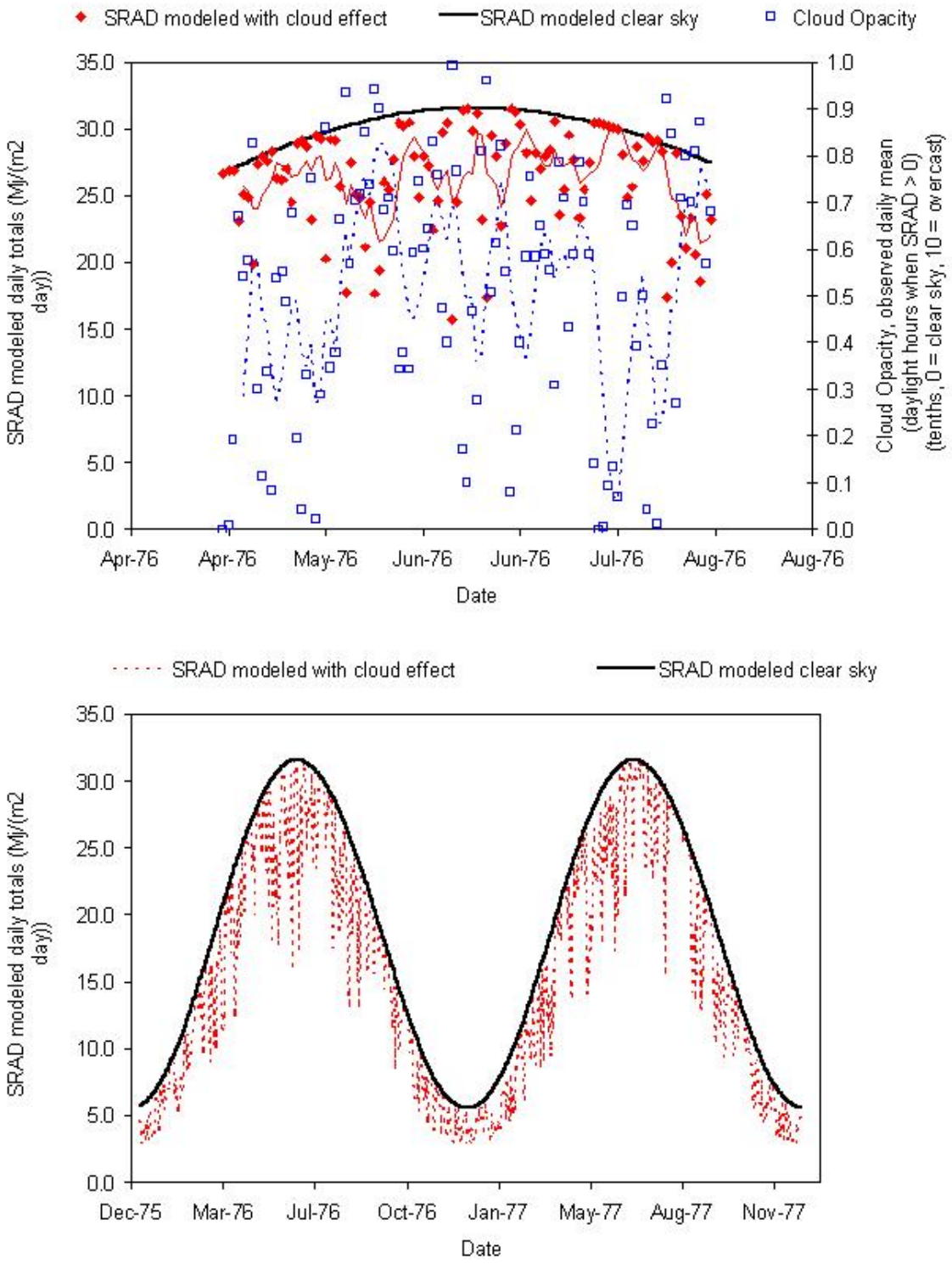

Figure 62 Solar radiation at Castlegar, BC (used for Grand Forks weather model) modeled from clear sky incident solar radiation, adjusted by cloud opacity based on solar radiation / cloud opacity model for Summerland, BC (1974-1975).

5.7. WEATHER INPUTS FOR RECHARGE MODEL

A stochastic weather generator produces artificial time series of weather data for a location based on the statistical characteristics of observed weather at that location. For each month, different model parameters are used in order to reflect seasonal variation in both the values of climatic variables and their cross-correlations (CEAA, 2003). There are two basic types of stochastic weather generator:

1. "Richardson" weather generator (WGEN) (Richardson, 1981; Richardson and Wright, 1984)
2. "Serial" (Racsko et al., 1991; Semenov et al., 1998)

Both types of weather generator require initial calibration based on observed station data (Richardson, 2000). Since WGEN is used in UnSat Suite together with HELP model for rain infiltration, a short description is necessary here. Eventually, a newer stochastic weather generator LARS-WG was used to model artificial weather series for this study.

5.7.1. RICHARDSON (WGEN) USED IN HELP: STOCHASTIC WEATHER GENERATOR

WGEN (provides daily generated values of precipitation (p), maximum temperature (tmax), minimum temperature (tmin), and solar radiation (r) for an n-year period at a given location (Richardson and Wright, 1984). The occurrence of rain on a given day has a major influence on temperature and solar radiation for the day. The approach that is used is to generate precipitation for a given day independently of the other variables. Maximum temperature, minimum temperature, and solar radiation are then generated according to whether a wet day or dry day was previously generated. The model is designed to preserve the dependence in time, the correlation between variables, and the seasonal characteristics in actual weather data for the location.

The precipitation component of WGEN is a Markov chain-gamma model. A first-order Markov chain is used to generate the occurrence of wet or dry days. When a wet day is generated, the two-parameter gamma distribution is used to generate the precipitation amount. With the first-order Markov chain model, the probability of rain on a given day is conditioned on the wet or dry status of the previous day. A wet day is defined as a day with 0.01 inch or rain or more. Thus, there are two precipitation classes (i.e., wet or dry) and these take into account precipitation occurrence on the previous day only. This process gives transition probabilities (of wet day occurring following of dry or wet day, P(W/W) or P(W/D)) calculated from observed data. If the precipitation is modeled to occur on a given day, the amount of precipitation is determined by using a predefined frequency distribution, most commonly the gamma distribution with two shape and scale parameters α and β (Wilks and Wilby, 1999). The remaining climate variables are calculated based on their correlations with each other and on the wet or dry status of each day.

Wilks (1992) suggested a methodology for adjusting the parameters of WGEN to account for climate change (change between base line and future climate). However, changes in future climate may change patterns of precipitation, and thus, any or all of these P and shape parameters (CICS, 2003). WGEN has been known for inadequate modelling of persistent wet or dry periods (Wilks and Wilby, 1999). In contrast, the serial weather generators (e.g., LARS-WG) avoid this shortcoming. These models determine sequences of dry and wet series of days, then generate other climatic variables.

The main reason why WGEN was first considered in this study is related to available software. The program UnSat Suite Plus (Waterloo Hydrogeologic Inc., 2003) is a user interface to both HELP model and to WGEN, and these operate together. UnSat Suite contains a database of weather stations, mainly in the USA, and associated WGEN parameters that date to 1984 and the work of Richardson and Wright, who developed the Fortran source code. Although the database is fully customizable, allowing the user to modify existing data or create new records to accommodate site specific weather conditions, there is no method for computing the WGEN parameters. Typically, a hydrogeologist would be interested in landfill design when using HELP model, for which it was originally developed, so a nearest weather station would be selected, then monthly precipitation and temperature means modified to a local weather station of interest that is not in the database. This approach was also followed by Allen (2001) in initial recharge estimates for Grand Forks.

However, the WGEN Markov chain gamma model parameters are not adjusted and the resulting synthetic weather is different from the observed local weather at the site of interest. Not only are the resulting time series different in frequency and amplitude of precipitation and temperature, but the monthly means do not add up to observed means, even if observed monthly means are entered into WGEN. The Grand Forks example of WGEN output compared to observed is shown in (Figure 63 and Figure 64). Generated precipitation in May, June, and November is very different from observed, and in other months there are smaller differences. This is troubling when considering climate scenario modelling applications using WGEN, because the predicted climate change amounts in monthly mean precipitation are on the order of magnitude of the differences between WGEN-modeled and observed weather, thus climate change scenarios will not be adequately resolved if so much uncertainty is present in weather generator alone.

In recharge modelling, not only are mean monthly rainfall amounts important, but also the duration / frequency of rainfall and intensity. In a semi-arid area, such as Grand Forks, recharge will occur, as will be shown by the results of this study, only when rainfall intensity is sufficient to both saturate the soil and infiltrate over the soil column depth to the water table. Thus, the length of wet and dry weather spells and rainfall intensities must be represented adequately by the weather generator that supplies inputs to HELP for recharge modelling to be accurate, especially for climate change scenarios.

Another potential problem with WGEN is solar radiation. It is generated using a simplistic approach where incident solar radiation is calculated from a function that estimates solar irradiance on cloudless sky conditions based on the location of station. For wet days, this value is simply decreased by a constant value to represent expected increase of cloudiness associated with occurrence of precipitation. However, precipitation is a daily average (including night and day), whereas incident solar radiation occurs only in daytime. Cloud cover often occurs without precipitation, and depending on local climate, intense precipitation can occur on a day with relatively large incident solar radiation averaged for a day. This is the expected case for Grand Forks, which has large number of small but intense convective rainfall events. WGEN does not take these into account at all. Since solar radiation is not measured directly at Grand Forks, it must be either estimated from cloud cover data (hourly) or other methods that modify the “cloudless sky” incident solar radiation, which can be reliably and accurately predicted for any location, while the cloud cover is the main complicating factor. Solar radiation is used to model evapotranspiration in HELP recharge model (together with temperature and precipitation). For Grand Forks, the mountainous terrain also decreases solar radiation (shortens the day) for some areas, but that is beyond the scope of complexity for this

Figure 63 Monthly precipitation normals for Grand Forks, observed and modeled in WGEN weather generator using 30 year run of historical climate.

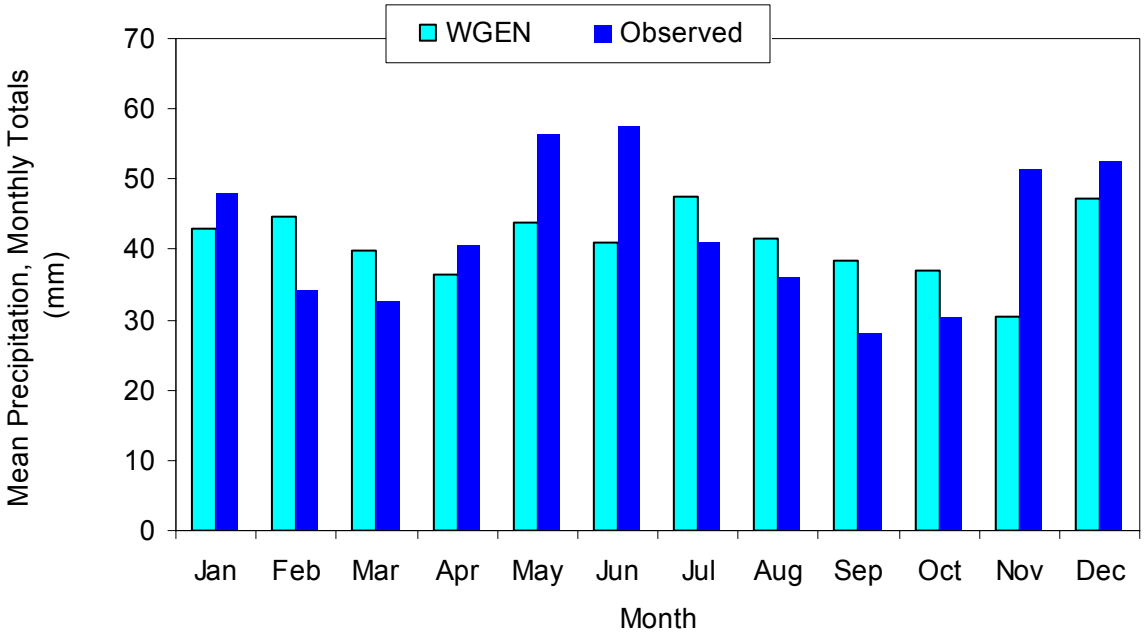

Figure 64 Monthly temperature normals for Grand Forks, observed and modeled in WGEN weather generator using 30 year run of historical climate.

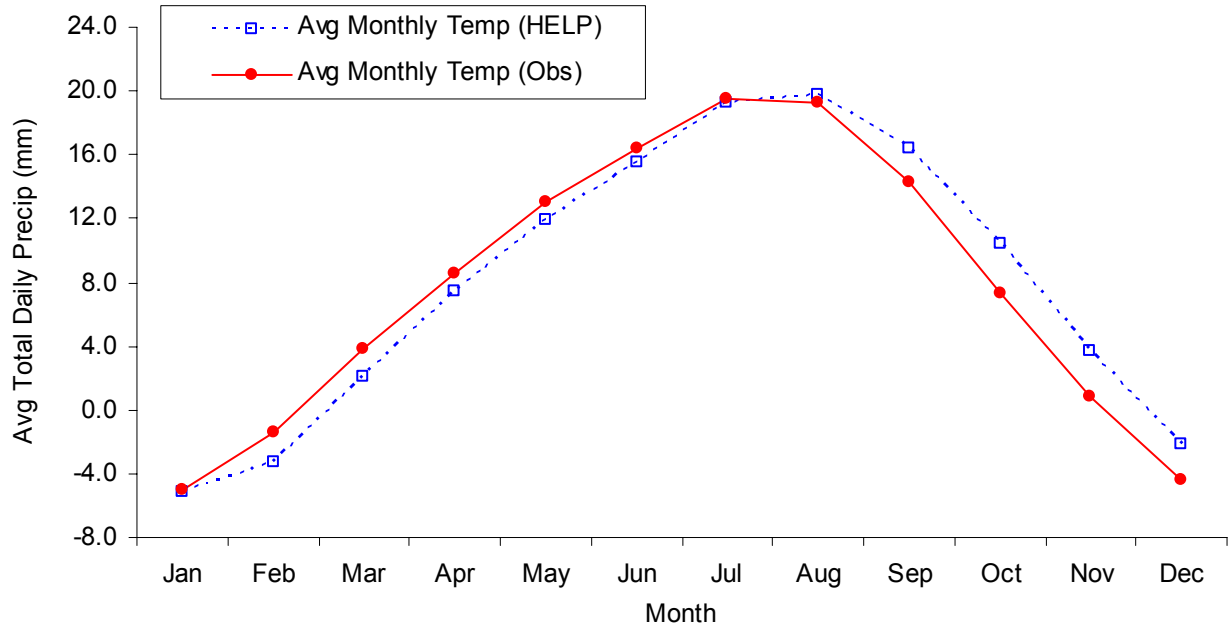

project. There are existing methods for modelling solar irradiance in presence of cloud cover, and these have been used in this project. By accounting for cloud cover, the evapotranspiration values should contain much less error than would otherwise be the case.

WGEN can be used to model weather using observed daily precipitation, temperature, and solar radiation, thus avoiding the problems with WGEN synthetic weather. However, this approach

requires that daily weather data be available from another weather generator, or downscaled in other ways, for future climate scenarios. In this study, WGEN is used only to provide weather input to the HELP model, but using historical observed data, and future "generated" daily data from other sources. That source will be the LARS-WG weather generator.

In WGEN, customized weather data can be entered manually, or imported from standard National Oceanic and Atmospheric Administration (NOAA) or Canadian Climate Centre (CCC) formats. In this case, CCC format was used. There was a limitation in UnSat Suite where only 2 years of data could be imported at any time, although multiple 2-year long daily data sets could be imported separately to make a 20 year weather record available in WGEN for weather inputs to HELP recharge model. Therefore, WGEN will be by-passed by writing daily weather directly to weather files for HELP model, in the same format at WGEN would have created. The weather input files for HELP have this naming convention:

_weather1.dat - Daily Precipitation,
_weather2.dat - Mean Daily Temperature,
_weather3.dat - Daily Solar Radiation, and
_weather4.dat - Evapotranspiration Parameters.

Formatting the first three files is 10 numbers in a row, 37 rows for a year. Custom code was written to write data into this format for precipitation and temperature. The evapotranspiration parameters are constants.

5.7.2. LARS-WG: STOCHASTIC WEATHER GENERATOR WITH SERIAL APPROACH TO PRECIPITATION

A stochastic WG allows the generation of synthetic daily weather data which will incorporate these changes, but which will be different from the original time series on a day-to-day basis, although the statistical characteristics will be (almost) identical. It also allows changes in climate variability to be incorporated, and not just changes in mean values. This is very important if actual predicted weather (best scientific guess) are to be simulated, and not just what-if scenarios of weather change (e.g., by certain percentage of mean value).

Stochastic weather generators were originally developed for two main purposes:

1. To provide a means of simulating synthetic weather time-series with statistical characteristics corresponding to the observed statistics at a site, but which were long enough to be used in an assessment of risk in hydrological or agricultural applications.

2. To provide a means of extending the simulation of weather time-series to unobserved locations, through the interpolation of the weather generator parameters obtained from running the models at neighbouring sites.

In LARS-WG manual, Semenov and Barrow (2002) noted that a stochastic weather generator is not a predictive tool that can be used in weather forecasting, but is simply a means of generating time-series of synthetic weather statistically 'identical' to the observations. New interest in local stochastic weather simulation has arisen as a result of climate change studies. At present, output from global circulation models (GCMs) is of insufficient spatial and temporal resolution and reliability to be used directly in impact models. A stochastic weather generator, however, can serve as a computationally inexpensive tool to produce multiple-year climate change scenarios at the daily time scale, which incorporates changes in both mean climate and in climate variability (Semenov & Barrow, 1997).

LARS-WG is a stochastic weather generator which can be used for the simulation of weather data at a single site (Racsko et al., 1991; Semenov et al., 1998; Semenov & Brooks, 1999), under both current and future climate conditions. These data are in the form of daily time-series for a suite of climate variables, namely, precipitation (mm), maximum and minimum temperature (°C) and solar radiation (MJm^{-2} day^{-1}).

LARS-WG is based on the series weather generator described in Racsko et al. (1991). It utilizes semi-empirical distributions (see Figure 65) for the lengths of wet and dry day series, daily precipitation and daily solar radiation. The simulation of precipitation occurrence is modelled as alternate wet and dry series, where a wet day is defined to be a day with precipitation > 0.0 mm. The length of each series is chosen randomly from the wet or dry semi-empirical distribution for the month in which the series starts. In determining the distributions, observed series are also allocated to the month in which they start. For a wet day, the precipitation value is generated from the semi-empirical precipitation distribution for the particular month independent of the length of the wet series or the amount of precipitation on previous days. Daily minimum and maximum temperatures are considered as stochastic processes with daily means and daily standard deviations conditioned on the wet or dry status of the day (Semenov and Barrow, 2002).

Such daily output fits perfectly in the recharge modelling scheme because the recharge is based on step-like climate scenarios, whereas in each scenario ("step"), the climate is the same and equivalent to predicted by GCMs / downscaled / stochastic-generated, and then recharge is averaged for the scenario by month. The GCMs ensure that physical processes are modeled spatially (on very coarse scale) and, more importantly, temporally. The downscaling ensures that processes and resulting values of variables are as close to site-specific as possible, while preserving the GCM predictions. The stochastic weather ensures that daily values of variables are realistic, consistent, site specific, and preserve both values and variability predicted to change from current to future climate scenarios by GCMs. The recharge model (HELP model in this project) uses daily inputs of weather to calculate daily recharge through soil columns. Thus, appropriate frequency, magnitude and duration of precipitation and other events are modeled. Typically 30 or more years are modeled within each climate scenario, and then monthly averages are computed to represent monthly variation of recharge that is representative of the climate regime being modeled. Because the stochastic weather generator requires more than 100 years of daily weather to be created to begin approaching the statistics specified for a climate scenario (and local weather), the recharge model will receive also that long time period of simulated weather, and the averages will be representative. See graphs comparing climate scenario inputs to LARS-WG model and outputs from 100 y weather run in Figure 69. The length of weather time series is not meant to model actual changing climate year-to-year, but to model climate change step-wise for each scenario and to generate long enough weather time series to preserve and properly represent statistical properties for the site and predicted climate for the scenario.

The groundwater model will be "transient", but only on monthly time steps due to computational limitations, although 10 day time steps could be modeled with some effort. Since most of the GCM summaries, downscaling tools, and stochastic weather generators are set-up for adjusting monthly statistics for daily weather, it makes sense to model transient groundwater flow also on monthly time steps. The actual groundwater flow model has more time steps, but inputs are modified and outputs generated on monthly time steps. Thus, monthly recharge is required as an input for each climate change scenario.

5.7.3. METHODOLOGY

1) extract daily P (and other if available) from the GCM model
2) site analysis to each GCM scenario
3) Qtest and compare time series
4) Calculate change in P variability between scenarios

Data were extracted from CGCM1 daily output, because that was available at the time for downloading. Data were obtained from Zwiers (2001). Available were three 21-year time series of daily precipitation amounts simulated by the CGCM1 climate model in each of three 21-year "windows" representing the climates of 1975-95, 2040-60 and 2080-2100. That is, a total of 3x (3x21)=189 years of simulated daily precipitation data are available. This climate modelling case was run to explore the changes in extremes in precipitation over Canada (Kharin and Zwiers, 2000).

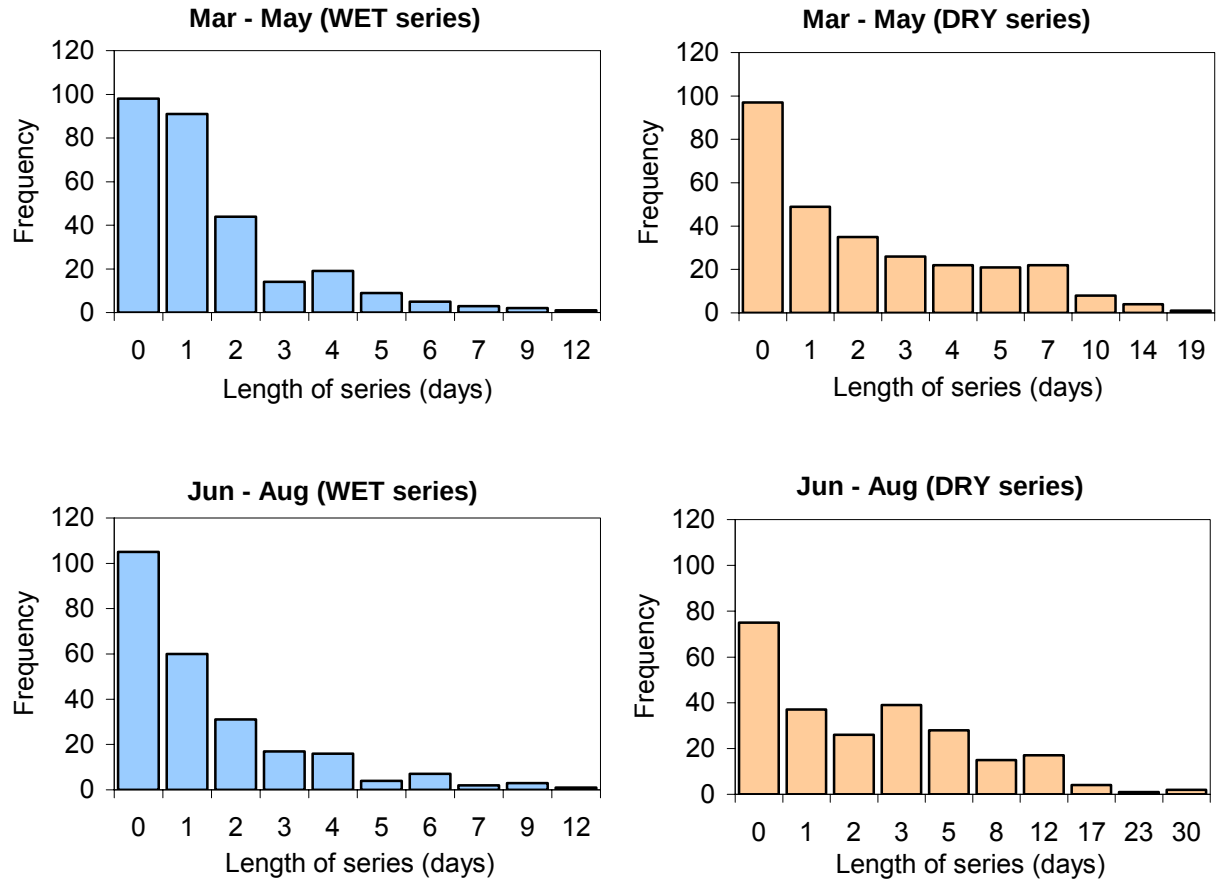

Figure 65 Precipitation distributions as WET and DRY series generated by LARS-WG for Grand Forks. The histograms show frequency distributions by length of days of WET / DRY series for two time periods Mar – May and Jun – Aug. This corresponds to 20 year weather calibrated to 1975-1995 observed.

5.7.4. CLIMATE SCENARIOS IN LARS-WG FROM SDSM DOWNSCALING

Table 17 Climate scenario input (scenario file example) from SDSM to LARS-WG stochastic weather generator. Shown is the base case current climate scenario and three future climate scenarios for Grand Forks, BC.

m.rain = precipitation relative change (future / base) or (base / base)
wet = WET spell length relative change
dry = DRY spell length relative change
tem = temperature absolute change
sd = standard deviation of temperature relative change
rad = solar radiation absolute change

[NAME]
base

[DATA]	m.rain	wet	dry	tem	sd	rad
Jan	1.00	1.00	1.00	0.00	1.00	0.00
Feb	1.00	1.00	1.00	0.00	1.00	0.00
Mar	1.00	1.00	1.00	0.00	1.00	0.00
Apr	1.00	1.00	1.00	0.00	1.00	0.00
May	1.00	1.00	1.00	0.00	1.00	0.00
Jun	1.00	1.00	1.00	0.00	1.00	0.00
Jul	1.00	1.00	1.00	0.00	1.00	0.00
Aug	1.00	1.00	1.00	0.00	1.00	0.00
Sep	1.00	1.00	1.00	0.00	1.00	0.00
Oct	1.00	1.00	1.00	0.00	1.00	0.00
Nov	1.00	1.00	1.00	0.00	1.00	0.00
Dec	1.00	1.00	1.00	0.00	1.00	0.00

[END]

[NAME]
GF_CGCM1_2010_2039

[DATA]	m.rain	wet	dry	tem	sd	rad
Jan	1.40	1.33	0.81	0.74	0.94	0.14
Feb	1.14	1.31	0.95	0.62	0.98	0.03
Mar	1.12	1.21	1.07	0.94	1.09	0.17
Apr	1.13	1.06	1.12	1.53	1.22	0.26
May	0.90	0.97	1.21	2.19	0.91	0.39
Jun	1.04	0.92	1.30	1.71	0.86	-0.08
Jul	0.83	1.10	1.01	1.00	0.78	0.15
Aug	1.19	1.27	0.95	0.41	0.85	-0.02
Sep	1.03	0.87	0.75	0.91	0.84	-0.24
Oct	0.97	1.17	1.24	1.27	0.94	0.11
Nov	1.04	1.17	1.29	1.33	0.84	0.00
Dec	1.21	1.02	0.82	1.15	0.92	-0.03

[END]

[NAME]
GF_CGCM1_2040_2069

[DATA]	m.rain	wet	dry	tem	sd	rad
Jan	1.44	1.49	0.87	2.18	1.27	0.19
Feb	1.28	1.38	0.91	2.30	1.05	0.05
Mar	1.37	1.30	0.90	2.13	1.22	0.27
Apr	1.45	1.14	0.94	3.48	1.19	0.40
May	1.00	0.83	1.16	4.07	0.96	0.40
Jun	0.86	0.99	1.31	3.63	0.82	-0.19
Jul	0.73	1.00	1.15	1.90	0.66	0.26
Aug	1.11	1.21	0.96	1.10	0.71	-0.17
Sep	0.92	1.23	0.80	2.74	0.78	-0.44
Oct	1.03	1.01	1.28	3.80	0.97	0.25
Nov	1.15	1.39	1.44	4.03	0.84	0.05
Dec	1.39	1.11	0.60	3.88	0.78	-0.07

[END]

[NAME]
GF_CGCM1_2070_2099

[DATA]	m.rain	wet	dry	tem	sd	rad
Jan	1.71	1.42	0.81	5.11	1.12	0.10
Feb	1.51	1.48	0.90	4.99	1.02	0.04
Mar	1.67	1.58	0.76	4.87	1.37	0.25
Apr	1.49	1.14	1.07	6.08	1.01	0.34
May	1.19	0.95	1.23	6.57	0.94	-0.31
Jun	0.65	0.84	1.37	5.82	0.65	-0.36
Jul	0.57	0.89	1.30	2.51	0.60	0.31
Aug	1.10	1.32	0.84	0.97	0.61	-0.56
Sep	1.27	1.53	0.71	3.93	0.55	-0.58
Oct	0.88	0.92	1.49	6.63	0.88	0.50
Nov	1.22	1.21	1.24	7.19	0.88	0.20
Dec	1.46	1.17	0.71	6.19	0.99	-0.12

[END]

5.8. CALIBRATION OF LARS-WG WEATHER GENERATOR

Model calibration notes and procedures are taken from LARS-WG manual, and excerpts are used here to give an overview of the calibration process.

Model calibration in LARS-WG involves a "site analysis" procedure whereby the observed weather data are analyzed to determine their statistical characteristics. LARS-WG is able to simulate artificial weather data based on as little as a single year of observed weather data. However, as the simulated weather data will be based on these observed data, the more data used the closer LARS-WG is likely to match the true climate for the site in question. Use of at least 20-30 years of daily weather data is recommended. In order to be able to capture some of the less frequent climate events (e.g., droughts) as long an observed record as possible should be used.

Note that unlike the DRY/WET series for precipitation, the air temperature is modelled in LARS-WG by using Fourier series, i.e., the annual cycle of temperature is described using sine and cosine curves. These curves can be constructed with information pertaining to only a small number of parameters (i.e., the mean value, amplitude of the sine/cosine curves and phase angle). Both maximum and minimum temperature are modelled more accurately by considering wet and dry days separately.

The QTest option carries out a statistical comparison of synthetic weather data generated using LARS-WG with the parameters derived from observed weather data. In order to ensure that the simulated data probability distributions are close to the true long-term observed distributions for the site in question, a large number of years of simulated weather data should be generated. The synthetic data are then analyzed, and parameter files produced which contain probability distribution, mean and standard deviation information.

The χ^2 , t- and F- tests assume that the observed weather is a random sample from some existing distribution, which represents the 'true' climate at the site. In the absence of any changes in climate, this true distribution could be estimated accurately from observed data over a very long time period. The simulated climate distribution is estimated from a long run of synthetic weather data generated by LARS-WG using the parameter files output during the model calibration process. The statistical tests carried out in QTest look for differences between the simulated climate and the 'true' climate. Each of the tests considers a particular weather statistic and compares the values from the observed and simulated data. All of the tests calculate a p-value, which is used to accept or reject the hypotheses that the two sets of data could have come from the same distribution (i.e., there is no difference between the 'true' and simulated climate for that variable). Therefore, a very low p-value means that the simulated climate is unlikely to be the same as the 'true' climate. If the p-value is not very low, it is plausible that the climates are the same, although statistical tests cannot prove this.

5.8.1. REASONS FOR DISCREPANCIES IN MODELLED WEATHER TO OBSERVED

Significant differences between simulated and observed data are likely to be due to LARS-WG smoothing the observed data. For example, LARS-WG fits smooth curves to the average daily mean values for minimum temperature and for maximum temperature. It does this in order to eliminate as much as possible the random noise in the observed data in order to get closer to the actual climate for the site. Differences are likely to be due to departures of the observed values from the smooth pattern for the data.

Random variation in the observed data: In the above example, May could have been unusually cold in the years covered by the observed data, and therefore, the data would not be typical of the true climate at that site. Random variations from month to month are likely to be greater when there is less observed data. If the differences are due to such random variations, the smoothing employed by LARS-WG will mean that the simulated weather is likely to be closer to the actual climate for the site than the observed data, and so the simulated data can be accepted. [LARS-WG assumes that the observed climate is stationary; if there are any trends in the observed data then these need to be removed before LARS-WG is used.]

Climate anomalies: The variations in the data may be due to some unusual climatic phenomenon and so the data may actually be typical of the climate for the site. It is likely that in this case LARS-WG will not match the climate for that part of the year. In this case, careful consideration is needed of the effect on your application of the differences between LARS-WG and the typical climate.

5.8.2. CALIBRATION TO RAINFALL PARAMETERS

In Figure 66 the mean monthly rainfall values for LARS-WG generated weather at Grand Forks are within 2 mm/month (within 5%) or closer for all months (compared to 40-50 mm/month precipitation values). The seasonal variation in rainfall shows very good fit to observed rainfall normals. Variability of rainfall (standard deviation of monthly precipitation) is also preserved in synthetic weather, but there are relatively small discrepancies between modeled and observed precipitation in May-Jul and Nov. This “error” is related to ability of LARS-WG to model rainfall intensities and wet/dry weather time series. The model’s ability to simulate WET and DRY series of weather, and extreme weather spells, was evaluated as suggested in LARS-WG manual and results are in Table 18. The chi-test gave very good results for WET/DRY precipitation series (small 1-p values for all seasons), indicating very good fit of modeled to observed data. The model performance for extreme weather spells was much worse. The science of weather generation is still evolving and even such models as LARS-WG cannot properly replicate the occurrence of rare and extreme weather spells (of cold and hot temperatures) because these are site-specific and occur due to unique weather conditions. However, the amounts of precipitation are not likely to be affected by the extreme weather events, even if poorly modeled. Precipitation distribution (histograms by month) were very well reproduced in the LARS-WG synthetic weather according to chi-test.

Figure 66 Monthly Rainfall at Grand Forks, BC, observed for period of record 1975-1995 (base climate scenario) and modeled with stochastic LARS-WG weather generator (20 year run): (a) Precipitation Amounts as mean monthly precipitation (b) Precipitation Variability as standard deviation of mean monthly precipitation.

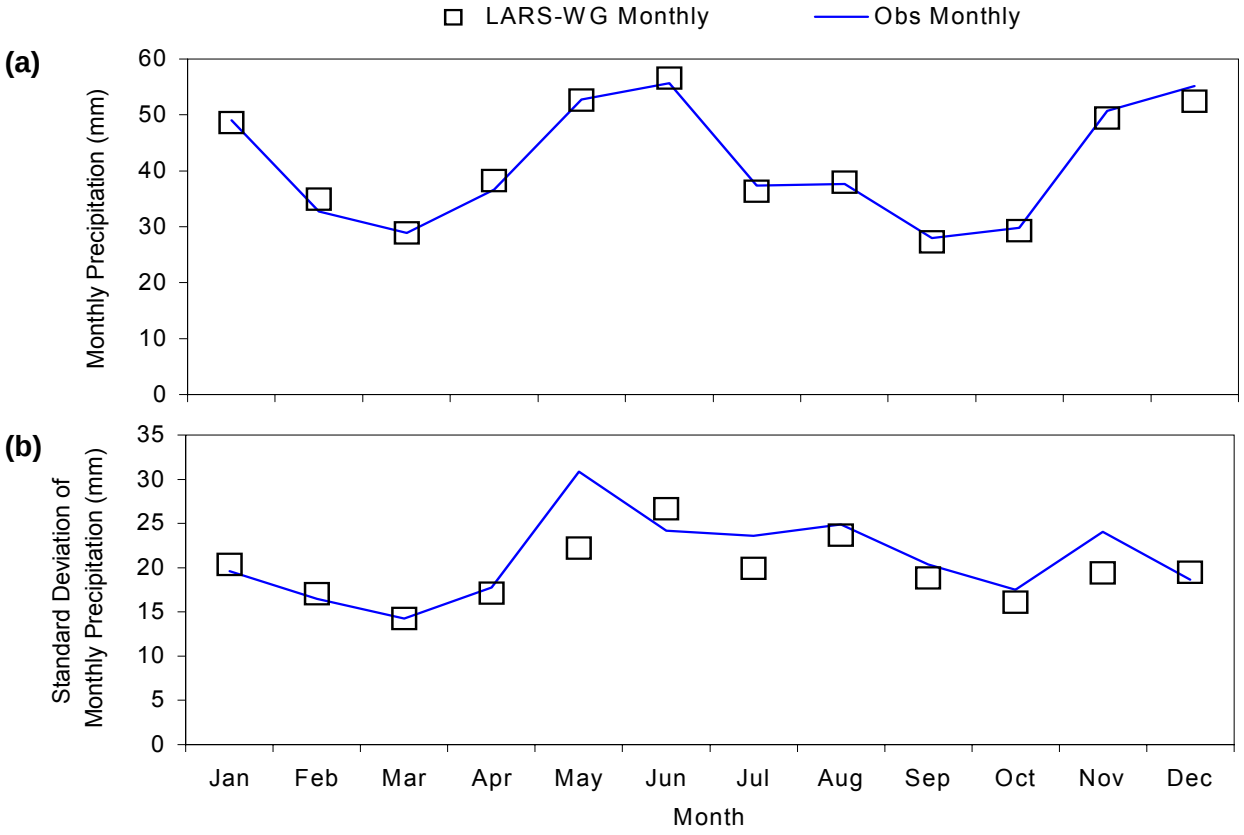

Table 18 Results of calibration of LARS-WG synthetic weather generator for Grand Forks precipitation. Q-test for WET / DRY series, extreme weather spells, and precipitation distributions by month (comparing synthetic weather and ability of LARS-WG to generate weather to observed weather).

WET / DRY precipitation series

Months	Weather Series	df	chi^2	1- p-value	Comments
Dec - Feb	WET	9	0.310	0.000	very good fit
	DRY	9	3.170	0.043	very good fit
Mar - May	WET	9	0.460	0.000	very good fit
	DRY	9	1.950	0.008	very good fit
Jun - Aug	WET	8	0.120	0.000	very good fit
	DRY	9	1.110	0.001	very good fit
Sep - Nov	WET	9	0.660	0.000	very good fit
	DRY	9	2.210	0.012	very good fit

Extreme Weather Spells

Months	Weather Series	df	chi^2	1- p-value	Comments
Dec - Feb	FROST	7	9.170	0.759	moderate fit
	HOT	0	0.000	0.000	no hot spells in winter
Mar - May	FROST	10	15.500	0.885	poor fit
	HOT	2	3.280	0.806	moderate fit
Jun - Aug	FROST	1	0.000	0.000	no frost in summer
	HOT	7	45.870	1.000	poor fit
Sep - Nov	FROST	11	25.820	0.993	poor fit
	HOT	3	10.590	0.986	poor fit

Precipitation distribution

Months	df	chi^2	1- p-value	Comments
Jan	6	0.770	0.007	very good fit
Feb	8	0.650	0.000	very good fit
Mar	10	1.980	0.003	very good fit
Apr	9	0.870	0.000	very good fit
May	8	0.660	0.000	very good fit
Jun	8	0.870	0.001	very good fit
Jul	6	0.920	0.011	very good fit
Aug	8	0.330	0.000	very good fit
Sep	9	0.480	0.000	very good fit
Oct	9	1.490	0.003	very good fit
Nov	9	0.870	0.000	very good fit
Dec	9	1.900	0.007	very good fit

* in the original LARS-WG output, low chi2 and p near 1.00 indicate good fit
the 1 - p-value was done to avoid confusion, where in most statistical tests low p-value indicates low probability that the result is due to random error

5.8.3. CALIBRATION TO TEMPERATURE PARAMETERS

The stochastic weather generator reproduced air temperatures very precisely as calibrated from the observed records. Monthly minimum and maximum temperatures (averages) of modeled and observed are almost identical on a graph in Figure 67 (a). Daily minimum and maximum temperature variability (standard deviation) were calculated both for daily values and for monthly (mean) values. In both cases, the modeled temperature variability was very close to observed. In winter months, LARS-WG produced 0.5 to 1.0 C cooler minimum temperatures than observed, when comparing variability in monthly values.

Figure 67 Monthly mean air temperature at Grand Forks, BC, observed for period of record 1975-1995 (base climate scenario) and modeled with stochastic LARS-WG weather generator (20 year run): (a) Mean Monthly Temperature as monthly averaged mean daily temperature (b) Temperature Variability as standard deviation of mean daily temperature, averaged monthly.

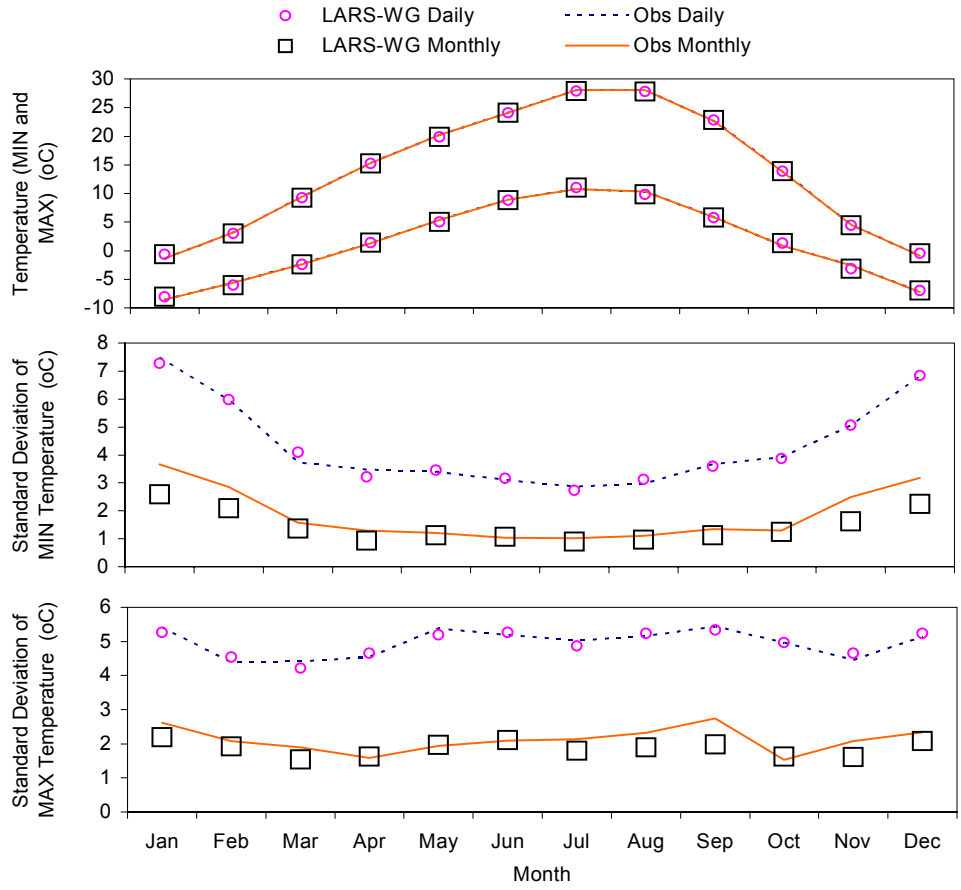

(a)

(b)

(c)

5.8.4. CALIBRATION TO SOLAR RADIATION PARAMETERS

Solar radiation was reproduced very well in stochastic weather of LARS-WG output. Mean solar radiation values in Figure 68 (b) in weather generator output were within 1% of observed values. Daily variability in daytime solar radiation was also reasonably well preserved in stochastic weather model, although daily values were under-predicted by 5 to 10%, compared to observed. This under-prediction might cause small error in evapotranspiration estimates in HELP recharge model, once the LARS-WG weather is input into HELP.

Figure 68 Monthly and daily solar radiation (based on daily values) at Grand Forks, BC, modeled using cloud opacity and clear sky radiation for period of record 1975-1995 (base climate scenario) and modeled with stochastic LARS-WG weather generator (300 year run): (a) Monthly mean of daily values of Solar Radiation (b) Solar Radiation Variability as standard deviation of daily values and monthly means (of daily values).

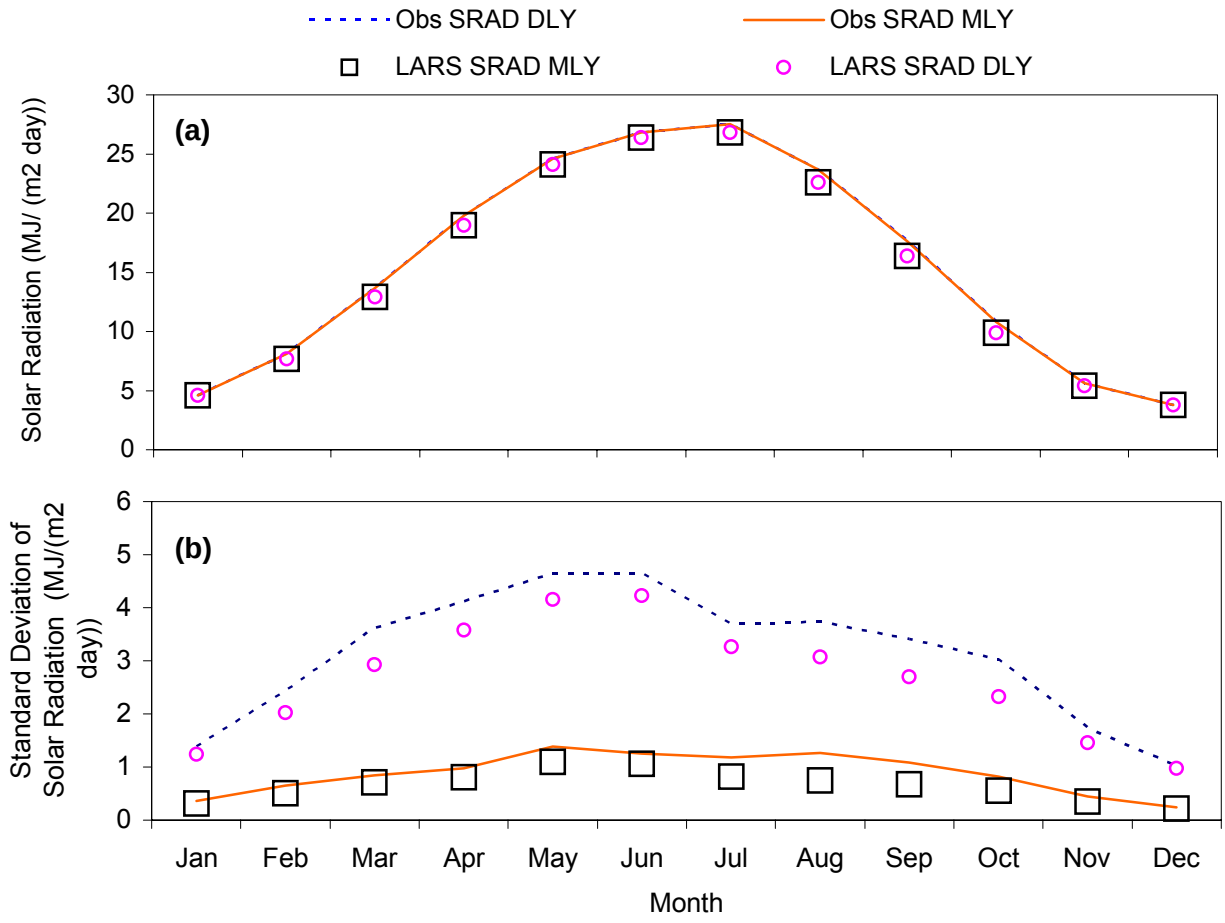

Figure 69 Comparing scenario input and LARS-WG output of 100 years of synthetic weather for 2010-2039 climate scenario: relative change in monthly precipitation, temperature, and solar radiation parameters compared to observed as test of LARS-WG model performance for Grand Forks weather generation.

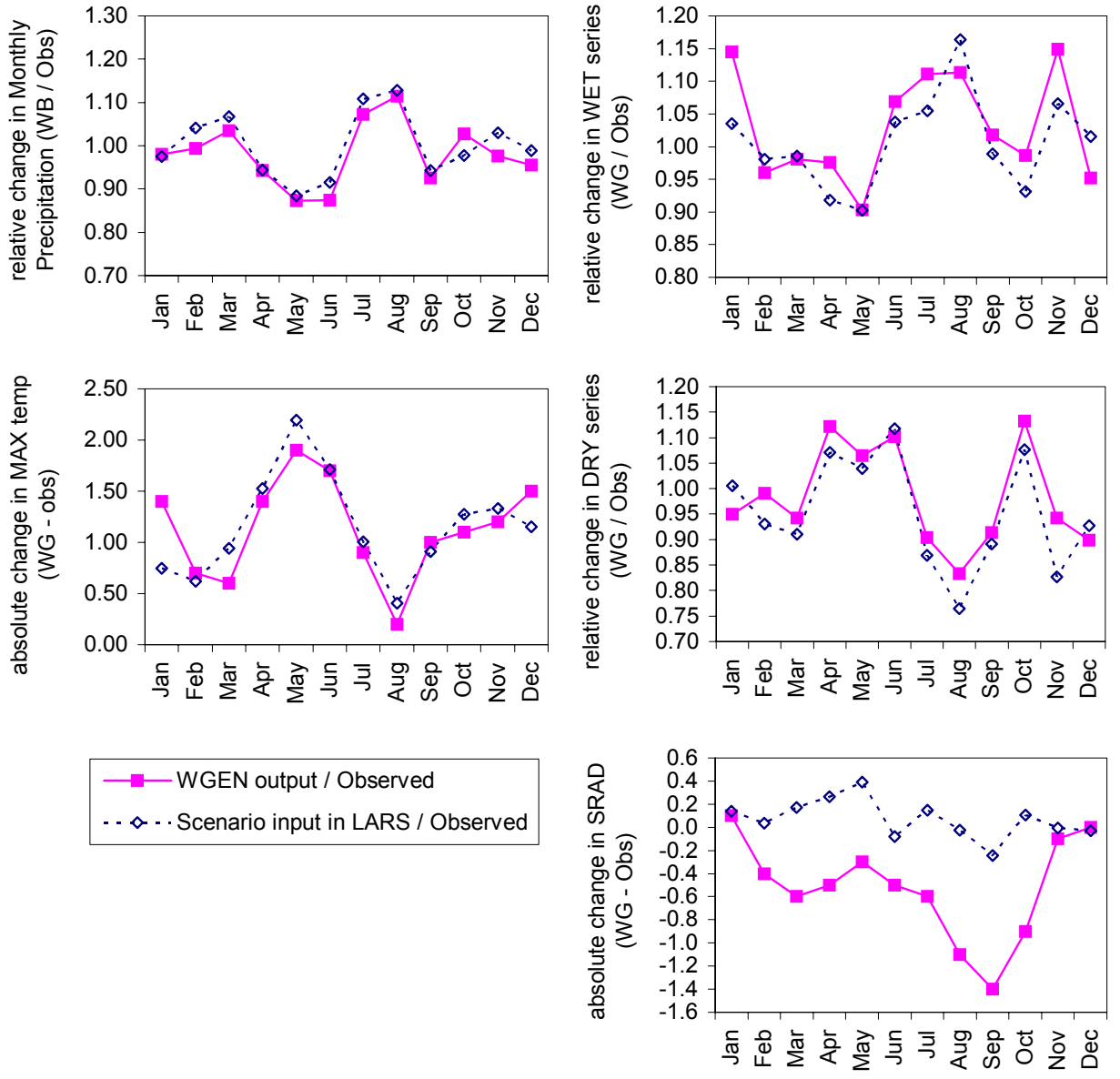

5.9. METHODOLOGY FOR RECHARGE MODELLING USING HELP

There are many physical properties of the subsurface that affect recharge to an unconfined aquifer and, as in other properties, they have three-dimensional distribution, and some change with time as well such as soil moisture and depth to water table. The available data constrains the choice of parameters with relatively good ground truthing, and other parameter values must be inferred from other information and essentially estimated.

The ground truth data currently available includes the list below. The parameters are presumably listed in order of importance in each group, but that will be explored further in HELP model sensitivity analysis to each. Usually, the type of local climate and, more specifically, seasonal distribution of precipitation will have dominant control on aerial recharge (at least the maximum possible recharge). The aquifer properties will control the actual amount of recharge into the aquifer, where the aquifer properties are assumed not to change with time, except unsaturated zone thickness, which will fluctuate seasonally. Ground surface properties, such as vegetation cover, have strong seasonality, and irrigation practices might have strong effect on local recharge rates.

Climatic variables:

1) precipitation (both depth and rate are important)
2) evapotranspiration
3) surface runoff

Aquifer media properties:

1) unsaturated zone hydraulic properties from lithology at point locations (estimated equivalent saturated hydraulic conductivity)
2) unsaturated zone thickness (depth to water table)
3) soil types
4) soil thickness
5) elevation and slope of ground surface (that affect runoff)

Ground surface properties (human modified):

1) vegetation cover (that affect evapotranspiration)
2) irrigation rates and areas affected (return flow to recharge)

There is a degree of uncertainty in each of these properties because data come from various sources and formats, which are discussed below. The authors of this report believe that the recharge model presented here is a best scientific guess at the actual values, and the only way to overcome the limitations of the assumptions, and to decrease uncertainty, is to collect more field data.

5.9.1. PREVIOUS WORK ON RECHARGE MODELS FOR GRAND FORKS AQUIFER

Previous recharge modelling for Grand Forks aquifer was done by Allen (2000), who used HELP model and WGEN weather to model mean annual recharge to surficial unconfined aquifer at Grand Forks, BC. The purpose of the model was to supply recharge values for steady-state groundwater flow model, which was then used to investigate sensitivity of groundwater levels to different climate change scenarios (thus, recharge scenarios). At the time, the Grand Forks aquifer model consisted of several hydrostratigraphic units (layers of similar hydraulic properties).

In all cases, 10 years of weather were generated for HELP scenarios. For the base case model of recharge, Allen (2000) estimated recharge as spatially uniform of 135.46 mm/year or about 28% of mean annual precipitation (see also Piteau and Associates, 1993). Recharge was computed from annual water balance in HELP, and then averaged over 10 years of results.

During sensitivity analysis, Allen (2000) discovered that the number of aquifer / aquitard layers specified in HELP does change the recharge estimates significantly (e.g. by 50%). At the time, on the basis of the available information, Allen (2000) concluded that it was not possible to determine which one better represents the actual recharge to the system. In other calibrations of HELP model, it was found that initial moisture content also caused significant changes (20%) on resulting mean annual recharge, but no other variables were investigated, and the time scale was annual which hides most of the temporal variation in recharge. Spatial variation of recharge was not accounted for at all, except for one scenario where effect of change in hydraulic conductivity was evaluated.

Allen (2000) was mostly interested in change in annual recharge at different climate scenarios, which were specified by shifted monthly precipitation and temperature normals in the WGEN. All the scenarios had the same HELP parameters (initial moisture, soil column configuration, etc). Here "low" T refers to small increase (1ºC) in predicted Temperature in Grand Forks due to doubling of CO_2 and "high" T refers to large change (3.5ºC). Similarly with precipitation, "low" refers to less than 15% increase, and "high" refers to 40% increase. Mean annual recharge was computed as:

Scenario	Recharge (mm)
Low T / low P:	127.93
High T / High P	149.71
High T / Low P	122.75
Low T / High P	170.28

5.9.2. NEW APPROACH TO RECHARGE MODELLING

A previous study that encompassed detailed aquifer architecture mapping and vulnerability mapping using the DRASTIC method (Allen et al., 2003) let to the development of a series of maps of showing variations in aquifer thickness, variations in aquifer media and properties over space, and variability in surficial materials, including soils. Compilation of this information has allowed for much more elaborate recharge modelling than had previously been possible. Thus, this study includes several "improvements" in methodology of recharge model for Grand Forks. First, several of the major factors that affect recharge are accounted for:

1) soil properties
2) hydraulic conductivity
3) depth of unsaturated zone (depth to water table)

Hydraulic conductivity was averaged from a completely updated and standardized well litholog database, and averages represent the ensemble of materials present, and their vertical distribution. Furthermore, hydraulic conductivity was interpolated over the unsaturated zone depth to give spatial distribution (as best as could be derived from available data). Soils were also spatially distributed, and so was the depth of unsaturated zone (depth to water table).

The temporal variation of precipitation was accounted for by calculating monthly recharge values (as opposed to annual only), which give relatively good temporal distribution of recharge

and capture the main inter-annual variation. Much better precipitation and other climate data were used (at higher temporal resolution), and a much more detailed climatological study was done to represent the climate change scenarios. The new LARS-WG weather generator allowed for better representation of dry and wet spells and provides a better fit to observed data. Higher resolution CRCM results, and stochastic weather from LARS-WG were used for climate scenarios:

1) monthly precipitation and other climatic variables
2) calibrated LARS-WG for weather generation
3) use of higher resolution CRCM for climate change scenarios
4) accounted for both change in mean values and variability of precipitation
5) overall much better climatic data input to HELP model

The use of spatial analysis tools in GIS environment allowed for spatial and temporal data integration. Therefore, the following results have both temporal and spatial components. This has not been done for any aquifer, especially regional aquifers, in BC. To the best of our knowledge, this type of comprehensive climate change modelling and recharge estimation for groundwater flow modelling has not been done yet in Canada.

5.9.3. ASSUMPTIONS

- AERIAL RECHARGE AND SCALE

Recharge varies spatially in real world, and is controlled by variations soil permeability (including effects of topography and surficial drainage), aquifer thickness to water table and hydraulic conductivity. In large regional aquifers, on the order of tens to hundreds of kilometres distance, there are usually strong trends in precipitation and temperature, further complicating recharge modelling efforts.

When averaged over time, precipitation is assumed not to vary significantly over area of Grand Forks aquifer, which may not be the case, but due to lack of data must be assumed. Considering the small spatial extent of the valley aquifer and only small variation in valley floor elevation (on the order of 50 m), the assumption is probably valid. Thus, spatially distributed recharge will be modeled and this will depend only on the spatial distribution of soil and aquifer properties. Since the HELP model predicts recharge at point locations in the aquifer, many different soil columns must be used, and the recharge solver in HELP used to determine representative recharge estimates as a function of soil and aquifer properties.

- AREAS OF ENHANCED RECHARGE

In this report, recharge refers to aerial recharge only. Surface water interactions with the aquifer, and the special case of groundwater seepage from valley slopes are considered separately in the Grand Forks aquifer groundwater flow models. Most of the valley slopes are very steep rock faces or steep forested slopes. Only a few small creeks have been mapped on the valley slopes and most channels are ephemeral and mostly dry during the summer, except during large rain events (Scibek and Allen, 2003). Small rain events usually do not produce visible streamflow or overland flow on these slopes, but more observations should be made during large rain storms.

The seepage from slopes is difficult to estimate. In the summer, if no streamflow occurs, the water may infiltrate the soil and remain in storage for a short time until the soils dry up, or it may flow downslope and contribute to aquifer recharge along the valley edges. This amount of

recharge may be larger along the valley walls than mean recharge from rainfall in the aquifer per unit area. However, this is only an assumption. Most of the downslope seepage may eventually channelize into streamflow of small creeks during and a short time after a major rain event due to thin soils on the valley slopes. Most of the valley slopes are bedrock outcrops, with some colluvium veneers and thin soils. Thus, any aquifer recharge from the slopes will occur only at small creek outlets into the valley and not along all valley walls. If overland flow (e.g., small waterfalls, small creeks, major seepage on slopes) is observed along most of the valley slopes during large rain events, then the recharge could be assumed evenly distributed. Allen (2000; 2001) employed a larger value of recharge to the groundwater model edges to account for added recharge from valley slopes.

To improve spatial resolution of recharge to the aquifer along valley edges, the valley walls may be observed during rain events and during dry periods for signs of seepage or overland flow, which would ultimately infiltrate the valley floor and not continue as channelized streamflow. If there is a high spatial density of such recharge areas, separated by dry slopes, then recharge zones can be defined and average recharge calculated. A regional groundwater flow model, such as the Grand Forks Aquifer model (Allen, 2000), uses grid cells 50x50 m or larger, and high spatial variability of recharge will probably not result in large differences in water table elevations along valley edges.

A second potential cause of enhanced recharge is irrigation return flow. A large proportion of groundwater use in the Grand Forks Valley is for irrigation. A portion of the pumped water that is used for irrigation may ultimately return to the aquifer if the plants are unable to use all of the water applied. A more detailed discussion and estimates of irrigation return flow are provided later in this report.

- THICKNESS OF VADOSE ZONE

The seasonal fluctuations of water table in Grand Forks outside the floodplain are small compared to thickness of vadose zone. There are high terraces outside the floodplain where water table is 5 to 20 m below ground. Recharge to unconfined aquifer in Grand Forks depends partly on thickness of vadose zone, but there is some maximum extinction depth (for effects of evapotranspiration). In theory, the problem of transient behaviour of the water table would cause non-linearities in model of unsaturated zone – its thickness would vary with time. However, the surficial sediments in this valley have high hydraulic conductivity, and the sands and gravels have probably low moisture content, and occasionally become saturated during intense precipitation events. Most aerial recharge probably occurs either during snowmelt or during large rainstorms. The sands and gravels probably drain very fast and the small variation of thickness of vadose zone probably does not affect aerial recharge significantly. The actual spatial variation of this thickness may affect recharge and the HELP will be shown in this report to be sensitive to thickness of unsaturated zone.

- SOIL HETEROGENEITY

The aquifer systems represent another source of land heterogeneity when considering the regional effects of climate change (York et al., 2002). Where aquifers have large aerial extent, on the order of several kilometres, the soils are usually heterogeneous over such large area, and discrete recharge zones exist. The different recharge zones can be characterized by infiltration rates or permeability of overlying soils, thickness of unsaturated units and depth to water table (unconfined aquifers). Therefore, the aquifer will be subdivided into a number of recharge zones. A recharge zone has a unique sediment column, and is based on a conceptual model that represents the average stratigraphy in that zone of unconfined aquifer. Recharge zones are derived from soil maps, extent of paved areas, and surficial geology maps. This requires integration of digital GIS coverages with published paper maps and reports, and interpretation of geologic cross-sections and/or standardized well lithologs.

- SATURATED HYDRAULIC CONDUCTIVITY

The Grand Forks aquifer is largely unconfined, and there is some heterogeneity of surficial materials that can be assumed to cause significant differences in infiltration rates. Infiltration of water is controlled by the unsaturated hydraulic conductivity and soil moisture of the surficial sediments. However, unsaturated hydraulic conductivity depends on the moisture content, thus a non-linear problem is posed. Unsaturated-saturated groundwater codes, such as HELP, vary the value of hydraulic conductivity used at any one time step according to the pressure, and thus, soil moisture distribution. These are related by characteristic curves that show hydraulic conductivity in variably saturated media as a function of soil moisture. Consequently, the maximum value of hydraulic conductivity, which is equivalent to the saturated hydraulic conductivity, K_{sat}, is input into HELP.

5.9.4. HELP MODEL SPECIFICS

The program WHI UnSat Suite (Waterloo Hydrogeologic Inc.), which includes the sub-code Visual HELP (US EPA Hydrologic Evaluation of Landfill Performance model), is used to estimate recharge to the Grand Forks aquifer. HELP is a versatile quasi-two-dimensional model for predicting hydrologic processes at landfills and testing the effectiveness of landfill designs, and enabling the prediction of landfill design feasibility. HELP is also effective in estimating groundwater recharge rates. Inputs consist of a representative sediment column with defined soil and sediment properties, engineering design features, surface slope, meteorological conditions, and evaporation rates. HELP uses numerical solution techniques that account for the effects of surface storage, snowmelt, runoff, infiltration, evapotranspiration, vegetative growth, soil moisture storage, and various engineering parameters (e.g., lateral subsurface drainage). The natural water balance components that the program simulates include precipitation, interception of rainwater by leaves, evaporation by leaves, surface runoff, evaporation from soil, plant transpiration, snow accumulation and melting, and percolation of water through the profile.

- SEDIMENT COLUMNS

For the soil and sediment columns, the materials must be defined and the user must specify:

1. Soil (porosity, field capacity, wilting point, and hydraulic conductivity)
2. Engineering design data (liners, leachate and runoff collection systems, surface slope)

The profile structure can be multi-layered, consisting of a combination of natural (soil) and artificial materials (e.g., waste, geomembranes). In the current application, HELP will use only natural geological materials consistent with those found in the Grand Forks aquifer.

Soil media is the upper weathered zones of the earth, which averages a depth of 6 feet or less from the ground surface (Osborn et al., 1998). Soil has a significant impact on the amount of recharge that can infiltrate into the ground. In general, the less the clay shrinks and swells, and the smaller the grain size of the soil, the less likely contaminants will reach the water table.

The overall percolation column design in this study includes only two layers:

1) Soil (vertical percolation layer)
2) Aquifer media (horizontal drainage layer or vertical percolation layer)

UnSat Suite includes a user interface to facilitate soil column design and project management (Figure 70 and Figure 71. There is a pre-existing database of soils and aquifer media with appropriate hydraulic properties, and new materials can be defined using the material editor (Figure 72). There is no difference in model performance whether the vertical percolation layer or the lateral drainage layer is used for the bottom layer if there is no specified lateral inflow into the percolation column (as in this case).

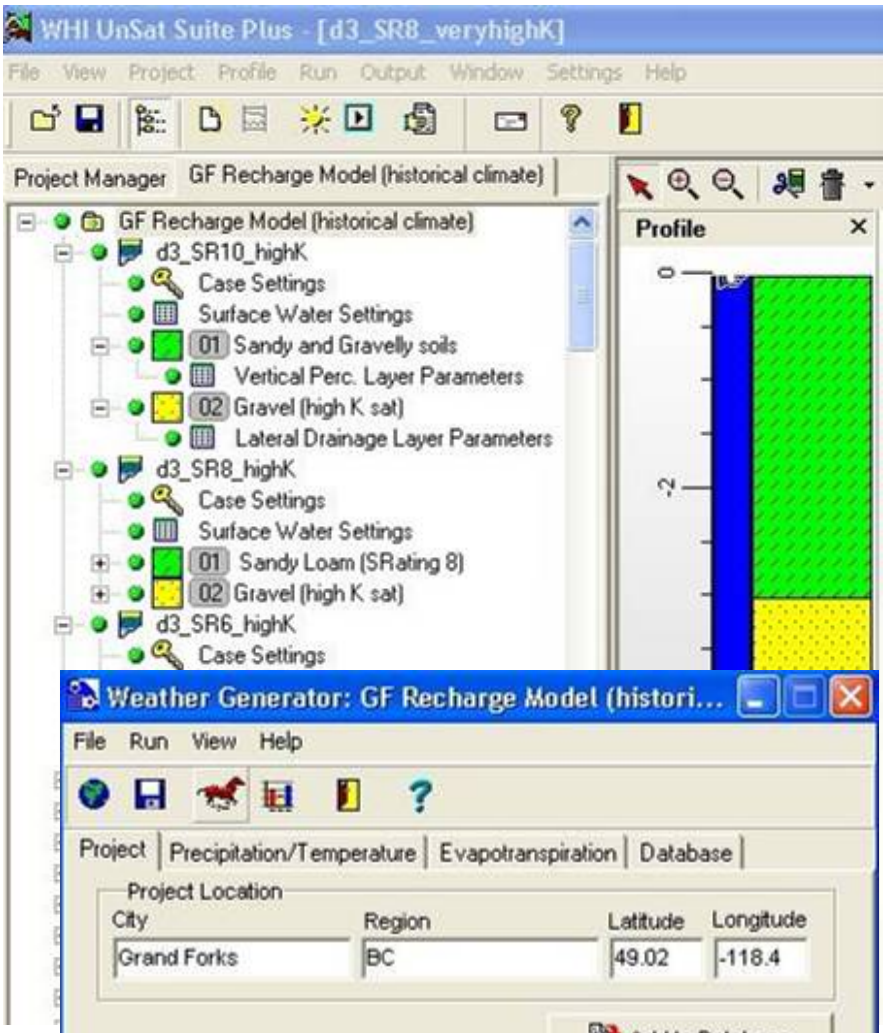

Figure 70 UnSat Suite interface: soil columns and scenarios for HELP model

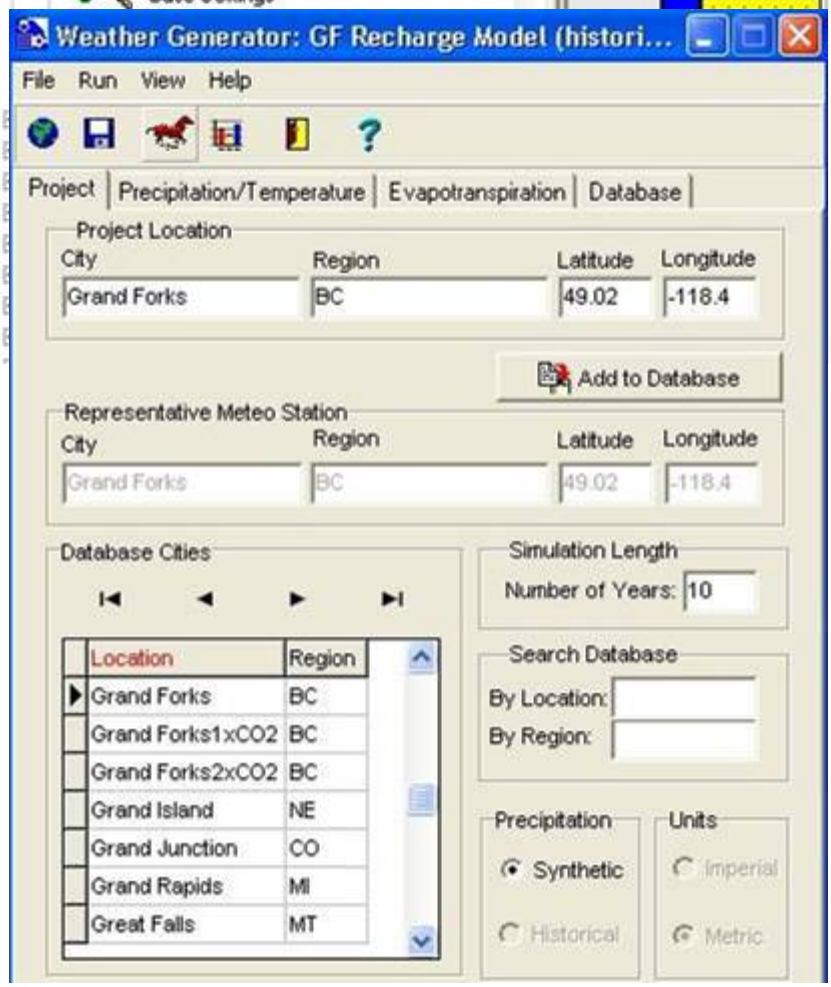

Figure 71 UnSat Suite interface: weather generator for climate change scenarios.

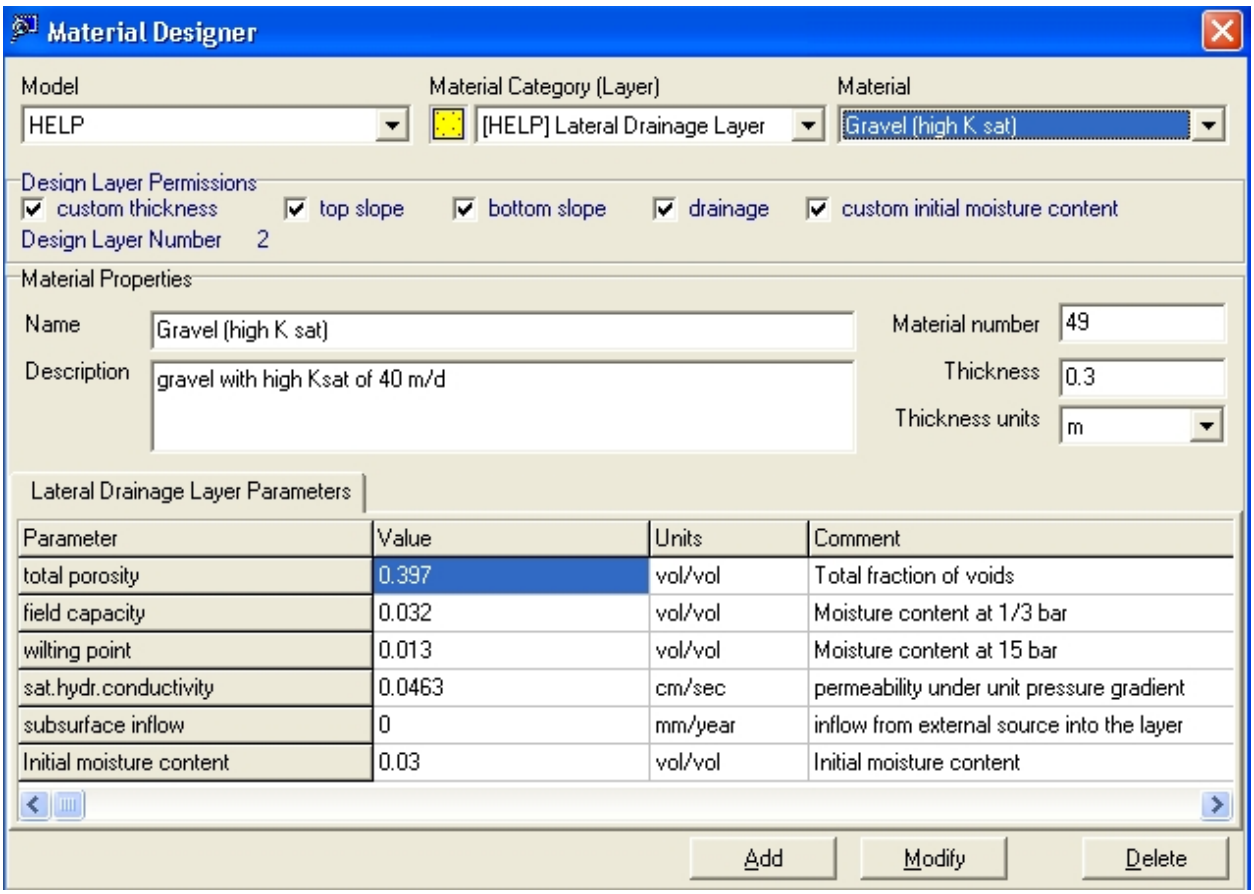

Figure 72 Material designer interface in UnSat Suite.

- INITIAL MOISTURE CONTENT

Before running the simulations, the initial water content of different layers should be specified. UnSat Suite gives the user the option to have the initial water content values specified by the user or computed by the model (as nearly steady-state values). With the latter, which is the default, UnSat Suite assigns realistic values for the initial water moisture storage of layers and simulates one year of hydrology. The values of moisture storage obtained from this simulation are then used as initial values, and the simulation starts again at year one.

- WEATHER INPUTS

HELP requires three different types of meteorological data that must be provided as daily values:

- Precipitation
- Solar radiation
- Mean air temperature

Data, representing meteorological conditions, can be imported from a particular meteorological station file or synthetically simulated with the Weather Generator. Most weather stations collect only temperature and precipitation measurements, as is the case with Grand Forks.

Air temperature

Mean air temperature can be input as daily time series or as monthly normals, and then modeled with weather generator (as in this case).

Solar radiation

Solar radiation is specified as daily time series. In this report, the solar radiation was modeled separately then combined with precipitation and temperature time series, for input to stochastic weather generator calibration.

Precipitation

Precipitation is applied from specified daily time series, or created by weather generator from monthly normals (as in this case). It is the most important climatic variable controlling recharge.

Evapotranspiration

Evapotranspiration is computed by HELP model at the soil-air interface of the upper layer in the soil column. The HELP model requires a set of parameters to simulate evapotranspiration that are constants for the duration of the simulation. The model uses a complicated multi-level procedure for calculating different types of evaporation and evapotranspiration. The subroutines of this model allow calculation of evaporation from snow, soil and leaves. In addition, the model calculated vegetation growth and transpiration. In total, around 70 equations describe these processes. Fortunately, the number of parameters which require the user's input are limited. These include:

- Evaporative zone depth
- Maximum leaf area index
- Growing Season start and end day
- Average wind speed
- Quarterly relative humidity

The evaporative zone depth is the maximum depth from which water can be removed by evapotranspiration. A value of 20 cm was used for these simulations. This value is at the lower end of the range of values possible and is characteristic of sandy soils. The other parameters are included in the Spokane, Washington climate database.

Runoff

For runoff calculations, it is necessary to specify the area over which runoff can occur and the type of surface vegetation. These two parameters remained fixed at 100% runoff area and a fair stand of grass, respectively, for all simulations. The rainfall-runoff processes in UnSat Suite are modelled using the USDA (US Department of Agriculture) Soil Conservation Service curve-number method, which is widely accepted and allows the user to adjust the runoff calculation to a variety of soil types and land management practices. The curve number (CN) is defined with respect to the runoff retention parameter (S), which is a measure of the maximum retention of rainwater after runoff starts (in inches):

$$CN = 1000 / (S + 10) \quad [16]$$

The maximum value of CN, which is 100, occurs when there is no infiltration. The smaller the CN is, the more rainwater will infiltrate the soil. The minimum realistic value for CN can be

assumed to be appropriately equal to 50. UnSat Suite uses different procedures to adjust the value of CN to surface slope, soil texture, and vegetation class. By default, the model automatically calculates the CN. The default condition was used for all simulations. For purposes of simplicity, zero slope was assigned to each model layer. The topography of the two aquifer surfaces is slightly undulating or sloping, but over small areas the surface is approximately horizontal. Steep escarpments are exceptions, but the relative area of these features is very small compared to the aerial aquifer extent.

5.9.5. SPECIFIC STEPS OF RECHARGE MODELLING

The overall methodology will be to select soil type representative of very high, high, medium, and low permeabilities. Similarly, four representative values of saturated hydraulic conductivity (K_{sat}) of the unsaturated aquifer media above water table are selected, through which recharge water percolates. The same or equivalent soil layers in HELP soil profiles are used as the capping soil units for recharge calculation. If recharge is sensitive to depth of percolation column, then representative depths are selected from depth statistics. A total of 4 x 4 x 4 = 64 scenarios of soil columns will be represented by the various combinations of depth, K_{sat}, and soil. Recharge is computed for all columns using the same weather data set for 10 years of weather, thus allowing for calculation of monthly and long term mean recharge for each column. Raster calculations are done to compute spatially distributed recharge for the base case (no climate change). The aquifer area is then classified using the scenarios and recharge values are linked to the classified aquifer map, obtaining spatially distributed recharge, which could be interpolated or smoothed as necessary. The final step involves transferring recharge values into the transient groundwater flow model.

It is important to calibrate the HELP weather generator to climate data set for Grand Forks (base case); this involves comparing the modeled and observed precipitation and temperature time series, adjusting the weather generator parameters, and recording them in the database (the calibrated weather generator database for Grand Forks). This is done because the nearest weather station in the HELP database is not at Grand Forks. The nearest station is in Spokane, Washington, which has a much drier climate than Grand Forks. The Access database must be modified with weather station parameters; this involves adjusting Spokane's parameters: input temperature and precipitation normals for Grand Forks, and calibrating the other parameters, such as probability of rainfall for each month.

For transient model, recharge varies with time, monthly time steps at the minimum, so the number of HELP analyses rises significantly. However, HELP already produces monthly recharge estimates (based on the average over the selected time scale, e.g., 10 years of weather from the weather generator). The same weather data set is used for all soil columns for a given climate scenario.

- STANDARDIZATION OF THE WATER WELL DATABASE LITHOLOGY LOGS

Lithology data, obtained directly from the BC Ministry of Water, Land and Air Protection Water Well Database, were standardized using an in-house standardization macro developed in MS Excel (described in Section 2.0).

-

CALCULATING VERTICAL SATURATED HYDRAULIC CONDUCTIVITY

Using the standardized well logs, a Visual Basic program was written to extract all units that lie above the water table depth. This resulted in a minimum of a single layer and up to several layers for each well. Up to three material descriptions, as described earlier under standardization, were retained. A spreadsheet recording values of saturated hydraulic conductivity (K_{sat}), specific storage (Ss) and specific yield (Sy) for each material type was created, based on estimates used in previous vulnerability mapping studies (e.g., Fraser Valley) as well as published values.

Table 19 shows the lithologic descriptions and the Ksat values for various material types, including dominant material types with qualifiers (e.g., silty sand). The geometric means of the Ksat values were calculated for each layer in each well where more than one material type was recorded (Table 20). Where only a single material type was recorded in the standardized well log, a single K_{sat} value for that layer was generated. A manual examination of the output data was carried out in order to ensure that the calculated hydraulic conductivities were consistent with the original well log descriptions. In only a few cases (<10) were modifications made as a result of the standardization scheme not correctly identifying the dominant material types. Only the two first material types were considered in this manual adjustment of K_{sat} values.

Each well consists of one or more layers, therefore, the approach used was to calculate an equivalent vertical K value, K_z, to represent the soil media above the water table. According to Leonards (1962), an equivalent vertical hydraulic conductivity (Kz), which is at right angles to stratification of assumed homogeneous and isotropic units, is given by formula:

$$Kz = \frac{\sum m_i}{\sum \left(\frac{m_i}{K_i} \right)} \qquad \textbf{[17]}$$

where m_i is the thickness of layer i having equivalent hydraulic conductivity K_i. Although other methods of averaging are available (Domenico and Schwartz, 1998), the K_i values for the layered media in standardized lithologs are not as reliable and numerous as to be able to perform more complex statistical analyses, thus the simple averaging method presented here was used. The units that are being averaged are imaginary concepts because the K_i values were derived from averaging of typical K values for material encountered within that unit, but without precise knowledge of the relative abundance of each material. The averaged units m_i are, by default, homogeneous and isotropic as represented by equivalent K_i. There are no data for the aquifer on micro-scale isotropy.

Figure 73 shows a histogram of K_z values for each well in the aquifer. K_z values in 285 wells ranged from a maximum of 1000 m/d to a minimum of $1x10^{-6}$ m/d, and median of 13 m/d and quartile values of 100 and 0.14 m/d (Table 21).

The K_{sat} in vadose zone were interpolated using Inverse Distance Weighed interpolator (power 2, number of points = 5, output cell size 100 m), and computed on representative vertically averaged LOG K_{sat} values at all available point locations where lithologs exist. After interpolation, 10^(Log K_{sat}) of the interpolated raster was computed. K_{sat} values were then converted to units of m/d. Four K_z classes were chosen as $1x10^{-6}$ to 0.14, 0.14 to 13 m/d, 13 to 100 m/d, and 100 to 1000 m/d (Map 2). The higher values mean that water will percolate more easily through the vadose zone during recharge events. Representative material K_{sat} in HELP soil columns will be 315, 40, 1.4, and 0.015 m/d (mid value in each class).

Table 19 Assigned hydraulic properties to material types in litholog standardization: hydraulic conductivity, specific yield (for unsaturated layers above water table), and specific storage.

Hydraulic Conductivity

Material	Min K	Max K	assign K	comments
	m/d			
gravel	100	5000	1000	
pebbles	100	5000	1000	assume same as Gravel
cobbles	100	5000	1000	assume same as Gravel
boulders	100	5000	1000	assume same as Gravel
sand	0.5	200	10	medium clean sand
silt	0.001	0.1	0.1	
clay	1.00E-07	5.00E-04	1.00E-06	
till	1.00E-07	5.00E-01	1.00E-04	glacial till

from Heath (1983) in Anderson and Woessner (1992)

Specific Yield

Material	Min Sy	Max Sy	Assign Sy	comments
gravel	0.13	0.40	0.28	fine gravel
pebbles	0.13	0.25	0.21	coarse gravel
cobbles			0.21	coarse gravel
boulders			0.21	coarse gravel
sand	0.16	0.46	0.32	medium clean sand
silt	0.01	0.39	0.20	
clay	0.01	0.18	0.06	
till	0.01	0.18	0.06	assume same as clay

from Morris and Johnson (1967) in Anderson and Woessner (1992)

Specific Storage

Material	Min Ss	Max Ss	Assign Ss	comments
	m-1			
gravel	1.00E-04	4.90E-05	7.45E-05	dense sandy gravel
pebbles	1.00E-04	4.90E-05	7.45E-05	dense sandy gravel
cobbles	1.00E-04	4.90E-05	7.45E-05	dense sandy gravel
boulders	1.00E-04	4.90E-05	7.45E-05	dense sandy gravel
sand	2.00E-04	1.30E-04	1.65E-04	assume dense sand
silt	2.60E-03	1.30E-03	1.95E-03	assume same as stiff clay
clay	2.60E-03	1.30E-03	1.95E-03	stiff clay
till	2.60E-03	1.30E-03	1.95E-03	assume same as clay

from Domenico (1972) in Anderson and Woessner (1992)

Table 20 Calculation of average vertical Ksat for Grand Forks aquifer layers above water table: (a) assigned Ksat values based on material types within each layer and average Kz for layer and average vertical Kz for each litholog, (b) table exported to GIS for spatial interpolation of Kz values

(a)

	Materials in layer			Depth		Elevation				Assigned Ksat			
well tag number	1	2	3	top of layer	bottom of layer	top of layer	bottom of layer	water table	layer thickness	Kz1	Kz2	Kz3	Average Kz for layer
	(standardized)			(ft)		(m a.s.l.)			(m)	(m/d)			
42043	sand	silt	clay	0.0	23.0	529.0	522.0	517.4	7.0	1.0E+01	1.0E-01	1.0E-06	1.0E-02
42043	sand	gravel		23.0	27.0	522.0	520.8	517.4	1.2	1.0E+01	1.0E+03		1.0E+02
42043	clay	silt	gravel	27.0	31.0	520.8	519.6	517.4	1.2	1.0E-06	1.0E-01	1.0E+03	4.6E-02
42043	sand			31.0	38.1	519.6	517.4	517.4	2.2	1.0E+01			1.0E+01
										avg Kz for above layers interval			1.6E-02
42044	clay	sand		0.0	31.0	528.5	523.6	518.8	4.9	1.0E-06	1.0E+01		3.2E-03
42044	gravel			31.0	31.8	519.1	518.8	518.8	0.3	1.0E+03			1.0E+03
										avg Kz for above layers interval			3.3E-03
42045	sand	gravel		0.0	13.0	527.5	523.5	518.0	4.0	1.0E+01	1.0E+03		1.0E+02
42045	gravel	cobbles		13.0	31.0	523.5	518.1	518.0	5.5	1.0E+03	1.0E+03		1.0E+03
42045	sand			31.0	31.2	518.1	518.0	518.0	0.1	1.0E+01			1.0E+01
										avg Kz for above layers interval			1.9E+02

(b)

WTN	Easting	Northing	Thickness	Layers	Kz	log Kz
5156	392446	5429280	9.5	3	7.13E-04	-3.15
5186	391306	5430708	1.4	1	1.00E+01	1.00
5280	392300	5429118	11.1	4	4.55E-06	-5.34
7869	394680	5429246	9.9	4	3.22E+00	0.51
7887	390136	5428746	5.2	3	2.74E+02	2.44
7972	394936	5429204	8.6	2	3.86E+01	1.59
14087	394339	5432150	2.6	2	1.07E-06	-5.97
14093	393678	5432540	6.4	2	1.27E+02	2.10
14654	393184	5431546	5.2	1	1.00E+03	3.00
18115	389304	5430202	35.8	8	7.83E-06	-5.11
...	...	...	...	...	...	...

Figure 73 Histogram of averaged vertical Kz (above water table) for all well locations in Grand Forks aquifer.

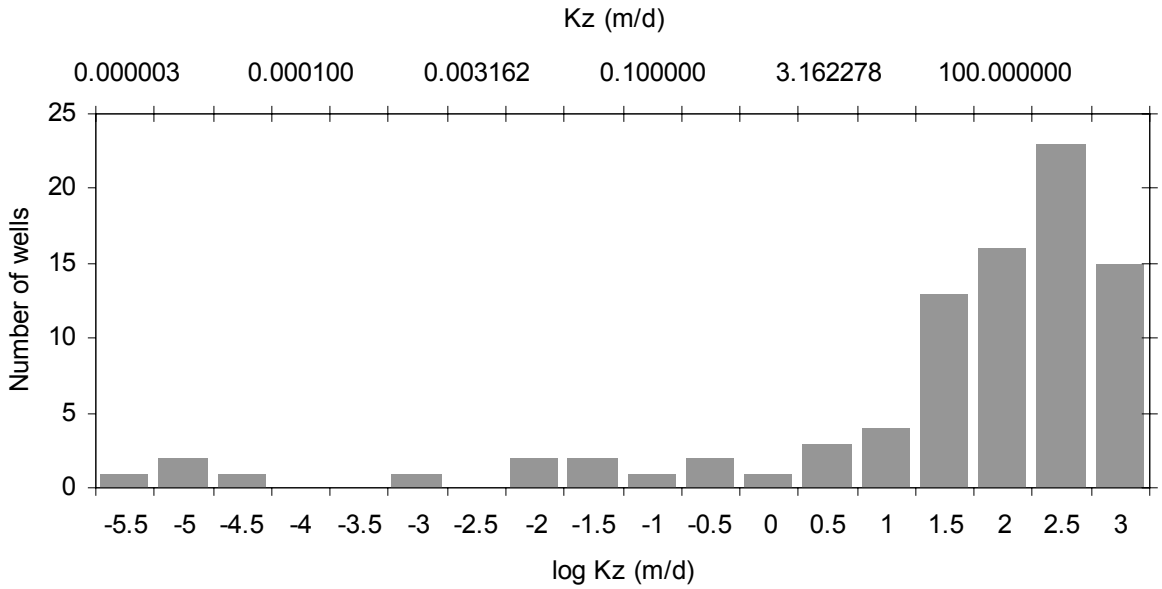

Table 21 Descriptive statistics of averaged vertical Kz (above water table) for all well locations in Grand Forks aquifer, and assignment of Kz categories for recharge modelling in HELP module in UnSat Suite.

	log Kz	Kz (m/d)
Mean	1.21	16.06
Median	1.69	48.98
Standard Deviation	1.93	
Range	8.97	1000.00
Minimum	-5.97	0.000001
Maximum	3.00	1000.00

Percentiles	log Kz	Kz (m/d)	Kz (cm/s)	K categories in HELP model
0.0%	-5.97	1.35E+00	0.00156	
13.9%	-0.31	1.07E-06	0.00000	**low**
25.0%	1.09	1.23E+01	0.01423	----------
23.2%	1.00	1.00E+01	0.01157	**mod**
50.0%	1.69	4.90E+01	0.05669	----------
56.9%	2.00	1.00E+02	0.11574	**high**
75.0%	2.15	1.42E+02	0.16405	----------
82.5%	2.44	2.74E+02	0.31735	**v high**
100.0%	3.00	1.00E+03	1.15741	

Map 19 Distribution of K_Z in unsaturated zone above water table in Grand Forks aquifer.

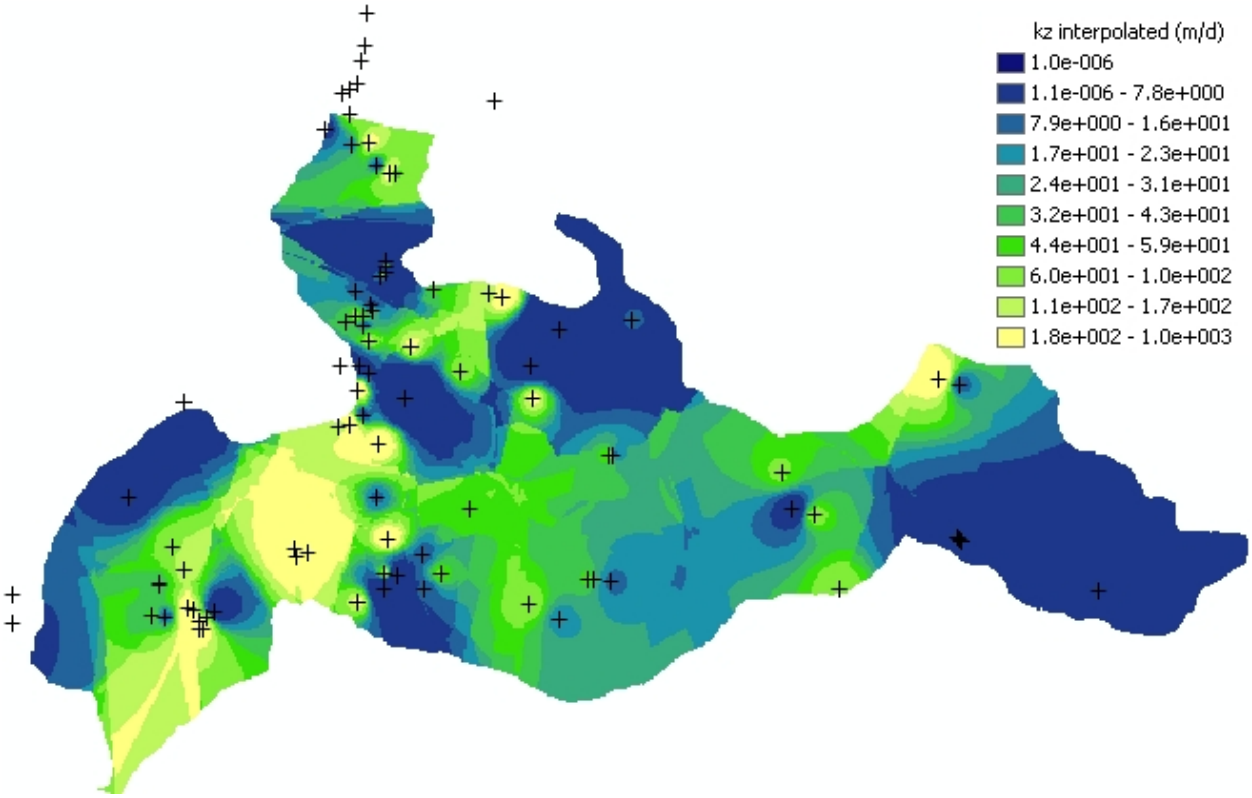

Map 20 Reclassed K sat map of unsaturated zone above water table in Grand Forks aquifer.

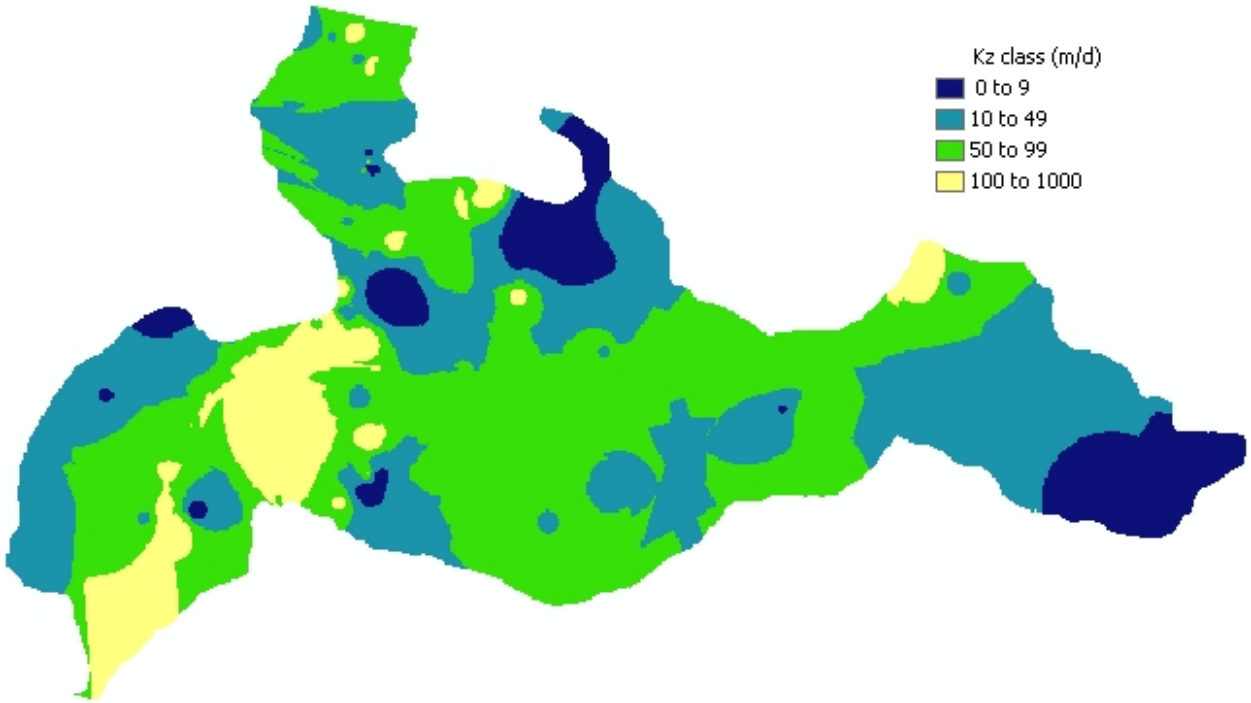

- SOIL TYPE (PERMEABILITY)

In the Grand Forks valley, soil information was taken from 1964 B.C. Soil Survey report by Sprout and Kelly (1964). The map in Map 21 of Canadian side of Grand Forks valley shows classified soil polygons identified by soil name and subgroup, and listing parent material and drainage properties. There are more than 15 types of mostly coarse-grained soils present in the valley. The most common and largest contiguous soil polygon is defined as Bubar sandy soil (Loamy Fine Sand, Sand, and Sandy Loam). This unit and the Marble Sand, derived from sandy glacial outwash and river deposits (shown in shades of yellow), are rapidly drained and cover south-central valley regions. The second most prominent soil type is McCoy Gravelly Sandy Loam, which has higher gravel content and is also rapidly drained (brown color on map). These gravelly soils are found along Kettle River and other parts of the valley. The most recent alluvial deposits are found in abundance adjacent to Kettle River and are named Saunier Complex (shown in gray). These soils are well to imperfectly drained where silty floodplain deposits are the capping materials. Along the north-east and western valley margins are prominent alluvial-colluvial fan deposits (Republic Gravelly Sandy Loam soils), which are also rapidly to moderately well drained. Other soil types include Spion Loamy Sand and Mires Gravelly sandy Loam, both well drained, and very small swampy areas in the eastern portion of valley, along Kettle River. There are no significant fine grained and poorly drained soils in the valley as mapped by Sprout and Kelly (1964).

Since most of these soils are rapidly drained, the unconfined surficial aquifer in the valley is directly connected to the ground surface such that rainfall and meltwater is expected to rapidly infiltrate and recharge the aquifer. Only along the Kettle floodplain is reduced infiltration expected due to higher content of fine grained sediments. Surface runoff may also occur along highly permeable but steeply sloping alluvial fans near valley walls. However, a small portion of the valley floor is occupied by community of Grand Forks, with associated transportation network and built-up areas. There, a large proportion of the ground surface is paved, compacted, or covered by structures, such that most of the rainfall and meltwater is redirected to stormflow network and removed. Infiltration to unconfined aquifer is limited in those areas.

The Bubar type soils (Orthic Dark Brown) are derived from sandy river terraces, and are described in detail by Sprout and Kelley (1964). The surface varies from level to irregular or moderate slopes. The parent material consists of calcareous and mildly alkaline fine to coarse sands. The sandy deposits are underlain at variable depths by outwash gravels. Gravels are scattered in the soil column, but cobbles are found only at the bottom of soil profile. The soils developed under bunchgrasses, which are now replaced by secondary grasses, weeds, or planted crops such as alfalfa, hay, grains, or potatoes. These crops are representative of moderately fine stand of grass in HELP model.

Soil maps for the Kettle River Valley (Sprout and Kelly, 1964) were digitized in ArcMap and linked to soil properties tables, where permeability was ranked from 1 to 12, using the categorical descriptors provided on soil documentation (e.g. “rapidly drained” = 1). Rock outcrops surround the aquifer outline, and very small outcrops occur within the aquifer area, as defined by BCWLAP. Rock outcrops were assigned special code for low permeability, relative to unconsolidated sediments in the valley that form the aquifer. Corresponding with the central city limits of Grand Forks is largely paved area, which was assigned decreased permeability.

Table 22 Soil types in Grand Forks aquifer area, soil properties, drainage and soil rating codes, and area covered in Grand Forks valley.

SYMBOL	Soil Name	Parent Materials	Grain Size	Drainage	Drain Code	S rating	Area (ha)
Bulfs	Bubar Loamy Fine Sand	Outwash & River Deposits	sandy	Rapidly drained	2	9	804
My	McCoy Gravelly Sandy Loam	Outwash & River Deposits	gravelly	Rapidly drained	2	10	472
Sa	Saunier Complex	Alluvium (recent)		Well to imperfectly well drained	6	5	465
Busl	Bubar Sandy Loam	Outwash & River Deposits	sandy	Rapidly drained	2	9	355
Bus	Bubar Sand	Outwash & River Deposits	sandy	Rapidly drained	2	10	297
Ma	Marble Sand	Outwash & River Deposits	sandy	Rapidly drained	2	10	267
Paved	Mostly impermeable surfaces			Decreased permeability	97	1	140
Re	Republic Gravelly Sandy Loam	Alluvial-Colluvial Fans		Rapidly to moderatelly well drained	4	8	100
In	Ingram Loam	River Terraces	silty	Well drained	4	6	91
Mi	Mires Gravelly Sandy Loam	Outwash & River Deposits	gravelly	Rapidly drained	2	10	86
Sp	Spion Loamy Sand	Outwash & River Deposits	sandy	Well to moderatelly well drained	5	6	57
B	Bluffs and Ravines			Rapidly drained	2	9	42
Sw	Swamps			Very poorly drained	12	1	41
Mr	Myncaster Silt Loam	Slopewash		Poorly drained	10	1	23
Fv	Fiva Sandy Loam	Alluvial-Colluvial Fans		Rapidly to well drained	3	8	22
F	Ferroux Sandy Loam	Alluvial-Colluvial Fans		Rapidly to well drained	3	8	20
Rm	Rough Mountainous Land	Bedrock		Low permeability	99	1	20
St	Stevens Loam	Glacial Till		Well to moderatelly well drained	5	5	19
Tz	Tuzo Gravelly Sandy Loam	Alluvial-Colluvial Fans		Rapidly drained	2	10	16
W	Wilkinson Silt Loam	River Terraces	silty	Well to moderatelly well drained	5	5	11
Bo	Boldue Gravelly Sandy Loam	Alluvial-Colluvial Fans		Moderatelly well drained	6	5	9
Wg	Wilgress Muck	Slopewash		Poorly to very poorly drained	11	1	9
Ro	Rock outcroppings	Bedrock		Low permeability	98	1	8

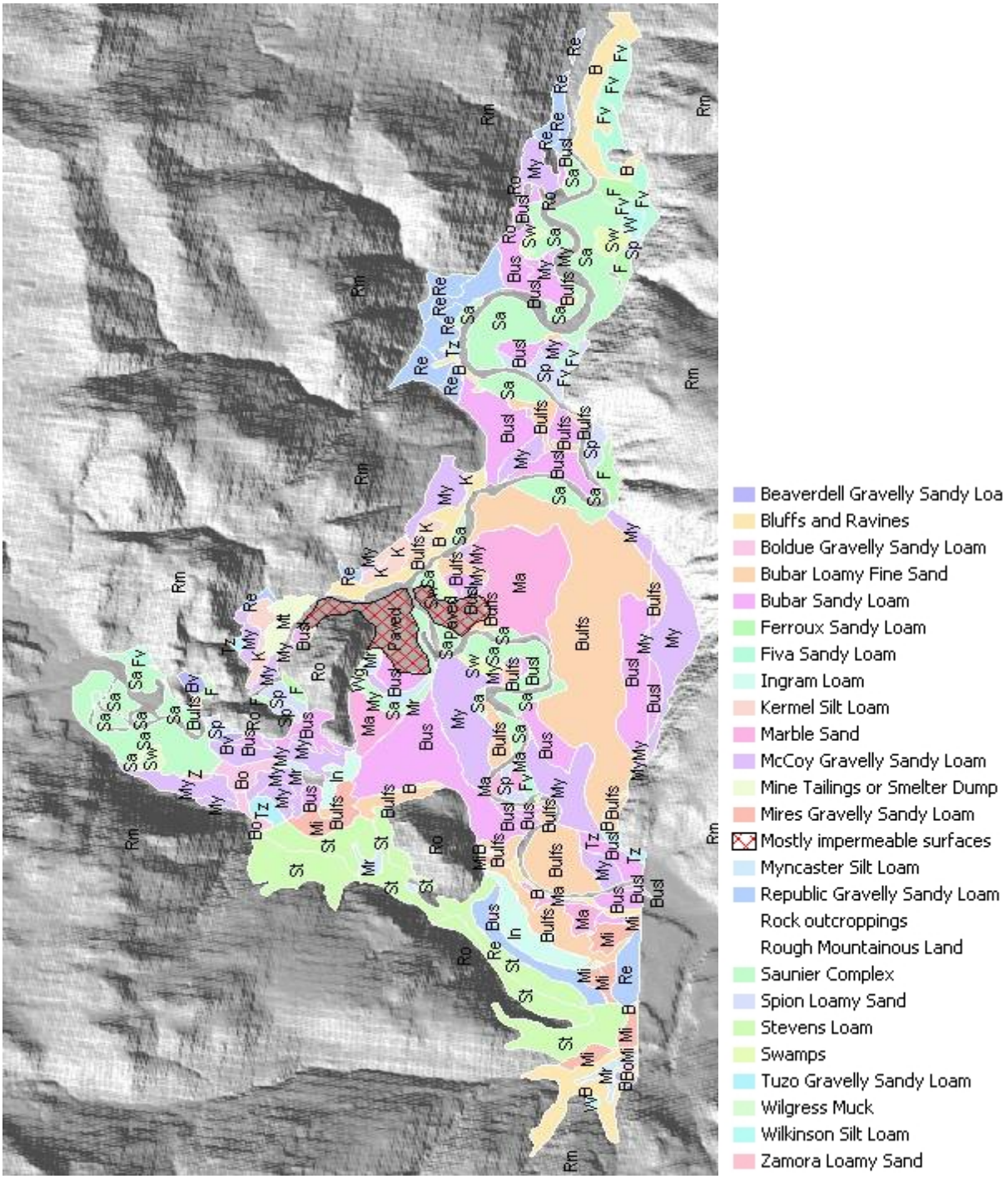

Map 21 Soil Map of Grand Forks Valley (Sprout and Kelly, 1964).

Drainage characteristics were included in the soil map legend and in the source documentation (Sprout and Kelly, 1964), and these represent average or typical soil permeabilities, although significant small-scale variation is expected. Since the recharge units are 50x50 m map pixels, the average properties are appropriate here. In the future these could be tested with permeameters.

Map 23 shows the soil permeability over the aquifer while more detailed listing is given in Table 22. T he dominant soils are Loamy Fine Sand and Gravelly Sandy Loam, covering almost 40 % of the aquifer. These are found on river terraces and floodplains, except in the eastern valley, where lower permeability (poorly drained) soils are present. Some floodplain soils along the Kettle River in central valley are also of poorer drainage. Note that there are several more soil types in the Grand Forks area, as on soil map sheet, but only soils found within defined Grand Forks aquifer area are listed in table (other soils were not used in recharge calculations).

For the purpose of recharge modelling, the GIS soil map was converted to raster format with 20 m resolution, then reclassified into 5 soil rating categories based on S-ratings[1] of soil in DRASTIC aquifer vulnerability mapping method. There were no soils with S-rating of 7, and only a few small patches with ratings below 6, which were then combined with those having rating of 6 as representing low permeability class. Paved areas and rock outcrops were given rating of 1 (lowest). This raster map was used as one of the variables that generated spatially-distributed recharge estimates for the aquifer. For the purpose of recharge analysis using the HELP vertical percolation columns, the soil types in the HELP model were matched by permeability class and assigned representative S-rating (see Table 23). Results are shown in Map 23. Vertical saturated K values were used as given in HELP database for various soil types that were selected. No actual soil infiltration or permeability data was available for Grand Forks area.

Table 23 Soil types in HELP model, soil hydraulic conductivities, and assigned S-rating and permeability class for recharge modelling.

Vertical percolation layer in HELP	Vertical Kz (sat)		SRating	Permeability
	(cm/s)	(m/d)		
Silty Loam	1.90E-04	0.164	5 to 6	low
Loam	3.70E-04	0.320		
Fine Sandy Loam	5.20E-04	0.449		
Sandy Loam	7.20E-04	0.622	8	moderate
Loamy Fine Sand	1.00E-03	0.864		
Loamy Sand	1.70E-03	1.469	9	high
Sandy Gravelly Soils (new type)	5.80E-03	5.011	10	v high

[1] S rating is used in the DRASTIC method of assessing intrinsic vulnerability of the aquifer. The S rating is a relative rating, with high values indicating higher relative ease of drainage. Scale of 1 to 10.

Map 22 Soil permeability over Grand Forks aquifer (digitized form soil maps).

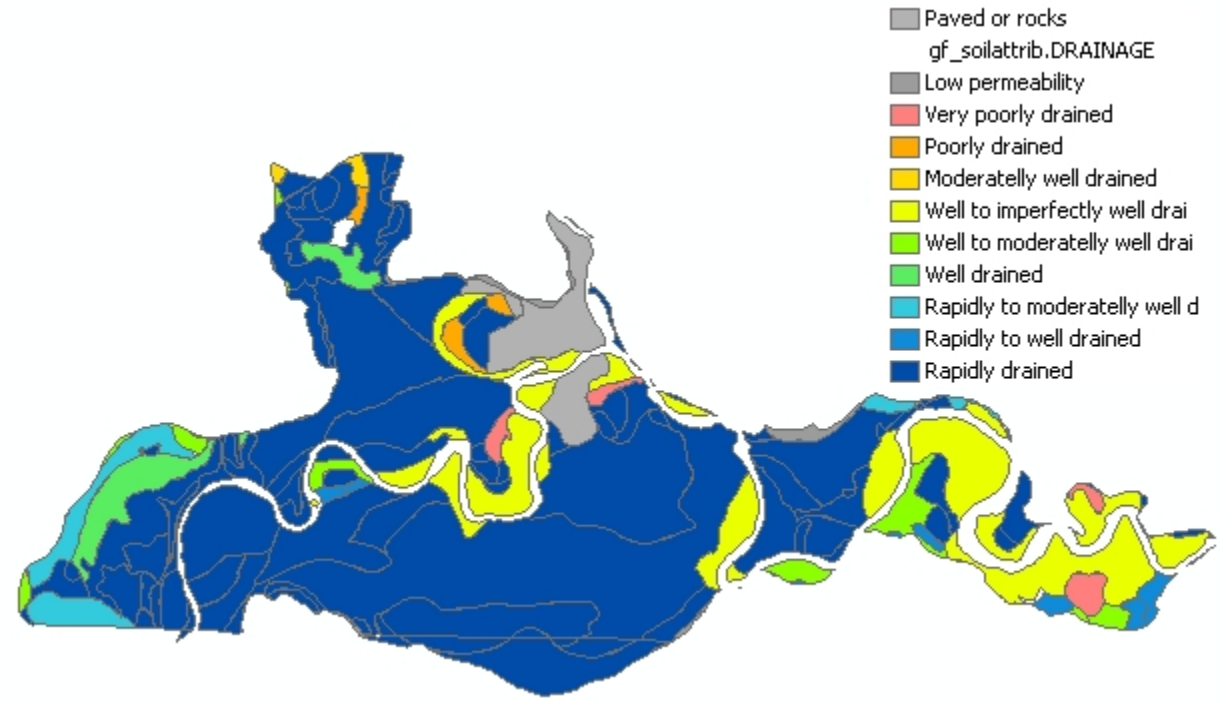

Map 23 Relative Soil permeability map derived from soil drainage map.

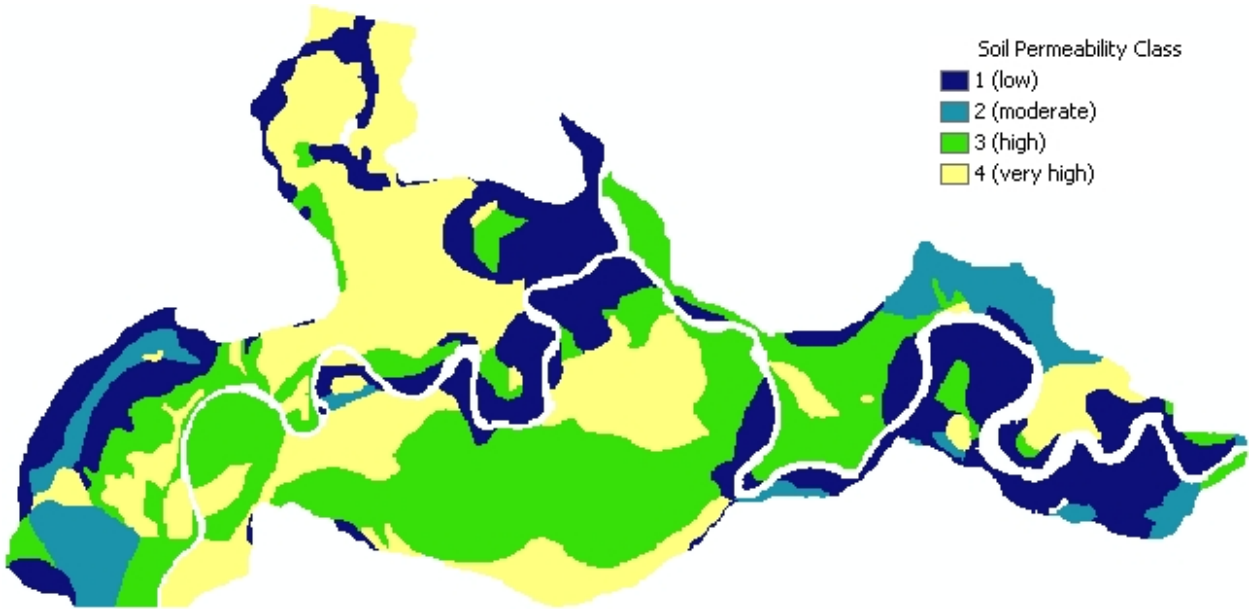

- SOIL THICKNESS

The vertical soil profiles and thicknesses are also important in determining soil permeability and recharge to deeper layers. There are two sources of information regarding soil thickness: well lithologs and soil pits. Although many drillers recorded the thickness of overburden and soil, only 55 out of 150 lithologs have estimate of soil thickness, not enough to get accurate spatial distribution of soil thickness. Soils are expected to vary in thickness over micro-topography of the valley, thus any valley-wide interpolation of thickness would have very large error (locally).

There are 22 soil pits near Grand Forks, but only 5 of them are in the valley. This was a soil survey project (EP822.02) – data obtained from a BC web site source. Locations of soil pits and locations of lithologs with soil thickness information are shown on Map 24, along with one possible soil thickness distribution (in this case interpolated with inverse distance method used on combined data set of soil pits and lithologs with overburden soil layers). The pits have depths to different soil horizons, but overall soil depths (to deepest horizon) were between 0.60 and 1.15 m, which is consistent with the histogram of soil depths extracted from well lithologs in Figure 74, which shows that median soil depth is just above 1.0 m and only few locations had thicker soils (up to 2.0 m). Over most of the valley, soil thickness was between 1.0 and 1.5 m.

The south-western valley area tends to have thin soils, where as south-central area has thicker soils. With exception of few anomalous locations, the soil thickness is rather similar over the valley; the mean for the interpolated soil thickness surface is 0.92 m, with 0.21 standard deviation. Where soils are absent, less moisture is stored in shallow subsurface and less evapotranspiration is expected to occur than in thick soil areas. For the modelling purposes, soil thickness will be assumed to be 1.0 m in all percolation columns, since there are not enough data to properly assign soil thickness at all points in the valley due to very likely high spatial variation (not represented by this scarce data set).

Map 24 Soil thickness distribution (one of interpolation methods) over Grand Forks aquifer. Soil pits are blue triangles and soil thickness data from well lithologs are crosses.

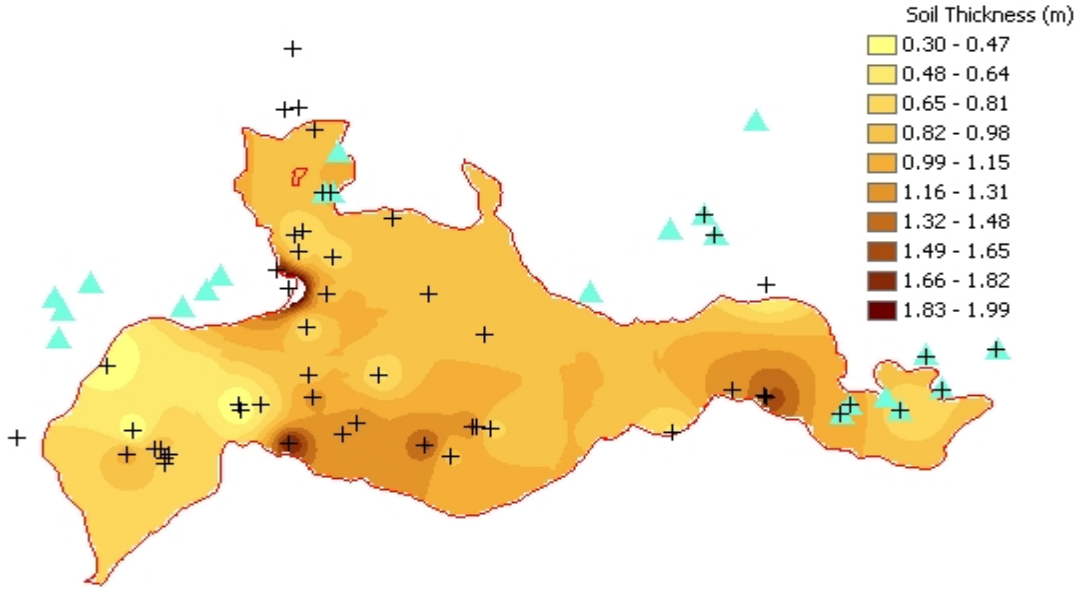

Figure 74 Thickness of soil and other sediments in standardized well lithologs in Grand Forks valley. Histograms of thickness of all litholog units in all wells and occurrence order in lithologs.

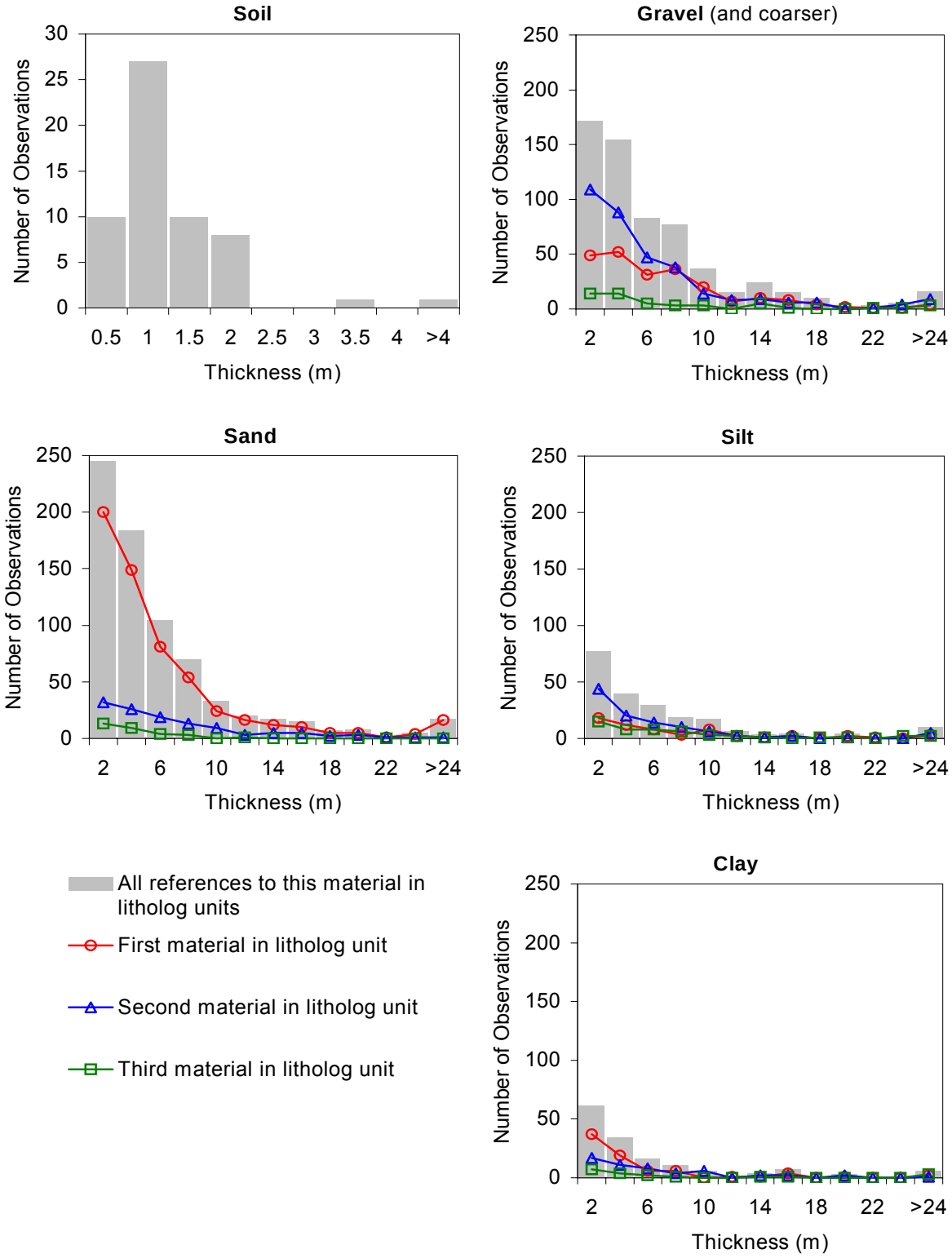

- DEPTH TO WATER TABLE

The depth to water is the distance (here in feet) from the ground surface to the water table. It determines the depth of material through which water must travel before reaching the water table. Depth to water was estimated for wells in the Grand Forks aquifer directly from the historic static water levels recorded in drillers' logs. Static water levels provide a one-time measure of the depth of water in the well. Normally, these measurements are made immediately following drilling, and therefore, can result in lower values that would be measured some time following drilling when the well has re-equilibrated with the surrounding aquifer water levels. The Grand Forks aquifer is a highly permeable aquifer, consequently, the hydraulic disturbance during drilling activities can be expected to dissipate fairly quickly. In this respect, it is reasonable to assume that post-drilling measurements of water level may be similar to those of the surrounding undisturbed aquifer. In addition to drilling disturbance, water levels vary throughout the year in an aquifer according to seasonal factors (e.g., changes in recharge and changes in storage). Because wells are drilled at different times of the year, the static water elevations recorded following drilling might be expected to vary depending on season. Notwithstanding, static water level measurements are assumed to be representative of groundwater levels in the aquifer, and act as a surrogate for ambient groundwater conditions in the aquifer.

Figure 75 Depth to water table from ground surface at well locations in Grand Forks aquifer (histogram and descriptive statistics).

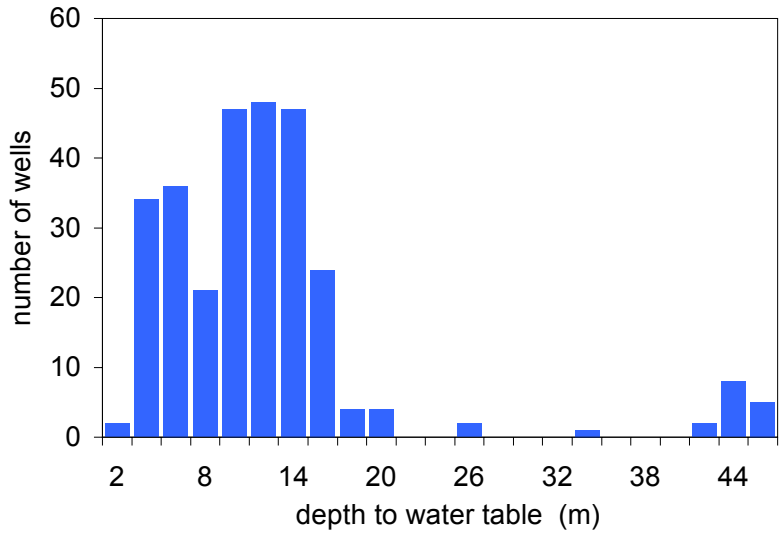

Statistic	(m)
Mean	11.4
Median	10.1
Standard Deviation	8.8
Minimum	1.5
Maximum	46.8

Count	285

Percentiles	(m)
13	4.2
25	6.1
33	8.3
50	10.1
63	11.8
75	12.9
87	14.7
94	24.8

Values of static water level (recorded as depth to water in a well), were imported into ARCGIS as point values that are representative of the water level at each well. The median depth was 10.1 m, but range was from 1.5 to 46.8 m (Figure 75).

A composite water surface was calculated using a geostatistical analysis involving interpolation between points, and extrapolation to the boundary of the aquifer. By subtracting the water table surface from the ground surface (using digital elevation model), a map of depth to water table was produced in 20 m raster format (shown in Map 25).

Map 25 Depth to water table from ground surface in Grand Forks aquifer.

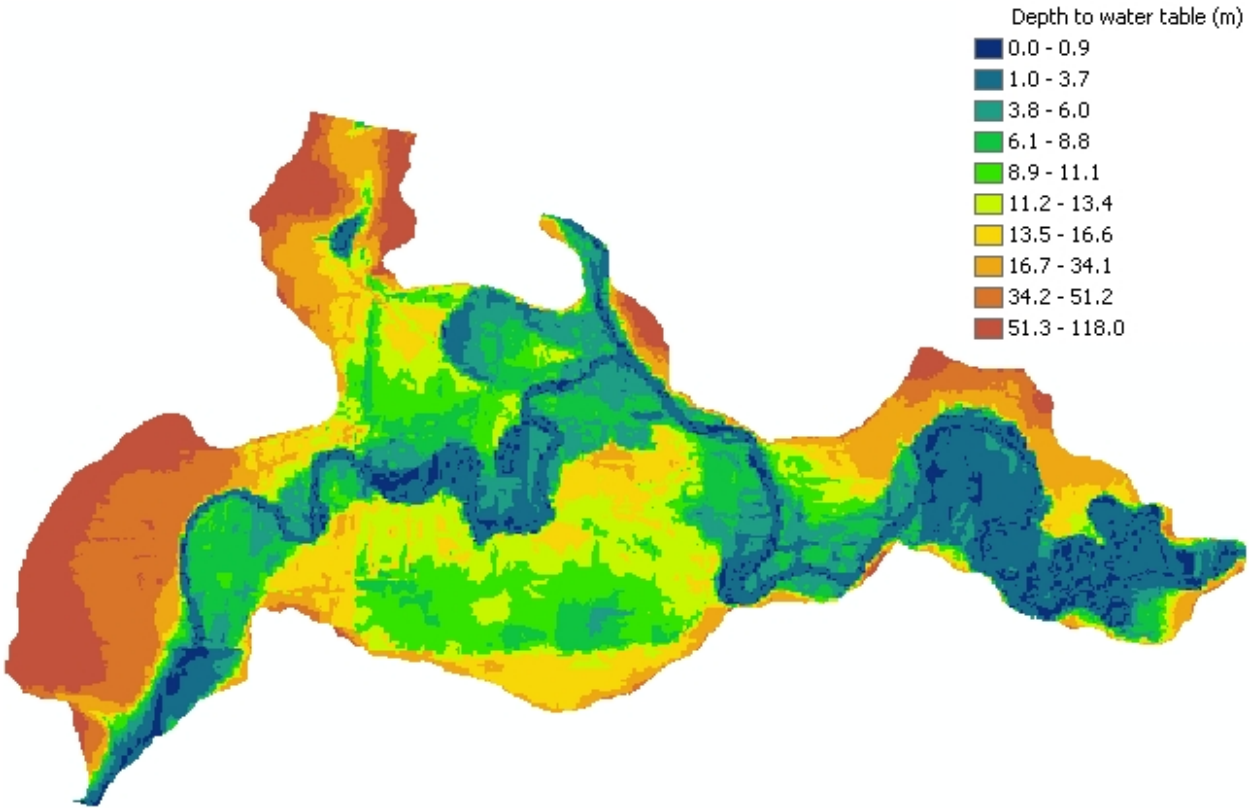

The “static” water table is very close to ground surface along the Kettle River, which is incised into the larger valley floodplain, and especially in eastern end of valley. However, the static groundwater levels in eastern end of valley were at or above ground surface of present Digital Elevation Model (DEM), resulting in 0 or negative values in subtraction of the water table surface from ground DEM. Thus, value of 0 was assigned in those cases for map cells for depth to water table. Whether the wells were artesian or surveying errors were made or data incorrectly digitized from old litholog forms, cannot be ascertained at this time. The water table is very near the ground surface in that part of valley, as evidenced by swampy ground, with multiple ponds and oxbow lakes and generally low-lying ground along the river. Above the floodplain, in central portion of valley, the water table is 5 to 15 m below surface.

Along the valley walls, the terraces are higher and ground slopes up faster than water table, producing much greater depths to water table, notably in western valley region, where depth up to 45 m are common. The main uncertainty of this map is in the interpolated water table surface from static levels, which were extrapolated to valley boundaries. In reality, the groundwater surface might slope up more sharply along valley walls, particularly if the surface runoff from valley slopes provides sufficient recharge, but that is not very likely over most part of the year in Grand Forks due to small precipitation levels and generally dry valley slopes. The water table surface was also smoothed out by the Kriging interpolation method, so random errors in static ground water surface (not being really static but seasonally variable) were minimized. Thus, the depth to groundwater map should be quite accurate given all considerations to source data and analysis methods.

Depth to water table determines the total thickness of HELP soil column for recharge computation. Five depths were selected using quantiles of the distribution of the depths (min and max bounding values). Depths to water table in 285 wells ranged from 1.5 m to 46.8 m, with median of 10.1 m and quartile values of 6.1 m and 12.9 m. The depth classes will be chosen as 0 to 6 m, 6.1 to 10 m, 10.1 to 12.9 m, 13 to 47 m, with roughly 25% of aquifer area in each category (four categories). Representative sediment columns will be 3, 8, 11, and 25 m in depth to water table.

5.9.6. RECHARGE SCENARIOS

Recharge scenarios were generated for all combinations of defined classes (4 categories each) of Kz, depth to water, soil type. The four Kz classes were “very high”, “high”, “moderate”, and “low” hydraulic conductivity of unsaturated zone aquifer media. Depth to water classes were used: 3, 8, 11, and 25 metres (coded as d3, d8, …). Soil classes were coded in terms of permeability, previously shown in Table 23, as “low”, “moderate”, “high”, and “very high”, and coded with S-rating values (of DRASTIC method) as SR10, SR9, … The percolation column scenario names were coded by specifying depth, soil type, and Kz as in the example: “d3_SR10_highK”.

Using ArcGIS, the aquifer was reclassified into percolation column scenario polygons, based on cross-referencing of 3 raster images for the 3 variables (classed maps). The conditional statement for raster calculation had 64 conditions specified, was rather long, and was constructed on a spreadsheet before using in ArcGIS. The resulting map of percolation column scenarios (Map 26 on next page) shows that there is relatively high spatial resolution of the differences between the 3 variables of aquifer media in most parts of the valley, except the eastern section where K_z had low variability due to low number of interpolated points (smother K_z distribution), and where depth to water table was small throughout. The higher the variability in these scenarios over space, the more accurate the recharge distribution will be.

More categories of K_z and depth could be added, but that would result in many more percolation columns in HELP model, thus more data analysis requirements. Note that there are only 4 discernible soil types over most of the area of the valley. K_z is interpolated and larger number of K_z classes would represent that interpolated K_z distribution more smoothly, but it would not improve the accuracy of the model because K_z distribution is not that well known; in itself it is heavily averaged and has many assumptions. Depth to water table is relatively well known, probably the best of these 3 parameters, but in areas where depth has low variation, the addition of more depth classes would not improve the resolution (the scenario map would look almost identical to present one).

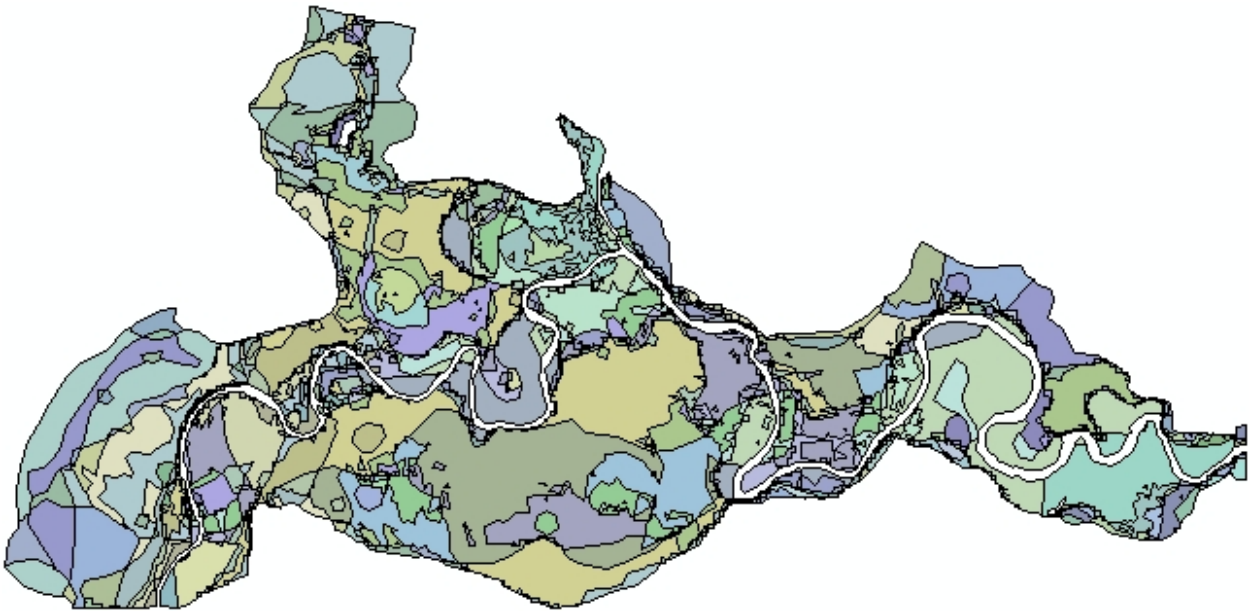

Map 26 Spatial distribution of aquifer media categories (recharge scenarios).

5.9.7. SENSITIVITY ANALYSIS OF RECHARGE TO HELP PARAMETERS (SOIL COLUMNS)

It is important to evaluate the sensitivity of HELP modeled recharge to soil column depth of aquifer media. If the effect is strong, for each month in the year the aquifer has to be reclassified into new assignments of the 27 categories of infiltration columns, using depths to water table at the end of previous month. The problem is that these are not known until the groundwater model is run in transient mode up to that month, but the groundwater flow model requires prior recharge inputs for it to predict the groundwater levels. This results in a circular problem. Figure 76 (and Figure 78 with recharge as percentage of monthly precipitation) and the following summarize the sensitivity of recharge to several parameters:

1. No noticeable or very small (< 5% change) effect on recharge (of percolation layer parameters):
    - stand of grass type
    - wilting point
    - field capacity
    - initial moisture content
2. Moderate effect on recharge:
    - soil thickness
    - porosity of percolation layer
3. Strong effect on recharge:
    - depth of vadose zone (percolation layer)
    - soil type
    - K sat of vadose zone

Figure 76 Sensitivity of HELP modeled recharge estimates to (a) saturated vertical hydraulic conductivity of vadose zone, (b) soil permeability, (c – d) depth of vadose zone and soil permeability, (e) soil thickness, (f) porosity of vadose zone material.

(a) effect of K sat on recharge (d = 3m, high soil perm.)

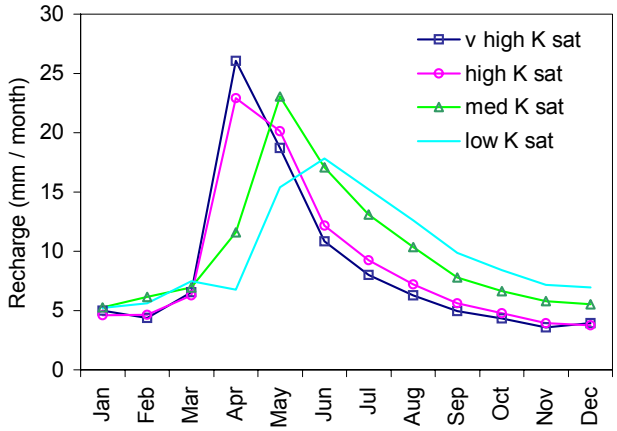

(b) effect of SOIL PERM. on recharge (d = 3 m, med K sat)

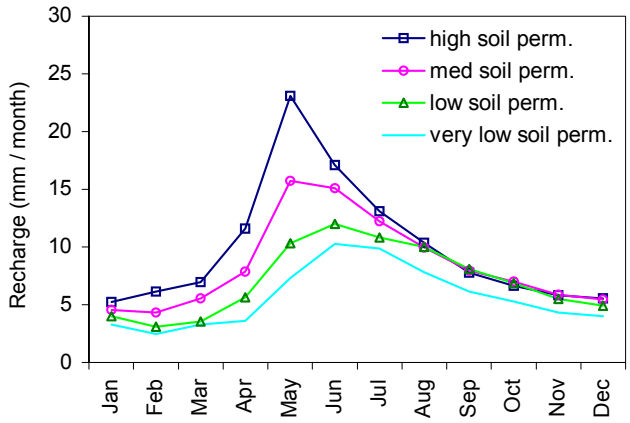

(c) effect of DEPTH on recharge (high Ksat, high soil perm.)

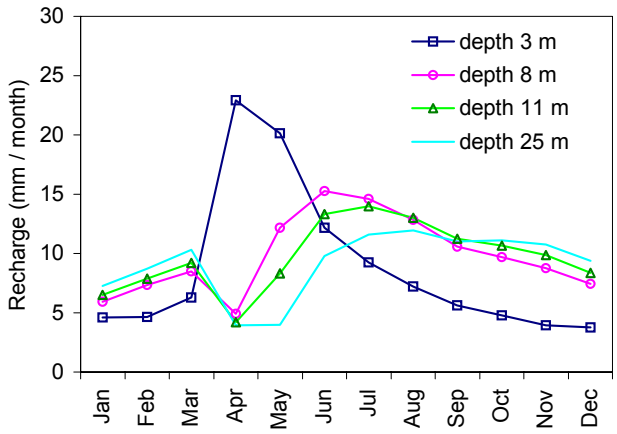

(d) effect of DEPTH on recharge (high Ksat, low soil perm.)

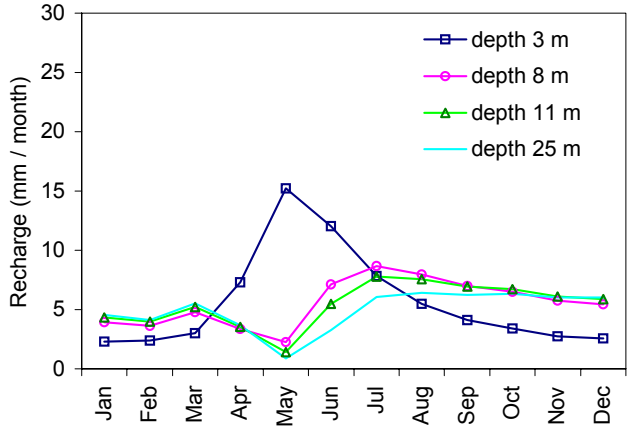

(e) effect of SOIL THICKNESS on recharge (d = 3 m, med Ksat)

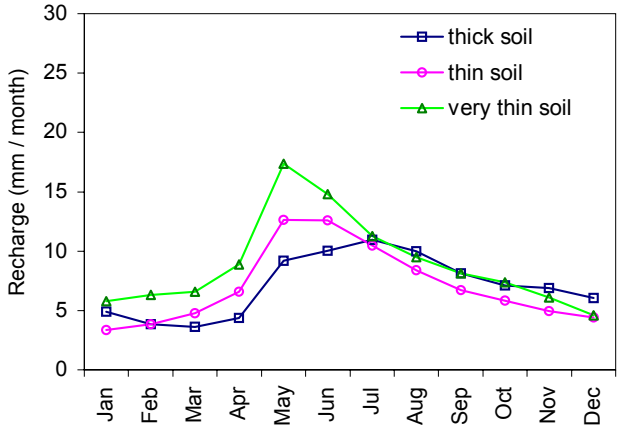

(f) effect of POROSITY of percolation layer on recharge (d = 3 m, med K sat, med soil perm.)

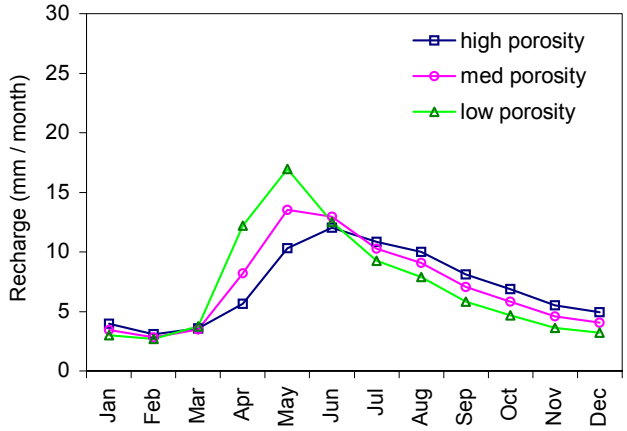

The unusual results shown in Figure 77 occurred in all HELP scenarios where K = “low” or when K = “low” or “med” and depth >= 11 m. The results seem to suggest that HELP kept increasing extinction depth, or kept changing moisture content of the vadose zone or some other effect. It would be expected that when vadose zone is deeper, it would take more water to commit to storage along the way during percolation, so less recharge would occur, but eventually, the soil would be near saturation below extinction depth and would remain that way (no ET). It is difficult to evaluate HELP performance here, but it is comparable to other hydrologic models and has been compared to other models (Scanlon et al., 2002a; 2002b). The HELP model underestimated measured runoff by ½ order of magnitude (which could be corrected by increasing K in model), had evapotranspiration (ET) error up to 30%, and storage estimate error of up to order of magnitude. The storage routing in HELP compared badly to Richards’ equation method in all other codes. Unsat-H outperformed HELP significantly and should be considered for in the future research.

Figure 77 Adjusted recharge for some HELP outputs where K sat of vadose zone was low and output was questionable (too high).

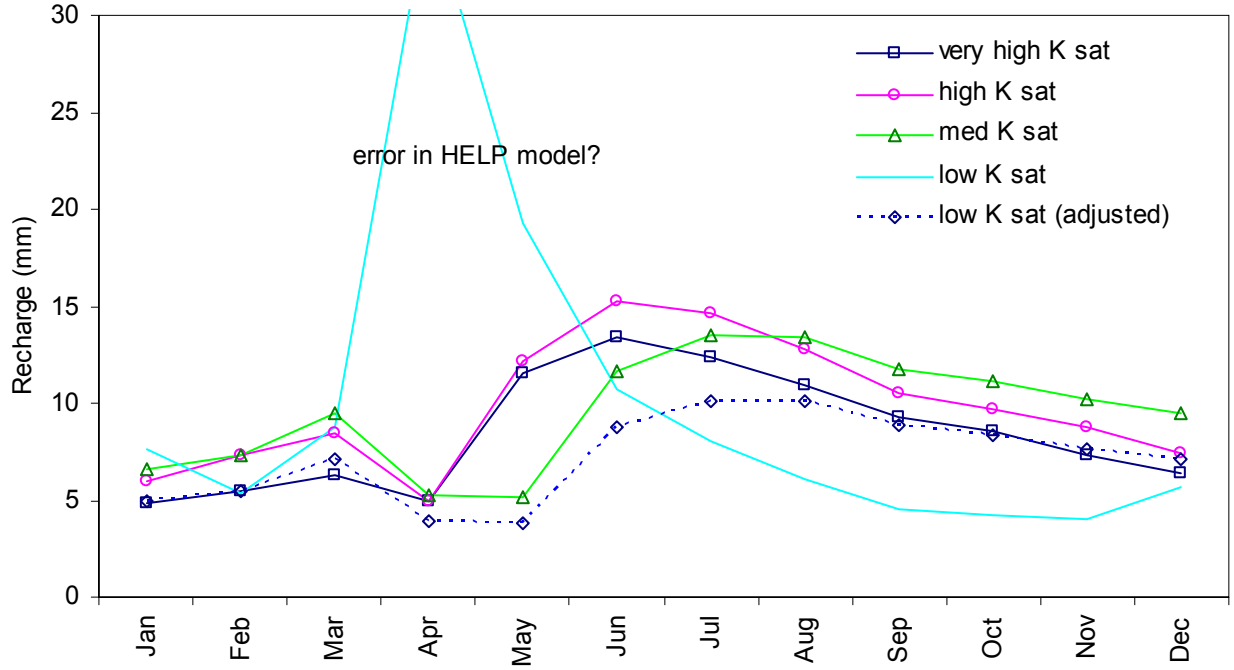

In terms of recharge as a percentage of monthly precipitation, Grand Forks receives between 10% and 80% of recharge from precipitation, according to HELP output. In spring time, it receives 40% to 80% recharge from precipitation depending on soil properties and K properties, and in summer the values are 30% to 50%. During late summer the aquifer receives 60% to 90% of precipitation, but overall recharge (in mm) is small because rainstorms are infrequent. The LARS-WG preserves the intensities of rain events, and what was observed was that if a high intensity event occurs during the late summer (such as a thunderstorm), it rains heavily and most of the water infiltrates the aquifer. Had it rained slowly and over a longer time, much more of it would evaporate. This type of relation may be very different in other climate regions and in other aquifers where high intensity rainfall events may lead to increased runoff and less infiltration. Figure 79 shows recharge as percentage of monthly precipitation for the most common recharge zones.

Figure 78 Sensitivity of HELP modeled recharge estimates, as percentage of monthly precipitation to (a) soil permeability, grouped by different K sat of vadose zone, (b) K sat of vadose zone, grouped by different soil permeability.

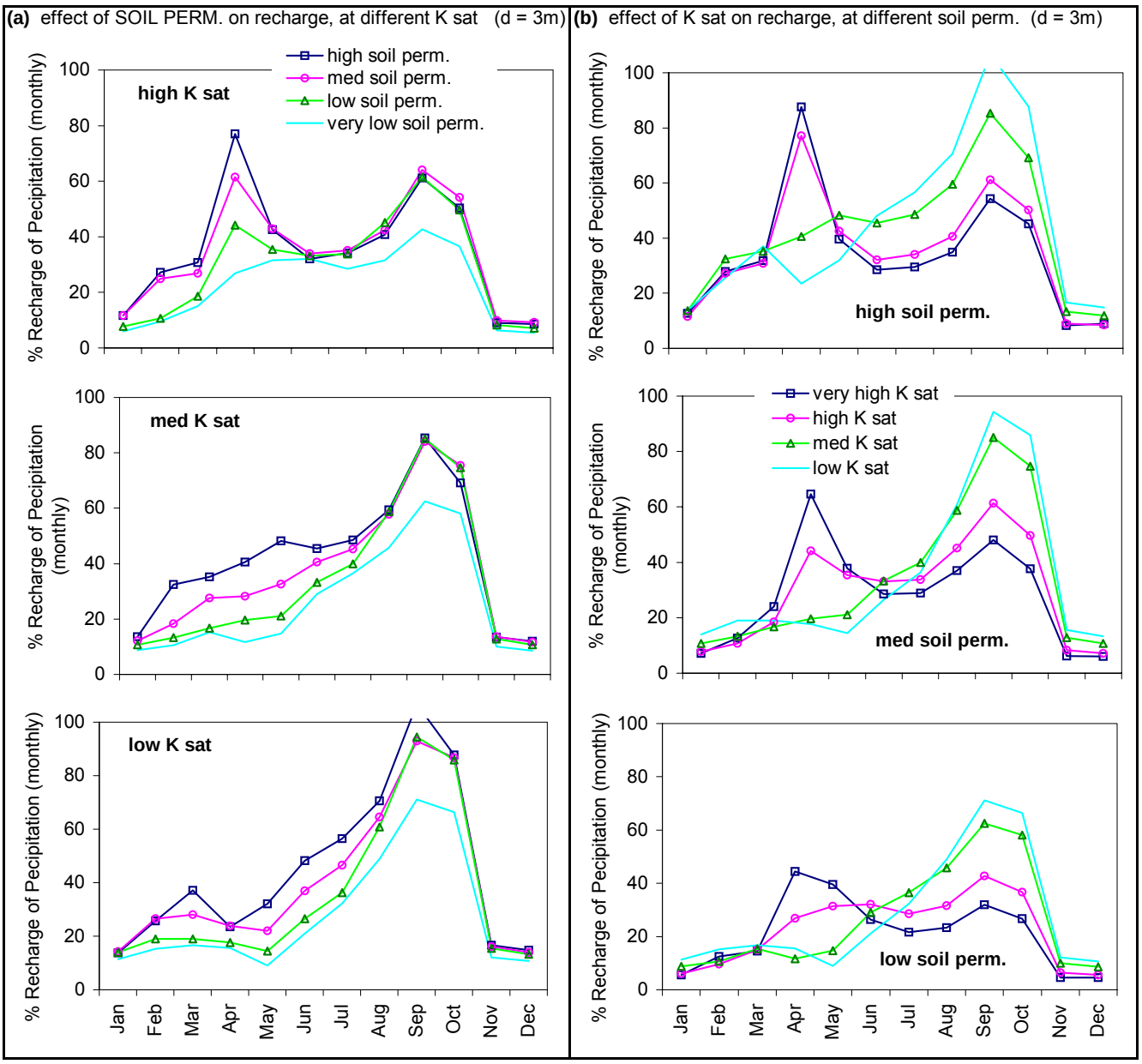

Figure 79 Recharge as percentage of monthly precipitation for most common recharge zones (numbered here S1 to S27) in Grand Forks aquifer, by month and by recharge zone. Historical climate scenario: (a) monthly for all recharge zones and historical climate only, (b) annual for all recharge zones and 3 climate scenarios.

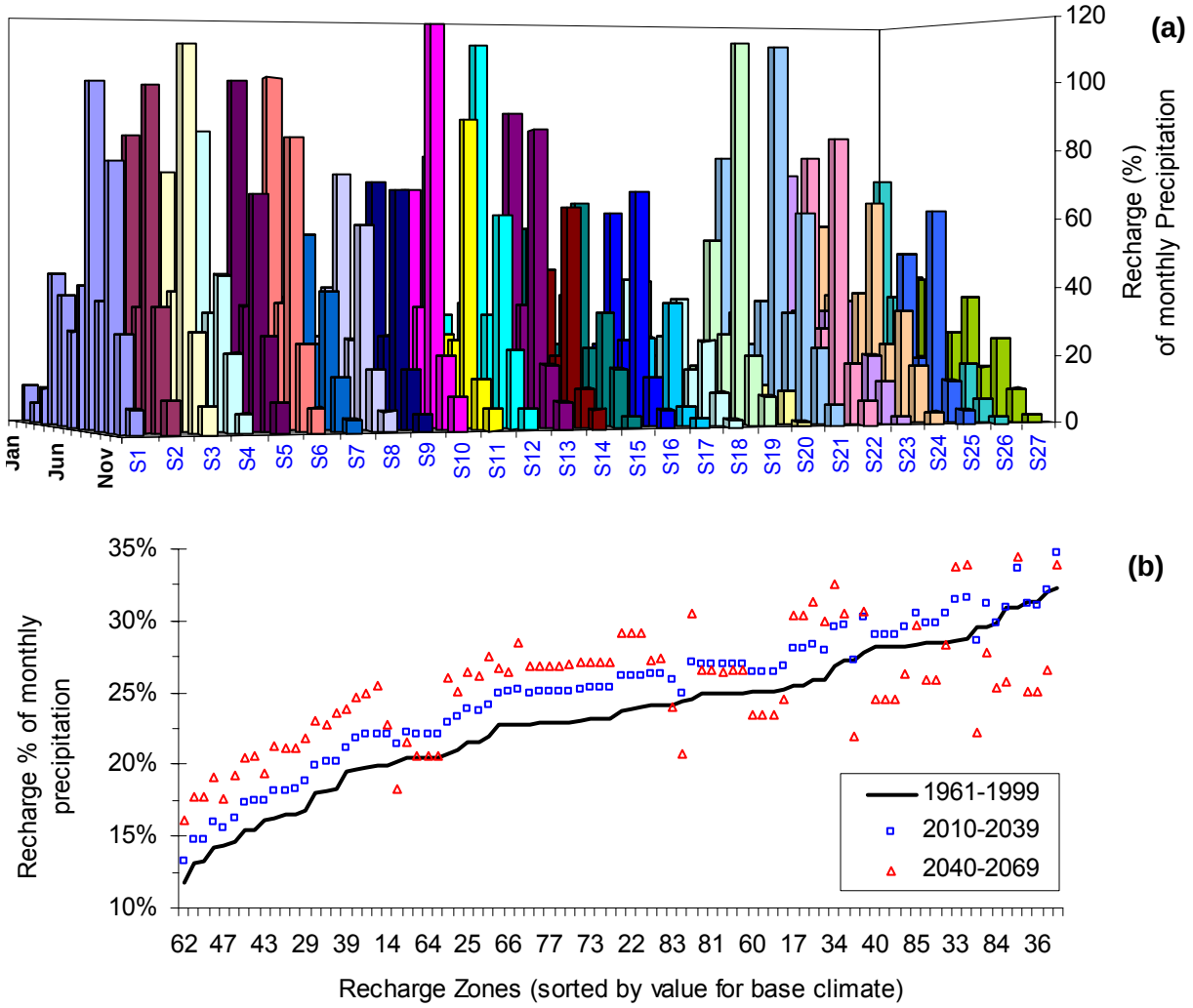

5.10. RECHARGE RESULTS FOR GRAND FORKS AQUIFER

Recharge values were modeled for present climate and 3 future climate scenarios (2010-2039, 2040-2069, 2070-2099). A summary table is provided in Appendix B. All predicted values were expressed as monthly average recharge. These values were summarized and mapped for 64 recharge zones, for each climate scenario. Figure 80 shows changes in recharge due to climate change in 3 different recharge zones, corresponding to zones 1, 38 and 4. These simulation results do not include irrigation return flow, which will be considered later.

Figure 80 Changes in recharge due to climate change in 3 different recharge zones (monthly mean recharge without irrigation return flow as applied to groundwater model).

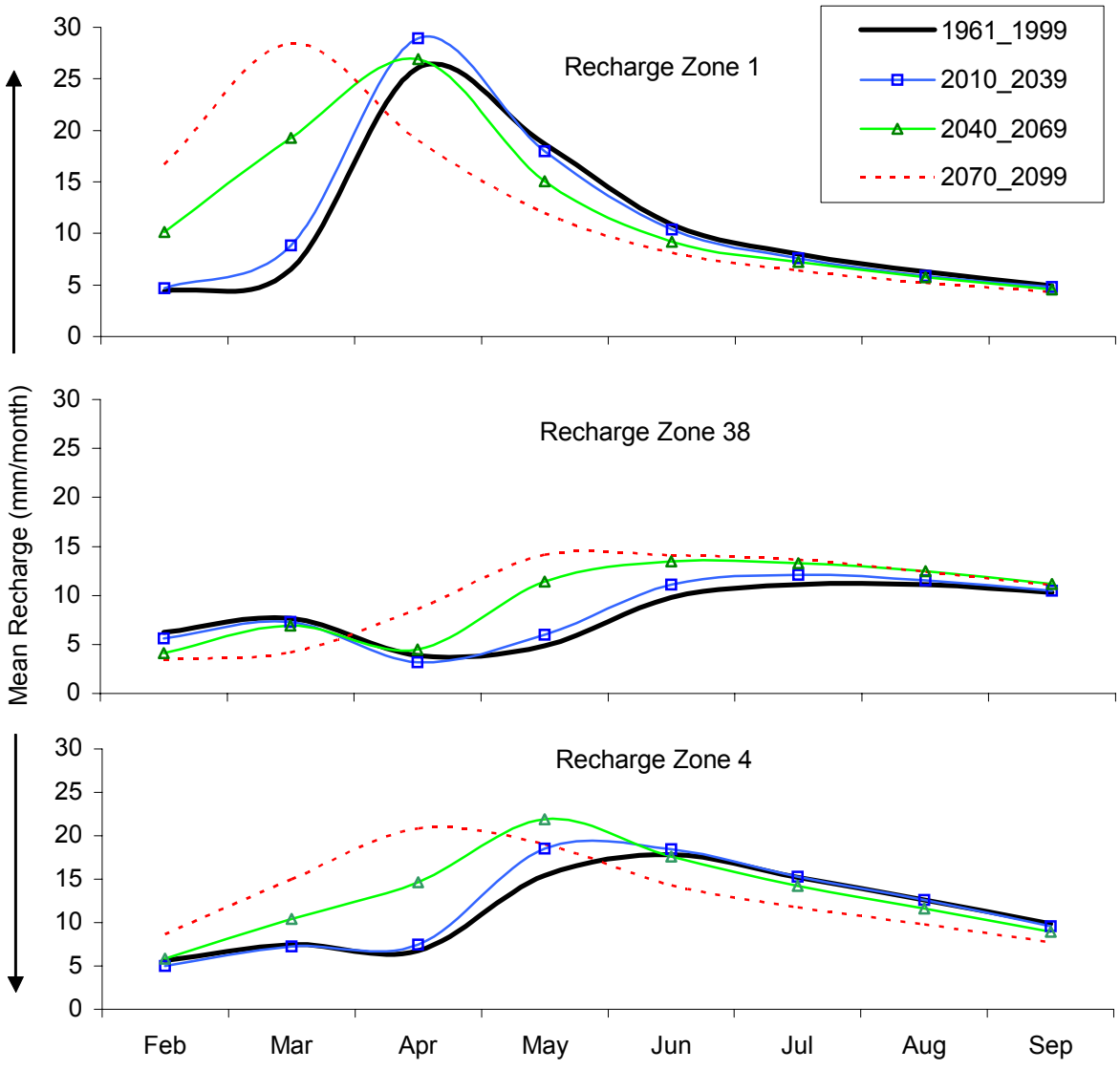

5.10.1. HISTORICAL CLIMATE

Map 27 (a) shows the spatially distributed mean annual recharge to the Grand Forks aquifer (mm/year). Values range from near 0 to 120 mm/year. The western and the northwestern portions of the aquifer receive the lowest recharge, while the highest recharge is received in the more central and eastern portions of the aquifer on river terraces, where as the floodplain areas receive lower recharge. According to HELP model results, in this climatic region there isn't enough precipitation to recharge the aquifer where there are thick sand and gravel terraces – most of the precipitation changes moisture content in these areas of thick gravels above water table, but little of it recharges the groundwater aquifer. This situation would be different if this was a wet climatic zone – most recharge would occur in most permeable areas with less influence on depth of sediment to water table.

Previous recharge modelling showed that the range of recharge determined for the Grand Forks aquifer is 76.56 mm/year to 165.71 mm/year, with a "representative" recharge[2] of 135.46 mm/year. The HELP modeling results and spatial distribution of recharge zones suggests the recharge value to be typically between 10 and 80 mm/year, showing strong zonation (floodplain versus terraces).

Mean monthly recharge to the inset area (see Map 27) of the aquifer is shown in Map 28. The lowest recharge occurs in January through May, the highest recharge occurs in June to September, while October through December receive moderate recharge. Recharge follows annual distribution of precipitation, when summer rainstorms supply most intense rainfall and most of recharge to aquifer from rainfall. The predicted changes in mean annual recharge were converted to percentage differences: (future – historical) / historical, and are included in Map 27 parts (b) and (c), and also graphed in separate maps for monthly recharge estimates.

5.10.2. MODELLED 2010-2039 CLIMATE

The 2010-2039 climate scenario has predicted 2 to 7 % increase from present mean annual recharge and there are no predicted decreases. Predicted mean monthly recharge to the inset area (see Map 27) of the aquifer is shown in Map 29 for the period 2010-2039. The lowest recharge occurs in January through May, the highest recharge occurs in June to September, while October through December receives moderate recharge. See section 7.4 for a comparison of these results with historic climate data.

5.10.3. MODELLED 2040-2069 CLIMATE

The 2040-2069 climate scenario has predicted 11 to 25 % increase from present mean annual recharge, also without any prediced decreases. Predicted mean monthly recharge to the inset area (see Map 27) of the aquifer is shown in Map 30 for the period 2040-2069. The lowest recharge occurs in January through May, the highest recharge occurs in June to September, while October through December receives moderate recharge. See section 7.4 for a comparison of these results with historic climate data and predicted data for 2010-2039.

[2] "representative" recharge was determined from the dominant aquifer media used in the soil column in HELP. This representative value was ultimately used by Allen (2001) as the base case for climate change impact modelling.

Map 27 Mean annual recharge to Grand Forks aquifer for historical climate scenario (1961-1999), modeled in HELP and assigned to recharge zones: (a) mean annual recharge values in mm/year, (b) percent change between 2010-2039 and historical, (c) percent change between 2040-2039 and historical.

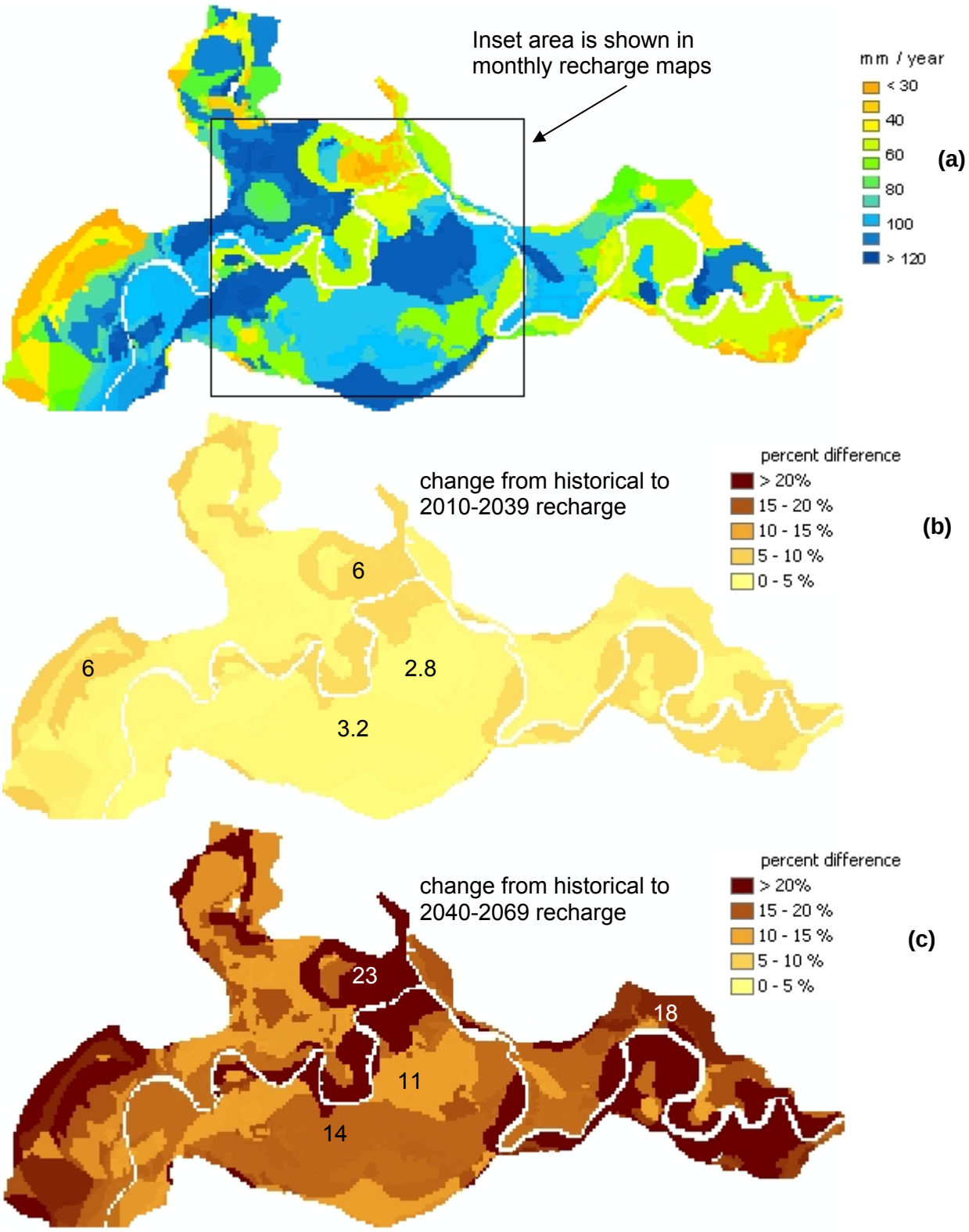

Map 28 Mean monthly recharge to Grand Forks aquifer for historical climate scenario (1961-1999), monthly maps for central portion of valley (see inset on mean annual recharge Map 27).

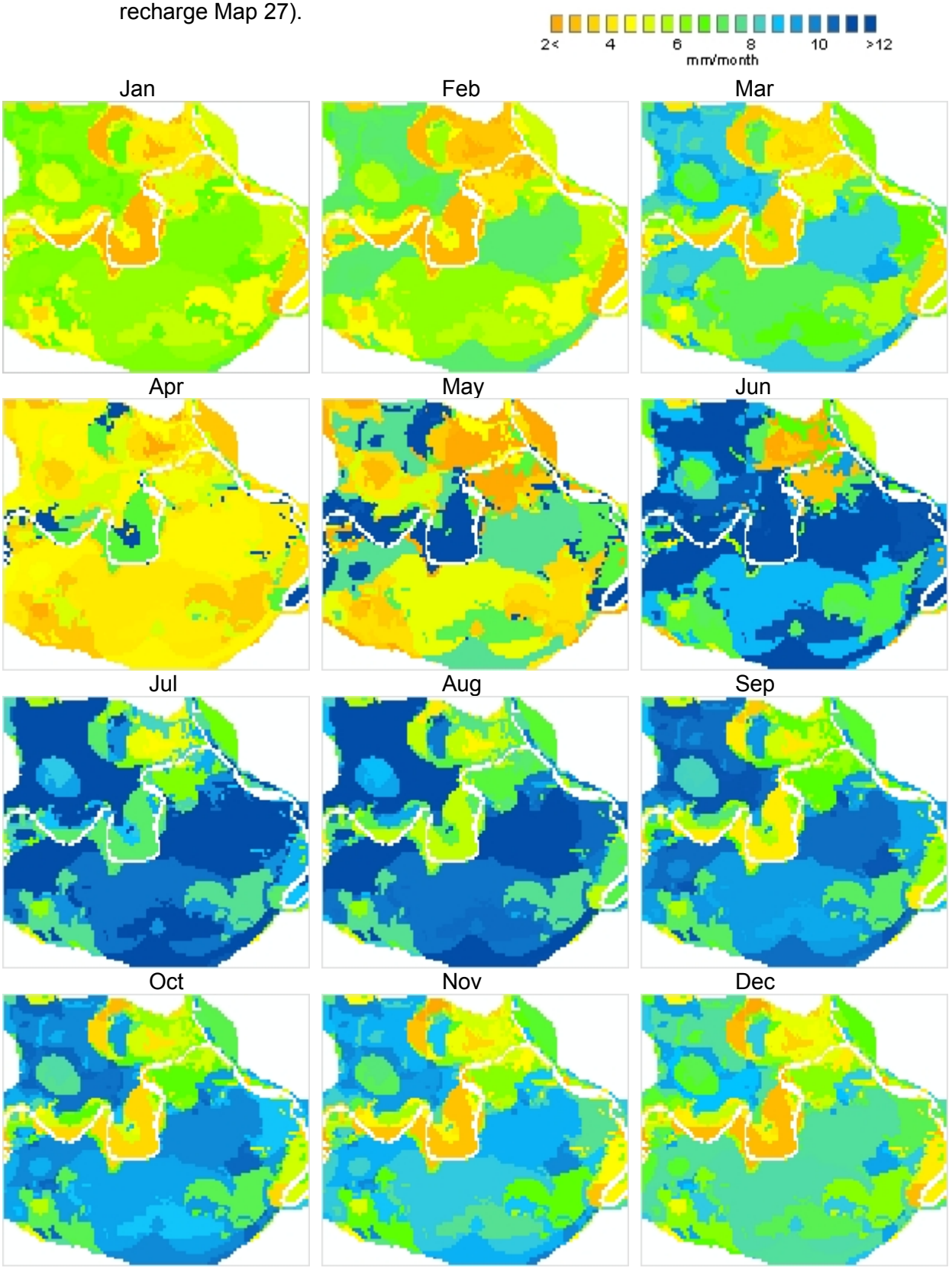

Map 29 Mean monthly recharge to Grand Forks aquifer for predicted climate scenario (2010-2039), monthly maps for central portion of valley (see inset on mean annual recharge Map 27).

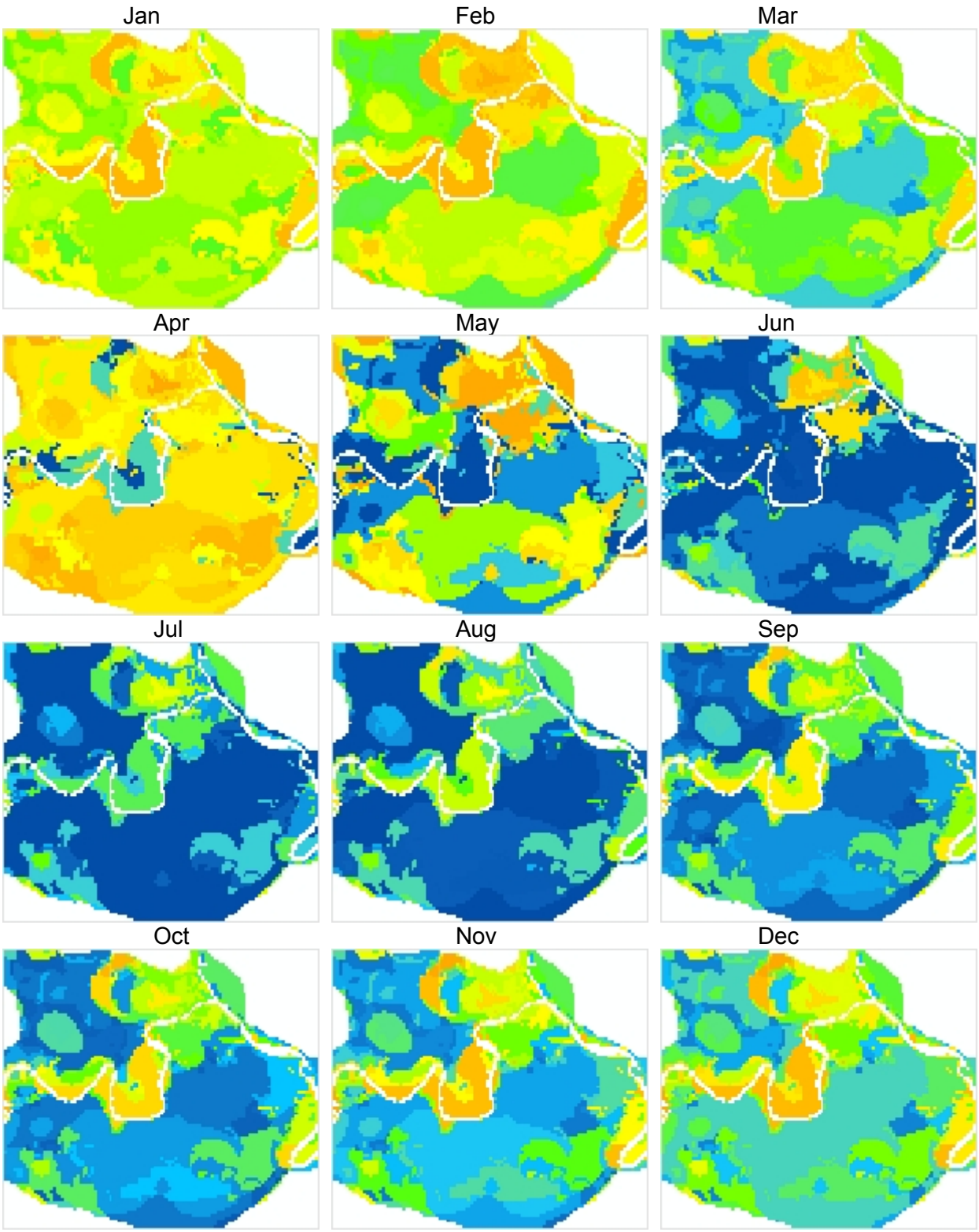

Map 30 Mean monthly recharge to Grand Forks aquifer for predicted climate scenario (2040-2069), monthly maps for central portion of valley (see inset on mean annual recharge Map 27).

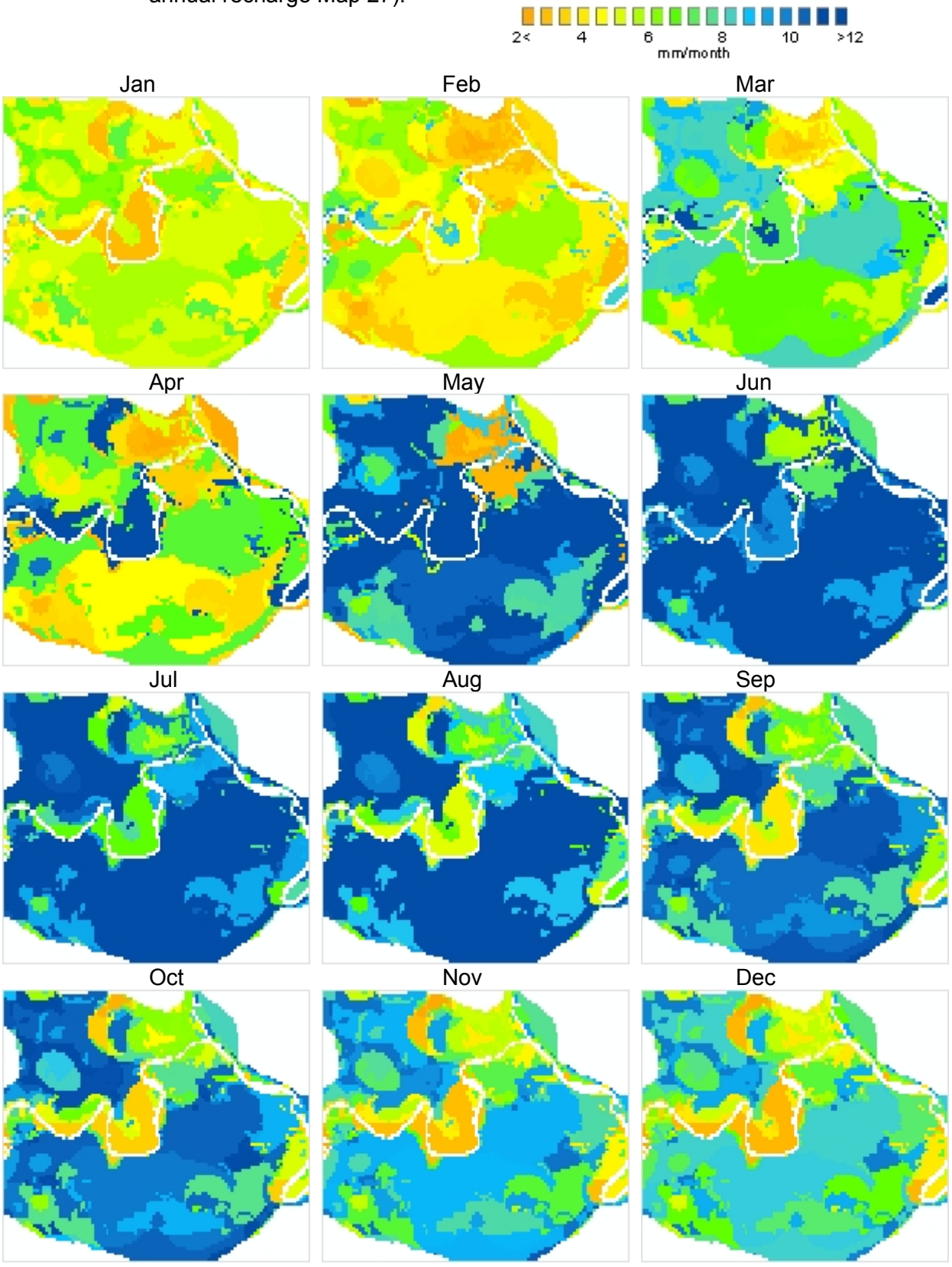

5.10.4. ADJUSTED RECHARGE FOR IRRIGATION RETURN FLOW

In all pumping model scenarios for groundwater model of the Grand Forks aquifer, the recharge zones were modified by including estimated irrigation return flow to the aquifer. The analysis of irrigation zones was done by Allen et al. (2003), included here as summary of methodology and results. Irrigation and pumping was applied only from June to August (in Grand Forks aquifer transient model these were times in Julian Day from 155 to 242).

Maps (hard copy) were provided by the Irrigation and Improvement Districts in the Grand Forks area. These were of varying quality. District boundaries were mapped and created polygon shapefiles in GIS, then to raster coverage, and used in new recharge zone classification. The new recharge zone classification was necessary for MODFLOW, which defines recharge zones by "value set" (each zone is unique in that is has unique recharge value or recharge schedule). To represent "modified" recharge schedules, a new recharge zone was created out of every combination of original 64 (non-irrigated) recharge zones from HELP model, and areas of irrigated fields with their different return flow estimates. In total 161 recharge zones (unique recharge schedules) were applied to transient Grand Forks recharge model.

- ESTIMATION OF RETURN FLOW (DEEP PERCOLATION LOSSES)

When undertaking a DRASTIC analysis, recharge is typically estimated in one of two ways. Often it is assumed that the same amount of recharge is applied to the entire map area. However, a better representation of recharge takes into account the amount of water that is returned to the aquifer when the land is irrigated. This is commonly referred to as return flow (from the aquifer perspective) or deep percolation losses (from an irrigation perspective).

Estimates of return flow were obtained through consultation with both experts in the field of irrigation. Two individuals were identified who by Agriculture Canada and the BC Ministry of Water, Land and Air Protection could provide assistance in this respect. Ultimately, Pat Brisbin, Golder Associates, Abbotsford was contacted, and John Parsons.

Pat Brisbin (personal communication) indicated that there are two main issues regarding the volume of return flow. First, is the issue of inefficient sprinkler systems, and second is the issue of excess application. Brisbin indicated that although there are no specific studies that have attempted to measure return flow in the Grand Forks area, he could provide us with justified estimates.

Brisbin described sprinkler systems as being inefficient because of the non-uniformity of area of application. Basically, irrigation is applied over a circular area, but the required land area is square. Additional irrigation water must be applied to the circular area in order to provide enough water to the outer edges (outside the circle). This results in excess water going into groundwater storage. Brisbin estimated that approximately 25-28% of applied water will go below the root zone in the central area. Of that amount, some (approx. 3%) is lost to evaporation, therefore, he estimated that approximately 22-25% could be the amount of return flow due to sprinkler system inefficiency.

Brisbin also estimated that most farmers probably over-irrigate because they cannot anticipate rainfall events. A farmer will apply a certain amount of irrigation so as to fill up the soil profile, and then find that it rains the next day. The irrigation water cannot be used by the plants and

therefore, the water infiltrates below the root zone and is added to the groundwater. Brisbin indicated that approximately 50% of water could be lost through such practices.

John Parson (personal communication), stated that he knew of no studies or information on the specific question of irrigation return flow in Grand Forks. From personal experience, but backed up with no data, he indicated that it is assumed there is return flow to the aquifer because through monitoring the aquifer for nitrates there are varying levels of nitrates under some of the agricultural fields. He suggested that most of this return flow is related to clean cultivated crops that are grown such as tree nurseries and potato fields; because this is where you see the most puddling of irrigation water. Pasture and hay fields that are irrigated on 24 hour sets may also experience some return flow. An unsubstantiated guess could put return flow on forage fields at 5% and clean cultivated fields at 10-15%, because plant use and evaporation would utilize the rest of the water. These estimates would be only for fields that do not have an impervious layer at a depth of 10 feet or lower. In consideration of both of these estimates for losses of irrigation water, we will assume an average return flow percent as 30%.

- IRRIGATION DISTRICTS AND IRRIGATED LAND

City of Grand Forks Water District

The Corporation of the City of Grand Forks was contacted and provided well use data for the year 2000. This dataset consisted of daily volumetric water extraction for each of city wells 2 through 5, and included monthly totals and averages.

As the City of Grand Forks provides water for both domestic and irrigation use, certain assumptions were necessary in order to generate an estimate for irrigation use from the totals provided. First, it was assumed that no irrigation takes place during the winter months and that water use over this period represents domestic use only (and that any increase in water use during the summer would represent water used for irrigation). Second, it was assumed that domestic water use remains relatively constant over the year and that seasonal variations (i.e., filling of swimming pools during summer) are insignificant. Finally, it was assumed that the majority of active irrigation in Grand Forks is performed June through August as these months have the highest temperatures and least precipitation (this assumption is supported by the observation that water volumes extracted by the City of Grand Forks were most strongly elevated during these months and generally constant over the remainder of the year).

Average monthly water use, September through May (assumed to represent domestic use only) was calculated to be 167,650 m^3. Average monthly water use June through August (assumed to represent domestic plus irrigation use) was calculated to be 418,267 m^3. The difference between these values (assumed to represent irrigation use only) is 250,617 m^3. As irrigation is assumed to be applied entirely during June, July and August, the yearly irrigation total would be equal to the three month summer total of 3 x 250,617 m^3 or 751,851 m^3.

Area of the City of Grand Forks Water District was measured from a GIS coverage to be 2,513,125 m^2, compared to total area of irrigation district of 10,529,922 m^2. Most of this area is not irrigated as determined from digital orthophotos, and the area of irrigated fields. The yearly volume was divided by the area of irrigated fields to generate an equivalent depth of water applied. This was calculated to be 299.17 mm/year. Assuming a 30% aquifer return flow, the final equivalent depth of water available for recharge is 89.75 mm/year.

Grand Forks Irrigation District (Big Y and Nursery Areas)

The Grand Forks Irrigation District was contacted and provided well use data for the years 1995 through 2001. This dataset consisted of yearly volumetric water extraction for each of wells Big Y#1 through #4 as well as Nursery #1 and #2. The Grand Forks Irrigation District also provided maps differentiating irrigated versus non-irrigated land within the Big Y and Nursery Areas.

In calculating irrigation water use estimates for the Big Y and Nursery areas, it was necessary to assume that the water extracted by the Grand Forks Irrigation District was all ultimately used for irrigation. This should be a reasonable assumption given the dominance of agricultural land use in the Big Y and Nursery areas.

Average yearly volumes of water pumped were calculated to be 2,020,140 m3 for the Big Y area and 516,240 m3 for the Nursery area. To determine an equivalent depth of water applied, the average yearly volume pumped by all wells in each area was divided by the total area of irrigated land in each. These area values were included as attributes in a GIS coverage, and totaled 4,778,093 m^2 for the Big Y area and 1,246,223 m2 for the Nursery area. Equivalent depths of water were calculated to be 422.79 mm/year for the Big Y area and 414.24 mm/year for the Nursery area. Assuming a 30% aquifer return flow, the final equivalent depths of water available for recharge are 126.84 mm/year for the Big Y area and 124.27 mm/year for the Nursery area.

Sion Improvement District

The Sion Improvement District was contacted and provided an irrigation estimate of 1.122 litres per second per hectare. The Sion Improvement District also provided maps differentiating irrigated versus non-irrigated land within the areas they service.

Assuming that the provided estimate is accurate and representative of all irrigated land within the Sion Improvement District, 1.122 litres per second per hectare converts directly to 884.58 mm/year. Assuming a 30% aquifer return flow, the final equivalent depth of water available for recharge is 265.37 mm/year.

Covert Irrigation District

The Covert Irrigation District was contacted and provided well use data for the years 1991 through 1998 for their larger (125 hp) pump and for the years 1991 through 2001 for their smaller (50 hp) pump. This dataset consisted of yearly volumetric water extraction for each of the wells mentioned. The Covert Irrigation District also provided a map differentiating irrigated versus non-irrigated land within their service area.

In calculating irrigation water use estimates for the Covert Irrigation District, it was necessary to assume that the water extracted was all ultimately used for irrigation. This should be a reasonable assumption given the dominance of agricultural land use in this area.

The average yearly volume of water pumped was calculated from the 1994 through 1998 data. These data range were selected as the bulk of the water extracted by the Covert Irrigation District is recorded to have been done with the 125 hp pump and (1) the pre-1994 pumping rates for this pump seem anomalously low and (2) the post-1998 pumping data for this pump are absent entirely. The average yearly volume of water pumped was calculated to be 207,875 m^3. To determine an equivalent depth of water applied, the average yearly volume of water pumped was divided by the total area of irrigated land in the Covert Irrigation District. This area was summed from the areas of individual irrigation lots included as an attribute in a GIS

coverage and totaled 629,538 m^2. The equivalent depth of water was calculated to be 330.20 mm/year. Assuming a 30% aquifer return flow, the final equivalent depth of water available for recharge is 99.06 mm/year.

Map 31 Irrigation districts of Grand Forks valley, with irrigated fields, overlaid on enhanced orthophotos.

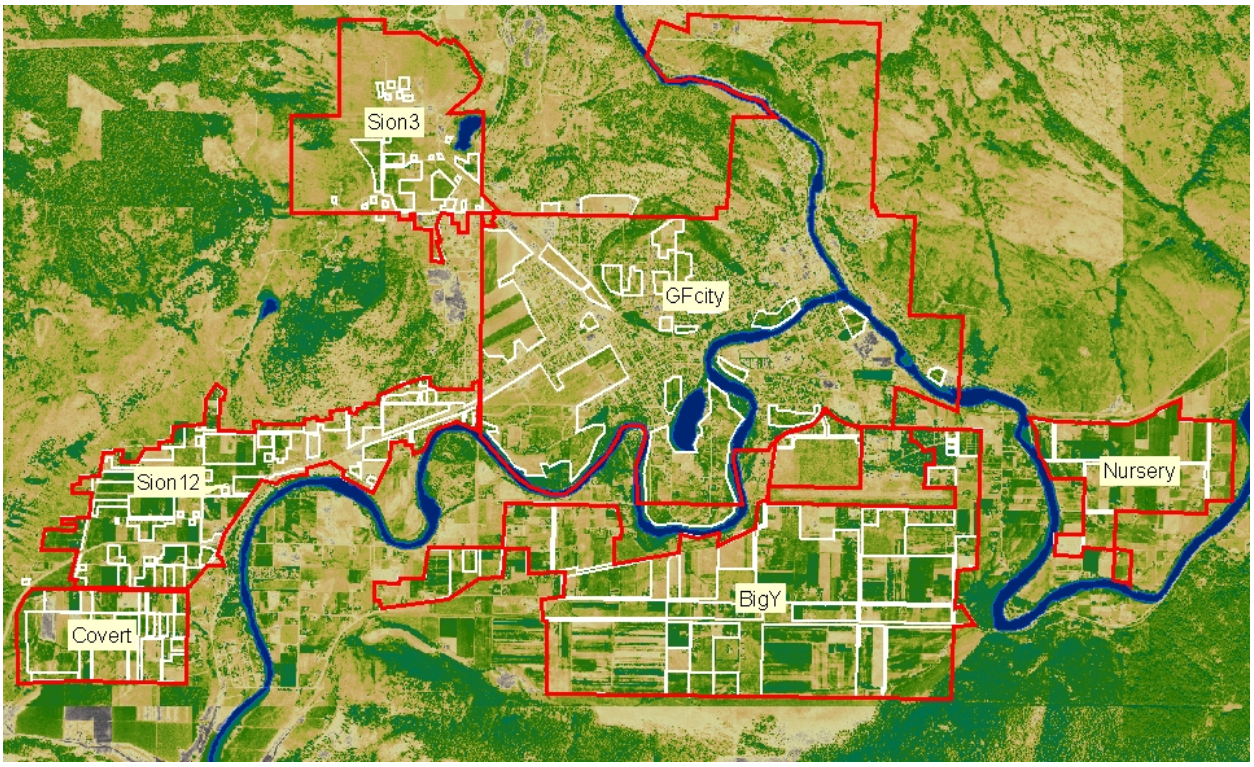

Map 32 Irrigation zones created from irrigated fields where irrigation return flow was estimated, in MODFLOW model of Grand Forks aquifer.

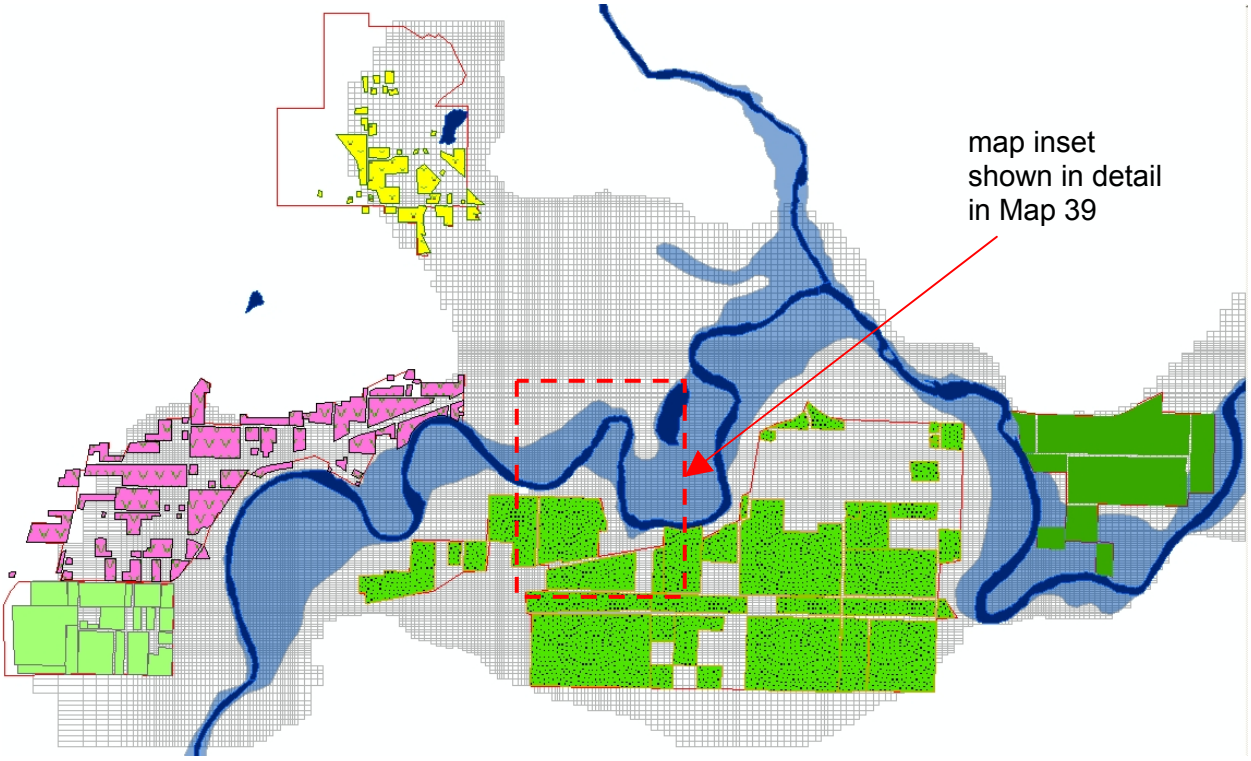

Return flow was expressed as net infiltration in mm/year, then converted to mm/month for MODFLOW recharge zones. Values for the irrigation districts are summarized in Table 24.

Table 24 Irrigation statistics and estimated irrigation return flow by irrigation district in Grand Forks valley.

Water District	Yearly Irrigation Volume (m^3/year)	Total Area of Irrigated Land (m^2)	Total Infiltraton (mm/year)	Losses to Evapo-transpiration (mm)	Net Infiltration (mm/year)
Big Y	2020140	4778093	422.79	295.95	126.84
Nursery	516240	1246223	414.24	289.97	124.27
Covert	207875	629538	330.20	231.14	99.06
Sion 12	–	–	884.58	619.21	265.37
Sion 3	–	–	884.58	619.21	265.37
City of Grand Forks	751852	2513125	299.17	209.42	89.75

6. MODEL DESIGN AND CALIBRATION

6.1. MODELING SOFTWARE

The groundwater flow model was implemented and solved by MODFLOW, a block-centered finite-difference code (McDonald and Harbaugh, 1988). MODFLOW views a three-dimensional system as a sequence of layers of porous material. The advantage of modflow is that is it widely used and its performance has been verified in numerous modeling studies. The regular grid design involves rectangular arrays for each layer, which are easy to modify using computer code, and are very easy to link with GIS (raster based) systems. Given the requirements of this project, of inputing spatially-distributed recharge, and of linking river models with groundwater models, and of mapping the results and spatialy-distributed inputs in GIS system, the finitie difference model type was selected.

Visual MODFLOW v 3.1.83 (Waterloo Hydrogeologic Inc.) was the modeling software environment for running MODFLOW 96 and 2000 and other packages such as ZBUD (Zone Budget), MODPATH (particle tracking). All recharge modeling was done outside of MODFLOW. The recharge and river inputs were modeled external of MODFLOW and are described in boundary condition chapter. All hydrostratigraphic modeling was done in GMS Groundwater Modeling System 4.0 and with aid of ArcGIS for spatial database and spatial interpolation and all other spatial analyses. Automated parameter estimation was not used here.

6.2. MODEL DOMAIN

In the groundwater flow model, the active cells were limited to valley sediments. All cells corresponding to valley walls (bedrock) were deactivated. The bedrock is considered a no-flow boundary here. The aquifer extent was originally defined by BC WLAP. The original surficial aquifer boundary considered surficial geology and known bedrock outcrops (Wei, personal communication). However, the digital soil map showed bedrock outcrops that constitute valley walls further beyond the aquifer boundary. After 3D hydrostratigraphic modeling, and after bedrock surface modeling, the valley walls were redefined. After the final editing of the MODFLOW grid and correction of DEM errors, the boundary of valley sediments and valley walls was redrawn. The sediments drape the valley slopes and thin upslope, so the new aquifer boundary stops where the sediment thickness falls below several meters (thin soil and sediment veneers on valley walls are not modelled in groundwater model because these are insignificant compared to the rest of the aquifer volume). To preserve consistency between the hydrostratigraphic model, the soil maps, the recharge maps, and the groundwater flow model grid design, the new aquifer extent was defined as shown on Map 33.

When looking in profile-cross-section view at the model domain, the vertical extent of valley sediments in the model is apparent. Visual MODFLOW 3D Explorer was used to produce a cut-away view in Map 34. The finite-difference grid is visible over all layers. The bedrock slopes (inactive cells) contain the active model area. The ground surface forms the upper model boundary.

Map 33 Grand Forks surficial aquifer extents: original BC WLAP aquifer extent, and modified extent for this modeling study.

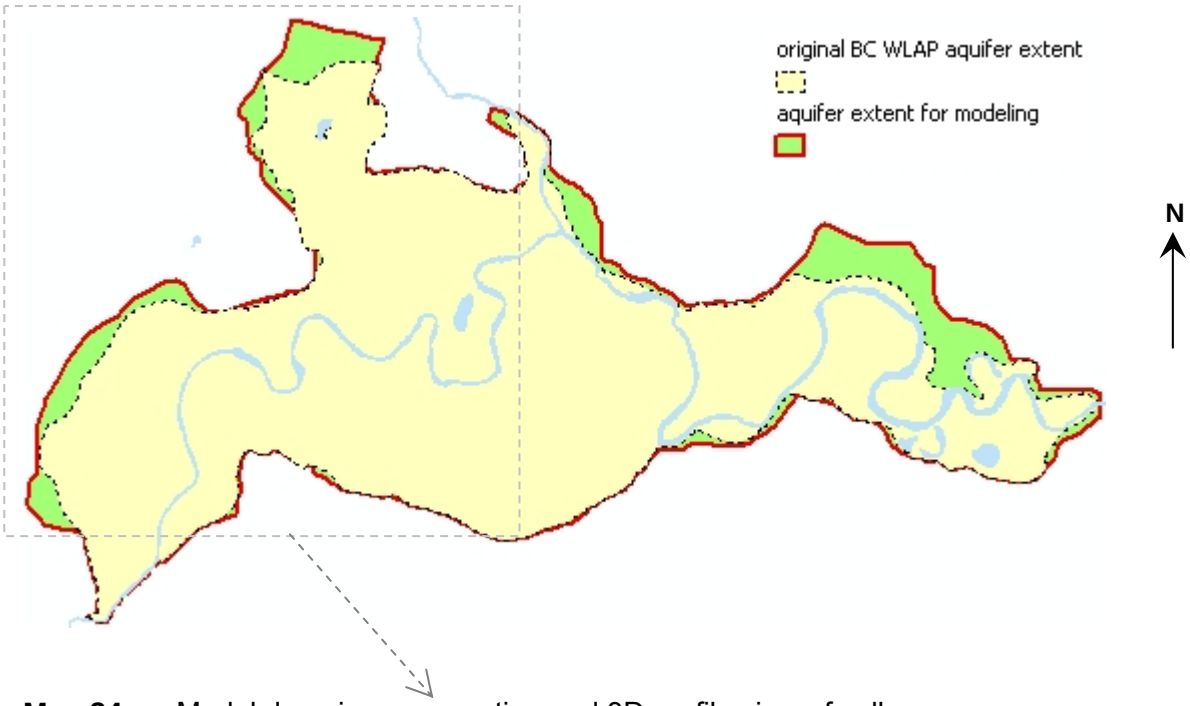

Map 34 Model domain cross-section and 3D profile view of valley.

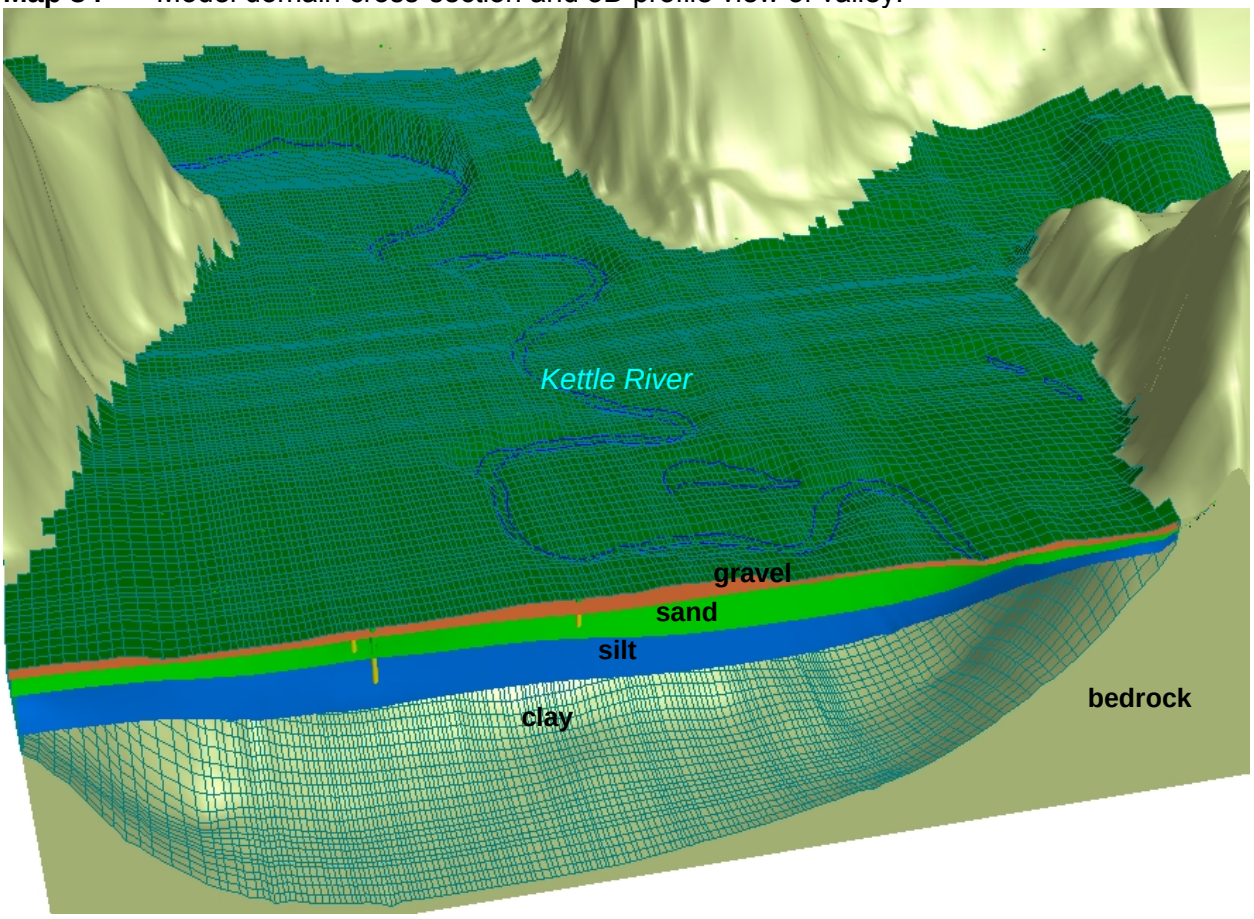

6.3. MODFLOW LAYERS AND GRID

A finite difference grid was constructed in three dimensions following standard grid-construction rules (Anderson and Woessner, 1992). Grid density (Map 35) dictates the resolution of the numerical solution. The grid was refined in areas where significant changes in the hydraulic heads were anticipated over short distances (e.g., near rivers and production wells), using standard telescopic mesh-refinement techniques. The horizontal grid spacing is customized in telescopic grid refinement to increase grid density near production wells and rivers.

The MODFLOW model of the Grand Forks aquifer was implemented in 5 layers (plus bedrock as layer 6) as seen in profile view of model domain cross-section in Map 37. Each layer represents a dominant sediment type, as was determined from borehole lithologs. Due to MODFLOW layer representation, the layered hydrostratigraphic units are assumed continuous in aerial extent. Where sediments of any type are absent, the layer was represented as thin. Near valley walls, the layers drape the bedrock slopes. Bedrock forms the bottom surface of the model domain.

Layer 1:
This is the top layer in the groundwater flow model and represents fluvial gravels (channels, floodplain, and eroded terraces). This layer has the highest hydraulic conductivity. In reality the gravels also contain sand and silt lenses and is covered by thin soils. Recharge is applied to this layer. The water table surface is below the bottom of this layer at some time during the year in about half of the aerial extent of the valley. All river channels and drain channels are in Layer 1 for consistency and to simplify import of recharge and river information. By definition, the top layer represents the floodplain and river channel gravelly fluvial deposits.

Layer 2:
The most dominant sediment in this layer is sand. The Grand Forks aquifer is composed of layers 1 and 2, but only Layer 2 is consistently saturated (below water table). The hydraulic conductivity is high, but is lower than Layer 1 because the occurrence of silt lenses increases and there is less gravel in this layer based on borehole lithology information. All modelled heads are exported from Layer 2 to avoid problems with dry cell representation. The hydraulic head in Layer 2 is approximately equivalent to water table elevation.

Map 35 MODFLOW grid spacing in model domain: (a) grid cell size map, (b) western and central model domain, (b) close-up near Sion production wells showing grid spacing.

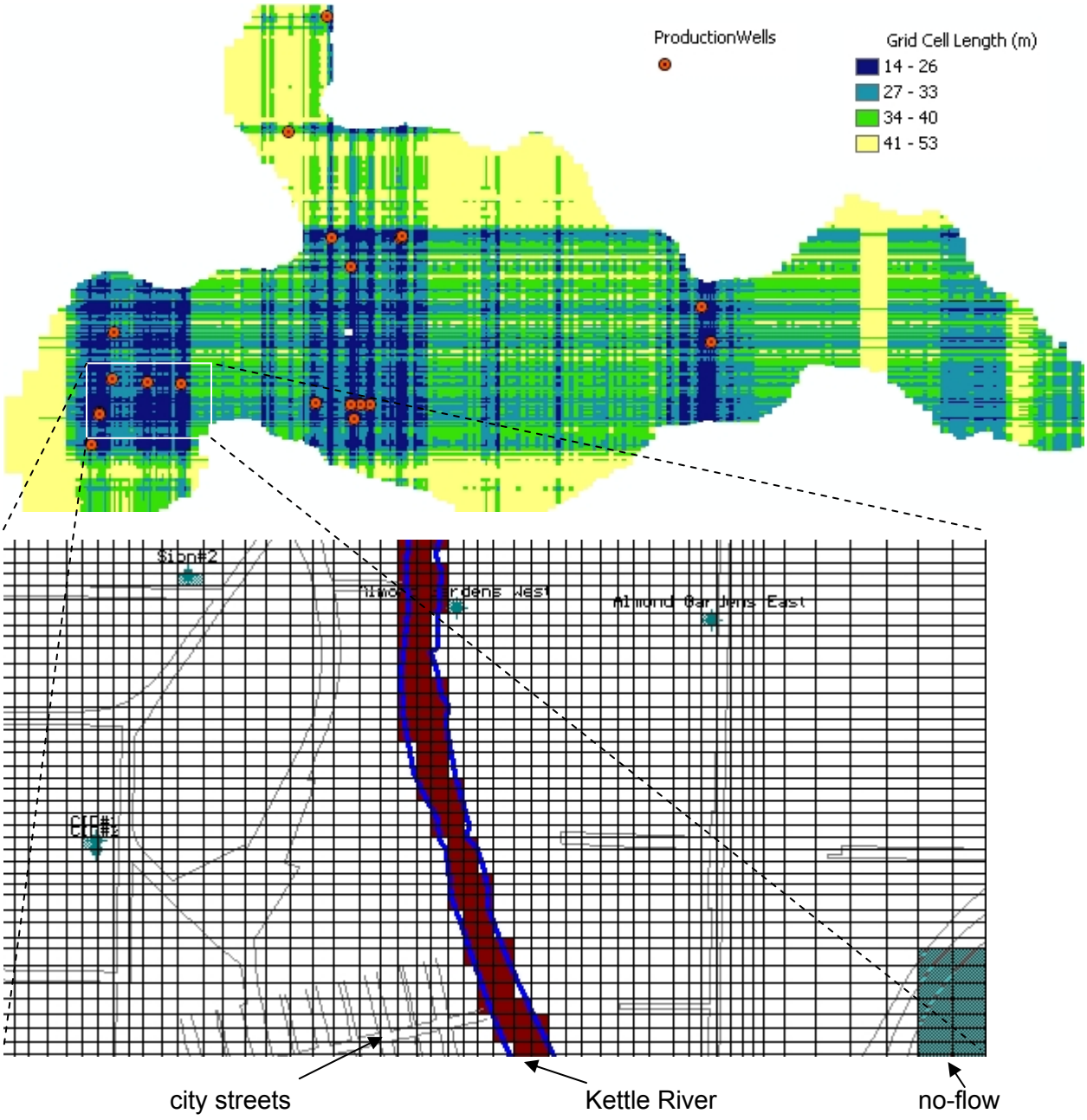

Map 36 Cross-section through MODFLOW model domain, showing layers, hydraulic conductivity zones, and bedrock surface.

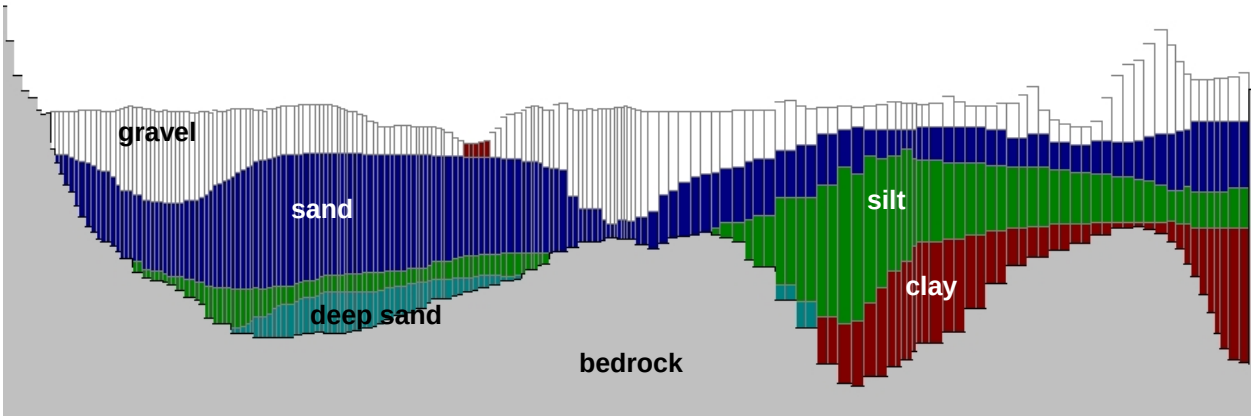

Layer 3:
In this layer the sediments have higher silt content, with some thick silty sand and silt intervals noted in borehole lithologs. There are still sand and gravel lenses (possibly from older and now buried river channels). Clay is also present in some areas. However, the dominant material is silty sand and silt, and the layer was called "silty" to account for it. Hydraulic conductivity is about one order of magnitude lower than in the above sand layer. Therefore, Layer 3 is an aquitard compared to Layer 2, but it still conducts significant flow volumes and can be considered part of the Grand Forks aquifer (relative to bedrock and Layer 4 – clay dominated sediments). Once exception is the absence of "silty" layer in the Ward Lake area (north-west valley extension). Here, the silt layer is absent and instead sand is present. This sand dominated area was represented by hydraulic conductivity (and storage) zone within Layer 3, and has the same hydraulic properties as sand Layer 2. The rest of layer 3 has properties of "silty sand".

Layer 4:
There is little information about the deepest sediments in the Grand Forks valley, but the predominance of clay in borehole lithologs at this depth led to representation of this layer as "clay", or "clay-dominant" sediments. Some sand lenses are still present but groundwater flow is probably much slower than in all above layers. This unit is an aquitard.

Layer 5:
This is an additional "layer" in which most cells are inactive except in the eastern portion of the valley where a deeper sand lens is found (possibly indicating a buried alluvial fan). Two of the lithologs indicate thick sand under a thin silt layer. Due to limitations in the geometry of MODFLOW grids, an additional layer had to be created to represent the contact between Layer 4 (clay) and underlying deep sand in that area.

Layer 6:
The bottom layer represents the bedrock under the valley sediments. Bedrock is assumed to have low permeability, and thus, all cells in bottom layer are inactive in the groundwater flow model. It is used to provide the bottom to Layer 5 and to help visualize the valley topography in cross sections.

6.3.1. ALTERNATIVE MODEL DESIGNS

The finite difference grid has many limitations, one being the “layered” approach and difficulty in representing lenses of materials. The new version of MODFLOW 2000 uses the HUV package which allows for representation of heterogeneities with hydraulic property arrays (the grid is uniformly or variably layered, but material types are represented by flow-properties alone – hydraulic conductivity and storage). The model then creates transition of properties where the solid model of materials shows transition between two different materials. This is easily implemented in GMS but not in Visual MODFLOW, although both support MODFLOW 2000. GMS also supports T-PROGS scenarios internally. T-PROGS is also stand-alone software, but it is difficult to integrate the output to MODFLOW model without specialized codes (or within GMS system).

Another alternative is to use a finite-element solution method as implemented in FEFLOW modelling system. A mesh is more flexible in representing complex surfaces than a 3D grid. The boundaries are more exact. GMS also supports mesh models.

The groundwater flow model solutions should be very similar in all these systems, but that should be investigated in the future. Future drilling or other aquifer characterization studies will undoubtedly improve the hydrostratigraphic model.

Map 37 Five layers of MODFLOW model, grid spacing, and active cell extent per layer.

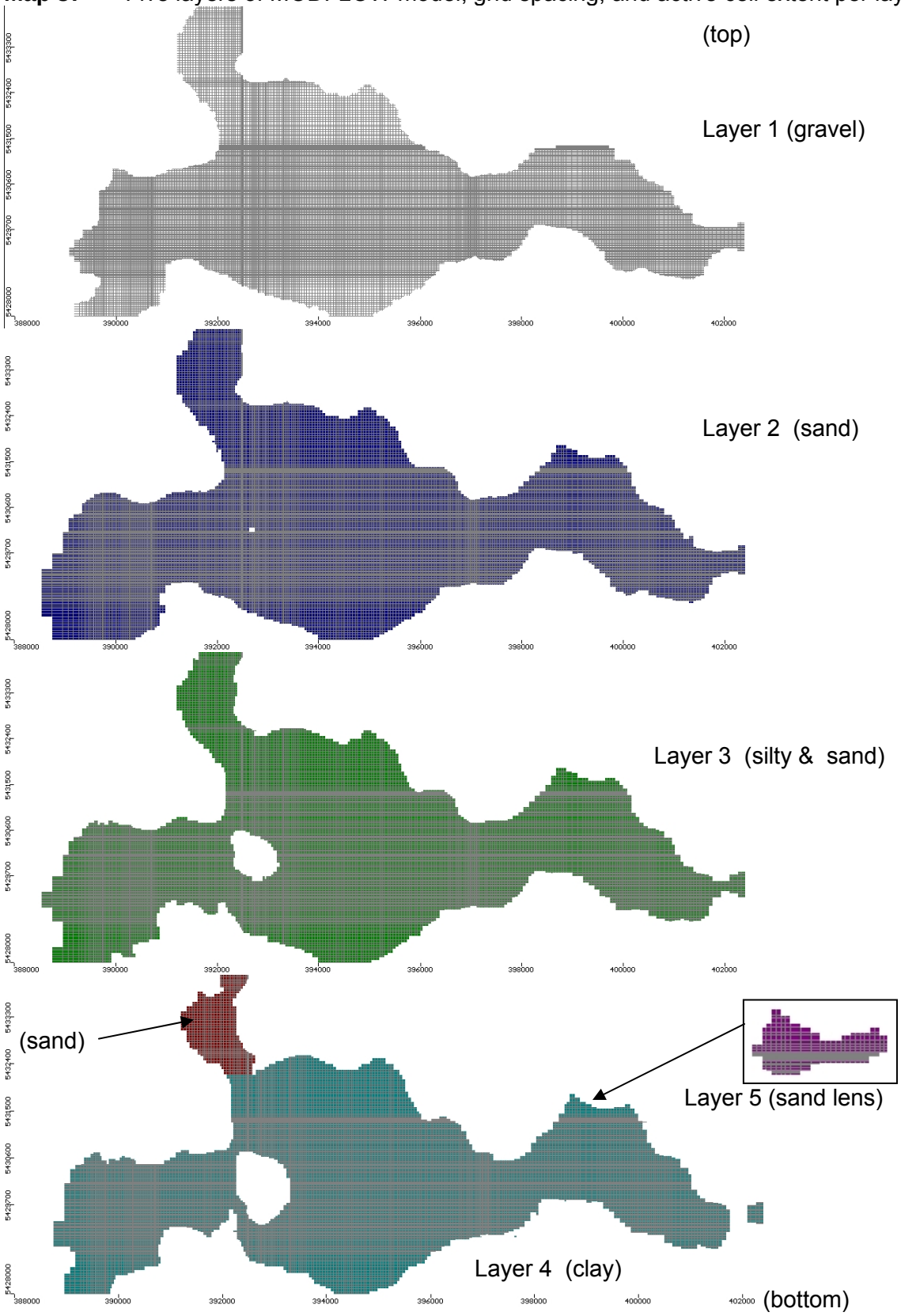

6.4. BOUNDARY CONDITIONS

6.4.1. BEDROCK WALLS AS NO-FLOW BOUNDARY

Overall, the hydraulic conductivity of the bedrock beneath and surrounding the valley is several orders of magnitude smaller than of aquitards in the valley fill sediments, and therefore can be considered as no-flow boundary in the model.

6.4.2. RECHARGE

Recharge to the model was calculated according to the methodology described in the last section. Figure 81 shows the frequency of occurrence of each of the 64 HELP recharge zones. More categories of Kz and depth could be added, but that would result in many more percolation columns in HELP model, thus more data analysis requirements. Note that there are only 4 discernible soil types over most of the area of the valley. Kz is interpolated, and larger number of Kz classes would represent the interpolated Kz distribution more smoothly, but it would not improve the accuracy of the model because Kz distribution is not that well known; in itself it is heavily averaged and has many assumptions. Depth to water table is relatively well known, probably the best of these 3 parameters, but in areas where depth has low variation, the addition of more depth classes would not improve the resolution (the scenario map would look almost identical to present one).

Figure 81 Frequency distribution of 64 HELP recharge zones by number of MODFLOW cells in transient model of Grand Forks aquifer (without irrigation return flow zone subdivisions).

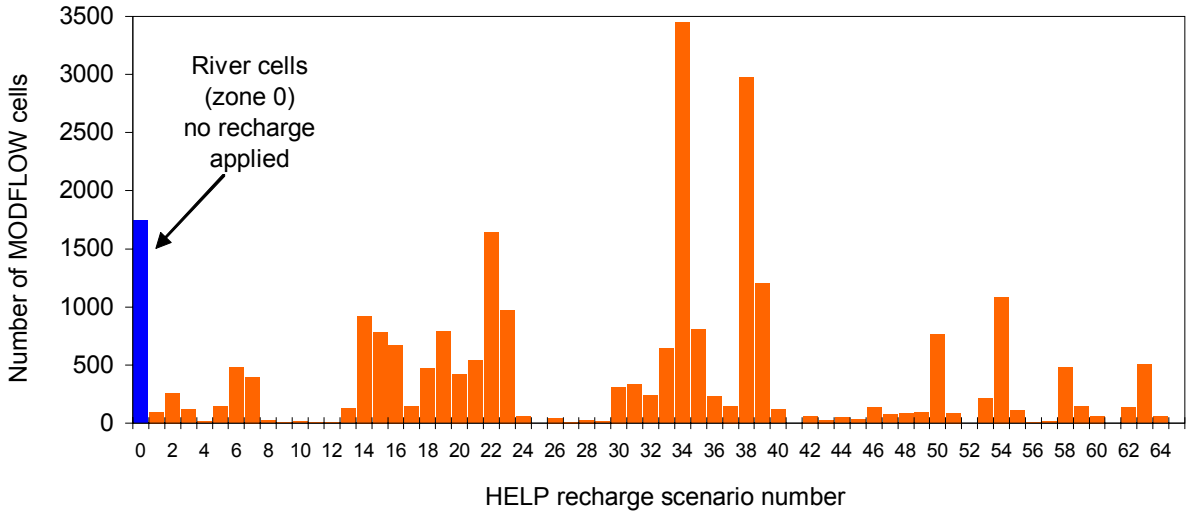

In all pumping model scenarios for groundwater model of the Grand Forks aquifer, the recharge zones were modified by including estimated irrigation return flow to the aquifer. The actual

process of extracting spatial information from a GIS system and mapping that onto MODFLOW cells was theoretically simple, but required development of custom code for reading and writing to/from MODFLOW grid files and boundary value files. In the top layer, mid cell-locations were read, then matched by location to mid-points of MODFLOW cells mapped in GIS as polygons as shown in Map 38. (MODFLOW grid row/column intersection coordinates provided vertices for those polygons). Each MODFLOW cell was assigned a unique ID number. A simple table join was performed in GIS, linking recharge polygons to MODFLOW cell midpoints, which picked up the recharge zone number and that was imported into recharge zone array in MODFLOW. The recharge zone definitions contained the recharge schedules for a given climate scenario for each recharge zone. Custom software was written to implement this whole import/export process and was successfully used for multiple transient models for multiple climate scenarios. Map 39 shows distributed recharge applied to the MODFLOW model for a zoomed in portion of the aquifer.

Map 38 Mapping of MODFLOW cell midpoints onto recharge scenario polygons.

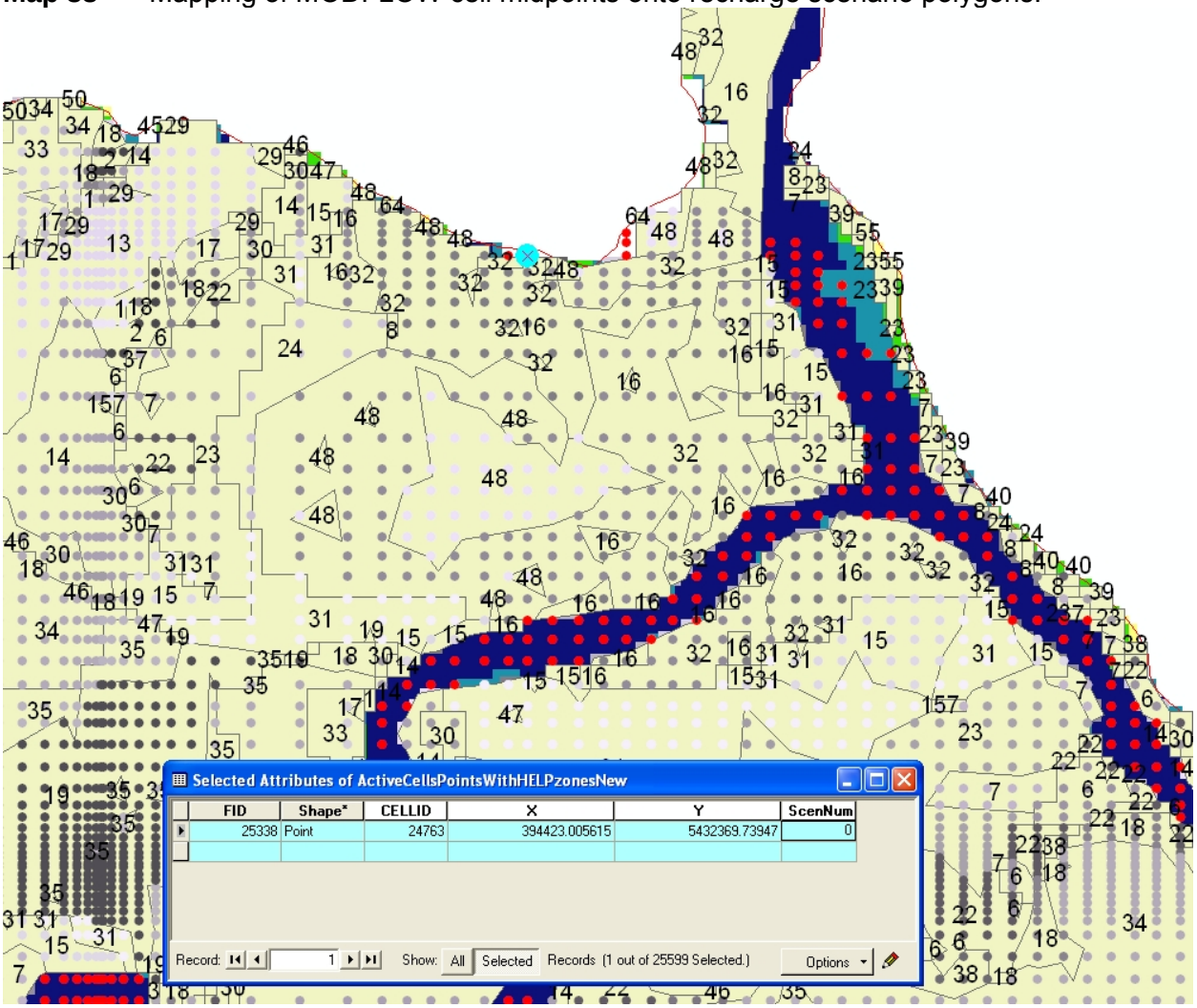

Map 39 Recharge zones in MODFLOW model: (a) south of Grand Forks and Kettle River, near Big Y irrigation district fields, showing additional recharge zones created from calculation of irrigation return flow effect, (b) cross-section of MODFLOW top layers with recharge zones and river cells.

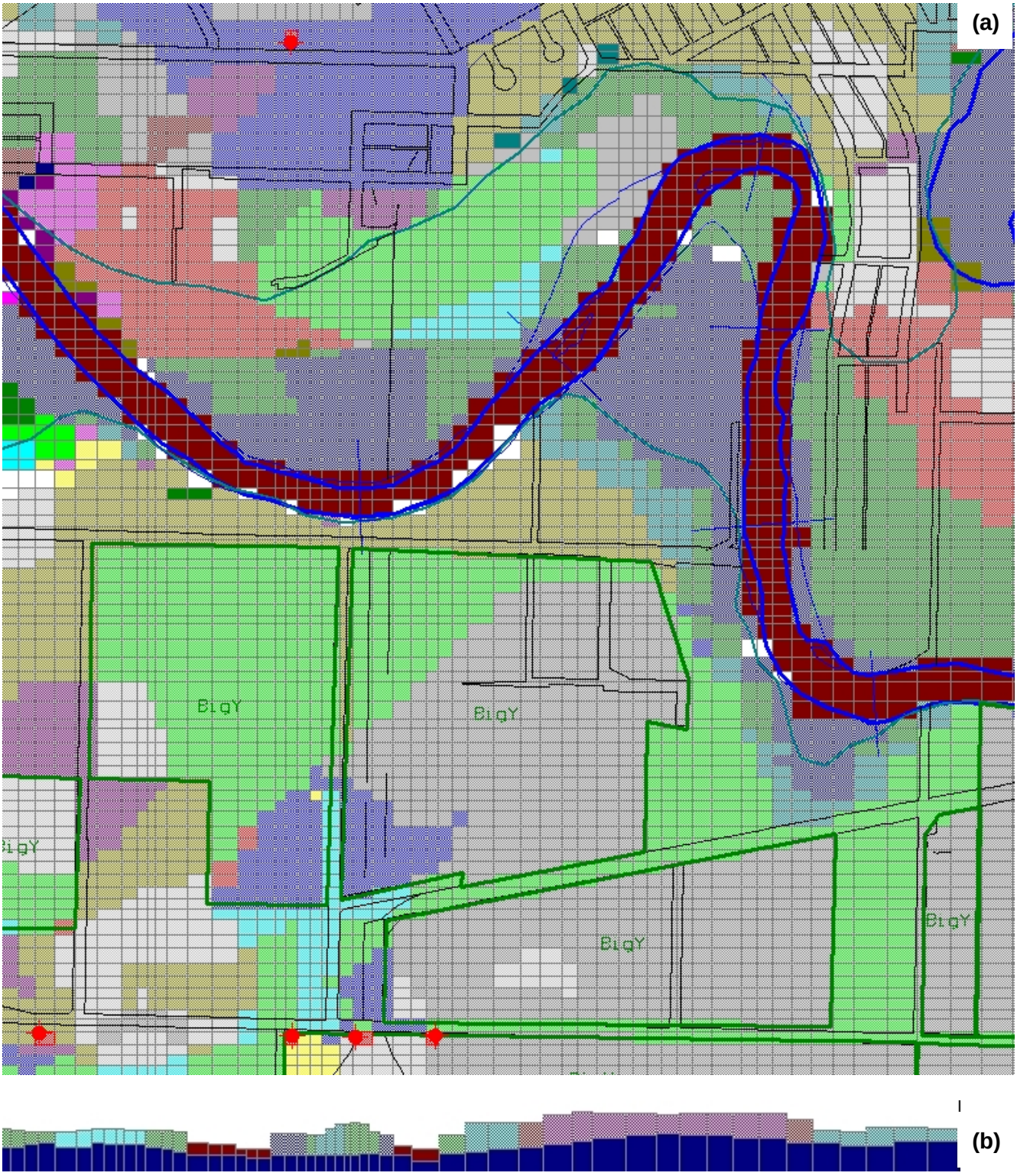

6.4.3. RIVERS

- EVIDENCE FOR HYDRAULIC CONNECTION WITH RIVERS

Interaction between the Kettle and Granby Rivers and the aquifer were not modeled specifically. This is because in a groundwater flow model, the rivers are normally treated as having some specified head (or head-dependent) boundary condition which is essentially unaffected by the groundwater regime. Unless a specialized code, such as MODBRANCH (USGS) is used, the feedback from the aquifer to the river cannot be simulated. It is assumed that the head in the river is held at a specified value regardless of how much water is taken from that surface water body. In the case of the Kettle and Granby Rivers, there is sufficient flow on a year-round basis to justify this assumption, and therefore, no need to implement a coupled flow code such as MODBRANCH.

Generally, the Kettle River is influent (contributes to the aquifer) in the western portion of the valley and effluent (receives groundwater from the aquifer) in the eastern portion of the valley. The steady state water balance calculated by Allen (2000) for different zones in the model (West, Central, North and East) confirm the nature of the connection. In the west, a large percentage of groundwater is derived from constant head nodes (i.e., the river), and in the east, a large percentage of groundwater exits the model via the constant head nodes.

As discussed previously, the groundwater hydrograph in well 217 (location and floodplain topography as in Map 40) displays regular seasonal pattern, similar to stage hydrograph of the Kettle River. The maximum groundwater level corresponds to maximum river stage during the spring freshet, while the lowest water tables occur during the winter months. The groundwater level in the well varied between 1 and 1.8 m over the period of record, where as the river experienced stage fluctuation of 3 meters. Records in this well were usually taken on the last or second last day of each month. The averaging process was similar to that used for Kettle River hydrographs (Scibek and Allen, 2003). The mean monthly water table elevation varied only by about 1 metre, with standard deviation of 0.2 m. The shape of well hydrograph was similar to Kettle River hydrograph, but the peak water level apparently was at end of July, rather than at end of June. However, the actual date of highest water level in well 217 is uncertain to at least 15 days, since the measurements are taken only once each month. For example, if well soundings were taken in the middle of the month, the peak would probably occur in the middle of June. The phase shift of the well hydrograph as induced by river hydrograph is at least 15 days, but could be up to 30 days.

The amplitudes of seasonal fluctuations are damped, which would be expected to increase with distance away from the river channel. It is one of the goals of groundwater model of the Grand Forks aquifer to provide numerical predictions of lag times in aquifer recharge, flow paths, and estimates of storage parameters.

Map 40 Floodplain topography at confluence of Kettle and Granby Rivers at Grand Forks with location of Observation Well 217 (wtn 14947) and nearby water wells.

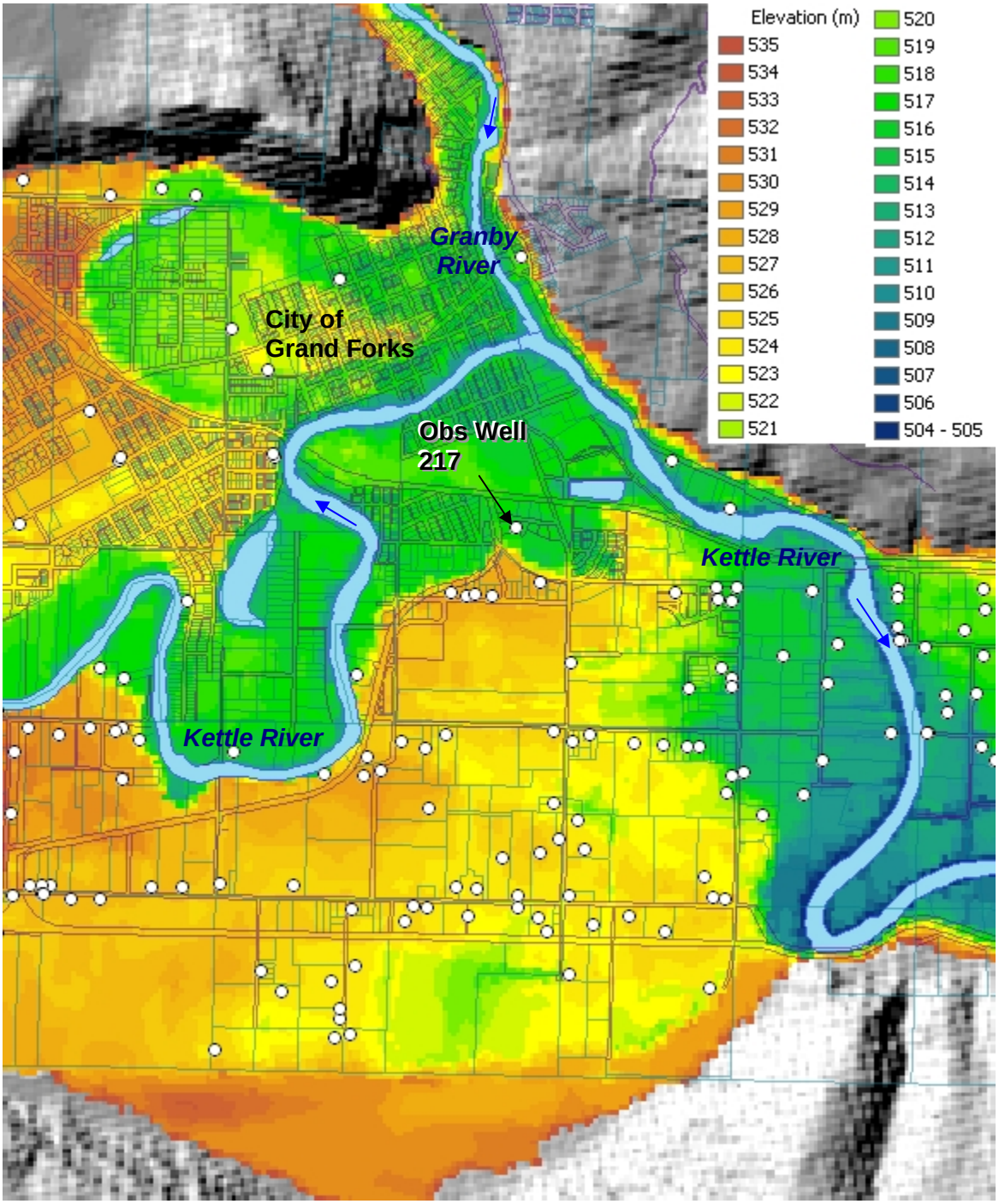

- GRAND FORKS VALLEY HYDROLOGY AND EFFECT ON RIVER STAGE

The hydrology of Grand Forks valley and watershed water balance was investigated in a report by Scibek and Allen (2003) to BC WLAP. The mean annual discharge of Kettle River in the Grand Forks Valley is on the order of 47 m^3/s, and that of Granby River is 30.5 m^3/s. The small tributaries contribute only 0.64 to 0.91 m^3/s mean annual discharge to the larger Kettle River,

within the extent of the Grand Forks aquifer. On an annual basis, this flow represents about 2% of the Kettle River flow, or 1% of the combined Kettle and Granby River flow downstream of Grand Forks. During the summer months, many of the smaller creeks become ephemeral, discharging water only after large rain events, and only a few maintain base flow in dry periods. The Kettle River low flow is about 12 m^3/s and is relatively constant from August to October. The low flows or no flow in the small creeks are expected to occur from June to October; longer than the Kettle River because it is assumed that snow melt occurs early in these low altitude small catchments.

In any case, the river discharge in both the Granby and Kettle Rivers will not be measurably affected by inflows from these small catchments in the Grand Forks Valley from Carson to Gilpin. Thus, water levels in Kettle and Granby will be controlled only by their very large upstream drainage basins (2000 km^2 for Granby and 6000 km^2 for the Kettle). This compares to a total of 95 km^2 for all catchments that provide flow into the valley at Grand Forks.

During high flow periods, the Kettle River carries 200 to 300 m^3/s, while estimated maximum discharge from all creeks into the valley was 4.12 m^3/s. At low flow in August, the Kettle River maintains between 10 and 14 m^3/s in most years compared to minimum discharge of 0.0137 m^3/s for the creeks. In terms of percentages, during the spring high flows, the small creeks contribute 1 to 2 % of Kettle River discharge in the valley. During the late summer low flow, the small creeks contribute about 0.1 % of the river flow in dry conditions, and may contribute more during localized rain storms. The maximum recorded runoff in creeks is during snowmelt in April to May. Although intense rain storms can produce creek discharge as high as one half of maximum recorded runoff from snowmelt, the atmospheric instabilities always affect a wide region. Consequently, the Kettle River stage would already be elevated from increased runoff and the creeks in this watershed would contribute 4.12 / 2 = 2.06 m^3/s to Kettle River conveying flow of 20 to 150 m^3/s. Therefore, at most, the creeks would provide 10% of the river discharge for a short time period, and that contribution would drop to 2% once dry conditions returned. Although the creeks have very little effect on the flow of Kettle River, they may be important for adding storage to the aquifer near valley edges away from the influence of the river on groundwater levels.

- TYPE OF RIVER BOUNDARY CONDITION IN MODFLOW

The correct selection of boundary conditions is a critical step in model design (Anderson and Woessner, 1992). The purpose of this section is to justify choices of types of boundary conditions in the transient groundwater flow model of the Grand Forks aquifer, which represent the rivers that flow through the Grand Forks Valley. Other physical and hydraulic boundaries of the Grand Forks aquifer model were described by Allen (2000).

Steady-state flow models are useful in evaluating long term-average groundwater flow conditions, and for sensitivity analysis of the model to various parameters (e.g., river stage, pumping rates, and evaporation rates). In steady-state simulations, the boundaries largely determine the flow pattern.

The original numerical model of the Grand Forks Aquifer was developed in Visual MODFLOW (version 2.60, Waterloo Hydrogeologic Inc.) by Allen (2000). This software is based on original USGS MODFLOW groundwater flow model (McDonald and Harbaugh, 1988), a three-dimensional block centered finite difference code that can simulate both confined and unconfined aquifers, but includes expanded graphical user interface. It also includes other modules, such as MODPATH for particle tracking.

The MODFLOW model contains two packages that account for leakage to and from rivers. The River package allows rivers to be represented with a stage fixed during a stress period with leakage to and from the aquifer (McDonald and Harbaugh, 1988). It requires an input value for streambed conductance to account for the length and width of river channel, the thickness of riverbed sediments, and their vertical hydraulic conductivity. New versions of MODFLOW (2000 or later) also include the Streamflow-Routing Package, which allows leakage to and from the stream, but it also maintains mass balance between the river and the aquifer. The Streamflow package assumes very simplified uniform rectangular geometry of river channel.

The bottom sediments of the Kettle and Granby Rivers above the Grand Forks aquifer consist of mostly gravels, with very little finer sediments. In effect, the aquifer is in direct contact with the river channel and there is no impediment to flow. The constant head nodes do not have any conductance coefficients, and thus assume perfect hydraulic connection between the river and the aquifer. The river can leak and receive water to and from the aquifer, but the river stage will not change as a result of such interaction. In other words, the river will act as an inexhaustible supply of water and will influence the aquifer water levels, but the aquifer will not have any effect on river discharge and stage, thus the term constant head.

Based on these observations, the combined aquifer and tributary contribution to the rivers have very small effect on Kettle and Granby River water levels, but the river water levels have strong effect on groundwater levels in the aquifer. Therefore, the rivers can be represented as specified head boundaries, such that the head schedules will represent the modeled river stage in transient Grand Forks aquifer models. The term “constant head” and “specified head” are equivalent here because the head is “constant” for the duration of a time step, but then is specified to change to different value with time. Therefore, the full transient river stage hydrographs can be represented by this type of boundary condition. The “river” boundary condition, which uses the “river package” in MODFLOW was not used because the conductance is not known, but is assumed to be very high (gravel river bed causes immediate groundwater connection of river and surrounding aquifer, relative to rates of change in river hydrograph).

- ALTERNATIVE TYPES OF BOUNDARY CONDITIONS FOR RIVERS

An alternative type of boundary is the specified flow boundary, which describes fluxes of water between the aquifer and the boundary. The major problem with this type of boundary is that water fluxes are unknown in the Grand Forks aquifer-river system. In fact, one of the purposes of the numerical model was to estimate the fluxes of water between the river and the aquifer. Moreover, the flux rate depends partly on hydraulic gradient near the river, thus it depends on both river stage and the groundwater heads near the river, both of which were unknowns before the implementation of transient groundwater flow model.

Transient simulations are needed to analyze time-dependent problems, such as the impact of climate-change induced shift in river hydrographs on the water levels in the Grand Forks aquifer. Boundary conditions influence transient solutions when the effects of the transient stress reach the boundary, and the boundaries must be selected to produce realistic simulated effect (Anderson and Woessner, 1992).

Where river channel geometry is important at the scale of the model, and where unsteady river flow conditions and aquifer interactions are studied, a truly coupled river-aquifer model may be required. One of such coupled models is the MODBRANCH model (Swain and Wexler, 1996) was developed by the USGS, and it couples the BRANCH river model with MODFLOW groundwater flow model. This model is especially useful for modelling intermittent flow systems where the river is periodically fed by groundwater or is completely drained by leakage to the aquifer (Swain and Wexler, 1996).

- RIVER STAGE SCHEDULES FROM BRANCH MODEL

The numerical flow model BRANCH (Schaffranek et al., 1981) and associated channel geometry analysis program CGAP (Regan and Schaffranek, 1985) of Kettle and Granby Rivers showed that channel geometry is variable and affects stage-discharge relation along the river channel. The calculated rating curves, together with an automated mapping of river water elevations to groundwater flow model of the valley aquifer, allows for modeling of seasonal variation of groundwater levels and their sensitivity of changed river hydrographs.

Modelled discharge hydrographs were converted to river stage hydrographs at each of 123 river segments, and interpolated between known river channel cross-sections. Stage-discharge curves were estimated using the BRANCH model and calibrated to observed historical data. River channels were represented in three-dimensions using a high grid density (14 to 25 m) in MODFLOW, which were mapped onto river segments. River stage schedules along the 26 km long meandering channel were imported at varying, but high, temporal resolution (1 to 5 days) for every cell location independently. CGCM1 downscaling was also used to predict basin-scale runoff for the Kettle River upstream of Grand Forks, and stage-discharge curves adjusted accordingly for different climate scenarios.

- BRANCH MODEL LIMITATIONS

Although the cross-section spacing along the Kettle River is dense, the river channel geometry varies greatly with location. There is a lack of consistency in high-water mark surveying along the cross-sections. It would be impossible for the surveyors to determine what flood magnitude caused each high-water mark at each survey location, and due to lack of more information, it can be assumed that not all the high-water level scour or debris on channel banks were caused by the same high flow at all points along the channel. At the same time, the model did not account for channel storage or variation of channel roughness with stage, or backing up of water along un-surveyed sections of the channel that could impact the surveyed locations. Therefore, neither the surveyed high-water marks nor the modelled stages are without error.

At low flow, there are small rapids in various places along the river channel (both Kettle and Granby Rivers), causing problems with solution of flow equations due to too steep channel slope. The BRANCH-network model was found to be difficult to work with and rather sensitive in its stability to a combination of control parameters, initial conditions, and boundary conditions. River flow through several of the cross-sections gave objectionable results and the curves were adjusted to fit the high-water mark regardless of BRANCH output.

- USING BRANCH OUTPUT AS BOUNDARY CONDITIONS IN MODFLOW GROUNDWATER FLOW MODEL

The MODFLOW grid subdivides the valley floor into grid cells of variable sizes (average 20 x 20 m long rivers). The channel width of Kettle River was one or two cell length at most locations (see Map 41). The actual thalweg or water-filled and flowing channel width may be less than two cell widths during low-flow months, but this schematization does not adversely affect the groundwater flow model.

The rivers were treated in the model as specified head boundary conditions. The rivers are best represented as specified head nodes in the model because the bottom sediments of the rivers are largely gravel, ensuring good hydraulic connection with the underlying aquifer. Modifications to the specified head boundary conditions (i.e., the rivers) had to be made to the original model (Allen, 2000; 2001) to account for slight variations in the surface topography of the model, as

this upper elevation had been modified as part of this study. Nevertheless, the only significant change to these boundary conditions was the layer to which the specified head was associated.

Map 41 River channels in MODFLOW grid in cross-section and model layers.

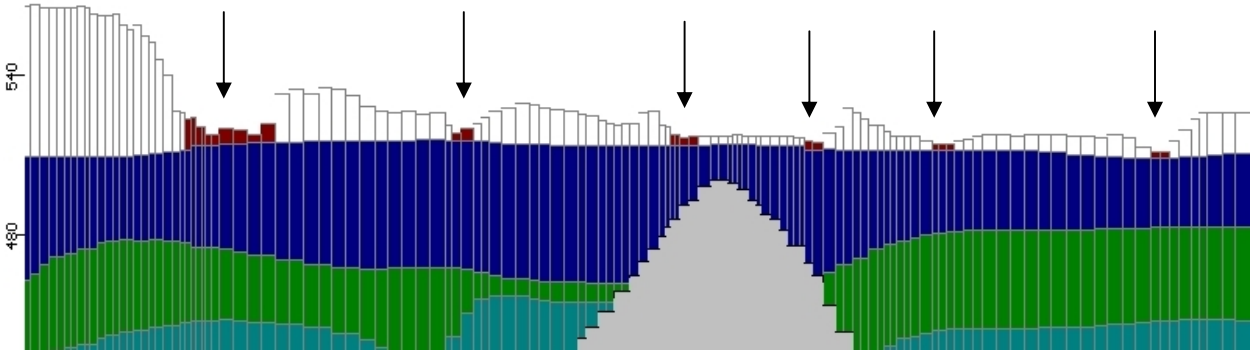

Adjacent cells in the MODFLOW grid were assigned to groups to represent river segments in raster format. Map 42 shows segments corresponding to MODFLOW cells for the Kettle and Granby Rivers. For each segment, the centroid location was estimated using GIS, and coordinates for the position were recorded as UTM easting (x) and northing (y) in metres relative to datum in UTM zone 11. The distance (Δx) was calculated using pythagorean distance formula between each segment. Distance along river channel was the running sum of inter-segment distances. For each segment (i), the program located the nearest upstream and downstream cross-section location for which the stage-discharge rating curve was used to calculate water elevation (z) from given discharge on input hydrograph. Linear interpolation was used to calculate water level representative of each segment between two cross-sections. The equation of the line describing water surface slope was calculated between two bounding cross-section locations, then solved for segment location. This process was carried out for all segments along the river and at all time intervals (Figure 82).

The program then updated the appropriate boundary file of Visual MODFLOW dataset using specified file format. The cells were identified by row, column, and layer number. For example, 365 day schedules of river stages were written to file as constant head boundaries, for each “river” cell in the aquifer model, to simulate the annual river hydrograph. Schedules of any time increment and length are possible as required by the groundwater model.

Map 42 River segments used in to link river stage predictions, along the sloping river channel, to MODFLOW model of the aquifer.

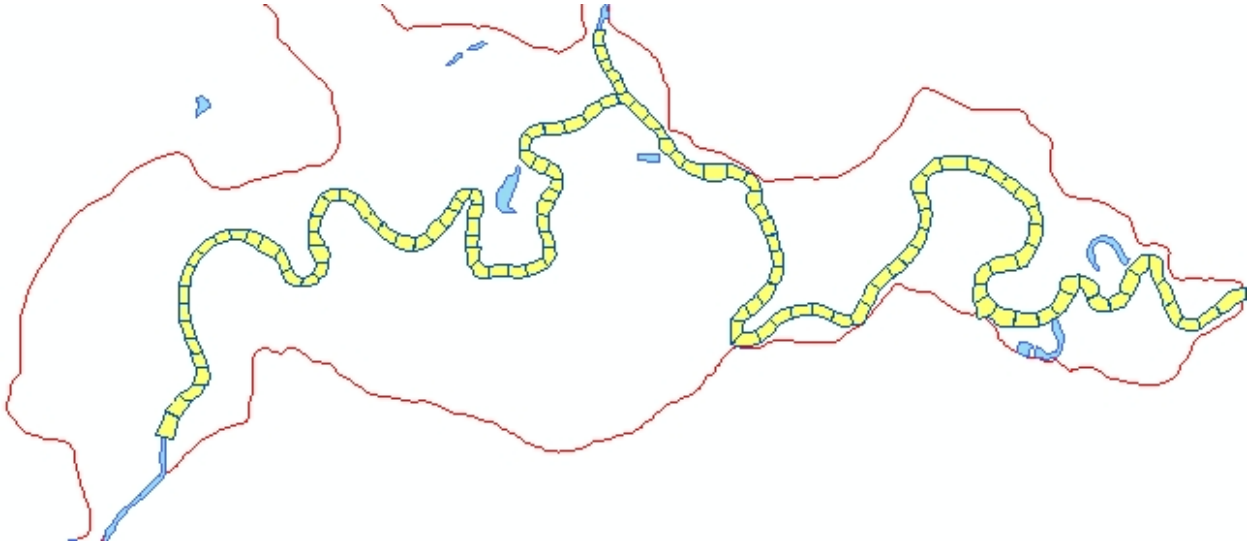

- ADJUSTING RIVER ELEVATION PROFILE

In 1990, river surveys were done on the Kettle River and Granby River in Grand Forks Valley by Surveys Section of Water Management Branch of Environment Canada. The river cross-sections are numbered 15 to 67, increasing upstream of Kettle River, and spaced (on average) approximately 600 m apart, but segment length varied between 1050 m and 200 m. For the Granby River, the cross-sections were numbered 1 to 12 in the upstream direction starting from confluence of the Granby River with Kettle River at Grand Forks, and ending about 2.3 km north of Grand Forks, with an average distance between cross-sections of 300 m.

Note that channel bottom elevation was the minimum elevation along cross-section. The channel bottom elevation profile along the length of the river (Figure 82) has jagged appearance because there are local depressions in the river channel, or perhaps surveying inaccuracies. It would be expected that channel bottom would decrease or remain level in downstream direction. This inconsistency of minimum channel bottom elevation profile caused problems in MODFLOW because the ground surface DEM and the river channels did not correspond (initially) to the surveyed channel bottom elevations and had to be modified along river channels. The river water elevation is calculated by adding river stage, computed from stage-discharge curve for a given discharge, to the channel bottom elevation. The irregularity of river channel bottom caused the water levels to also have jagged (sometimes increasing downstream) profile. In reality, river water elevation always decreases downstream, regardless of total depth of channel – the river compensates by changing flow velocity to conduct the same flow volume. The river stage must also be below floodplain levels to produce accurate water table elevation along the river (always below ground surface) in groundwater flow model. Consequently, the river channel bottom profile was smoothed out to ensure that calculated minimum and maximum stage were always decreasing downstream.

Another condition of this calibration was river stage below local floodplain elevation (since extreme floods are not modelled here). Floodplain elevations were read from the most accurate source available – the floodplain maps for Kettle River. The provincial DEM (20 m grid) was rather inaccurate in the valley. River floodplain elevations were too low in many places, the

river channels were poorly defined and usually represented the river water elevation and not the river channel bottom elevation – as would be expected from Kriging interpolation of digitized contour lines (and points) on topographic maps. The actual solution in MODFLOW does not require that ground surface be represented exactly, because flow is modelled in saturated zone only (unless the new Surfact package is used – WHI 2004, or similar). As long as the ground surface is high enough to be above computed water table, the solution will be correct. The river channel is gravelly and the assumption was that river is well connected hydraulically to the aquifer. MODFLOW layers were edited along all river channels to put all constant head boundary cells in first layer (gravel) of the model. The channels were also deeper than on original DEM surface of the valley, and more similar to the surveyed channel profiles.

Figure 82 Elevation profile of Kettle River in Grand Forks valley. Surveyed channel bottom elevations, floodplain elevations from maps and DEM model, and fitted channel profile for MODFLOW model of the aquifer.

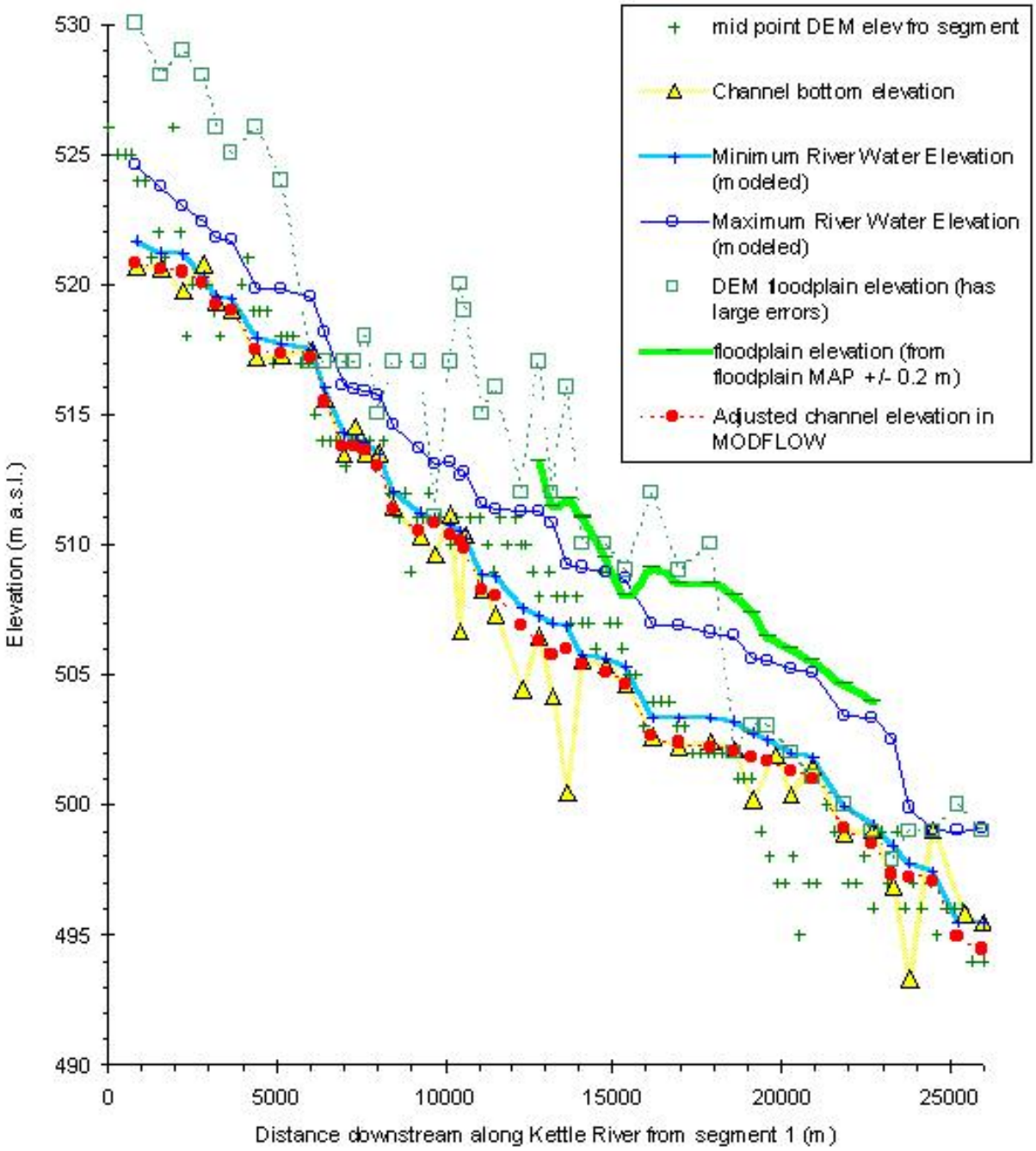

Figure 83 Surveyed profiles of Kettle River channel cross-sections (selected for part of valley), and example of stage-discharge curve fitted from BRANCH model output and to observed high-water mark on river cross-section.

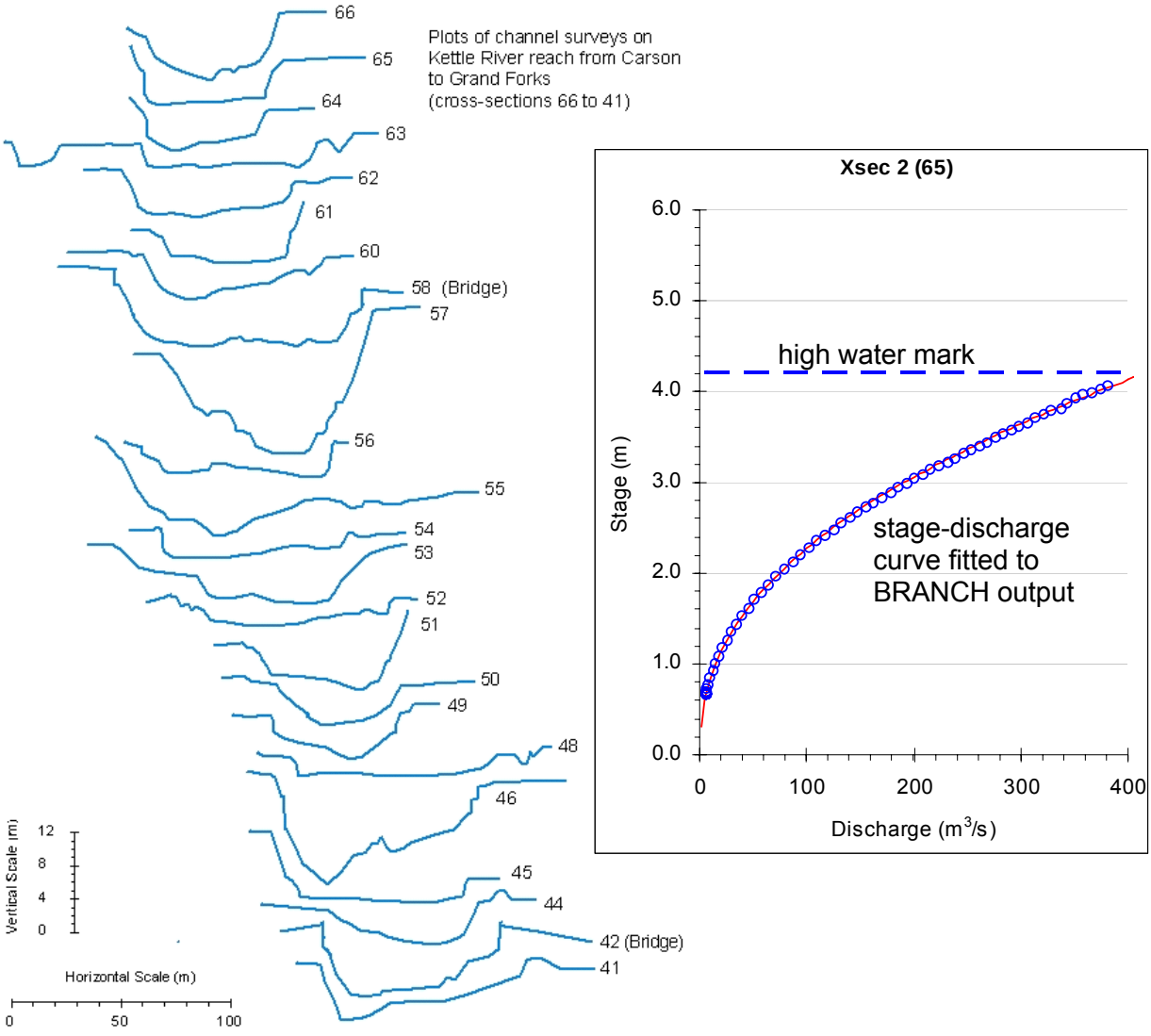

6.4.4. DRAINS

Drain boundary conditions were used for small lakes and large drains or swamps (Map 43). Lake and drain elevations were taken from floodplain maps. Drains were used only in areas where the flow model calculated heads were too high above ground (or lake) surface, and drains were used to tie-in the water table elevations to lake and drain elevations. Default drain conductance was specified as 5 m/d for all drains. The purpose of drain boundary condition is to force groundwater levels in groundwater flow model to not exceed the drain elevation (if given high enough drain conductance to drain all excess water).

Map 43 Drains and specified head boundaries in layer 1 of Grand Forks aquifer model.

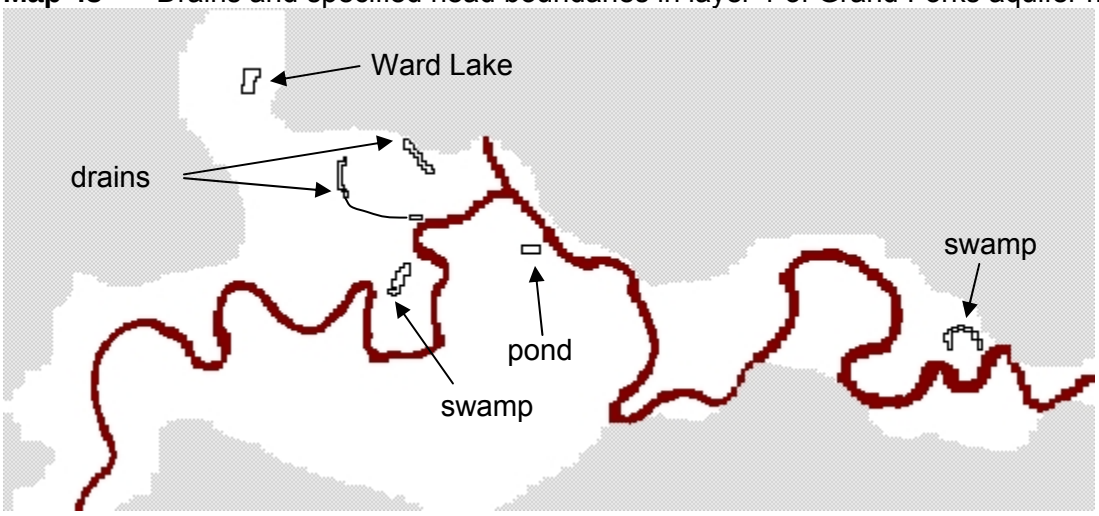

6.4.5. PUMPING WELLS

The major production wells in the Grand Forks aquifer include the Sion Improvement District wells (Sion#1, #2, and #3); Covert Improvement District wells (CID#1, #2 and #3); City of Grand Forks wells (GF#2, #3, #4, and #5); Grand Forks Irrigation District wells (BigY#1, #2, #3, #4, and 87-2) as well as the two Nursery wells (#1 and #2). Well locations are positioned on Map 44. These wells were assigned revised pumping rates based on values reported by the various operators for summer peak operating conditions. In most cases, the values were similar to those used in the previous modeling study (Allen, 2000). These pumping rates are provided in Table 25. In the transient model with pumping, the pumps were active only from June to August, as determined from monthly water use statistics (see example for Grand Forks water district in Figure 85.

Productions wells have theoretical well yields that are usually higher than measured (and estimated) discharge during summer months (Figure 84), when irrigation demand is at maximum. There is also a large range in well productivity. Drawdown associated with pumping will vary depending on well location and aquifer properties. For example, the two Nursery District wells have very small drawdown because these are adjacent to Kettle River. The Big Y wells have high pumping rates and the effect is additive for adjacent wells so drawdown will be larger. There are many domestic wells pumping from Grand Forks aquifer, but the discharges are much smaller than in production wells.

Map 44 Locations of production wells in Grand Forks aquifer.

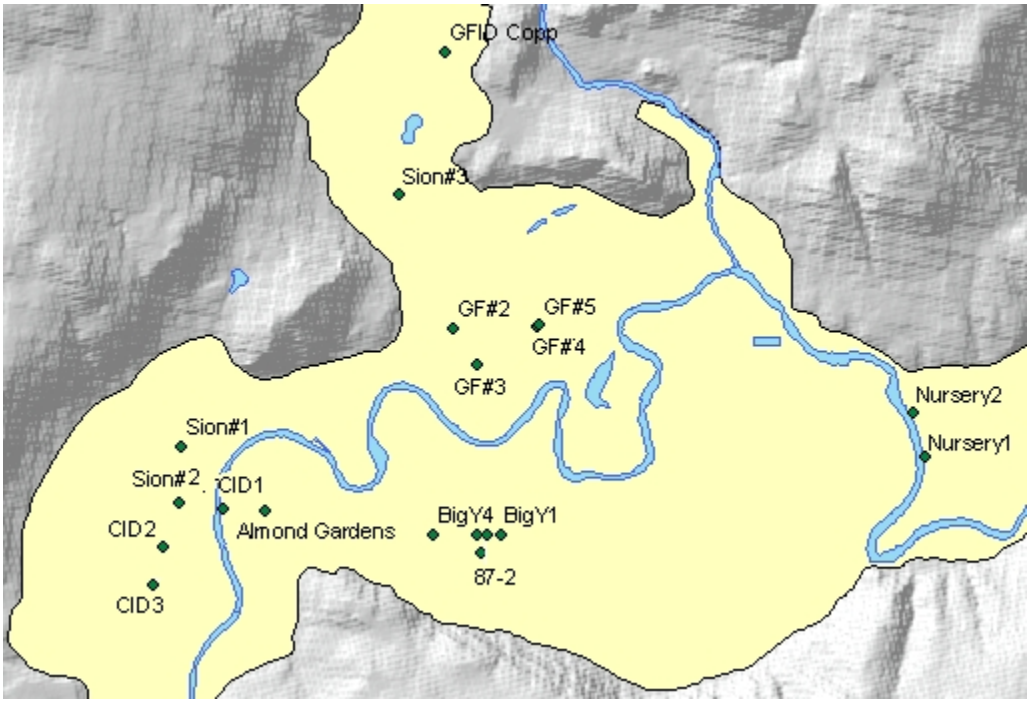

Notes:

wells GF5 and GF4 are adjacent

wells BigY1 to BigY3 are adjacent along a road (only two are labeled on map)

Table 25 Pumping Rates for Major Production Wells in Grand Forks

Well	Reported Well Yield (m^3/s)	Average Winter Q (m^3/s)	Average Summer Q (m^3/s)	Q used for irrigation (m^3/s)	Theoretical Max Yearly Use (m^3/year)	Actual Yearly Use (m^3/year)
CGF 2	0.0379	0.0089	0.0167	0.0078	1,195,214	338,499
CGF 3	0.0757	0.0023	0.0633	0.0610	2,387,275	546,007
CGF 4	0.0303	0.0069	0.0117	0.0048	955,541	252,915
CGF 5	0.0908	0.0465	0.0696	0.0231	2,863,469	1,626,228
Big Y1	0.0513	0.0000	0.0522	0.0522	1,617,797	405,540
Big Y2	0.0421	0.0000	0.0570	0.0570	1,327,666	443,340
Big Y3	0.0513	0.0000	0.0429	0.0429	1,617,797	333,720
Big Y4	0.1893	0.0000	0.1077	0.1077	5,969,765	837,540
Nursery 1	0.0757	0.0000	0.0483	0.0483	2,387,275	375,300
Nursery 2	0.0268	0.0000	0.0181	0.0181	845,165	140,940
Covert 125hp	0.0757	0.0000	0.0265	0.0265	2,387,275	206,116
Covert 50hp	0.0606	0.0000	0.0002	0.0002	1,911,082	1,759
Sion 1	0.0505	0.0000	0.0861	0.0861	1,592,568	669,224
Sion 2	0.0394	0.0000	0.0671	0.0671	1,242,518	522,128
Sion 3	0.0325	0.0000	0.0411	0.0411	1,024,920	319,486

Figure 84 Pumping discharge estimated for summer months for production wells in Grand Forks aquifer – comparing well yield to actual discharge.

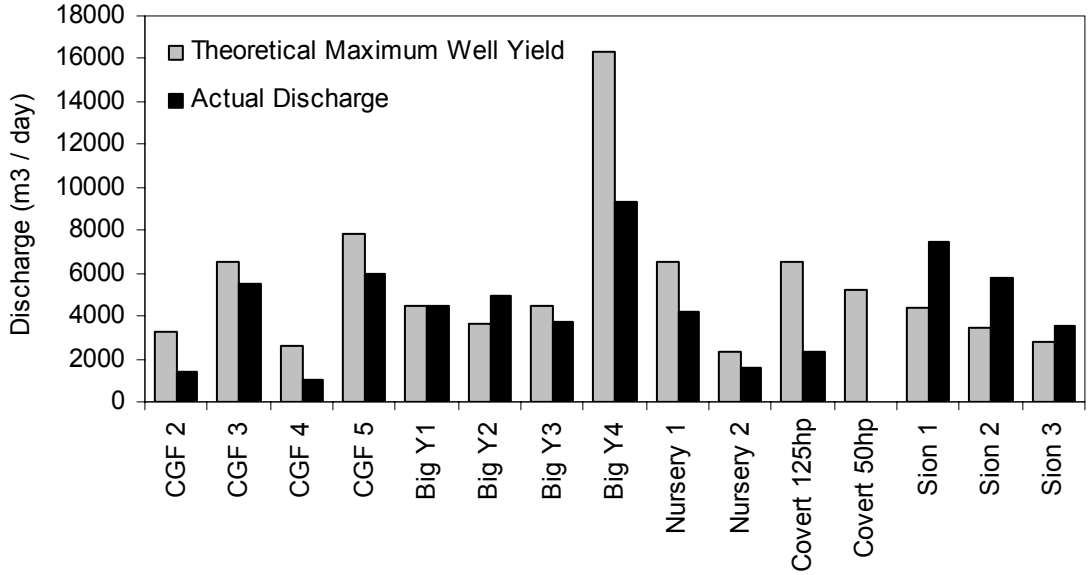

Figure 85 Monthly Total Water Use for the City of Grand Forks Water District.

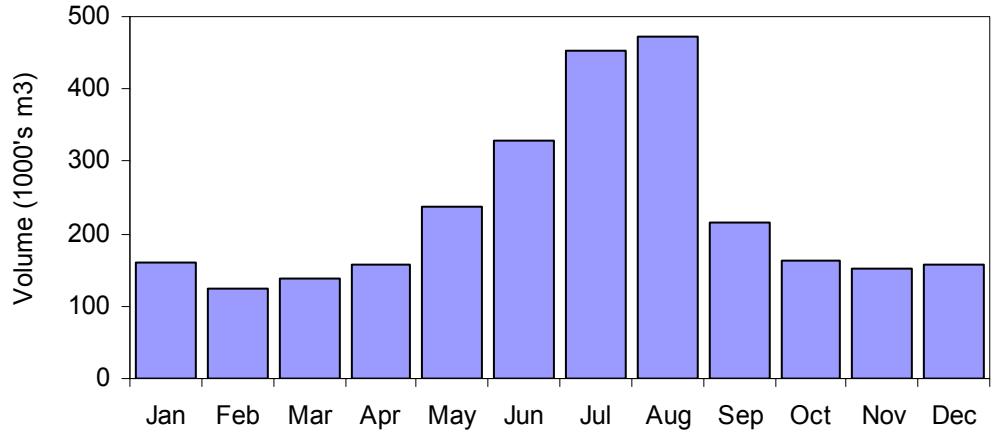

6.5. TRANSIENT MODEL SETTINGS

6.5.1. INITIAL HEADS

Initial head distribution is required to achieve model convergence at first time step of first stress period, and the solver is very sensitive to initial head distribution. The initial estimate of heads may cause non-convergence if specified improperly. The Grand Forks aquifer model experienced non-convergence initially, which was solved only after testing a variety (5) different solvers, adjusting solver parameters, and re-importing initial heads from any successful stress period head output in previous model runs. As a first attempt, initial heads were imported form interpolated water table from static water elevations in all wells, with added winter river levels.

In later test models, initial heads were used from previous model runs, and slowly improved. This process took about 50 model runs, during which the model grid was also edited in problem areas (smoothing out of layers in some places).

The final initial head distribution was also changed during model calibration, which proved to be sensitive to initial head distribution. After model calibration, the last model output (day 365) was assigned as initial head for next model run (day 1), to assure transient model consistency of annual behaviour of the groundwater system. This iterative calibration process produced the final initial head distribution, which was used in all climate change scenarios. There were several "test" transient models developed and tested and calibrated. All actual climate scenarios have identical initial head distributions as well as all other model and solver parameters, except differences in river stage, recharge and return flow and pumping schedules.

6.5.2. STRESS PERIODS AND TIME STEPS

Stress period start and end times were selected at unequal intervals because of river stage behaviour. When the water level in rivers changes rapidly, stress period duration should be more frequent to help the model converge on solutions. A total of 65 stress periods were used, corresponding the time in days as shown in Table 26.

Each stress-period is divided into a user-defined number of Time Steps at which the model computes the head solution using the solver. The time step Multiplier is the factor used to increment the time step size within each stress period (ratio of length of time step to preceding time step). During early model development, there were 10 time steps and multiplier of 1.2 (for time step expansion), but these were changed to 5 time steps and multiplier of 1.3 due to technical difficulties with saving files when MODPATH was run, and excessive run times, with no apparent difference in results. For example, Visual MODFLOW exceeded 2.1 GB composite budget data file .BCF when MODPATH was run, because MODPATH forced output of flow terms and heads at all time steps and all stress-periods. The .BCF file is required for MODPATH in transient simulations only.

Table 26 Stress periods and Julian Days of transient model runs.

SP	Day	SP	Day	SP	Day	SP	Day	SP	Day	SP	Day	SP	Day
1	0.11	11	96	21	146	31	156	41	185	51	255	61	330
2	21	12	101	22	147	32	157	42	190	52	265	62	335
3	32	13	106	23	148	33	158	43	195	53	270	63	345
4	41	14	111	24	149	34	159	44	205	54	275	64	355
5	51	15	116	25	150	35	160	45	210	55	285	65	360
6	60	16	121	26	151	36	165	46	215	56	295	66	365
7	61	17	126	27	152	37	170	47	225	57	300		
8	71	18	131	28	153	38	175	48	235	58	305		
9	81	19	136	29	154	39	180	49	240	59	315		
10	91	20	141	30	155	40	182	50	245	60	325		

6.5.3. SOLVER SETTINGS

All available solvers in Visual MODFLOW were tested, but ultimately the PCG2 (the new Generalized Preconditioned Conjugate-Gradient Package) had the most success in converging on solutions, and was used for all simulations. This solver is a general-purpose iterative solver based on the generalized conjugate gradient method. The solver was used with modified incomplete Cholensky preconditioning, and using the following head and head change residual criteria for convergence (abbreviations are for this report only and differ from MODFLOW code):

Max outer iterations (MXITER)	= 500
Max inner iterations (ITER)	= 100
Residual criterion (RC)	= 0.001 m
Head change criterion (HC)	= 86.4
Damping factor (DAMP)	= 0.6
Upper bound of estimate (NPBOL)	= 1 (calculate estimate)

The RC value is used to judge the overall solver convergence in any time step. A typical value is 0.01 m. The HC value is unit-dependent and is typically 864 if the unit of time is days and unit of length is meters, and it is used to judge convergence of inner iterations.

During cell re-wetting, the model often ran over 100 to 200 outer iterations without convergence, thus the unusually large value of MXITER (normally it is 25). Similarly number of inner iterations was increased to 100 (from typical 10) because of problems with convergence at these RC and HC criteria and during re-wetting of dry cells. During falling water levels in rivers, cell re-wetting wasn't a problem, and typically the model would perform 10 to 20 outer iterations per time step, with 100, 70, 30, 10, 5 …. 1 inner iterations decreasing during convergence, but it would do 100 to 80 inter iterations per outer iteration during periods of fast changes in river stage and dry-cell re-wetting.

The initial model mass balance at residual criterion 0.01 m and head change criterion of 864 m^3/d were found to produce up to 20% mass balance discrepancies, although all outputs looked plausible. The convergence criteria were reduced by factor of 10, to the assigned values.

The damping factor is used to restrict head change from one iteration to the next, and is useful in solving non-linear problems, because at DAMP < 1, the solution changes slowly (called under-relaxation).

Recharge setting was selected to apply recharge to the highest active (non-dry) cell in each vertical column. This approach must be used if dry cells are present and recharge can percolate through unsaturated zone.

<u>Layer type settings were kept as default:</u>

Layer 1 (type 1) Unconfined - the transmissivity of the layer varies and is calculated from the saturated thickness and hydraulic conductivity. The storage coefficient is constant, and specific yield (Sy) value is used.

Layer 2 to 5 (type 2) Confined/Unconfined, variable T, Constant T - the transmissivity of the layer is constant, while storage coefficient may alternate between confined and unconfined values. The layer 2 in this model has only a few dry cells around valley walls, which stay dry for

the entire duration of model run in all scenarios (could have been de-activated completely), thus this layer is saturated all the time (saturated thickness does not change during model run).

Anisotropy settings were all assigned “by layer”, and the ratio was always Ty/Tx = 1 for all layers, due to lack of any data about layer horizontal anisotropy in Grand Forks. The borehole data are too sparse and of too poor quality to give indication of y/x anisotropy.

6.5.4. RE-WETTING SETTINGS

For accurate modeling of water table in aquifers, the re-wetting option must be turned on. However, this option also causes the solution to be much more unstable in the Grand Forks model (as in other aquifers as mentioned by MODFLOW manual). The re-wetting options were set as follows:

Wetting threshold = 0.001 m
Wetting inverval = 30 iterations
Wetting method = from sides and below
Wetting head = calculated from threshold
Wetting factor = 1
Head value in dry cells = 0.001 m
Minimum saturated thickness for bottom layer = 0.001 m

Wetting threshold was set equal to the precision of solver in head convergence, to be consistent. This would cause re-wetting at every wetting intverval. The wetting interval was large to allow the model to non-rewet automatically during most iterations, in order to allow convergence. This was necessary after experiencing frequent non-convergence in this model. Re-wetting was eventually done manually, by lowering the head convergence criterion in the solver during run-time to very small number (0.000000001). In effect this involved setting > 30 outer iterations in model solution to stabilize the heads prior to cell re-wetting, then re-wetting would occur at iteration 30, and the solver HC was changed back to 0.001 value, after which the model would converge at that time step and continue solving. Re-wetting was specified during stress-periods as follows (mostly during rise in river hydrographs in spring time, and always at first stress period, and always during recovery from pumping in pumping models):

10, 12, 16, 20, 24, 26, 28, 3, 36, 40, 44 (and for pumping models: 50, 52, 58, 64)

During fall in river hydrographs, cells would become dry over time in layer 1 and re-wetting did not make any difference in the results, but only caused problems with convergence at intermediate time steps.

The wetting method (from all sides and below) was selected because this option is useful where a dry cell is located above a no-flow cell, which is the case near valley walls on steep slopes in this model. Wetted head was calculated from threshold:

Head = Zbot + Wetting factor * (Wetting threshold)

which is less reasonable then computing it from neighbouring cells (less accurate), but much more stable and as it causes less non-convergence. It had to be used to allow the solver to solve during cell re-wetting in this model. The head value in dry cells was assigned to just above cell bottom (instead of large negative value by default) to avoid large residuals during re-wetting and improve convergence of model.

6.6. MODEL CALIBRATION

The primary objective of model calibration is to verify the model by comparing observed known values against model derived values. In hydrogeologic models, this procedure typically involves calibrating against known water levels, either under steady state conditions or transient conditions.

The Grand Forks steady state numerical model had been calibrated to within 8% of observed static water level measurements and successfully reproduced observed data obtained from a few pumping tests (Allen, 2000; 2001). However, several modifications to the physical structure of the model, including a refinement of the layering, use of distributed recharge rather than a single value applied to the top surface of the model, and adjustment of the grid near rivers, were made for the purposes of this study. Thus, recalibration was necessary. In addition, the current model incorporates time varying boundary conditions (i.e., recharge river stage) and it is necessary to recalibrate to transient data sets. Specifically, the addition of time varying observation well data will be used.

Model calibration is undertaken normally by varying model input parameters; aquifer properties, recharge, etc. within acceptable ranges in order to determine the best combination of these parameters that reproduce the observed data. Because river stage and recharge parameters had been established following a rigorous methodology (Scibek and Allen, 2003; 2004), only the aquifer properties (hydraulic conductivity, specific storage, and specific yield) were varied during calibration. It is also important to note that specific storage and specific yield are not required for steady state model calibration as these two parameters only appear in the relevant transient groundwater flow equation.

6.6.1. HYDRAULIC CONDUCTIVITY DISTRIBUTIONS

- HOMOGENOUS LAYERED AQUIFER MODEL

The layered model of Grand Forks valley sediments assumes uniform or homogeneous hydraulic conductivity and storage properties in each layer. Each layer has an average hydraulic conductivity, initially assigned based on average hydraulic properties computed from pump test data, but later modified during model calibration (within reasonable range). This model type does not have “distributed” K as was done for “heterogeneous aquifer” model (see next section). Layers are required in MODFLOW implementation of aquifer model and the easiest approach to modelling aquifers where heterogeneity is difficult to characterize and where data are scarce is to assume homogeneous properties within each layer.

Prior to transient model calibration, the transient model was built from the same layers and had the same hydraulic properties as the steady-state model of this aquifer done by Allen (2000; 2001). The steady state model did not require S or Sy values, therefore these values had to be determined during transient calibration. After many modifications, reshaping of layer boundaries, expanding the model domain, re-importing bedrock and ground surface at higher resolution and with corrected model boundaries (where sediments thin out along valley slopes), the hydraulic properties were eventually changed during transient model calibration. It is important to see what hydraulic properties the model started (listed in Table 27) with to values after calibration to one observation well (Table 28), and also to compare to distributed K-fields in heterogeneous aquifer representation (Map 45) based on pump test data in production wells.

Table 27 Values of K used in the first steady state Groundwater Flow Model for Grand Forks (Allen, 2000), and later changed during transient model calibration.

Layer	K_x (m/s)	K_y (m/s)	K_z (m/s)
1 - gravel	1.0E-3	1.0E-3	1.0E-4
2 - sand	1.5E-4	1.5E-4	1.5E-5
3 - silt	7.0E-7	7.0E-7	7.0E-8
4 - clay	1.0E-7	1.0E-8	1.0E-8

Values for clay and silt were estimated from the literature on account of there being no values from hydraulic tests conducted in those units. K values for the upper portion of the subsurface, which is the active portion of the aquifer (i.e., the gravel and upper sand units comprising the Grand Forks aquifer) provide a good model calibration under steady-state conditions (see model calibration results in Table 28.

Table 28 Values of K calibrated in transient groundwater flow model of the Grand Forks aquifer.

		Kx,y		Kz		Sy
Layer	Units	(m/d)	(m/s)	(m/d)	(m/s)	
1	gravel	80	9.3E-04	30	3.5E-04	0.12
2	sand	20	2.3E-04	10	1.2E-04	0.12
3	silt	3.0	3.5E-05	0.5	5.8E-06	0.05
4	clay	0.05	5.8E-07	0.01	1.2E-07	0.06
5	deep sand	20	2.3E-04	10	1.2E-04	0.12

- HETEROGENEOUS LAYERED AQUIFER MODEL

In the Grand Forks valley, only a few wells had pump tests carried out over the history of groundwater resource evaluation in the area. Reports on these hydrogeologic studies were made available by BC MWLAP. For a few other wells, various consultants and drillers had estimated the specific capacity (SC) of wells, and from these, estimated the transmissivity (T) of aquifer at the well location, according to the methodologies described below (BC MWLAP, 1999). The wells were mostly production wells with high yields, and thus, offered high aquifer T values. In most cases, T was calculated from the SC of a well, and hydraulic conductivity (K), was then calculated by assuming that aquifer thickness is equal to maximum saturated thickness in well (equation 2). In other instances, T was estimated directly from pumping tests.

Table 29 summarizes the hydraulic properties at all wells where data are available, as part of previous capture zone delineation study by BC MWLAP for the Grand Forks Aquifer Protection Committee.

Specific Capacity is defined as the yield of a well divided by the drawdown. Typically, units are of drawdown are $m^3/s/m$ (or m^2/s). SC is often determined when production wells are installed, and empirical relations exist that relate SC to T. The alternative method of assessing T is by pump testing a well. The well is pumped for several hours and the drawdown as a function of time is measured. The Theis method of analysis (Theis, 1963) provides an estimate of T for a

confined aquifer based on some limiting assumptions, and if an observation well is available, the storativity (S) can also be estimated. Hydraulic conductivity (K) is related to T as:

$K = T / b$ (here expressed in m/day)

and specific storage (S_s) is related to S by:

$S_s = S / T$ (m^{-1})

The calculated K value thus depends on aquifer thickness at the well location, which was estimated. Hydraulic conductivity derived from the Theis method are considered homogeneous and isotropic (Kx = Ky = Kz). In this study, Kx = Ky, but Kz is treated separately and is initially assumed 0.25 of Kxy value, due to presence of silt lenses in the aquifer which retard vertical groundwater flow (based on previous modelling by Piteau Associates, 1988).

The values reported range from 14 m/d to 613 m/d, but the spatially distributed average (not counting repeating measurements in adjacent wells) is between 25 and 100, depending on interpolation method. Spatial interpolation assumes that these points are a good sample of aquifer properties, which is not likely due to aquifer heterogeneity, but the interpolation can be used for visualizing potential distribution of K in the aquifer. Inverse distance interpolation of log K values was used in ArcGIS to prepare the K distribution map (Map 45) of pump test data from. The range of K values was used in the model calibration process. Note that the table lists the observation well 217 with the calibrated value for Layer 2 of model (this aquifer layer is assumed to correspond to the aquifer from which pump test data are obtained). It is consistent with low range of K values.

Map 45a shows the distribution of K from pump test data (inverse distance of log K values). Map 45b shows the distribution of K from both pump test data and the calibrated model K value in Layer 2 from observation well 217. The addition of calibrated value of hydraulic conductivity only changes the local interpolated K field. The observation well is located as shown on Map 45b, which also plots the location of Kettle River for better orientation of well location on the floodplain. Contours are at 20 m/d intervals and values were extrapolated to aquifer bounds. Note that the Nursery wells and one of Big Y irrigation district wells have relatively high hydraulic conductivities compared to other areas of the aquifer.

Table 29 Hydraulic properties estimated in selected wells in Grand Forks aquifer. Source: BC well capture zone tables (BC MWLAP, 1999)

WTN	Well Name	X (UTM E)	Y (UTM N)	SC (m^2/s)	T (m^2/s)	b (m)	K xy (m/d)	K z
56888	87-2	392758	5429120		0.06930	39.9	150.06	?
58671	BigY1	392957	5429302		0.06930	39.9	150.06	?
58638	BigY2	392824	5429300		0.06930	39.9	150.06	?
58733	BigY3	392721	5429302		0.06930	39.9	150.06	?
58745	BigY4	392299	5429308	0.06530	0.12730	34.4	319.73	?
21752	CID1	389682	5429188	0.01420	0.01470	55.5	22.88	?
57771	CID3	389586	5428807	0.01270	0.01330	55.5	20.70	?
19226	GF#2	392484	5431297	0.01780	0.01850	24.8	64.45	?
22427	GF#3	392720	5430952	0.01060	0.01110	29.0	33.07	?
37325	GF#4	393316	5431312		0.01260	49.1	22.17	?
58625	Nursery1	397065	5430052	0.01300	0.09722	13.7	613.12	?
58601	Nursery2	396951	5430476	0.00730	0.02890	6.7	372.68	?
20502	Sion#1	389860	5430156	0.01490	0.01550	63.5	21.09	?
21189	Sion#2	389827	5429610	0.01120	0.01160	71.3	14.06	?
20497	Sion#3	391972	5432588	0.01840	0.01910	40.5	40.75	?
14947	Obs 217	395159	5431005				20.00	5.00

WTN	SC source	T source	Aquifer thickness
56888	consultant report	est from SC	max in well
58671	?	consultant report	sat thick in well
58638			
58733	drillers test in well log	est from SC	max in well
58745	?	consultant report (geom mean of 4 wells)	max in well
21752	pumping records	consultant report	max in well
57771	L/s/m, from pump test	consultant report	max in well
19226	pumping records	consultant report	max in well
22427	?	?	
37325	consultant report	est from SC	max in well
58625	consultant report	est from SC	max in well
58601	consultant report	est from SC	max in well
20502	drillers test in well log	est from SC	max in nearby wells (min)
21189	pump test	est from SC	max in nearby wells (min)
20497	?	?	
14947	?	K xy from transient model	

Map 45 Distribution of K (in m/d) (inverse distance of log K values): (a) pump test data only, (b) pump test data and observation well 217 with calibrated model K value in Layer 2. Contours are at 20 m/d intervals and values were extrapolated to aquifer bounds.

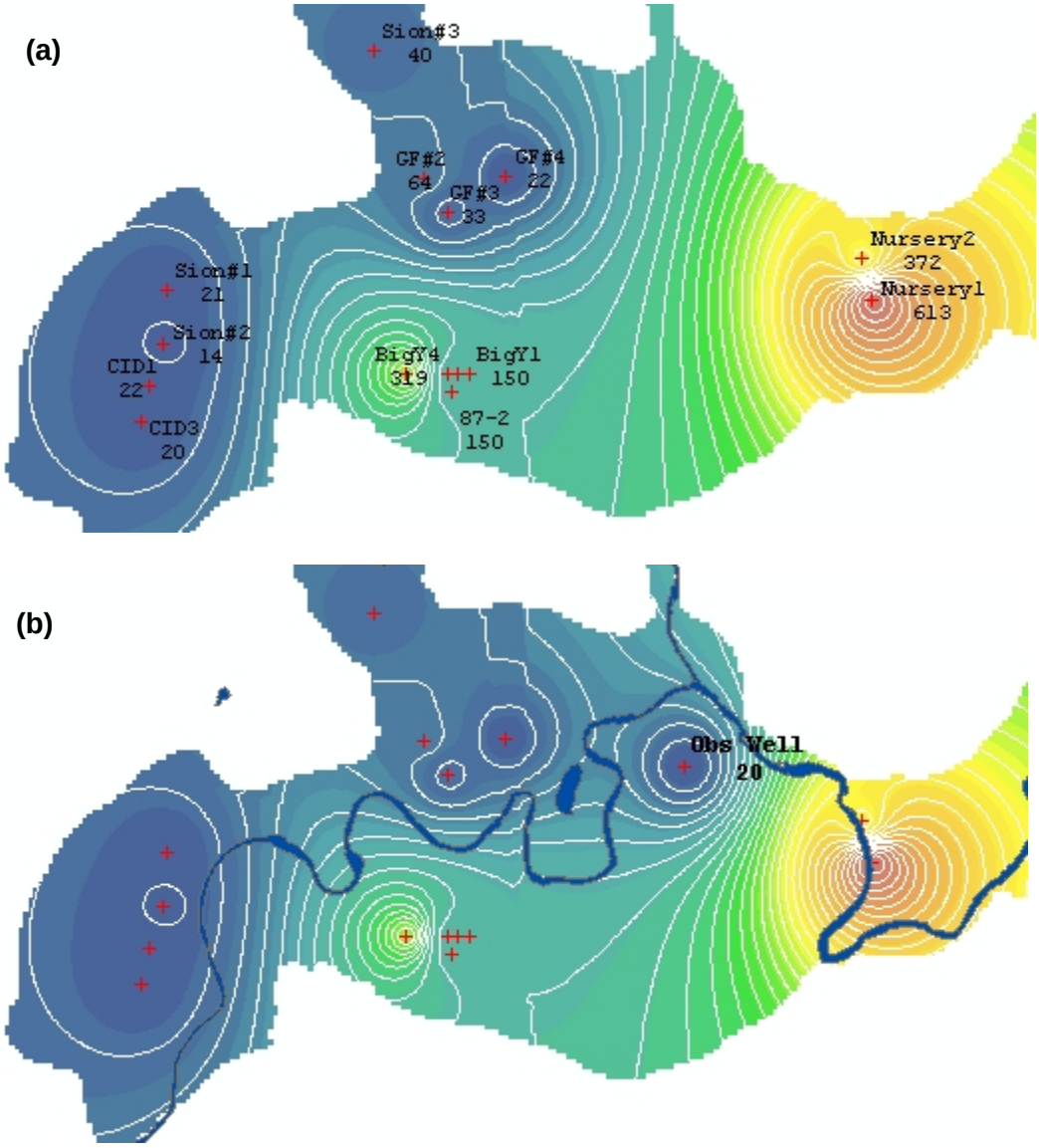

6.6.2. STATIC WATER LEVELS

In the Grand Forks area there are roughly 300 wells with static hydraulic head values for model calibration. These well include all of the domestic water wells, of varying depth, in addition to the production wells, that have been drilled in the area. The wells are well-distributed spatially throughout the aquifer (Map 46), and thus, provide an excellent means for steady-state and model calibration. It is important to recognize however, that the water elevations used for model calibration were determined at the time of drilling, and therefore, may not be representative of current groundwater conditions. In this respect, the ability of the model to accurately represent local detail is lower that it would be had the calibration data and river elevation data been collected at the same instant in time.

Map 46 Wells with static groundwater levels in BC database, and location of observation well 217 with monthly water records.

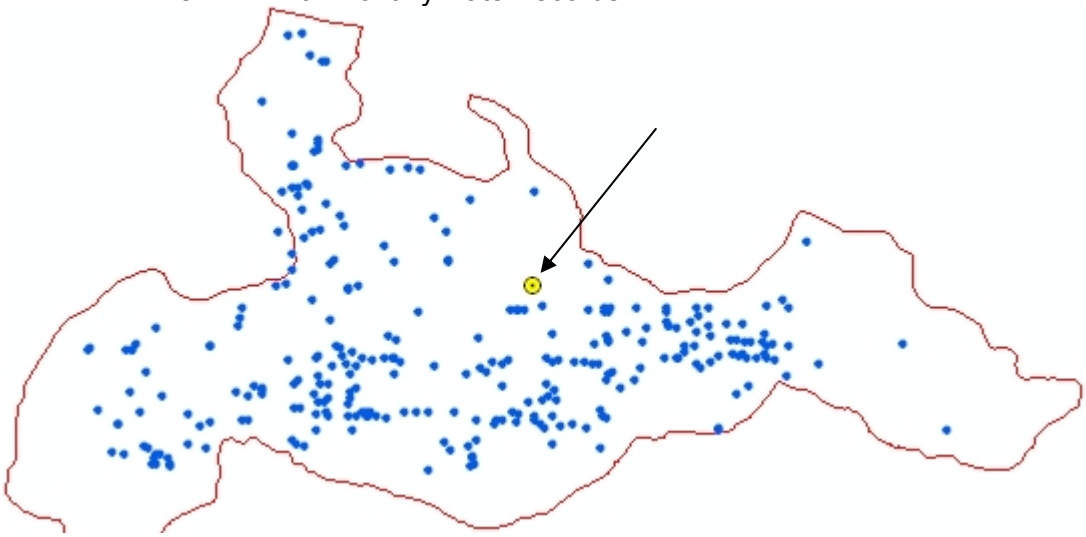

In the MODFLOW model, the ground surface was imported from a 20 m digital elevation model grid (BC province DEM). As a quality assurance step, the reported well elevations were compared to the available ground DEM surface. In Figure 86 the histogram of differences between well elevation and DEM elevation has approximately normal distribution. Although the histogram alone would suggest that random measurement errors could account for differences between well elevations and the DEM, the spatial distribution of such differences (Map 47) reveals trends and clusters. The high terraces in western and north-western valley ends have large negative differences meaning that reported well elevation is below DEM surface. These wells were checked against topographic maps, and in particular against highly accurate floodplain maps. This investigation concluded that the provincial DEM is inaccurate in many parts of the Grand Forks valley, and that most of reported well elevations appear to be correct. A few very large positive differences are clearly errors in DEM surface near steep valley walls – valley walls protrude too far inside valley floor and are a result of poor interpolation or digitizing of topographic maps that served as source for DEM. Most differences between well elevations and DEM in the central valley and over most of the floodplain are relatively small (within few meters). Again, the DEM is not as accurate as the flooplain maps, which mostly agree with well elevations.

The model residuals were computed for original well elevations (observation wells in MODFLOW), from which static groundwater levels were derived by subracting depth to static

water level from well top elevation. There is small error in this analysis because there are no data on whether the depths to water table were corrected for height of well casing or not. The same observation wells were also corrected in a separate calibration run to correspond to ground surface DEM to test whether the model would agree more closely or not with such modified static water levels. The calibrated model was better calibrated to original well elevations than to modified ones, and given the evidence of poor DEM quality and good correspondence of reported well elevations to floodplain maps, the original well elevations were kept for model calibration.

Figure 86 Histogram of inconsistencies in well elevations as compared to DEM elevation at Grand Forks aquifer.

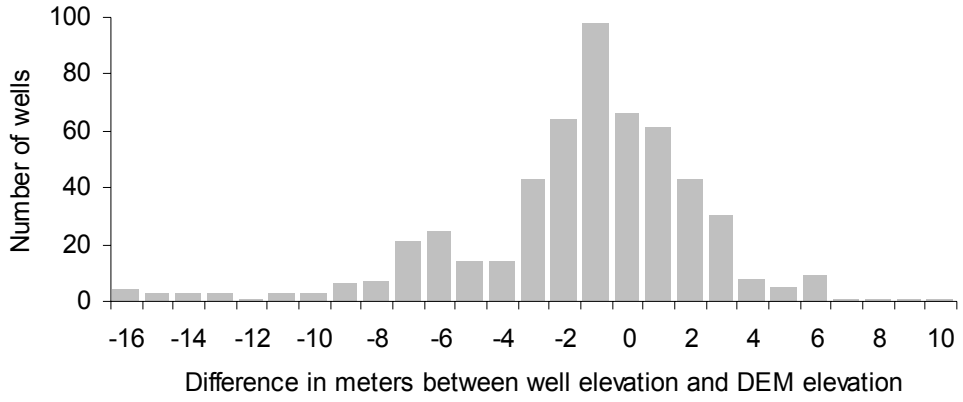

Map 47 Differences between reported well elevation and DEM elevation at the same location in Grand Forks valley.

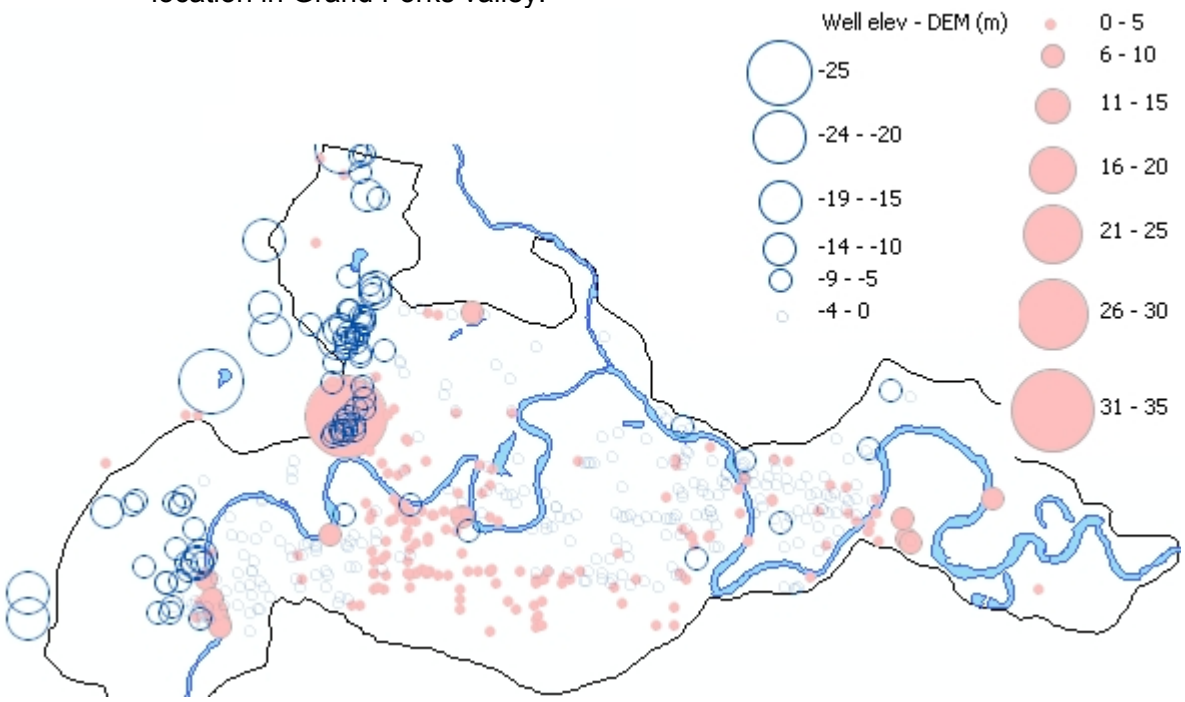

The static water level map was interpolated using both Kriging and inverse distance methods, with similar results in crentral valley but different results near valley edges. Kriging was used because it smoothed out the local variability in static water levels and it was able to extrapolate the surface reasonably well to valley edges. Contours at 0.5 m interval were added to final map and colour shading highlights the elevation differences (see Map 48).

Groundwater elevation in unconfined aquifer slopes downward from west to east, following the slope of Kettle River and valley ground surface. High density contours suggest high hydraulic gradients, which tend to occur along breaks in slope of ground surface where groundwater seeps into the river from higher terraces, setting up a large gradient in water table surface. This map was the first estimate of hydraulic heads in the aquifer for the purpose of model calibration; however, modelled heads were used in subsequent initial head inputs to consecutive calibration runs. This type of map can be considered accurate where static level observation point density is high, and is very inaccurate away from static points toward valley walls or in any other extrapolated direction.

Map 48 Static water table interpolated from all well records in Grand Forks valley, and also tied to river surface elevations at average flow levels.

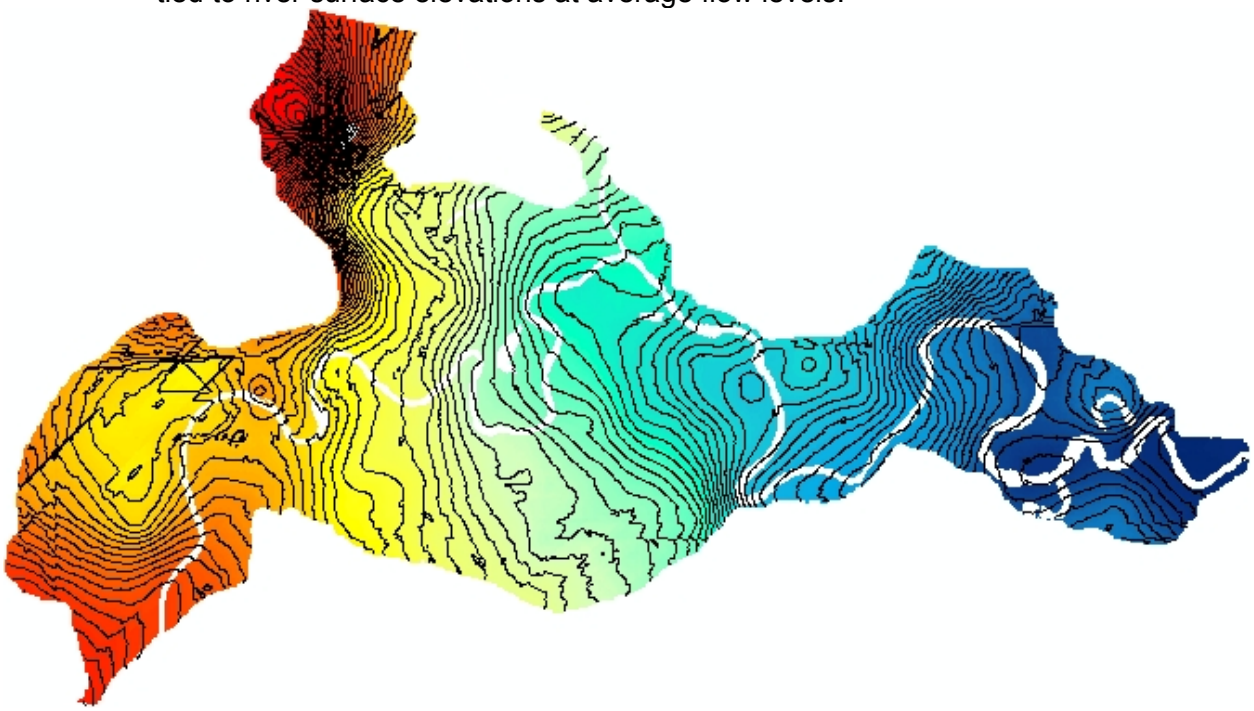

6.6.3. TRANSIENT WATER LEVELS

Transient water levels were only available for the river stage (modelled) and Observation well 217. Figure 87 shows a plot of average monthly groundwater elevations at Observation well 217 showing the statistics for this well. These data are the only data available for calibrating the transient groundwater flow model.

Figure 87 Groundwater elevations at Observation Well 217: graph of descriptive statistics of monthly observations for period of record.

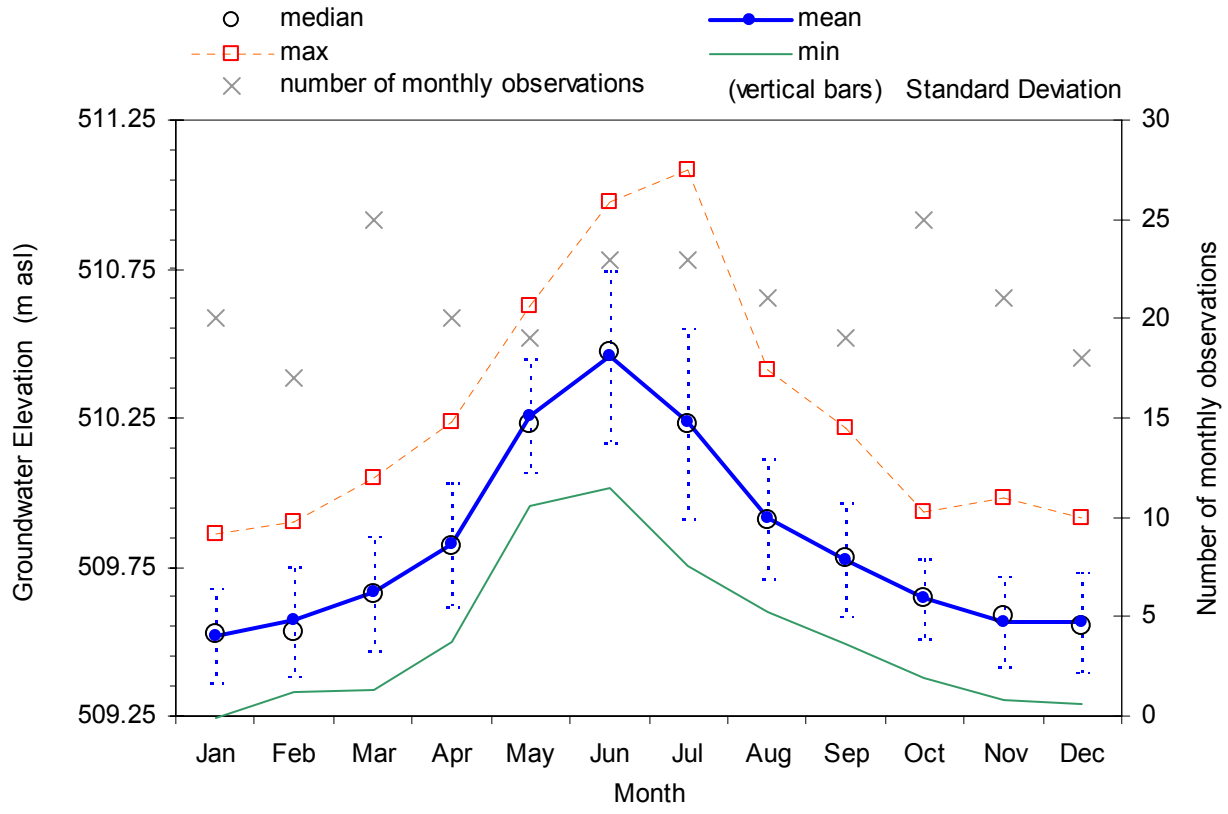

6.6.4. CALIBRATION STRATEGY

- CALIBRATION TARGETS

Model calibration employed the following strategy:

1. Matching the observed hydrograph in the observation well to that produced by the model. Two aspects were considered:

   vertical position (absolute elevation) of the hydrograph. The vertical position of the simulated hydrograph may not match the observed elevation due to well surveying errors and river channel bottom model errors. Calibration to vertical position was attempted by making small adjustments to the river channel curve near that area. As a final step, the well elevation was adjusted within known range of uncertainty only (by a maximum of 0.2 m).

   amplitude and phase shift of hydrograph were matched, allowing for model bias from observed to modelled river hydrograph (assume same bias between calibrated and observed water levels in well).

2. Considering the spatial distribution of residuals: these are static groundwater levels in all wells in GF valley. These are expected not to match perfectly due to static groundwater level errors (well elevation, location, time of sampling, pumping effects, and data entry errors).

3. Calculating the RMS of residuals and other estimates of goodness of fit (statistics).

- CALIBRATION VARIABLES AND SCENARIOS

More than 50 runs of transient model were completed, using different combinations of aquifer layer properties, and comparing the calculated groundwater hydrograph to that observed at well 217 location, comparing RMS values, and checking residual distributions over aquifer area. This section summarizes the calibration process and results. Table 30 lists the calibration model runs, horizontal and vertical hydraulic conductivities assigned to layers 1 to 4, and specific yield assigned to these model layers.

The first transient model run used the same K ans Sy values as applied to original steady-state model for Grand Forks aquifer (Allen 2000). The first models were physically identical to Allen (2000) aquifer models except for transient river and recharge boundary conditions. These early models were designated Model 1 (a to z), but are not included here because those were exploratory in nature.

Model 3 was a totally refurbished structure: all layers were edited in trouble areas, especially along valley walls, and between layer contacts to smooth out irregularities caused by import and interpolation errors between GMS and Visual MODFLOW. A new ground surface DEM was imported at resampled 10 m resolution, and all river channels were edited to correspond to surveyed river channels (roughly). The MODFLOW grid was changed and increased in density to improve river channel representation and production well locations were moved to correct locations. Observation wells were re-imported. Surface DEM was also edited in several spots after consultation with floodplain maps – more accurate topographic maps than the DEM. An additional model layer was added below layer 4 (clay) and shaped to create deep sand lens in eastern part of valley (elsewhere the layer was inactive). River cells and recharge zones were re-mapped based on newly acquired orthophotos (TRIM river outlines were often in wrong locations) and re-imported to MODFLOW files. In effect, the all parts of the model were modified from the original steady-state model, yet preserving the general valley hydrostratigraphy. The third model was further modified by adjusting river channel elevation.

InTable 30 the model runs are grouped into 3 groups: A, B, and C that correspond to Model 2, Model 3, and fine tuned Model 3 calibration runs. The first group (A) used Model 2 of aquifer and explored a wide range of model behaviour at different K and Sy values, and it used the original river channel elevations in the model – river channel bottom elevations partially control the vertical shift in groundwater hydrograph at observation well 217 location, and are not precisely known despite many river surveying lines across the channel. The second group (B) used the improved Model 3 and attempted to calibrate to observation well 217. The third group used Model 3 after adjustment of river channels because the transient model in calibration runs with Model 3 (group B in table) could not match the modelled and observed hydrographs in the observation well. The final Model 3 (with adjusted river channel elevations) was successfully calibrated to the observation well, and is listed separately in the table of results. Groundwater level calibration graphs at well 217 can be found in Figure 94.

The calibration runs, and the final calibrated transient model used the historical climate scenario for recharge, where recharge was spatially distributed in 65 zones and did not include irrigation

return flow (production wells were inactive). Recharge was not adjusted during model calibration, as considerable effort had been made to calculate distributed recharge using physical constraints and accurate climate forcing using HELP. Sensitivity analyses to recharge values proved that in Grand Forks recharge has very small effect on groundwater levels in the floodplain area where Obs well 217 is located. Recharge is only applied to the top active layer (or the top-most active cell if cells above are dry or inactive).

Hydraulic conductivity:

A layered MODFLOW aquifer model was used for the Grand Forks aquifer, where each layer has homogeneous hydraulic conductivity distribution (there is no distribution, only one value per layer). The values were varied within observed range in pump tests as follows, listed by layer:

Values in (m/d)

	min Kxy	**max Kxy**	**typical Kxy**	**min Kz**	**max Kz**
layer 1	30	100	50	10	40
layer 2	5	40	20	1	10
layer 3	0.5	5	1	0.05	1
layer 4	0.05	0.1	0.05	0.01	0.01

The section on the heterogeneous aquifer model provides details on spatially-distributed interpolated hydraulic conductivities and specific yields in top two layers of Grand Forks aquifer model. That type of model was not calibrated to any extent other than using calibrated K and Sy values for other layeres (from calibration results presented in this chapter), and by inclusion of "calibrated" K and Sy values at the location of observation well 217, but allowing variation of K and Sy in other areas of the aquifer according to pump test data (layer 2) or to lithology data at water table elevation (layer 1).

Specific yield and specific storage:

In the unconfined aquifer the storage property is specific yield (Sy), and the MODFLOW model was only sensitive to Sy and not to specific storage because the aquifer is largely unconfined. Specific storage values were kept at reasonable values appropriate for these types of sediments, but were not adjusted in model calibration, only Sy was. Calibration values ranged from were 0.06 to 0.20.

6.6.5. CALIBRATION RESULTS

- OBSERVATION WELL HYDROGRAPH

The calibration graph for Observation Well 217 in Grand Forks (Figure 88) displays graphically the observed long term monthly mean water elevation and modelled groundwater elevation after model calibration (1961-1999 scenario 1A). Also shown are observed and simulated discharge hydrographs for nearby Kettle River for corresponding time period.

Figure 88 Calibration graph for Observation Well 217 in Grand Forks showing observed long term monthly mean water elevation and modelled groundwater elevation after model calibration (1961-1999 scenario 1A). Also shown are observed and simulated discharge hydrographs for nearby Kettle River for corresponding time period.

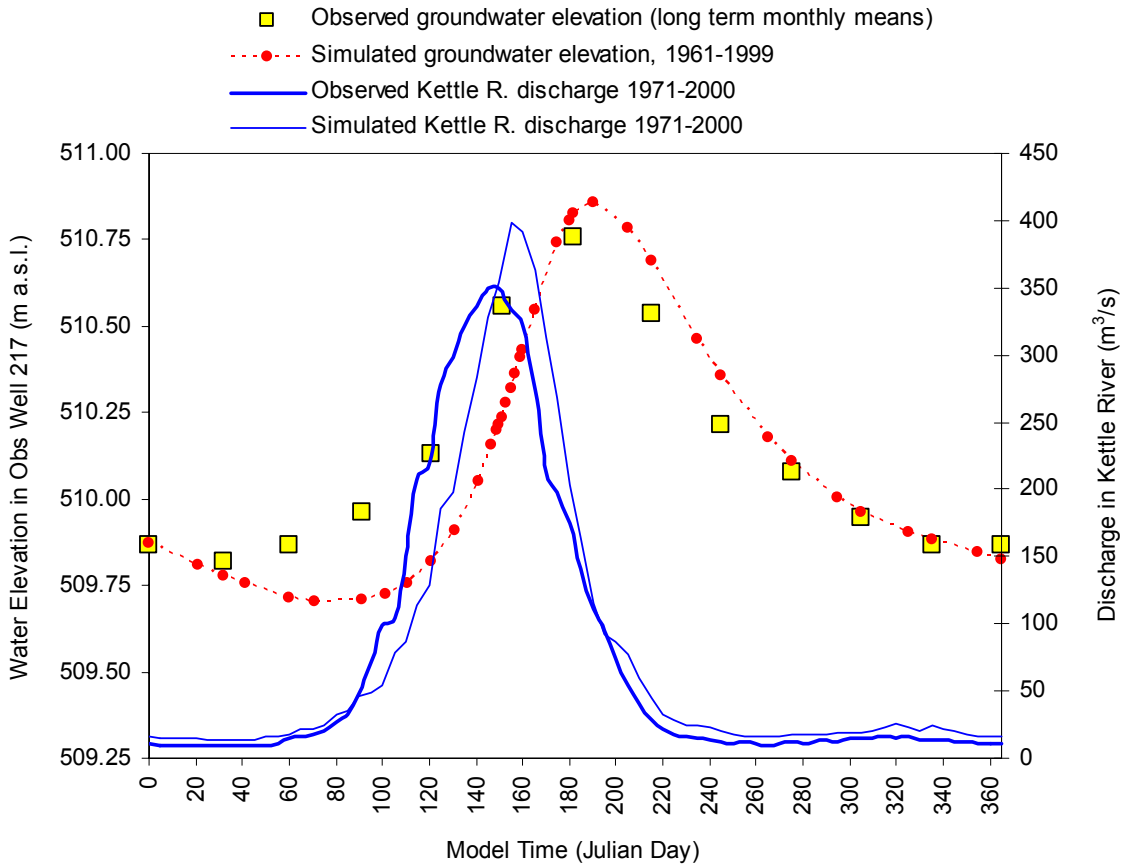

Vertical Shift of Hydrograph: The absolute elevation of the top of casing of Observation well 217 is not known, and was originally determined from detailed (0.1 m contours) floodplain maps (Wei, personal communication). The well was installed in 1970's and was never surveyed precisely with differential GPS or other tools. Thus, there is some error expected in this well elevation, on the order of +/- 0.2 m at least. The floodplain maps of Kettle River in Grand Forks (map sheet 5) plot the position of well 217 near the 515.0 m contour; near 513.6 m high point. The reported well elevation, as referenced to measured water levels, is 513.5 m. The water levels are measured with 1.0 cm accuracy by water level recorder and datalogger.

Amplitude of Hydrograph (peak): During calibration, in terms of calculated groundwater level at location of Observation well 217, the model was most sensitive to changes in specific yield (Sy) and horizontal hydraulic conductivity (Kxy) in Layer 2. As Sy changed from 0.04 to 0.20, the amplitude of the hydrograph decreased and the slope of the decreasing hydrograph also flattened, ending with higher groundwater levels at end of year, thus suggesting more stored groundwater in aquifer. However, as Kxy was lowered, keeping Sy constant, the same effect was observed (showing inverse relation of Sy to Kxy at that point).

Phase shift of hydrograph (time of rise and fall): The groundwater hydrograph in Observation well 217 is shifted due to the delay of groundwater flow across the distance from the Kettle River (in 3 directions, as the well is within river meander bend on the floodplain).

Modelled Groundwater Levels in Spring: The transient model consistently predicted lower than observed groundwater elevations in Observation well 217. It is important to recognize that the river discharge hydrographs do not show the stage of the river. The BRANCH model that computed stage-discharge elevations assumed ice-free conditions in the river, and only ice-free river stages (for obvious reasons) were used in stage-discharge curves in the past for this river. In spring time, the ice breakup on the river causes an increase in river stage due to icing of channel, resulting in higher actual river stage than would be predicted by given discharge. The modelled water levels do not account for this effect because the groundwater model uses modelled river stage that is computed from river discharge, without accounting for ice effects. Therefore, it is expected that modelled groundwater levels would decline from day 1 to day 60 when river discharge begins to increase due to snowmelt. In reality, the observed river stage is probably higher in spring due to ice damming and icing of the channel, but still passes the same discharge.

Another factor in higher groundwater levels in spring is direct recharge from snowmelt. Although the air temperatures are below freezing in winter in Grand Forks, snowmelt occurs in late winter and recharges the aquifer. The recharge model in HELP deals with snowmelt, but not in rigorous way, thus the soil is assumed to be unfrozen all winter. The HELP output already overestimates recharge in winter conditions at Grand Forks because of assumption of non-frozen soils. Furthermore, recharge was observed to have minor effect on groundwater levels in Grand Forks. Thus, aside from model error, the only plausible explanation for this discrepancy is the ice effect in river channel. We do not know of any other source of model error that would result in such a discrepancy, since the model appears to behave well for other parts of the year and the MODFLOW code has been verified and used extensively by hydrogeologic community.

River Model Bias: The groundwater model is calibrated to the modelled (not observed) discharge and stage in Kettle River (Figure 89). If there was no bias in river model (observed to modelled), the well hydrograph would also match the observed. The modelled peak of groundwater was maintained at a level slightly higher than observed to account for this positive bias in modelled versus observed river discharge (and thus stage). Similarly, the modelled hydrograph is shifted to a later date. The calibrated model is also shifted by the same number of days to account for this bias. In fact, it was not possible to calibrate the model to match the observed hydrograph in the observation well by matching amplitude, shape and phase of the peak.

We believe that the groundwater model is very well calibrated at the location of observation well 217. However, this does not mean that it is well calibrated for other regions of the aquifer. Other measures of goodness of fit were used for that. Ultimately, installation of more groundwater observation wells and their transient records would help calibrate the model to all regions of aquifer, and K and S parameters would have to be spatially-distributed.

Figure 89 Mean hydrograph of water table elevation (total head) in Observation Well 217 in Grand Forks aquifer and water surface elevation of Kettle River at cross-section 17 (400 m from well 217).

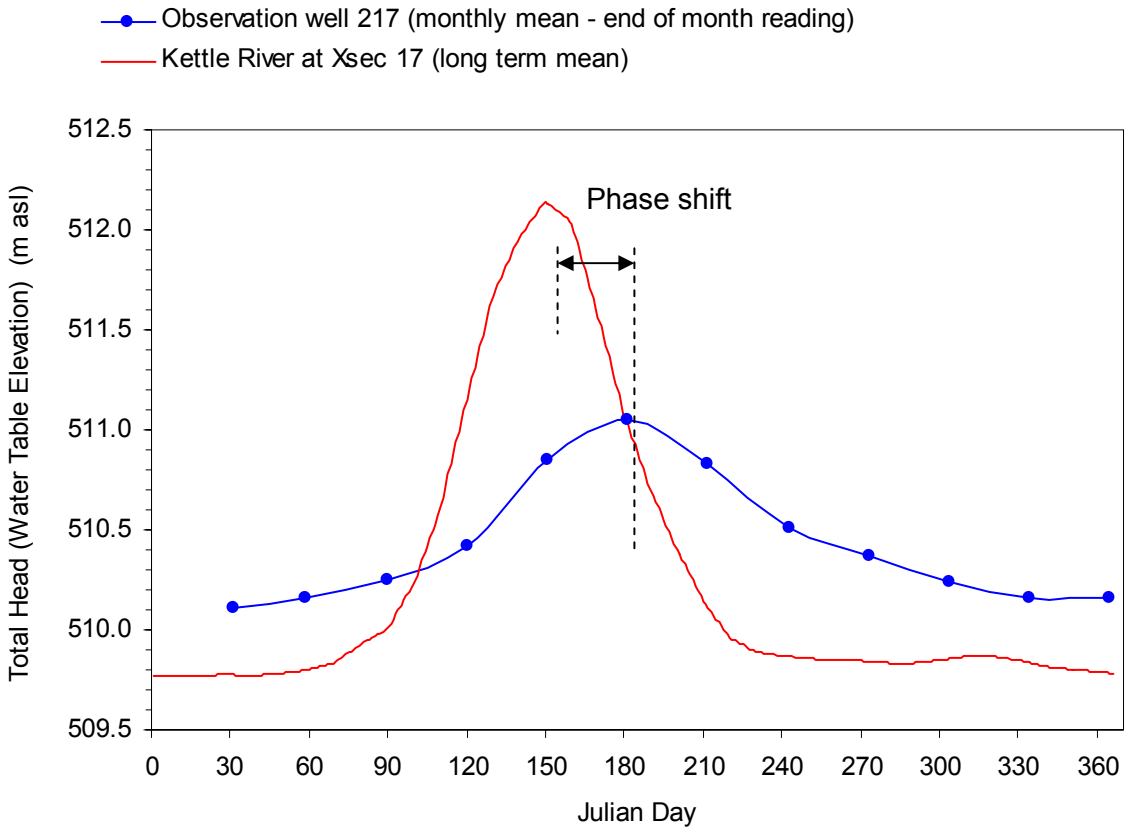

Heads (calculated and observed water levels) are compared for model cells that contain observation wells. The observation wells were screened over the entire thickness of the aquifer, and Visual MODFLOW calculates heads at nodes in the middle of cells (block centered model). The relatively fine model grid of 2.5 m by 2.5 m grid cells ensures that all observation wells are placed in separate grid cells and the position error between actual well location and cell node location is small.

Map 49 shows a map of the residuals (difference between model water levels and observed static water levels) for the calibrated model. These residuals correspond to time 160 (Julian Day), high river stage. The map suggests that there is roughly an even distribution between positive and negative residuals, which is important in order to demonstrate that the model is equally in error in all portions of the domain. Residuals tend to be high near the model boundaries, which might be anticipated due to lack of lack of physical data in these areas with which to constrain the conceptual model. Observation wells where residuals were very large (> 5 m) were examined in detail; looking at well location, elevation on the floodplain map and DEM surface. For these suspect wells the static water level was compared to nearby observation wells, to a possible range of river water levels if the well was adjacent to the river, and ground surface elevation and the expected water table surface in that area. At least 11 observation wells were identified that had suspect static water levels reported in BC well database. The errors could be data entry errors (e.g., using depths in feet where metres should be used and vice versa), incorrect static water depths reported, incorrect well casing elevations, and anomalous hydrogeologic events (e.g., pumping) near the wells. The residual map without anomalous wells is plotted in Map 49b. Figure 90 shows a graph of the same results (calculated

versus observed head – water level). An excellent fit was obtained (most data fall within the 95% confidence interval). Figure 91 shows a plot of the residuals for all time steps.

Map 49 Residuals from calibrated model water table and static water levels in wells at model time 160 (Julian Day) – high river stage: (a) all observation points, (b) excluded observation points with suspect static water levels.

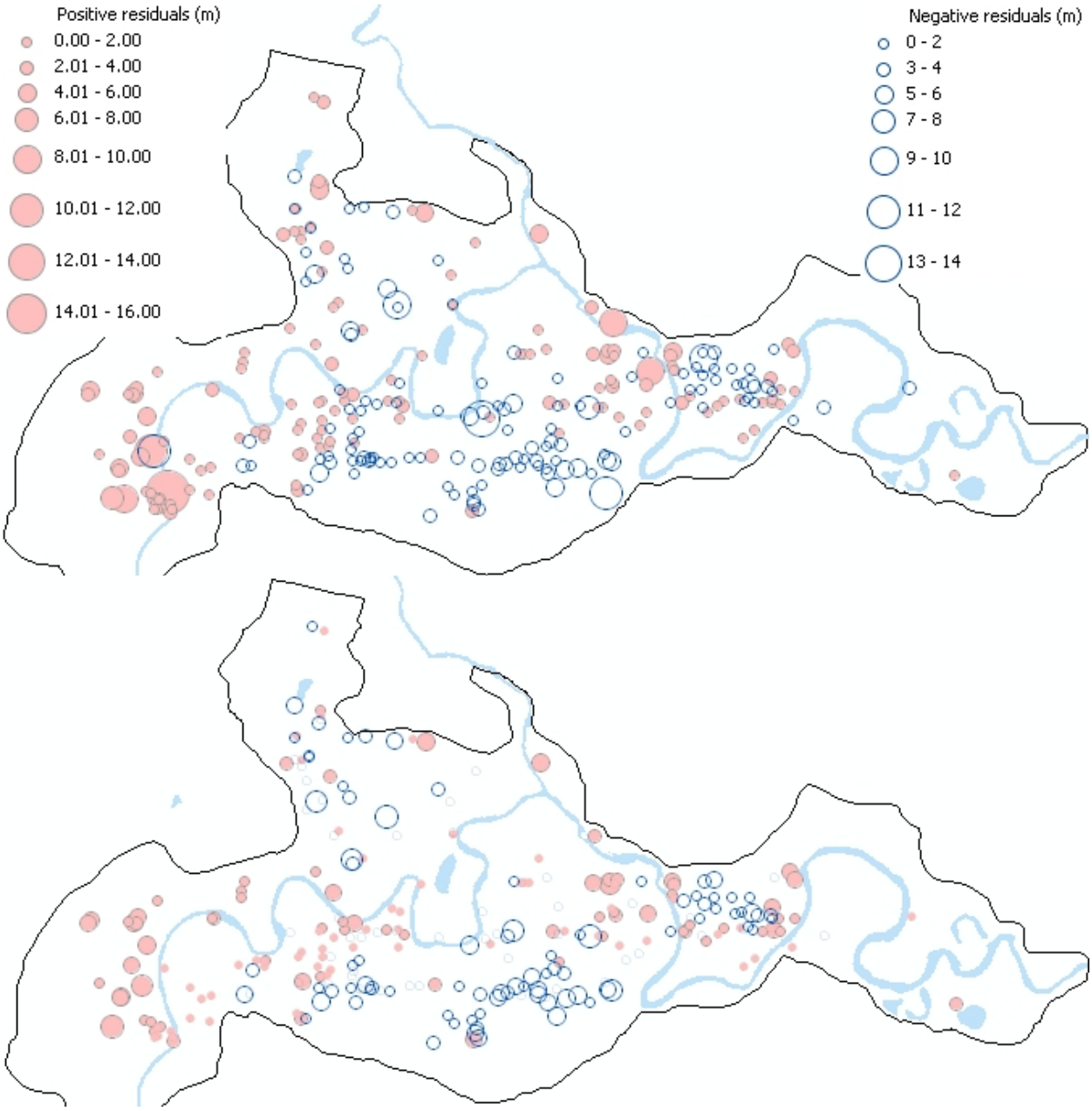

Figure 90 Residuals at model time 160 (Julian Day) from transient model run for 1961-1999 climate (scenario 1A).

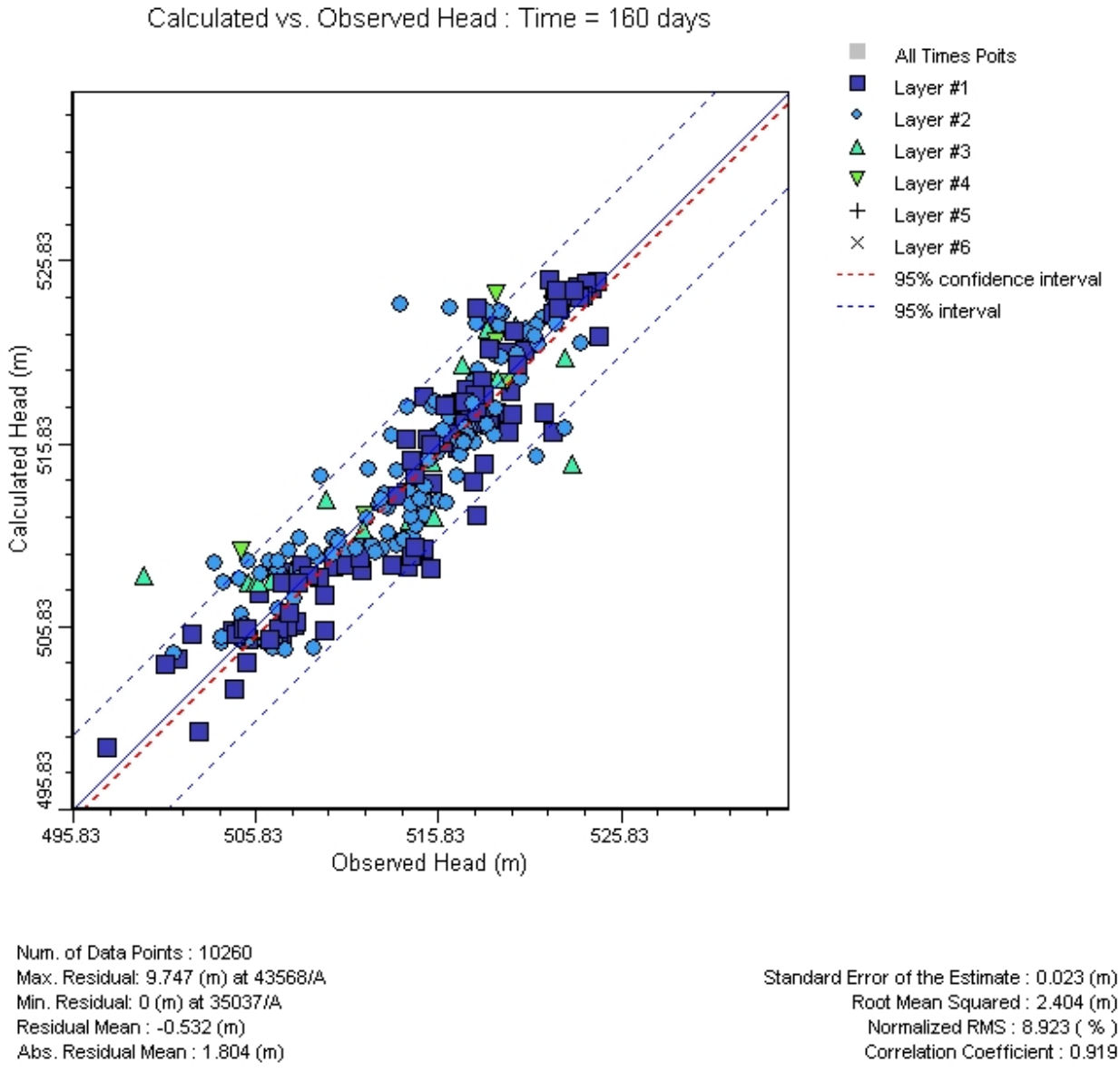

Figure 90 gives a graph of the same results (calculated versus observed head – water level). The normalized RMS for residuals between calculated and observed head was 8.9% for time step 160, and it was reduced to about 8% if large and anomalous residuals were excluded. (most data fall within the 95% confidence interval). Figure 91 shows a plot of the residuals for all time steps. The data points in Figure 90 have different symbols for model layers 1 to 4 (there is one well in layer 5 and no wells in layer 6). The graph is a scatterplot of calculated versus observed heads at time 160 of transient model run, both in elevations in metres above sea level (m.a.s.l.). Most of the points fall very close to 1:1 line, showing good correspondence between calculated and observed water levels (head in the unconfined aquifer). The graphs for different time steps look very similar, but there are small shifts in point positions and the statistics change slightly. The same points but for all time steps in transient model were graphed in Figure 91.

Figure 91 Residuals at all time steps from transient model run for 1961-1999 climate (scenario 1A).

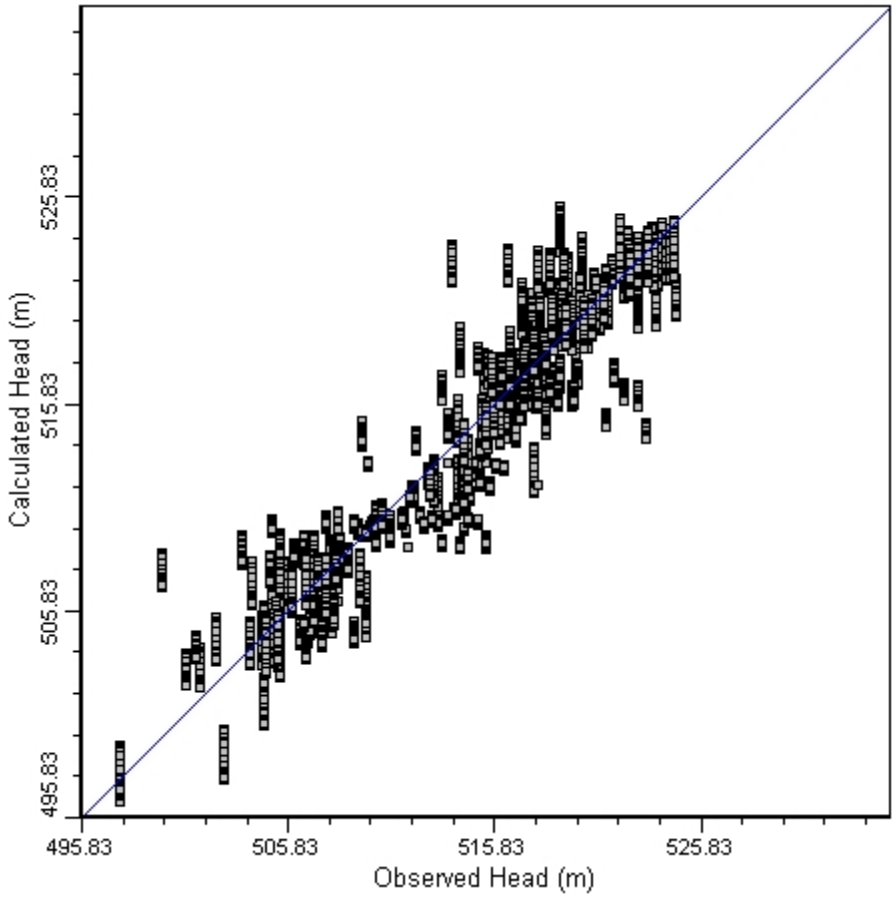

- OVERALL TRANSIENT MODEL CALIBRATION ERRORS VERSUS TIME

The model residuals (calc – obs) should have a normal distribution if the error distribution is normal and random errors are the cause. If the distribution is skewed and not normal, then some model areas have systematic errors that result from poor model calibration. A transient model would ideally have normally distributed residuals at all stress periods (model times), but that is not expected when static water levels are used because these tend to be collected during well installation, which tends to occur over warm parts of the year (late spring to early fall).

Each calibration run produced "goodness of fit" statistics that compared calibrated to observed head values and their distribution across the site. The acceptable solution should be between 5 and 10% normalized root mean square error (RMS), where RMS is:

$$\text{RMS Error} = [\ 1/n \sum_{i=1}^{n} (h_m - h_s)_i^2]^{1/2} \qquad \textbf{[18]}$$

Here n is number of observed and calculated value pairs (equal to number of observation wells with static water levels), h_m is the measured head, and h_s is the simulated head.

At all times of the transient model, residuals have close to normal distribution at times 1, 60, 121, 160, 305, 365 days (Figure 92). The mean residual is always negative, but is small (0 to -2 m). This indicates that there are more wells where modelled heads (water table in top two layers) were less than observed, but the locations of these points are not indicated. This is true at all times of transient model, thus it is not related to river stage.

As a time series in Figure 93, the calibration errors ARM (absolute residual mean) and RM (residual mean) had temporal trends such that residuals were smaller when river stage was larger (day 150 to 180) than at other times of the year. This indicates that static groundwater levels in wells were closer to modelled groundwater levels during late spring and early summer of the high water stages in Kettle River. It is likely that most static water levels were collected also during late spring months during well installation. Wells are installed for domestic and irrigation use, and it is reasonable to assume that most wells are installed prior to summer growing season, or before house construction. The RM error was always negative, agreeing with frequency distributions that the model underpredicts water levels in greater than 50% of wells. The ARM error is just the positive number of RM, given that RM was negative. The RMS (Root Mean Square Error) is the best estimate of model fit for the entire model, and it shows a value of 2.5 (note that RMS is always positive). Therefore, on average, the modelled water levels were off by 2.5 m from observed water levels, which in this aquifer system may not mean much because the static well elevations may have very large errors (sometimes > 20 m) due to poor control of well location and elevation. In the floodplain, river stage variation of several meters has also something to do with such calibration error. The RM showed that during high river stages, the positive and negative residuals are balanced (giving near zero RM).

Figure 92 Frequency distribution histogram of calibration of residuals (cal – obs) for different time periods in transient model.

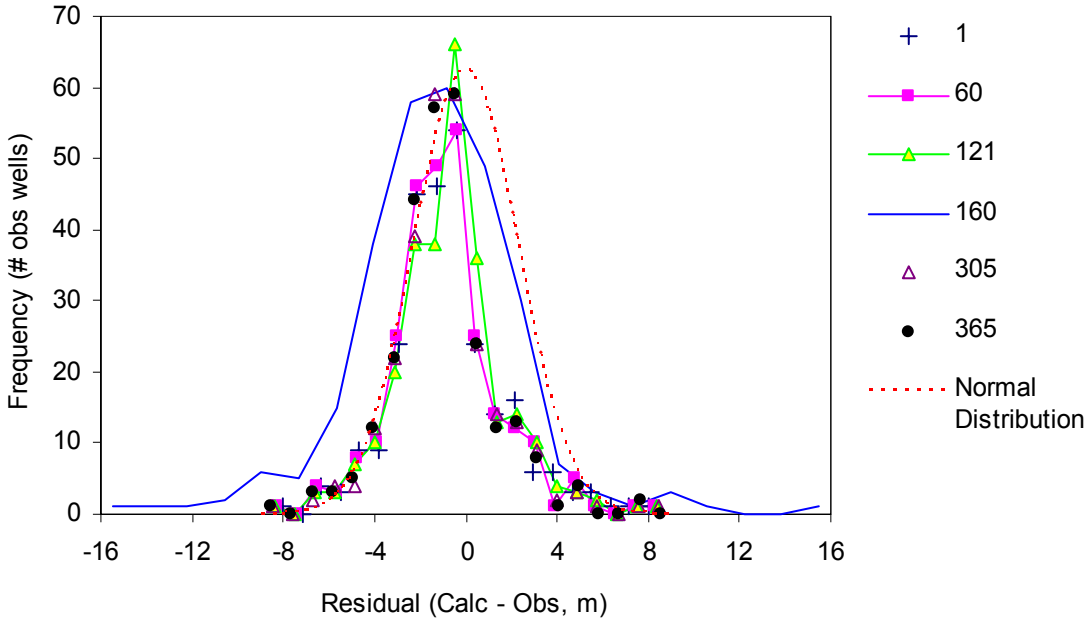

Figure 93 Calibration errors time series (versus model time) for transient model.

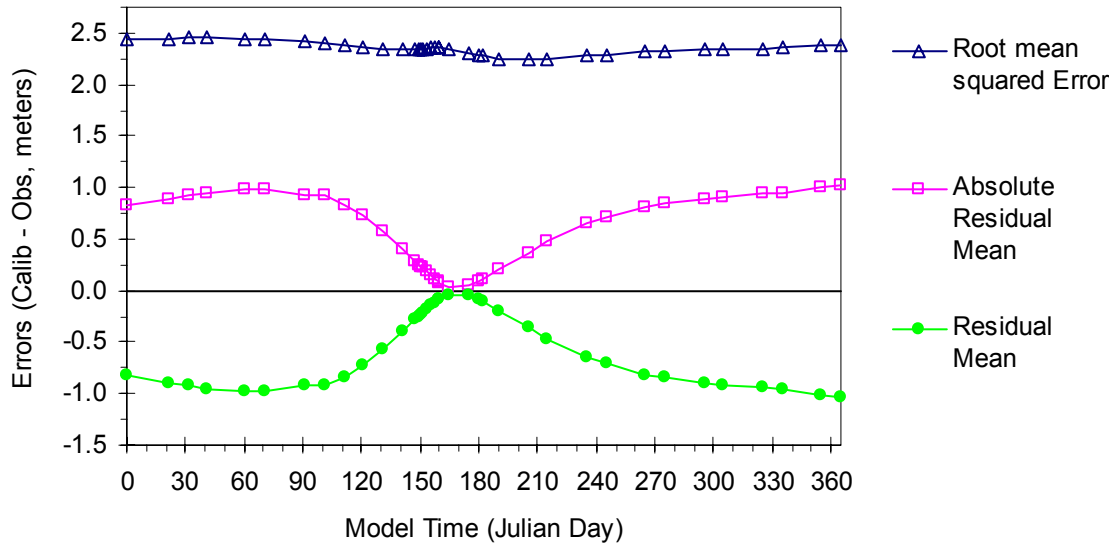

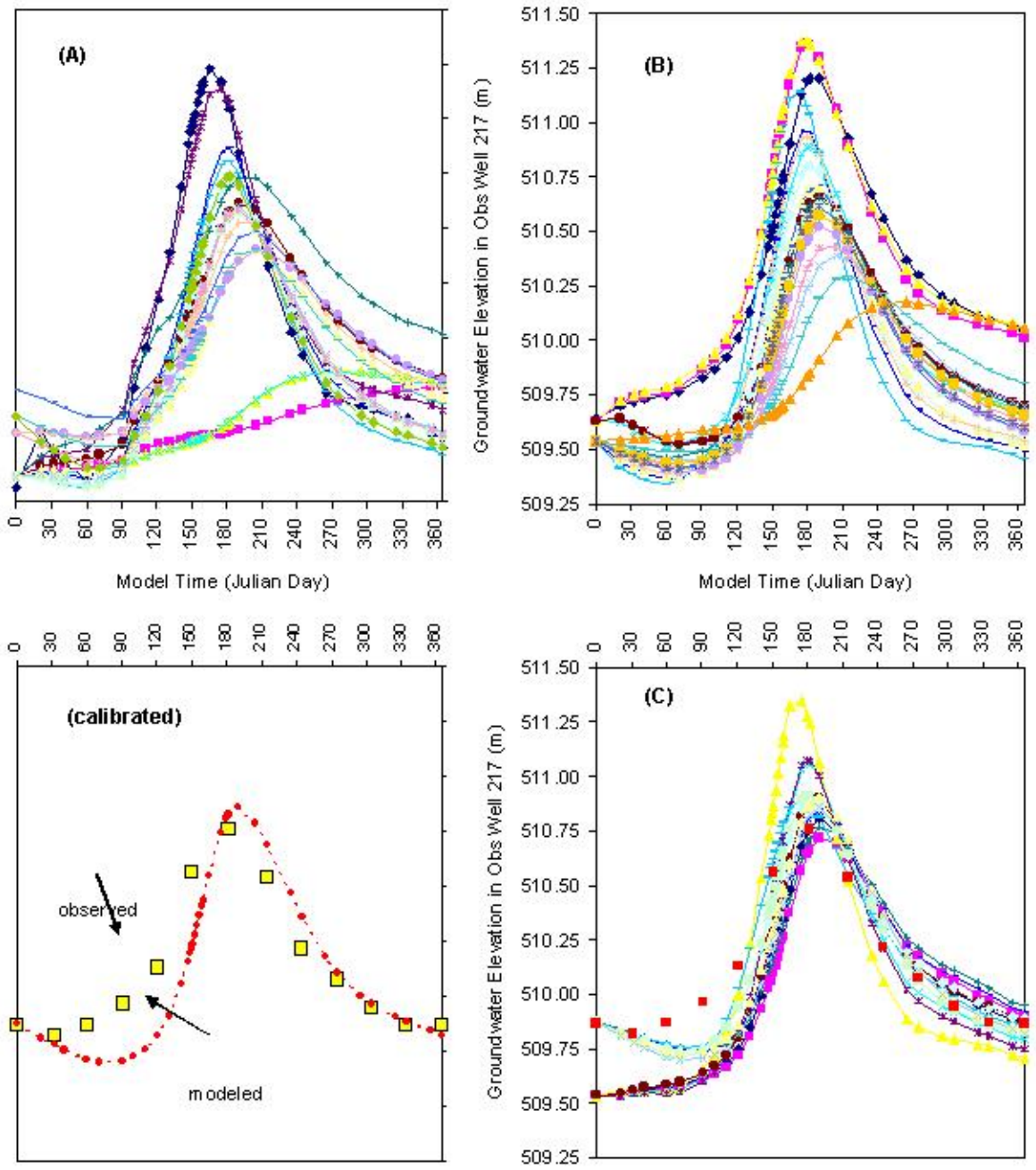

Figure 94 Calibration graphs for modelled groundwater levels (hydraulic heads in unconfined Layer 2) for calibration series A, B, and C, and calibrated transient model to Obs Well 217 in the floodplain.

Table 30 Calibration scenarios for transient Grand Forks aquifer model.

	K x,y m/d				**Kz** m/d				**Sy**				
	layer1	layer2	layer3	layer4	layer1	layer2	layer3	layer4	layer1	layer2	layer3	layer4	
Model2a	50	5	0.5	0.05	16	1	0.05	0.01	0.25	0.3	0.2	0.06	
Model2b	30	10	0.5	0.05	16	1	0.05	0.01	0.25	0.3	0.2	0.06	
Model2c	30	10	1	0.05	20	7	0.8	0.01	0.25	0.3	0.2	0.06	
Model2d	50	5	0.5	0.05	16	1	0.05	0.01	0.01	0.01	0.01	0.06	
Model2e	50	5	0.5	0.05	16	1	0.05	0.01	0.05	0.05	0.05	0.06	
Model2f	50	15	0.5	0.05	16	1	0.05	0.01	0.03	0.03	0.05	0.06	
Model2g	50	15	0.5	0.05	16	1	0.05	0.01	0.04	0.04	0.05	0.06	
Model2h	75	15	1	0.05	16	2	0.8	0.01	0.04	0.04	0.05	0.06	(A)
Model2i	50	15	1	0.05	16	2	0.8	0.01	0.05	0.05	0.05	0.06	
Model2j	50	15	1	0.05	16	2	0.8	0.01	0.07	0.07	0.05	0.06	
Model2k	50	10	1	0.05	16	2	0.8	0.01	0.08	0.08	0.05	0.06	
Model2l	80	15	1	0.05	30	5	0.8	0.01	0.07	0.07	0.05	0.06	
Model2m	80	15	1	0.05	30	5	0.8	0.01	0.07	0.07	0.05	0.06	
Model2n	80	7	1	0.05	30	2	0.8	0.01	0.07	0.07	0.05	0.06	
Model2o	80	7	1	0.05	30	2	0.8	0.01	0.07	0.05	0.05	0.06	
Model2p	80	7	1	0.05	30	2	0.8	0.01	0.07	0.06	0.05	0.06	
Model2q	80	10	1	0.05	30	2	0.8	0.01	0.07	0.08	0.05	0.06	
Model2r	80	13	1	0.05	30	2	0.8	0.01	0.04	0.04	0.05	0.06	
Model3 (a)	80	13	1	0.05	30	5	0.8	0.01	0.06	0.06	0.05	0.06	
Model3 (b)	80	13	1	0.05	30	5	0.8	0.01	0.04	0.04	0.05	0.06	
Model3 (c)	80	13	1	0.05	10	1.5	0.8	0.01	0.04	0.04	0.05	0.06	
Model3 (c2)	80	13	1	0.05	10	1.5	0.8	0.01	0.04	0.04	0.05	0.06	
Model3 (d)	80	13	1	0.05	30	5	0.8	0.01	0.07	0.07	0.05	0.06	
Model3 (e)	80	13	1	0.05	50	10	0.8	0.01	0.08	0.08	0.05	0.06	
Model3 (f)	80	20	1	0.05	30	5	0.8	0.01	0.07	0.07	0.05	0.06	
Model3 (g)	100	25	3	0.05	50	10	1	0.01	0.07	0.07	0.05	0.06	
Model3 (h)	100	25	3	0.05	50	10	1	0.01	0.04	0.04	0.05	0.06	
Model3 (i)	100	25	3	0.05	50	10	1	0.01	0.1	0.1	0.05	0.06	
Model3 (j)	100	25	3	0.05	50	10	1	0.01	0.15	0.15	0.05	0.06	
Model3 (k)	100	30	5	0.1	50	10	1	0.01	0.15	0.15	0.05	0.06	(B)
Model3 (L)	80	15	3	0.05	50	10	1	0.01	0.15	0.15	0.05	0.06	
Model3 (m)	100	25	3	0.05	50	10	1	0.01	0.2	0.2	0.05	0.06	
Model3 (n)	100	30	3	0.05	75	20	1	0.01	0.2	0.2	0.05	0.06	
Model3 (o)	80	20	3	0.05	30	5	1	0.01	0.06	0.06	0.05	0.06	
Model3 (p)	80	20	3	0.05	30	5	1	0.01	0.1	0.1	0.05	0.06	
Model3 (q)	80	13	3	0.05	30	5	0.5	0.01	0.15	0.15	0.05	0.06	
Model3 (r)	80	20	3	0.05	30	10	0.5	0.01	0.12	0.12	0.05	0.06	
Model3 (s)	80	20	1	0.05	80	15	0.1	0.01	0.12	0.12	0.05	0.06	
Model3 (t)	30	5	1	0.05	30	5	0.1	0.01	0.12	0.12	0.05	0.06	
Model3 (r2)	30	5	1	0.05	30	5	0.1	0.01	0.12	0.12	0.05	0.06	
Model3 (r3)	30	5	1	0.05	30	5	0.1	0.01	0.12	0.12	0.05	0.06	
Model3 (s)	80	20	3	0.05	30	10	0.5	0.01	0.12	0.12	0.05	0.06	
Model3 (t)	80	20	3	0.05	30	10	0.5	0.01	0.14	0.14	0.05	0.06	
Model3 (u)	80	40	1	0.05	30	20	0.5	0.01	0.07	0.07	0.05	0.06	
Model3 (v)	80	40	1	0.05	30	20	0.5	0.01	0.14	0.14	0.05	0.06	(C)
Model3 (u)	80	20	3	0.05	30	5	0.5	0.01	0.05	0.05	0.05	0.06	
Model3 (v)	40	20	3	0.05	40	10	0.5	0.01	0.1	0.1	0.05	0.06	
Model3 (w)	80	20	3	0.05	30	10	0.5	0.01	0.14	0.14	0.05	0.06	
Model3 (x) (calibrated)	80	20	3	0.05	30	10	0.5	0.01	0.12	0.12	0.05	0.06	

7. GROUNDWATER MODELLING RESULTS

7.1. GROUNDWATER FLOW

7.1.1. SCENARIOS

The final calibrated transient model was used for all climate change impacts scenarios and all sensitivity scenarios (to aquifer heterogeneity and recharge distribution assumptions). In this report a modelling "scenario" refers on one instance of a transient model run with one set of inputs:

1) recharge for one selected climate, either historical or predicted future climate

2) river hydrograph, either historical or predicted for future conditions

3) pumping or no-pumping

4) type of recharge distribution over the aquifer area

5) type of aquifer representation (homogeneous or heterogeneous K distribution)

Refer to Table 31 for a complete list of modeling scenarios and scenario series in this report.

There were five scenario "series" (all numbered) which group together similar models. The first series represents "natural conditions" without pumping effects. The second series represents pumping conditions. Both series 1 and 2 have the four climate scenarios (labelled with letters A to D; where A is historical climate, and B to D are future climates), one for historical climate, and three for future climates, where both river and recharge depend on the climate being represented. In all cases recharge is spatially and temporally distributed over the aquifer. The "code" for modelling scenario has two characters, the first one is the "series number" and the second is the "scenario label". On many maps and graphs the scenarios are identified by "code", for example, 1A for series 1 (non-pumping) and historical climate (A). In summary, in scenario series 1 to 4 the scenario "letters" represent climate: A = historical climate, B = 2010-2039 climate, C = 2040-2069 climate, D = 2070-2099 climate.

Scenario series 3 and 4 are analogous to series 1 and 2 in that each has four climate scenarios; one is for non-pumping (3) and one is for pumping models (4). However, both 3 and 4 run on a very different aquifer model, where aquifer heterogeneity is represented by spatial distribution of hydraulic parameters (K and Sy) in the top two layers, which correspond to the unconfined aquifer. In layer 2 of this model, the hydraulic conductivity and specific yield were interpolated from pump test data. In layer 1 (top layer and usually unsaturated), the K-values were interpolated from estimated K-values at the water table elevation from classified and interpreted borehole lithologs, using standard material types and typical average K and Sy values for a given material type.

Series 5 has two model scenarios, each designed to test the sensitivity of the model results to (A) temporal distribution of recharge, and (B) spatial distribution of recharge. This is accomplished by comparing the 5A model to 1A model results and subtracting head maps for all corresponding time steps in selected model layer (usually layer 2). The only difference between 1A and 5A is that in 5A the recharge has mean annual value for the whole year, for all time

steps of transient model, while 1A has full temporal distribution (at monthly steps). The only difference between 1A and 5B is spatial distribution of recharge by recharge zones in 1A, but only one large recharge zone in 5B (both have temporal variation in recharge).

In total 18 fully-transient models were run for 1 year of flow in the Grand Forks aquifer. Two different aquifer heterogeneity representations were used, but model layering and hydrostratigraphic model (aquifer architecture) are identical in all of these models.

Table 31 Transient model scenarios for Grand Forks climate change impacts modeling. Summary table.

Scenario series	Code	Climate	Pumping	Comments	Visual Modflow model name
1	1A	1961-1999		spatially-distributed recharge in 65 zones	tr_1961-1999
	1B	2010-2039			tr_2010-2039
	1C	2040-2069			tr_2040-2069
	1D	2070-2099			tr_2070-2099
2	2A	1961-1999	yes	spatially-distributed recharge in > 65 zones	tr_1961-1999_2
	2B	2010-2039	yes		tr_2010-2039_2
	2C	2040-2069	yes		tr_2040-2069_2
	2D	2070-2099	yes		tr_2070-2099_2
3	3A	1961-1999		Heterogeneous K distribution (L2 from pump tests, L1 from lithology as indicator at water table elevation)	tr_heterogenousL12_1961
	3B	2010-2039			tr_heterogenousL12_2010
	3C	2040-2069			tr_heterogenousL12_2040
4	4A	1961-1999	yes	Heterogeneous K distribution (L2 from pump tests, L1 from lithology as indicator at water table elevation)	tr_heterogenL12_1961_2
	4B	2010-2039	yes		tr_heterogenL12_2010_2
	4C	2040-2069	yes		tr_heterogenL12_2040_2
5	5A	1961-1999		constant recharge (mean annual) in one zone (no spatial variation)	tr_1961_1999_constrech
5	5B	1961-1999		mean monthly recharge in one zone (no spatial variation)	tr_1961_1999_nospatialrech

7.1.2. WATER TABLE SURFACE

The modeled water table elevations were exported from Visual MODFLOW as heads in layer 2 of the unconfined aquifer (where most cells are saturated). Two time periods from transient model output are displayed in Map 50. The elevations of the water table range from low of 497 m in eastern part of valley to high of 530 m in western and north-western sections of valley. Water table elevation follows roughly the ground surface elevation contours, except where there are high terraces that are mostly dry (western part and along valley walls). Dry cells have anomalously high water elevation values and have dense contour spacing and should be ignored.

At day 160 the river water levels are at an annual high and so are groundwater levels. At day 235, the river water elevation is close to baseflow and is still decreasing. Water table elevations in the aquifer are also lower, but the overall pattern of a sloping water table from west to east remains the same.

The calculated water table elevation can be compared to static water table elevation, which was interpolated from water well records at time of construction, as described in model calibration section of this report. Map 51 represents the “differences” between calculated water table and static water table. Areas where modelled heads were much higher than static were in western end of valley, but most significantly in eastern part of floodplain. The eastern part of floodplain had significant differences between ground surface DEM used in the MODFLOW model and actual floodplain elevation (about 1 to 3 meters), but the main problem lies with lack of static well data in that part of valley, so the static water table interpolation there was not valid. In most of the central valley the model predicted very similar groundwater levels to static ones. However, in north-west valley near Ward Lake, the modelled water elevations were much lower than static, which could be caused by wrong recharge inputs and incorrect hydraulic conductivity estimates for that part of valley.

7.1.3. GROUNDWATER FLOW PATTERNS AND GRADIENTS

Groundwater flow in the aquifer is predominantly from west to east, in the same direction as Kettle River flow. In Map 52 there are flow directions at two time steps (day 131 and day 160) of the transient model. The flow directions are for layer 2 of the unconfined aquifer and all vector arrows are identical in size (flow velocity is not shown on this map). Blue arrows have in-plane direction, whereas red arrows show out-of-plane directions. At day 131 (May 11), the production wells are inactive and flow patterns approximate natural conditions. Flow directions are indeed mostly from west to east, but there are local flow patterns usually away from the rivers, or flowing between river meander bends in the floodplain areas. In the north-west portion of valley the flow is north to south, following the ground surface slope of valley (and also bedrock surface topography). At day 131 the river stage is rising, therefore flow is usually outward from the river and into adjacent areas (water is put into temporary storage in the aquifer). At day 160, the pumps are active and the river is just past peak flow. Flow directions at day 160 are either away from the river, between river meanders, or toward pumping wells. The influence of pumping wells is clearly visible on groundwater flow patterns, but it appears to be localized. The river still controls the flow patterns in the valley.

Map 50 Water table elevations calculated by transient model of Grand Forks aquifer. Time steps at days 160 and 235. Historical climate input and non-pumping conditions. Contours are 0.5 m and elevations range from 497 m to 530 m.

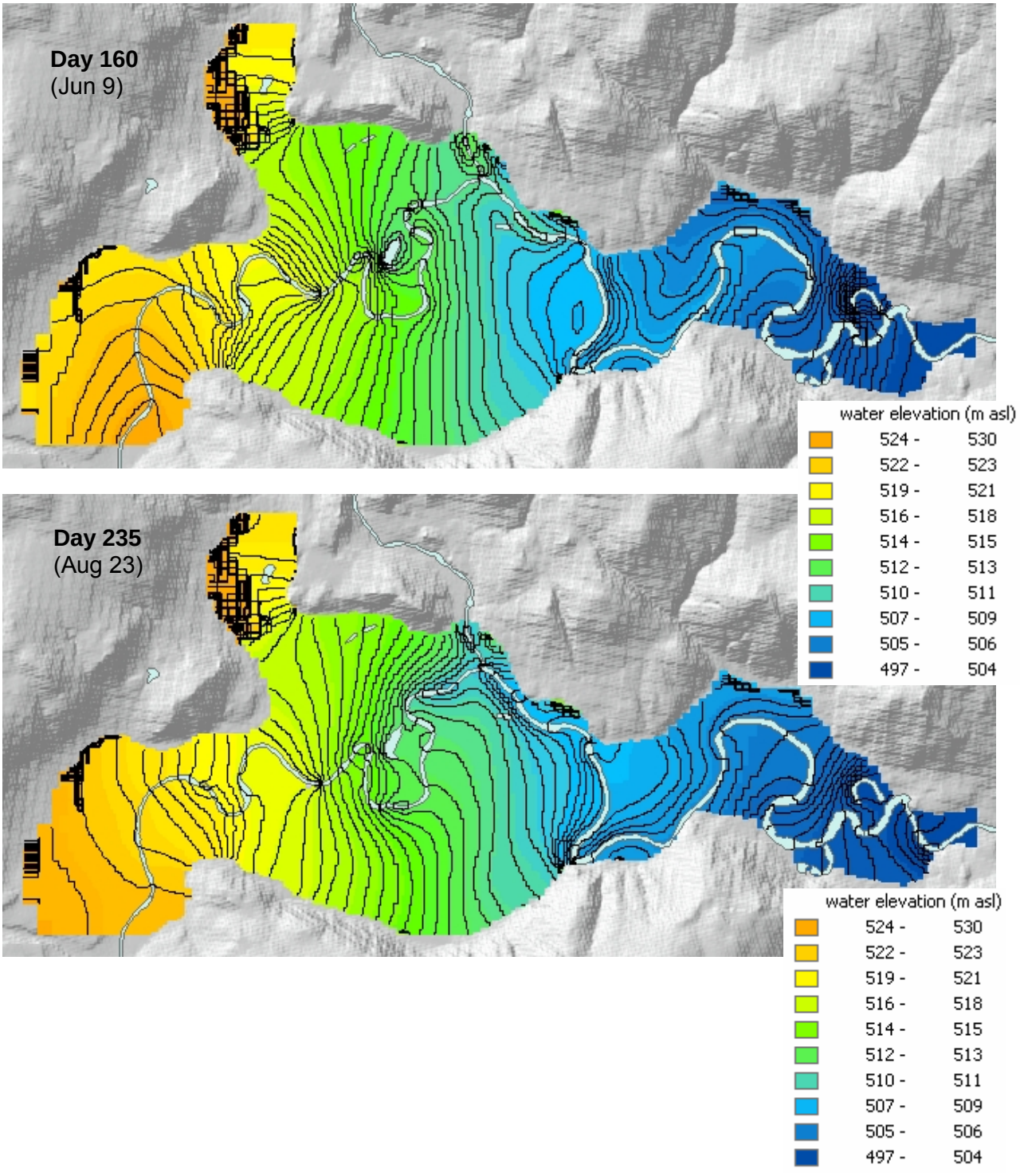

Map 51 Differences between calculated head in layer 2 and interpolated static water table elevation from well records, of unconfined aquifer at time step day = 160 in transient model (scenario 1A).

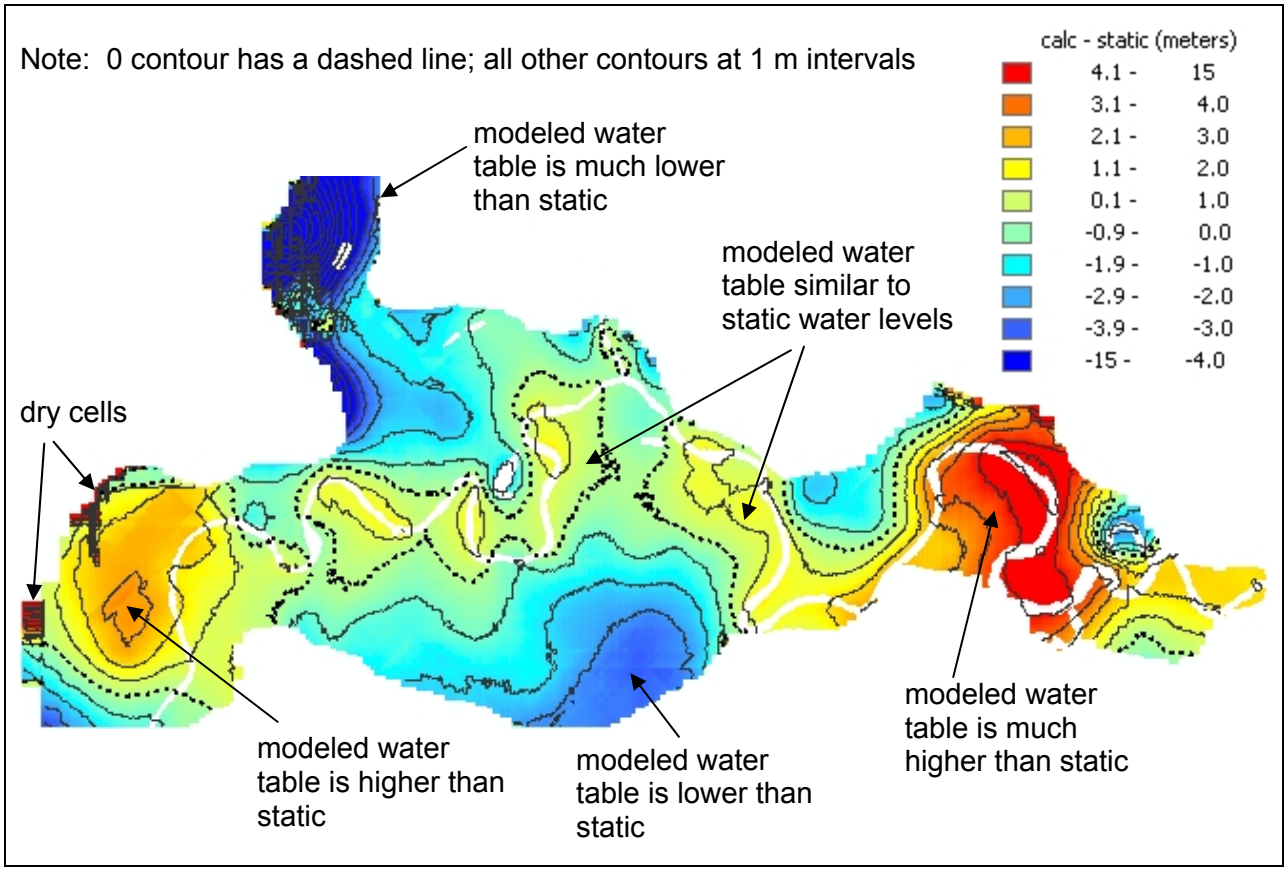

In cross-section view (along xz plane) of the valley, the groundwater directions vary with depth and location along a West-East line along the valley (see Figure 95). The profile view has been vertically exaggerated by 20 times, but flow directions are not changed. Flow velocities (magnitudes of vectors) for the West-East profile are shown in Figure 97. The very large downward pointing vectors occur near dry cells and are probably a result of an erroneously large hydraulic gradient there, related to problems of solution near dry cells. One North-South profile (Figure 95) shows flow directions between river channels as some channels loose water and others gain water. Layer boundaries also affect flow directions due to contrasts of hydraulic conductivity. These profile maps were produced directly from Visual MODFLOW and illustrate the general trends in groundwater flow through the valley.

Map 52 Groundwater flow direction vectors (not scaled to magnitude) in W-E cross-section over most of the Grand Forks aquifer at time step day = 131 and 160 in transient model with active pumping (scenario 2A). Arrow colours are for in-plane (red) and out of plane (blue) directions.

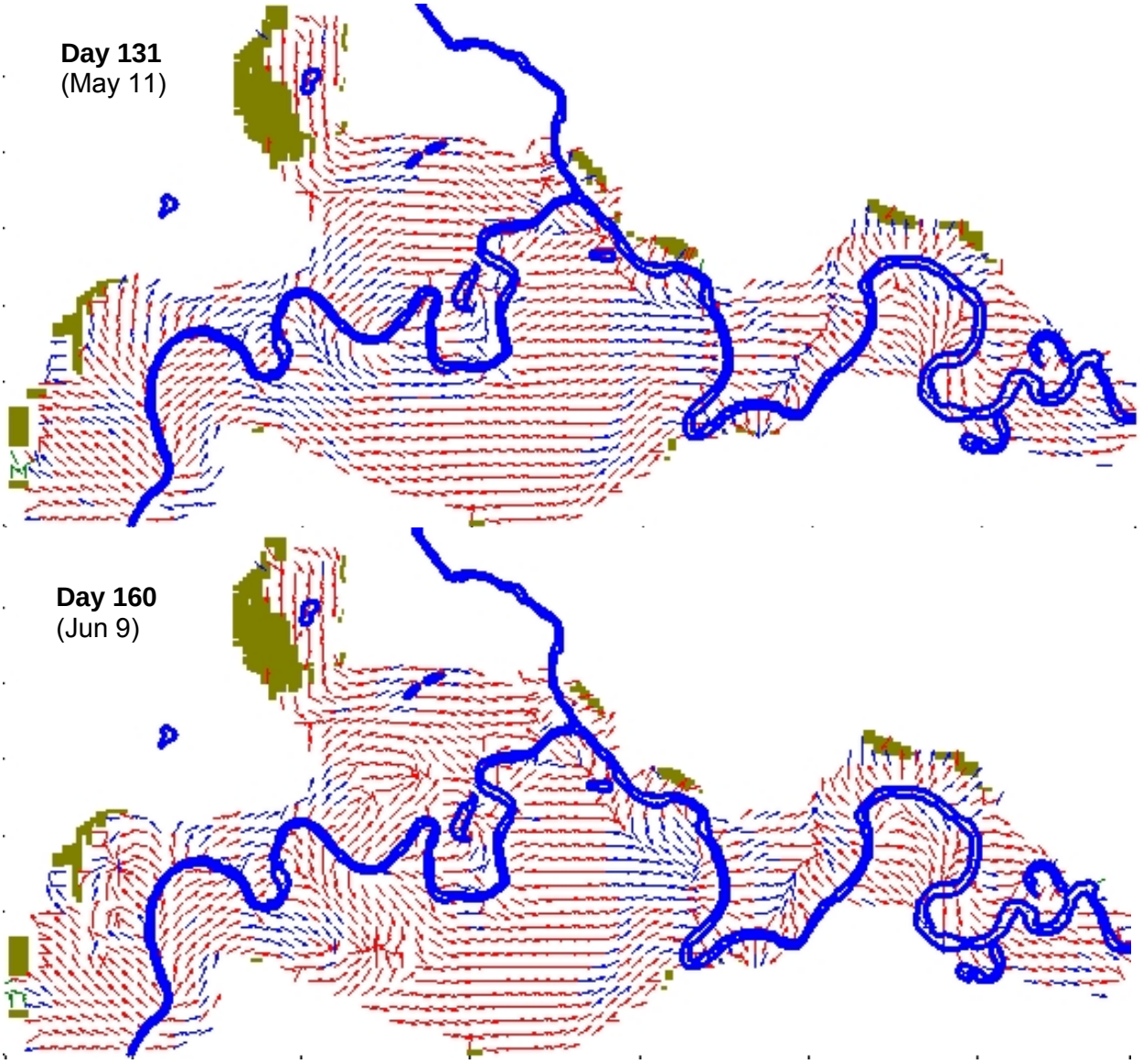

Figure 95 Groundwater flow direction vectors (not scaled to magnitude) in W-E cross-section over most of the Grand Forks aquifer at time step day = 160 in transient model with active pumping (scenario 2A). Arrow colours are for in-plane (red) and out of plane (blue) directions.

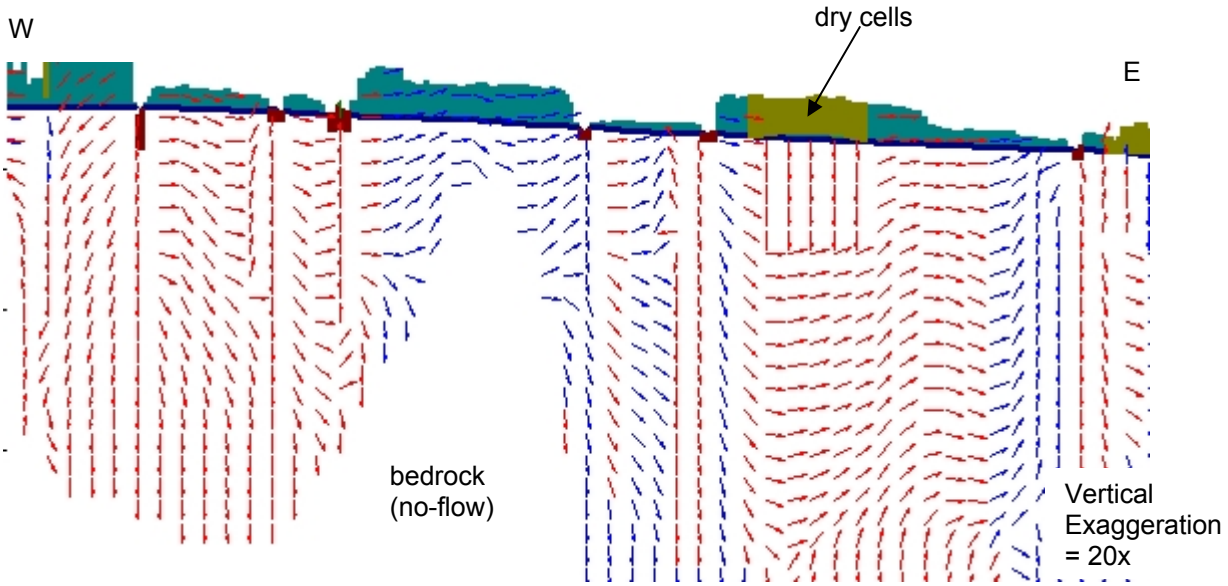

Figure 96 Groundwater flow direction vectors (not scaled to magnitude) in N-S cross-section over most of the Grand Forks aquifer at time step day = 160 in transient model with active pumping (scenario 2A). Arrow colours are for in-plane (red) and out of plane (blue) directions.

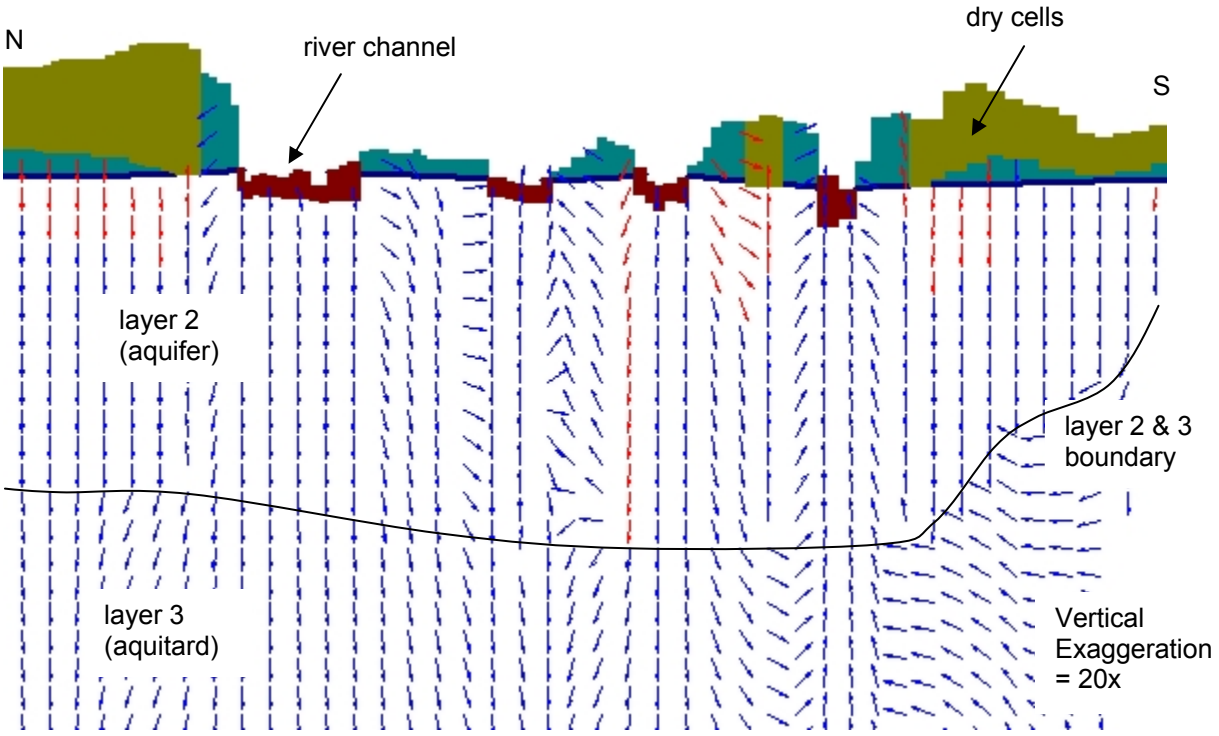

- HYDRAULIC GRADIENTS

Groundwater flow velocities in this unconfined aquifer are controlled by hydraulic gradients. The modelling software Visual MODFLOW computes flow vectors for both direction and magnitude, and the resulting vectors can be displayed with vector arrows scaled to magnitude and oriented in the direction of flow. Flow directions are indicated by arrows of constant length, whereas magnitudes have scaled arrows. There was a problem in displaying the magnitudes of flow for this aquifer because some areas had much higher flow rates near the rivers and near dry cells, than in most of the aquifer area. Therefore, only flow directions were shown and exported from Visual MODFLOW. Flow magnitudes were shown indirectly by estimating the hydraulic gradient at the water table in the surficial aquifer (layer 2 in model).

Flow velocities were difficult to extract from MODFLOW files as these combined all layers and all 3 vector components (xyz) into one large ascii file. Nevertheless, at one time step the horizontal (xy) flow velocities were imported to GIS and converted to a raster image as shown in Map 53. Horizontal flow velocities are typically 0.2 to 0.4 m/day, but near active pumps and along river channels the velocities may reach 0.5 to > 1 m/day.

At shallow depths, the gradient was approximated by calculating the slope of water table in GIS from head distribution maps exported from MODFLOW output of the transient model run. The historical climate model with pumping was used for this purpose. Gradients represent hz/hxy calculated from slope of the water table surface and expressed as % in ArcGIS v 8.13. The maps were reclassified and colour-coded. Two time steps for day 160 and 235 of the transient model (scenario 1A), and one time step (day 160) for the heterogeneous transient model (scenario 4A) are shown in Map 54.

Hydraulic gradient maps correspond very closely with the flow velocity map, validating this visualization approach. The maps show that the highest gradients occur near active pumps, along river channels where there are high terraces above the river and a large change in slope of the groundwater surface, and also in areas near valley walls where the groundwater surface is steep. The central-western portion of aquifer has generally steep hydraulic gradients because the river channel also has steep gradient. This relation is caused by the good hydraulic connection between the river and the surficial aquifer.

The heterogeneous model represents spatially-distributed K and S values for the aquifer, and differs from the "homogeneous" aquifer model in the following aspects: 1) the production wells in the south-central valley, south of the Kettle River, have much smaller gradients due to smaller modelled drawdown in the heterogeneous aquifer, 2) in most areas of the aquifer the hydraulic gradients are smaller, with the exception of a large area in the central valley. Overall the hydraulic gradients are similar in magnitude and spatial distribution for both types of models.

Figure 97 Groundwater flow magnitude vectors in W-E cross-section over most of the Grand Forks aquifer at time step day = 160 in the transient model with active pumping (scenario 1A).

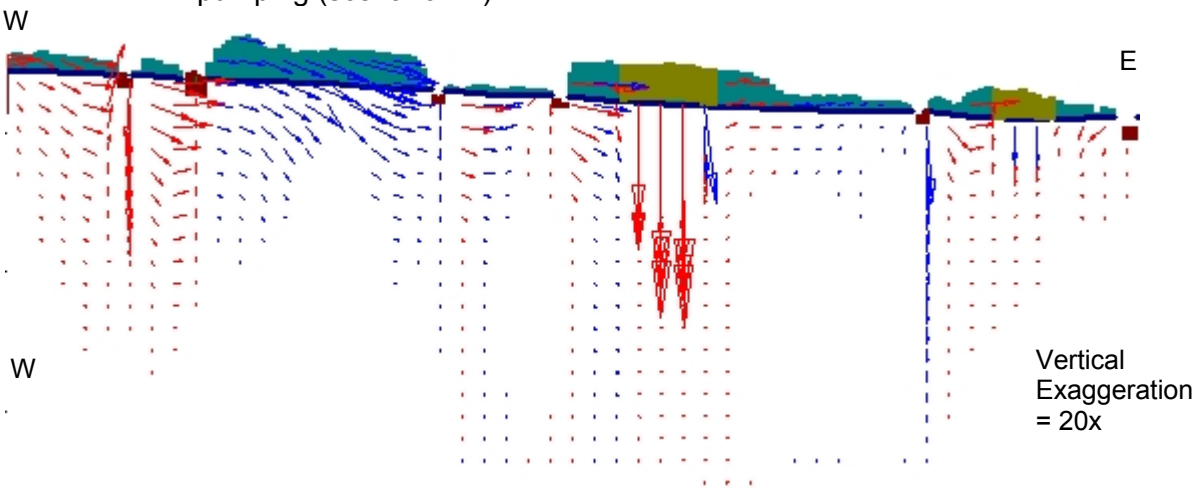

Map 53 Horizontal flow velocities for layer 2 of the unconfined aquifer under pumping conditions for historical climate, at time step 160. Velocities mapped in GIS from MODFLOW output.
Lines on map are areas where MODFLOW output did not convert to a raster image and should be ignored in interpretations. Compare with Map 54.

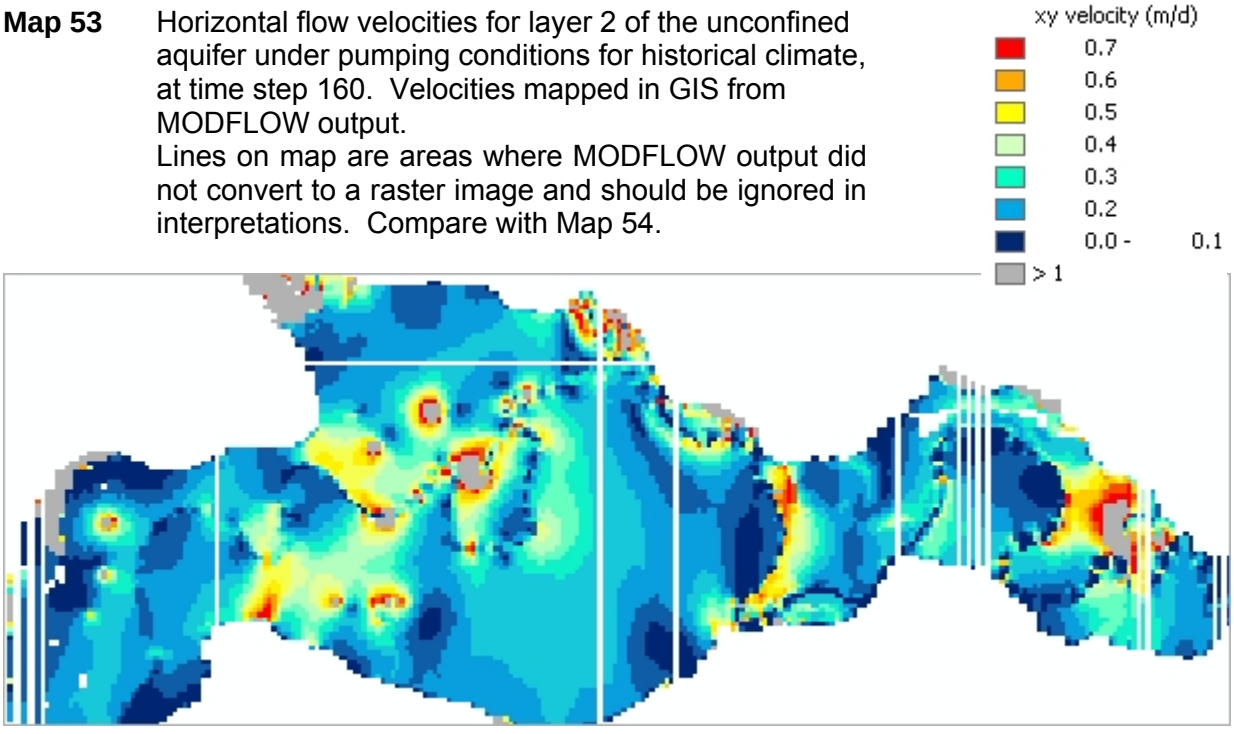

Map 54 Vertical hydraulic gradients (calculated from heads in layer 2 of unconfined aquifer) under pumping conditions for historical climate. Maps by time step in days 160 and 235: (a) homogeneous aquifer model, (b) heterogeneous aquifer model. Gradients were computed in GIS from water table maps and are shown at % values (hz/hxy * 100).
Linear features are residual effects of slope calculation and should be ignored in interpretations (assume the values are smoothly distributed).

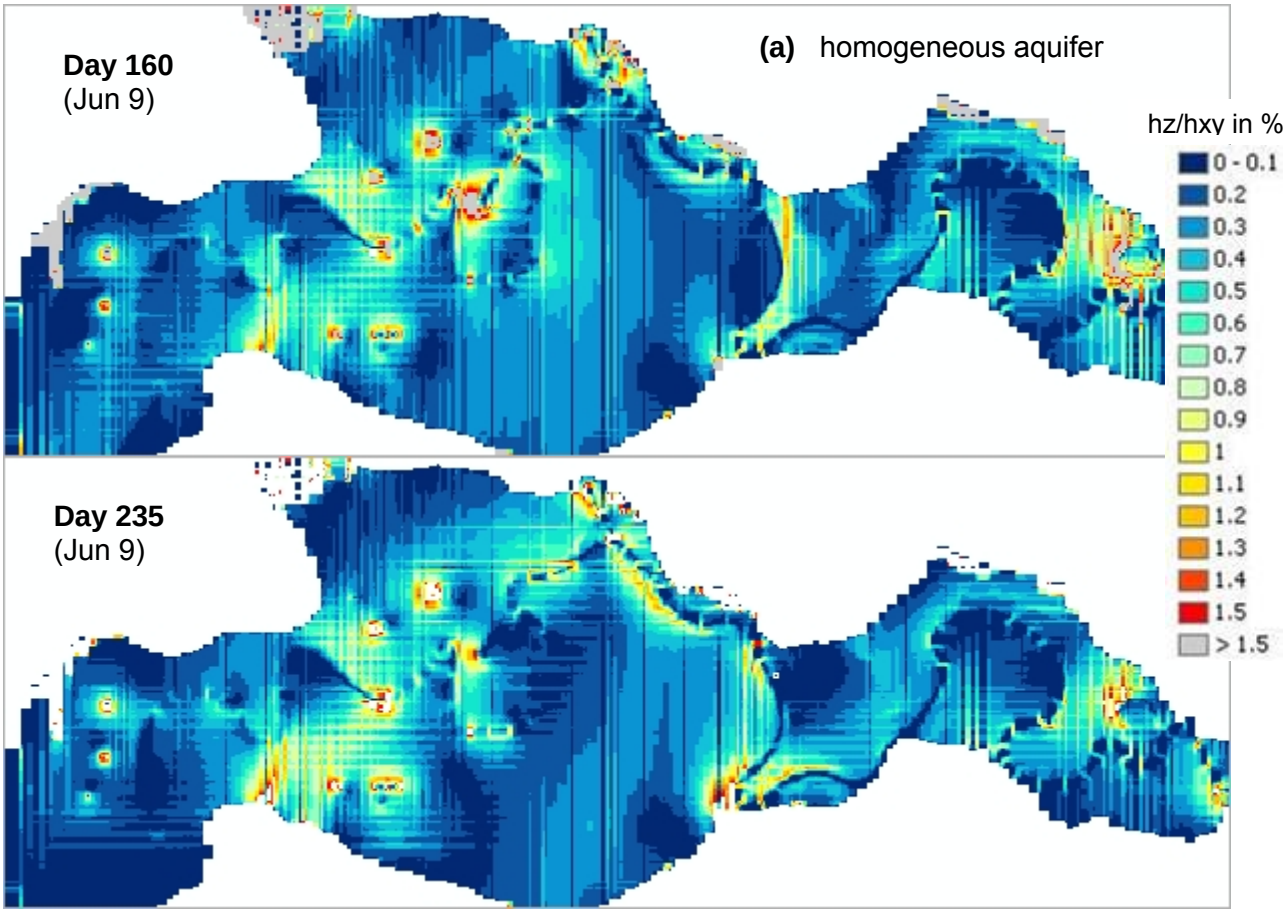

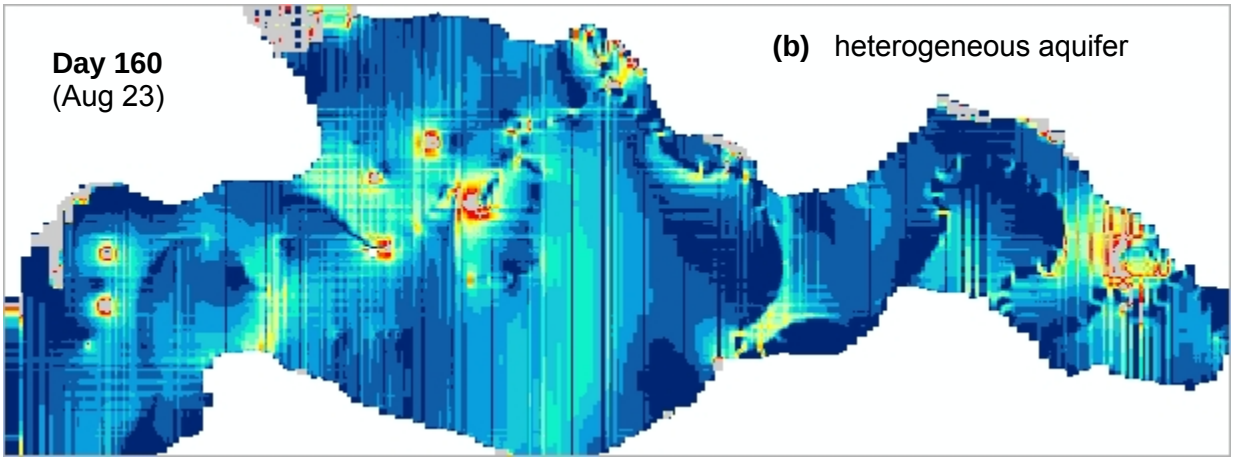

- FLUXES BETWEEN LAYERS

Groundwater flux between model layers was computed by MODFLOW and exported to GIS for mapping. Two time steps were selected: day 160 for pumping conditions at high river stage (see Map 55), and day 265 after stopping of production well pumps and decreasing river stage in the same model (Map 56). The transient model was taken from model scenario 2A (historical climate + pumping). Each map set shows the flux for 3 model layers. The flux represents vertical groundwater flow between model layers. Positive values indicate gain of water to layer cells (flux into layer) and negative values signify loss of water from layer cells (flux out of layer). The units are m/day and maps are colour coded from blue (negative) to red (positive), with white for dry or inactive cells. The positive flux (red) areas along Kettle River in Layer 1 and 2 mean outflow of water from the river into the aquifer (water loosing river reaches). The negative (blue) areas along the river suggest gaining river reaches where aquifer supplies baseflow to river as seepage. The pattern is complex. To isolate the river interactions, the composite of flux in layer 1 and layer 2 (used layer 2 flux when layer 1 had dry cells) were extracted for river channels only and mapped for 2 time steps (day 160 and 265) - see Map 57.

In layer 1, there are high flux values in western and central part of the valley and along river channels. The western part has mostly positive values (aquifer layer 1 is gaining water, mostly from the Kettle River, but also from inter-zonal flow). There is a large area of dry cells in central valley, south of the City of Grand Forks, and to east of that area, a dry cell area the layer 1 is loosing water due to downward flow into layer 2. In eastern valley floodplain the fluxes are near 0, except alternating positive and negative along river channels.

In layer 2, flow activity is also the greatest in western and central valley (southwest of the City of Grand Forks). Layer 2 flux map shows the loosing and gaining river reaches very clearly because the background flux values are much lower than along rivers or pumping wells. Production well pumping can be detected by either positive or negative large flux values in small circular patterns (usually with white dot in the middle for dry cells at maximum drawdown). Most wells pump from layer 2 directly, and cause negative flux values indicated on flux map (outflow from model cells in layer 2).

In layer 3, the flux is much less than in the upper layers of aquifer model. The largest groundwater flows occur near river channels that are along valley walls, and also in western part of valley. The protruding, but buried below ground surface rock outcrop, that separates western and central valley in layer 3 and below, causes increased flux on the downslope or lee side of the outcrop. This can be explained by groundwater traveling downward around the bedrock outcrop as the flow from west to east is interrupted by the outcrop. Pumping effects are very minor in layer 3, except in north-west section where layer 3 has a "sand aquifer" zone of hydraulic conductivity and where a production well is pumping.

During non-pumping conditions (pumps stop at day 242) in day 265 of transient model, the river stage is near baseflow conditions and is still decreasing. The flux patterns are significantly different in all layers than were observed earlier at day 160. In layer 1 there are more negative flux areas indicating outflow from layer 1 (water released from storage). The extent of dry cells is larger, which is expected as water levels decline. More areas in western part of valley have low fluxes than occurred earlier in the year. In layer 2, the flux magnitudes are much smaller too, and in many places the flux directions have been reversed compared to day 160. Pumping effects are absent. In layer 3, groundwater flow is greatly diminished, and in north-west area near Ward Lake the flux is reversed as water is leaving layer 3 and is re-wetting the large drawdown in above layers (and dry cells in layer 1 and 2) that were caused by pumping.

Map 55 Groundwater fluxes between MODFLOW layers in model scenario 2A (historical climate and active pumping) and time step day = 160. Maps by model layer 1 to 3.

Day 160 (Jun 9)

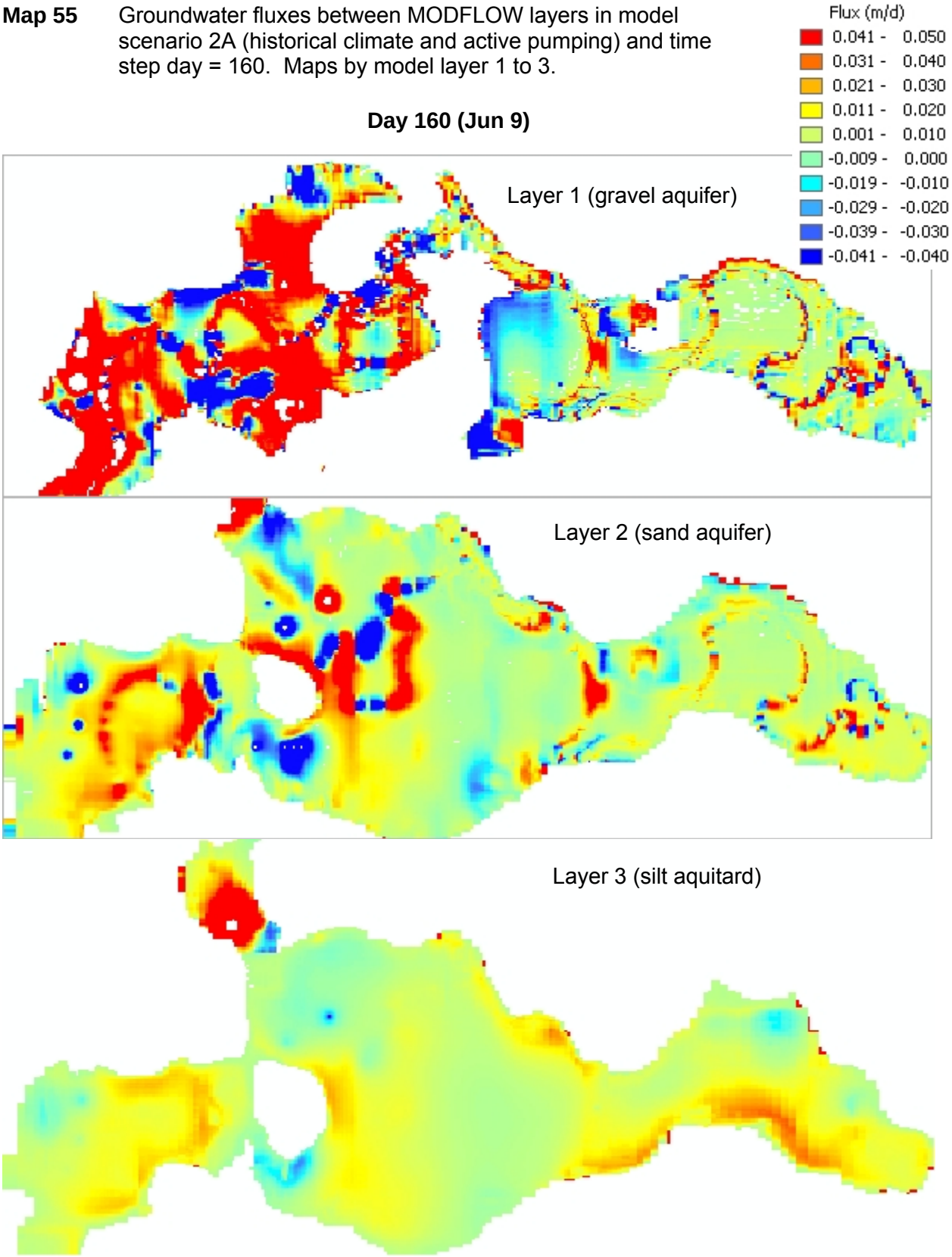

Map 56 Groundwater fluxes between MODFLOW layers in model scenario 2A (historical climate and active pumping) and time step day = 265 (pumping stopped at day = 242). Maps by model layer 1 to 3.

Day 265 (Aug 23)

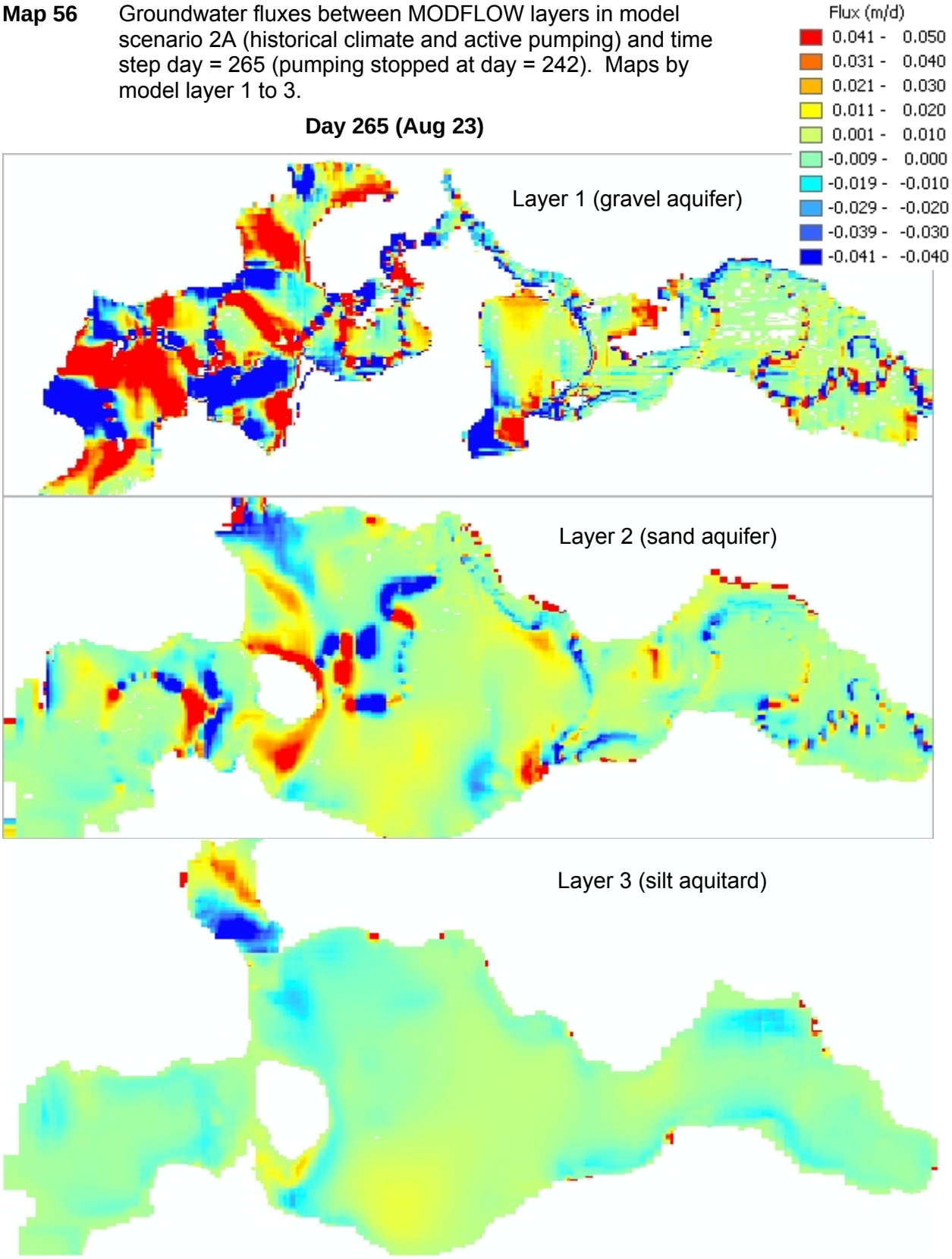

Map 57 Groundwater fluxes between MODFLOW layers along river cells only, showing graining and loosing river reaches. Model scenario 2A (historical climate and active pumping) and time step day = 265 (pumping stopped at day = 242). Maps by model layer 1 to 3.

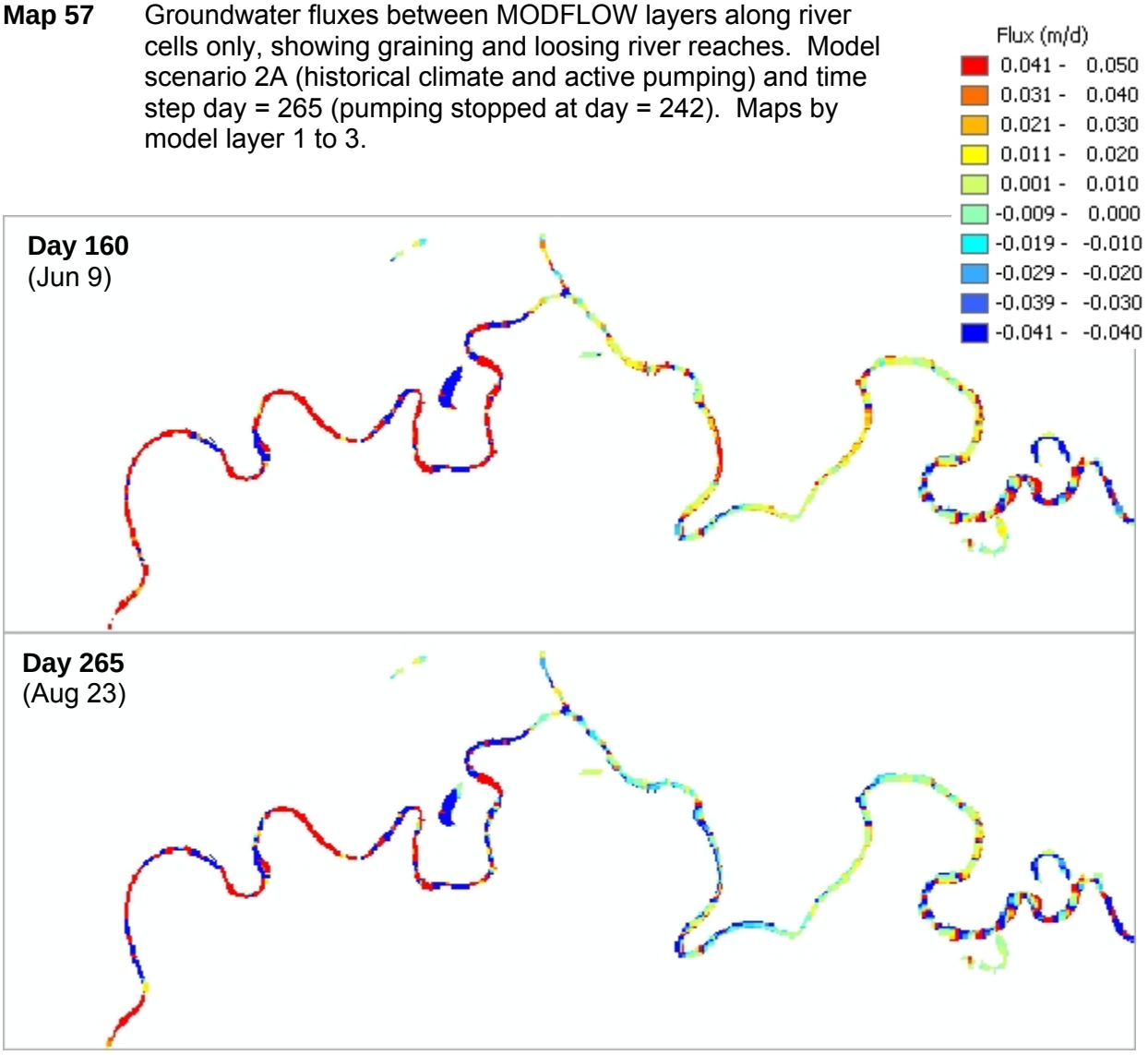

- CELL RE-WETTING

The final map set in this chapter (Map 58) compares the dry cell distributions in layer 1 at low river stage or low groundwater levels in the valley at day 32, and at high river stage and high groundwater levels at day 160. The dry cells are mostly present in layer 1, partly by model design. All river cells and most of the dry unconfined aquifer were designed to be in layer 1 of model to reduce model instabilities during solution. Layer 2 has very few dry cells and these are concentrated on high terraces along valley walls or west of Ward Lake in NW part of valley, where main aquifer layer is layer 3 (with redefined K zone). The cell re-wetting is significant only along river floodplain and it extends 100 to 200 m on each side of Kettle River. Most water levels (heads) were exported from layer 2 to avoid dry cell problems in the representation of results. In the unconfined aquifer the groundwater heads in layer 2 are approximately equal to the heads in saturated areas in layer 1, because layer 1 is relatively thin and saturated zone depth is thin also.

Map 58 Dry cells in Grand Forks aquifer model for layer 1 and 2, at time steps day = 32 and 160. Non-pumping and historical climate conditions.

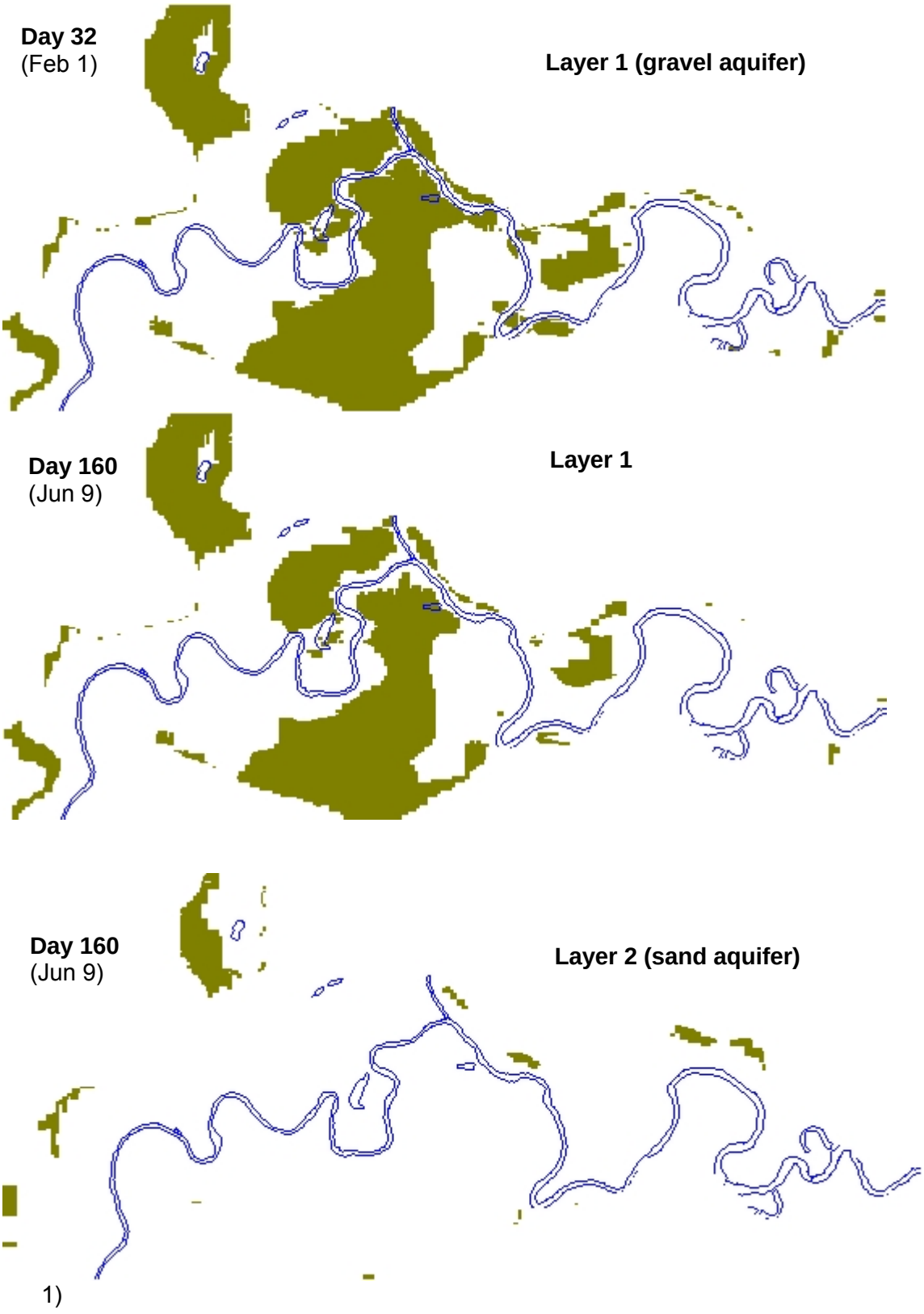

7.2. MASS BALANCE OF MODEL

7.2.1. ZBUD ZONES

Zone Budget (ZBUD) in MODFLOW calculates sub-regional water budgets using results from MODFLOW simulations. ZBUD is documented in detail in Harbaugh (1988). Visual MODFLOW provides a graphical interface for assigning budget zones in model domain, layer by layer. Zones are numbered 1 to 10 in this model as described in Table 32, and the spatial extent of each zone in layer 1 of the model is shown in Map 59.

In the top two aquifer layers, ZBUD (zone budget) areas were delineated for all cells. Zone 1 includes the Grand Forks (GF) irrigation district and other areas outside other irrigation districts (and ZBUD zones). In the five irrigation districts, polygons of irrigated areas (fields) were also used for ZBUD zone delineation, taking into account areas that are irrigated in the large districts. Flow budget zones in these districts only apply to actually irrigated areas, and not whole districts. The river floodplain was given separate zone. It is meant to account for river-aquifer exchanges in the low-lying areas that have head values very similar to river elevations and react very quickly to changes in river water levels.

7.2.2. MASS BALANCE ERRORS

Mass balance is one of the key indicators of a successful simulation. If the mass balance error for a simulation is less than 2% the results may be considered to be acceptable, provided the model is also calibrated (WHI, Visual MODFLOW manual). If error is greater than 2%, then there may be instability in the solution, and thus, inconsistencies in the results. Mass balance error will vary with time in a transient model and with location (e.g., within each ZBUD zone). Since the MODFLOW model is based on flow equations that assume conservation of mass, the discrepancy between IN and OUT flow volumes and rates in model cells can be used to evaluate model performance. Mass flow discrepancy is expressed as percentage of total flow into and out of the entire system as a whole. The listing is organized by source and sink terms, such as constant head (cells) and recharge, which are included both in IN and OUT list of terms.

The magnitude of discrepancy is somewhat related to zone size. The whole of Layer 5 of the model (zone 9 representing the clay layer) has the largest mass balance errors, and often > 2% error at time steps for days 270 to 365. The floodplain zone also has errors near 2% (whether positive or negative) when the river water levels are changing most rapidly, but the mass balance is acceptable (within 2%). All other ZBUD zones for the various irrigation districts have relatively small mass balance discrepancies. In models with heterogeneous aquifer properties, the mass balance errors were larger, particularly for pumping models and during recovery periods, but usually only zone 9 had errors > 2%. Discrepancies for most zones and most time periods were between 0 and 0.2 % (positive or negative).

Table 32 Water budget zones

Zone	Zone Name	Description	Model Layers
1	GF + background	Grand Forks Irrigation district + high terraces and areas away from river that are not assigned to any other budget zone	1 and 2
2	Floodplain	Entire floodplain of Kettle and Granby Rivers, selected within low floodplain elevations as delineated from Floodplain maps	1 and 2
3	Sion 1	Irrigation district "Sion 1" (only irrigated fields)	1 and 2
4	Sion 2 and3	Irrigation districts "Sion 2 and 3" (only irrigated fields)	1 and 2
5	Big Y	Irrigation district "Big Y" (only irrigated fields)	1 and 2
6	Covert	Irrigation district "Covert" (only irrigated fields)	1 and 2
7	Nursery	Irrigation district "Nursery" (only irrigated fields)	1 and 2
8	Silty Layer	Layer of lower hydraulic conductivity than overlying sandy and gravelly layers	3
9	Clayey Layer	Layer interpreted as aquitard and which fills the lower portions of sediments in valley	4
10	Deep sands	Local aquifer zones that either exist instead of clayey layer, or are deep and below the clayey layer	5

Map 59 Water budget zones for ZBUD package in MODFLOW model of Grand Forks aquifer (top layer shown).

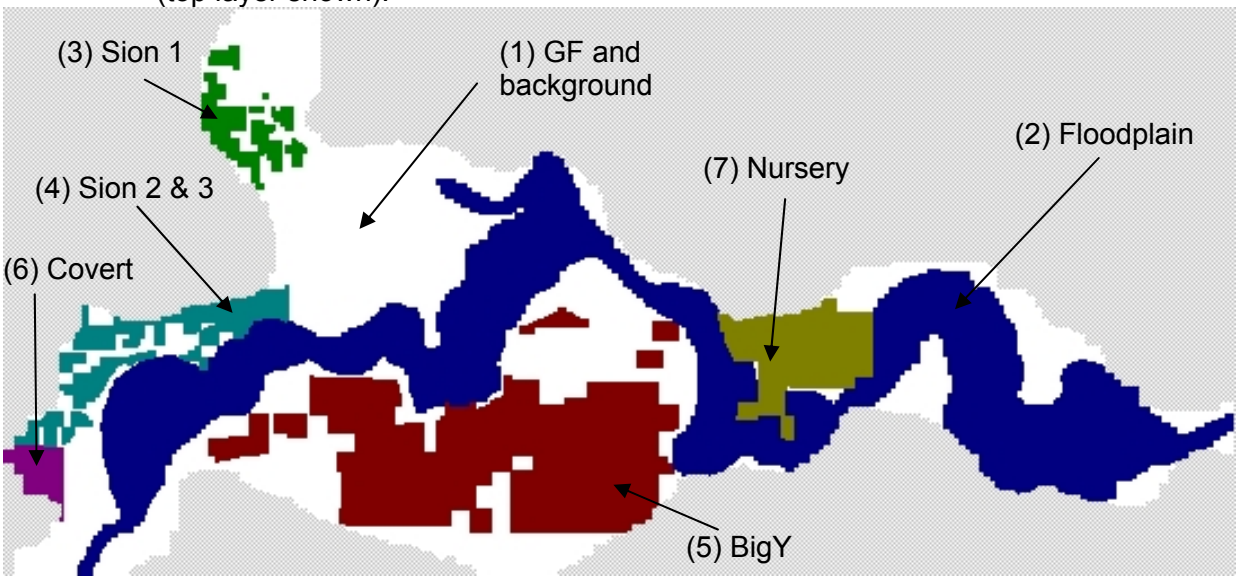

7.2.3. RECHARGE TO ZBUD ZONES

In the Grand Forks aquifer (ZBUD zones) the recharge flow rate was between 1 and 7% of other flow components, such as flow between zones and storage. This section provides graphs for each zone that compare all flow components, including recharge. In this section, recharge is discussed. Appendix C provides graphs of recharge for all zones. All climate change scenarios are compared, both for pumping and non-pumping models (non-pumping are always shown as lines and pumping as symbols only). All graphs have the same symbology, but each zone has different flow volume (y-axis) scale. Irrigation return flow can be observed by differences between pumping and non-pumping recharge for any one climate scenario.

- TRANSIENT RECHARGE TRENDS

In most zones represented in this analysis recharge increases from winter to summer, then remains high until late autumn and decreases toward winter months. Many zones also have bi-modal distribution, with a smaller peak of recharge in late winter, which corresponds to snowmelt in the valley, but then there is a low rate of recharge between day 100 and 150. The peak hydrograph of river stage/discharge also occurs between day 100 and 150, but it's not clear how the decrease in recharge during this time period is related to peak hydrograph (it may be either a computational error in ZBUD or an actual effect).

- RECHARGE AND CLIMATE CHANGE

The predicted future climate for the Grand Forks area from the downscaled CGCM1 model will result in more recharge to the unconfined aquifer from spring to summer seasons. The largest predicted increase is from day 100 to day 150, when it is predicted to increase by factor of 3 or more from present levels, according to ZBUD results from all zones. In the summer months, recharge is also predicted to be approximately 50% greater than at present (in most zones). In the autumn season the recharge is predicted to increase (10 to 25%) or remain the same as present, depending on location in Grand Forks valley. In the winter the CGCM1 weather predictions suggest less precipitation in winter and less recharge to aquifer.

If different models of climate change are used, the groundwater system may react differently, but the goal of this project was to demonstrate the behaviour of this groundwater-hydrologic-climate system and impacts of climate change as indicated by predictive methods available at this time. In this aquifer, the effect of changing recharge on groundwater levels is very small compared to changes in timing of basin-scale snowmelt events in the Kettle River and subsequent shift in hydrograph.

- IRRIGATION RETURN FLOW

Irrigation return flow has very insignificant effect of recharge to GF zone 1 or the floodplain zone 2. Zone 1 is very large and irrigation return flow is relatively small compared to overall recharge (irrigated fields cover small area in this large zone). The silt layer (zone 8), which underlies the surficial aquifer, receives recharge from the overlying units when the overlying model cells are "dry", thus giving direct recharge to next saturated layer – the silt layer. Note that the recharge flow volumes are small for such a large ZBUD zone compared to other flow terms (recharge is 2% of other flow rates, such as flow to/from other zones for this zone). In the late time steps of

the model year, the recharge rates for the pumping model are higher than for non-pumping model, possibly as a result of drawdown in some areas. Drawdown would create more "dry" cells in overlying aquifer layers in MODFLOW model, and redirect more recharge to the silt layer below. Zone 9 (clay aquitard) does not receive any recharge and was not graphed here.

Irrigation return flow begins in after day 150 and is clearly visible in the plots for zones 4, 5 and 7, where recharge increases by 10 to 20% due to irrigation return flow (compare pumping to non-pumping recharge). Return flow is constant for any climate scenario because it was calculated from present irrigation use of groundwater in each district (return flow component does not increase with climate change even if recharge changes). Zone 3 has a strong drawdown effect in late summer and fall as the number of dry cells increases; less recharge is counted in this ZBUD zone because it does not extend to underlying model layer (that recharge goes to the silt layer in zone 8). Clearly this is anomalous result (limited to methodology of ZBUD and counting of various flow components) and not typical of other irrigation districts, and has nothing to do with climate change effects. In zone 6, the irrigation return flow is small relative to calculated recharge. Small return flow would occur if well discharge rates were small compared to irrigation district area.

7.2.4. GROUNDWATER STORAGE AND FLOW BETWEEN ZONES (PUMPING AND NON-PUMPING SCENARIOS – HISTORICAL CLIMATE)

In this section, results are discussed in relation to changes in groundwater storage and flow between zones for both pumping and non-pumping scenarios. Only the historical climate scenario is considered. All graphs are provided in Appendix C. These graphs are in two forms: 1) the sum of flow between all adjacent model cells in the aquifer, and 2) "changes" to the zone, calculated from OUT – IN difference in ZBUD terms. In the case of the second set of graphs, positive values on the y-axis mean net water flow into storage or to other zones (there is always flow in two directions, but OUT > IN is positive on this graph). Negative values mean net water flow out of storage or into this zone from other zones. The graph series are symmetric about the 0 value line and indicate the relation between storage and flow to-and-from this zone, and effects of discharge to pumping wells.

- ZONE 1: GF AND OTHER UPLAND AREAS

The GF and other background zones encompass all areas outside the river floodplain, but exclude the prinmary irrigation districts and areas with irrigation return flow. The most dominant flow components are flows between adjacent zones, mainly from the floodplain, and also from the largest zones (4 and 5). As the Kettle River stage begins to increase (day 90), the flow into Zone 1 increases faster than outflow. This excess water is put into storage. At day 175 this process is reversed as the river stage falls, and for the rest of summer and into autumn water is released from storage in Zone 1 and ends up draining (through other zones) back to the river. When well discharge occurs in the pumping model, more water enters and leaves this zone, as it supplies the other irrigation district ZBUD zones where pumping takes place, except for pumping that occurs in the GF district. Note that more water is taken out of storage in the summer pumping season than in non-pumping model.

During spring freshet in the Kettle River, the rise in river stage causes inflow of water to this zone (after passing through the floodplain area). This excess water is stored in the aquifer. As

river stage drops, the hydraulic gradient is reversed and water is released from storage in this zone and leaves mostly to the floodplain zone as it returns to river as baseflow. Pumping was started as the river stage began to decrease, and most pumping occurred when water was being released from storage. But, during pumping even more water is taken from storage to supply the pumping wells. When pumps are turned off at day 242, there is not much excess water left in storage so almost no net flow occurs out of this zone. As most of the pumping water is lost to evapotranspiration on irrigated fields, there is small reduction in baseflow component to the Kettle River during the pumping period.

- ZONE 2: RIVER FLOODPLAIN

The Floodplain zone lies within the floodplain limits of the Kettle River and Granby River in the Grand Forks valley. It is not surprising that the dominant flow components are between the river and the surficial aquifer in this zone. The "inflow from river" zone budget term follows very closely the river hydrograph during the rise in river stage. As the river stage levels off and begins to decrease, the flow direction is reversed within 10 days, and the "flow into river" term begins to rise and then dominate for the rest of the year, as water previously stored in aquifer drains back to river as baseflow seepage. Storage rates are about 25,000 m^3/day, or less than half of flow rates to/from other zones from the floodplain, and 15 to 20% of flow from/to the river. Even less (up to 15,000 m^3/day or 4 m^3/s) drains out of the aquifer through drains, as defined in this model (large ditches, lakes, swamps, connected to river).

During peak flow on Kettle River, the river discharge is about 200 m^3/s upstream of the Granby River confluence and about 350 m^3/s below the confluence. This is subject to inter-annual variation and represents long-term historical averages. The river-aquifer interaction has maximum flow rate of 150,000 m^3/day or 41 m^3/s, which translates to between 11 and 20 % of river flow during spring freshet (mid value is most likely, or 15%). Therefore, the river puts about 15% of its spring freshet flow into storage in Grand Forks valley aquifer alone, for a short time, and close to 100% of that stored water (minus evapotranspiration loss and long-term storage if any) is eventually released back to river flow. Within 30 to 60 days, about 75% of that stored water is released back into the river flow. The long term storage in this groundwater system can be calculated by comparing the area under storage "from" component to area under storage "to" flow component. As the areas under the graphs are approximately equal, there is no long term storage. Long term storage would result in long-term changes in average static groundwater levels in the valley.

Pumping has a small (but significant) effect on flow budget in the floodplain zone. There are two wells in the Nursery Irrigation district, which are on the boundary of the floodplain zone. The pumping rates from these two wells are insignificant compared to other flow components in this entire zone and were not graphed (would graph very close to 0 m^3/day mark). Pumping in adjacent zones causes a reduction of return flow from other zones (into floodplain) and an increase in outflow from floodplain to other zones. The flow difference graph is a better indicator of pumping effects on groundwater flow balance in floodplain area. The storage is not affected by pumping because pumping discharge occurs in other zones and takes water out of storage there and not in floodplain. During pumping, slightly more water is taken from the river and passed through floodplain zone and less water is returned to river as baseflow. This water eventually flows through the aquifer and replenishes the water taken out of storage for pumping discharge.

- ZONE 3: SION 1 IRRIGATION DISTRICT

The Sion 1 irrigation district was assigned to Zone 3 in ZBUD module of MODFLOW. This area lies on the uplands away from Kettle River and is not influenced by river stage variation. There is a small lake below this zone (Ward Lk.) which was modeled as a drain. This zone is very different from all other ZBUD zones in this model as will be apparent from flow rate graphs versus time.

Under natural conditions (without pumping from wells) the flow from and to this zone are almost balanced, but there is some loss of water from storage to supply this difference, and in the summer most of that water enters the local hydrologic system from recharge. The late winter and spring discrepancy between flow in and out of this zone can be explained by transient model behaviour; it is likely that initial heads in the transient model in that area are too high, and basically there is an excess of stored water in the local aquifer portion near zone 3 that drains to other zones until day 180 of model run, thus creating that difference between in and out terms. In later part of the year, the difference can be explained by draining of recharge water that infiltrates from rainfall.

Pumping wells pump from the deep sand aquifer in this area, which is not part of ZBUD zone 3. However, the ZBUD zone 3 is directly connected to this underlying aquifer and pumping discharge is supplied from storage and from inflow from nearby zones (this zone 3 and other zones). During pumping, there is increased release from storage and subsequent outflow from this zone (vertically down to deep sand aquifer which is being pumped). This behaviour is interesting because it shows the rapid and direct connectivity of aquifer regions and response to pumping (in this case of deep wells).

- ZONE 4: SION 1 AND 2 IRRIGATION DISTRICTS

Zone 4 encompasses many irrigated fields in Sion 2 and 3 irrigation districts, located on terraces above the river floodplain. These terraces are close to the river in horizontal distance, but the high hydraulic gradient upslope from river channel means that only some of that area is influenced by river water level changes. During high river stage, the flow of water through Zone 4 doubles, and about 30% of that water is stored in aquifer in this zone. As river stage drops, water drains from storage and out of the zone back to floodplain area. Pumping causes increased inflow from other zones to replenish the aquifer (drawdown increases hydraulic gradients and flow rates). When the pumps stop, there is still inflow of water into the zone down the hydraulic gradient toward drawdown depressions, and that is temporarily stored, then drained slowly until end of year. When pumping occurs, the water is supplied mostly by flow from other zones and to lesser extent by depletion of storage. The same behaviour was observed for Zone 5 (Big Y irrigation district). Zone 5 is also located on terraces above the floodplain, but is large in area and the flow rates are larger than in zone 4. The rebound of storage after stopping of pumps is also larger.

- ZONE 5: BIG Y IRRIGATION DISTRICT

Zone 5 is the largest irrigation district in terms of irrigated field areas and volume of water pumped from well fields. It covers most of south-central valley, on mostly flat terraces and lowlands. The river is demonstrably hydraulically connected to the surficial aquifer in this zone. During high river stage, the flow of water through Zone 4 increases by 1/3, but only for inflow into this zone. This water is then stored in the aquifer. Without pumping this stored water in spring season is drained slowly (released from storage) by flow out of the zone and back to floodplain and river. Aerial recharge is significant in this zone and accounts for half the water

drained out of the zone (the rest is released from storage), but only from day 160 to end of year. From day 90 to 180 river effects dominate.

During pumping water is immediately lost from storage and also supplied from inflow to the zone. However, outflow from the zone also increases during pumping as water is transferred from parts of zone 5 to other zones that are also pumping. About half of pumped discharge originates from stored aquifer water and half from inflow from other zones. After pumping ceases, the hydraulic gradients toward drawdown areas persist for a month and there is still inflow of water into the zone causing temporary storage. The stored water is then drained slowly until end of year.

- ZONE 6: COVERT IRRIGATION DISTRICT

The smallest ZBUD zone is zone 6 of Covert Irrigation District, located on high terrace in western end of Grand Forks valley. Depth to water table is large (about 20 m) but the groundwater levels are directly connected to nearby Kettle River water levels. From day 120 to 180 the high water levels of river cause large net inflow of water into this zone and storage in aquifer media. After day 180 this stored water is drained through other zones back to the river. Recharge is very small compared to other flow components. Pumped water is taken from storage and supplied from other zones in approximately equal flow rates. After pumping stops, there is very small rebound of storage, but mostly a small flow of water continues draining until end of the year and equals the recharge rate from rainfall. Zones 6 and 5 demonstrate that storage and inter-zonal flow relations are independent of zone size.

- ZONE 7: NURSERY IRRIGATION DISTRICT (PUMPING WELLS ADJACENT TO RIVER)

This irrigation district lies in close proximity to Kettle River, within a large river meander. The irrigated fields are relatively high above the river floodplain, but water table elevation is close to river water levels and is very strongly controlled by river stage variation. The best evidence is that both inflow from floodplain zone (and other zones, but mostly the floodplain) and storage respond almost immediately and identically to changes in the river hydrograph. No other irrigation zone has this strong connection to the river as Zone 7 (Nursery Irrigation District). As the river stage drops near day 180 the stored water is released from storage and flows out of zone 7 and mostly into floodplain zone. Recharge is significant but does not control seasonal flow variation. What is very different in this zone is the response to well pumping. In fact, there is no apparent response at all because the two production wells are located adjacent to Kettle River and pump almost directly from the river. Therefore, well discharge in or near the river floodplain takes groundwater almost directly from the river through very fast hydraulic connection between the gravel bed of the river channel and the surficial aquifer from which well pump water.

- ZONE 8: SILT MODEL LAYER UNDERLYING ALL SURFICIAL AQUIFER LAYERS AND IRRIGATION ZONES

In the silt zone (layer 3 of model), the flow rates are relatively large in this very large volume of modeled valley sediments. Inter-zonal flow shows river effects (stage variation), but storage is also very important (flow rates to/from storage are 30 to 50% of inter-zonal flow rates). Transient flow trends and relations are similar to those at other ZBUD zones.

- ZONE 9: CLAY LAYER (AQUITARD AT VALLEY BOTTOM)

The clay aquitard layer has smaller flow rates through it than the overlying silt layer, but flow still occurs according to the groundwater flow model. There is also a hydraulic connection to river water levels, but unlike in all other zones of surficial aquifer, the aquitard zone supplies all inter-zonal flow from storage. All water incoming to zone 9 goes into storage in zone 9. All water flowing out of zone 9 is taken out of storage from zone 9. The total flow volume involved seems large, but this is a function of total volume of this zone, which is very large (most of valley sediments). Flow volume per unit volume of aquifer/aquitard will be much smaller in this zone than in all other zones, due to differences in hydraulic conductivity and storativity.

7.2.5. GROUNDWATER STORAGE AND FLOW BETWEEN ZONES (PUMPING AND NON-PUMPING SCENARIOS – MODEL PREDICTIONS IN FUTURE CLIMATE SCENARIOS)

The impacts of climate change on groundwater flow were represented as time series graphs of change in storage (flow rate) and change in inter-zonal flow rate, for both non-pumping and pumping models, for all 4 climate scenarios (Appendix C). Each ZBUD zone has 2 figures and 4 graphs. With different climate inputs to the model, through control of river hydrograph and aerial recharge from precipitation, the temporal trends of flow rates shift to different days of the year and also change peak values slightly. There are also some "random" changes between each climate scenario, which have to do with local effects of groundwater flow within each zone.

In all zones there is an inverse relation between net storage flow rate and net inter-zonal flow. Several zones show similar responses to climate change scenarios modeled here. As the climate impacts are mainly driven by river stage (and its shifts to earlier date), any ZBUD zone that has strong hydraulic connection to the river, and which shows temporal variation of flow rates driven by changes in river hydrograph, will have the largest climate-driven changes. As the river peak flow shifts to an earlier date in any year, the “hydrographs” for flow rates also shift by the same interval. These shifted flow rates are superimposed on pumping effects, which were not shifted in time for future climates.

The smallest climate change effect is found in Zone 3. This zone is not hydraulically connected to Kettle River. Therefore, the only climatic changes are those to recharge. Those changes in flow rates for storage and inter-zonal flow are very small (<5% difference for any time of year) between historical climate and future predicted climates.

7.2.6. EFFECT OF AQUIFER HETEROGENEITY ON GROUNDWATER STORAGE AND FLOW BETWEEN ZONES (PUMPING AND NON-PUMPING SCENARIOS AND CHANGES WITH CLIMATE)

In this section we discuss the sensitivity of groundwater flow model results (ZBUD flow rates by zone) to method of representation of aquifer heterogeneity. In the layered MODFLOW model, the top two layers form the surficial aquifer, whereas the bottom layers are silt and clay aquitards (except deep sand aquifers in the bottom layer). The "homogeneous" aquifer model has the same MODFLOW layers as the "heterogeneous" aquifer model. In heterogeneous representation the hydraulic conductivity and specific yield are spatially distributed within each of the top two layers (as described previously). This contrasts to one hydraulic conductivity value and one specific yield value assigned per layer in "homogeneous" approach, which was the default model type in this project.

The same climate and pumping scenarios were input into models with heterogeneous aquifer representation, and ZBUD results were subtracted between scenario series 4 models (A to C for climate change scenarios) representing heterogeneous aquifer and scenario series 2 models (also A to C for climate scenarios). Only pumping models were used because these are the most realistic, and pumping drawdown is sensitive to aquifer heterogeneity distributions. Both net change in storage flow rate (OUT – IN) within each zone and the net inter-zonal flow rates (OUT – IN) were graphed. Thus, there two graphs in one figure per ZBUD zone. These graphs are shown in Appendix C. The graphs show only effect of heterogeneity (all other temporal and climatic trends are subtracted). It does not mean that the "difference" between homogeneous and heterogeneous models are the same for all climate scenarios (they aren't). The graphs were also kept at the same xy scales as the flow rate change graphs in previous sections to allow visual inspection and comparing of relative importance of heterogeneity on the groundwater system flow components.

The various ZBUD zones have different sensitivity to aquifer heterogeneity representation in the model, in terms of flow to storage and inter-zonal flow. Magnitudes of changes differ because zones have different sizes (volumes of aquifer media), but also there is a different change in groundwater flow if heterogeneity is considered – by definition, heterogeneity varies over the aquifer area so different effects are expected for various zones of aquifer. The vertical scales of the graphs are similar to those for the homogeneous aquifer model net change in storage and inter-zonal flow rates for corresponding zones. Therefore, if graphed "differences" resulting from aquifer heterogeneity plot near the 0 line, the changes are relatively small compared to natural variation modelled in the models, but if the plotted lines fill the graph area, the effect is as large as the original variation in flow rates. In latter case, it would mean doubling flow rates as a result of increases heterogeneity (usually increased hydraulic conductivity within a zone).

- EFFECTS OF HETEROGENEITY IN ZONE 1 AND 2 (GF + BACKGROUND AND FLOODPLAIN)

In Zone 1 (GF Irrigation District + background) there were significant differences attributed to heterogeneous aquifer representation. More flow occurred in spring time (both into storage and out of the zone). This increase of flow was between 5 and 10 x 1000 m^3/day, as compared to maximum net change flow rates (storage or inter-zonal) of about 50 x 1000 m^3/day. Over most of the year, the % differences were less than 50% (except on days when flow rate trends shifted in time and created large % differences – these are temporal changes rather than absolute changes – we see spikes in % differences values).

In floodplain zone 2, storage was not affected significantly by heterogeneity of the aquifer, but inter-zonal flow was very different and very much larger than in the homogeneous model. In the spatially-distributed Kxy-field the surficial aquifer is much better hydraulically connected to the river and much more flow occurs between the floodplain (and river) and other zones of aquifer. The flow rates for inter-zonal flow increase by 30,000 m^3/day (or 50 to 75%) as a result of including aquifer heterogeneity. The river-effects reach further and are stronger away from the river floodplain. Therefore, climate change impacts are larger under heterogeneous model than in homogeneous model.

- EFFECTS OF HETEROGENEITY IN ZONES 2 TO 9

In zone 3 (Sion 1 irrigation district), flow rates were greater in winter and spring than for zone 4 (Sion 2 & 3 irrigation district), for example. The flow rates were 50 to 75% greater in late spring and summer as a result of including aquifer heterogeneity in the climate scenario models, but during pumping discharge the heterogeneous aquifer provided more water from storage and more water inflowing from adjacent zones for pumping, and less drawdown would be expected than in homogeneous model.

A large effect of aquifer heterogeneity is predicted for south-central Grand Forks valley, where Zone 5 (Big Y irrigation district) is located. The pump tests in production wells in this district have large hydraulic conductivity estimates and interpolating these over space greatly increases flow rates in the aquifer, compared to lower values assigned to the aquifer layers in homogeneous models. The drawdown is expected to be much smaller and closer to observed in heterogeneous aquifer scenarios than in the original model scenarios. The difference in flow rates in spring time (high flow on Kettle River) are of the same magnitude as modelled in scenario series 2, so the heterogeneous scenario series 4 would have double the flow rates, with some differences between climate scenarios - but the same magnitudes of heterogeneity effect on flow. Much more water would be stored and much more water would flow to and from other zones through this area of aquifer. The hydraulic connection to Kettle River would be much greater, and larger impacts of climate change (shifts of river hydrograph) are expected in the heterogeneous model.

Zones 6, 8, and 9 have small to moderate differences between heterogeneous and homogeneous aquifer models, but not nearly as large as in zone 5. Overall, the flow rates would increase.

Zone 7 (Nursery irrigation district) is also proximal to Kettle River and increased hydraulic conductivity as interpolated from pump test data in heterogeneous model would cause larger flow rates and better connection with the river. The effect would be larger than in zones 6, 8 and 9 but less than in zone 5.

It can be concluded that including aquifer heterogeneity in this model creates better connections between most zones and with the river, creates higher flow rates, less drawdown due to pumping, and causes larger responses to river hydrograph changes as a result of predicted climate changes. These results will be confirmed by spatial maps of head differences between heterogeneous and other model outputs from transient MODFLOW model runs of the aquifer model).

7.2.7. EFFECT OF RECHARGE DISTRIBUTION AND TEMPORAL VARIATION ON GROUNDWATER STORAGE AND FLOW BETWEEN ZONES (NON-PUMPING SCENARIOS AND CHANGES WITH CLIMATE)

In this section we discuss the sensitivity of groundwater flow model results (ZBUD flow rates by zone) to method of representation of recharge, and in particular to spatial and temporal distribution of recharge. Two sensitivity scenarios were run: 5A and 5B. The 5A scenario has mean annual recharge as the recharge input and the values are spatially distributed among the recharge zones (there is spatial variation in mean annual recharge). The 5B scenario has temporally variable recharge rates, but there is uniform spatial distribution (one recharge zone).

Only non-pumping historical climate scenarios were used to test sensitivity of model results to recharge distribution. Both net change in storage flow rate (OUT – IN) within each zone and the net inter-zonal flow rates (OUT – IN) were graphed. Thus, there two graphs in one figure per ZBUD zone. These graphs are provided in Appendix C. The graphs show only effect of recharge distribution (all other temporal and climatic trends are subtracted). It does not mean that the "difference" between the distributed recharge in model 1A and either 5A or 5B models are the same for all climate scenarios (they aren't).

The various ZBUD zones have different sensitivity to recharge representation in the model, in terms of flow to storage and inter-zonal flow. Magnitudes of changes differ because zones have different sizes (volumes of aquifer media), but also there is a different change in groundwater flow under the two recharge schemes. The vertical scales of graphs are similar to those for scenario 1A with spatially and temporally variable recharge, for net change in storage and inter-zonal flow rates for corresponding zones. Therefore, if graphed "differences" resulting from recharge distribution plot near the 0 line, the changes are relatively small compared to natural variation modeled in the 1A scenario, but if the plotted lines fill the graph area, the effect is as large as the original variation in flow rates.

There are ZBUD zones where the spatial distribution of recharge has the same (and small) control on flow rates into storage as the temporal distribution of recharge; these zones are 1, 2, 4, and 8 and 9. Storage flow rates show some significant response to recharge in zones 3, 5, 7. The spatial distribution of recharge has consistently greater control on flow rates than temporal distribution of recharge (monthly variation versus mean annual value).

7.3. WATER LEVELS AND CHANGES WITH CLIMATE

7.3.1. METHODOLOGY FOR HEAD DIFFERENCE MAPS

The effects of climate change are difficult to observe on head distribution maps because the high hydraulic gradient in the Grand Forks valley dominates all other trends. The climate-induced changes in water elevations are on the order of 0.5 m, while the gradient in the valley spans about 30 m elevation, so any changes would just shift the water table contours slightly and would be difficult to read. Thus, it was necessary to develop a different strategy for displaying any changes induced by climate, which would exclude the hydraulic gradient of the valley (and valley topography) and compare directly changes from present conditions. Accordingly, head difference maps were prepared to show only differences due to climate change between future climate scenario model outputs and present climate scenario model outputs, separately for pumping and non-pumping models. The pumping effects were also subtracted out in these maps because drawdown was identical in all climate scenarios (pumping rates were constant in all models for the pumping time period).

In Visual MODFLOW, heads in layer 2 were exported at 10 different stress-periods, at the following Julian Days of model output: 101, 131, 160, 170, 180, 190, 205, 245, 265, 305. Heads were saved as ASCII files (default export format in Visual MODFLOW). These contain X,Y coordinates for cell and Head value. Points of intersection of cell boundaries (row and column breaks) were read from the MODFLOW grid file, and coordinate points calculated for each rectangular MODFLOW cell in Layer 2 (and other layers where heads were read). These were converted to .dbf file and imported into ArcGIS, and converted to polygons. Polygons were mapped using spatial-join operations to mid-cell coordinates of MODFLOW output for heads, and a link was established for mapping head values over space. Code was written to import head files and compute differences in head for all cells per layer between future climate scenario output and historical climate. The polygons of cells, via table join operation of head difference outputs at mid-cell points, were converted to 25 m raster grids for display and further analyses. Contours of head differences were generated from raster maps.

The GIS environment provides better integration with all other spatial data than Visual MODFLOW, and there is much more control of mapping of MODFLOW results. GIS grids, polygons and contour lines in shapefile format are also better for data interchange for other purposes for users that do not have Visual MODFLOW access, and present a ready result format rather than xyz data tables of MODFLOW exports.

Each map shows the difference in hydraulic head between a future climate scenario and a present climate scenario, all under pumping conditions. Positive contours are shown at 0.1 m interval. The zero contour is dashed line. Negative contours not shown. The darkest blue colours indicate values < -0.5 m (along rivers only). At day 101, difference map (not shown) has values within 0.1 m of zero.

Each climate scenario is illustrated with 6 maps for six model time steps, starting from day 131 when the river hydrograph is near peak flow (and peak stage), and ending on day 305 when river water levels have almost returned to baseflow conditions of late fall and winter. The maps are grouped into two "Map" captions (to fit into report format), each with 3 time-snapshot maps of differences in groundwater levels.

7.3.2. CHANGES IN WATER ELEVATIONS DUE TO CLIMATE CHANGE (PUMPING AND NON-PUMPING MODELS)

- 2010-2039 CLIMATE SCENARIO (DIFFERENCE FROM PRESENT)

For the 2010-2039 climate scenario, the results of transient model simulations are plotted in Map 60and Map 61. At day 131 the water levels are higher along the floodplain than at the same day in 1961-1999 historical climate scenario. The main cause is a shift in river hydrograph peak flow to earlier date, thus creating positive difference in water levels between the 2010-2039 and 1961-1999 models at day 131. In other words, in future the peak river stage would be earlier and water levels would be higher in floodplain at an earlier date (also in day 131). This excess water flows into surficial aquifer and is stored there, as was demonstrated in flow budget section of this report. The zone of storage is roughly along river floodplain and also in areas where there are higher river terraces. Within a month the peak flow passes and river water levels begin to drop rapidly. By day 160, the river water levels are similar in both 2010 and historical climate models, but only along the river channel. Away from the river channel water levels are elevated by 30 to 40 cm (stored water) which continue to drain until day 180. Away from the river, the water levels are still very similar (within 10 cm) to present day water levels at that time of year. By day 180, the river stage has dropped below typical river stage at present climate (again, due to the shift in hydrograph), and the water levels in floodplain in 2010 climate are lower by 10 to 40 cm at day 180 than at present climate at that day.

At day 205, the 2010 river water level is still 10 to 20 cm below present at that day, but the increased recharge in 2010 climate over historical climate causes up to 10 cm higher water levels away from the river. This spatial pattern of slightly elevated water levels away from the floodplain relative to present climate continues to day 235 (Aug 23), but by day 305 (Nov 1) the water levels in unconfined aquifer are almost identical to present levels at that time of year. Overall, the climate change effects for 2010-2039 scenario relative to present are limited to floodplain and to early part of the year when river hydrograph shifts and is at peak flow levels, but small increase of water levels due to increase in recharge forecast for 2010 climate.

- 2040-2069 CLIMATE SCENARIO (DIFFERENCE FROM PRESENT)

For the 2040-2069 climate scenario, the results of transient model simulations are plotted in Map 62 and Map 63. At day 131 the water levels are higher along the floodplain than at the same day in 1961-1999 historical climate scenario. The main cause is a shift in river hydrograph peak flow to an earlier date, thus creating positive difference in water levels between the 2040-2069 and 1961-1999 models at day 131. The hydrograph shift is larger than in the 2010-2039 climate scenario, so the computed differences to historical climate are also larger. Water levels are over 50 cm above normal, but only along the floodplain. The term "above normal" means "occurring earlier in year," but the maximum water levels associated with the peak hydrograph are very similar to present climate because the peak discharge is not predicted to change, only the timing of it. This excess water flows into surficial aquifer and is stored there, as was demonstrated in flow budget section of this report. The zone of storage is roughly along river floodplain and also in areas where there are higher river terraces. Within a month the peak flow passes and river water levels begin to drop rapidly.

By day 160, the peak flow in river has passed and subsided at an earlier time than at present conditions, and there are > 50 cm lower water levels in floodplain close to the river channel at day 160. But, outside the floodplain the water levels remain elevated above normal for that time

of year. The stored water accounts for the 20 to 40 cm elevated water levels just outside the floodplain (see orange-red areas on map). This stored water drains within 1 month back to the river. By day 180 the shift in river hydrograph in this climate scenario results in lower (> 50 cm) than at present water levels in floodplain (not entire floodplain) and still slightly higher water levels (10 to 20 cm) in other areas.

At day 205, the 2040 river water level is still 20 to 50 cm below present at that day, but the increased recharge in 2040 climate over historical climate causes up to 10 cm higher water levels away from the river. This spatial pattern of slightly elevated water levels away from the floodplain relative to present climate continues to the end of year (longer than in 2010-2039 scenario). Overall, the climate change effects for 2040-2069 scenario relative to present are limited to floodplain and to early part of the year when river hydrograph shifts and is at peak flow levels, but a small increase of water levels due to increase in recharge forecast for 2040 climate.

7.3.3. EFFECT OF PUMPING ON WATER ELEVATIONS AT DIFFERENT CLIMATE SCENARIOS

Pumping effect was calculated by subtracting pumping model output (head maps) in layer 2 of the sand aquifer, from non-pumping model outputs, for each time step. There were only few isolated cells where cells were dry in one model but not another, and therefore, head values near dry cells were different – these “errors” are related to numerical solution differences, which had to do with cell re-wetting, which may have differed slightly between the pumping and non-pumping scenarios, all other solver parameters being equal. In 99.99% of model cells, the head change due to pumping was equal in all climate scenarios

Head differences for pumping – nonpumping maps were calculated using raster algebra in GIS system. These values are essentially drawdown values because both model series (pumping and non-pumping) are identical to day 142 prior to pumping. Two sets of maps are shown in Map 64 for times 131 to 205, and Map 65 for times 235 to 365. Colour scale is used only as an indicator of drawdown areas, and 0.5 m contours are used to show magnitude of drawdown. Maximum drawdown in this model varied between 3 and 8 m depending on well location. It should be noted that actual pumping effects are probably different than in the “calibrated layer” model, because hydraulic conductivity near each well is different and has spatial distribution. The heterogeneous model series will show other possible drawdown maps for this aquifer. Nevertheless, the pumping effect is independent of climate scenario, and will vary with pumping rates and aquifer properties near the wells. These maps show the extent of pumping effects and their temporal variability in this aquifer.

Since the drawdown due to pumping for present climate is practically identical to drawdown in future climate scenarios, the difference maps subtract the pumping effect out and drawdown is not apparent in these maps. There are separate maps showing only the effect due to pumping (essentially drawdown maps – computed by subtracting nonpumping modelled heads from pumping modelled heads for any given climate scenario and time step). All climate scenarios had identical drawdown effect (at a given K distribution), so only one set of drawdown maps is shown for present climate scenario. In conclusion, the pumping effect, as in drawdown, is identical for a given time step (day) in all climate scenarios. This is expected, because the pumps pump identical amounts of water.

Map 60 Water level differences (measured as head in layer 2 of unconfined aquifer) between future and present climate (2010-2039, scenario 2B) under pumping conditions. Maps by time step in days 131 to 180.
Positive contours shown at 0.1 m interval. Zero contour is dashed line. Negative contours not shown. Darkest blue colours indicate values < -0.5 m (along rivers only). At day 101, difference map (not shown) has values within 0.1 m of zero. Compare with Map 68 for effects of aquifer heterogeneity on this prediction.

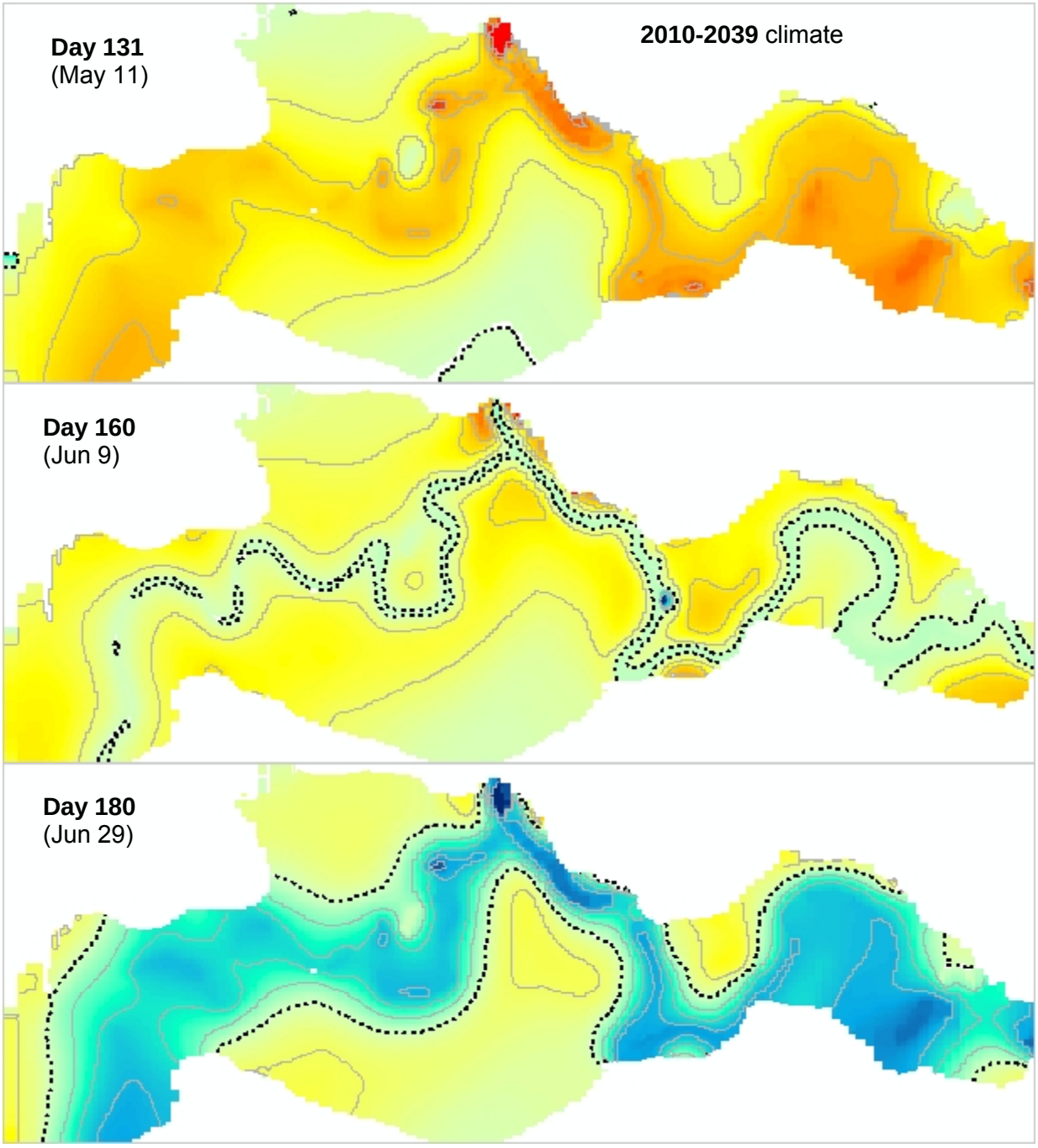

Map 61 Water level differences (measured as head in layer 2 of unconfined aquifer) between future and present climate (2010-2039, scenario 2B) under pumping conditions. Maps by time step in days 205 to 305.
All contours at 0.1 m interval. Zero contour is dashed line. Compare with Map 69 for effects of aquifer heterogeneity on this prediction.

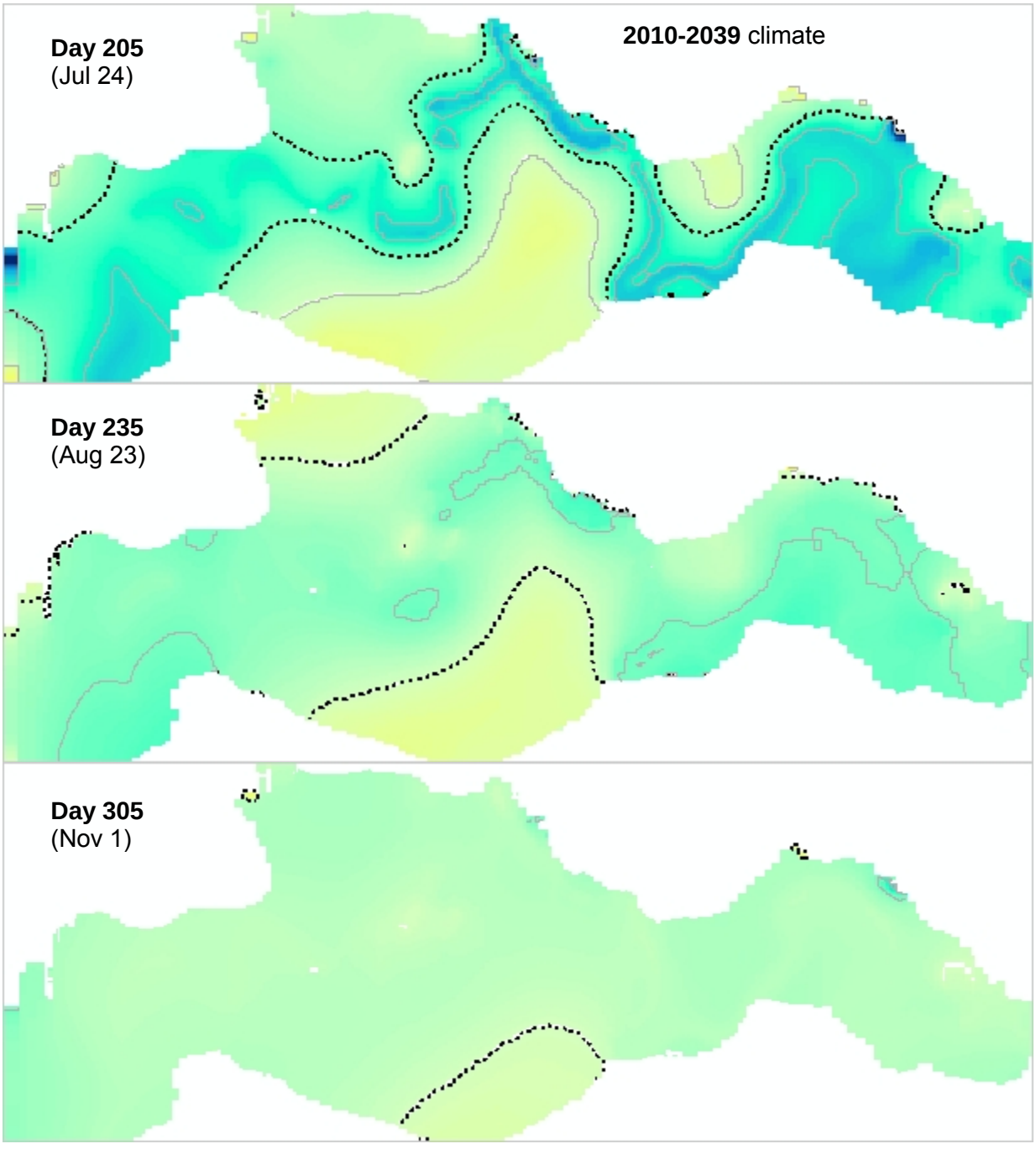

Map 62 Water level differences (measured as head in layer 2 of unconfined aquifer) between future and present climate (2040-2069, scenario 2C) under pumping conditions. Maps by time step in days 131 to 180.
Positive contours shown at 0.1 m interval. Zero contour is dashed line. Negative contours not shown. Darkest blue colours indicate values < -0.5 m (along rivers only). At day 101, difference map (not shown) has values within 0.1 m of zero.

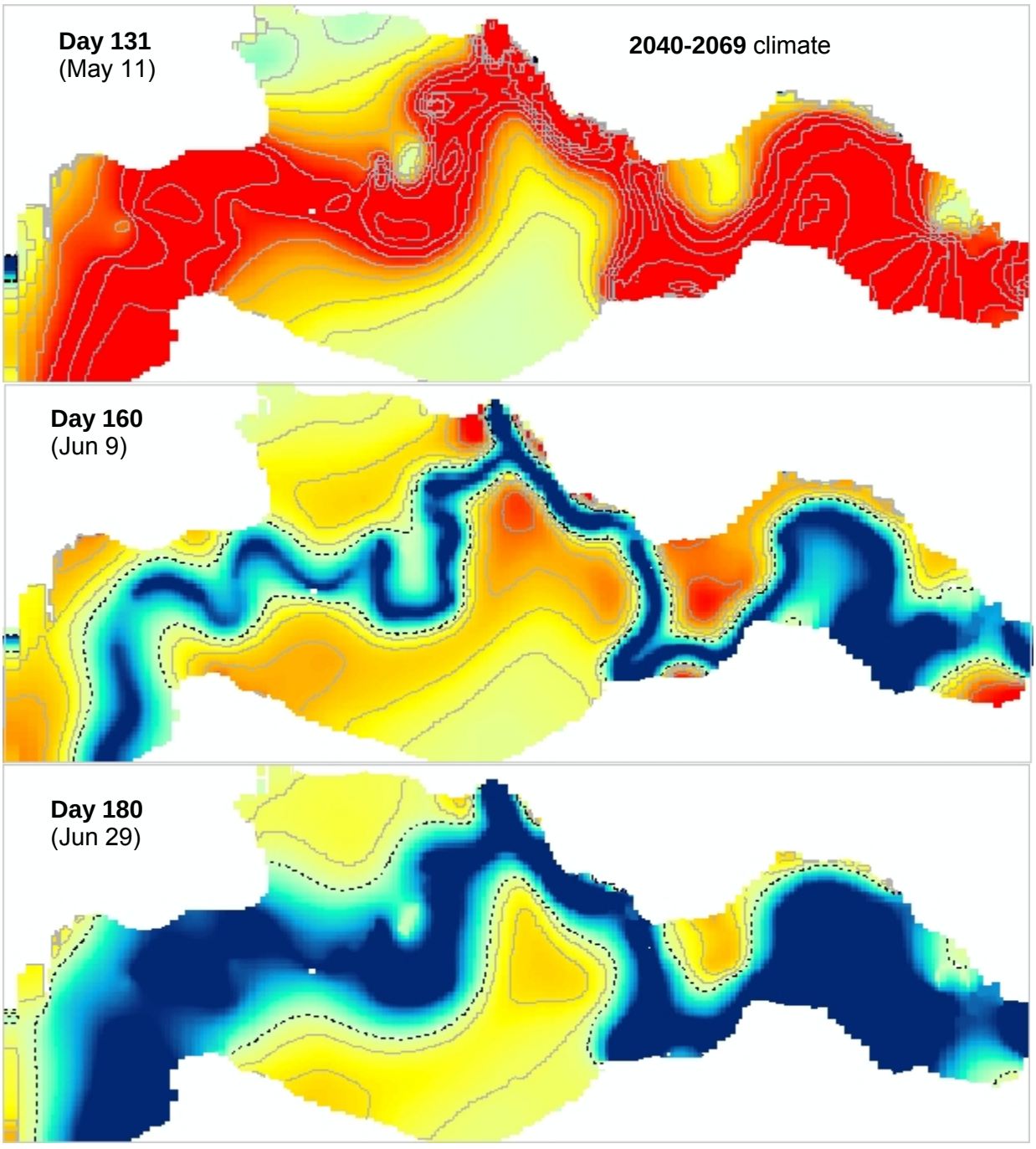

Map 63 Water level differences (measured as head in layer 2 of unconfined aquifer) between future and present climate (2040-2069, scen 2C) under pumping conditions. Maps by time step in days 205 to 305.
All contours at 0.1 m interval. Zero contour is dashed line.

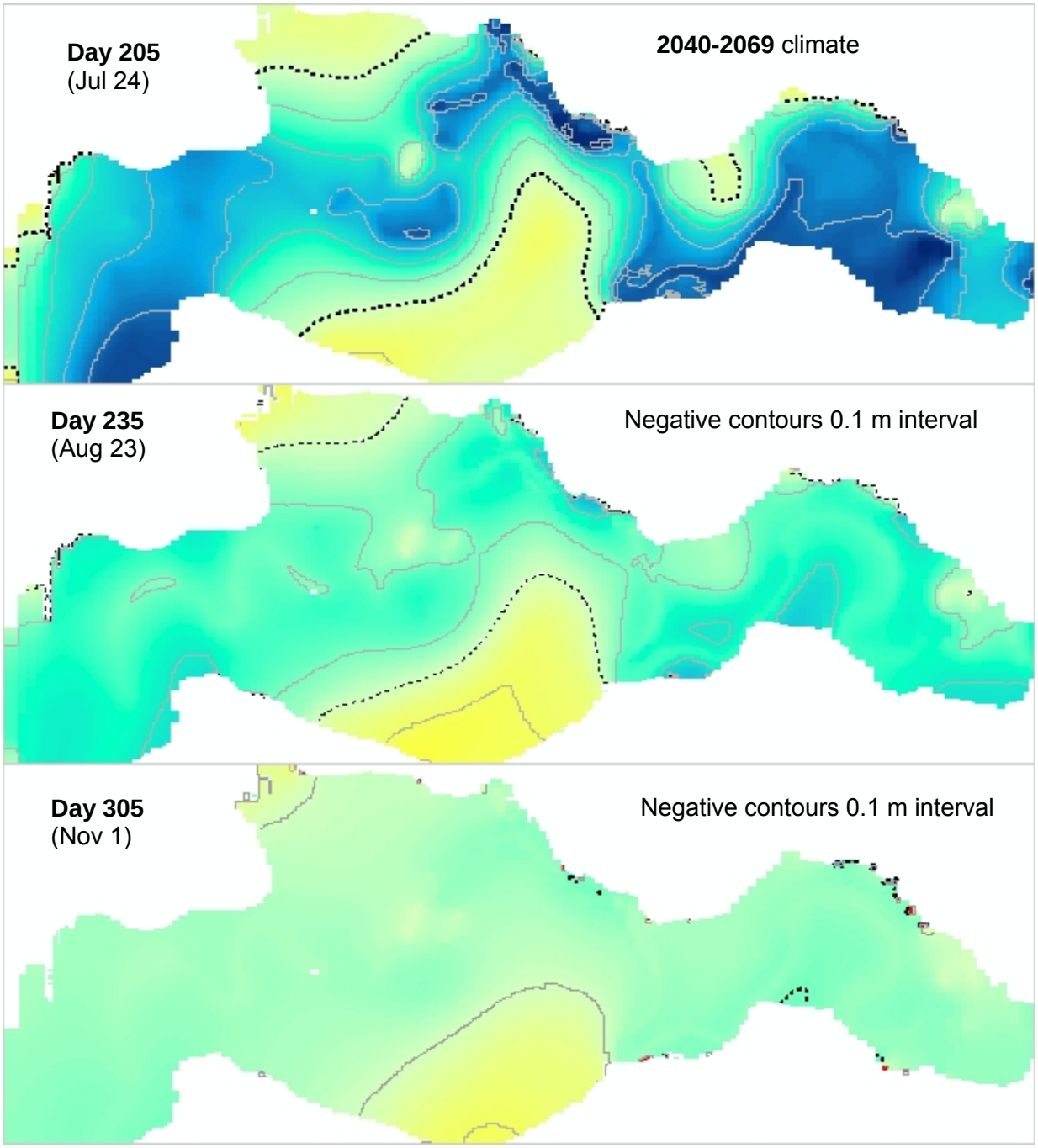

Map 64 Difference in hydraulic head between pumping and non-pumping scenarios (for any climate scenario) by selected time steps (maps for days 131 to 205).

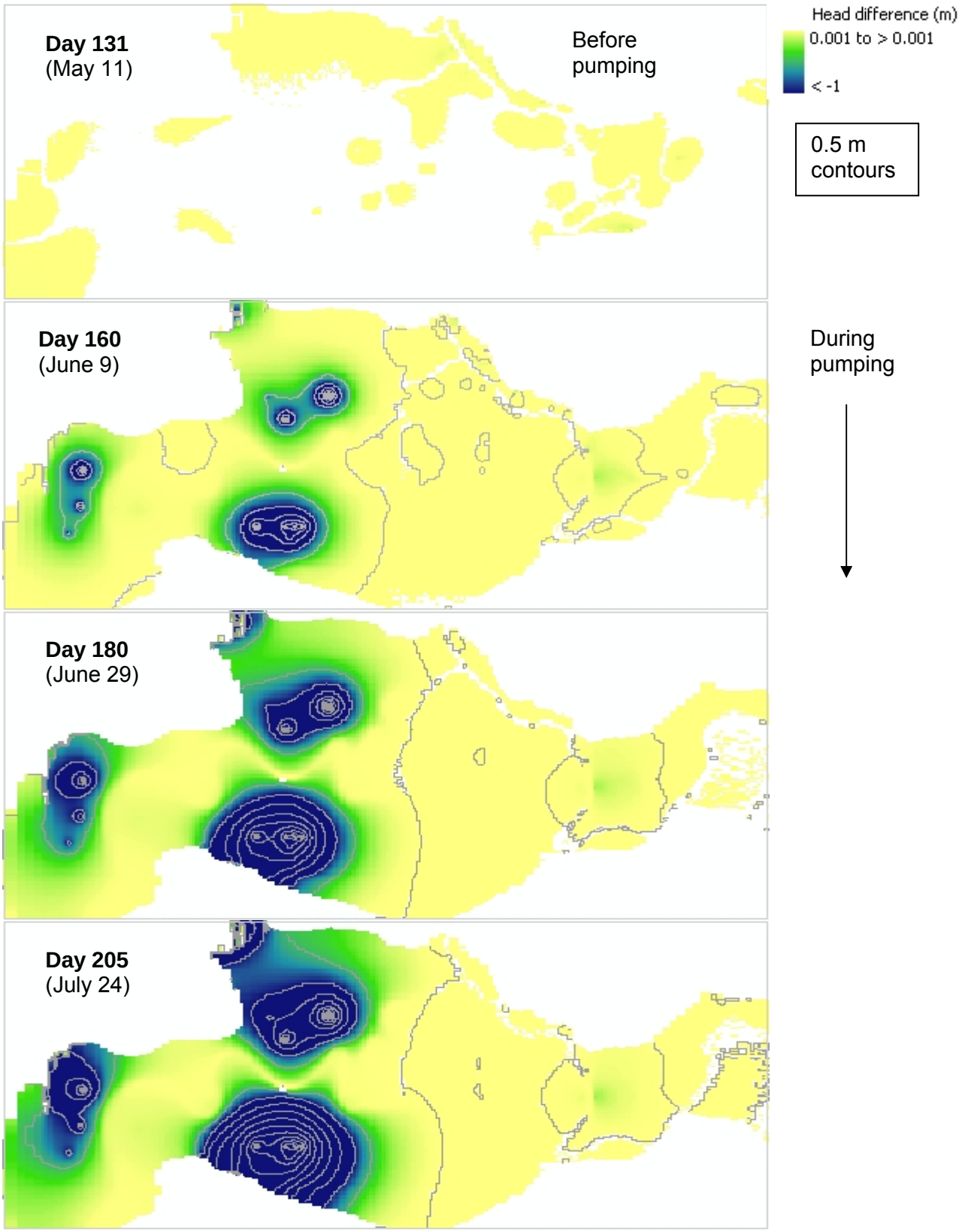

Map 65 Difference in hydraulic head between pumping and non-pumping scenarios (for any climate scenario) by selected time steps (maps for days 235 to 305).

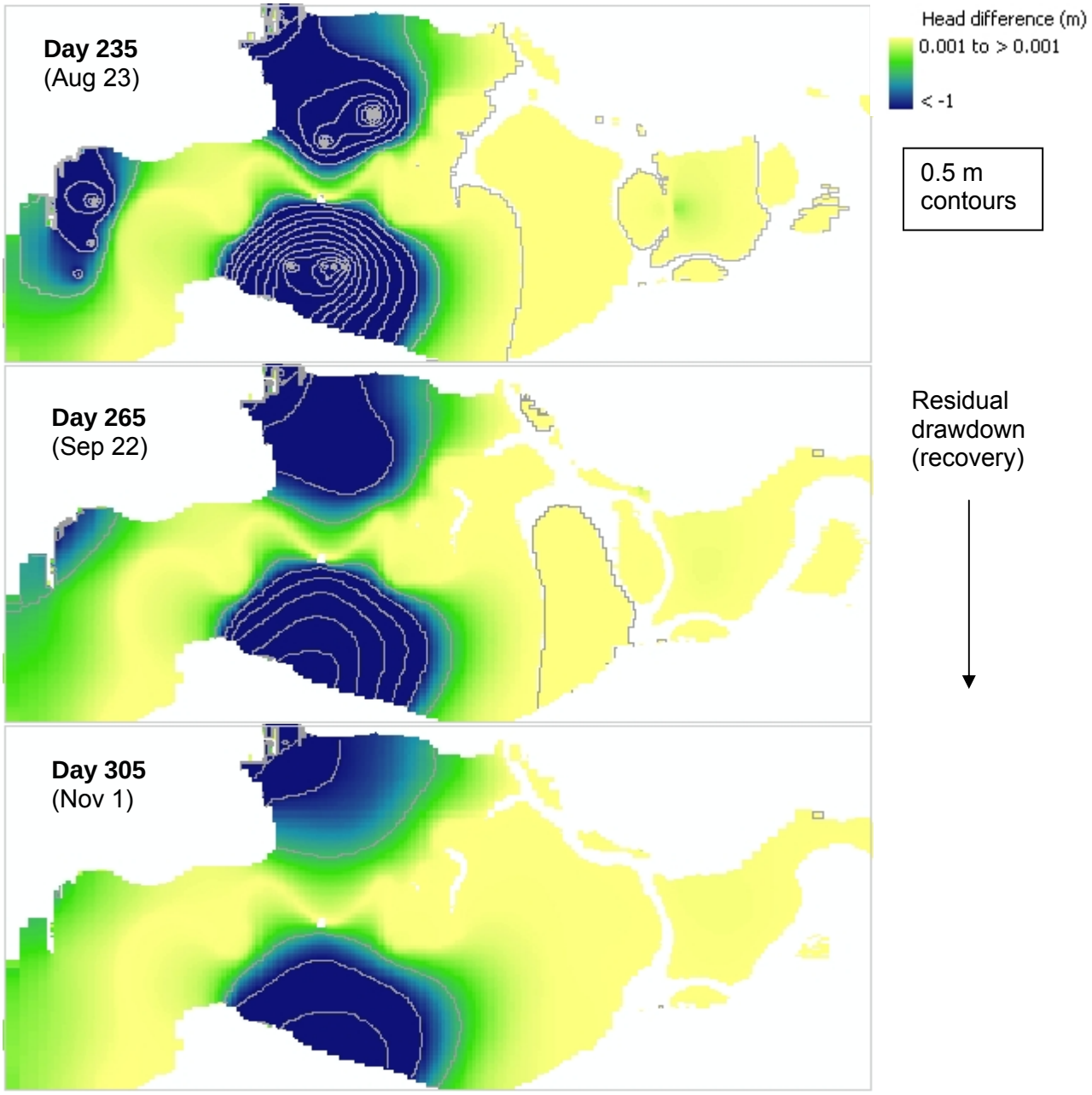

7.3.4. WATER ELEVATION PROFILES

Groundwater elevation (water table) profiles are based on head values in unconfined Layer 2 (sand aquifer) of the model output. Custom code was written and used to extract and aided to graph profiles along a selected row or column (this is much easier to implement than diagonal profiles due to the rectangular grid of MODFLOW). Profiles were selected for different areas in the aquifer, and should give a good sample of water table profiles and transient behaviour, and also present impacts due to climate change, superimposed on typical temporal trends of present conditions. There are 5 water table elevation profiles as shown on Map 66.

- Profile 1 runs N-S and then S-W, away from the Kettle River. Water elevations were extracted at observation well points from model output to explain variation in water elevation, and especially storage effects with increasing distance from the river.
- Profile 2 is the longest and spans most of W-E aquifer extent. It crosses two well fields; Sion wells near Kettle River in the western end, and Big Y wells in the central area, and also extends to the aquifer area distant from pumping influence.
- Profile 3 crosses two pumping wells in Grand Forks district and also crosses the Kettle River. This area has different hydraulic conductivity and pumping rates and is higher in elevation above the river than in Big Y district (of profile 1 and 2). The eastern end intersects the location of observation well 217, which was used to calibrate the transient model storage properties.
- Profile 4 crosses the floodplain between meanders of Kettle River and runs near the Nursery production wells.
- Profile 5 runs N-S and represents the Ward Lake area with two nearby production wells. This area is not influenced by river behaviour, rather only by recharge and pumping.

Map 66 Water elevation profiles (profile locations in Grand Forks aquifer).

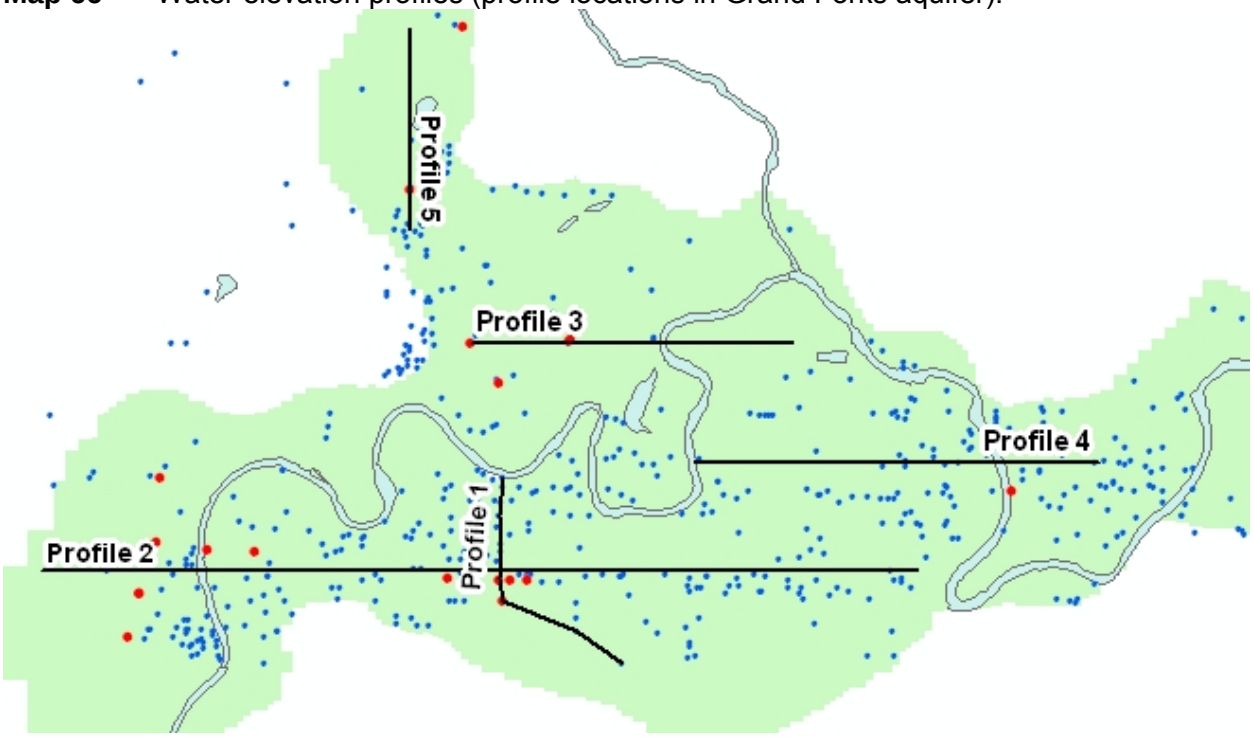

- PROFILE 1 (BIG Y IRRIGATION DISTRICT)

There are two figures for this water table profile. Figure 98 graphs temporal variation in water table elevation, expressed as difference from Day 1 (for each point along the profile), for different distances away from Kettle River. Non-pumping model output was used for the historical climate scenario. Kettle River stage hydrograph was computed for nearest river cross-section and graphed as "River" on the graph at 0 distance. The next nearest point is 20 m away, just outside the river channel.

The modelled water level has almost immediate response to the river, although peak amplitude is lower than that of river, showing effects of groundwater storage. Further away from the river, the amplitude of the hydrograph decreases and also shifts to a later day. The furthest observation point (1886 m) is only slightly influenced by river stage variation. The results here depend on choice of hydraulic conductivity and specific yield for the aquifer layer, and represent modelled results. There are no measured data to confirm this model behaviour, and it is shown here to illustrate storage effects in the calibrated layered model of Grand Forks aquifer. These data could be used to back calculate aquifer transmissivity.

Figure 98 Change in water elevation over 1 year of transient model run, relative to day 1 water elevation. Modeled variation of groundwater levels with distance away from river along Profile 1. Non-pumping model and historical climate scenario.

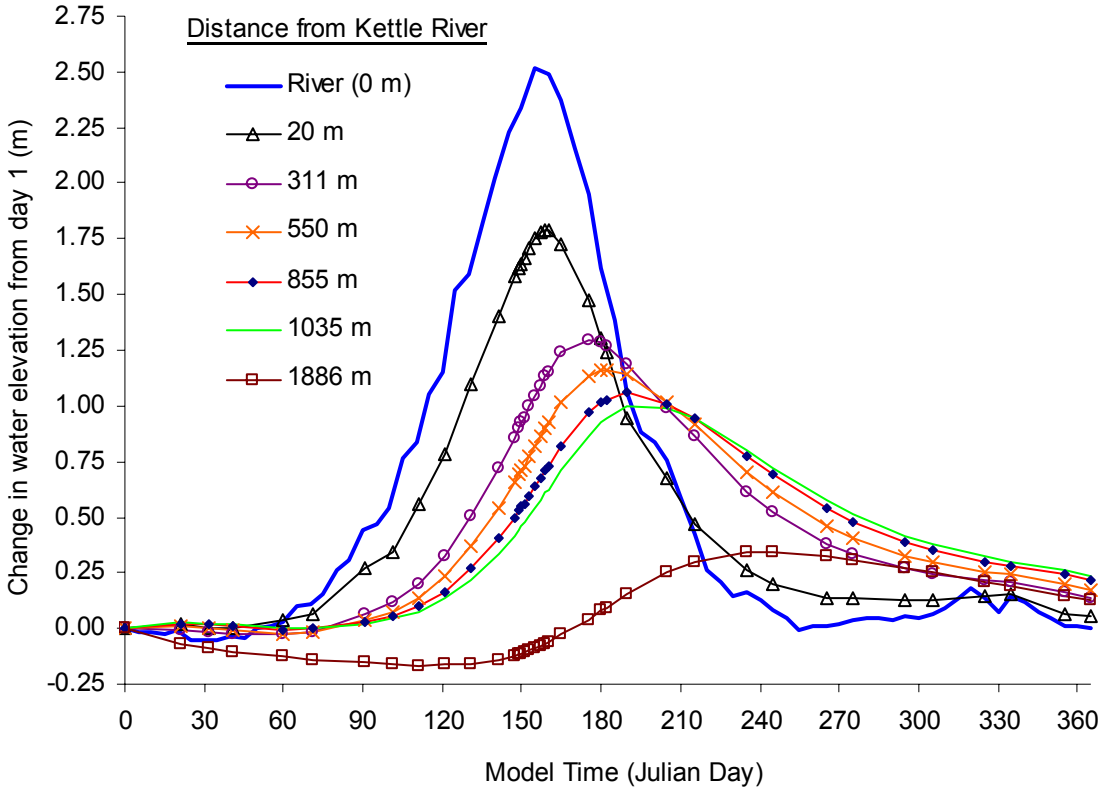

The actual water table elevation cross-section is graphed in Figure 99. Both pumping and non-pumping conditions are represented in "Site A" along the profile close to pumping wells in Big Y district. "Site B" is at the far end of Profile 1 at a point furthest away from the river, and is not significantly influenced by drawdown due to pumping. Note that vertical scale is different for both "sites" and that actual groundwater elevation was used.

Figure 99 Effect of climate change under pumping and non-pumping conditions on groundwater elevations in unconfined aquifer: Site A (close to pumping wells), Site B (away from pumping wells).

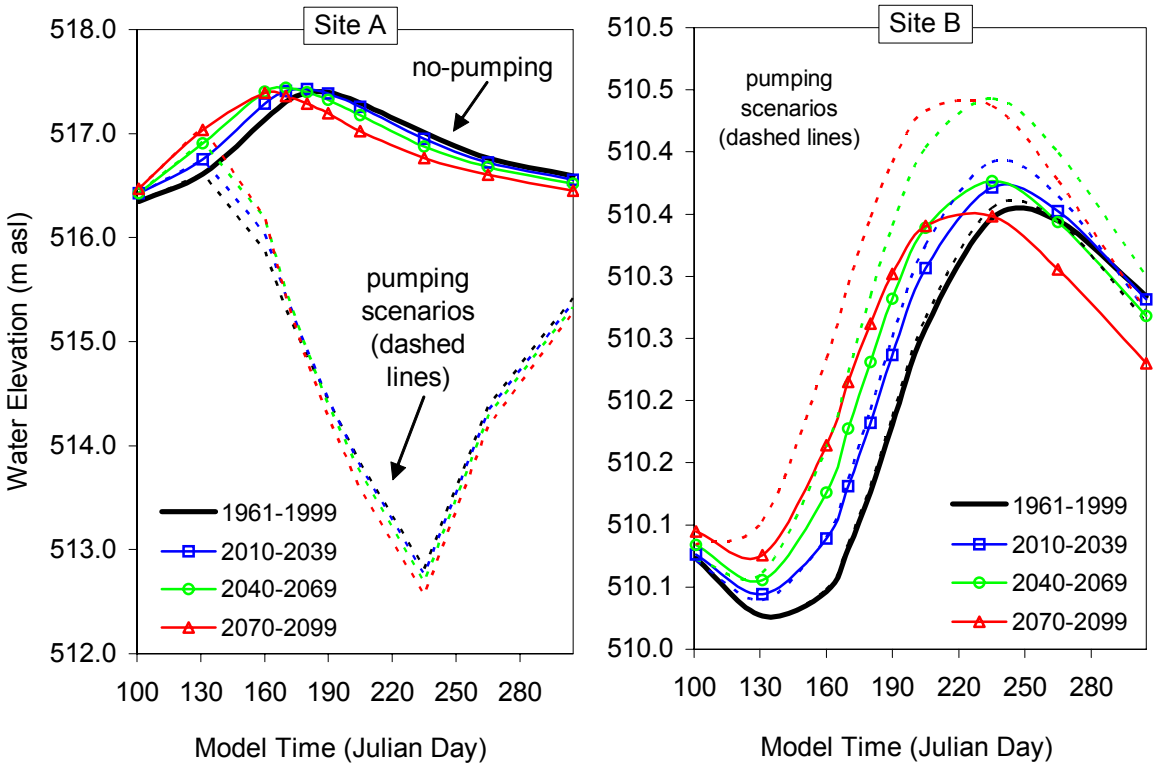

The climate change effect at both sites without pumping effect is different because of different distance to river of each site. As the river hydrograph shifts to earlier peak day in future climates, the groundwater levels follow. There is also a small effect of changing recharge in future climate. This is a layered aquifer model with calibrated hydraulic properties. In the heterogeneous-aquifer model, the drawdown is much smaller because the K and Sy are more site-specific. This figure shows that climate change effects (river + recharge) are much smaller in magnitude than typical seasonal variation, but are significant.

Profile 1 does not show the effects of heterogenous aquifer assumption (distributed K), but those were computed for other profiles in water elevation.

- PROFILE 2

The next three 3 figures (Figure 100, Figure 101, Figure 102) present combined graphs and maps of water table elevation (expressed as deviation from Day 1, for all model cells separately along the transect). The elevations were expressed as deviation from Day 1 to remove the elevation differences along the profile, which would overwhelm any attempt to show the effects of climate change because of the strong hydraulic gradient in this aquifer, and therefore, steep water table profile. Deviations are also more useful in showing and comparing strengths of temporal variation and climate change effects at each point along the profile. Selected time steps were for days 101 (prior to pumping), 160, 205, 235 all during pumping, and day 305 during recovery from pumping. The “Map View” shows water table contours at 1 m spacing and all are colour coded for elevation to help visualize low and high elevations. Pumping production wells are shown as red dots. The water table profile is a black line. All graphs use the same vertical and horizontal scale, legend coding and map colour shading.

Again what is seen are relatively small impacts due to climate change, compared to natural variation in water table elevations. In this homogeneous K model, the drawdown is very large, but the system almost recovers by day 305 (it does recover completely by day 365 and it resets itself for next annual cycle). If actual water elevations were to be predicted for future, the model would need accurate pumping schedules and would have to be run for multiple years continuously to predict inter-annual trends. This model does not do that. It runs only for 1 year.

What the graphs show, by day:

- Day 101 (prior to pumping) – climate change impacts are strongest close to river, but very small away from river (thus, recharge variation has weak effect here).
- Day 160 (pumps ON) – at this time the river is at the high stage of hydrograph and pumps cause large drawdown near production wells. River stage change causes as much change in water levels as does pumping according to this homogeneous K model (see heterogeneous K model for different result). Climate change scenarios have identical "natural + pumping" trends, with small climate change effects superimposed to produce final water table profile.
- Day 205 to 235 (pumps ON) – same conclusions as for day 160, but drawdown increases.
- Day 305 (pumps OFF at day 242) – quick recovery of water table after pumping and very small changes due to climate change effects

Figure 100 Differences groundwater elevation (hydraulic head in layer 2 of model) from Day 1 elevation, along Profile 2, for all climate scenarios. Showing water table elevation map and cross-section: Day 101.

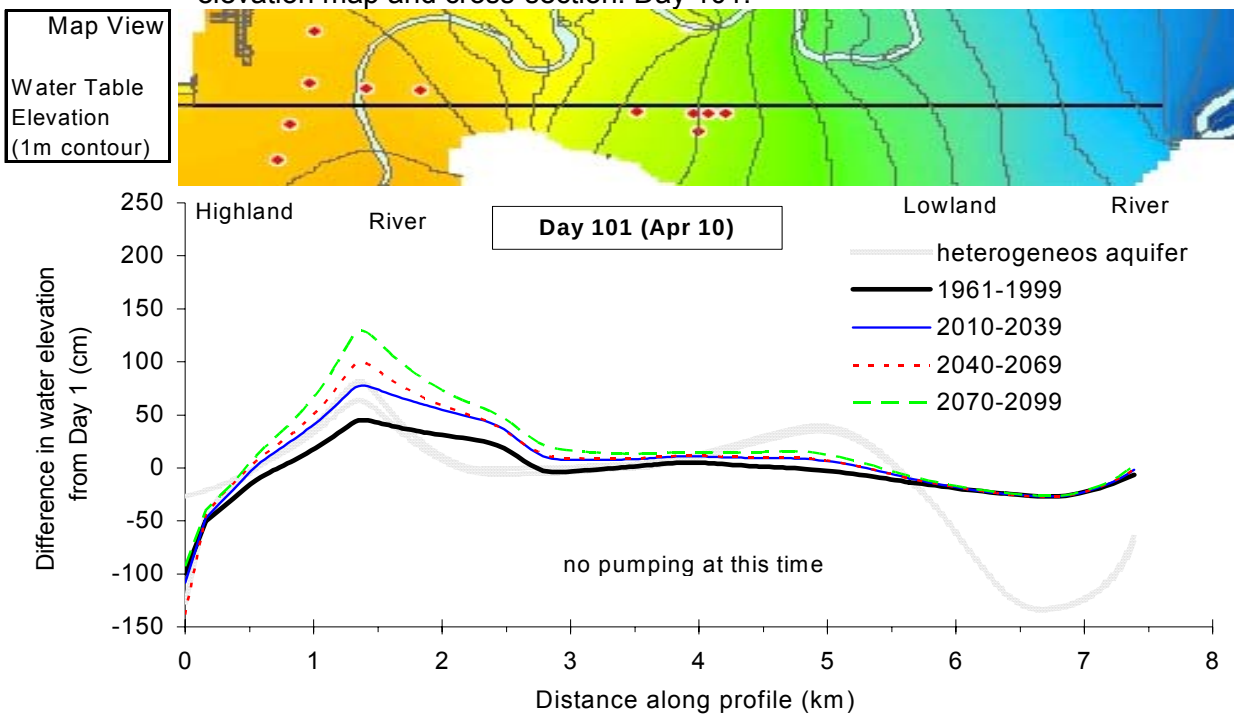

Figure 101 Differences groundwater elevation (hydraulic head in layer 2 of model) from Day 1 elevation, along Profile 2, for all climate scenarios. Showing water table elevation map and cross-section: Day 160 and Day 205.

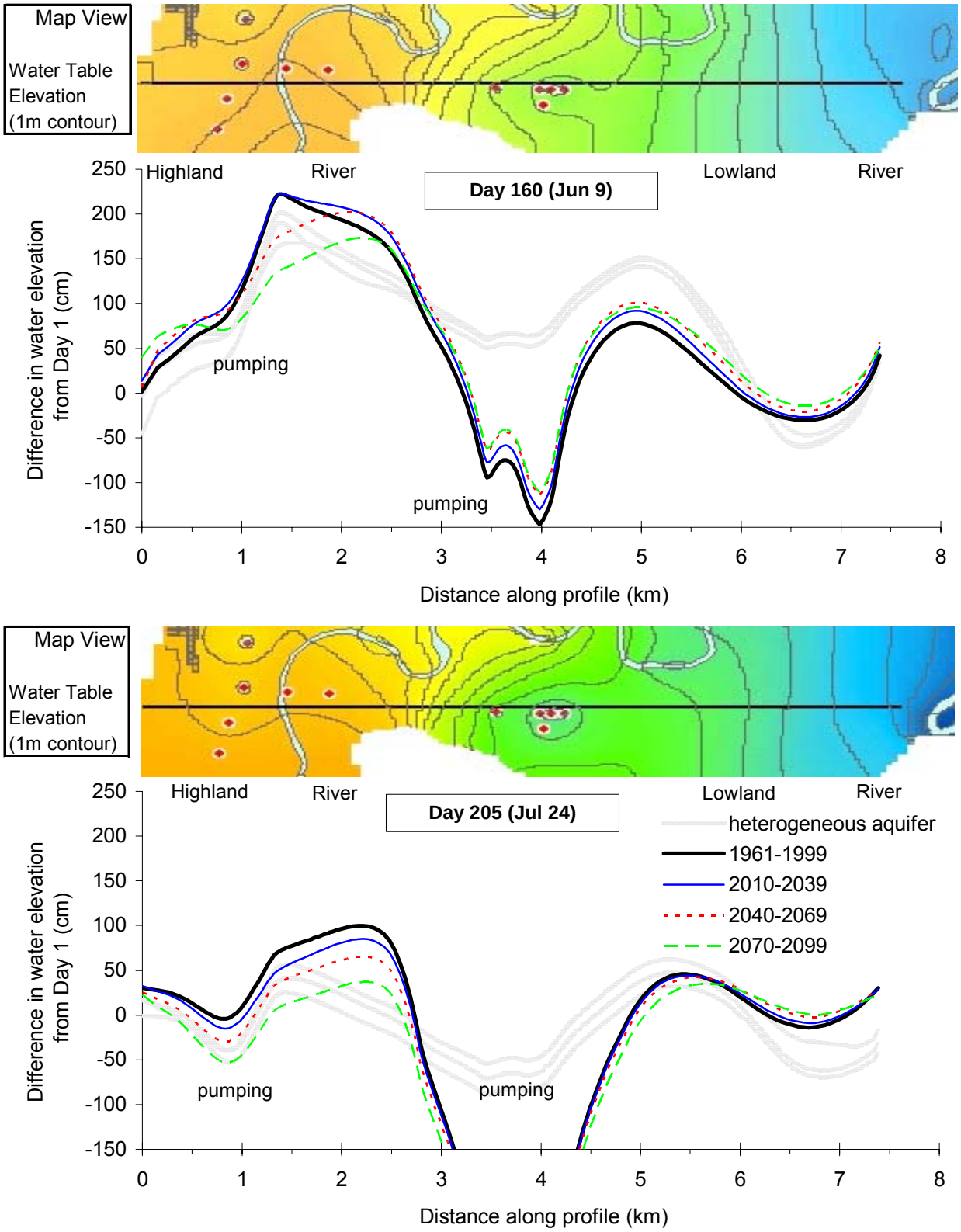

Figure 102 Differences groundwater elevation (hydraulic head in layer 2 of model) from Day 1 elevation, along Profile 2, for all climate scenarios. Showing water table elevation map and cross-section: Day 235 and Day 305.

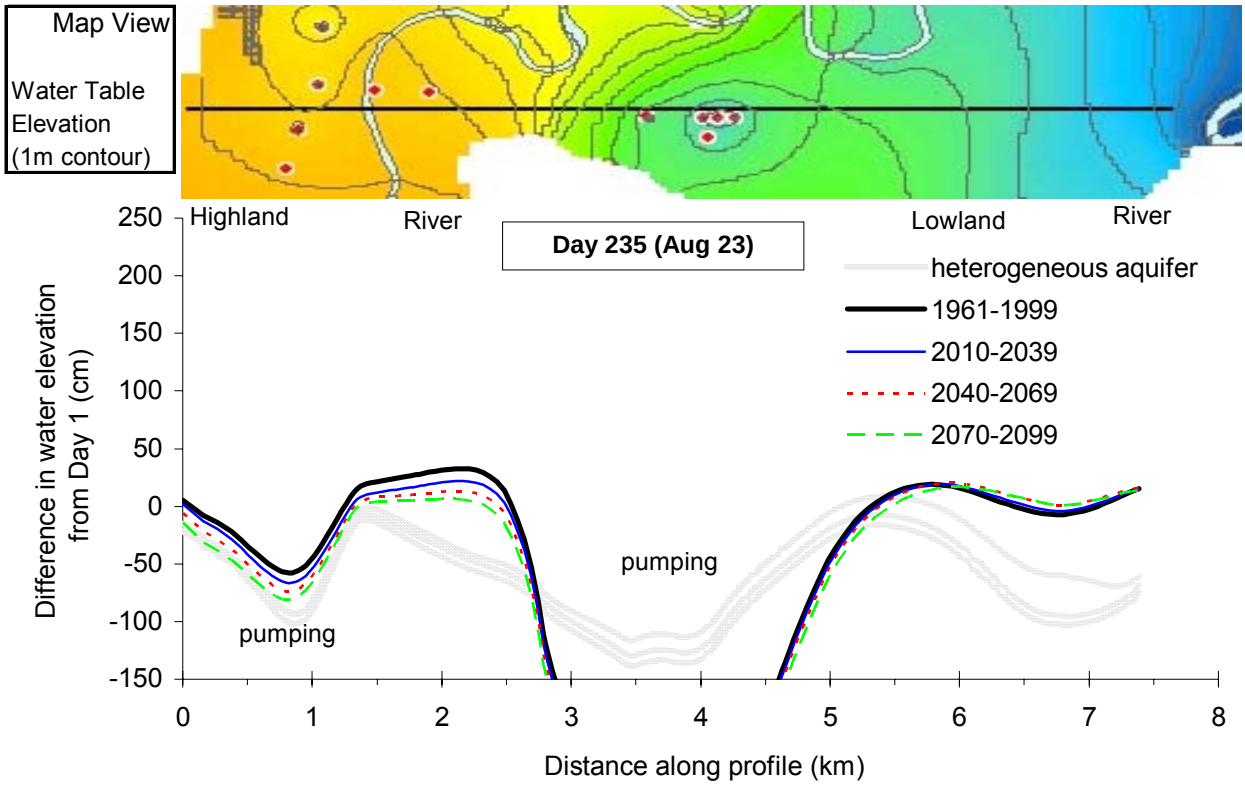

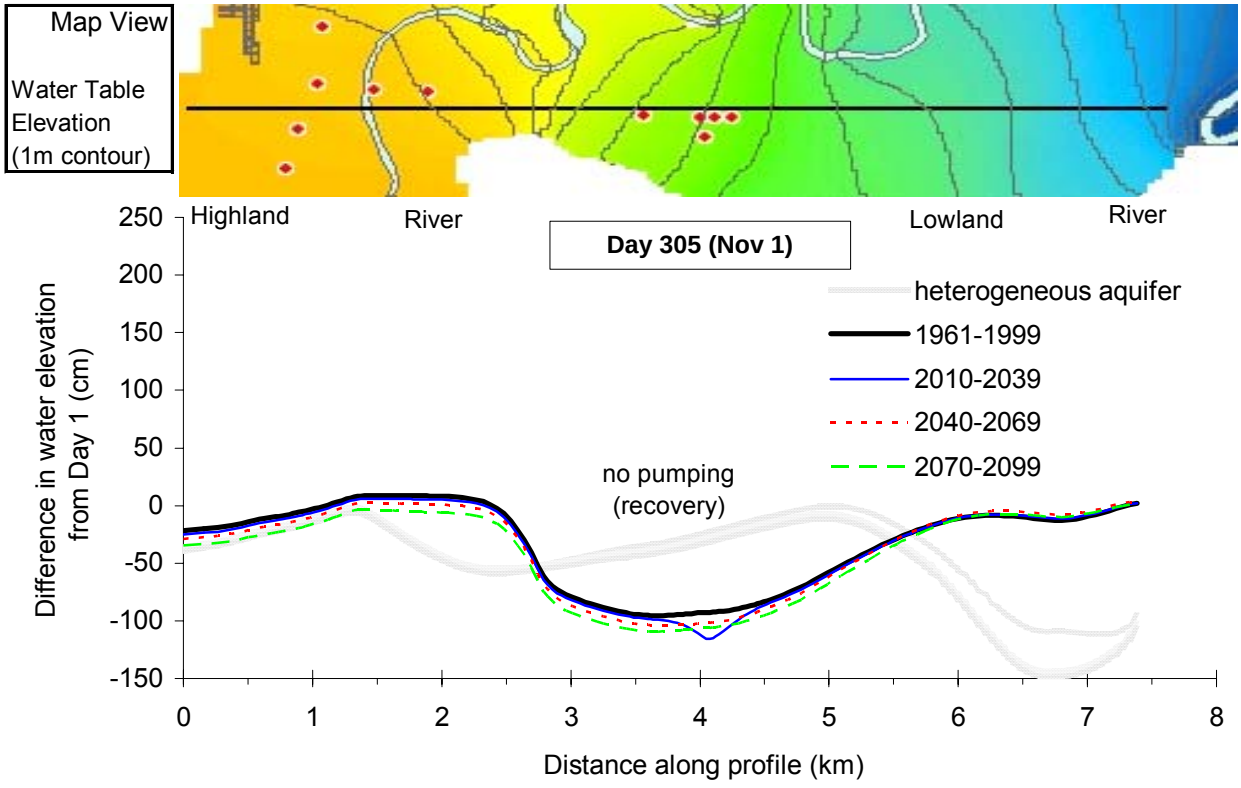

- PROFILE 3

As with water table elevation profile 2, the Profile 3 is shown in 3 figures (Figure 103, Figure 104, Figure 105) containing combined graphs and maps of water table elevation (expressed as deviation from Day 1, for all model cells separately along the transect). The elevations were expressed as deviation from Day 1 to remove the elevation differences along the profile, which would overwhelm any attempt to show the effects of climate change because of strong hydraulic gradient in this aquifer, and therefore, steep water table profile. Deviations are also more useful in showing and comparing strengths of temporal variation and climate change effects at each point along the profile. Selected time steps were for days 101 (prior to pumping), 160, 205, 235 all during pumping, and day 305 during recovery from pumping. The "Map View" shows water table contours at 1 m spacing and all colour coded for elevation (to help visualize low and high elevations). Pumping production wells are shown as red dots. The water table profile is a black line. All graphs use the same vertical and horizontal scale and legend coding and map colour shading.

- At day 101, prior to pumping of wells in Grand Forks district, the water table elevation is similar to that at beginning of the year, except for change in river stage and associated raising of groundwater elevation away from the river in the floodplain. Strong river effect on water levels extends approximately 0.5 km on both sides of the river channel. Further away the static groundwater levels are above the highest river stage and the river effects are diminished and related to changes in hydraulic gradient but not actual river water levels. As was observed in Profile 2, there are relatively small impacts due to climate change, compared to natural variation in water table elevations. In this homogeneous K model, the drawdown is very large, but the groundwater levels recover quickly and by day 305 they are only 50 cm lower than prior to pumping. By day 365 the recovery is total.

- Day 160 (pumps ON) – at this time the river is at high stage of hydrograph and pumps cause large drawdown near production wells. River stage change causes as much change in water levels as does pumping according to this homogeneous K model (see heterogeneous K model for different result). Climate change scenarios have identical "natural + pumping" trends, with small climate change effects superimposed to produce final water table profile.

- Day 205 to 235 (pumps ON) – same conclusions as for day 160, but drawdown increases.

- Day 305 (pumps OFF at day 242) – quick recovery of water table after pumping and very small changes due to climate change effects.

- 7.3.4. PROFILES 4 AND 5

These water elevation profiles look very similar to profiles 1 to 3, and were not included in this report as graphs. Similar sections could be drawn across any area of aquifer. Sections 4 and 5 were done for completeness and did not reveal any new or unexpected trends.

Figure 103 Differences groundwater elevation (hydraulic head in layer 2 of model) from Day 1 elevation, along Profile 3, for all climate scenarios. Showing water table elevation map and cross-section: Day 101.

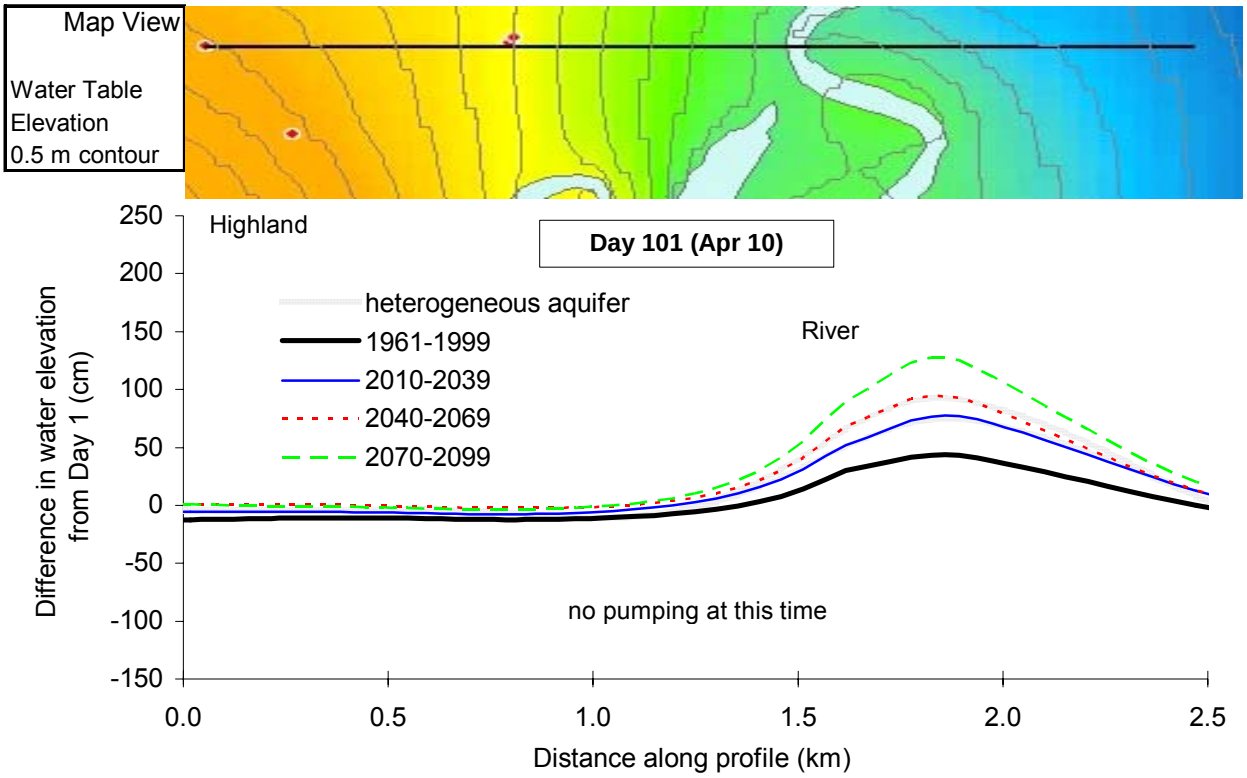

Figure 104 Differences groundwater elevation (hydraulic head in layer 2 of model) from Day 1 elevation, along Profile 3, for all climate scenarios. Showing water table elevation map and cross-section: Day 160 & 205.

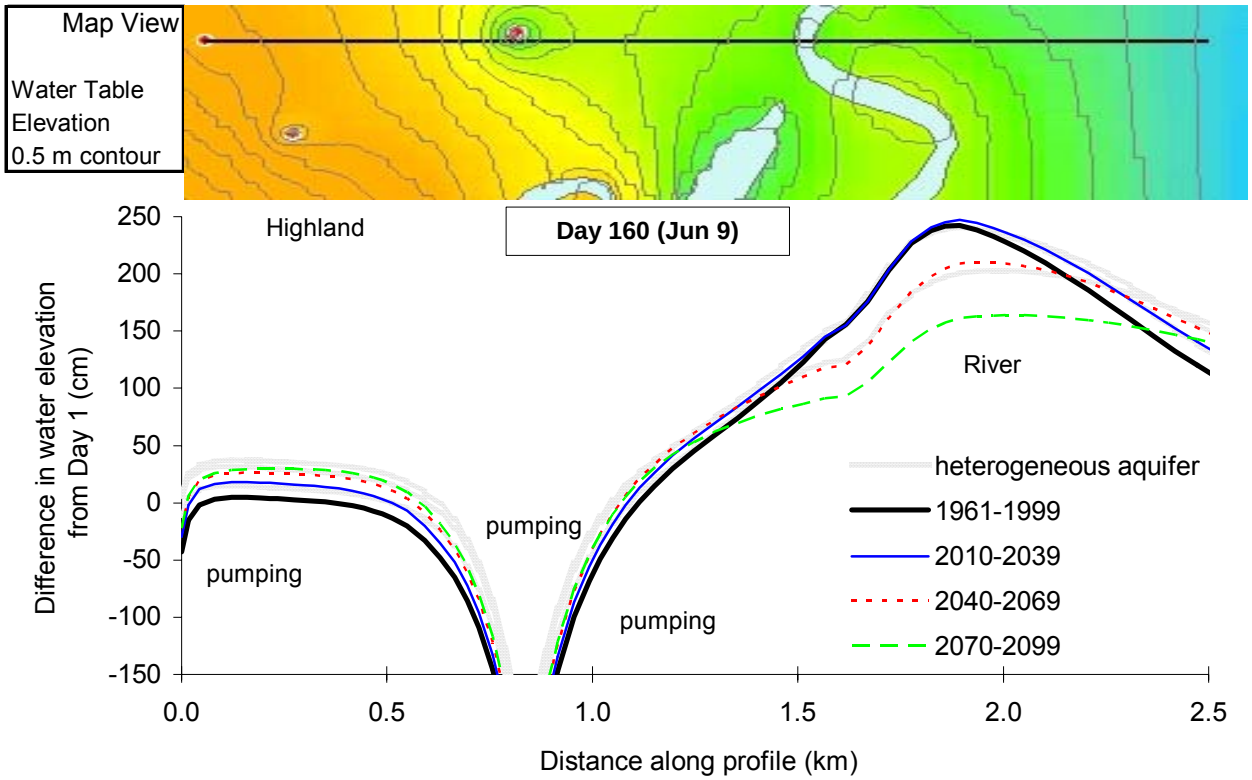

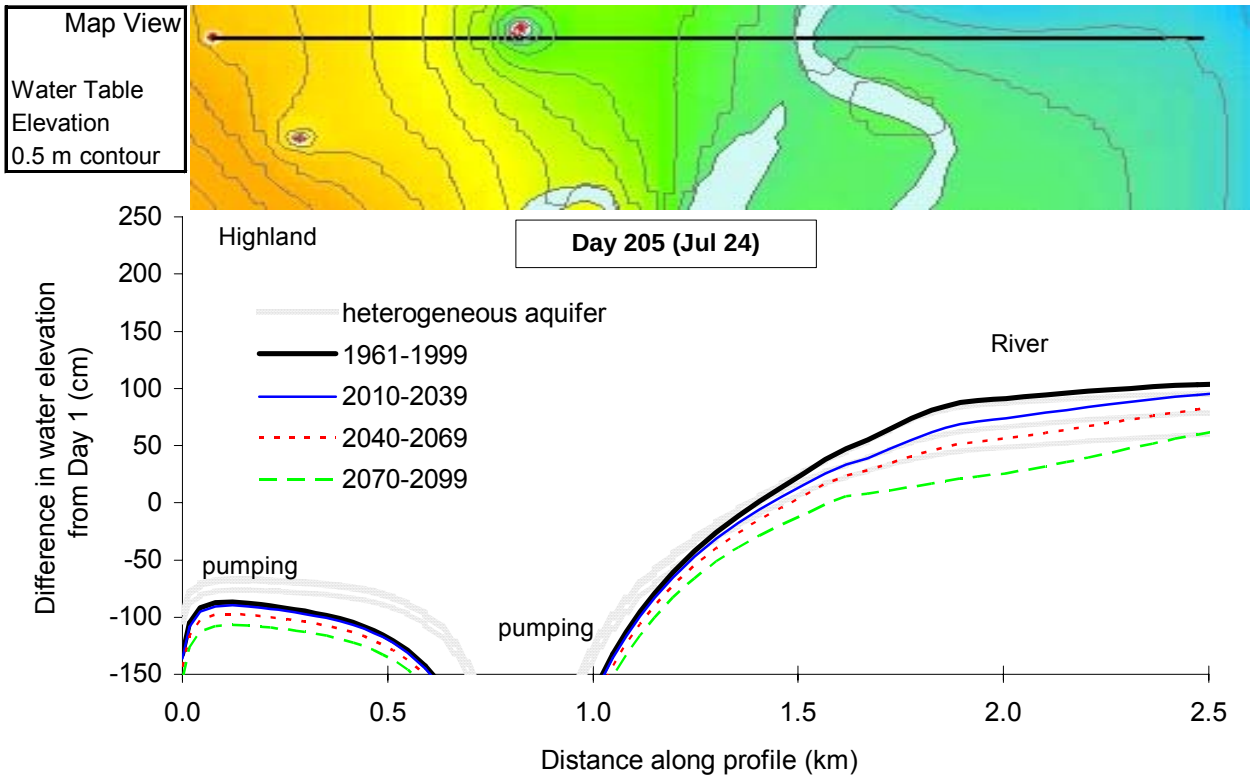

Figure 105 Differences groundwater elevation (hydraulic head in layer 2 of model) from Day 1 elevation, along Profile 3, for all climate scenarios. Showing water table elevation map and cross-section: Day 235 & 305.

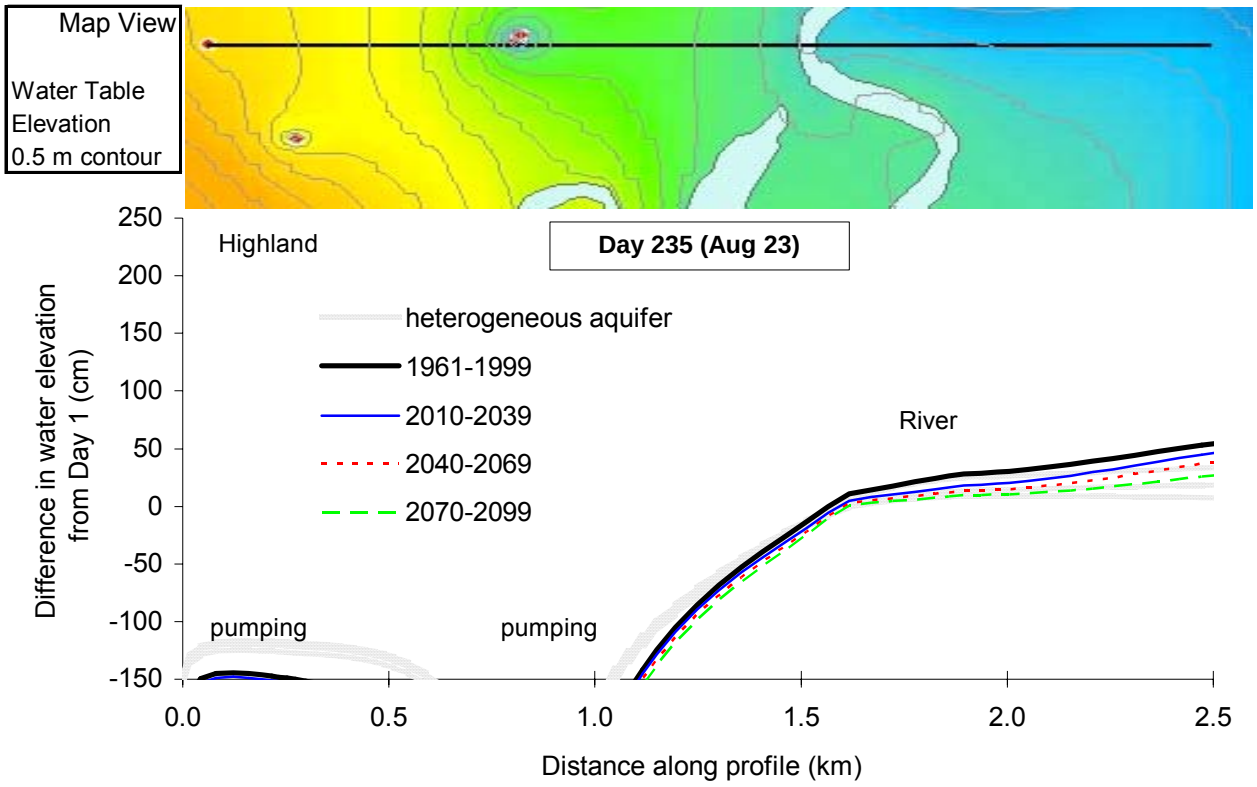

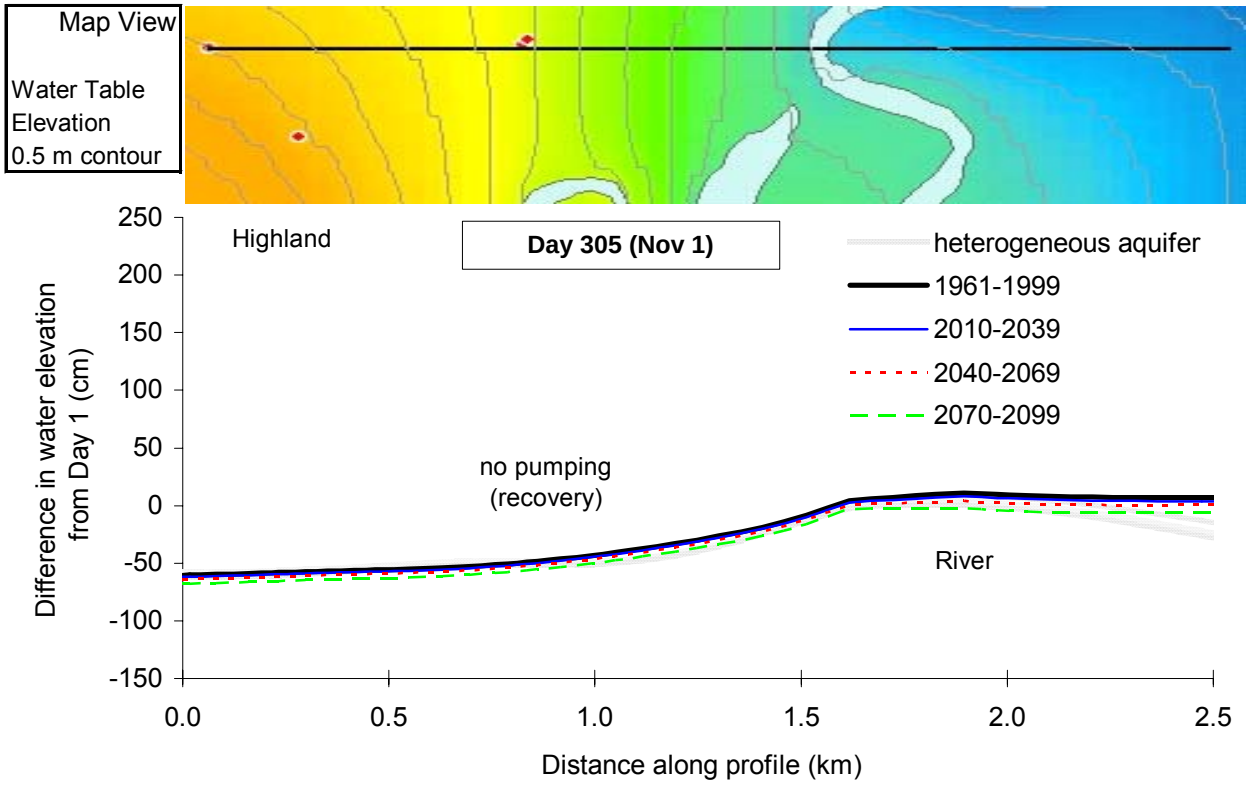

7.4. AQUIFER HETEROGENEITY AND CLIMATE CHANGE

7.4.1. QUANTIFYING EFFECTS OF AQUIFER HETEROGENEITY ON WATER LEVELS

The effects of aquifer heterogeneity were quantified similarly to the effect of climate change on water levels in the unconfined aquifer of the Grand Forks valley. All climate scenarios were re-run as separate model series (series 4), but the models were modified to include aquifer heterogeneity, which was represented by distributed hydraulic conductivity fields in top two aquifer layers. Climate change impacts were computed by taking a difference between future and present climate water levels at selected model time steps, using a method identical to that used for the homogeneous aquifer model.

Each map shows difference in hydraulic head between a future climate scenario and the present climate scenario, all under pumping conditions. Positive contours shown at 0.1 m interval. The zero contour is dashed line. Negative contours are not shown. The darkest blue colours indicate values < -0.5 m (along rivers only). At day 101, the difference map (not shown) has values within 0.1 m of zero.

Each climate scenario is illustrated with 6 maps for six model time steps, starting from day 131 when the river hydrograph is near peak flow (and peak stage), and ending on day 305 when river water levels have almost returned to baseflow conditions of late fall and winter. The maps are grouped into two "Map" captions (to fit into report format), each with 3 time-snapshot maps of differences in groundwater levels.

7.4.2. CLIMATE CHANGE PREDICTIONS ON WATER LEVELS (ASSUMING DISTRIBUTED K VALUES)

- 2010-2039 CLIMATE SCENARIO (DIFFERENCE FROM PRESENT)

Water level differences between 2010-2039 climate scenario and present climate, in the heterogeneous aquifer model, are displayed in Map 67, Map 68 and Map 69. The latter two maps can be compared to corresponding maps for homogeneous aquifer model (Map 60 and Map 61). The effect of aquifer heterogeneity was also quantified by subtracting the results for heterogeneous from results of homogeneous aquifer models, for the appropriate climate scenarios and pumping models (see Map 70 and Map 71).

The following discussion of maps is similar to the one for homogeneous (original) aquifer model, but any major differences are mentioned.

At day 131 the water levels are higher along the floodplain than at the same day in the 1961-1999 historical climate scenario. The main cause is a shift in river hydrograph peak flow to an earlier date, thus creating positive difference in water levels between the 2010-2039 and 1961-1999 models at day 131. The increased heterogeneity caused stronger hydraulic connection with the river over most of the valley area, especially in south-central valley, south of Grand Forks (in Big Y irrigation district of ZBUD zone 5). The excess water is now stored in a much larger area that extends far beyond the floodplain, as compared to its smaller extent in the homogeneous aquifer model.

Within a month the peak flow passes, and river water levels begin to drop rapidly. By day 160, the river water levels are similar in both the 2010 and historical climate models, but the pattern is more complex in heterogeneous aquifer and there is more variation in groundwater levels as a response to changes in river stage. Away from river channel water levels are elevated by 30 to 40 cm (stored water), which continue to drain until day 180. Away from the river, the water levels are either up to 30 cm higher than at present or are similar to present - where high hydraulic conductivity "conduits" to the river are present and water levels respond very fast to river water levels. By day 180, the river stage has dropped below typical river stage at present climate (again, due to shift in the hydrograph), and the water levels in floodplain in the 2010 climate are lower by 20 to over 50 cm at day 180 compared to present climate at that day, showing more spatial variability in heterogeneous aquifer. The eastern floodplain and adjacent areas are very well connected to river, causing fast drainage of stored water from previously high river water levels that recharged the surficial aquifer. In western and northern parts of valley, the hydraulic conductivity field has lower values, and water remains in storage with a longer lag time for draining as response to dropping river water levels.

At day 205, the 2010 river water level is still at least 10 cm below present at that day, but the increased recharge in 2010 climate over historical climate causes up to 10 cm higher water levels away from the river (but now only in areas with low hydraulic conductivity). This spatial pattern of slightly elevated water levels away from the floodplain relative to present climate continues to day 235 (Aug 23), but by day 305 (Nov 1) the water levels in unconfined aquifer are almost identical to present levels at that time of year over most of the aquifer extent. However, there are smaller areas where water levels are either lower or higher than expected. The "low" area in south-central valley is unexplained.

Overall, the climate change effects for the 2010-2039 scenario relative to present are no longer limited to floodplain, but extent over most parts of the valley in this heterogeneous aquifer model. Areas where an increase in recharge creates higher water levels than at present conditions are only limited to high terraces in west and north parts of aquifer. The effect of heterogeneity on water levels is arguably as strong as the shift of river hydrograph due to climate change.

- 2040-2069 CLIMATE SCENARIO (DIFFERENCE FROM PRESENT)

For the 2040-2069 climate scenario, the results of transient model simulations are plotted in Map 70 and Map 71. At day 131 the water levels are higher along the floodplain than at the same day in the 1961-1999 historical climate scenario. The main cause is a shift in river hydrograph peak flow to an earlier date, thus creating a positive difference in water levels between the 2040-2069 and 1961-1999 models at day 131. The hydrograph shift is larger than in the 2010-2039 climate scenario, so the computed differences to historical climate are larger too. Water levels are 40 to 80 cm above normal, mostly along the floodplain, but areas away from the floodplain are also affected due to better hydraulic connection with the river in a heterogeneous aquifer model. The term "above normal" means "occurring earlier in year," but the maximum water levels associated with the peak hydrograph are very similar to present climate because the peak discharge is not predicted to change, only the timing of it. This excess water flows into surficial aquifer and is stored there, as was demonstrated in flow budget section of this report. The zone of storage includes all of the floodplain and large areas of river terraces in the valley. Within a month the peak flow passes and river water levels begin to drop rapidly.

By day 160, the peak flow in river has passed and subsided at an earlier time than under present conditions, and there are > 50 cm lower water levels in floodplain close to the river channel at day 160, but outside the floodplain the water levels remain elevated above normal for

that time of year. The stored water accounts for the 20 to 40 cm elevated water levels just outside the floodplain (see orange-red areas on map). This stored water drains within 1 month back to the river. By day 180 the shift in the river hydrograph in this climate scenario results in lower (> 50 cm) than at present water levels in entire floodplain and beyond. In the homogeneous aquifer model the water levels were only low along parts of the floodplain.

At day 205, the 2040 river water level is still 20 to 50 cm below present at that day in most parts of the valley, but the increased recharge in the 2040 climate scenario over historical climate causes up to 20 cm higher water levels away from the river. This spatial pattern of slightly elevated water levels away from the floodplain relative to present climate continues to end of year (longer than in 2010-2039 scenario). Overall, the climate change effects for 2040-2069 scenario relative to present extend over most of the valley and are strongest near the floodplain, especially in the eastern part of valley. The largest changes occur in early part of the year, but large changes persist up to day 205, and smaller changes occur even to end of year.

- EFFECTS OF AQUIFER HETEROGENEITY ON WATER LEVELS

In addition to climate change effects, the effect of assumption of aquifer heterogeneity was also isolated by taking the differences between corresponding heterogeneous and original homogeneous (one K value per layer) aquifer models. Results are shown i n Map 72 and Map 73.

The differences between heterogeneous (distributed K field) aquifer and homogeneous (one K value per layer) aquifer are very large, and similar in magnitude to climate change impacts alone (the color scales in the maps are identical). The effects of heterogeneity are somewhat randomly distributed over the valley. Some areas have much higher or much lower water levels than in the homogeneous aquifer model results.

Areas that have negative differences have a higher hydraulic conductivity in the heterogeneous model than in the homogeneous layered model. Accordingly, these areas are much better connected to the river water levels and tend to have lower water levels than other areas. Large positive differences are usually associated with pumping effects, or rather the reduction of drawdown in a heterogeneous model to more realistic drawdown. The Grand Forks and Big Y water district well fields have much smaller drawdown if K-values from pump tests are interpolated over the aquifer.

Another way of looking at changes in water levels under different climate scenarios is in cross-sections, by showing water table differences from day 0 of a model run. The results for the heterogeneous aquifer model were graphed together with homogeneous aquifer model results and were included in water table profile graphs in previous section (see Figure 100 to 105).

Map 67 Water level differences (measured as head in layer 2 of unconfined aquifer) between future and present climate (2010-2039, scenario 4B) under pumping conditions, and with heterogeneous hydraulic conductivity distribution. Maps by time step in day 101 (this is an additional map).

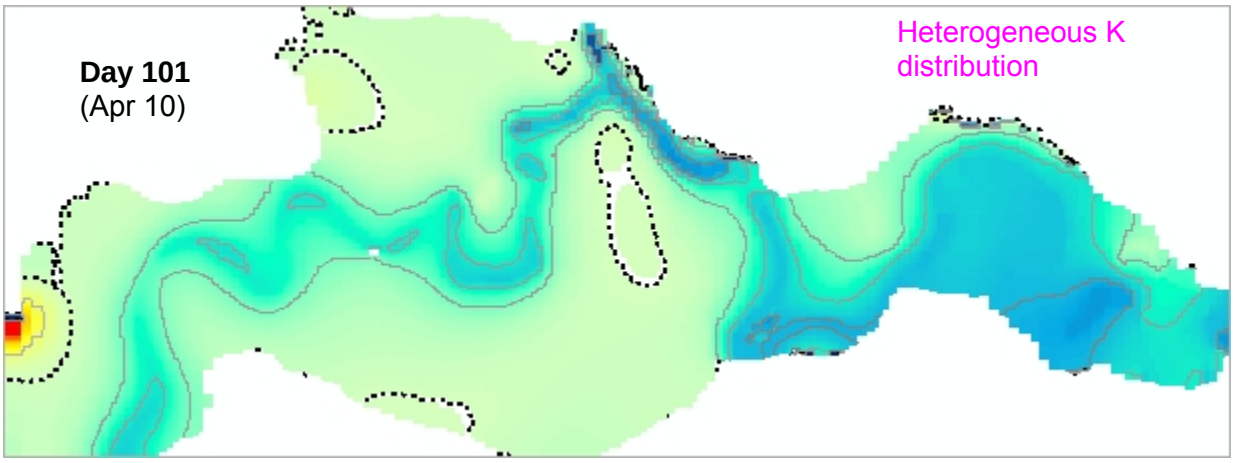

Map 68 Water level differences (measured as head in layer 2 of unconfined aquifer) between future and present climate (2010-2039, scenario 4B) under pumping conditions, and with heterogeneous hydraulic conductivity distribution. Maps by time step in days 131 to 180.
Positive contours shown at 0.1 m interval. Zero contour is dashed line. Negative contours not shown. Darkest blue colours indicate values < -0.5 m (along rivers only).

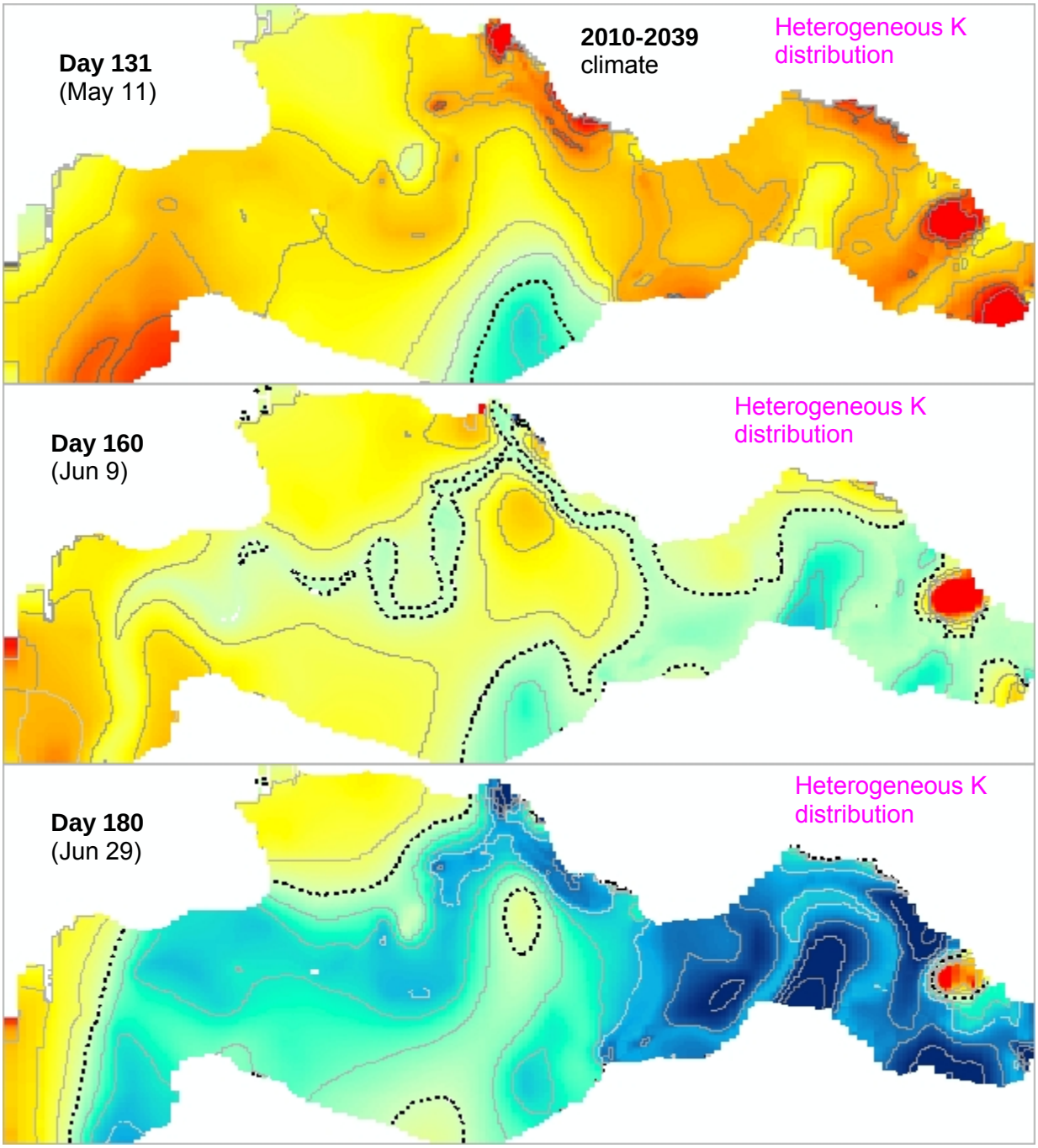

Map 69 Water level differences (measured as head in layer 2 of unconfined aquifer) between future and present climate (2010-2039, scenario 4B) under pumping conditions, and with heterogeneous hydraulic conductivity distribution. Maps by time step in days 205 to 305.
All contours at 0.1 m interval. Zero contour is dashed line.

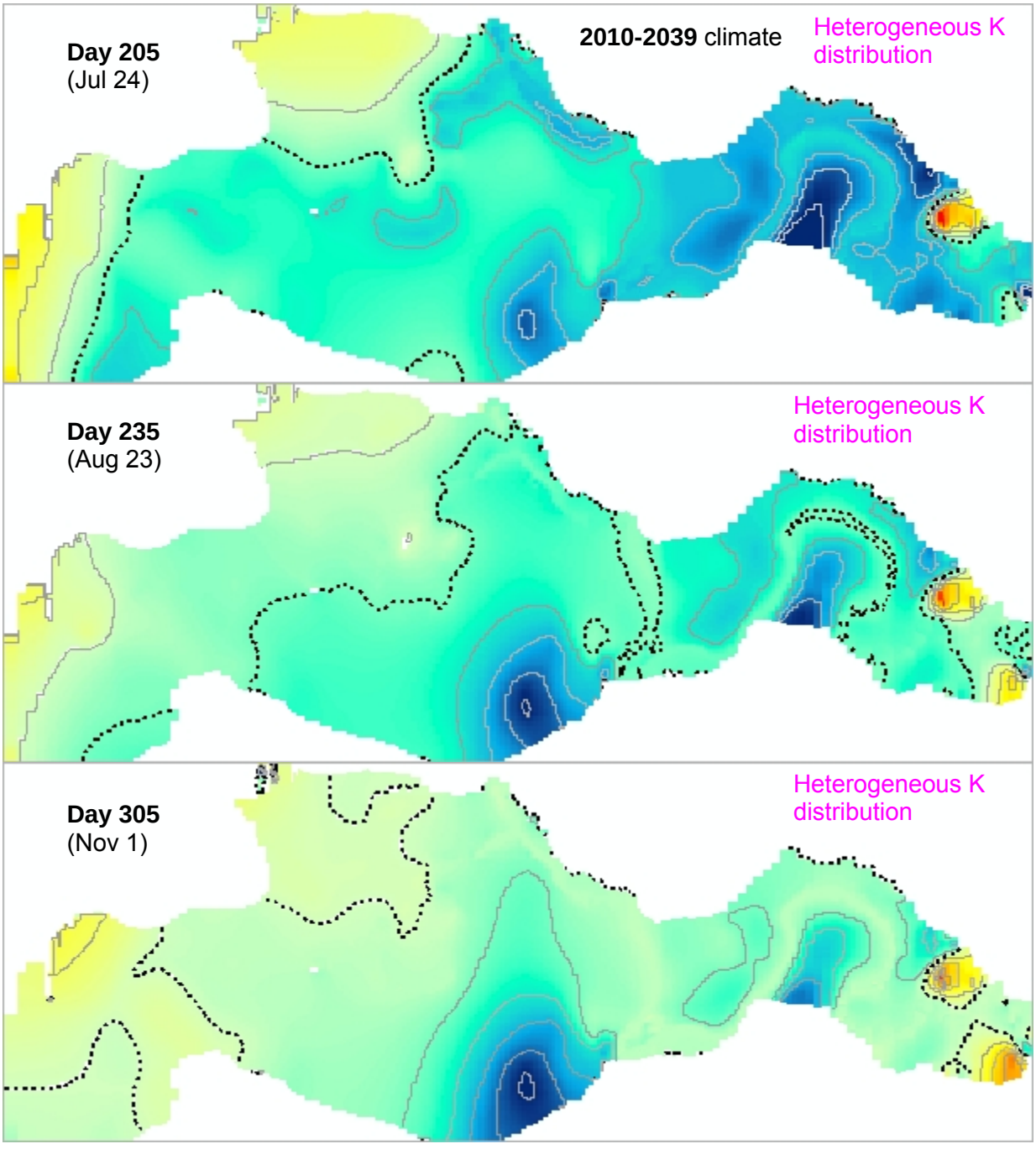

Map 70 Water level differences (measured as head in layer 2 of unconfined aquifer) between future and present climate (2040-2069, scenario 4C) under pumping conditions, and with heterogeneous hydraulic conductivity distribution. Maps by time step in days 131 to 180.
Positive contours shown at 0.1 m interval. Zero contour is dashed line. Negative contours 0.1 m interval but not shown below -0.5 m (darkest blue colours along rivers only). At day 101, difference map (not shown) has values within 0.1 m of zero.

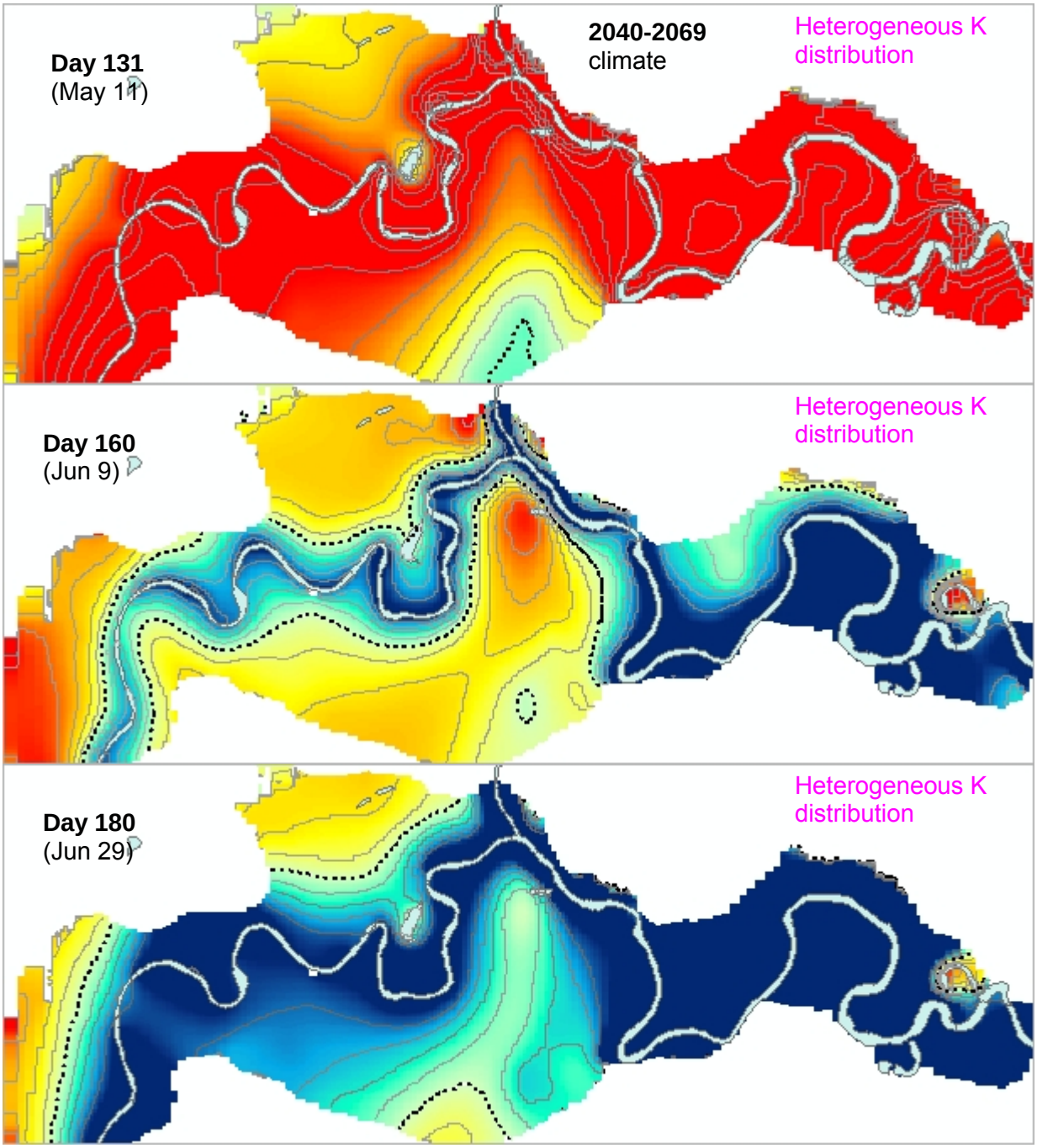

Map 71 Water level differences (measured as head in layer 2 of unconfined aquifer) between future and present climate (2040-2069, scenario 4C) under pumping conditions, and with heterogeneous hydraulic conductivity distribution. Maps by time step in days 205 to 305.
All contours at 0.1 m interval. Zero contour is dashed line.

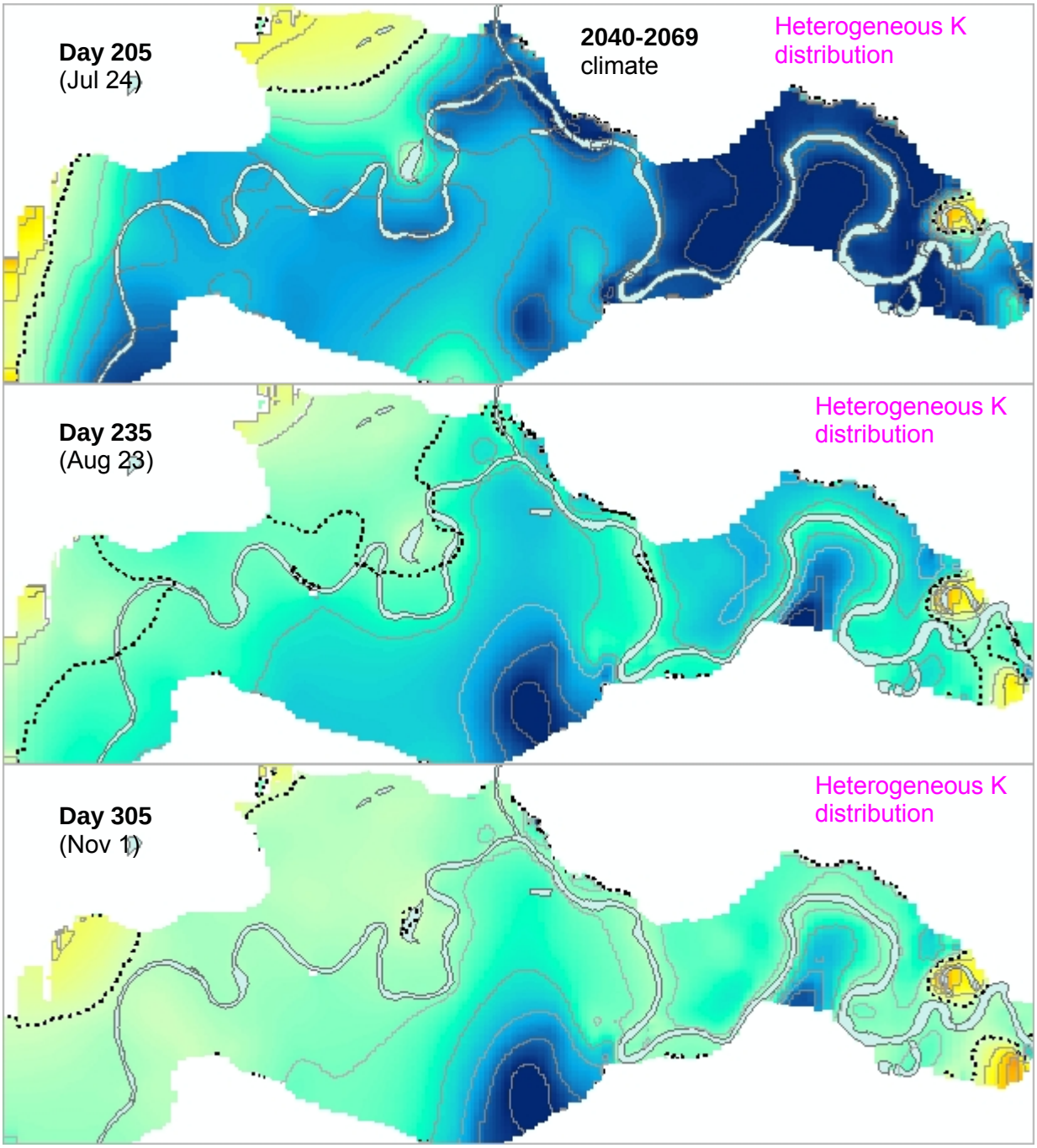

Map 72 Differences between homogeneous K model and heterogeneous K model for different time steps in transient model under present climate and with pumping. Values based on head values in aquifer layer 2. Maps by time step in days 101 to 160.

All contours at 0.1 m interval. Zero contour is dashed line.

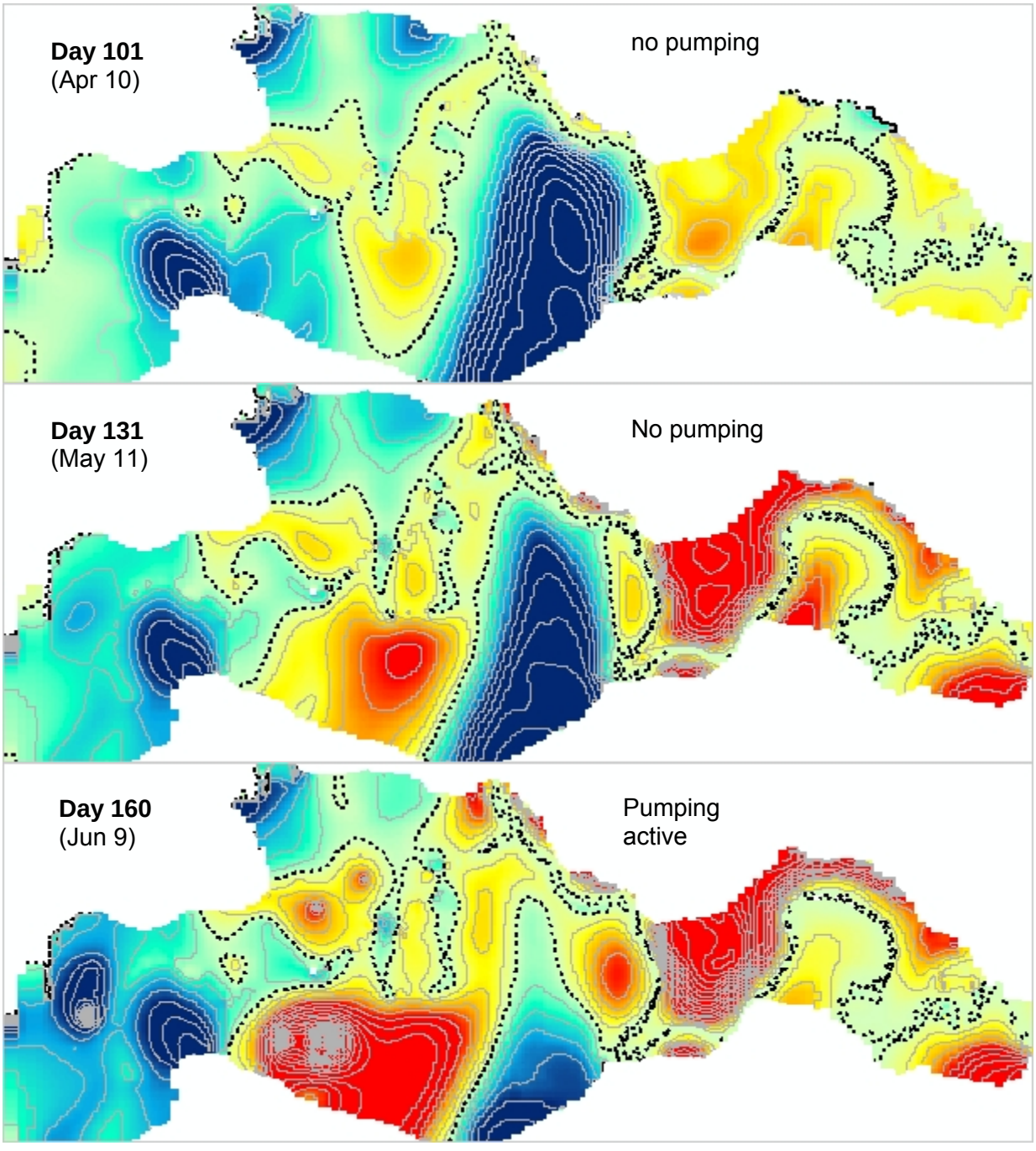

Map 73 Differences between homogeneous K model and heterogeneous K model for different time steps in transient model under present climate and with pumping. Values based on head values in aquifer layer 2. Maps by time step in days 205 to 265.

All contours at 0.1 m interval. Zero contour is dashed line.

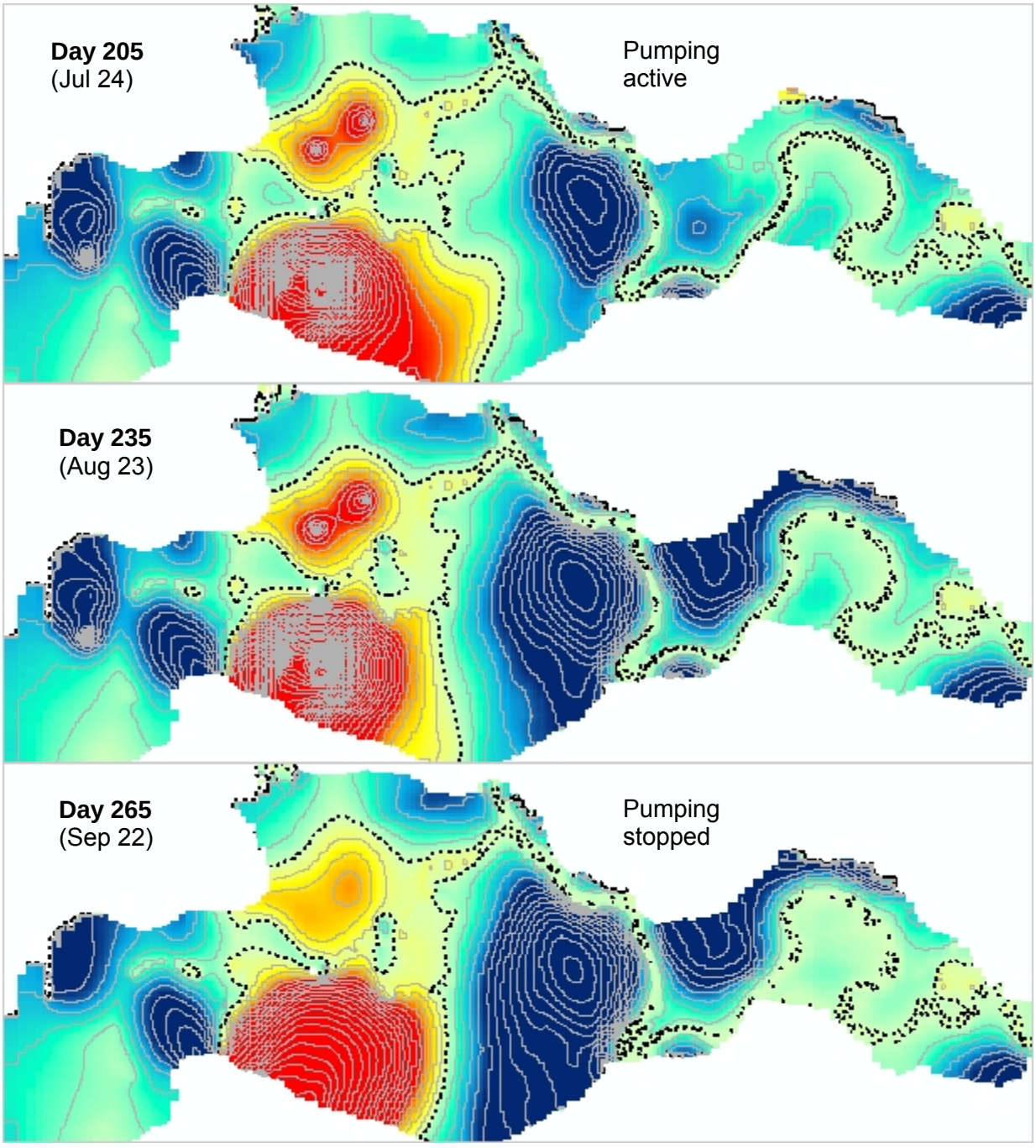

7.4.3 SENSITIVITY OF GROUNDWATER LEVELS TO RECHARGE DISTRIBUTION (SPATIAL AND TEMPORAL)

In model scenario 5A, recharge has a mean annual value for all time steps of the transient model. This scenario is designed to test the sensitivity of the model results to temporal variation in recharge in the Grand Forks aquifer. The methodology was similar for climate change scenarios, where the two models (5A and 1A) were compared at each time step and head difference maps for layer 2 were calculated. Results are shown in Map 74 and 75 for 6 time steps.

Areas of aquifer where temporal variation in recharge does not significantly affect model output are along river floodplains. There, water levels are almost entirely controlled by river water levels. In areas distal from the river, the effect is relatively small, but significant, and it varies over the year. At days 101, 131, 265, and 305, and presumably in winter, the difference in water levels away from the river are less than 10 cm between models 5A and 1A. Thus, if mean annual recharge value was applied due to lack of climate data or good recharge estimates over the year, then modelled water levels would be within 10 cm of that modelled with temporally variable recharge. At days 160 and 205 there are areas where water levels would differ by 20 cm or more (e.g., south-central valley, and north-west section). Overall, compared to the effects of river stage variation over the year, the control of recharge variation over the year on water levels is small.

In model scenario 5B, the only difference between 1A and 5B is spatial distribution of recharge by recharge zones in 1A, but only one large recharge zone in 5B (both have temporal variation in recharge). The one recharge zone in 5B is that of "high" recharge, or representing shallow depth to water table and high hydraulic conductivity of the unsaturated zone. In most areas of the aquifer the variation in depth to the water table and soil permeability class would produce a range of recharge zones, from high to low recharge values as modelled in HELP. The one “high recharge” zone is expected to have higher recharge than scenarios with 65 recharge zones.

Results are in Map 64 and 65 for 6 time steps also. The impact of spatial distribution of recharge on water levels is much larger than of temporal variation in recharge (as in model 5A). All differences in Map 76 to 77 are positive and typically between 10 and 20 cm. The interpretation is that recharge zonation in this case reduces recharge from maximum to a range of values depending on recharge zone. In the Grand Forks aquifer, the model is sensitive to recharge only away from river floodplain and the maximum change expected (within the range of recharge values between the 65 recharge zones as used in this report) in water table elevation is between 10 and 50 cm, but typically about 20 cm.

Map 74 Water level differences (measured as head in layer 2 of unconfined aquifer) between scenario 5A and 1A (effect of spatially distributed recharge), and with heterogeneous hydraulic conductivity distribution. Maps by time step in days 101 to 160.
Positive contours shown at 0.1 m interval. Zero contour is dashed line. Negative contours not shown. Darkest blue colours indicate values < -0.5 m (along rivers only).

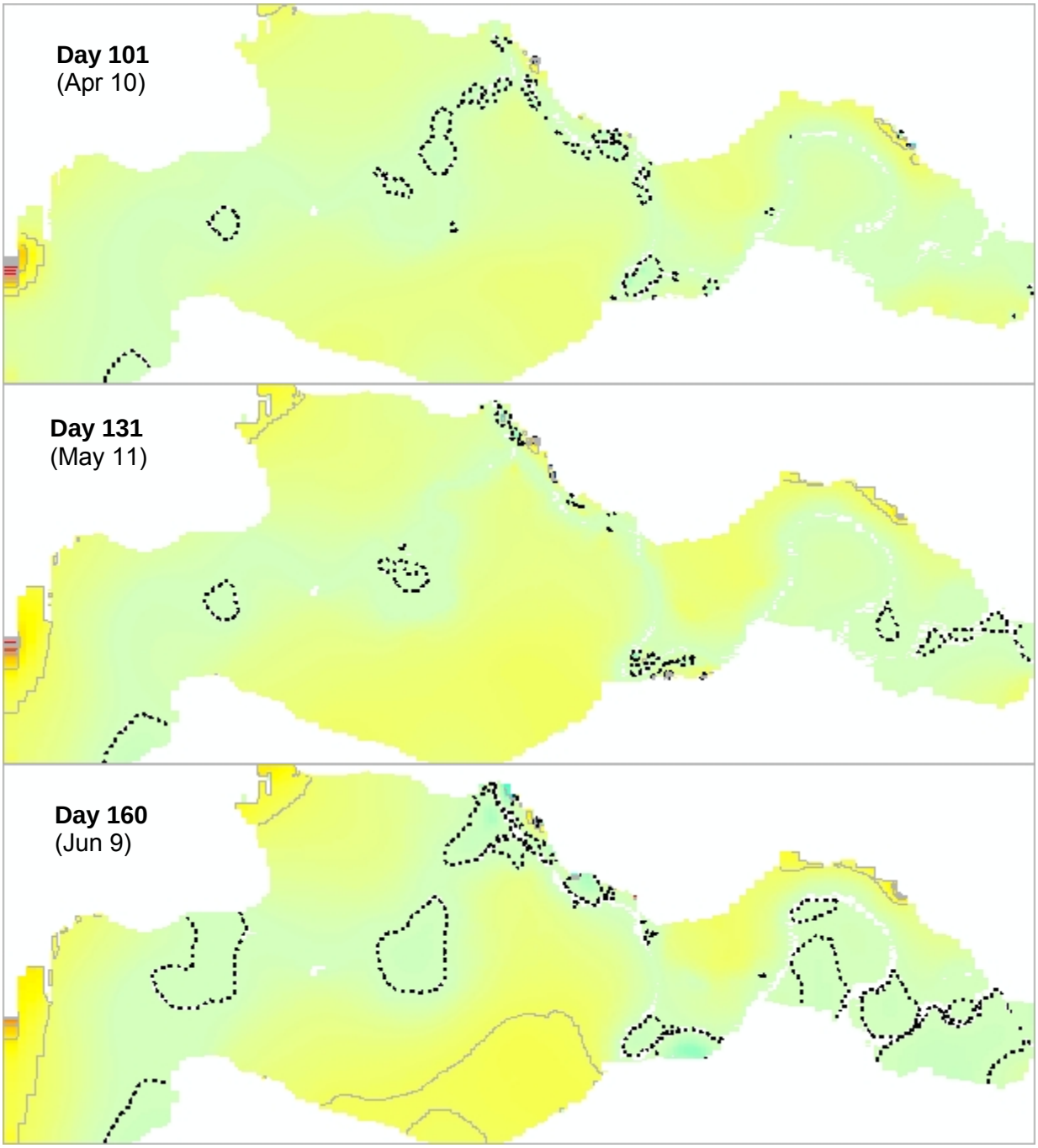

Map 75 Water level differences (measured as head in layer 2 of unconfined aquifer) between scenario 5A and 1A (effect of spatially distributed recharge), and with heterogeneous hydraulic conductivity distribution. Maps by time step in days 205 to 305.
Positive contours shown at 0.1 m interval. Zero contour is dashed line. Negative contours not shown. Darkest blue colours indicate values < -0.5 m (along rivers only).

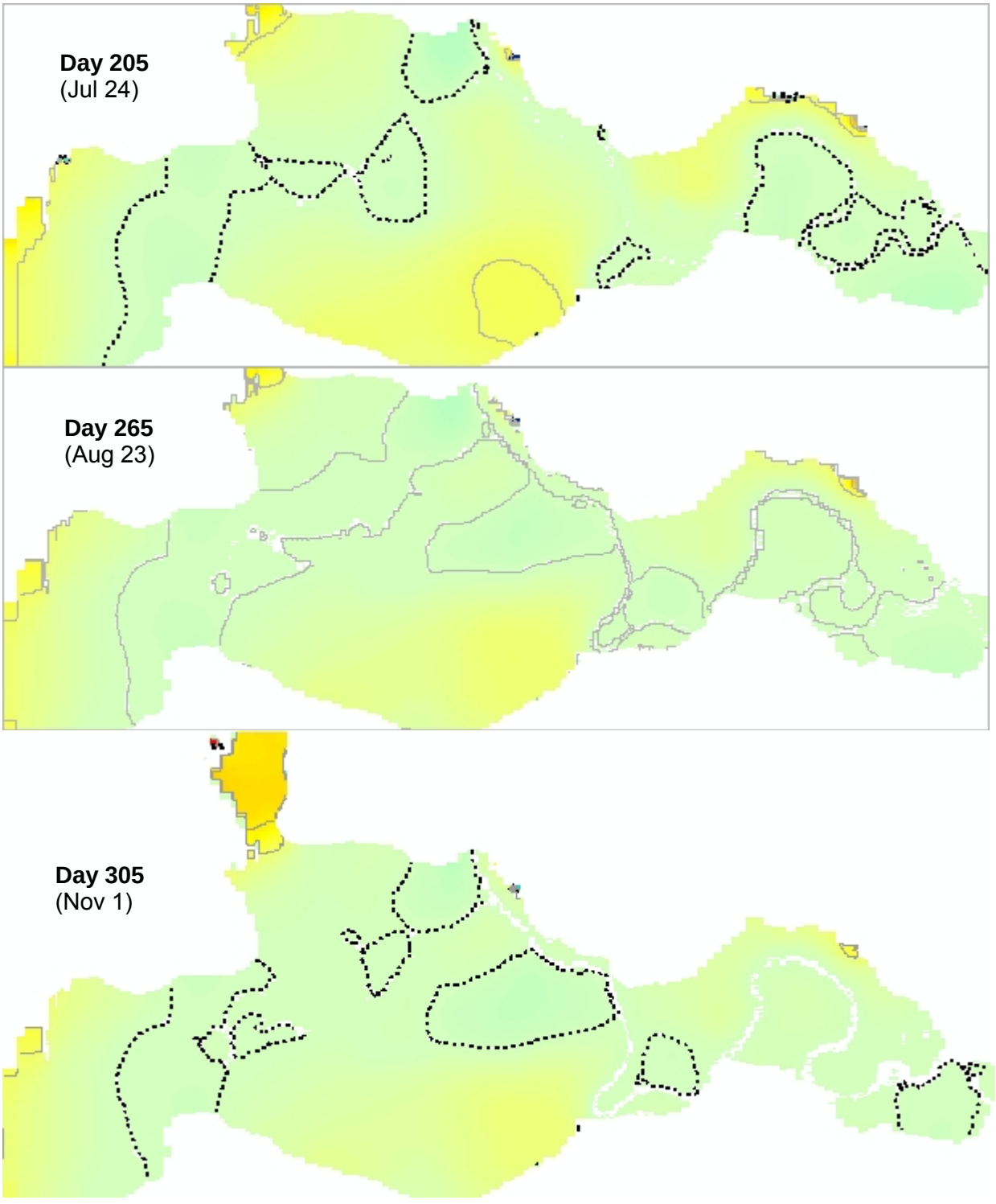

Map 76 Water level differences (measured as head in layer 2 of unconfined aquifer) between scenario 5B and 1A (effect of spatially distributed recharge), and with heterogeneous hydraulic conductivity distribution. Maps by time step in days 101 to 160.
Positive contours shown at 0.1 m interval. Zero contour is dashed line. Negative contours not shown. Darkest blue colours indicate values < -0.5 m (along rivers only).

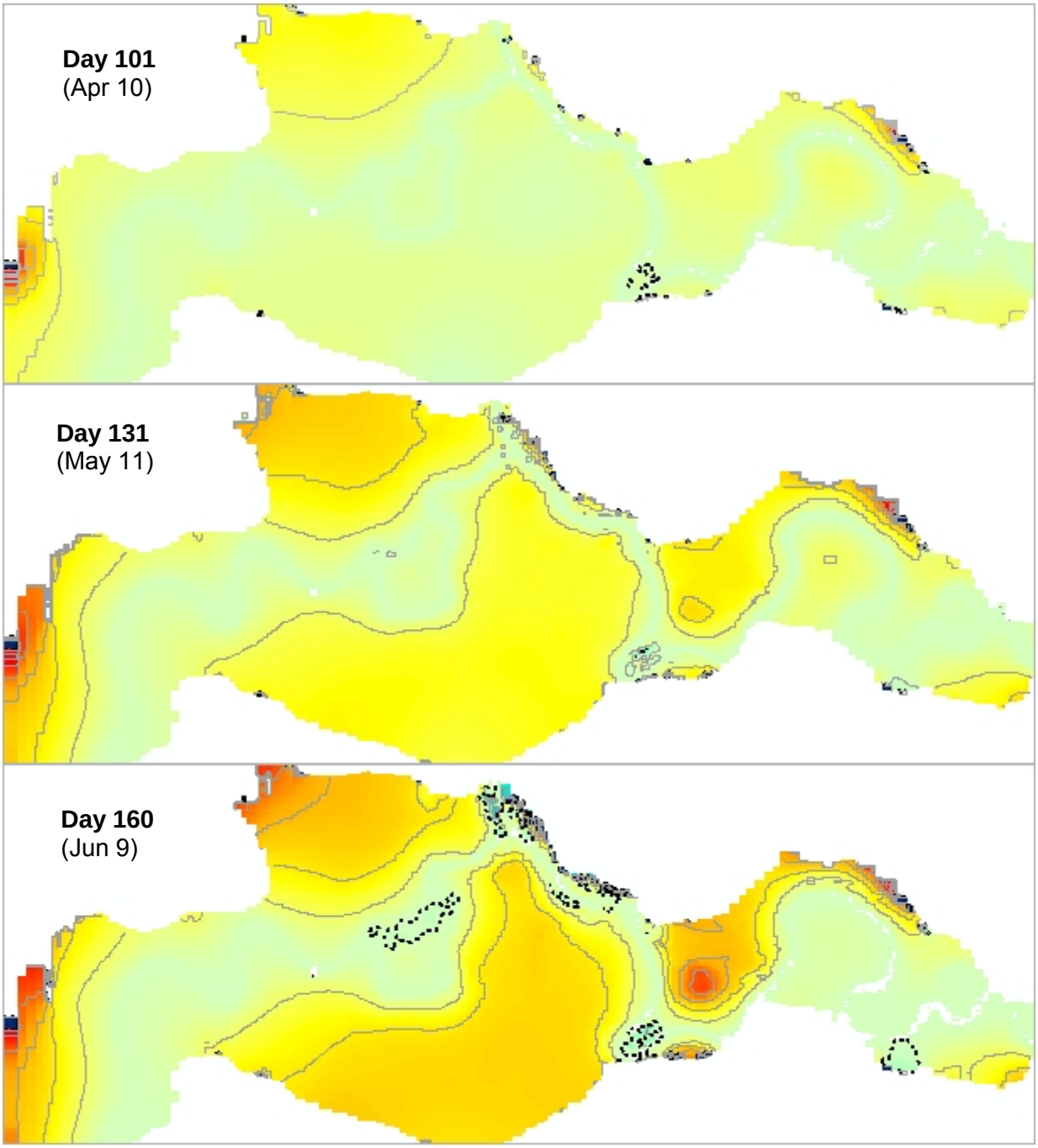

Map 77 Water level differences (measured as head in layer 2 of unconfined aquifer) between scenario 5B and 1A (effect of spatially distributed recharge), and with heterogeneous hydraulic conductivity distribution. Maps by time step in days 205 to 305.
Positive contours shown at 0.1 m interval. Zero contour is dashed line. Negative contours not shown. Darkest blue colours indicate values < -0.5 m (along rivers only).

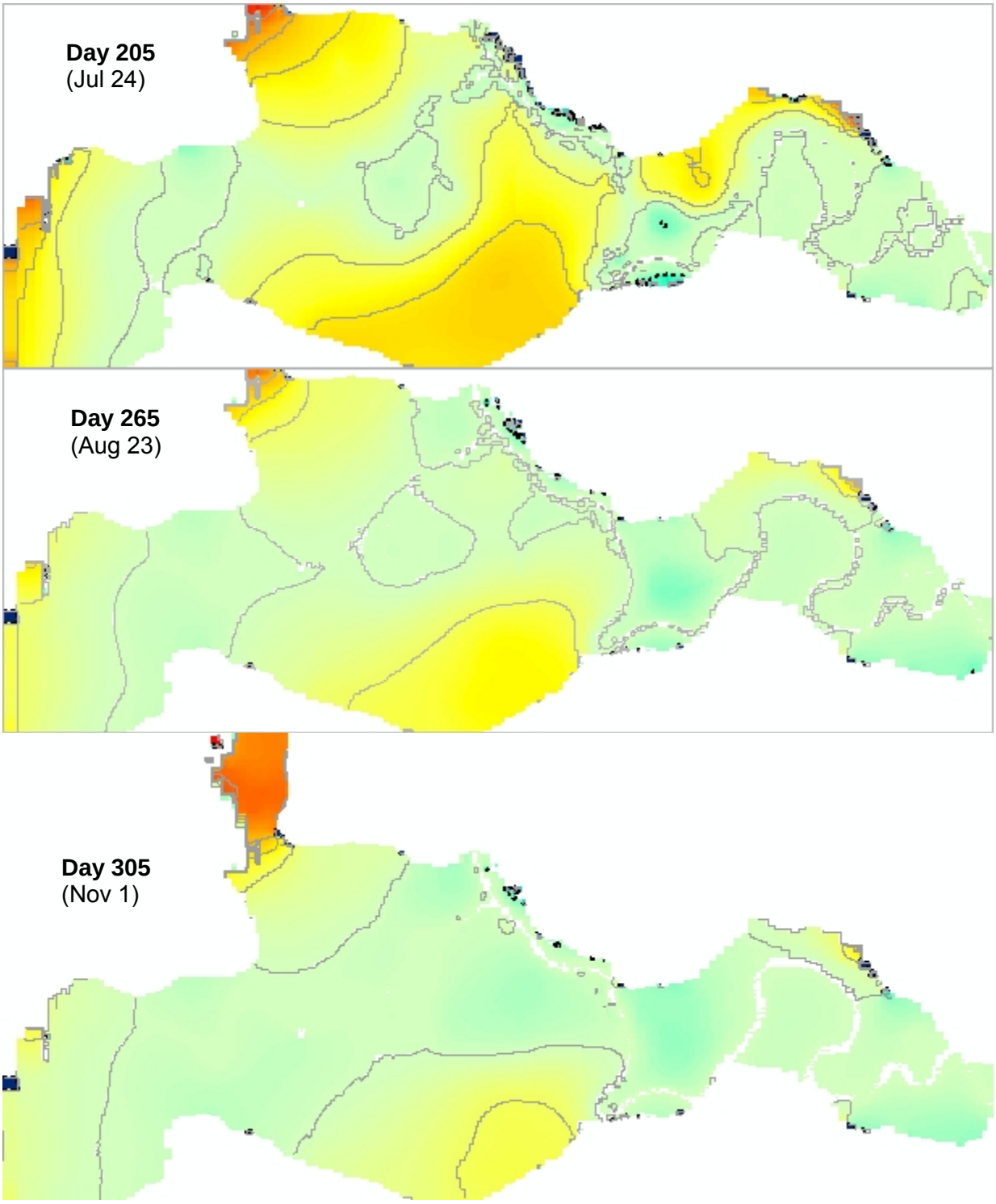

8. SIMILAR AQUIFERS IN BC

The final component of this research was use existing information on aquifers in BC to identify other aquifers within the province that may behave similarly to Grand Forks under climate change conditions. As described throughout this report, the Grand Forks aquifer has a high degree of interaction with the Kettle and Granby Rivers under current climate conditions. Modelling has demonstrated the high degree of impact under climate change due to changes in river stage alone. Thus, it might be inferred that similar aquifers (i.e., those that have strong potential interaction with surface water and that are unconfined and permeable) might exhibit similar types of responses.

8.1. AQUIFER CLASSIFICATION

Many aquifers in BC have been classified by the BC Ministry of Water, Land and Air Protection. The aquifer classification system has two components, of which the classification component is directly relevant to the current study. The classification component categorizes aquifers according to level of development (use) and vulnerability to contamination categories. The composite of these two categories is the Aquifer Class.

The level of development of an aquifer is determined by subjectively assessing demand verses the aquifer's yield or productivity. A high (I), moderate (II), or low (III) level of development can be designated. The vulnerability of an aquifer to contamination from surface sources, or equivalently to potential climate change, is assessed based on: type, thickness and extent of geologic materials overlying the aquifer, depth to water (or top of confined aquifers), and the type of aquifer materials. A high (A), moderate (B), or low (C) vulnerability can be designated. The combination of the three development and three vulnerability categories results in nine aquifer classes. For example, a class IA aquifer would be heavily developed with high vulnerability to contamination, while a IIIC would be lightly developed with low vulnerability. A priority is implied where IA aquifers are the highest priority aquifers in the province and IIIC aquifers are the lowest.

The Aquifer Classification System provides a useful screening and prioritizing tool for the management and protection of developed aquifers in the province. The resultant aquifer classification maps are also an effective tool to educate the public and decision makers about the occurrence and general nature of aquifers in a given region. To-date, over 450 developed aquifers have been identified, delineated and classified in British Columbia. Potential aquifers that have not been developed have not been identified nor classified due to lack of data. Roughly 10% of the aquifers are subjected to heavy use and a third of the aquifers are considered highly vulnerable to contamination. It’s estimated that over half of the 750,000 persons reliant on groundwater obtain water from unconfined, highly vulnerable aquifers. Over 90% of these aquifers are used for drinking water.

8.2. IDENTIFYING AQUIFERS

Information on classified aquifers in BC is available to the public through the internet (http://www.elp.gov.bc.ca/wat/aquifers/index.html). Aquifers on the site are classified according to the methodology above. In collaboration with Mike Wei (BC MWLAP), BC aquifers were identified that meet all the following criteria:

1. type "A" aquifers (generally unconfined and consisting of permeable geologic materials),
2. are heavily (Type I) to moderately (Type II) used,
3. have a strong potential for interaction with surface water (generally with rivers or streams, but in a few cases with lakes).

Table 33 summarizes the results of that work, and lists the BC aquifer number and name, the BC classification, and the name of the river (stream or lake) that is expected to interact with the aquifer. Note that in some instances Type IIIa aquifers are included because they are located in high potential growth areas. Some Type I or Type II aquifers were not included due to their relatively small size. A few aquifers are bounded by the ocean, but are not included.

Several aquifers are identified in bold face in Table 33 because of a high degree of certainty in interaction. The results indicate that aquifers that meet the criteria are widely distributed across the province (Map 78); however, the degree to which interaction occurs and also the degree to which climate change may impact groundwater are not possible to ascertain without more detailed studies at each site. Nevertheless, these aquifers (particularly those aquifers identified in bold type) should be targeted for long-term monitoring. Many of these aquifers have provincial observation wells situated nearby, which could be used for more in depth studies of climate variability and climate change impacts on the aquifers. In addition, it would be worthwhile holding stakeholder meetings in selected areas to discuss climate change impacts on groundwater resource sustainability and providing guidance for long-term monitoring and study.

Map 78 Map of British Columbia showing the location aquifers that may be sensitive to climate change through river interaction.

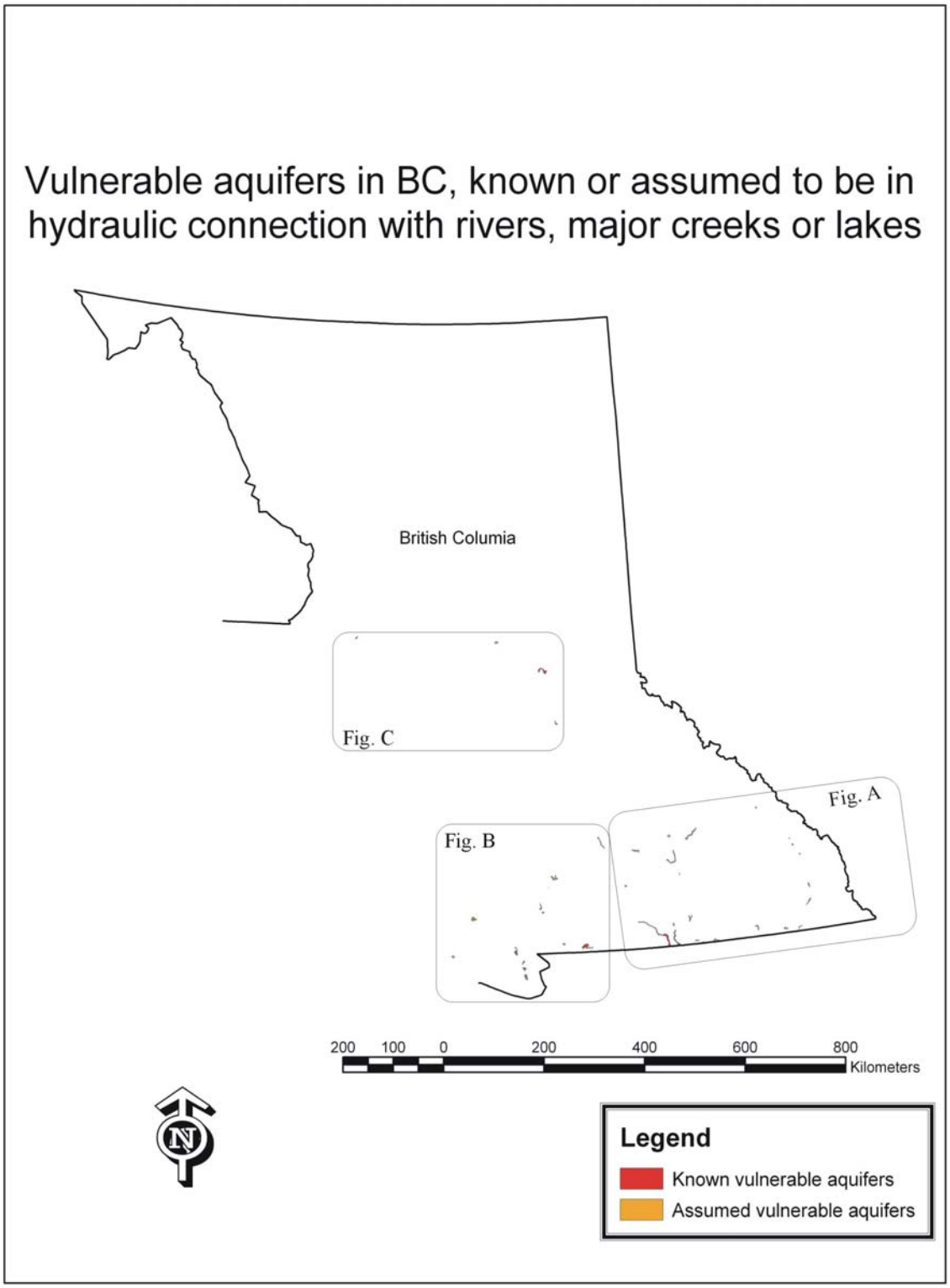

Map 79 Fig. A inset map (refer to Map 78)

Fig. A

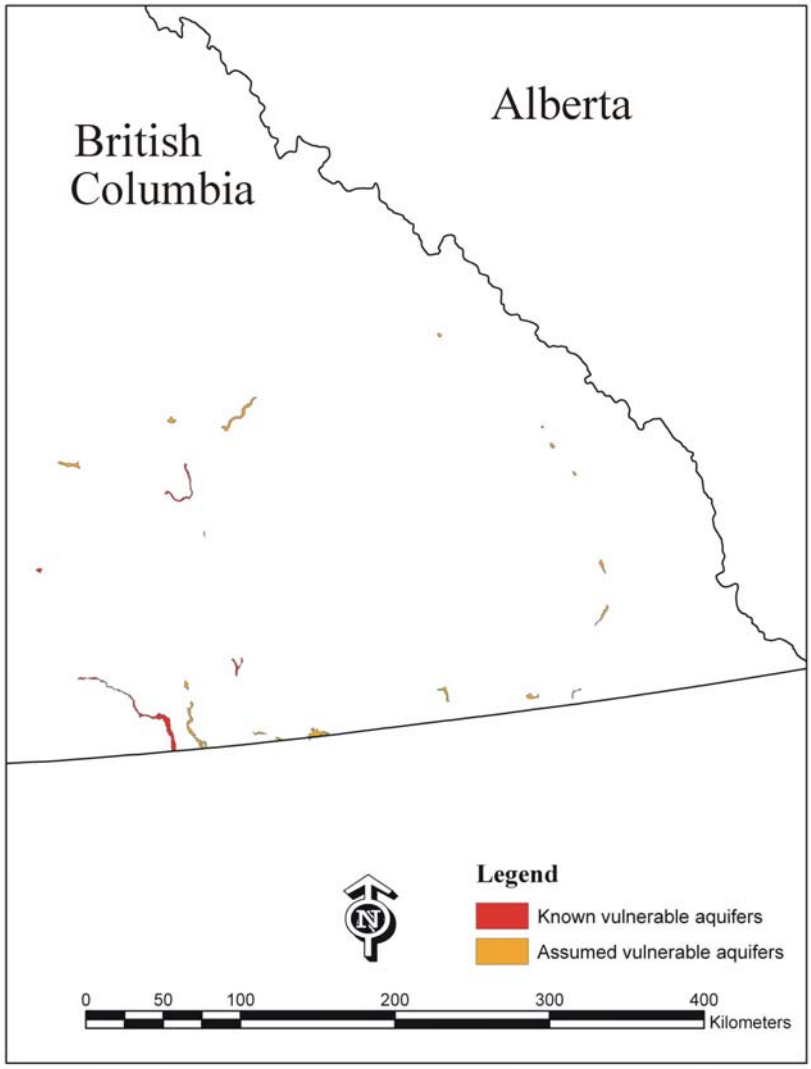

Map 80 Fig. B inset map (refer to Map 78)

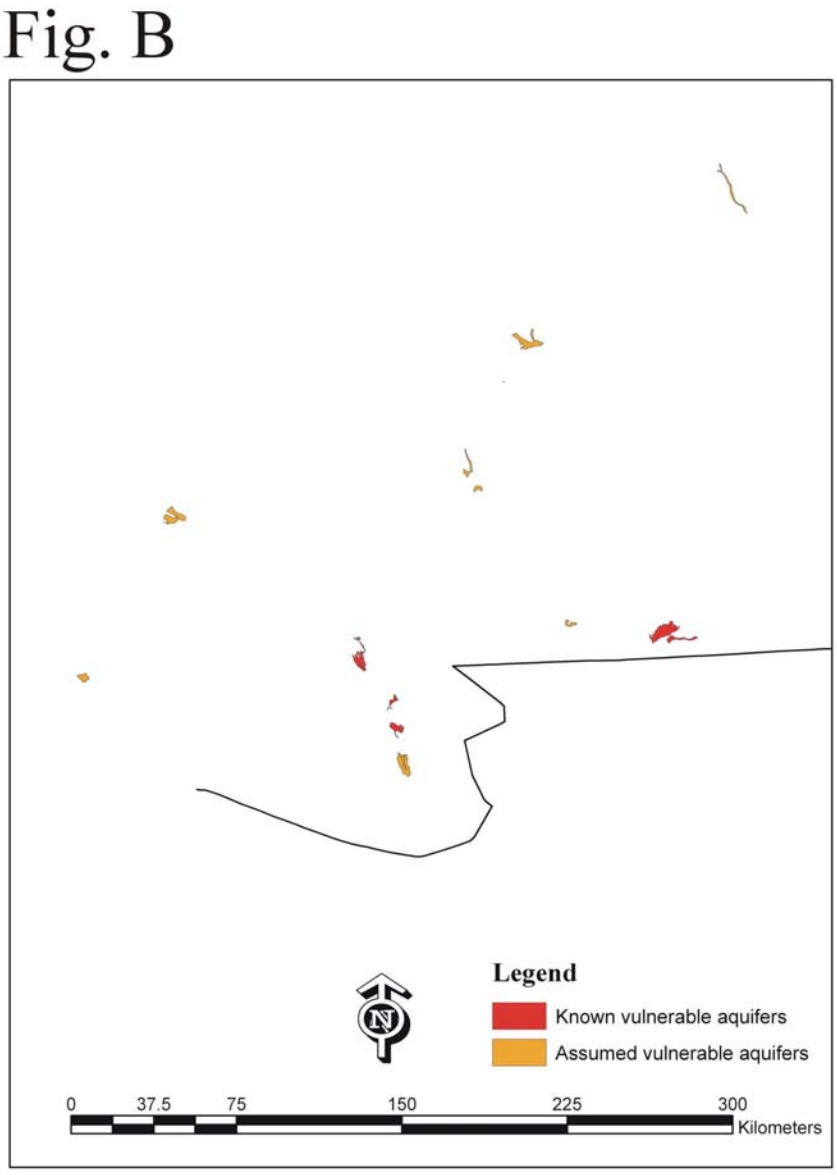

Map 81 Fig. C inset map (refer to Map 78)

Fig. C

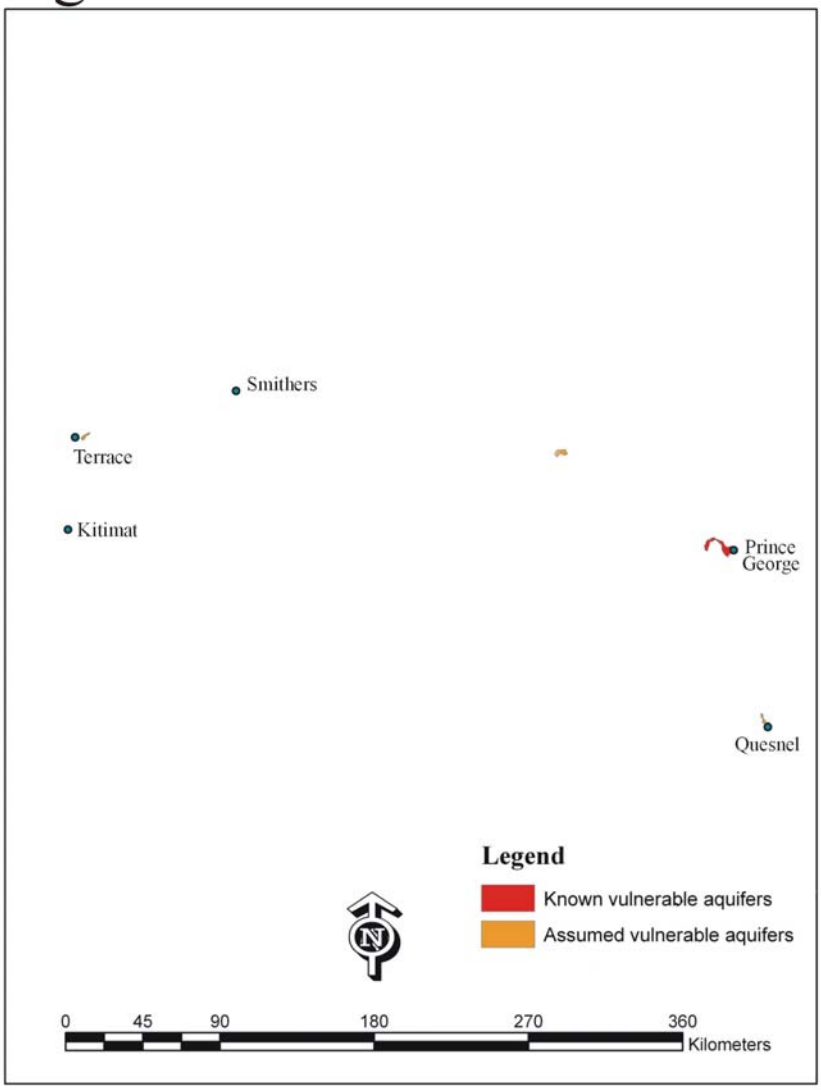

Table 33 Vulnerable[1] aquifers in BC that are known (bold type) or assumed (normal type) to be in hydraulic connection with Rivers, major Creeks or Lakes

Aquifer Number	Aquifer Name	Aquifer Classification	River(s) Interaction
008/009	Chilliwack – Vedder Crossing	IA / IIA	Chilliwack River
036	**Fort Langley**	**IIA**	**Fraser River**
074	Merritt	IA	Nicola and Coldwater Rivers
092	Prince George	IA	Fraser and Nechacko Rivers
097	Salmon River near Armstrong	IIA	Salmon River
115	**Quesnel**	**IIA**	**Quesnel River**
134	**Cache Creek**	**IA**	**Cache Creek**
158	**Grand Forks**	**IA**	**Kettle and Granby Rivers**
159	**Uclulet**	**IIA**	**Lost Shoe Creek**
161	Cassidy	IIA	Nanaimo River
172	Chemainus	IIA	Chemainus River
186	Duncan	IA	Lower Cowichan River
193 /194	**Osoyoos**	**IIA**	**Osoyoos Lake**
203	**Shawnigan Lake**	**IIA**	**Shawnigan Lake**
229	**Scotch Creek**	**IIA**	**Scotch Creek**
254	**Oliver**	**IA**	**Osoyoos Lake**
255	**Tugulniut Lake**	**IA**	**Tugulniut Lake to Vaseux Lake**
259	Princeton - Keremeos	IIA	Similkameen River
263	**Okanagan Falls**	**IIA**	**Skaha Lake**
282	**North Kamloops**	**IIIA**	**Thompson River**
307	**Malakwa**	**IIA**	**Eagle River**
326	**Pemberton**	**IIIA**	**Lillooet River**
346	**Vernon**	**IA**	**Kalamalka Lake**
370	**Quesnel**	**IIA**	**Fraser River**
373	**Fort Saint James**	**IIA**	**Nahounli Creek**
390	**Green Lake N of Whistler**	**IA**	**Green Lake**
396/401	**Squamish**	**IIIA**	**Cheakamus River**
398	**Mamquam**	**IIIA**	**Mamquam Creek**
401	**Cheakamus**	**IIA**	**Cheakamus River**
413	**Courtenay**	**IIA**	**Trent River**
417	**Courtenay**	**IIIA**	**Comox Lake**
454	**Nicholson**	**IIA**	**Columbia River**
459	**Fairmont Hot Springs**	**IIA**	**Columbia River**
477/478	**Midway**	**IIA**	**Kettle River**
482	Beaverdell	IIIA	Beaverdell River
487	**Creston**	**IIIA**	**Goat River**
491/492	**Curzon/Yahk**	**IIIA/IIA**	**Moyie River**
496	**Salmo**	**IIA**	**Salmo River**
524	**Cranbrook**	**IIA**	**Joseph Creek**
540	**Wasa**	**IA**	**Kootenay River**
571	**Thornhill**	**IIA**	**Skeena River**
602	**Radium**	**IIA**	**Columbia River**
603	**Invermere**	**IIA**	**Windermere Lake**

[1] Vulnerability is here defined to be an aquifer that is classified as a Type IA or IIA aquifer, where I denotes highly used, II denotes moderately used, and a denotes permeable and unconfined. In some cases Type IIIa aquifers are included as these are located in potential high population growth areas. Some Type I or II aquifers are not included as they were considered very small. Aquifers that are bounded by the ocean are not included.

9. SUMMARY AND CONCLUSIONS

9.1. HYDROGEOLOGY OF THE GRAND FORKS AQUIFER

The bedrock surface of Grand Forks valley was eroded by glacial processes during the Wisconsin glaciation, and by pre-glacial fluvial erosion. The valley shape was modelled using profile extrapolation, constrained with well lithologs, and geostatistical interpolation. The valley attains a maximum depth of 250 m below ground surface, but typical sediment thickness is about 100 m. The gravel in layer 1 is mostly of fluvial origin and has been reworked by the meandering Kettle River. The sand in layer 2 may be of fluvial or glaciofluvial (more likely) origin – some type of outwash. The silt layer refers most likely to glaciolacustrine silt, which may have been deposited in a ponded glacial lake as the Cordilleran Ice Sheet melted. The clay layer 4 could represent glacial till or combination of till and glaciolacustrine and other sediments, but clay is abundant. It is probably not continuous as suggested by the layered model here. The unconsolidated sediments thicken toward the middle of the valley, have presumed horizontal stratigraphy, and the topmost coarse grained sediments form the Grand Forks Aquifer. The stochastic simulation of valley hydrostratigraphic units (T-PROGS) from interpreted borehole lithologs suggests that the aquifer is much larger and deeper than represented in the layered model. It is also more complex in structure and much more heterogeneous. The Markov-chain stochastic model is much more true to original litholog data (classified) and is locally exact, but interpolates between lithologs producing complex lens configurations, which differ between model realizations. Where there is a high density of boreholes, the results tend to agree between different realizations.

9.2. HYDROLOGY

The streamflow hydrographs were dominated by a spring snow melt event, followed by low flow until early winter. The Granby River basin has larger runoff, thus, it is a wetter catchment than any of the sub-basins of the Kettle River. There were also small differences in runoff between stations on Kettle River. Since the hydrograph shape changes past the confluence of Kettle and Granby Rivers, the hydrograph derived for upstream section of Kettle River in Grand Forks valley was downscaled from more complete flow records upstream of the valley. The hydrograph derived for the downstream section of Kettle River was the sum of Kettle and Granby Rivers. The watershed of the Kettle River reacts similarly to climate change at different catchment scales. The most noticeable trend is of lower discharge in the latter decade for hydrograph months May to February. The largest decrease in flow occurred in the early fall months, establishing a new date for lowest river flows in mid-September (from previous lowest flow in January).

The water balance and the relation of water levels in the observation well in the valley aquifer and the Kettle River, established that the valley aquifer is hydraulically linked to the river. Kettle River discharge is much greater than the inflow of tributaries in the valley watershed, but many of the water balance components in the valley aquifer are not quantified. The numerical flow model of Kettle and Granby rivers, BRANCH, showed that channel geometry is variable and affects stage-discharge relation along the river channel. The calculated rating curves, together with an automated mapping of river water elevations to groundwater flow model of the valley aquifer, allowed for modeling of seasonal variation of groundwater levels and their sensitivity of changed river hydrographs.

CGCM1 downscaling was also used to predict basin-scale runoff for the Kettle River upstream of Grand Forks. The streamflow hydrographs were analysed and compared. The streamflow hydrographs were dominated by a spring snow melt event, followed by low flow until early winter. In future climate scenarios the hydrograph peak is shifted to an earlier date, although the peak flow remains the same. Changes to the river hydrograph are predicted to be much larger by 2040-2069 than by 2010-2039 years, compared to historical 1961-1999 time period. The hydrograph derived for the downstream section of Kettle River was the sum of Kettle and Granby Rivers. Kettle River discharge is much greater than the inflow of tributaries in the valley watershed, but many of the water balance components in the valley aquifer are not quantified.

9.3. RECHARGE

This report also detailed the methodology developed for modelling recharge to the Grand Forks aquifer under both current climate and predicted climate scenarios. The approach consisted of deriving climate parameters from a downscaled a CGCM1 model, using these climate parameters to drive a weather generator, and using the output climate as input to a hydrologic model (HELP). A limitation of the existing climate model (CGCM1) was identified when calibration of historic data was undertaken. We observed that CGCM1 is unable to adequately model precipitation for Grand Forks, especially in the summer months, giving an underestimate of precipitation up to 40% compared to observed, even after downscaling with a well-calibrated model (Figure 30). These are fundamental limitations of CGCM1 predictions and considered "model bias", where the model is the general circulation model.

The downscaling of CGCM1 results was accomplished using 2 independently calculated methods: 1) using SDSM software (at Simon Fraser University by authors of this report), and 2) by Environment Canada using an altogether different method. Summer precipitation is predicted to increase in July and August, but in other months there are either no changes or decreases. The % of wet days in summer months is predicted to increase in future climate scenarios. For temperature, the results are simple and consistent: temperatures are predicted to increase in all months from present to future. The two downscaling methods used agree that summer temperatures will increase at relatively constant rate of 1ºC per 30 years.

The use of spatial analysis tools in a GIS environment allowed for spatial and temporal data integration. Therefore, the following results have both temporal and spatial components. This has not been done for any aquifer in BC, especially regional aquifers. The temporal variation of precipitation was accounted for by calculating monthly recharge values (as opposed to annual only), which give a relatively good temporal distribution of recharge and capture the main inter-annual variation. Most aerial recharge probably occurs either during snowmelt or during large rainstorms. Much better precipitation and other climate data were used (at higher temporal resolution), and a much more detailed climatological study was done to represent the climate change scenarios. The new LARS-WG weather generator allowed for better representation of dry and wet spells and provides a better fit to observed data. Higher resolution CRCM1 results and stochastic weather from LARS-WG were used for climate scenarios: Overall, the recharge model in HELP accounted for soil properties, hydraulic conductivity, depth of unsaturated zone.

According to the HELP model results, in this climatic region there isn't enough precipitation to recharge the aquifer where there are thick sand and gravel terraces – most of the precipitation changes moisture content in these areas of thick gravels above water table, but little of it recharges the groundwater aquifer. This situation would be different if this was a wet climatic zone – most recharge would occur in most permeable areas with less influence on depth of sediment to water table. The HELP modeled-recharge is similar in magnitude but smaller than

previously estimated, and results indicate that Grand Forks receives between 10% and 80% of recharge from precipitation.

HELP was set up to model recharge to 64 combinations of site conditions, which encompassed variations in depth to water, soil type and vadose zone permeability. Ultimately, distributed recharge maps were generated for Grand Forks, which capture the spatial and temporal variability of this critical model input parameter. The temporal variation of precipitation was accounted for by calculating monthly recharge values (as opposed to annual only); this gave a relatively good temporal distribution of recharge and captured the main inter-annual variation. The new LARS-WG weather generator was used rather than WGEN (the weather generator within HELP). This allowed for better representation of dry and wet spells and provided a better fit to observed data. Higher resolution CRCM results and stochastic weather from LARS-WG were used for climate scenarios.

It was observed that the HELP model is sensitive to depth of vadose zone (percolation layer), soil type, K sat of vadose zone. Therefore, in order to achieve accurate results for recharge, it is important that the spatial variability of these key variables be known.

Spatially distributed mean annual recharge to the Grand Forks aquifer (mm/year). Values range from near 0 to 100 mm/year. The western and the northwestern portions of the aquifer receive the lowest recharge, while the highest recharge is received in the more central and eastern portions of the aquifer. According to HELP model results, in this climatic region there isn't enough precipitation to recharge the aquifer where there are thick sand and gravel terraces – most of the precipitation changes moisture content in these areas of thick gravels above water table, but little of it recharges the groundwater aquifer. This situation would be different if this was a wet climatic zone where most recharge would occur in most permeable areas with less influence on depth of sediment to water table. Previous recharge modelling showed that the range of recharge determined for the Grand Forks aquifer is 76.56 mm/year to 165.71 mm/year, with a "representative" recharge of 135.46 mm/year. The HELP modeling results and spatial distribution of recharge zones suggests the recharge value to be typically between 10 and 80 mm/year, showing strong zonation (floodplain versus terraces).

In terms of recharge as a percentage of monthly precipitation, Grand Forks receives between 10% and 80% of recharge from precipitation, according to HELP output. In spring time, it receives 40% to 80% recharge from precipitation depending on soil properties and K properties, and in summer the values are 30% to 50%. During late summer the aquifer receives 60% to 90% of precipitation, but overall recharge (in mm) is small because rainstorms are infrequent. The LARS-WG preserves the intensities of rain events; we observe that if a high intensity event occurs during the late summer (such as a thunderstorm), it rains heavily and most of the water infiltrates the aquifer. Had it rained slowly and over a longer time, much more of it would evaporate. This type of relation may be very different in other climate regions and in other aquifers where high intensity rainfall events may lead to increased runoff and less infiltration.

9.4. GROUNDWATER MODELLING RESULTS

9.4.1. MODEL DESIGN AND CALIBRATION

The layered hydrostratigraphic model of Grand Forks valley sediments assumes uniform or homogeneous hydraulic conductivity and storage properties in each layer. Each layer has an average hydraulic conductivity, initially assigned based on average hydraulic conductivity values determined from pump test data, but later modified during model calibration (within reasonable range). A second hydrostratigraphic model was constructed where the hydraulic properties were distributed in top two aquifer layers. This model was called “heterogeneous aquifer” model.

The transient model incorporates the updated valley and aquifer architecture compared to earlier steady-state layer models which were based on simplified three dimensional structure. All layers were edited in trouble areas, especially along valley walls, and between layer contacts to smooth out irregularities caused by import and interpolation errors between GMS and Visual MODFLOW. A new ground surface DEM was imported at re-sampled 10 m resolution, and all river channels were edited to correspond to surveyed river channels (roughly). The MODFLOW grid was changed and increased in density to improve river channel representation, and production well locations were moved to correct locations. Observation wells were re-imported. The surface DEM was also edited in several spots after consultation with floodplain maps – more accurate topographic maps than the DEM. An additional model layer was added below layer 4 (clay) and shaped to create deep sand lens in eastern part of valley (elsewhere the layer was inactive). River cells and recharge zones were re-mapped based on newly acquired orthophotos (TRIM river outlines were often in wrong locations) and re-imported to the MODFLOW files. In effect, the all parts of the model were modified from the original steady-state model, yet preserving the general valley hydrostratigraphy.

During calibration, in terms of calculated groundwater level at the location of Observation well 217, the model was most sensitive to changes in specific yield (Sy) and horizontal hydraulic conductivity (Kxy) in Layer 2. Calibration was done to the "modelled" river hydrograph, which has model bias to actual observed. Mass balance discrepancies for most zones and most time periods were between 0 and 0.2 %, which is very good for the purposes of this modelling study. The normalized RMS for residuals between calculated and observed head was 8.9% for time step 160, and it was reduced to about 8% if large and anomalous residuals were excluded. Static water levels in observations wells contained many poor-quality data, where static water levels had unexplained and large errors. The provincial DEM is inaccurate in many parts of the Grand Forks valley, and that most of reported well elevations appear to be correct. A few very large positive differences are clearly errors in DEM surface near steep valley walls – valley walls protrude too far inside valley floor and are a result of poor interpolation or digitizing of topographic maps that served as source for DEM.

9.4.2. GROUNDWATER FLOW PATTERNS

Groundwater elevation in the unconfined aquifer slopes downward from west to east, following the slope of Kettle River and valley ground surface. Hydraulic gradient maps correspond very closely with the flow velocity map. The highest gradients occur near active pumps, along river channels where there are high terraces above the river and large changes in slope of groundwater surface, and also in areas near valley walls where the groundwater surface is steep. The central-western portion of aquifer has generally steep hydraulic gradients because

the river channel also has steep gradient. This relation is caused by good hydraulic connection of river and surficial aquifer. In the heterogeneous model the gradients near production wells in south-central valley, south of Kettle River are much smaller (smaller drawdown in higher hydraulic conductivity field). In areas away from pumping wells, the hydraulic gradients are similar in magnitude and spatial distribution for both types of models. The positive flux areas along Kettle River in Layer 1 and 2 indicate outflow of water from the river into the aquifer (water loosing river reaches). The negative areas along the river suggest gaining river reaches where the aquifer supplies baseflow to river as seepage. The pattern is complex along the length of the river channel in the valley and outside the floodplain. The model predicts that there are many gaining and loosing river reaches.

9.4.3. CHANGES IN RECHARGE TO AQUIFER IN PREDICTED CLIMATE SCENARIOS

In most zones, recharge increases from winter to summer, then remains high until late autumn and decreases into the winter months. Many zones also have bi-modal distribution, with a smaller peak of recharge in late winter, which corresponds to snowmelt in the valley. The predicted future climate for Grand Forks area from downscaled CGCM1 model will result in more recharge to the unconfined aquifer from spring to summer seasons. The largest predicted increase is from day 100 to day 150, when it is predicted to increase by factor of 3 or more from present levels, according to ZBUD results from all zones. In summer months recharge is also predicted to be approximately 50% greater than at present (in most zones). In the autumn season the recharge is predicted to increase (10 to 25%) or remain the same as present, depending on location in Grand Forks valley. In the winter the CGCM1 weather predictions suggest less precipitation in winter and less recharge to aquifer. Irrigation return flow begins in after day 150 causing increase of aquifer recharge by 10 to 20% in most irrigation district zones.

If different models of climate change are used, the groundwater system may react differently, but the goal of this project was to demonstrate the behaviour of this groundwater-hydrologic-climate system and impacts of climate change as indicated by predictive methods available at this time. In this aquifer, the effect of changing recharge on groundwater levels is very small compared to changes in timing of basin-scale snowmelt events in the Kettle River and subsequent shift in hydrograph.

9.4.4. GROUNDWATER FLOW COMPONENTS AND IMPACTS OF CLIMATE CHANGE

- INTERPRETATIONS ZBUD RESULT INTERPRETATIONS FOR IRRIGATION DISTRICTS OUTSIDE RIVER FLOODPLAIN

During spring freshet on the Kettle River, the rise in river stage causes inflow of water to various irrigation ZBUD zones (after passing through the floodplain area). This excess water is stored in the aquifer. As river stage drops, the hydraulic gradient is reversed and water is released from storage and leaves mostly to the floodplain zone as it returns to river as baseflow. Pumping was started as the river stage began to decrease, and most pumping occurred when water was being released from storage, but during pumping even more water is taken from storage to supply the pumping wells. When pumps are turned off, there is not much excess water left in storage so almost no net flow occurs out of the zone. As most of the pumping water is lost to evapotranspiration on irrigated fields, there is a small reduction in baseflow component to the Kettle River during the pumping period.

- INTERPRETATIONS OF ZBUD RESULT FOR RIVER FLOODPLAIN

The rate of inflow of groundwater from the river and into aquifer along the floodplain zone follows very closely the river hydrograph during the rise in river stage. As the river stage levels off and begins to decrease, the flow direction is reversed within 10 days and the rate of inflow from the river to the aquifer begins to rise, and then dominates for the rest of the year, as water previously stored in aquifer drains back to river as baseflow seepage. Storage rates are less than half of flow rates to/from other zones from the floodplain, and 15 to 20% of flow from/to the river. Even less water drains out the aquifer through drains, as defined in this model (large ditches, lakes, swamps, connected to river).

During peak flow on the Kettle River, the river discharge is about 200 m^3/s upstream of the Granby River confluence and about 350 m^3/s below the confluence. The river-aquifer interaction has maximum flow rate of 41 m^3/s, which translates to between 11 and 20% of river flow during spring freshet (mid value is most likely 15%). Therefore, the river puts about 15% of its spring freshet flow into storage in Grand Forks valley aquifers alone, for a short time, and almost all of that stored water (minus evapotranspiration loss and long-term storage, if any) is eventually released back to river flow – most is released within 30 to 60 days. The long term storage in this groundwater system can be calculated by comparing the area under the storage "from" component to area under the storage "to" flow component. As the areas under the graphs are approximately equal, there is no long term storage. Long term storage would result in long-term changes in average static groundwater levels in the valley. However, the models at this time cannot adequately resolve long term storage trends, given the uncertainties involved. Long term storage should be computed from transient model runs on actual river hydrographs and not averaged ones.

- IMPACTS OF CLIMATE CHANGE:

As the climate impacts on the aquifer are mainly driven by river stage, and because river stage shifts to an earlier date, any ZBUD zone that has strong hydraulic connection to the river, and which shows temporal variation of flow rates driven by changes in the river hydrograph, will have the largest climate-driven changes. As the river peak flow shifts to an earlier date in a year, the "hydrographs" for flow rates also shift by the same interval. These shifted flow rates are superimposed on pumping effects, which were not shifted in time for future climates. Impacts are smallest in zones least connected to the river (away from the river and at higher elevation).

9.4.5. EFFECTS OF AQUIFER HETEROGENEITY ON FLOW COMPONENTS AND IMPACTS OF CLIMATE CHANGE

The various ZBUD zones have different sensitivity to aquifer heterogeneity representation in the model, in terms of flow to storage and inter-zonal flow. Magnitudes of changes differ because zones have different sizes (volumes of aquifer media), but also there is different change in groundwater flow after inclusion of heterogeneity – by definition, heterogeneity varies over the aquifer area, so different effects are expected for various zones of aquifer.

In floodplain zone 2, storage was not affected significantly by heterogeneity of aquifer, but inter-zonal flow was very different and very much larger than in the homogeneous model. In the spatially-distributed Kxy-field the surficial aquifer is much better hydraulically connected to the river and much more flow occurs between the floodplain (and river) and other zones of aquifer.

The flow rates for inter-zonal flow increase by 50-75% as a result of including aquifer heterogeneity. The river-effects extend further from and are stronger away from the river floodplain. Therefore, climate change impacts are larger under heterogeneous model than in homogeneous model.

In zone 3, flow rates were greater in winter and spring than for other zones of similar size. The flow rates were 50 to 75% greater in late spring and summer as a result of including aquifer heterogeneity in the climate scenario models, but during pumping the heterogeneous aquifer provided more water from storage and more water inflowing from adjacent zones, and consequently, less drawdown would be expected than in the homogeneous model.

A large effect of aquifer heterogeneity is predicted for south-central Grand Forks valley, where Zone 5 (Big Y irrigation district) is located. The pump tests in production wells in this district have large hydraulic conductivity estimates and interpolating these over space greatly increases flow rates in the aquifer, compared to lower values assigned to the aquifer layers in the homogeneous models. The drawdown is expected to be much smaller and closer to observed in heterogeneous aquifer scenarios than in original model scenarios. The difference in flow rates in spring time (high flow on Kettle River) are of the same magnitude as modelled in scenario series 2, so the heterogeneous scenario series would have double the flow rates, with some differences between climate scenarios - but the same magnitudes of heterogeneity effect on flow. Much more water would be stored and much more water would flow to and from other zones through this area of aquifer. The hydraulic connection to the Kettle River would be much greater, and larger impacts of climate change (shifts of river hydrograph) are expected in heterogeneous model. Other zones have small to moderate differences between heterogeneous and homogeneous aquifer models, but not nearly as large as in zone 5. Overall, the flow rates would increase.

It can be concluded that including aquifer heterogeneity in this model would create better connections between most zones and with the river, create higher flow rates, less drawdown due to pumping, and cause larger responses to river hydrograph changes as a result of predicted climate changes. These results will be confirmed by spatial maps of head differences between heterogeneous and other model outputs from transient MODFLOW model runs of the aquifer model.

9.4.6. IMPACTS OF CLIMATE CHANGE ON WATER LEVELS IN UNCONFINED AQUIFER

The effects of climate change are difficult to observe on head distribution maps because the high hydraulic gradient in the Grand Forks valley dominates all other trends. The climate-induced changes in water elevations are on the order of 0.5 m, while the gradient in the valley spans about 30 m elevation, so any changes would just shift the water table contours slightly and would be difficult to read. Thus it was necessary to develop a different strategy for displaying any changes induced by climate, which would exclude the hydraulic gradient of the valley (and valley topography) and compare directly the changes from present conditions. Accordingly, head difference maps were prepared to show only differences due to climate change between future climate scenario model outputs and present climate scenario model outputs, separately for pumping and non-pumping models. The pumping effects were also subtracted out in these maps because drawdown was identical in all climate scenarios (pumping rates were constant in all models for the pumping time period).

- 2010-2039 SCENARIO

At day 131 the water levels are higher along the floodplain than at the same day in 1961-1999 historical climate scenario. The main cause is a shift in river hydrograph peak flow to an earlier date, thus creating a positive difference in water levels between 2010-2039 and 1961-1999 models at day 131. In other words, in the future the peak river stage would be earlier and water levels would be higher in the floodplain at an earlier date (also in day 131). This excess water flows into the surficial aquifer and is stored there, as was demonstrated in flow budget section of this report. The zone of storage is roughly along the river floodplain and also in areas where there are higher river terraces. Within a month the peak flow passes and river water levels begin to drop rapidly. By day 160, the river water levels are similar in both 2010 and historical climate models, but only along the river channel. Away from the river channel water levels are elevated by 30 to 40 cm (stored water), which are still draining until day 180. Away from the river, the water levels are still very similar (within 10 cm) to present day water levels at that time of year. By day 180, the river stage has dropped below typical river stage at present climate (again, due to shift in hydrograph), and the water levels in floodplain in 2010 climate are lower by 10 to 40 cm at day 180 than at present climate at that day.

At day 205, the 2010 river water level is still 10 to 20 cm below present at that day, but the increased recharge in 2010 climate over historical climate causes up to 10 cm higher water levels away from the river. This spatial pattern of slightly elevated water levels away from the floodplain relative to present climate continues to day 235 (Aug 23), but by day 305 (Nov 1) the water levels in unconfined aquifer are almost identical to present levels at that time of year. Overall, the climate change effects for 2010-2039 scenario relative to present are limited to the floodplain and to the early part of the year when the river hydrograph shifts and is at peak flow levels. A small increase of water levels due to the increase in recharge is forecast for 2010 climate.

- 2040-2069 SCENARIO

The hydrograph shift is larger than in 2010-2039 climate scenario, so the computed differences to historical climate are similarly larger. Water levels are over 50 cm above normal, but only along the floodplain. The term "above normal" means "occurring earlier in year" but the maximum water levels associated with the peak hydrograph are very similar to present climate because the peak discharge is not predicted to change, only the timing of it. This excess water flows into the surficial aquifer and is stored there, as was demonstrated in flow budget section of this report. The zone of storage is roughly along the river floodplain and also in areas where there are higher river terraces. Within a month the peak flow passes and river water levels begin to drop rapidly. The spatial pattern of slightly elevated water levels away from the floodplain relative to present climate continues to end of the year (longer than in the 2010-2039 scenario). Overall, the climate change effects for the 2040-2069 scenario relative to present are limited to the floodplain and to the early part of the year when the river hydrograph shifts and is at peak flow levels. A small increase of water levels due to increase in recharge is forecast for 2040 climate.

All climate scenarios had identical drawdown effects (at a given K distribution), because the same pumping rates were applied in all pumping scenarios. If pumping rate predictions were available, the drawdown effects would differ in each climate change scenario - but there is no information on predictions of pumping rates in Grand Forks for the future.

9.4.7. SENSITIVITY OF MODEL RESULTS TO AQUIFER HETEROGENEITY REPRESENTATION AND ON PREDICTED IMPACTS DUE TO CLIMATE CHANGE ON WATER LEVELS IN UNCONFINED AQUIFER

At day 131 the water levels are higher along the floodplain than at the same day in 1961-1999 historical climate scenario. The main cause is a shift in river hydrograph peak flow to earlier date, thus creating positive difference in water levels between the 2010-2039 and 1961-1999 models at day 131. The increased heterogeneity caused stronger hydraulic connection with the river over most of the valley area, especially in south-central valley part south of Grand Forks (in Big Y irrigation district of ZBUD zone 5). The excess water is now stored in much larger area that extends far beyond the floodplain, as compared to the smaller extent in homogeneous aquifer model.

Within a month the peak flow passes and river water levels begin to drop rapidly. By day 160, the river water levels are similar in both the 2010 and historical climate models, but the pattern is more complex in the heterogeneous aquifer and there is more variation in groundwater levels as a response to changes in river stage. Away from the river channel water levels are elevated by 30 to 40 cm (stored water), which are still draining until day 180. Away from the river, the water levels are either up to 30 cm higher than at present or are similar to present - where high hydraulic conductivity "conduits" to the river are present and water levels respond very fast to river water levels. By day 180, the river stage has dropped below typical river stage at present climate (again, due to shift in hydrograph), and the water levels in floodplain in 2010 climate are lower by 20 to over 50 cm at day 180 than at present climate at that day, showing more spatial variability in heterogeneous aquifer. The eastern floodplain and adjacent areas are very well connected to the river, causing fast drainage of stored water from previously high river water levels that recharged the surficial aquifer. In the western and northern parts of valley, the hydraulic conductivity field has lower values and water remains in storage with a longer lag time for draining as a response to dropping river water levels.

At day 205, the 2010 river water level is still at least 10 cm below present at that day, but the increased recharge in 2010 climate over historical climate causes up to 10 cm higher water levels away from the river (but now only in areas with low hydraulic conductivity). This spatial pattern of slightly elevated water levels away from the floodplain relative to present climate continues to day 235 (Aug 23), but by day 305 (Nov 1) the water levels in unconfined aquifer are almost identical to present levels at that time of year over most of the aquifer extent, but there are smaller areas where water levels are either lower or higher than expected. The "low" area in south-central valley is unexplained.

Overall, the climate change effects for 2010-2039 scenario relative to present are no longer limited to the floodplain, but extent over most parts of the valley in this heterogeneous aquifer model. Areas where increase in recharge creates higher water levels than at present conditions are only limited to high terraces in west and north parts of aquifer. The effect of heterogeneity on water levels is arguably as strong as the shift of river hydrograph due to climate change.

9.4.8. CLIMATE CHANGE IMPACTS ON WATER LEVELS IN CROSS-SECTION PROFILES

The modelled water level has an almost immediate response to the river, although peak amplitude is lower than that of river, showing effects of groundwater storage. Further away from the river, the amplitude of the hydrograph decreases and also shifts to a later day. The furthest

observation point 2 km from river is only slightly influenced by river stage variation. Climate change effects (river + recharge) are much smaller in magnitude than typical seasonal variation, but are significant.

Prior to pumping in the spring season the climate change impacts are strongest close to river, but very small away from river (thus, recharge variation has a weak effect here). During high river stage and during active pumping from production wells, the change in river stage causes as much change in water levels as does pumping, according to this homogeneous K model, although the heterogeneous model shows a different result. The natural groundwater level variation and pumping drawdown are much larger than climate change effects. After pumping stops, there is quick recovery of water table and climate change impacts remain small.

9.4.9. SENSITIVITY OF MODEL RESULTS TO RECHARGE DISTRIBUTION

There are ZBUD zones where the spatial distribution of recharge has the same (and small) control on flow rates into storage as the temporal distribution of recharge. These zones are 1, 2, 4, and 8 and 9. Storage flow rates show some significant response to recharge in zones 3, 5, 7. The spatial distribution of recharge has consistently greater control on flow rates than temporal distribution of recharge (monthly variation versus mean annual value).

Areas of aquifer where temporal variation in recharge does not significantly affect model output are along river floodplains. In those areas, water levels are almost entirely controlled by river water levels. In areas distal from the river, the effect is relatively small, but significant, and it varies over the year. It can be said that if mean annual recharge value was applied due to lack of climate data or good recharge estimates over the year, then modelled water levels would be within 10 cm of modelled with temporally variable recharge. At day 160 and 205 there are areas where water levels would differ by 20 cm or more (e.g., south-central valley, and north-west section). Overall, compared to the effects of river stage variation over the year, the control of recharge variation over the year on water levels is small.

The impact of spatial distribution of recharge on water levels is much larger than of temporal variation in recharge. Recharge zonation in this case reduces recharge from a maximum to a range of values depending on recharge zone. In the Grand Forks aquifer, the model is sensitive to recharge only away from river floodplain and the maximum change expected (within the range of recharge values between the 65 recharge zones as used in this report) in water table elevation is between 10 and 50 cm, but typically about 20 cm.

10. REFERENCES

Allen, D.M., Mackie, D.C. and Wei, M. (2003). "Groundwater and climate change: A sensitivity analysis for the Grand Forks aquifer, southern British Columbia, Canada." *Hydrogeology Journal, on line publication, June 2003*

Allen, D.M., Scibek, J. and Bishop, T.W. (2003). A collection of Geographical Information System (GIS) maps and related documentation showing the geologic architecture of the Grand Forks aquifer, the vulnerability of the aquifer using DRASTIC, and numerical modelling results for groundwater flow. Provided to the BC Ministry of Water, Land and Air Protection (website address: forthcoming).

Allen D.M., Scibek J., Mackie D.C., Wei M. (2002) "Modelling the impact of climate change on a groundwater system: a case study for south central British Columbia" In Proceedings of the Canadian Geotechnical Society - International Association of Hydrogeologists Joint Annual Meeting, Niagra Falls, Ontario.

Allen D.M. (2000) "Numerical Modelling of the Grand Forks Aquifer, Southern British Columbia." Final report prepared for Groundwater Section, Water Management Branch, BC Ministry of Environment, Lands and Parks (July 2000), Queen's Printer, Victoria.

Allen D.M. (2001) "Groundwater and Climate Change: A Case Study Sensitivity Analysis for the Grand Forks Aquifer, Southern British Columbia." Final report prepared for Groundwater Section, Water Management Branch, BC Ministry of Environment, Lands and Parks (July 2001), Queen's Printer, Victoria.

Allen, R.G., L.S. Pereira, D. Raes, M. Smith (1998) "Crop Evapotranspiration-Guidelines for computing crop water requirements-FAO Irrigation and Drainage", Paper 56. Rome, Food and Agriculture 796, Organization of the United Nations, 797.

Anderson M.P. and W.W. Woessner (1992) "Applied Groundwater Modeling: Simulation of Flow and Advective Transport." Academic Press, 381 pgs

Arnold J.G., R. Srinivasan, R.S. Muttiah, and J.R. Williams (1998) "Large area hydrologic modelling and assessment, Part I. Model development." *Journal of the American Water Resources Association*, 34, 73-89.

Augustinus P.C. (1992) "The influence of rock mass strength on glacial valley cross-profile morphometry: a case study from the Southern Alps, New Zealand." *Earth Surface Processes and Landforms*, 17, 39-51.

Barnett, T.P. and R.W. Preisendorfer (1978) "Multifield analog prediction of short-term climate fluctuations using a climate state vector." *Journal of Atmospheric Science,* 35, 1771–1787.

Beersma J, M Agnew, D Viner, and M Hulme (Eds.) (2000) "Climate Scenarios for Water-related and Coastal Impacts." ECLAT-2 Workshop Report No. 3, Published by Climatic Research Unit, UEA, Norwich, UK.

Boer, G.J., Flato, G.M. and Ramsden, D. (2000) "A transient climate change simulation with historical and projected greenhouse gas and aerosol forcing: projected climate for the 21st century." *Climate Dynamics,* 16, 427-450.

Boer, G.J., Flato, G.M., Reader, M.C., and Ramsden, D. (2000a) "A transient climate change simulation with historical and projected greenhouse gas and aerosol forcing: experimental design and comparison with the instrumental record for the 20th century." *Climate Dynamics*, 16, 405-425.

Boer, G.J., N.A. McFarlane, and M. Lazare (1992) "Greenhouse Gas-induced Climate Change Simulated with the CCC Second-Generation General Circulation Model." *J. Climate*, 5, 1045-1077.

British Columbia Ministry of Water, Land and Air Protection (2002a) “Indicators of climate change for British Columbia,” Victoria, BC.

British Columbia Ministry of Water, Land, and Air Protection (2002b) “Hydrograph analysis of observation well 217 ”http://wlapwww.gov.bc.ca/wat/gws/obswell/obsw217.html.

British Columbia Ministry of Sustainable Resources Management (2002), River Forecast Centre, http://srmwww.gov.bc.ca/aib/wat/rfc/river_forecast/graphs/dgokkesi.html.

BC MWLAP (1999) “Preliminary Capture Zones for Grand Forks Community Wells, BC.” Government Document prepared for L. Thompson, Grand Forks Aquifer Protection Committee, July 28, 1999, obtained from BC Ministry of Water Land and Air Protection (WLAP) in 2003.

British Columbia Ministry of Environment, Lands and Parks (1999) “A Water Conservation Strategy for British Columbia.” http://www.elp.gov.bc.ca/wat/wrs/strategy/strategy.html.

British Columbia Ministry of Environment (1992) “Floodplain Mapping, Kettle & Granby Rivers, Grand Forks Area”, NTS Map No 82E/1,2, Drawing No 90-34-4 to 7, Sheets 4 to 7 out of 9, produced by Acres International Limited, Vancouver, BC, Canada.

Brodie R.S. (1999) "Integrating GIS and RDBMS technologies during construction of a regional groundwater model." *Environmental Modelling & Software*, 14, 119-128.

Brugman, M.M., Raistrick, P. and Pietroniro, A. (1997). Glacier related impacts of doubling atmospheric carbon dioxide concentrations on British Columbia and Yukon. In: Responding to Global Climate Change in British Columbia and Yukon. Volume I of the Canada Country Study: Climate Impacts and Adaptation, E. Taylor and B. Taylor (Eds.), Environment Canada and BC Ministry of Environment, Lands and Parks.

Campbell A.N. (1971) “Geohydrology of Grand Forks, British Columbia.” Unpublished report about Grand Forks aquifer, copy at Simon Fraser University, obtained from BCWLAP.

Cannon A.J. and P.H. Whitfield (2002) “Downscaling recent streamflow conditions in British Columbia, Canada using ensemble neural network models.” *Journal of Hydrology*, 259, 136-151.

Cannon A.J. and P.H. Whitfield (2002) “Downscaling recent streamflow conditions in British Columbia, Canada using ensemble neural network models.” *Journal of Hydrology*, 259, 136-151.

Carle, S. F., E. M. LaBolle, G. S. Weissmann, D. Van Brocklin and G. E. Fogg (1998). "Conditional simulation of hydrofacies architecture: A transition probability/Markov approach." In G. S. Fraser and J. M. Davis (Eds.), *Hydrogeologic Models of Sedimentary Aquifers, Concepts in Hydrogeology and Environmental Geology*, No. 1, SEPM (Society for Sedimentary Geology) Special Publication, 147-170.

Carlson A.B., Kratz D.P., Stackhouse P.W. (2002) “Release 3 NASA Surface Meteorology and Solar Energy Data Set For Renewable Energy Industry Use.” http://eosweb.larc.nasa.gov/sse/

Caya, D. and Laprise, R. (1999) "A semi-implicit semi-Lagrangian regional climate model: the Canadian RCM."" *Monthly Weather Review* 127, 341-362.

CCCma (2003) Canadian Climate Centre for Modelling and Analysis, CGCM1 information." website (http://www.cccma.bc.ec.gc.ca/models/cgcm1.shtml)

CCIS Canadian Climate Impacts Scenarios (2002) http://www.cics.uvic.ca/scenarios/i

CEAA, Canadian Environmental Assessment Agency (2003) “Stochastic Weather Generators, Appendix E” www.ceaa-acee.gc.ca/0010/0001/0002/0004/appendixE_e.htm

Changnon S.A., F.A. Huff, C-F Hsu (1988) "Relations between precipitation and shallow groundwater in Illinois." Journal of Climate, 1, 1239-1250.

Chen X. (2001) “Migration of Induced-Infiltrated Stream Water into nearby aquifers due to seasonal ground water withdrawal.” *Ground Water*, Vol 39 no 5 pg 721-728

Chen Z., S.E. Grasby, K.G. Osadetz (2002) "Predicting average annual groundwater levels from climatic variables: an empirical model." *Journal of Hydrology*, 260, 102-117.

CICS, Canadian Institute for Climate Studies (2003) “Canadian Climate Change Scenarios”, www.cics.uvic.ca/scenarios/

CICS, Canadian Institute for Climate Studies (2003b) Downscaling Tools, SDSM www.cics.uvic.ca/scenarios/sdsm/

Clague J.J. (1981) "Late Quaternary geology and geochronology of British Columbia, 2. Summary and discussion of radiocarbon-dated Quaternary history." *Geological Survey of Canada Paper* 80-35, 41 pp.

Coulson, H. (1997). The impacts of climate change on river and stream flow in British Columbia and Southern Yukon. In: Responding to Global Climate Change in British Columbia and Yukon. Volume I of the Canada Country Study: Climate Impacts and Adaptation, E. Taylor and B. Taylor (Eds.), Environment Canada and BC Ministry of Environment, Lands and Parks.

Daly C., R.P. Neilson, and D.L. Phillips (1994) "A statistical-topographic model for mapping climatological precipitation over mountainous terrain." *J. Appl. Meteor.*, 33, 2, 140-158.

Danard, M., and J. Galbraith. (1997) "High resolution analyses of daily precipitation amounts and temperatures in Southwestern British Columbia 31 Oct 1971 to 29 June 1995." Report prepared for BC Hydro by Atmospheric Dynamics Corporation, Victoria, BC.

Davies J.A., D.C. McKay (1982) “Estimating solar irradiance and components.” *Solar Energy*, 29, 1, p 55-64

Eheart J.W., D.W. Tornil (1999) "Low-flow frequency exacerbation by irrigation withdrawals in the agricultural midwest under various climate change scenarios." *Water Resources Research*, 35, 7, 2237-2246.

Environment Canada (1997). "Responding to Global Climate Change in British Columbia and Yukon. Volume I of the Canada Country Study: Climate Impacts and Adaptation." E. Taylor and B. Taylor (Eds.), Environment Canada and BC Ministry of Environment, Lands and Parks.

Eyles N. and H.T. Mullins (1997) 'Seismic-stratigraphy of Shuswap Lake, British Columbia, Canada." *Sedimentary Geology*, 109, 283-303.

Eyles N., H.T. Mullins, A.C. Hine (1991) "The seismic stratigraphy of Okanagan Lake, British Columbia; a record of rapid deglaciation in a deep 'fiord-lake' basin." *Sedimentary Geology*, 73, 13-41.

Fayer M.J., G.W. Gee, M.L. Rockhold, M.D. Freshley, and T.B. Walters (1996) "Estimating recharge rates for a groundwater model using a GIS." *Journal of Environmental Quality*, 25, 3, 510-518.

Flato, G.M., Boer, G.J., Lee, W.G., McFarlane, N.A., Ramsden, D., Reader, M.C., and Weaver, A.J. (2000) "The Canadian Centre for Climate Modelling and Analysis Global Coupled Model and its Climate." *Climate Dynamics*, 16, 451-467.

Flato, G.M., G.J. Boer, W.G. Lee, N.A. McFarlane, D. Ramsden, M.C. Reader, and A.J. Weaver, (2000) "The Canadian Centre for Climate Modelling and Analysis Global Coupled Model and its Climate." *Climate Dynamics*, 16, 451-467.

Flato, G.M., G.J. Boer, W.G. Lee, N.A. McFarlane, D. Ramsden, M.C. Reader, and A.J. Weaver, (2000) "The Canadian Centre for Climate Modelling and Analysis Global Coupled Model and its climate." Climate Dynamics 16, 451-467.

Fogg, G. E., S. F. Carle and C. Green (2000). A connected-network paradigm for the alluvial aquifer system. In: D. Zhang (Ed.), Theory, Modeling and Field Investigation in Hydrogeology: A Special Volume in Honor of Shlomo P. Neuman's 60th Birthday, Geological Society of America Special Publication.

Fogg G.E. (1986) "Groundwater Flow and Sand Body Interconnectedness in a Thick, Multiple-Aquifer System." *Water Resources Research*, 22, 5, 679-694.

Fogg, G. E., S. J. Seni and C. W.Kreitler (1983). "Three-dimensional ground-water modeling in depositional systems, Wilcox Group, Oakwood Salt Dome area, East Texas." The University of Texas at Austin, Bureau of Economic Geology Report of Investigations No. 133. 55 pages.

Frind E.O., D.S. Muhammad, and J.W. Molson (2002) "Delineation of Three-Dimensional Well Capture Zones for Complex Multi-Aquifer Systems." *Ground Water*, 40, 6, 586-598.

Fulton R.J., B.G. Warner, H.J. Kubiw, and R.A. Achard (1989) "Geology and paleoecology of early Holocene lacustrine deposits in the Columbia River valley near Fauquier, southern British Columbia." *Canadian Journal of Earth Sciences*, 26, 257-265.

Fulton R.J. (1984) "Quaternary glaciation, Canadian Cordillera." *Geological Survey of Canada Paper* 84-10, pg 39-48

Fulton R.J. and G.W. Smith (1978) "Late Pleistocene stratigraphy of south-central British Columbia." *Canadian Journal of Earth Sciences*, vol 15, pg 971-980

Gleick P.H. (1986) "Methods for evaluating the regional hydrologic impacts of global climatic changes." *Journal of Hydrology*, 88, 97-116.

Global Change Strategies International Inc. and Environment Canada (2000). "Vulnerability and Adaptation to Climate Change." Environment Canada.

Goode, Daniel J., Appel, Charles A. (1992) "Finite-difference interblock transmissivity for unconfined aquifers and for aquifers having smoothly varying transmissivity" USGS, *Water Resources Investigations Report*, 92-4124, 79 pp.

Graf W.L. (1970) "The geomorphology of the glacial valley cross-section." *Arctic and Alpine Research*, 2, 4, 303-312.

Gregory, J.M., Wigley, T.M.L., Jones P.D. (1993) "Application of Markov models to area-average daily precipitation series and interannual variability in seasonal totals." *Climate Dynamics*, 8, 299-310.

Guillet, D.W. and Skinner, W.R. (1992) "The state of Canada's climate: temperature change in Canada 1895-1991". Environment Canada, SOE Report 92-2

Hager W.H. and Huang H.Q. (1996) "Alluvial channel geometry. Theory and applications." *Journal of Hydraulic Engineering*, vol 122 no 12 p 750

Halford, K.J. (1999) "Effects of Steady-State Assumption on Hydraulic Conductivity and Recharge Estimates in a Surficial Aquifer System." *Ground Water*, 37, 1, 70-79.

Harbor J.M, B. Hallet, C.F. Raymond (1988) "A numerical model of landform development by glacial erosion." *Nature*, 333, 347-349.

Harbor J.M. and D.A. Wheeler (1992) "On the mathematical description of glaciated valley cross-sections." *Earth Surface Processes and Landforms*, 17, 477-485.

Herzog B.L., D.R. Larson, C.C. Abert, S.D. Wilson, and G.S. Roadcap (2003) "Hydrostratigraphic Modeling of a Complex Glacial-Drift Aquifer System for Importation into MODFLOW." *Ground Water*, 41, 1, 57-65.

Hewitson, B.C. and R.G. Crane (1996) "Climate downscaling: techniques and application." *Climate Research*, 7, 85-96.

Hirano M., and M. Aniya (1988) "A rational explanation of cross-profile morphology for glacial valleys and of glacial valley development." *Earth Surface Processes and Landforms*, 13, 707-716.

Huth, R., J. Kysely, and M. Dubrovsky (2001) "Time structure of observed, GCM-simulated, downscaled, and stochastically generated daily temperature series." *Journal of Climate*, 6, 4047-4061.

Iqbal, M. (1983) "An introduction to solar radiation." Academic Press, Toronto, 390 pp.

Jones, P.D. (1994) "Hemispheric Surface Air Temperature Variations: A Reanalysis and an Update to 1993." *J. Climate*, 7, 1794-1802.

Jones N.L., T.J. Budge, A.M. Lemon, and A.K. Zundel (2002) "Generating MODFLOW Grids from Boundary Representation Solid Models." *Ground Water*, 40, 2, 194-200.

Jyrkama M.I., J.F. Sykes, and S.D. Normani (2002) "Recharge Estimation for Transient Ground Water Modelling." *Ground Water*, 40, 6, 639-649.

Kalnay, E., M. Kanamitsu, R. Kistler, W. Collins, D. Deaven, L. Gandin, M. Iredell, S. Saha, G. White, J. Woollen, Y. Zhu, M. Chelliah, W. Ebisuzaki, W. Higgins, J. Janowiak, K.C. Mo, C. Ropelewski, J. Wang, A. Leetmaa, R. Reynolds, R. Jenne, and D. Joseph, (1996) "The NCEP/NCAR 40-Year Reanalysis Project." Bulletin of the American Meteorological Society 77, 437-471.

Kalnay, E., Kanamitsu, M., Kistler, R. et al. (1996) "The NCEP/NCAR 40-year reanalysis project." *Bulletin of the American Meteorological Society,* 77, 437-471.

Kennedy E.J. (1964) "Discharge ratings at gaging stations.", Techniques of Water-Resources Investigations of the United States Geological Survey, Chapter Al0, Book 3, Applications of Hydraulics

Kharin, V.V. & F.W. Zwiers (2000). "Changes in the extremes in an ensemble of transient climate simulation with a coupled atmosphere-ocean GCM", *Journal of Climate*, 13, 3760-3788.

Kruger A., U. Ulbrich, and P. Speth (2001) "Groundwater Recharge in Northrhine-Westfalia Predicted by a Statistical Model for Greenhouse Gas Scenarios." *Physics and Chemistry of the Earth Part B: Hydrology Oceans and Atmosphere*, 26, 11-12, 853-861.

Landman, W.A., Mason S.J., Tyson P.D., Tennant W.J. (2001) "Statistical downscaling of GCM simulations to streamflow." *Journal of Hydrology*, 252, 221-236.

Laprise, R., Caya, D., Giguere, M., Bergeron, G., Cote, H., Blanchet, J.-P., Boer, G.J. and McFarlane, N.A. (1998) "Climate and climate change in Western Canada as simulated by the Canadian Regional Climate Model." *Atmosphere-Ocean*, 36, 119-167.

Leith R.M. and P.H. Whitfield (1998) "Evidence of climate change effects on the hydrology of streams in south-central BC." *Canadian Water Resources Journal*, 23, 3, 219-230.

Leith R.M. and P.H. Whitfield (2000) "Some effects of urbanization on streamflow records in a small watershed in the Lower Fraser Valley, BC." *Northwest Science*, 74, 1, p. 69.

Li Y., G. Liu, Z. Cui (2001) "Glacial valley cross-profile morphology, Tian Shan Mountains, China." *Geomorphology*, 38, 153-166.

Little H.W. (1957) "Kettle River, east half, British Columbia." Geological Survey of Canada Map 6-1957.

Loaciga H.A., D.R. Maidment, J.B. Valdes (2000) "Climate-change impacts in a regional karst aquifer, Texas, USA." *Journal of Hydrology*, 227, 173-194.

Loaiciga H.A., J.B. Valdes, R. Vogel, J. Garvey, H.H. Schwarz (1996) "Global warming and the hydrologic cycle." *Journal of Hydrology*, 174, 1-2, 83-128.

Lockington D.A. (1999) "Response of unconfined aquifer to sudden change in boundary head." *J. of Irrigation & Drainage Engineering*, 123, 1, 24.

Logan C., H.A.J. Russell, D.R. Sharpe (2002) "Regional 3D geological modelling of the Oak Ridges Moraine area, southern Ontario." Geological Survey of Canada, Ottawa.

Luttmerding H.A. (1980) "Soils of the Langley-Vancouver Map Area." Report no 15 of British Columbia Soil Survey, BC Ministry of Environment, Soil Map Mosaics and Legend, Lower Fraser Valley, RAB Bulletin 18, Volume 1, maps 1 to 3, 13 to 15.

McFarlane, N.A., G.J. Boer, J.-P. Blanchet, and M. Lazare (1992) "The Canadian Climate Centre Second-Generation General Circulation Model and its Equilibrium Climate." *J. Climate*, 5, 1013-1044.

Malcolm R., and C. Soulsby (2000) "Modelling the potential impact of climate change on a shallow coastal aquifer in northern Scotland." In Robins N.S. and Misstear B.D.R. (Eds.) *Groundwater in the Celtic Regions: Studies in Hard Rock and Quaternary Hydrogeology*. Geological Society, London, Special Publications, 182, 191-204.

Marino M.A. (2001) "Conjunctive management of surface water and groundwater." Regional Management of Water Resources (Proceedings of a symposium held during the Sixth IAHS Scientific Assembly at Maastricht, The Netherlands, IAHS AISH Publication, 268, 165-173.

Martin P.J. and E.O. Frind (1998) "Modeling a Complex Multi-Aquifer System: The Waterloo Moraine." *Ground Water*, 36, 4, 679-690.

Morris D.A., and Johnson A.I. (1967) "Summary of hydrologic and physical properties of rock and soil materials as analyzed by the Hyrologic Laboratory of the USGS 1948-1960." USGS *Water Supply Paper* 1839-D.

Mullins H.T. and E.J. Hinchey (1989) "Erosion and infill of New York Finger Lakes: implications for Laurentide ice sheet deglaciation." *Geology*, 17, 622-625.

Mullins H.T., N. Eyles, E.J. Hinchey (1990) "Seismic reflection investigation of Kalamalka Lake: a 'fiord lake' on the Interior Plateau of southern British Columbia." *Canadian Journal of Earth Sciences*, 27, 1225-1235.

NASA Surface meteorology and Solar Energy Data Set (Carlson et al, 2002). Grand Forks, BC Lat 49.01 Lon -118.26

National Solar Radiation Data Base User's Manual (1961-1990) http://rredc.nrel.gov/solar/pubs/NSRDB/background.html

Pacific Field Corn Association (2002) Evapotranspiration estimates for selected locations, based on Environment Canada climate data. http://www.farmwest.com

Paillet, F.L., and R.S. Reese (2000) "Integrating borehole logs and aquifer tests in aquifer characterization." *Ground Water*, 38, 5, 713-725.

Parrish R.R., S.D. Carr, D.L. Parkinson (1988) "Eocene extensional tectonics and geochronology of the southern Omineca Belt, British Columbia and Washington." *Tectonics*, 7, 2, 181-212.

Piteau Associates (1988) “City of Grand Forks and Kerr Wood Leidal Associates Design Construction and Testing of Grand Forks Production Well, PW5 – consultants report.” Piteau Associates Engineering Ltd. March, project 87-971-B.

Piteau Associates Engineering Ltd. (2002) Dakin Report vol 3, March 11 (hydrological assessment of the Grand Forks Aquifer and its future use)

Preto V.A. (1970) "Structure and petrology of the Grand Forks Group, British Columbia." *Geological Survey of Canada Paper* 69-22, 80 pp.

Pruitt, W. O. and Doorenbos, J. (1977) "Background and Development of Methods to Predict Reference Crop Evapotranspiration (ETo)." Appendix II in FAO-ID-24, 108-119.

Quick, M.C. (1995) “The UBC watershed model.” In: V.P. Singh (ed.), “Computer Models Of Watershed Hydrology.” Water Resources Publications, pp. 233-280.

Rantz S.E. (1982) “Measurement and Computation of Streamflow: measurement of stage and discharge.” USGS Water Supply Paper 2175, Volume 1

Reader, M.C., and Boer, G.J., 1998: The modification of greenhouse gas warming by the direct effect of sulphate aerosols. *Climate Dynamics*, 14, 593-607.

Regan R.S. and R.W. Schaffranek (1985) “A computer program for analyzing channel geometry.” USGS Water-Resources Investigations Report 85-4335, 49 pp.

Rhodes B.P., and E.S. Cheney (1981) "The low-angle Kettle River fault: The eastern contact of Kettle Dome, northeast Washington." *Geology*, 9, 366-369.

Richardson C.W. (1981) “Stochastic simulation of daily precipitation, temperature, and solar radiation.” *Water Resources Research*, 17, 182-190.

Richardson C.W. (2000) “Data requirements for estimation of weather generation parameters.” *Transactions-of-the-American-Society-of-Agricultural-Engineers*, 43, 4, 877-882.

Richardson C.W., and D.A. Wright (1984) "WGEN: A model for generating daily weather variables." ARS-8, Washington DC, USDA Agricultural Research Service.

Riggs H.C. (1972) “Low-flow investigations.” Techniques of Water-Resources Investigations of the United States Geological Survey, Chapter Bl, Book 4.

Riggs H.C. (1982) “Regional analyses of streamflow characteristics.” Techniques of Water-Resources Investigations of the United States Geological Survey, Chapter B3, Book 4

Ritzi, R.W., D.F. Jayne, A.J. Zahradnik, A.A. Field, and G.E. Fogg (1994). "Geostatistical modeling of heterogeneity in glaciofluvial, buried-valley aquifers," *Ground Water*, 32, 4, 666-674.

Ritzi, R.W., D.F. Dominic, and K. Kausch (1996) "Aquitard distribution in a northern reach of the Miami Valley aquifer: 1) three-dimensional geostatistical evaluation of physical heterogeneity." *Journal of Hydrogeology*, 4, 2, 12-24.

Rivera A. (2000) "Groundwater management in Canada." Geological Society of America annual meeting, Abstracts with Programs - Geological Society of America, 32, 7.

Ryder J.M. (1971) "Some aspects of the morphometry of paraglacial alluvial fans in south-central British Columbia." *Canadian Journal of Earth Sciences*, vol 8, pg 1252-1264

Ryder J.M. and M. Church (1987) "The Lillooet terraces of Fraser River: a peleoenvironmental equiry." *Canadian Journal of Earth Sciences*, 23, 869-884.

Ryder J.M., R.J. Fulton, J.J. Clague (1991) "The Cordilleran ice sheet and the glacial geomorphology of southern and central British Columbia." *Geographie Physique et Quaternaire*, vol 45, no 3, pg 365-377

Scanlon, B. R., Christman, M., Reedy, R. C., Porro, I., Simunek, J., and Flerchinger, G. N. (2002a) “Intercode comparisons for simulating water balance of surficial sediments in semiarid regions.” *Water Resources Research*, 38, 1323–1339.

Scanlon, B. R., Healy, Rick, and Cook, P. G. (2002b) “Choosing appropriate techniques for quantifying groundwater recharge.” *Hydrogeology Journal*, 10, 18–39.

Schaffranek R.W., Baltzer R.A., and D.E. Goldberg (1981) “A Model for Simulation of Flow in Singular and Interconnected Channels.” Techniques of Water-Resources Investigations of the USGS. Chapter C3, Book 7, 110 pages

Schueler, T.R. and R.A. Claytor (1996) "Design of Stormwater Filter Systems." Center for Watershed Protection, Silver Spring, MD.

Scibek J. and Allen, D.M. (2003). Groundwater Sensitivity to Climate Change (Part I): Analysis of Watershed Water Balance and River-Aquifer Interactions for the Grand Forks Aquifer, Southern British Columbia. Report to be submitted to BC Ministry of Water, Land and Air Protection.

Scibek J. and Allen, D.M. (2004). Groundwater Sensitivity to Climate Change (Part II): Analysis of Recharge for the Grand Forks Aquifer, Southern British Columbia. Report to be submitted to BC Ministry of Water, Land and Air Protection.

Scibek, J., Allen D.M., and Whitfield, P. (2004) Groundwater Sensitivity to Climate Change (Part III): Climate Change Modelling Results for the Grand Forks Aquifer, Southern British Columbia. Report to be submitted to BC Ministry of Water, Land and Air Protection.

Semenov MA, Brooks RJ, Barrow EM & Richardson CW (1998) “Comparison of the WGEN and LARS-WG stochastic weather generators for diverse climates.” *Climate Research*, 10, 95-107.

Simmers I. (1998) "Groundwater recharge: an overview of estimation 'problems' and recent developments. In *Groundwater Pollution, Aquifer Recharge and Vulnerability*, N.S. Robins (Ed). Geological Society, London, Special Publication, 130, 107-115.

Sminchak, J.R., D.F. Dominic, and R.W. Ritzi, (1996) "Indicator geostatistical analysis of sand interconnections within a till." *Ground Water*, 36, 5, 1125-1131.

Soil Conservation Service (1985) "National Engineering Handbook: Section 4-Hydrology." Washington DC, US Department of Agriculture.

Sprout P.N. and C.C. Kelley (1964) "Soil Survey of the Kettle River Valley in the Boundary District of British Columbia." British Columbia Soil Survey report no 9, BC Department of Agriculture, Canada Department of Agriculture, Ottawa, Cat no A57-418, includes Soil Map of Kettle River Valley, British Columbia.

Swain E.D. and Wexler E.J. (1996) “A Coupled Surface-Water And Ground-Water Flow Model (MODBRANCH) For Simulation Of Stream-Aquifer Interaction.” Techniques of Water-Resources Investigations of the USGS. Chapter A6

Tarboton, K. C., W. W. Wallender, G. E. Fogg and K. Belitz. (1995) "Kriging of regional hydrogeologic properties in the western San Joaquin Valley, California." *Journal of Hydrogeology*, 3, 1, 5-23.

US watershed maps from: http://gisdata.usgs.net/ and http://gisdata.usgs.net/website/National_Map/viewer.htm

Vanderburgh S., and M.C. Roberts (1996) "Depositional systems and seismic stratigraphy of a Quaternary basin: north Okanagan Valley, British Columbia." *Canadian Journal of Earth Sciences*, 33, 917-927.

Vermulst J.A.P. and W.J. De Lange (1999) "An analytic-based approach for coupling models for unsaturated and saturated groundwater flow at different scales." *Journal of Hydrology*, 226, 262-273.

Waterloo Hydrogeologic Inc. (1996). Visual MODFLOW.

Watkins D.W., D.C. McKinney, D.R. Maidment, and M. Lin (1996) "Use of geographic information systems in groundwater flow modelling." *Journal of Water Resources Planning and Management*, 122, 2, 88-96.

Wei M., A.P. Kohut, D. Kalyn, and F. Chwojka (1994) "Occurrence of nitrate in groundwater, Grand Forks, British Columbia." *Quaternary International*, 20, 39-49.

Weissmann, G. S. and G. E. Fogg (1999) "Multi-scale alluvial fan heterogeneity modeled with transition probability geostatistics in a sequence stratigraphic framework." *Journal of Hydrology*, 226, 48-65.

Weissmann, G.S., S.A. Carle, and G.E. Fogg (1999). "Three-dimensional hydrofacies modeling based on soil survey analysis and transition probability geostatistics." *Water Resources Research*, 35, 6, 1761-1770.

Weissmann, G. S. and G. E. Fogg. (1999) "Multi-scale alluvial fan heterogeneity modelled with transition probability geostatistics in a sequence stratigraphic framework." *Journal of Hydrology*, 226, 48-65.

Wheeler D.A. (1984) "Using parabolas to describe the cross-sections of glaciated valleys." *Earth Surface Processes and Landforms*, 9, 391-394.

Wheeler J.O. (1966) "Eastern tectonic belt of Western Cordillera in British Columbia." in Tectonic history and mineral deposits of the Western Cordillera, Canadian Institute of Mining Met., Special Volume 8, 27-45.

Whitfield P. and A. Cannon (2003) Personal communictaion. Environment Canada, Vancouver, BC.

Whitfield P.H. and A.J. Cannon (2000) “Recent variations in climate and hydrology in Canada.” *Canadian Water Resources Journal*, 25, 1, 19-65.

Whitfield P.H., A.J. Cannon, J.Y. Wang, and C.J. Reynolds (2002) “Modelling hydrologic conditions in present and future climates – model performance for recent conditions in Coastal British Columbia.” (paper submitted to AMS conference – also Environment Canada report).

Whitfield, P.H. and A.J. Cannon (2000) "Recent Variations in Climate and Hydrology in Canada." *Canadian Water Resources Journal,* 25, 19-65.

Whitfield, P.H. and E. Taylor (1998) "Apparent recent changes in hydrology and climate of coastal British Columbia." In: Y. Alila (Ed.), Mountains to Sea: Human Interactions with the Hydrologic Cycle. Proceedings of the 51st Canadian Water Resources Conference, 22-29.

Wilby, R.L. and Wigley, T.M.L. (1997) “Downscaling general circulation model output: a review of methods and limitations.” *Progress in Physical Geography*, 21, 530-548.

Wilby, R.L., Dawson, C.W., and Barrow, E.M. (2002) SDSM – a decision support tool for the assessment of regional climate change impacts.” Environmental and Modelling Software, 17, 145-157.

Wilks D.S. (1992) "Adapting stochastic weather generation algorithms for climate change studies." *Climatic Change*, 22, 67-84.

Wilks D.S. and Wilby R.L. (1999) “The weather generation game: a review of stochastic weather models.” *Progress in Physical Geography*, 23, 329-357.

Winter T.C. (1983) "The interaction of lakes with variably saturated porous media." *Water Resources Research*, 19, 5, 1203-1218.

Woessner W.W. (2000) “Stream and fluvial plain ground water interactions: rescaling hydrogeologic thought.” *Ground Water*, 38, 3, 423-429.

Xiao Q., S.L. Ustin, and W.W. Wallender (1996) "A spatial and temporal continuous surface-subsurface hydrologic model." *Journal of Geophysical Research*, 101, D23, 29565-29584.

Xu C (1999) “From GCMs to river flow: a review of downscaling methods and hydrologic modelling approaches.” *Progress in Physical Geography*, 23, 2, 229-249.

York J.P., M. Person, W.J. Gutowski, T.C. Winter (2002) "Putting aquifers into atmospheric simulation models: an example from the Mill Creek Watershed, northeastern Kansas." *Advances in Water Resources*, 25, 221-238.

Yusoff, I., Hiscock, K. M.; Conway, D. (2002) "Simulation of the impacts of climate change on groundwater resources in eastern England." *Sustainable Groundwater Development*, Geological Society of London, United Kingdom Geological Society Special Publications, 193, 325-344.

Zektser I.S., H.A. Loaiciga (1993) "Groundwater fluxes in the global hydrologic cycle: past, present, and future." *Journal of Hydrology*, 144, 405-427.

Zhang L., W.R. Dawes, T.J. Hatton, P.H. Reece, G.T.H. Beale, and I. Packer (1999) "Estimation of soil moisture and groundwater recharge using the TOPOG_IRM model." *Water Resources Research*, 35, 1, 149-161.

Zwiers F. (2001) “Climate Change - Case Study: Projected Changes in Extreme 24-hour Precipitation.” Canadian Centre for Climate Modelling and Analysis, http://www.math.mcmaster.ca/peter/sora/case_studies_01/climate.html

Software manuals

ESRI (2004) "ArcGIS 8.13 User Manual and Documentation.” Environmental Systems Research Institute (ESRI).

EMRL (2004) “GMS 4.0 User Manual and Documentation.” Environmental Modeling Research Laboratory (EMRL) at Brigham Young University is part of the Civil and Environmental Engineering Department.

Waterloo Hydrogeologic Inc. (2000) "WHI UnSat Suite User's Manual: 1-D Unsaturated Zone Groundwater Flow and Contaminant Transport Modeling using VLEACH, PESTAN, VS2DT, and HELP." Waterloo, Canada.

Waterloo Hydrogeologic Inc. (2000). "Visual MODFLOW v 3.0: User Manual." Waterloo, Canada.

Regan R.S. and R.W. Schaffranek (1985) A computer program for analyzing channel geometry. USGS Water-Resources Investigations Report 85-4335, 49 pp.

Schaffranek R.W., Baltzer R.A., and D.E. Goldberg (1981) A Model for Simulation of Flow in Singular and Interconnected Channels. Techniques of Water-Resources Investigations of the USGS. Chapter C3, Book 7, 110 pp.

McDonald M.G. and A.W. Harbaugh (1988) "A modular three-dimensional finite-difference ground-water flow model." USGS Techniques of Water Resources Investigations Book 6, Chapter A1, Reston, Virginia, USGS.

Harbaugh A.W. (1988) A Computer Program for Calculating Subregional Water Budgets Using Results from USGS MODFLOW model.' USGS report.

Swain E.D. and Wexler E.J. (1996) "A Coupled Surface-Water and Ground-Water Flow Model (MODBRANCH) for Simulation of Stream-Aquifer Interaction." Techniques of Water-Resources Investigations of the USGS. Chapter A6.

Carle S.F. (1999) "T-PROGS: Transition Probability Geostatistical Software Version 2.1" University of California, Davis.

Textbooks

Domenico P.A., and F.W. Schwartz (1998) "Physical and Chemical Hydrogeology." 2nd ed., J. Willey & Sons Inc.

Freeze R.A., J.A. Cheery (1979) "Groundwater." Prentice-Hall Inc. Englewood Cliffs, New Jersey, 604 pp.

Leonards (1962) "Leonards G.A. (1962) Engineering Properties of Soils. In G.A. Leonards (ed.) Foundation Engineering. McGraw-Hill, NY, 66-240.

Tarboton, K. C., W. W. Wallender, G. E. Fogg and K. Belitz. (1995) "Kriging of regional hydrogeologic properties in the western San Joaquin Valley, California." *Journal of Hydrogeology*, 3, 1, 5-23.

Knighton D. (1984) "Fluvial Forms and Processes." Arnold, London, 217 pp.

Embleton C. and C.A.M. King (1975) "Glacial and Periglacial Geomorphology." Willey & Sons, New York, 203 pp.

Data sources

BC Ministry of Water, Land and Air Protection

- Cadastral layers for city of Grand Forks
- River surveys and cross-sections (Kettle and Granby Rivers)
- TRIM maps, base maps, well locations
- Well Litholog Database
- Digital Elevation Model for Fraser Valley, 50 m grid
- Digital Elevation Model for Fraser Valley, 20 m grid
- pumping and irrigation statistics for production wells in Grand Forks area
- summaries of pump test data and previous well capture zone delineation studies
- original Grand Forks aquifer extent (as dxf map)
- floodplain mapping of Kettle River valley near Grand Forks
- locations of aquifers in BC

BC Energy & Mines Mapplace

- Surficial Geology - Kootenay Region, 1:250 K

Environment Canada

- climate normals for Canadian weather stations
- climate data for selected climate stations
- stage and discharge data for selected hydrometric stations
- climate change scenarios (Whitfield P. and Gunn A. pers comm.)
- Digital Elevation Model for Grand Forks area, 20 m grid
- water levels in piezometers, ditches, streams in Abbotsford area
- pump tests for Abbotsford aquifer

Canadian Institute for Climate Studies (CICS)

- all CRCM and CGCM1 data
- downscaling software SDSM and link to downloading LARS-WG

McElhanney Consulting Services Ltd.

- digital orthophotos (B/W 1 m res.) for Grand Forks valley (map sheets 82E008, 82E009)

USGS (public domain data accessed from GeoCommunity website)

- Digital Elevation Model for Boundary Mountain quadrangle, 20 m
- Digital orthophotos (B/W 1 m res.)
- groundwater wells south of Grand Forks, BC (in WA state)

Digital data produced at Simon Fraser University (2004) from analysis results and other primary non-digital sources

- 3D hydrostratigraphic models of Grand Forks aquifer in GMS
- layer surfaces, sediment thickness maps
- standardized and interpreted litholog database (various versions)
- all groundwater modeling results in vector and raster format (converted from MODFLOW outputs), including MODFLOW grid cells mapped to GIS, and other links (river, recharge)

- soil map polygons, recharge scenario zones, depth to water table
- updated river extents, streams, river cross-section locations, updated water bodies
- irrigation districts, irrigated fields (from orthophotos)
- combined bedrock surface model with ground surface DEM (both US and Canada)
- valley cross-section lines
- contour maps (ground surface, water table, differences between heads in modeling scenarios)
- complete cliimate data sets and analyses, downscaling, etc... for Grand Forks
- Kettle River flow model and results, inputs to MODFLOW for all climate scenarios
- recharge model and results for Grand Forks valley for all climate scenarios
- various base maps, 3D maps, animations, all spatial analyses presented in this report
- aquifer vulnerability maps and analyses

Carlson A.B., Kratz D.P., Stackhouse P.W. (2002) “Release 3 Nasa Surface Meteorology And Solar Energy Data Set For Renewable Energy Industry Use.” Abstract, data from http://eosweb.larc.nasa.gov/sse/

Western Climate Center (2002) Digital data for climate normals and station information.

APPENDIX A:

HYDROMETRIC STATIONS FOR SMALL CATCHMENTS

Station ID:	Station name:	Latitude	Longitude	POR	POR (years)	Basin Area (km^2)	Mean Basin Elevation (m asl)	Runoff, mean annual (mm)	Runoff, max daily rate (mm)	Discharge , min (m^3/s)	Discharge, mean (m^3/s)	Discharge , mean (m^3/s)
08NE111	Little Sheep Creek near Rossland	49.098	117.828	1971-1974	4	1.3		182	1.2		0.0073	0.0073
08NE027	Ferguson Creek near Edgewood	49.850	118.169	1925-1959	35	1.9		846	5	0.0151	0.0515	0.0515
08NE112	Record Creek near Rossland	49.061	117.868	1971-1974	4	5.4		970	3.2	0.00814	0.1670	0.1670
08NN009	Dan O'Rea Cr.	49.030	118.371	1921	1	7.8		36	0.29	0.000571	0.0090	0.0090
08NM074	Ellis Creek near Penticton	49.471	119.387	1933-1955	23	9.1		2710	6.8	0.0411	0.7790	0.7790
08NN021	Moody Creek near Christina	49.051	118.273	1971-1984	14	13.5		324	5.5	0.007	0.1380	0.1380
08NM229	Loch Katrine Creek at outlet of Grayston	49.984	118.871	1977-2002	26	16.1	2029	731	22	0	0.3730	0.3730
08NM126	Haynes Creek near Osoyos	49.024	119.386	1912-1964	45	17.6		87	0.92	0	0.0489	0.0489
08NM210	Pooley Creek above Pooley Ditch	49.748	119.337	1973-1979	6	18.1		846	10	0.003	0.4850	0.4850
08NN020	Trapping Creek at 1220 m contour	49.667	118.910	1970-1981	10	22.8		657	18	0.0111	0.4750	0.4750
08NN018	July Creek	49.014	118.541	1965-1974	10	45.6		221	3.9	0.00686	0.3200	0.3200
08NE039	Cayuse Creek near Deer Park	49.407	117.989	1955-1958	4	51.3		691	2.6	0.0131	1.1200	1.1200
08NE082	Inkaneep Creek near Oliver	49.119	119.361	1941-1977	37	70.4		164	1.9	0.006	0.3670	0.3670
08NM172	Pearson Creek near the mouth	49.887	119.062	1970-1987	18	73.6		410	6.2	0.0399	0.9560	0.9560
08NN016	SUTHERLAND CREEK NEAR FIFE	49.066	118.189	1960-1973	14	88.1		282	2.7	0.0139	0.7870	0.7870
12407520	Deer Creek near Valley	48.118	117.798			93.2	2006				0.5169	0.5169
12408420	Haller Creek near Arden	48.467	117.907			95.8	1600				0.2095	0.2095
12407000	Sheep Creek at Loon Lake	48.060	117.653			98.2	2370				0.0668	0.0668
08NM171	Vaseux Creek above Solco Creek	49.249	119.321	1970-2002	33	117.0	1829	252	9.6	0.0386	0.9370	0.9370
12444100	Whitestone Creek near Tonasket	48.785	119.433			143.5	1180				0.0813	0.0813
12439300	Tonasket Creek at Oroville	48.943	119.413			155.7	960				0.0876	0.0876
12402500	Curlew Creek near Malo	48.767	118.653			173.0					0.5494	0.5494
08NE028	Renata Creek near Renata	49.421	118.109	1912-1931	20	195.0		25	0.0053	0.071	0.1570	0.1570
12408500	Mill Creek near Colville	48.579	117.866			215.0	1950				1.3578	1.3578
12407700	Chewelah Creek at Chewelah	48.283	117.714			243.7	1674				1.0256	1.0256
12444490	Bonaparte Creek near Wauconda	48.657	119.201			250.2	2300				0.1381	0.1381
08NN007	Rock Creek near Rock Creek	49.056	118.999	1915-1984	70	280.0		230	2.2	0.00943	2.0400	2.0400
12408300	Little Pend Oreille River near Colville	48.466	117.748			341.9	1983				1.6790	1.6790
08NM082	Big Sheep Creek near Rossland	49.013	117.944	1971-1974	5	347.0	1507	512	8.2	0.241	5.6300	
12409500	Hall Creek at Inchelium	48.311	118.211			417.0	1420				2.0157	2.0157
08NN001	Boundary Creek near Greenwood	49.079	118.687	1912-1980	69	479.0		218	4.7	0.0437	3.3200	3.3200
12399600	Deep Creek near Northport	48.930	117.750			494.7	1310				2.9846	2.9846
12400500	Sheep Creek near Northport	48.944	117.781			582.7	1295				6.1806	
08NN002	Grand Forks	49.044	118.438									

Source: Environment Canada and US Geological Survey, 2002

Table A1 Summary statistics for hydrometric stations on small catchments near Grand Forks, BC. (Canadian and US data). Estimated mean annual discharge.

Creeks on BC side

Catchment number	Estimated area (ha)	Estimated area (km^2)	Dominant aspect	Stream order	Slope	Estimated annual Q (m^3/s)
1	579	5.79	SE	2	mod	0.030
2	110	1.10	S	1	steep	0.006
3	193	1.93	S	0	rock face	0.010
4	48	0.48	S	1	steep	0.002
5	848	8.48	SE	3	mod	0.044
6	90	0.90	S	1	rock face	0.005
7	1500	15.00	SE	3	mod	0.078
8	149	1.49	S	1	steep	0.008
9	319	3.19	S	1	steep	0.017
10	60	0.60	SW	1	mod	0.003
11	34	0.34	NE	0	steep	0.002
12	50	0.50	S	0	rock face	0.003
13	65	0.65	NW	1	low	0.003
14	96	0.96	E	0	rock face	0.005
15	270	2.70	E	1	mod	0.014
16	73	0.73	SE	0	rock face	0.004
17	303	3.03	SE	1	steep	0.016
18	173	1.73	SE	1	rock face	0.009
19	71	0.71	NE	0	rock face	0.004
20	43	0.43	NW	0	rock face	0.002
21	271	2.71	N	1	rock face	0.014
22	54	0.54	N	0	rock face	0.003
Creeks on US side						
25		25.56	N	3	mod	0.133
26		8.57	N	3	steep	0.045
27		1.42	N	1	rock face	0.007
28		1.52	N	1	rock face	0.008
29		2.28	N	1	steep	0.012
30		1.42	N	1	rock face	0.007
Totals		94.762				0.493

note: estimates are from regression equation of mean annual discharge to catchment area: m.a. Q = 0.0052 Area, where area is in km^2 and Q is in m3/s

Table A2 Small catchments discharging into Grand Forks Valley: area, aspect, slope, stream order, and estimated annual discharge.

APPENDIX B:

HELP- MODEL SENSITIVITY ANALYSIS

Table B2 HELP recharge model scenarios for soil columns and physical parameters: sensitivity analysis to secondary soil properties.

Scenario		Depth of column	Soil Type	vertical Ksat						
(number)	(name)	(depth to water table)	(S rating of soil; permeability)	(of vadose zone)	soil depth	initial moisture content	porosity	field capacity	wilting point	grass stand
		(m)	(10 to 6)	(m/d)	(m)	(vol/vol)	(vol/vol)	(vol/vol)	(vol/vol)	
65	d3_thicksoil	3	8	med	1.5	0.03	0.397	0.032	0.013	good
66	d3_thinsoil	3	8	med	0.5	0.03	0.397	0.032	0.013	good
67	d3_verythinsoil	3	8	med	0.2	0.03	0.397	0.032	0.013	good
68	d3_highmoist	3	8	med	1	0.12	0.397	0.032	0.013	good
69	d3_modmoist	3	8	med	1	0.1	0.397	0.032	0.013	good
70	d3_lowmoist	3	8	med	1	0.08	0.397	0.032	0.013	good
71	d3_medporosity	3	8	med	1	0.03	0.32	0.032	0.013	good
72	d3_lowporosity	3	8	med	1	0.03	0.25	0.032	0.013	good
73	d3_highFC	3	8	med	1	0.03	0.397	0.038	0.013	good
74	d3_lowFC	3	8	med	1	0.03	0.397	0.028	0.013	good
75	d3_highWP	3	8	med	1	0.03	0.397	0.032	0.015	good
76	d3_lowWP	3	8	med	1	0.03	0.397	0.032	0.01	good
77	d3_poorstandgrass	3	8	med	1	0.03	0.397	0.032	0.013	bare
78	d3_excelstandgrass	3	8	med	1	0.03	0.397	0.032	0.013	excellent
79	d3_highmoist_highKsat	3	8	high	1	0.12	0.397	0.032	0.013	good
80	d3_modmoist_highKsat	3	8	high	1	0.1	0.397	0.032	0.013	good
81	d3_lowmoist_highKsat	3	8	high	1	0.08	0.397	0.032	0.013	good
82	d3_thicksoil_highKsat	3	8	high	1.5	0.03	0.397	0.032	0.013	good
83	d3_thinsoil_highKsat	3	8	high	0.5	0.03	0.397	0.032	0.013	good
84	d3_verythinsoil_highKsat	3	8	high	0.2	0.03	0.397	0.032	0.013	good
85	d3_thicksoil_highKsat_SR10	3	10	high	1.5	0.03	0.397	0.032	0.013	good
86	d3_thinsoil_highKsat_SR10	3	10	high	0.5	0.03	0.397	0.032	0.013	good
87	d3_verythinsoil_highKsat_SR10	3	10	high	0.2	0.03	0.397	0.032	0.013	good

APPENDIX C:

ZONE BUDGET MODELLING RESULTS

GRAPHS SHOWING RECHARGE TO ZBUD ZONES

Figure C1 Transient model flow volumes for Zones 1, 2, 8. Calculated for ZBUD RECHARGE only in Grand Forks aquifer. Comparing non-pumping to pumping and all climate scenarios.
Symbol legend applies to both graphs. Horizontal axis is time in days, vertical axis is flow volume in 1000's m^3/day. Different vertical scale on graphs.

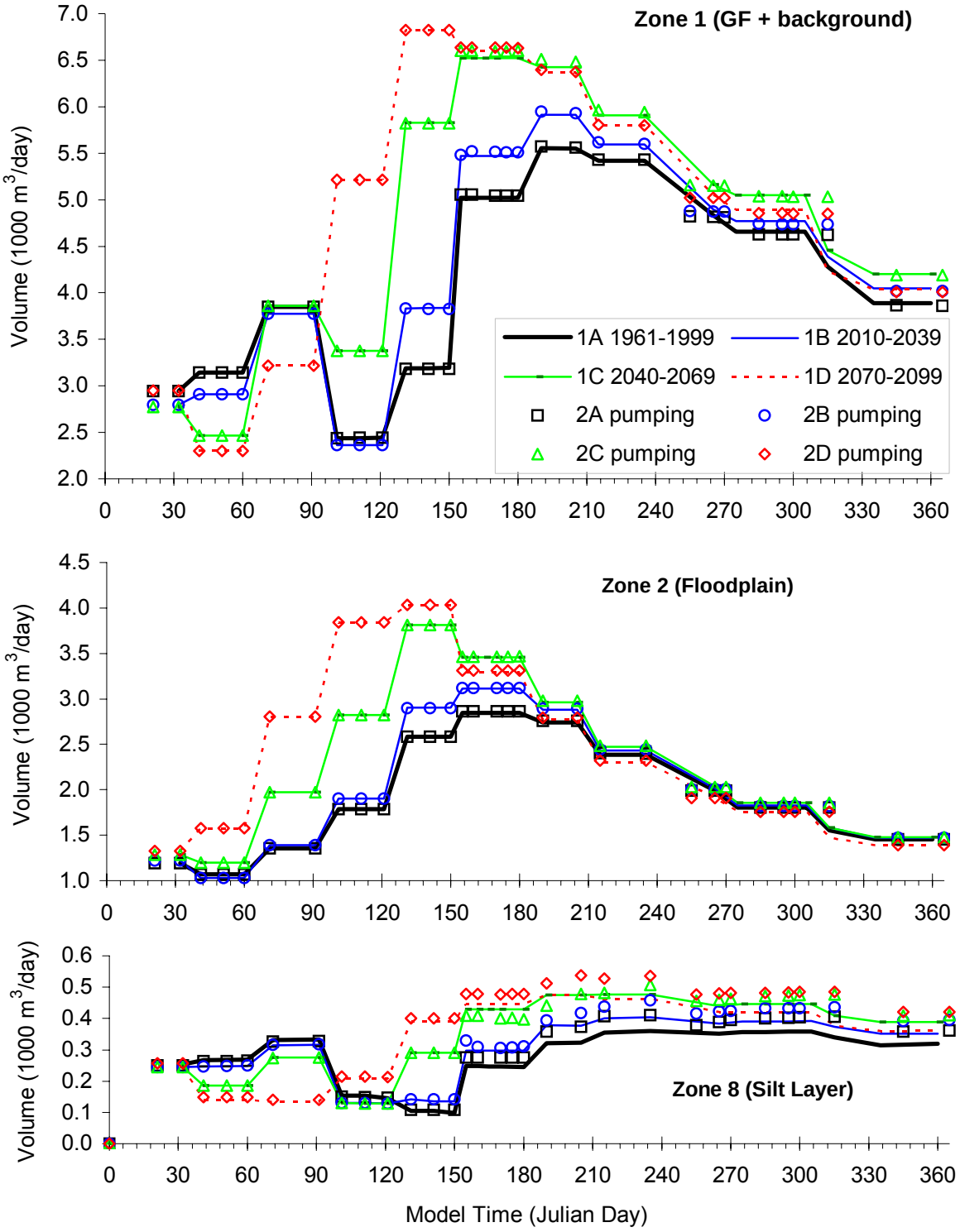

Figure C2 Transient model flow volumes for Zones 3, 4, 5. Calculated for ZBUD RECHARGE only in Grand Forks aquifer. Comparing non-pumping to pumping and all climate scenarios.
Symbol legend applies to both graphs. Horizontal axis is time in days, vertical axis is flow volume in 1000's m^3/day. Different vertical scale on graphs.

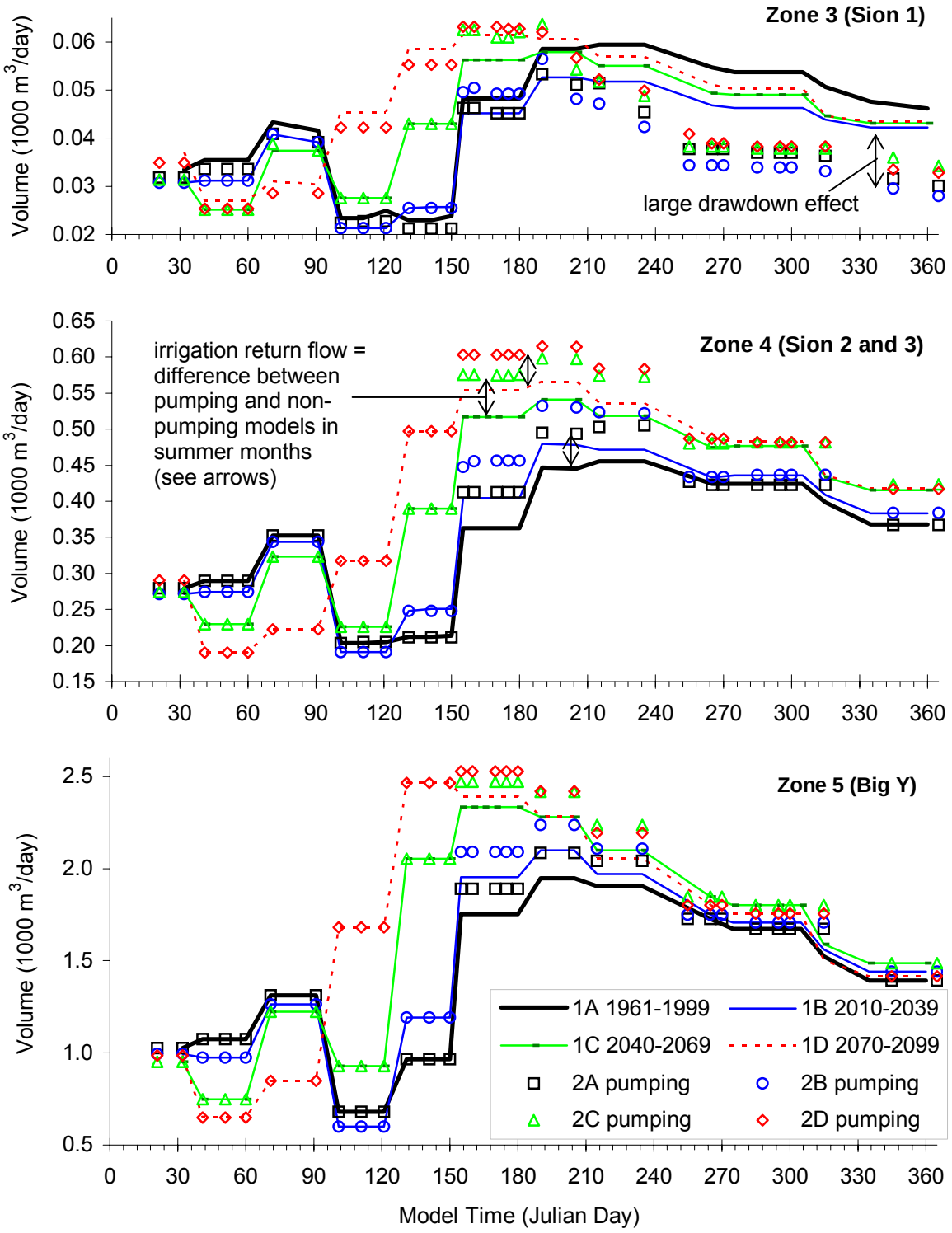

Figure C3 Transient model flow volumes for Zones 6, 7. Calculated for ZBUD RECHARGE only in Grand Forks aquifer. Comparing non-pumping to pumping and all climate scenarios.
Symbol legend applies to both graphs. Horizontal axis is time in days, vertical axis is flow volume in 1000's m^3/day. Different vertical scale on graphs.

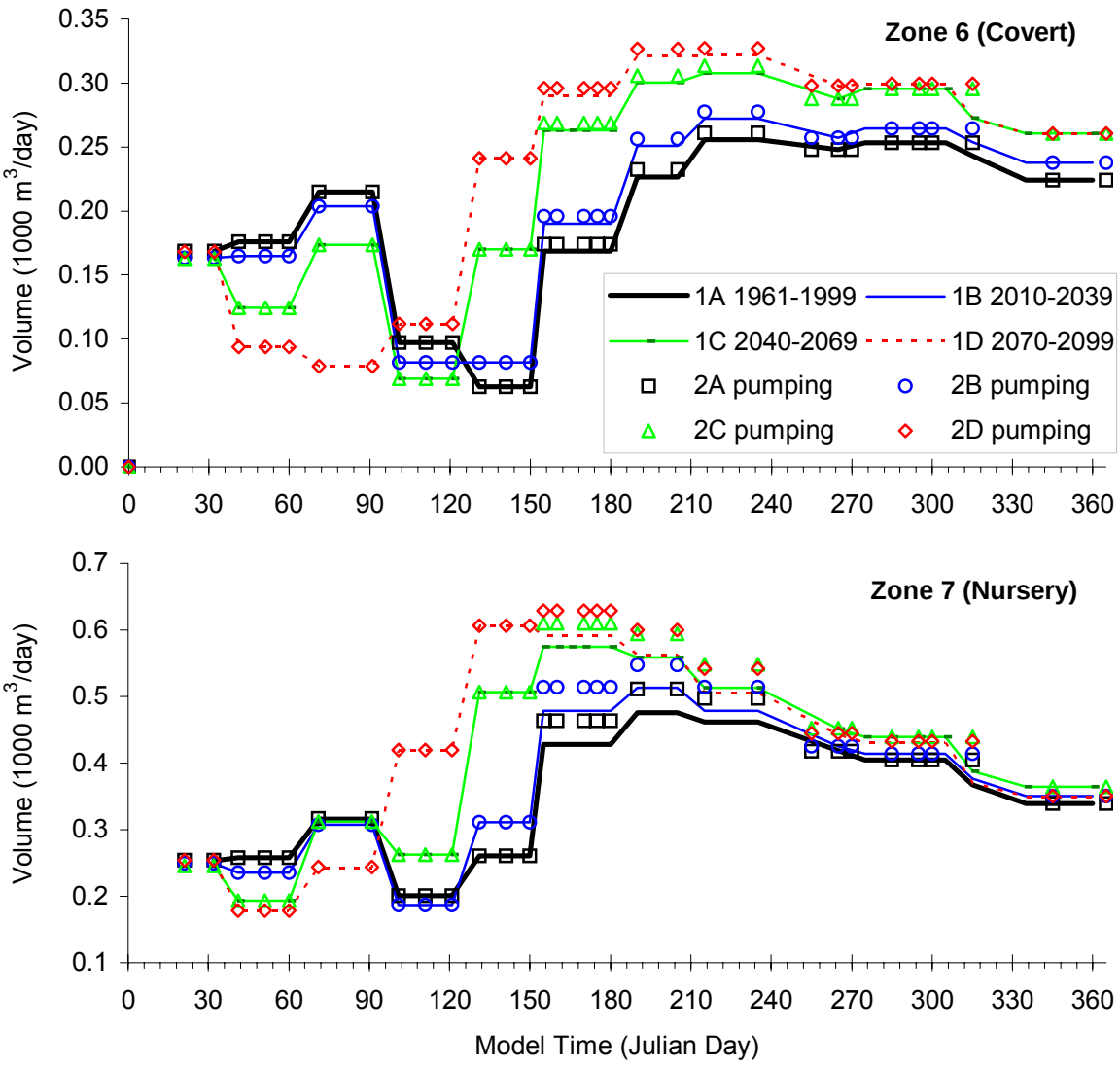

GRAPHS SHOWING GROUNDWATER STORAGE AND FLOW BETWEEN ZONES (PUMPING AND NON-PUMPING SCENARIOS – HISTORICAL CLIMATE)

Figure C4 Transient model flow volumes for Zone 1 (Grand Forks + background areas) calculated for ZBUD IN and OUT components in Grand Forks aquifer. Comparing non-pumping to pumping scenarios for historical climate. Symbol legend applies to both graphs, except for "well discharge" which applies only to pumping scenario results. Horizontal axis is time in days, vertical axis is flow volume in 1000's m^3/day. Same scales on both graphs.

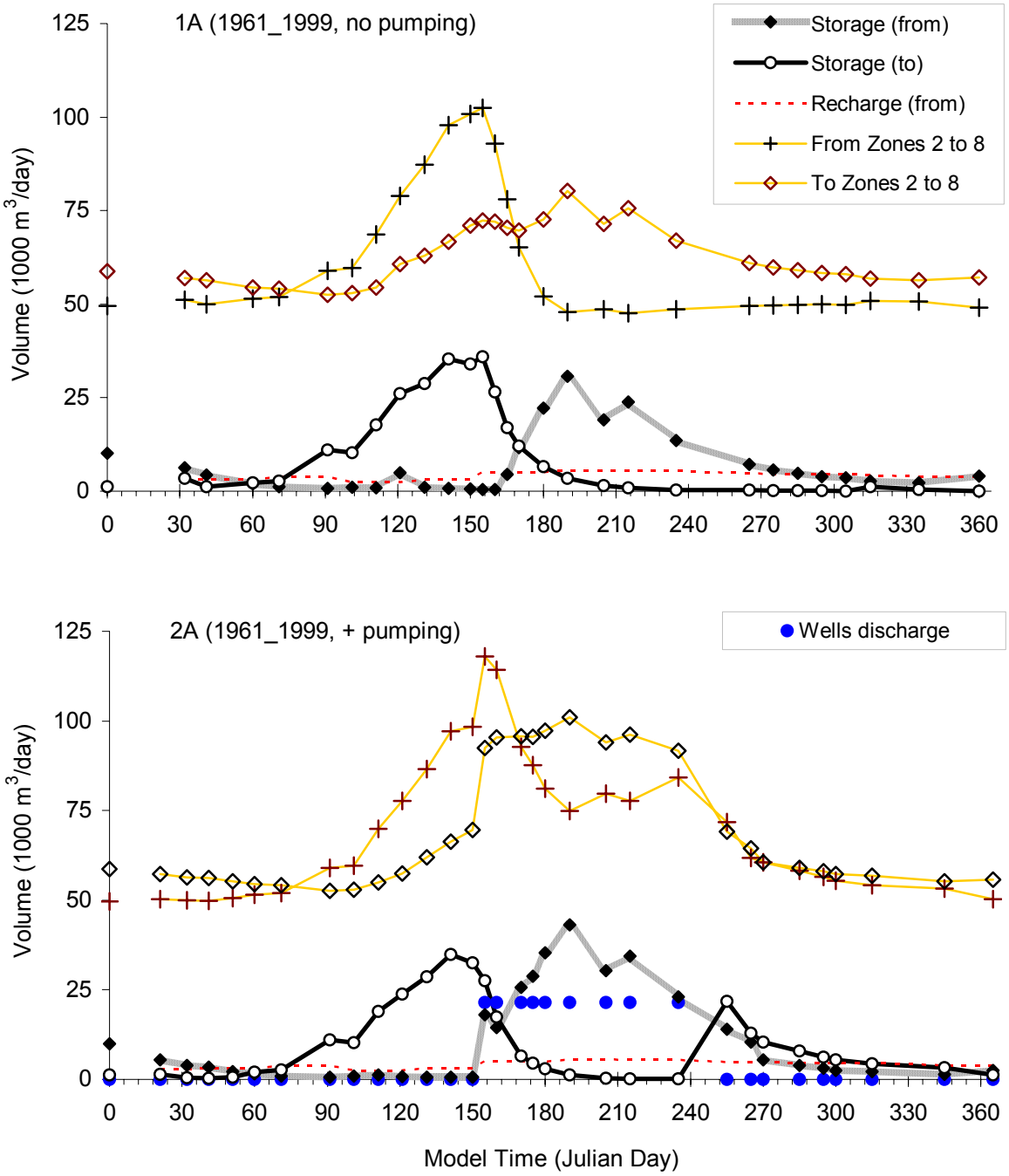

Figure C5 Transient model differences between OUT and IN flow volumes for Zone 1 (Grand Forks + background areas) calculated for ZBUD components in Grand Forks aquifer. Comparing non-pumping to pumping scenarios for historical climate.
Symbol legend applies to both graphs, except for "well discharge" which applies only to pumping scenario results. Horizontal axis is time in days, vertical axis is flow volume in 1000's m^3/day. Same scales on both graphs.

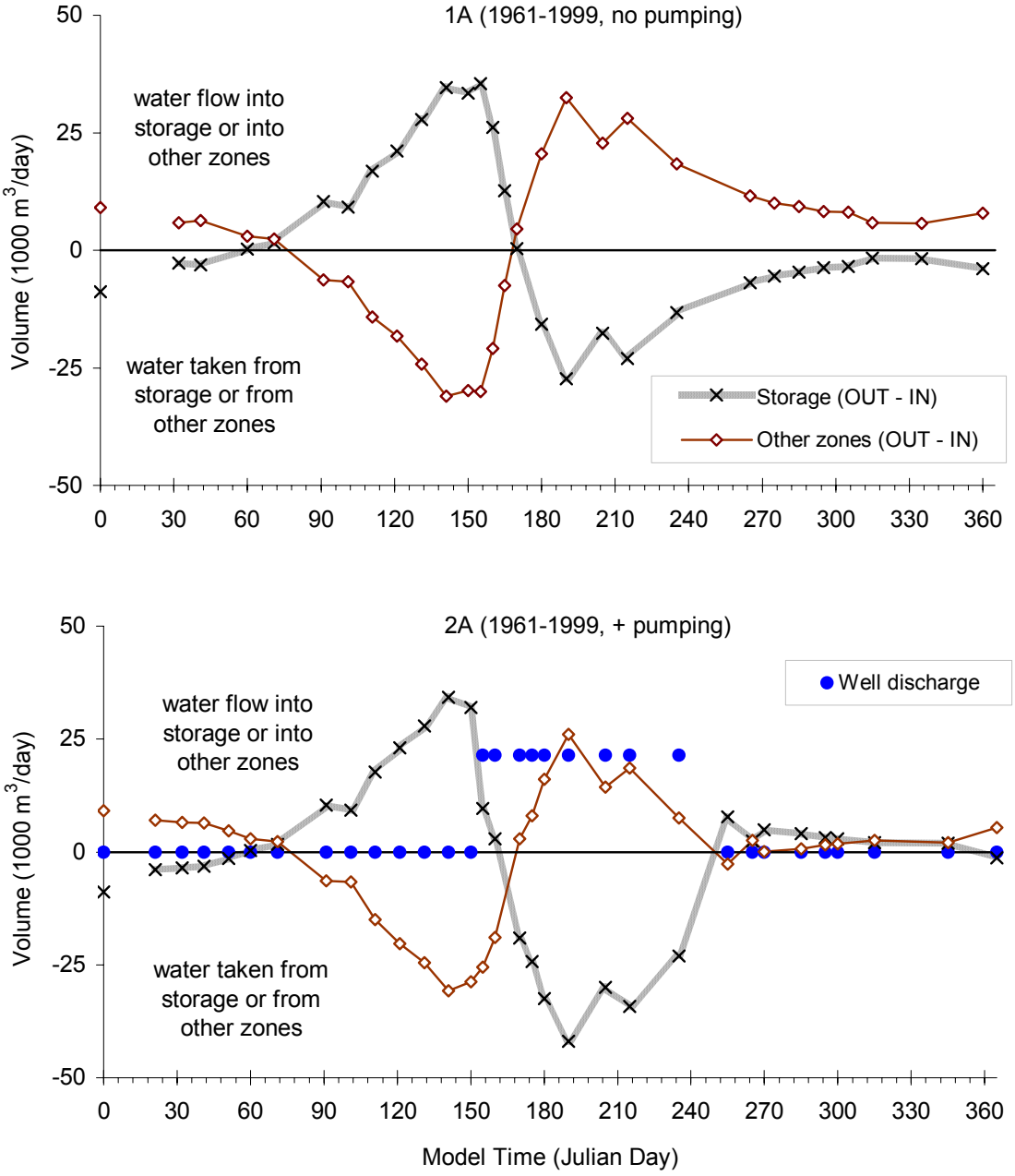

Figure C6 Transient model flow volumes for Zone 2 (River Floodplain) calculated for ZBUD IN and OUT components in Grand Forks aquifer. Comparing non-pumping to pumping scenarios for historical climate.
Symbol legend applies to both graphs. Horizontal axis is time in days, vertical axis is flow volume in 1000's m^3/day. Same scales on both graphs. There are no pumping wells in this ZBUD zone.

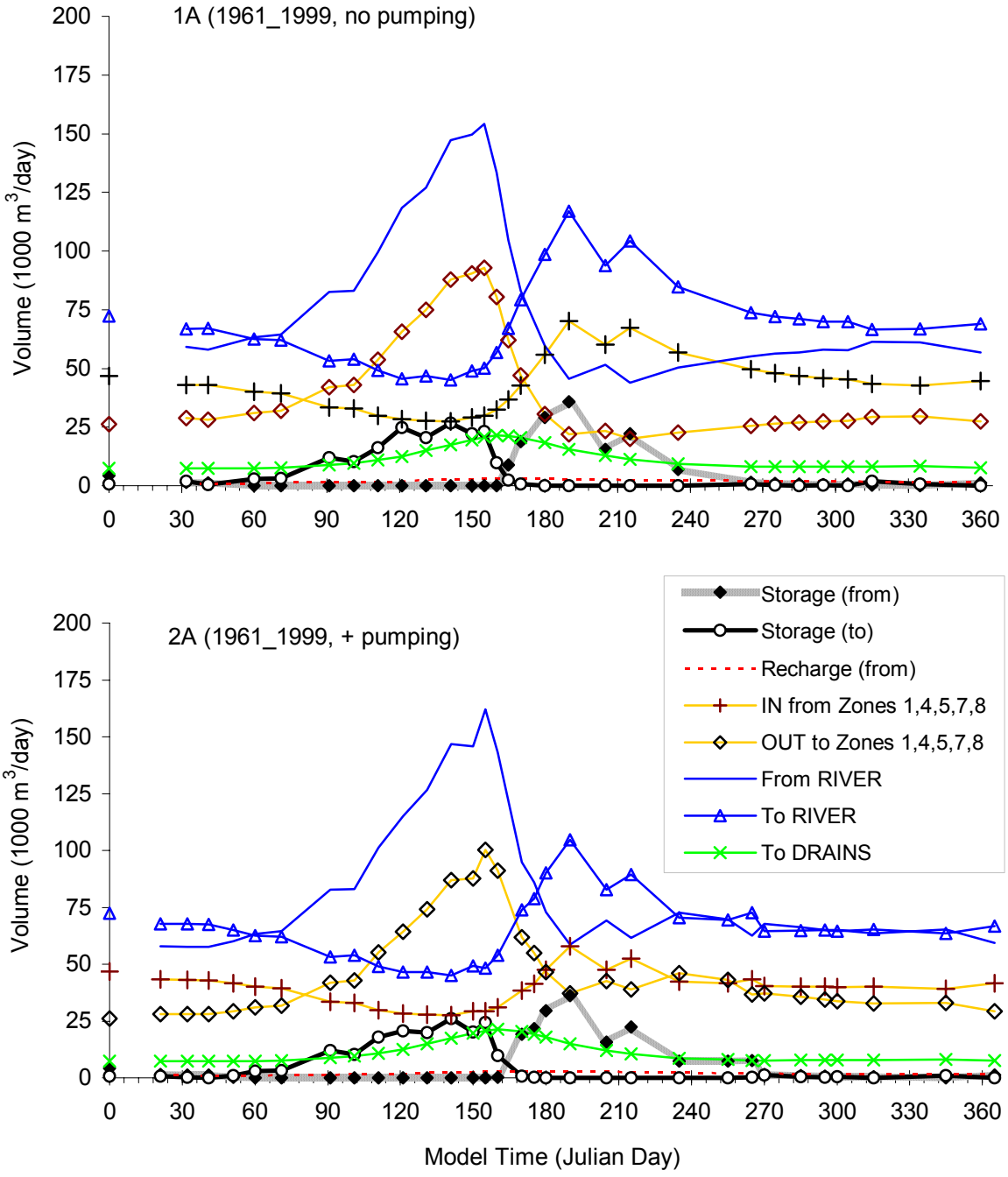

Figure C7 Transient model differences between OUT and IN flow volumes for Zone 2 (River Floodplain) calculated for ZBUD components in Grand Forks aquifer. Comparing non-pumping to pumping scenarios for historical climate.
Symbol legend applies to both graphs. Horizontal axis is time in days, vertical axis is flow volume in 1000's m^3/day. Same scales on both graphs. There are no pumping wells in this ZBUD zone.

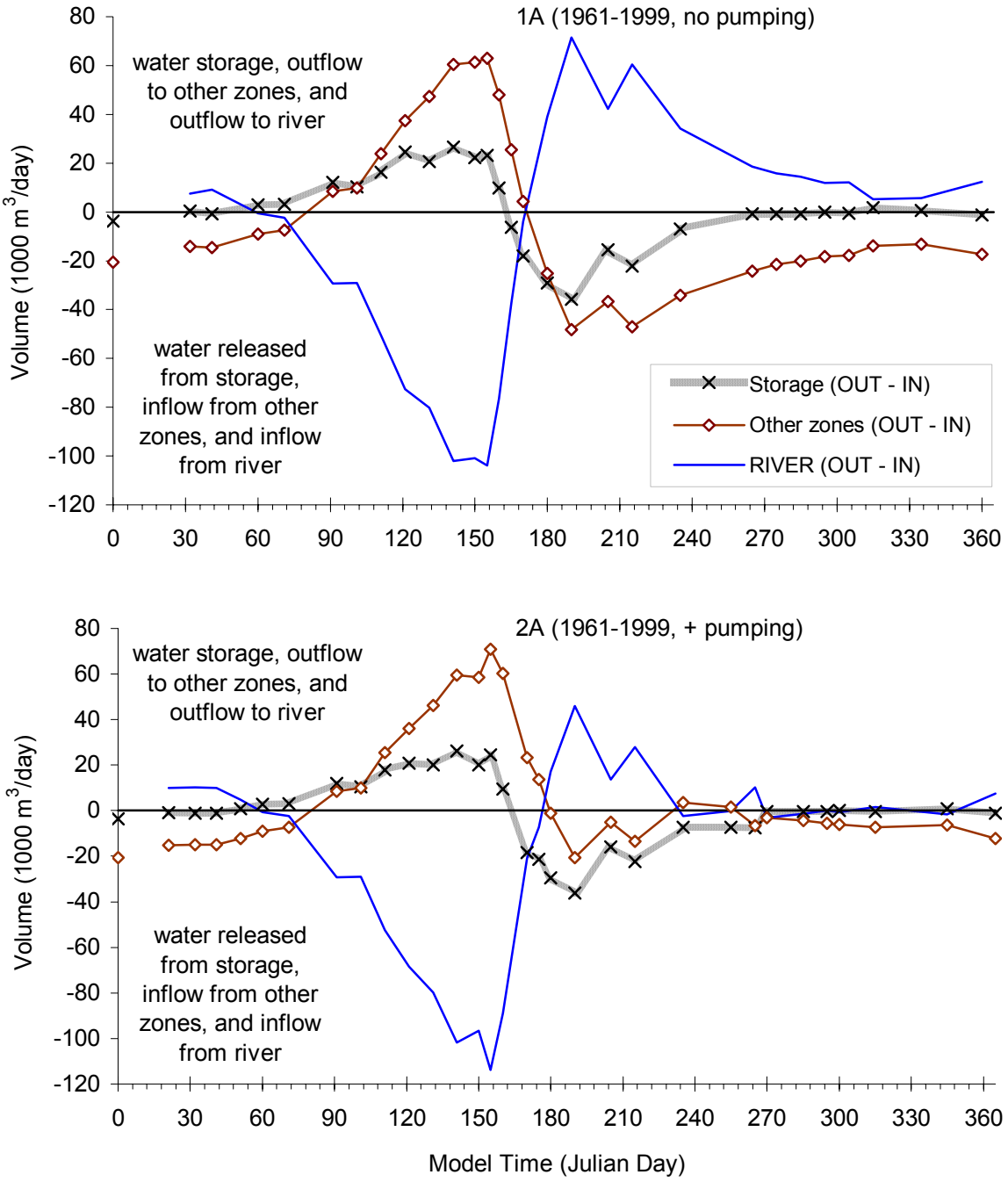

Figure C8 Transient model flow volumes for Zone 3 (Sion 1 Irrigation District) calculated for ZBUD IN and OUT components in Grand Forks aquifer. Comparing non-pumping to pumping scenarios for historical climate.
Symbol legend applies to both graphs. Horizontal axis is time in days, vertical axis is flow volume in 1000's m^3/day. Same scales on both graphs. There are no pumping wells in this ZBUD zone.

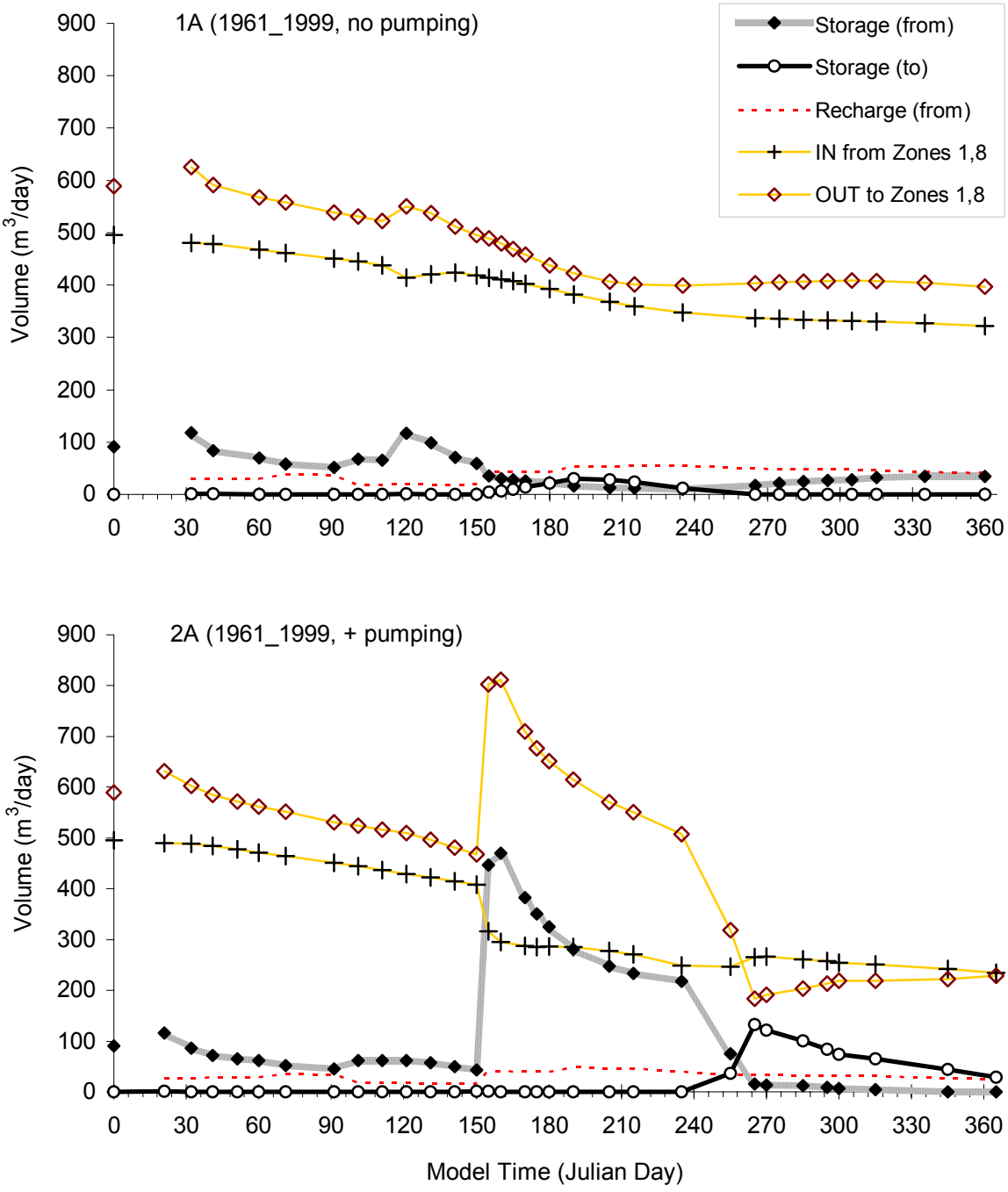

Figure C9 Transient model differences between OUT and IN flow volumes for Zone 3 (Sion 1 Irrigation District) calculated for ZBUD components in Grand Forks aquifer. Comparing non-pumping to pumping scenarios for historical climate. Symbol legend applies to both graphs. Horizontal axis is time in days, vertical axis is flow volume in 1000's m^3/day. Same scales on both graphs. There are no pumping wells in this ZBUD zone.

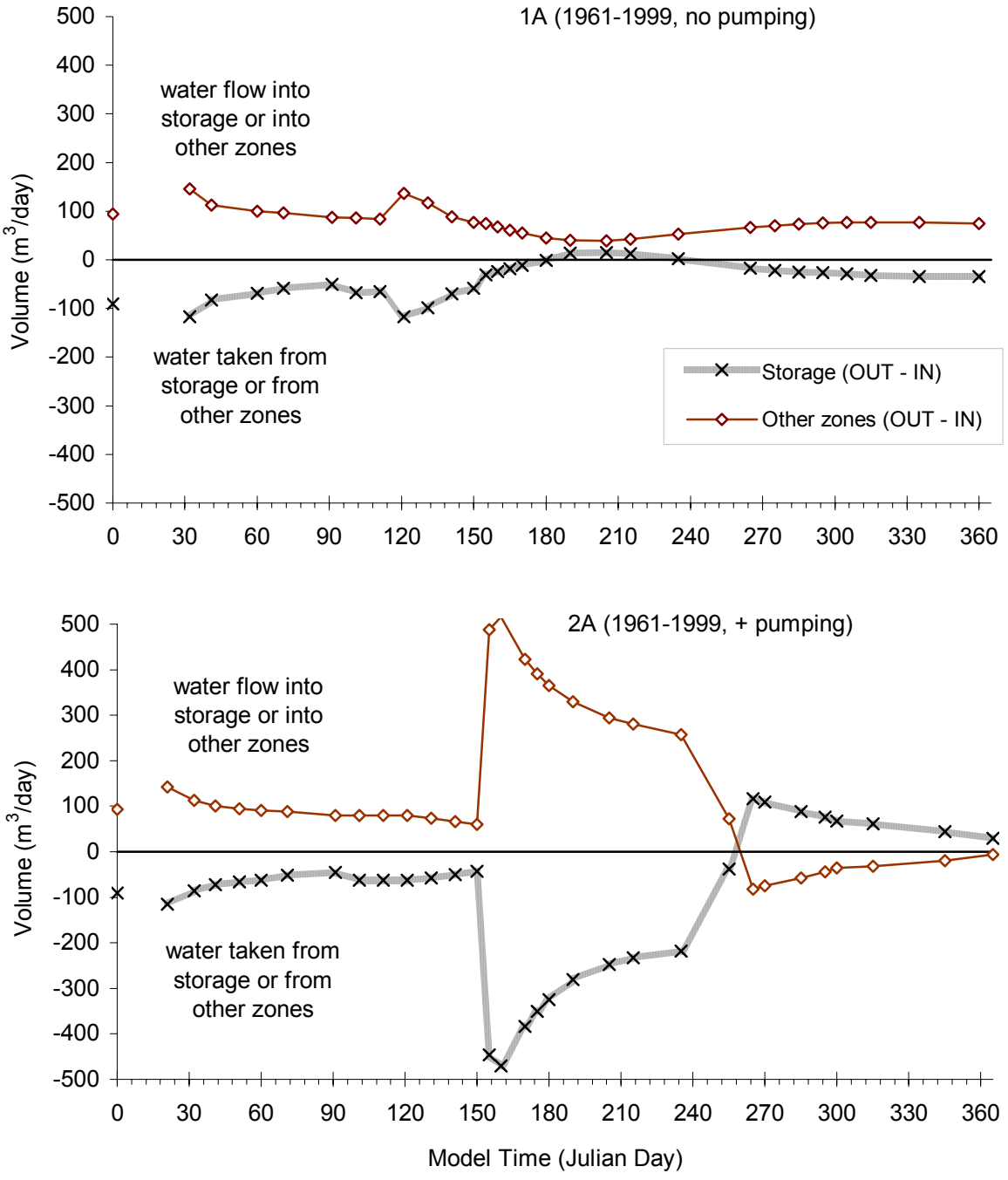

Figure C10 Transient model flow volumes for Zone 4 (Sion 2 and 3 Irrigation Districts) calculated for ZBUD IN and OUT components in Grand Forks aquifer. Comparing non-pumping to pumping scenarios for historical climate. Symbol legend applies to both graphs, except for "well discharge" which applies only to pumping scenario results. Horizontal axis is time in days, vertical axis is flow volume in 1000's m^3/day. Same scales on both graphs. There are pumping wells in this ZBUD zone but wells pump from "deep sand" layer, which is not part of this ZBUD zone.

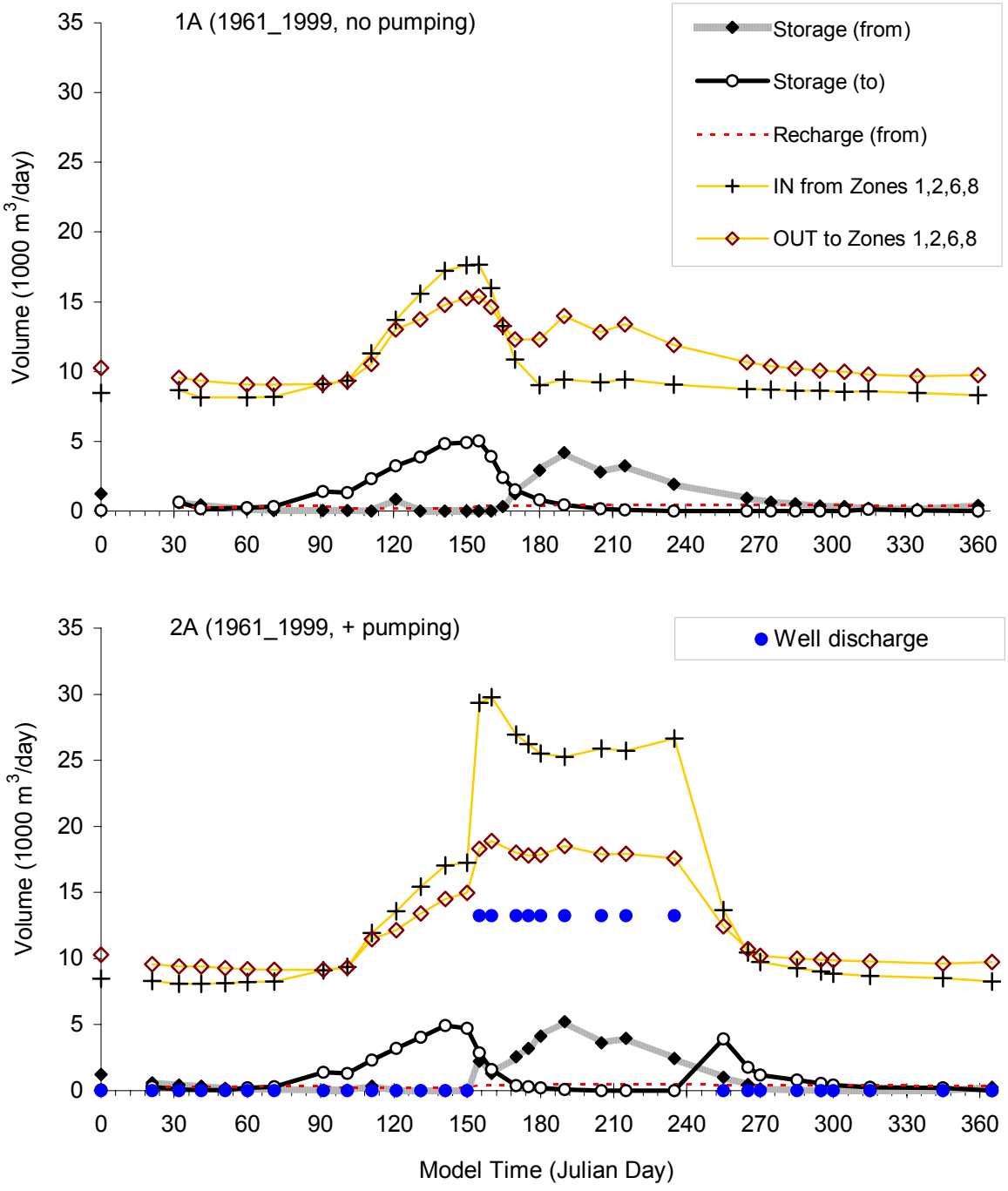

Figure C11 Transient model differences between OUT and IN flow volumes for Zone 4 (Sion 2 and 3 Irrigation Districts) calculated for ZBUD components in Grand Forks aquifer. Comparing non-pumping to pumping scenarios for historical climate. Symbol legend applies to both graphs, except for "well discharge" which applies only to pumping scenario results. Horizontal axis is time in days, vertical axis is flow volume in 1000's m^3/day. Same scales on both graphs. There are pumping wells in this ZBUD zone but wells pump from "deep sand" layer, which is not part of this ZBUD zone.

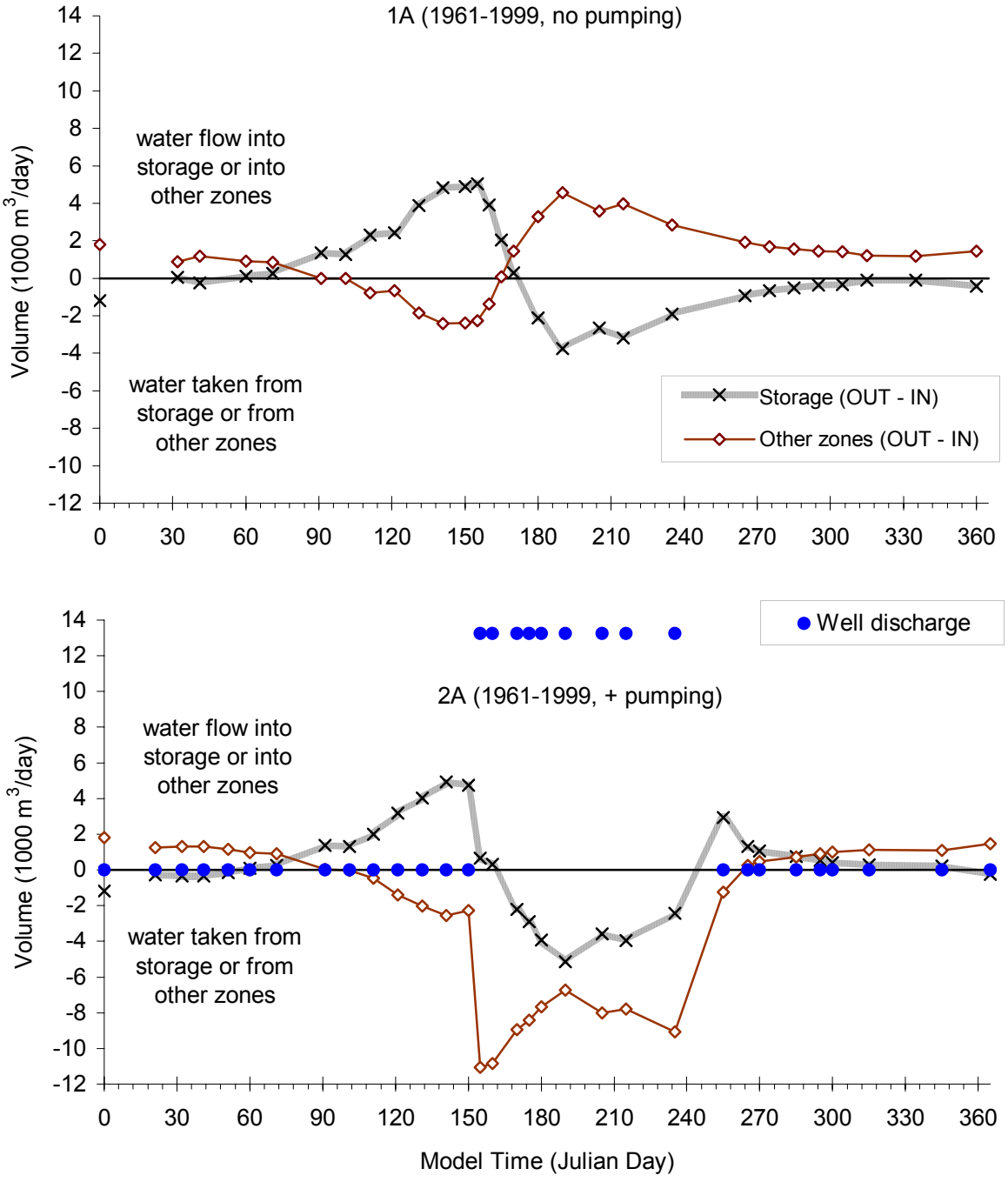

Figure C12 Transient model flow volumes for Zone 5 (Big Y Irrigation District) calculated for ZBUD IN and OUT components in Grand Forks aquifer. Comparing non-pumping to pumping scenarios for historical climate.
Symbol legend applies to both graphs, except for "well discharge" which applies only to pumping scenario results. Horizontal axis is time in days, vertical axis is flow volume in 1000's m^3/day. Same scales on both graphs.

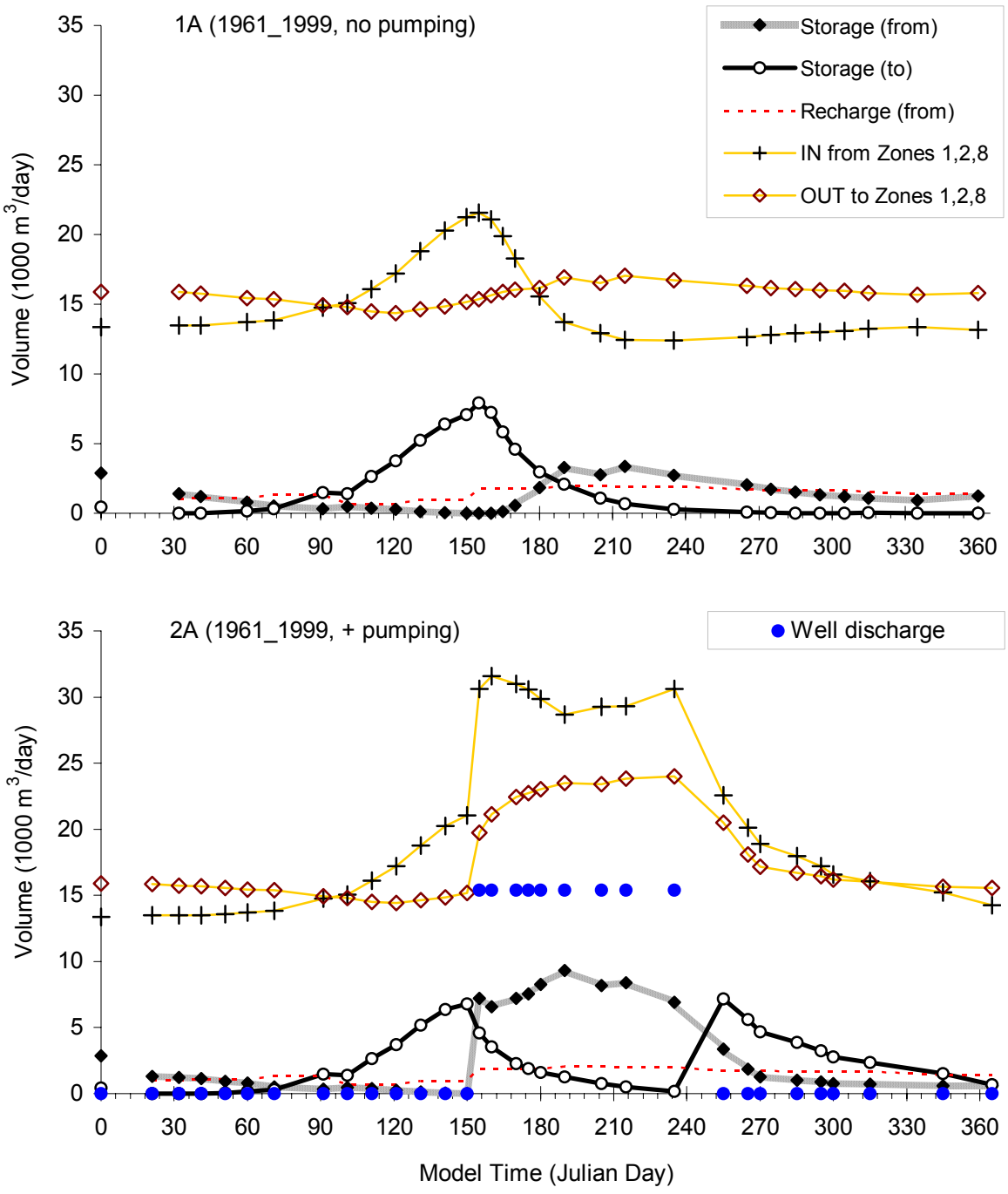

Figure C13 Transient model differences between OUT and IN flow volumes for Zone 5 (Big Y Irrigation District) calculated for ZBUD components in Grand Forks aquifer. Comparing non-pumping to pumping scenarios for historical climate. Symbol legend applies to both graphs, except for "well discharge" which applies only to pumping scenario results. Horizontal axis is time in days, vertical axis is flow volume in 1000's m^3/day. Same scales on both graphs.

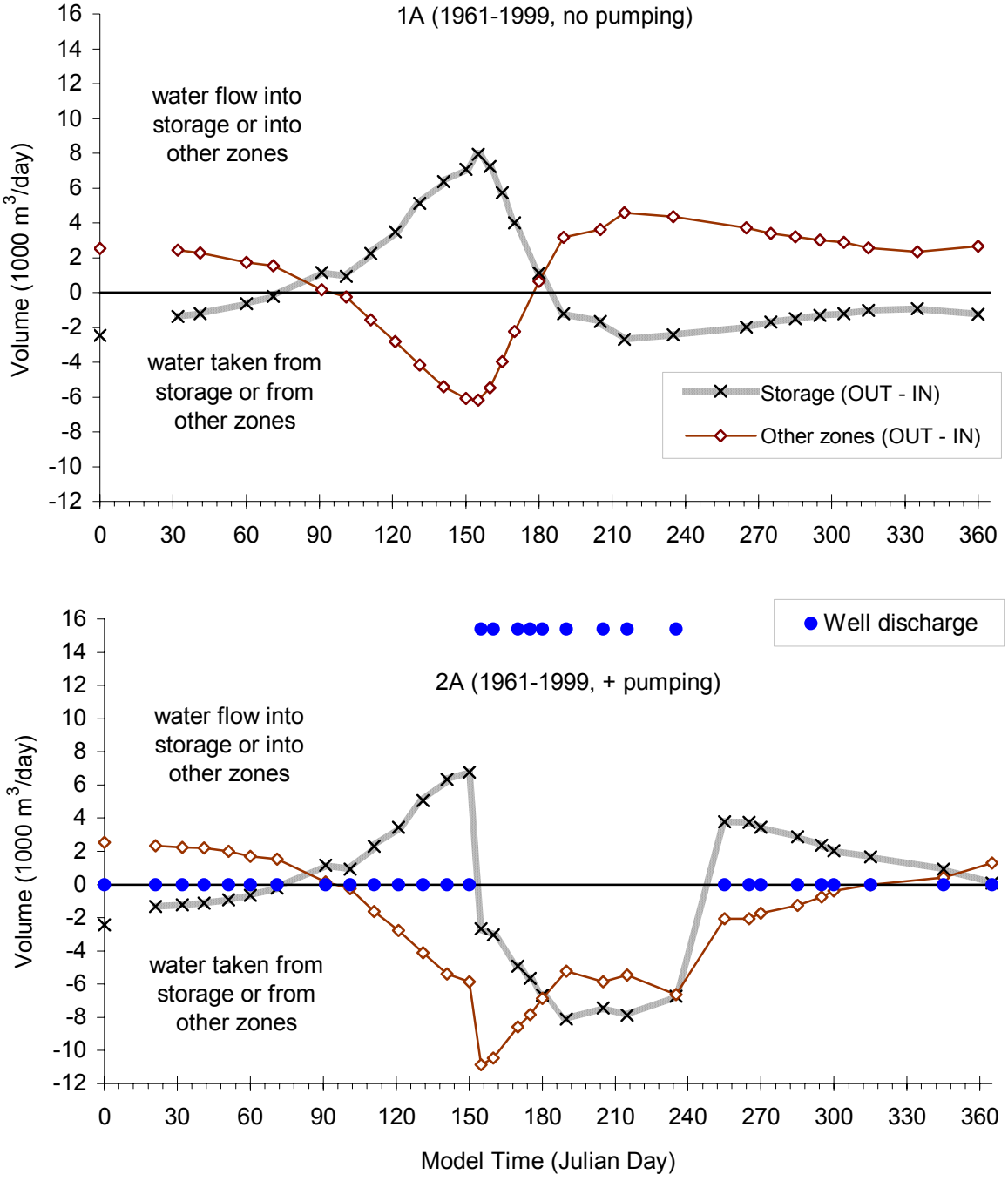

Figure C14 Transient model flow volumes for Zone 6 (Covert Irrigation District) calculated for ZBUD IN and OUT components in Grand Forks aquifer. Comparing non-pumping to pumping scenarios for historical climate.
Symbol legend applies to both graphs, except for "well discharge" which applies only to pumping scenario results. Horizontal axis is time in days, vertical axis is flow volume in 1000's m^3/day. Same scales on both graphs.

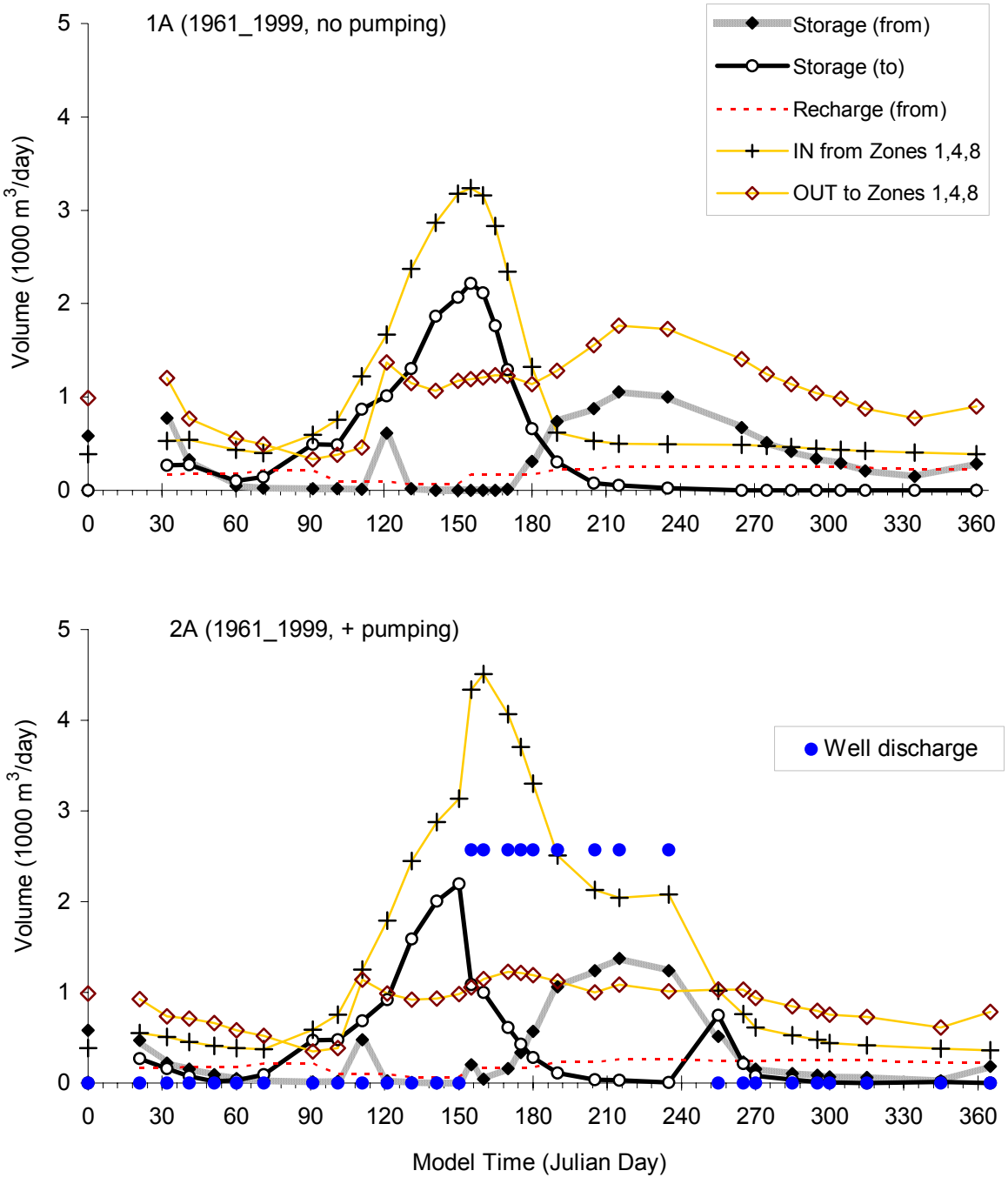

Figure C15 Transient model differences between OUT and IN flow volumes for Zone 6 (Covert Irrigation District) calculated for ZBUD components in Grand Forks aquifer. Comparing non-pumping to pumping scenarios for historical climate. Symbol legend applies to both graphs, except for "well discharge" which applies only to pumping scenario results. Horizontal axis is time in days, vertical axis is flow volume in 1000's m^3/day. Same scales on both graphs.

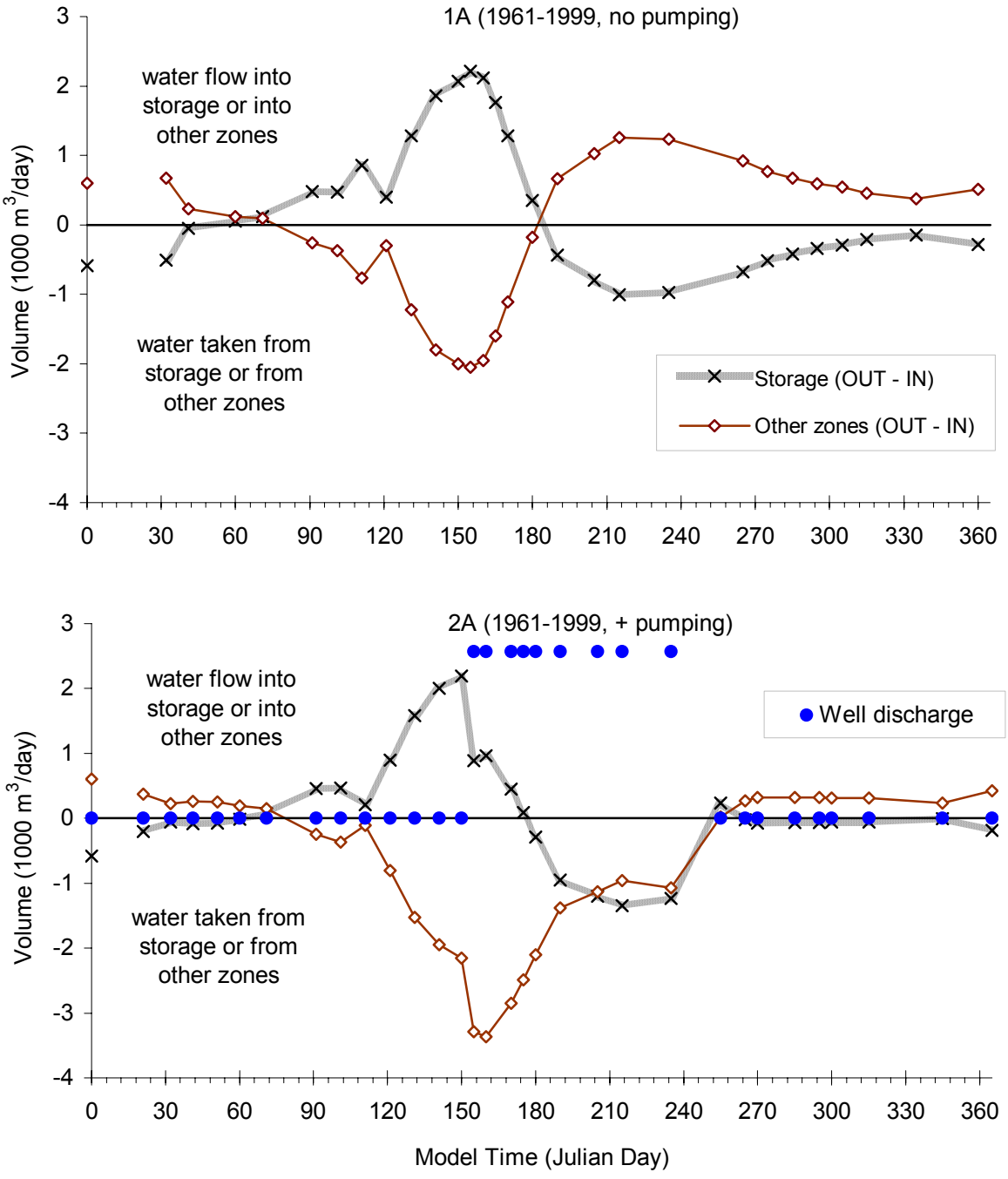

Figure C16 Transient model flow volumes for Zone 7 (Nursery Irrigation District) calculated for ZBUD IN and OUT components in Grand Forks aquifer. Comparing non-pumping to pumping scenarios for historical climate.
Symbol legend applies to both graphs. Horizontal axis is time in days, vertical axis is flow volume in 1000's m^3/day. Same scales on both graphs. There are no pumping wells in this ZBUD zone (Nursery wells are pumping in Floodplain Zone adjacent to Kettle River).

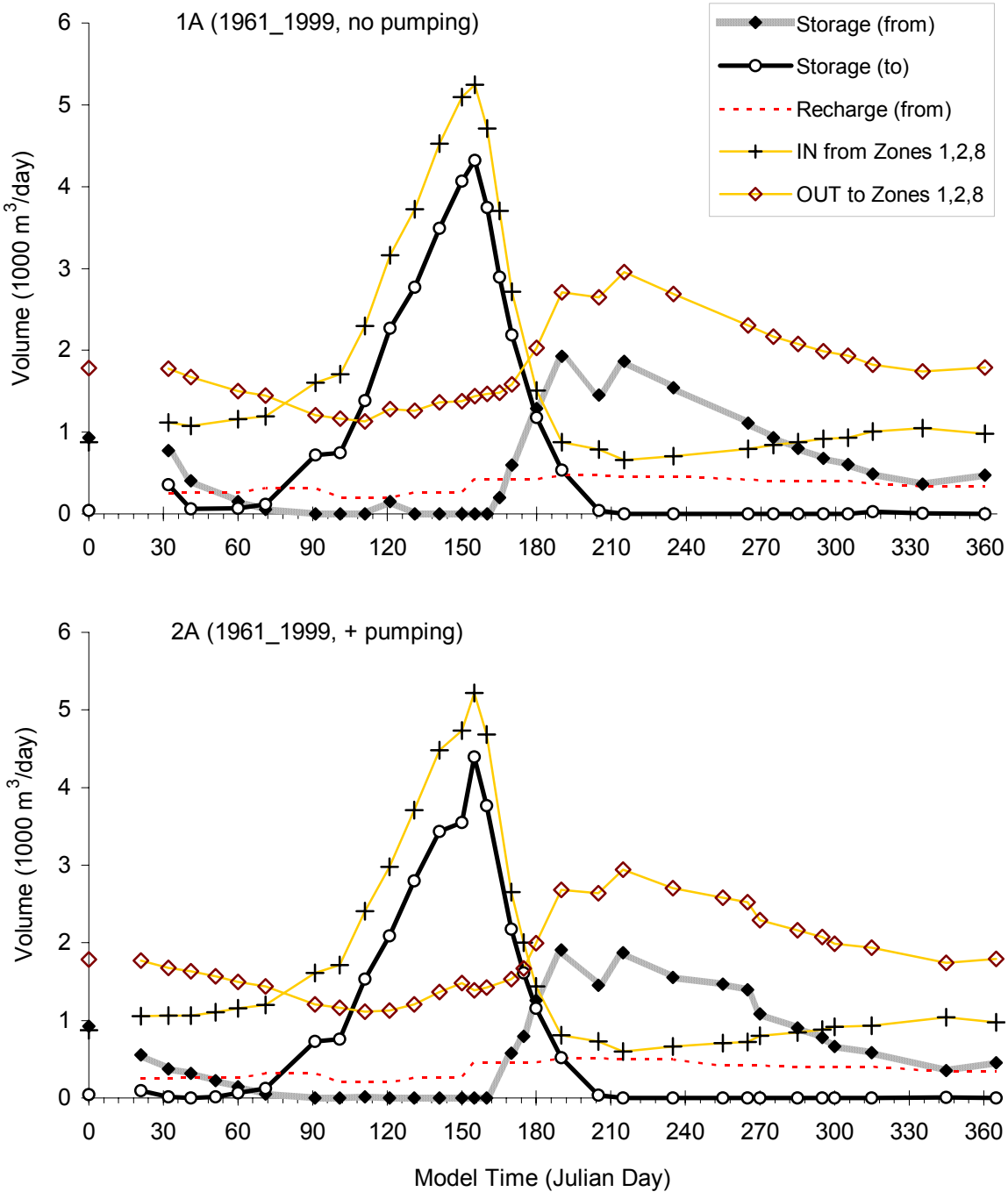

Figure C17 Transient model differences between OUT and IN flow volumes for Zone 7 (Nursery Irrigation District) calculated for ZBUD components in Grand Forks aquifer. Comparing non-pumping to pumping scenarios for historical climate. Symbol legend applies to both graphs. Horizontal axis is time in days, vertical axis is flow volume in 1000's m^3/day. Same scales on both graphs. There are no pumping wells in this ZBUD zone (Nursery wells are pumping in Floodplain Zone adjacent to Kettle River).

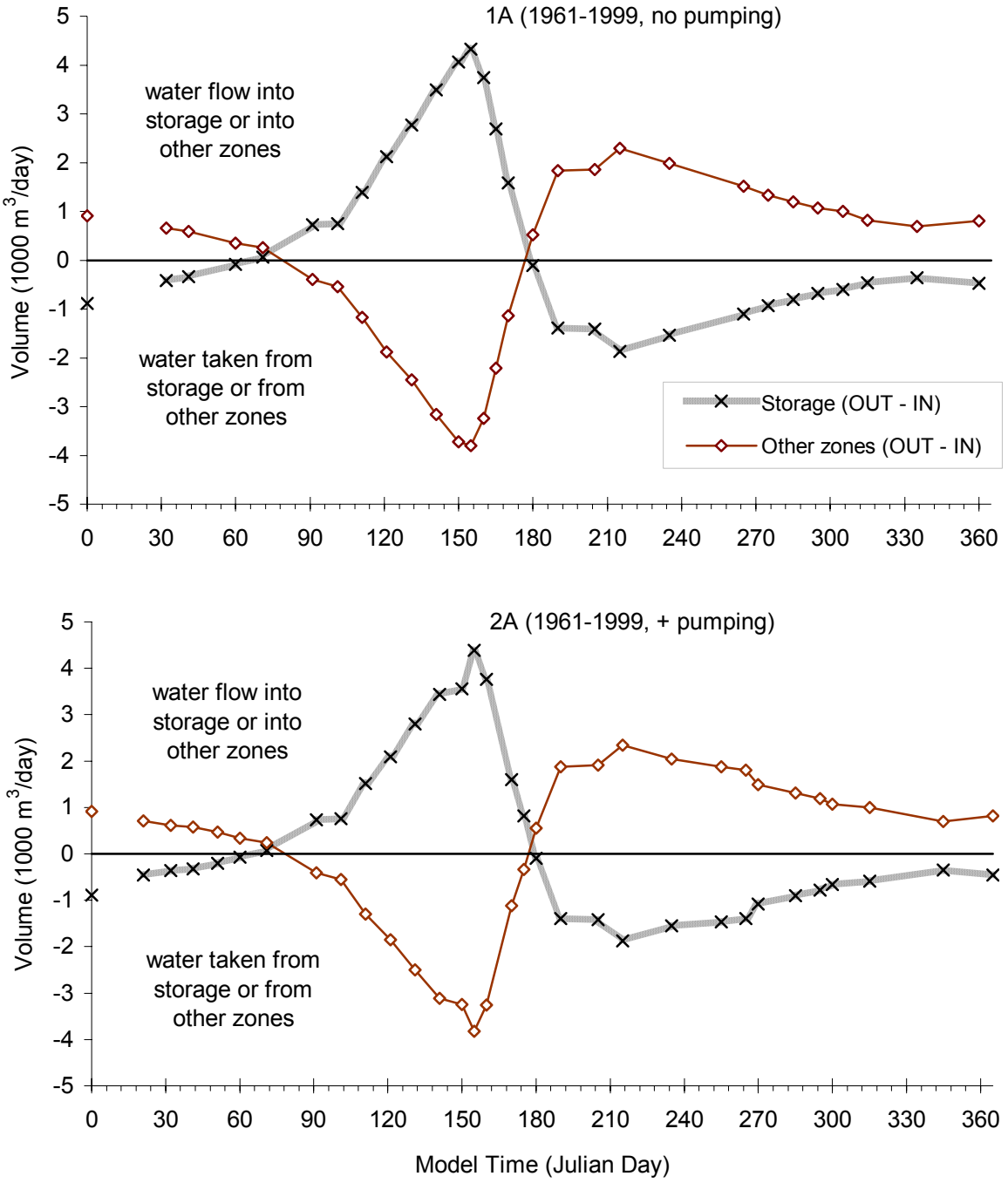

Figure C18 Transient model flow volumes for Zone 8 (Silt Layer) calculated for ZBUD IN and OUT components in Grand Forks aquifer. Comparing non-pumping to pumping scenarios for historical climate.
Symbol legend applies to both graphs. Horizontal axis is time in days, vertical axis is flow volume in 1000's m^3/day. Same scales on both graphs.

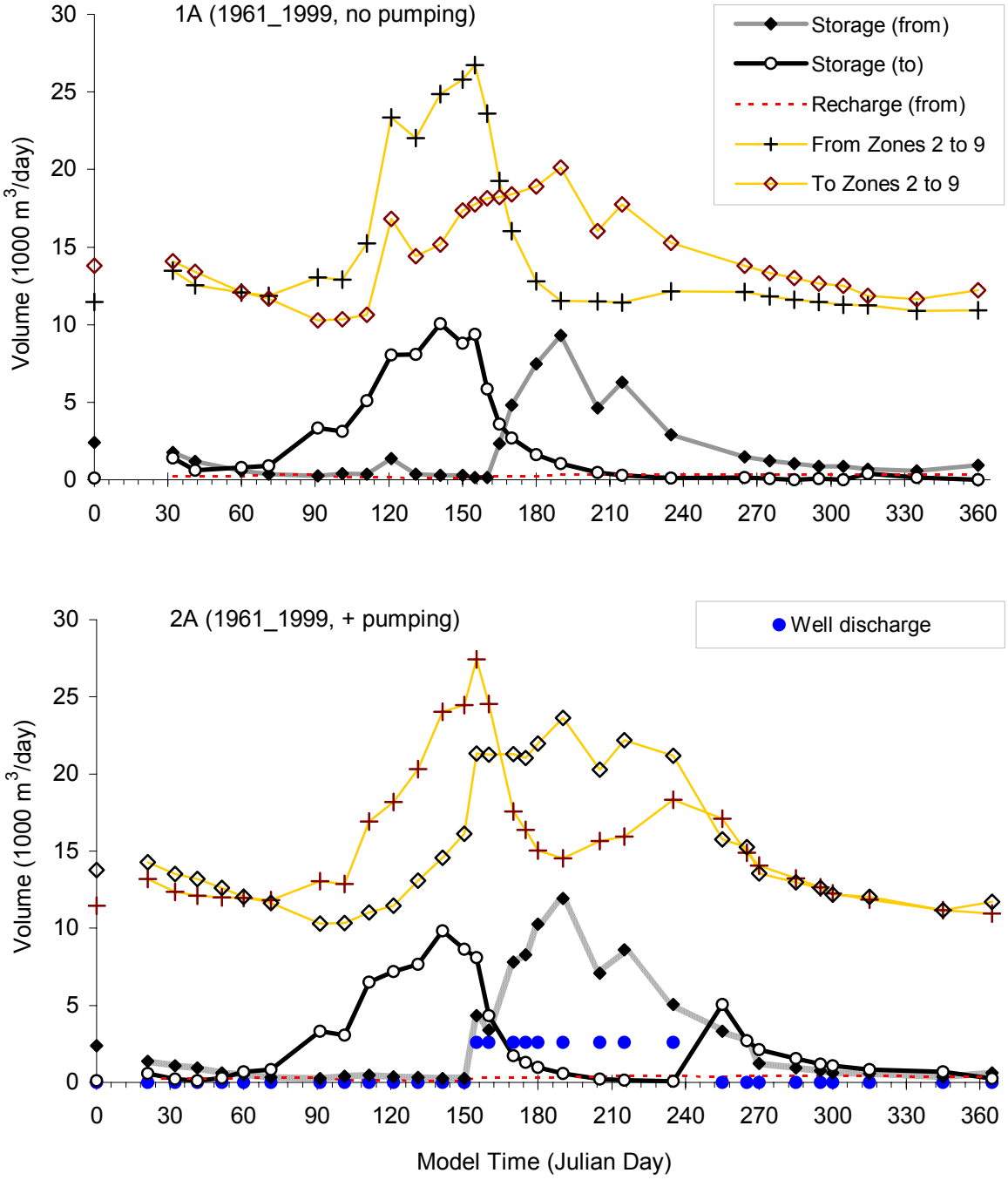

Figure C19 Transient model differences between OUT and IN flow volumes for Zone 8 (Silt Layer) calculated for ZBUD components in Grand Forks aquifer. Comparing non-pumping to pumping scenarios for historical climate.
Symbol legend applies to both graphs. Horizontal axis is time in days, vertical axis is flow volume in 1000's m^3/day. Same scales on both graphs.

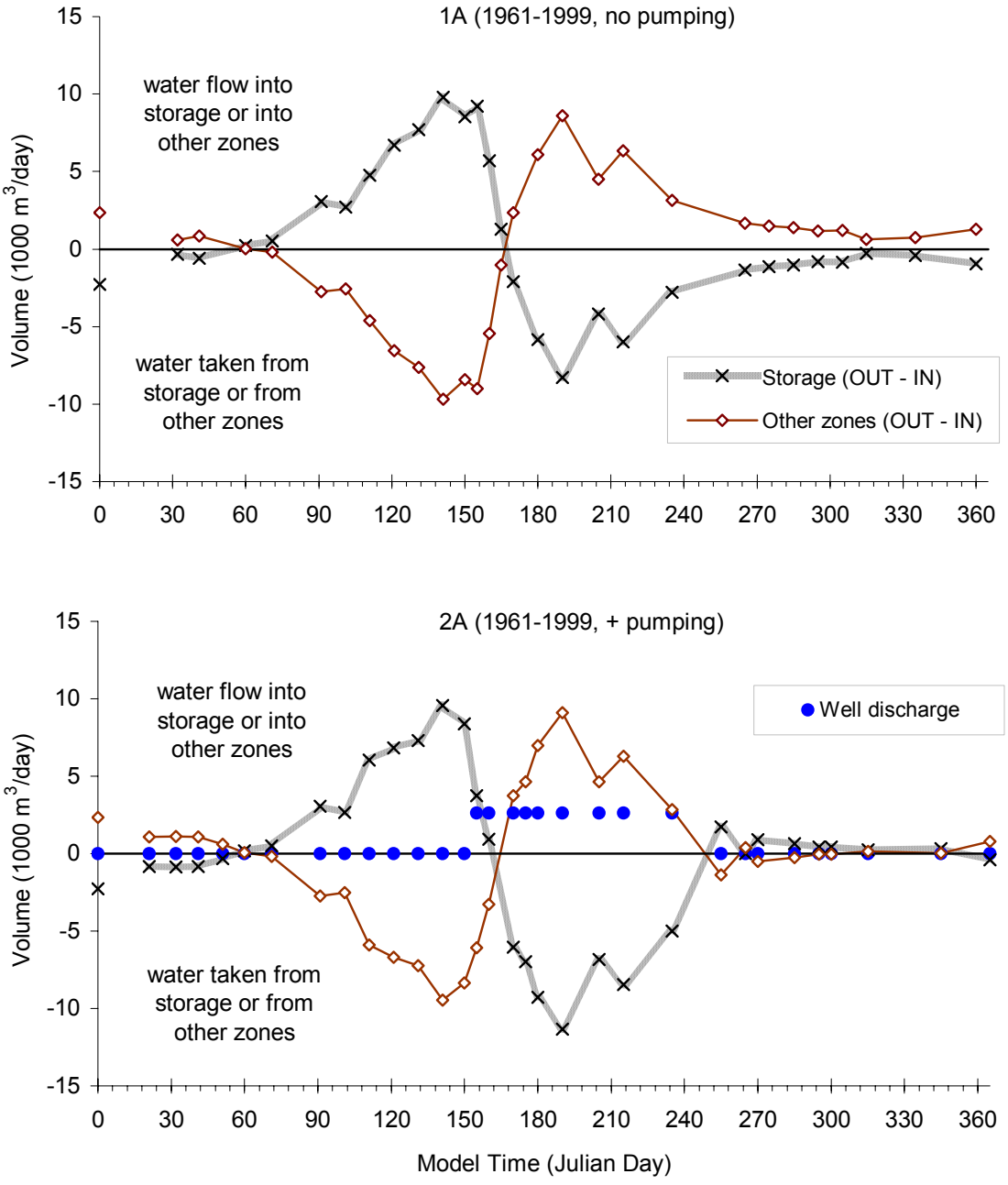

Figure C20 Transient model flow volumes for Zone 9 (Clay Layer) calculated for ZBUD IN and OUT components in Grand Forks aquifer. Comparing non-pumping to pumping scenarios for historical climate.
Symbol legend applies to both graphs. Horizontal axis is time in days, vertical axis is flow volume in 1000's m^3/day. Same scales on both graphs. There are no pumping wells in this zone.

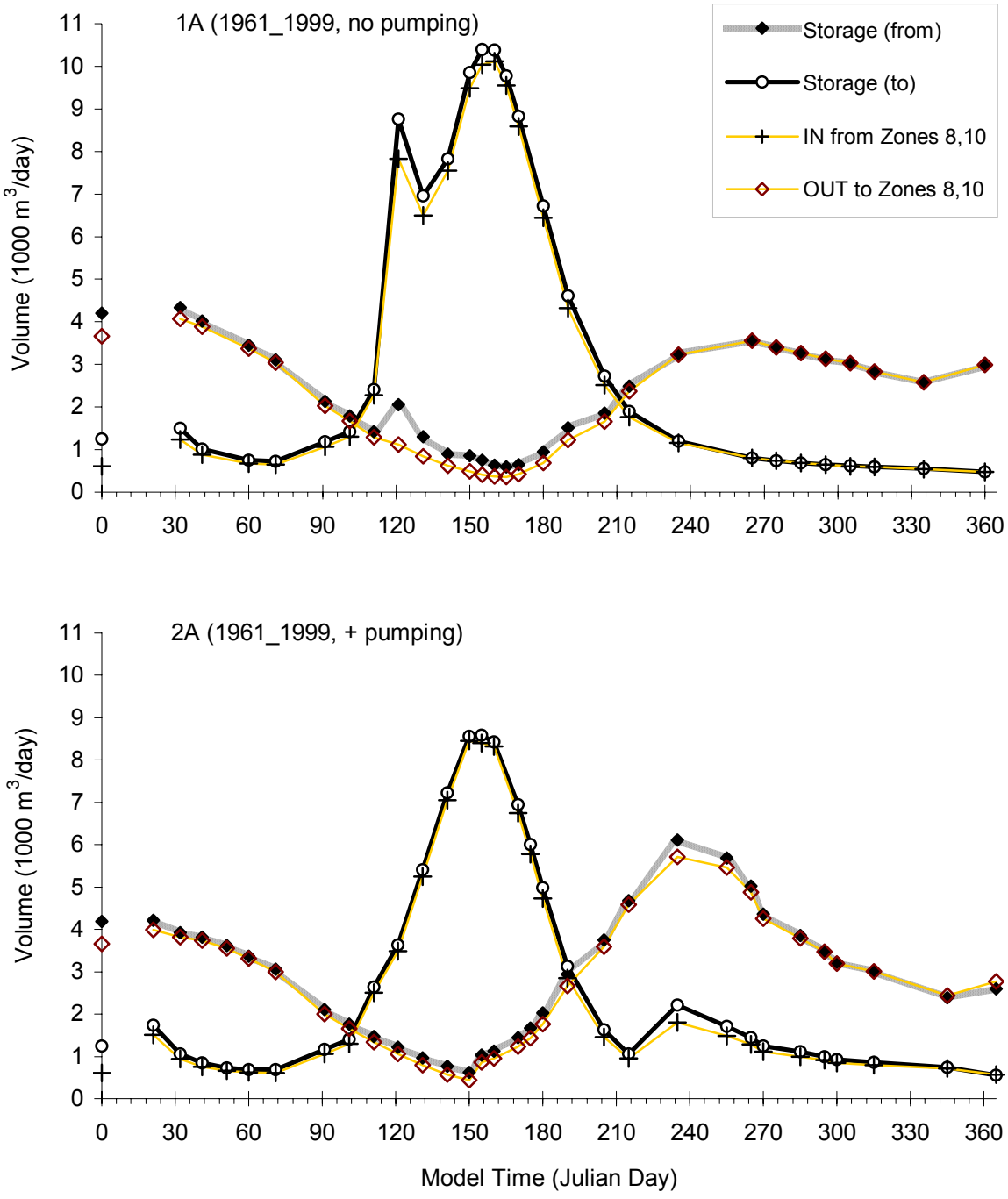

Figure C21 Transient model differences between OUT and IN flow volumes for Zone 8 (Silt Layer) calculated for ZBUD components in Grand Forks aquifer. Comparing non-pumping to pumping scenarios for historical climate.
Symbol legend applies to both graphs. Horizontal axis is time in days, vertical axis is flow volume in 1000's m^3/day. Same scales on both graphs. There are no pumping wells in this zone.

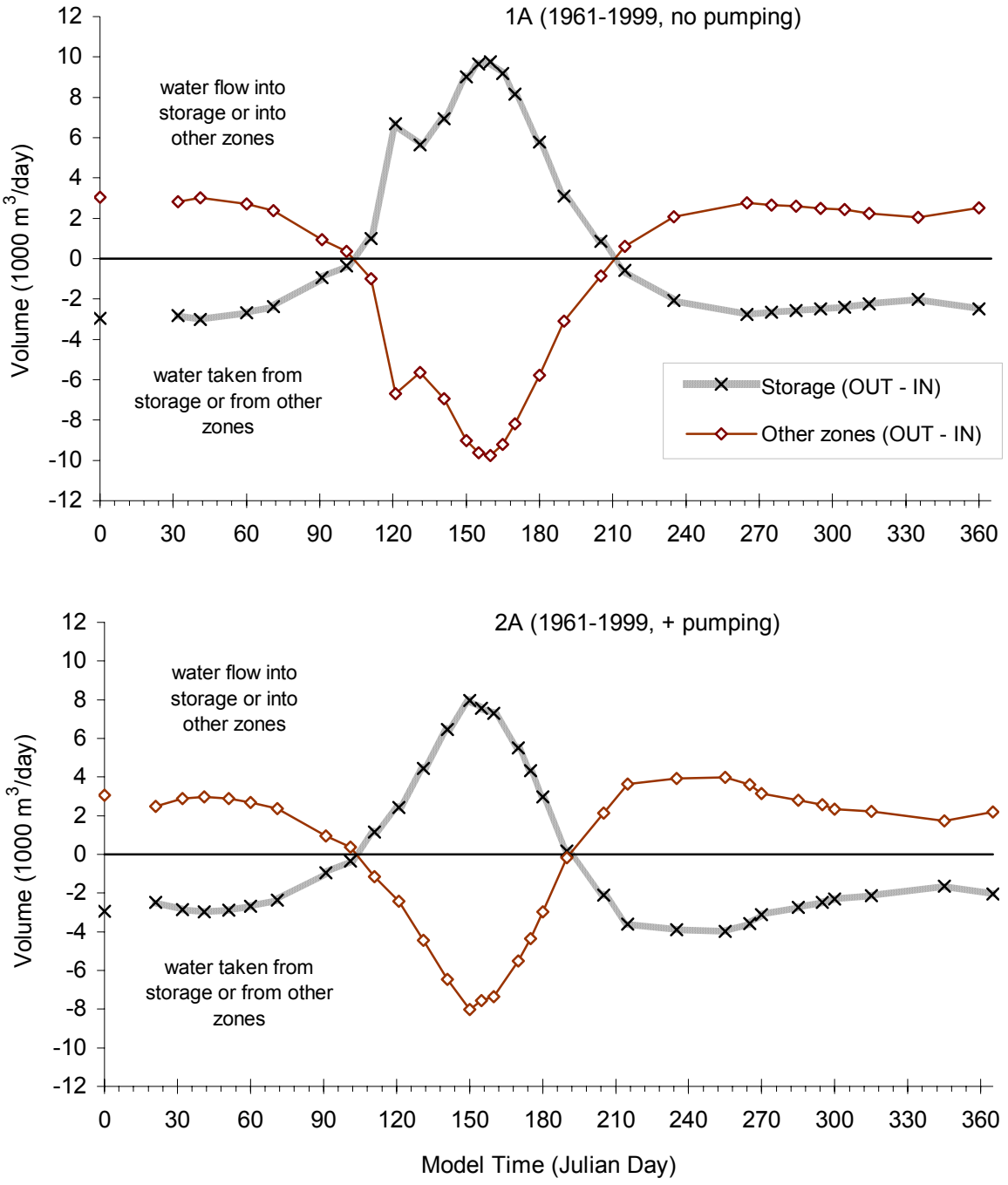

GRAPHS SHOWING GROUNDWATER STORAGE AND FLOW BETWEEN ZONES (PUMPING AND NON-PUMPING SCENARIOS – MODEL PREDICTIONS IN FUTURE CLIMATE SCENARIOS)

Figure C22 Transient model water Storage component of ZBUD for Zone 1 (GF Irrigation District and background) in Grand Forks aquifer. Comparing non-pumping to pumping and all climate change scenarios.
Symbol legend applies to both graphs. Horizontal axis is time in days, vertical axis is flow volume in 1000's m^3/day. Same scales on both graphs.

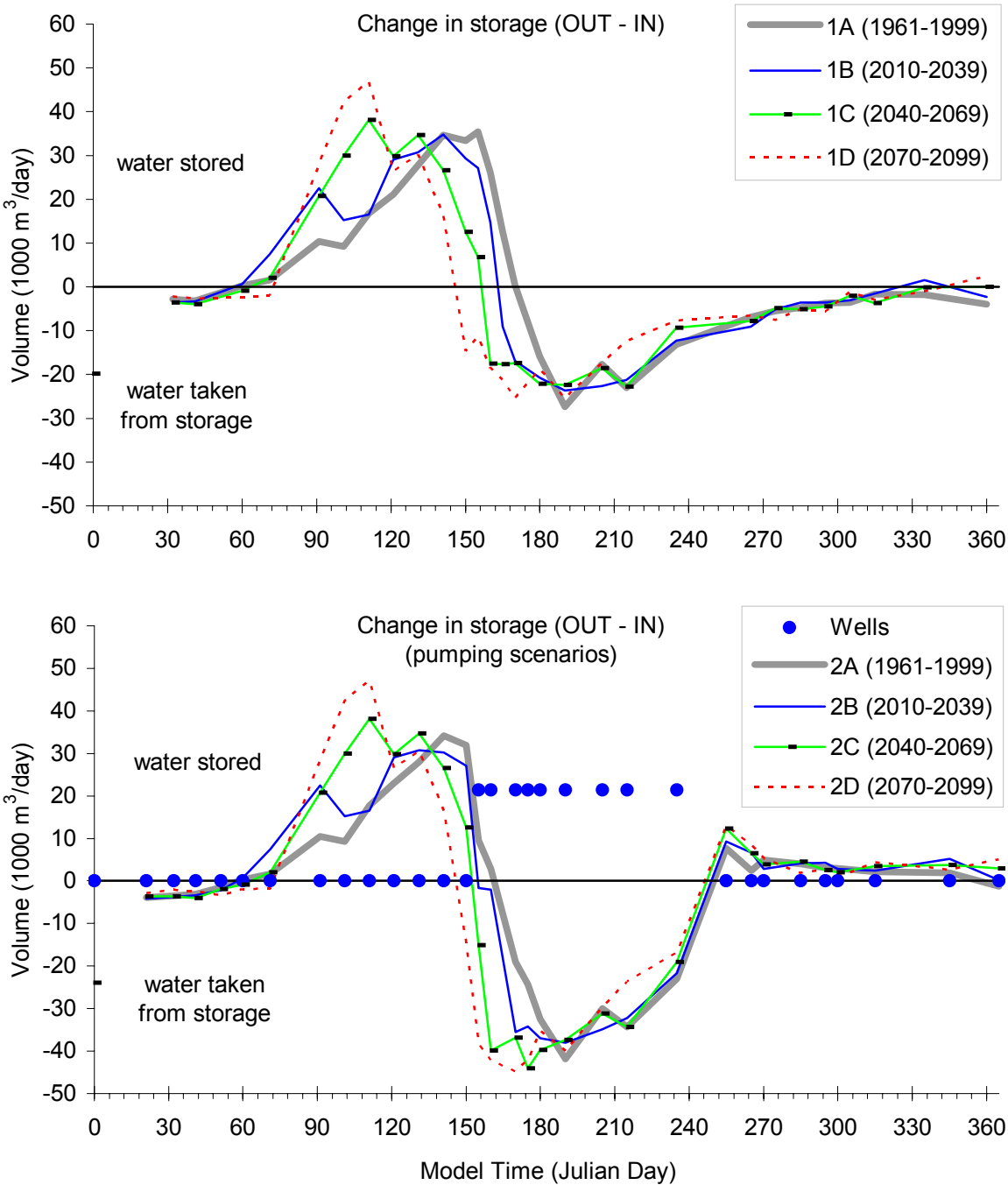

Figure C23 Transient model water flow to/from other zones for Zone 1 (GF Irrigation District and background) in Grand Forks aquifer. Comparing non-pumping to pumping and all climate change scenarios.
Symbol legend applies to both graphs. Horizontal axis is time in days, vertical axis is flow volume in 1000's m^3/day. Same scales on both graphs.

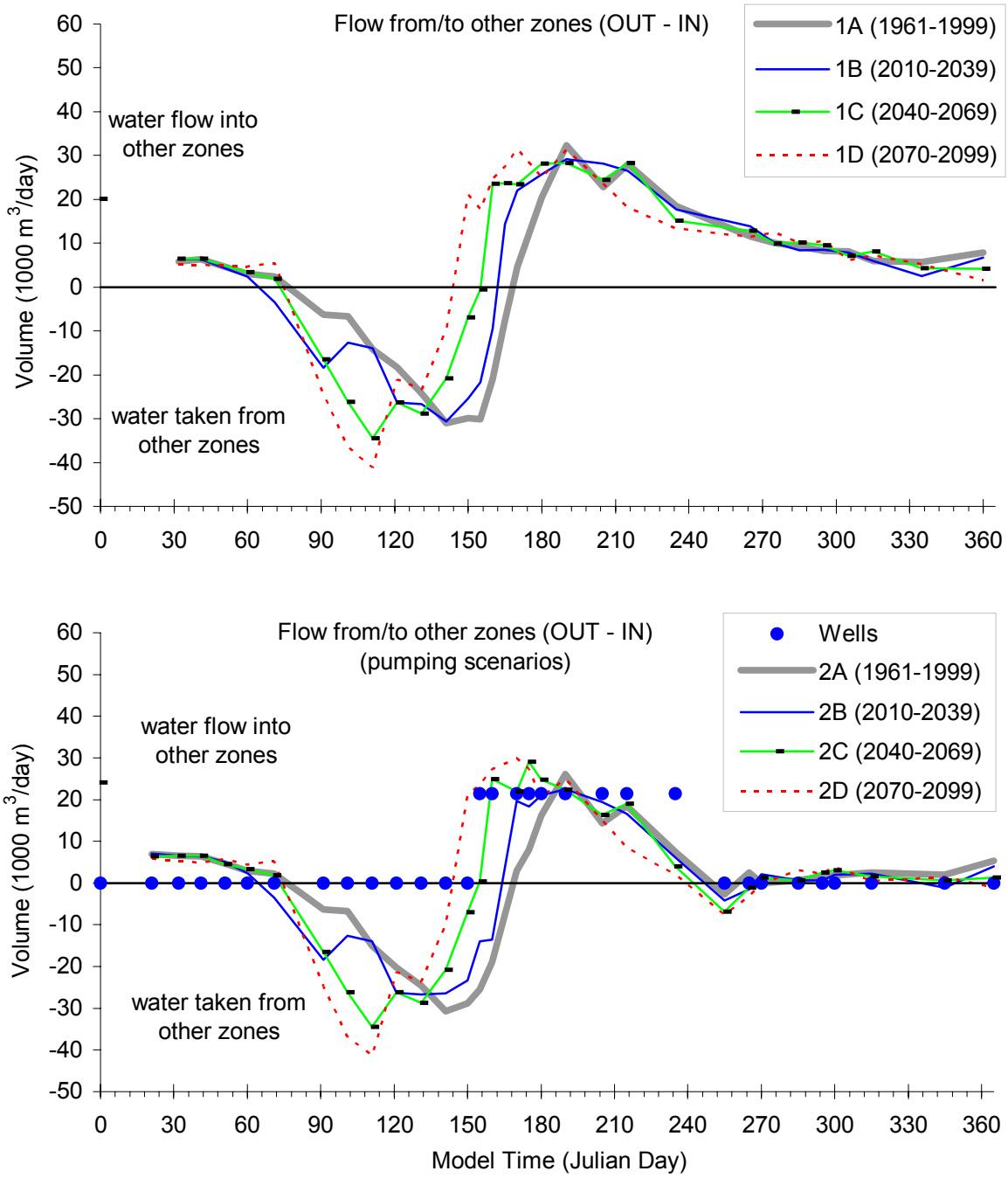

Figure C24 Transient model water Storage component of ZBUD for Zone 2 (Floodplain) in Grand Forks aquifer. Comparing non-pumping to pumping and all climate change scenarios.
Symbol legend applies to both graphs. Horizontal axis is time in days, vertical axis is flow volume in 1000's m^3/day. Same scales on both graphs.

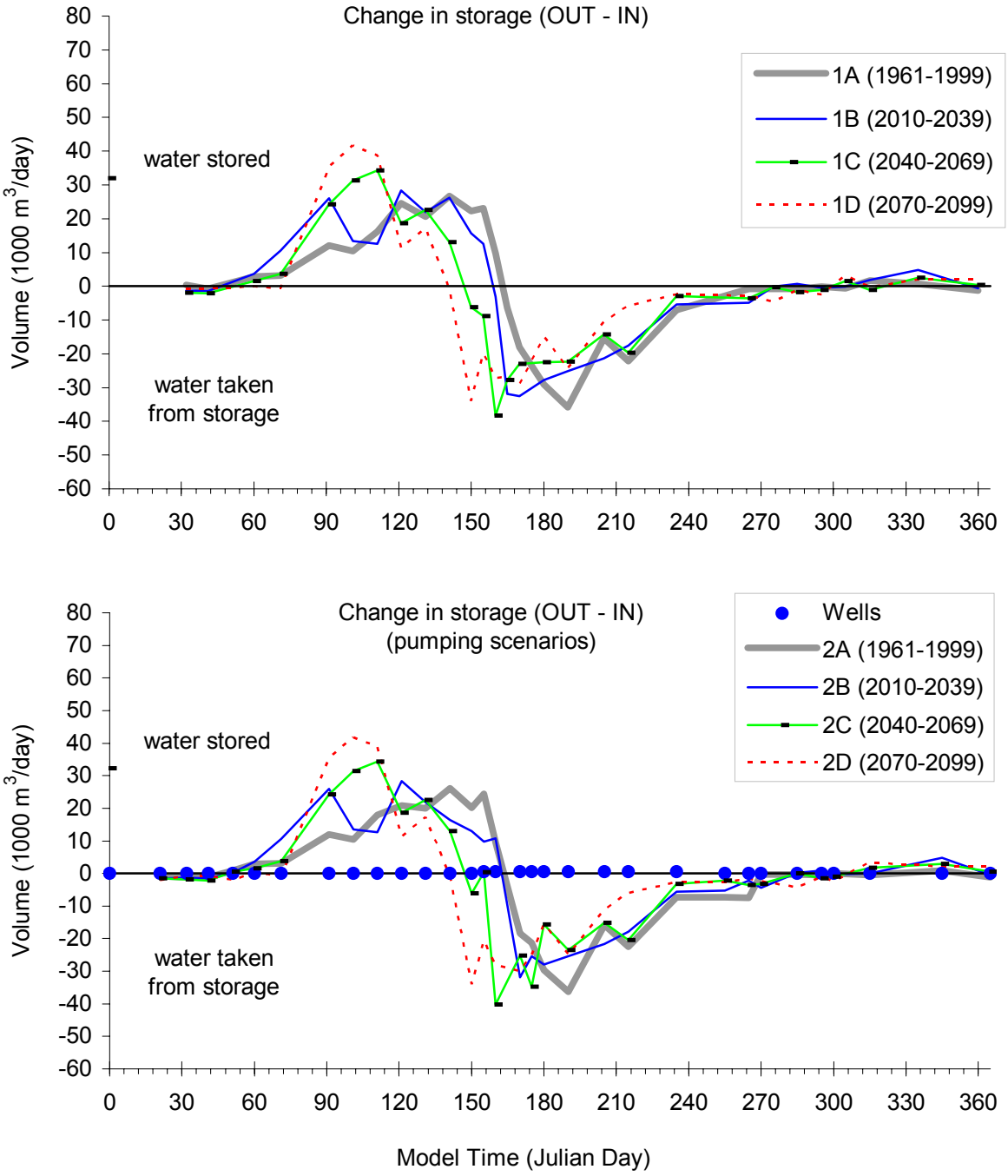

Figure C25 Transient model water flow to/from other zones for Zone 2 (Floodplain) in Grand Forks aquifer. Comparing non-pumping to pumping and all climate change scenarios.
Symbol legend applies to both graphs. Horizontal axis is time in days, vertical axis is flow volume in 1000's m^3/day. Same scales on both graphs.

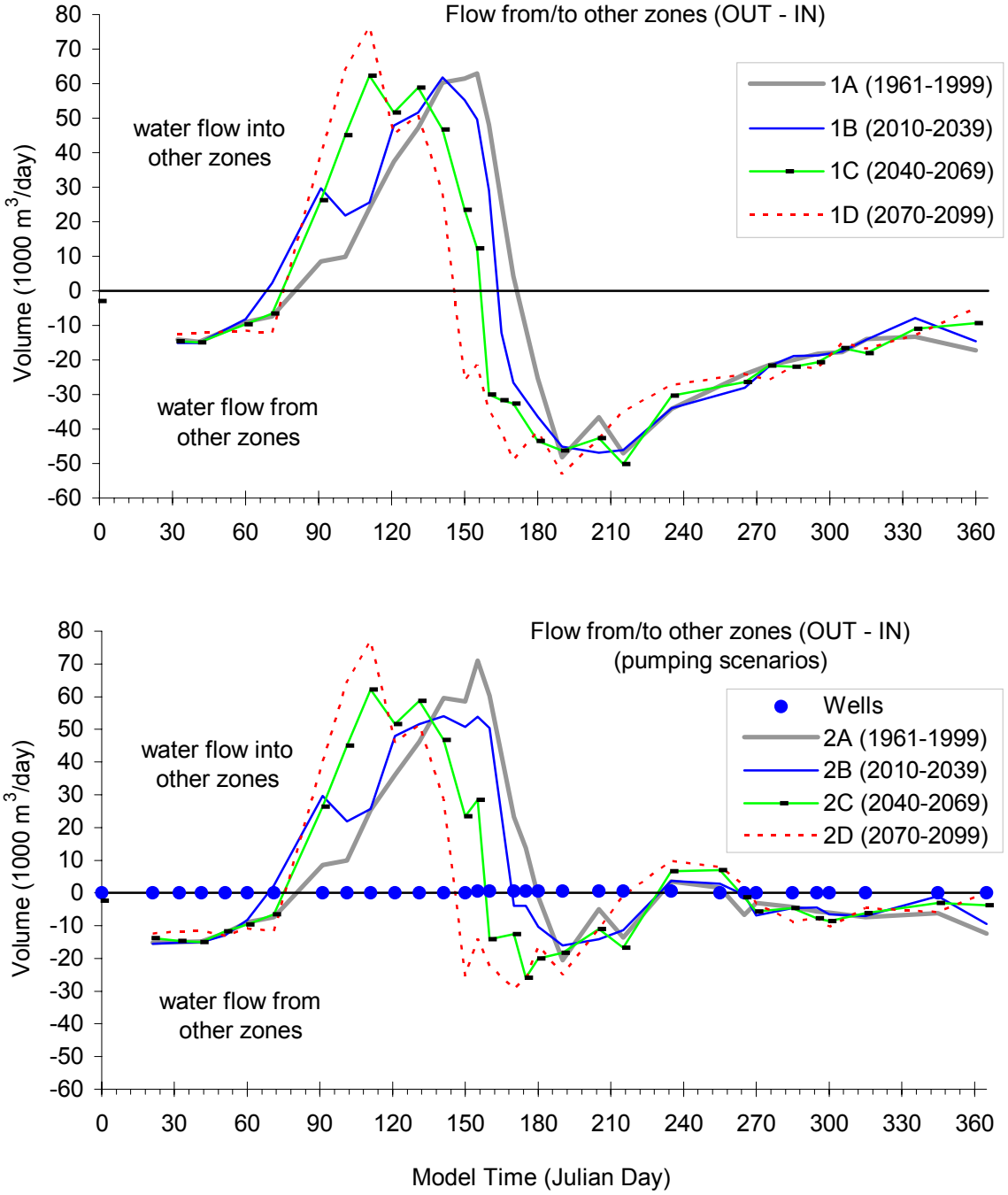

Figure C26 Transient model water Storage component of ZBUD for Zone 3 (Sion 1 Irrigation District) in Grand Forks aquifer. Comparing non-pumping to pumping and all climate change scenarios.
Symbol legend applies to both graphs. Horizontal axis is time in days, vertical axis is flow volume in 1000's m^3/day. Same scales on both graphs.

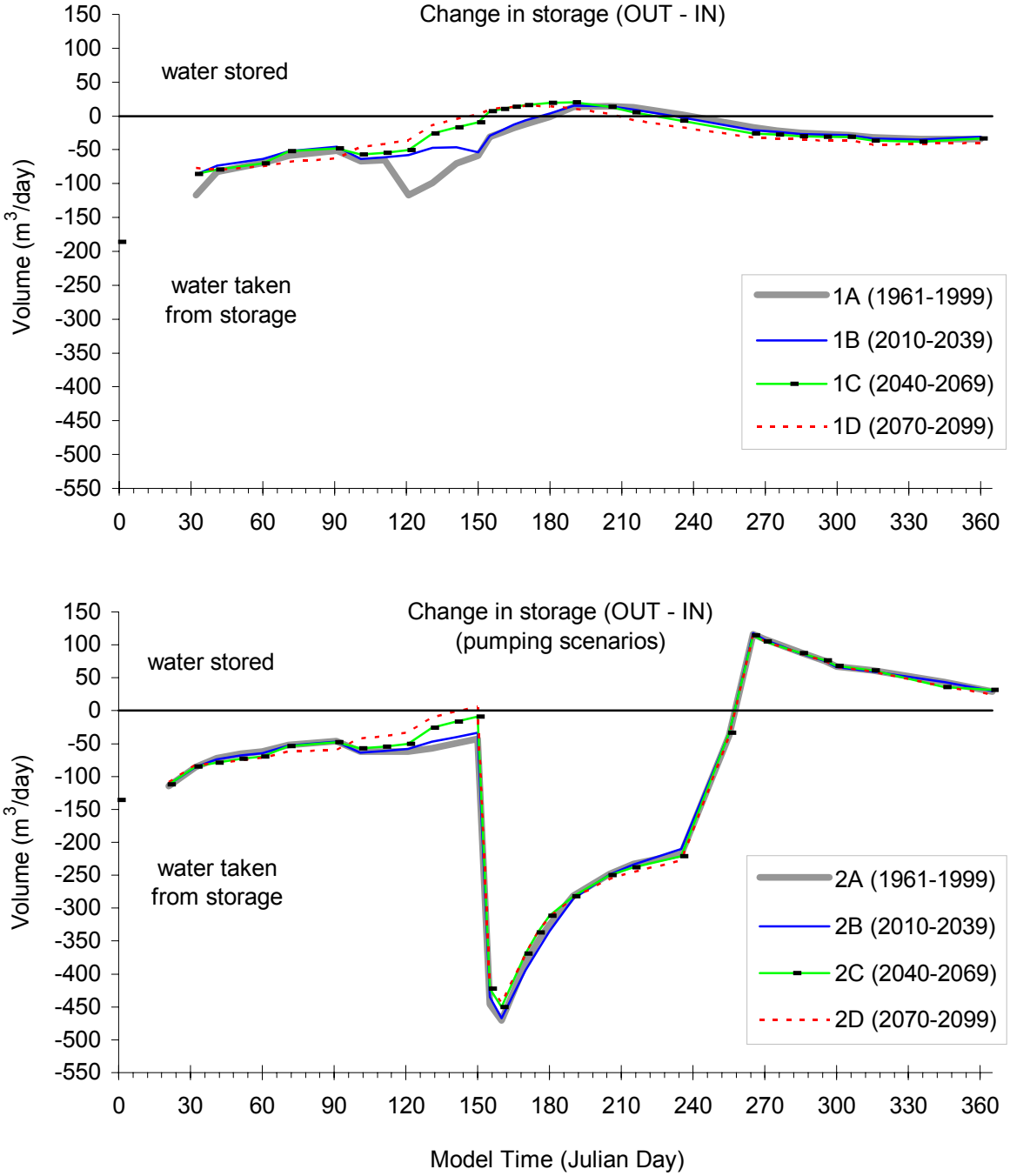

Figure C27 Transient model water flow to/from other zones for Zone 3 (Sion 1 Irrigation District) in Grand Forks aquifer. Comparing non-pumping to pumping and all climate change scenarios.
Symbol legend applies to both graphs. Horizontal axis is time in days, vertical axis is flow volume in 1000's m^3/day. Same scales on both graphs.

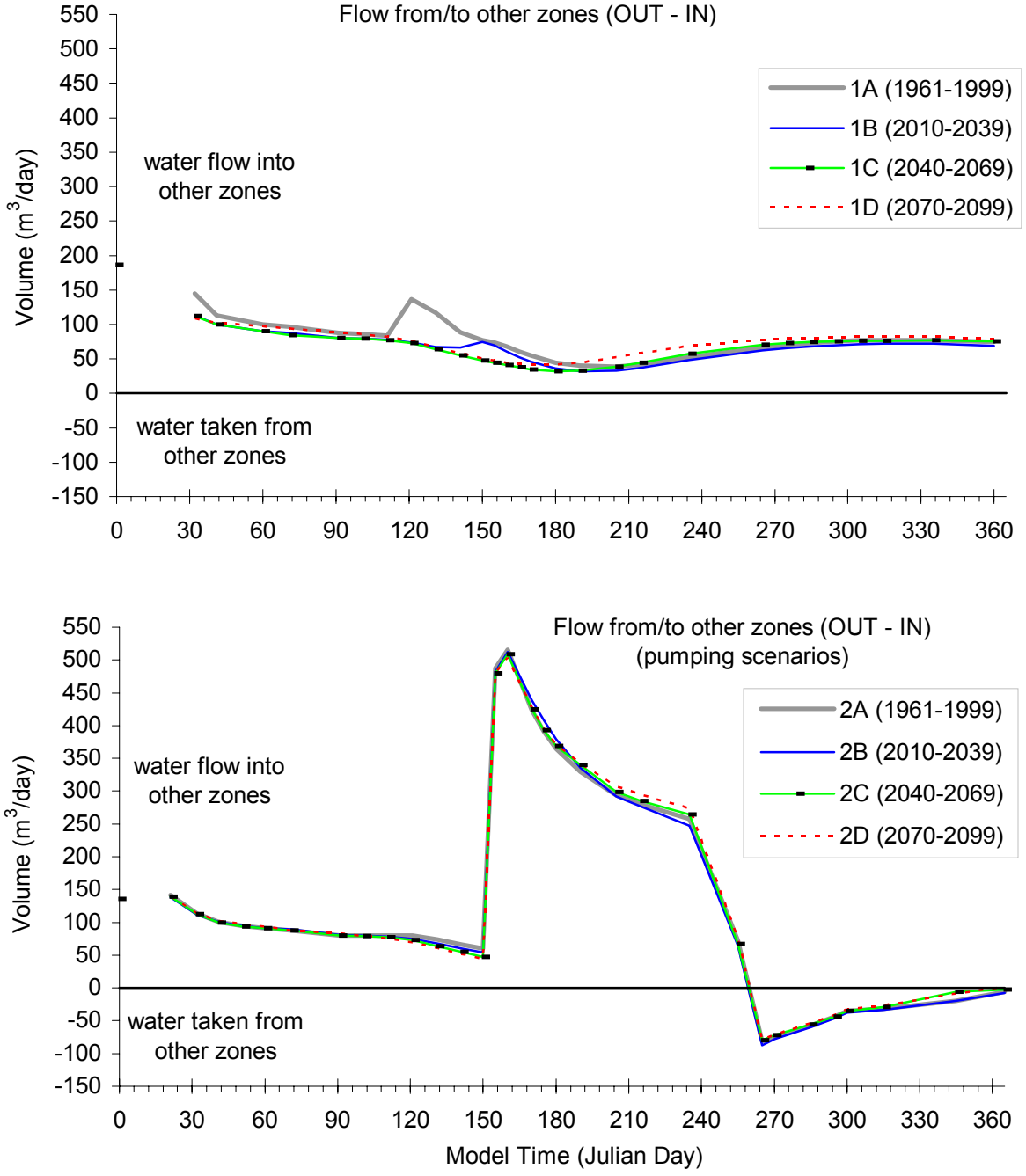

Figure C28 Transient model water Storage component of ZBUD for Zone 4 (Sion 2 & 3 Irrigation Districts) in Grand Forks aquifer. Comparing non-pumping to pumping and all climate change scenarios.
Symbol legend applies to both graphs. Horizontal axis is time in days, vertical axis is flow volume in 1000's m^3/day. Same scales on both graphs.

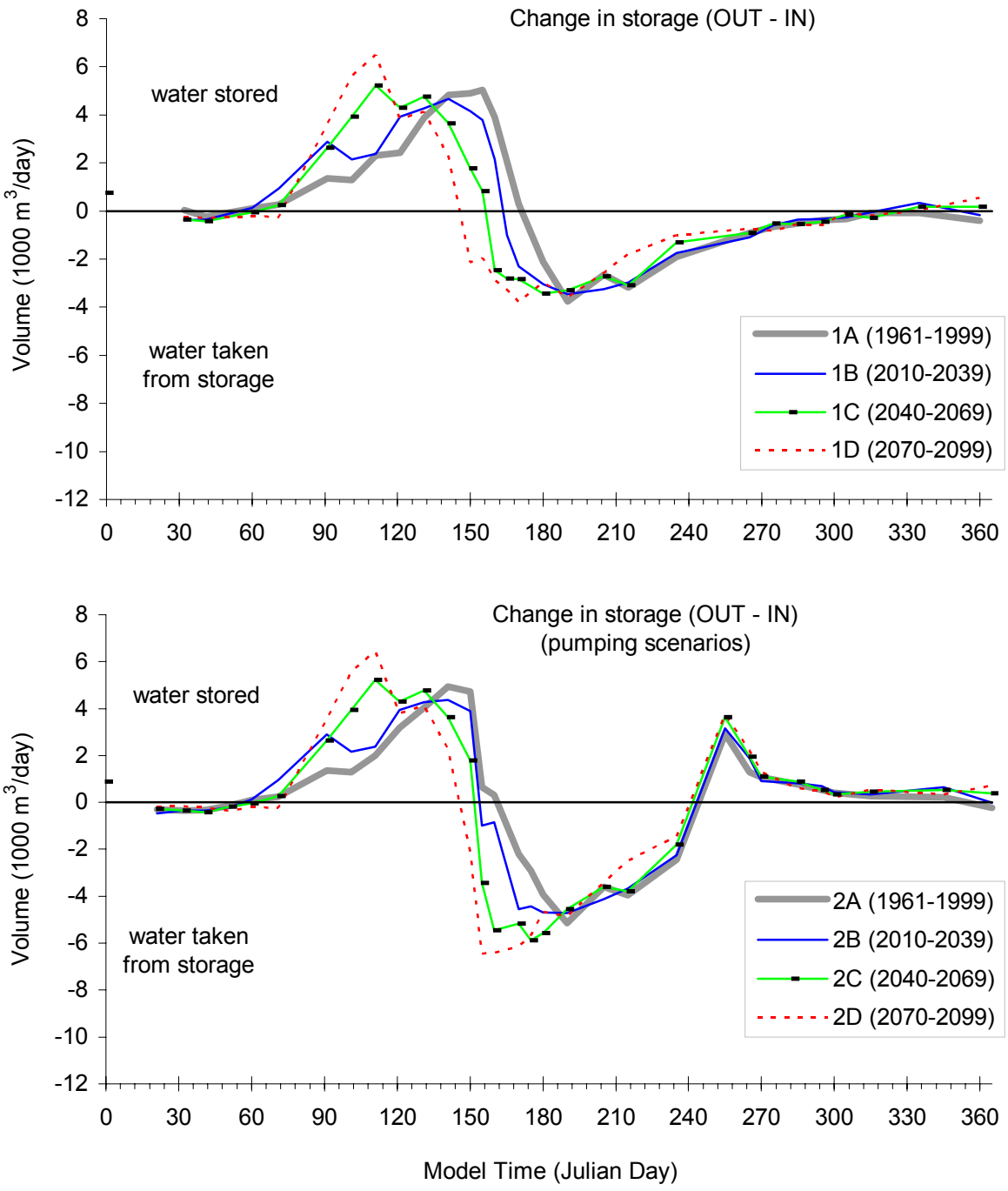

Figure C29 Transient model water flow to/from other zones for Zone 4 (Sion 2 & 3 Irrigation Districts) in Grand Forks aquifer. Comparing non-pumping to pumping and all climate change scenarios.
Symbol legend applies to both graphs. Horizontal axis is time in days, vertical axis is flow volume in 1000's m^3/day. Same scales on both graphs.

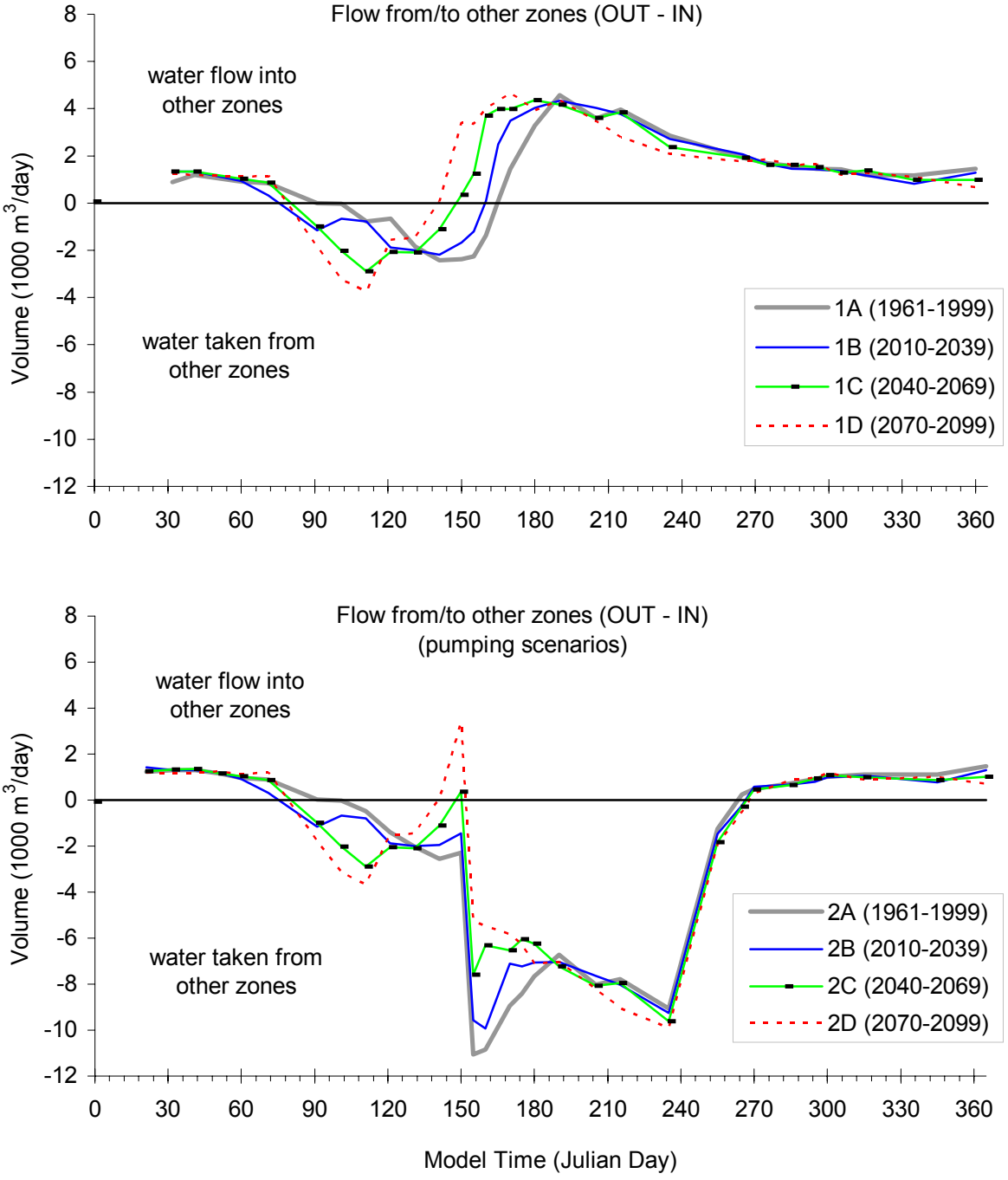

Figure C30 Transient model water Storage component of ZBUD for Zone 5 (Big Y Irrigation District) in Grand Forks aquifer. Comparing non-pumping to pumping and all climate change scenarios.
Symbol legend applies to both graphs. Horizontal axis is time in days, vertical axis is flow volume in 1000's m^3/day. Same scales on both graphs.

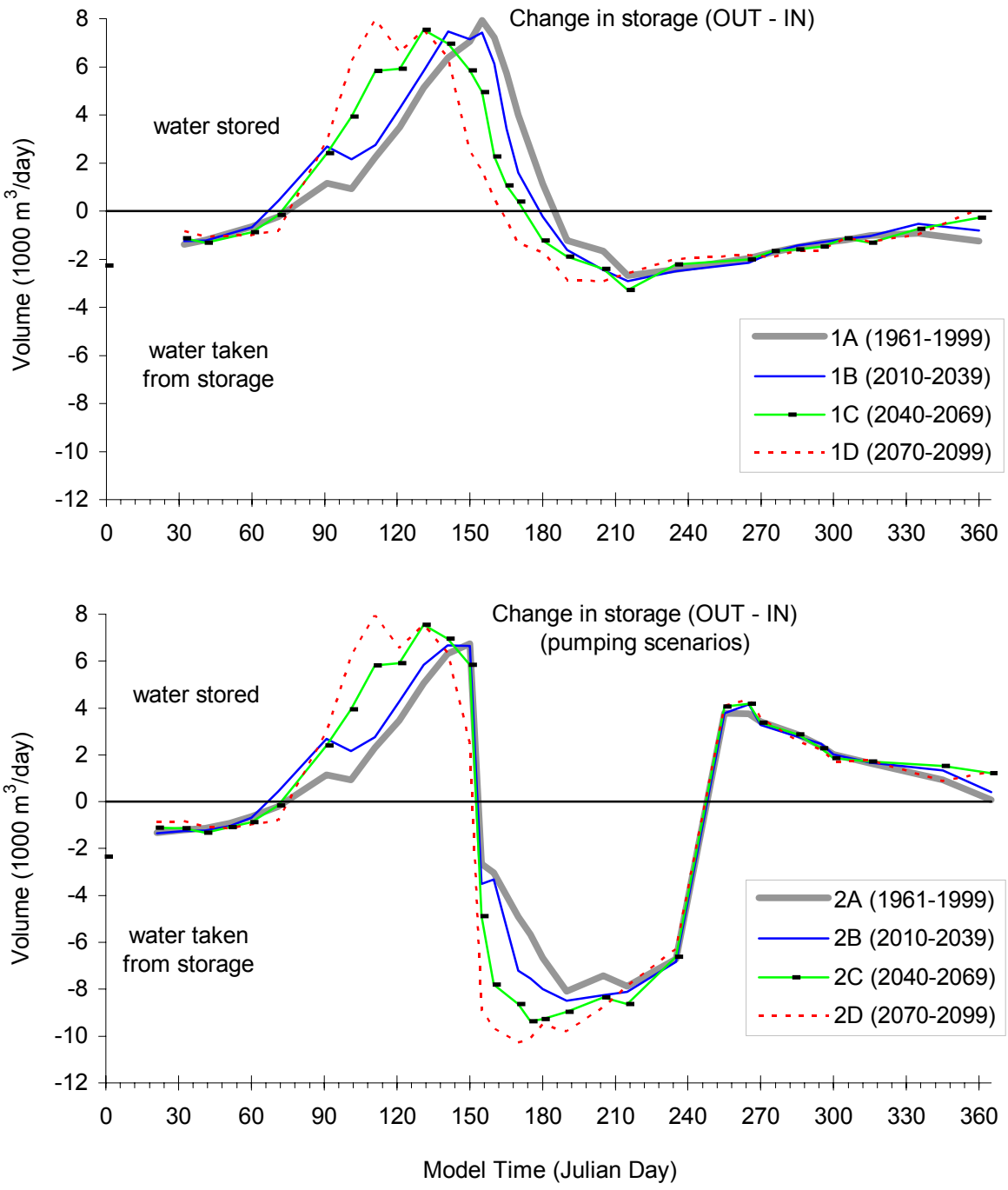

Figure C31 Transient model water flow to/from other zones for Zone 5 (Big Y Irrigation District) in Grand Forks aquifer. Comparing non-pumping to pumping and all climate change scenarios.
Symbol legend applies to both graphs. Horizontal axis is time in days, vertical axis is flow volume in 1000's m^3/day. Same scales on both graphs.

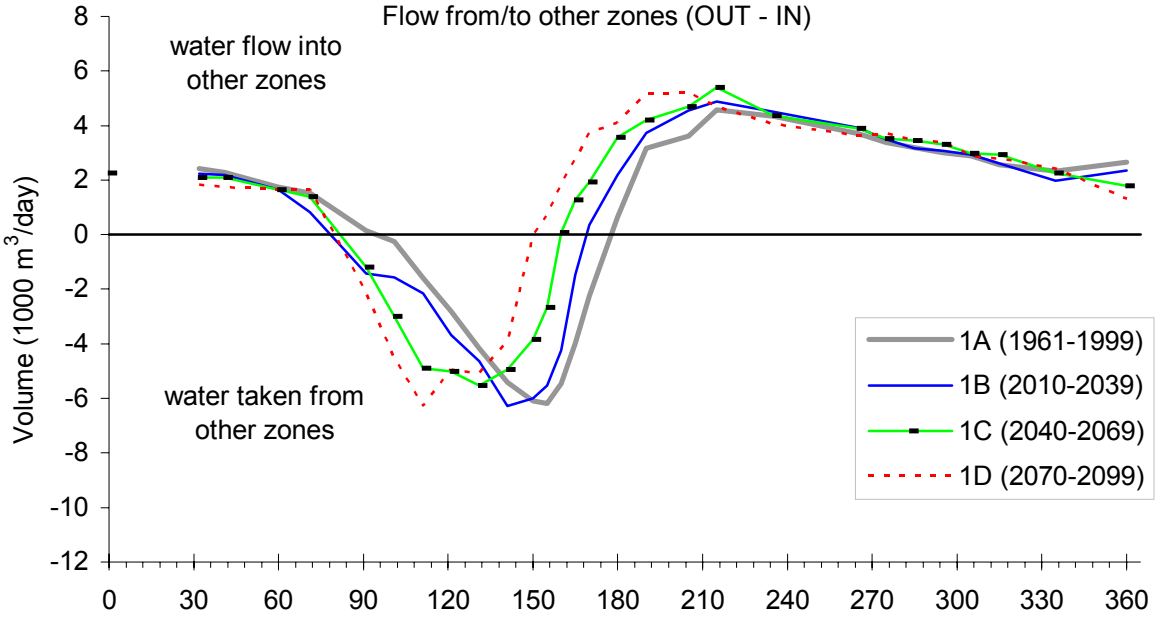

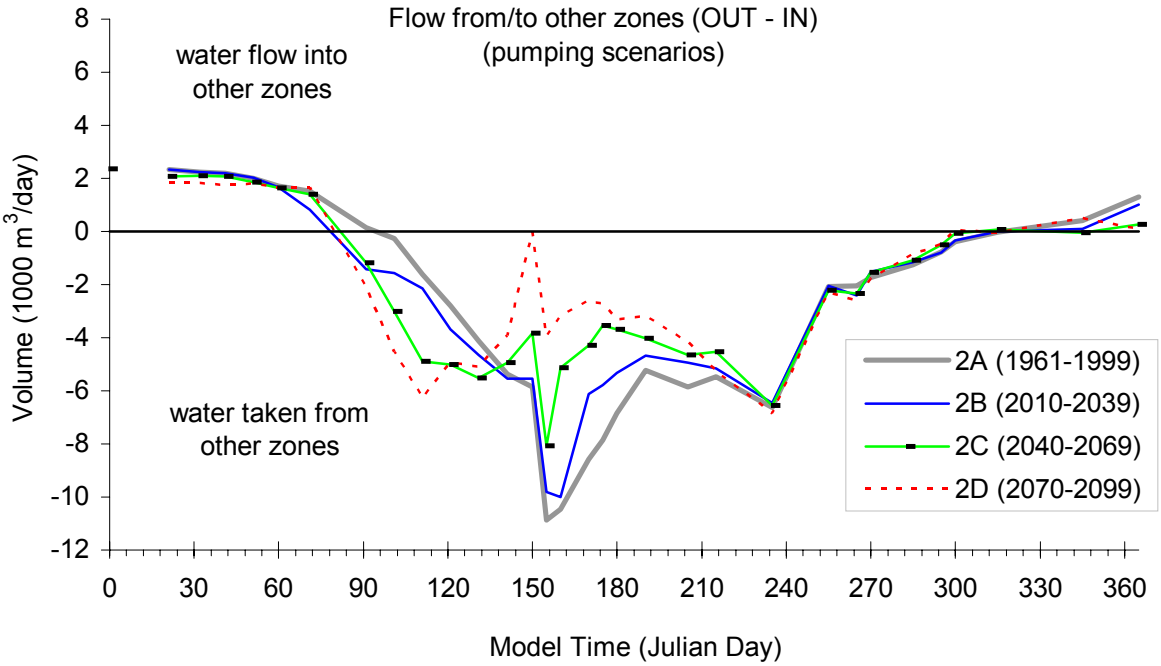

Figure C32 Transient model water Storage component of ZBUD for Zone 6 (Covert Irrigation District) in Grand Forks aquifer. Comparing non-pumping to pumping and all climate change scenarios.
Symbol legend applies to both graphs. Horizontal axis is time in days, vertical axis is flow volume in 1000's m^3/day. Same scales on both graphs.

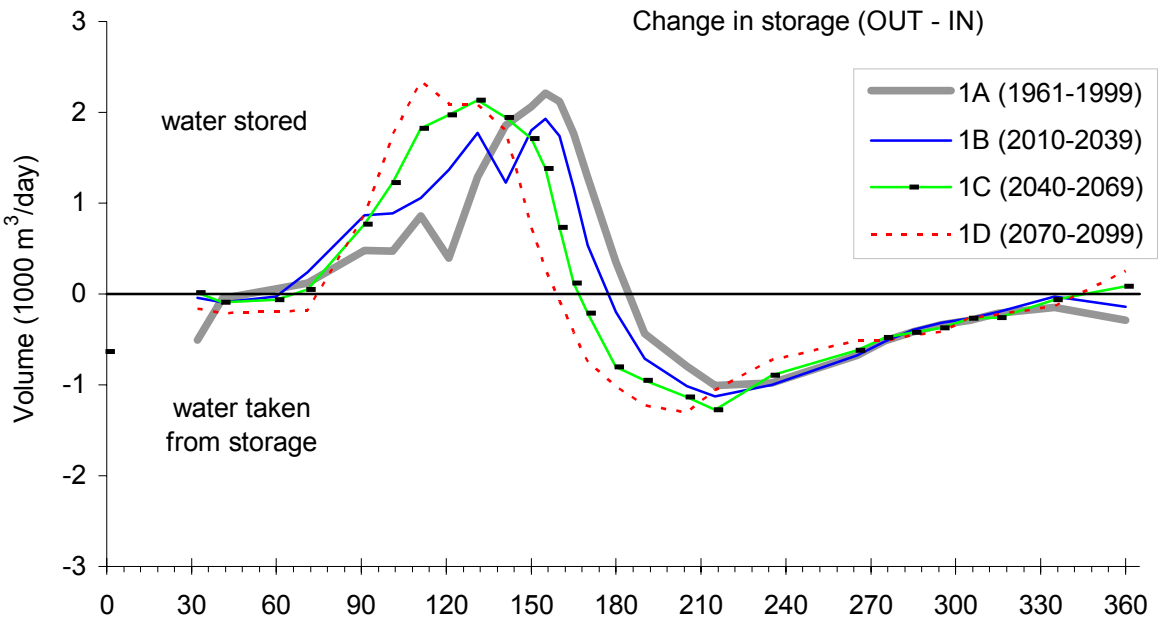

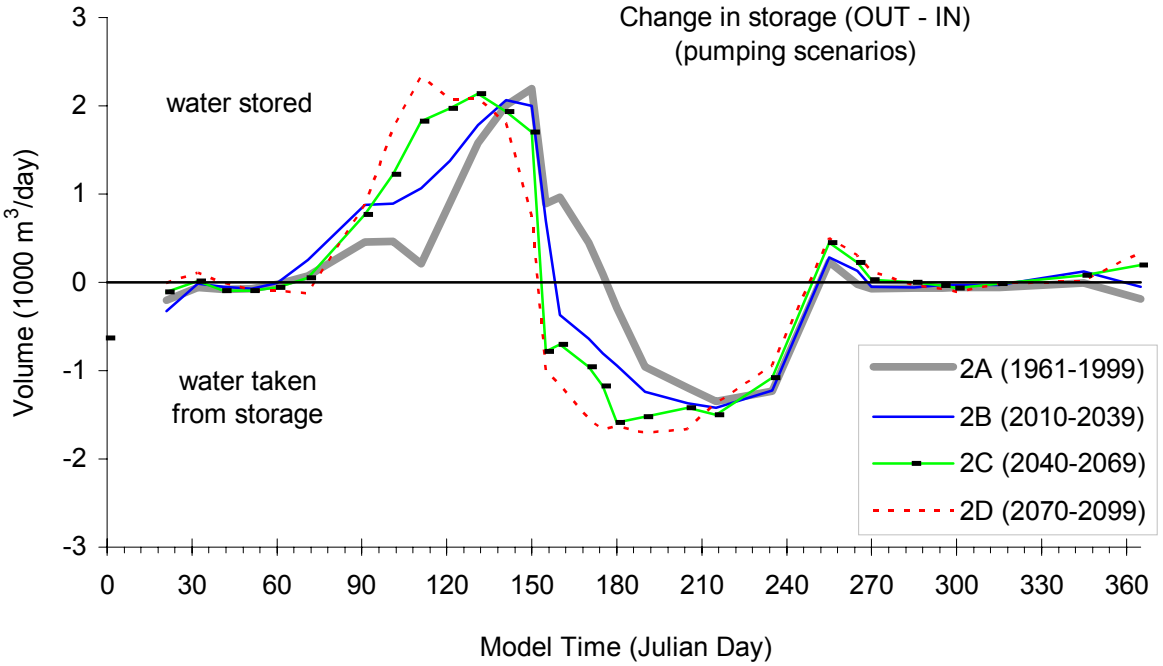

Figure C33 Transient model water flow to/from other zones for Zone 6 (Covert Irrigation District) in Grand Forks aquifer. Comparing non-pumping to pumping and all climate change scenarios.
Symbol legend applies to both graphs. Horizontal axis is time in days, vertical axis is flow volume in 1000's m^3/day. Same scales on both graphs.

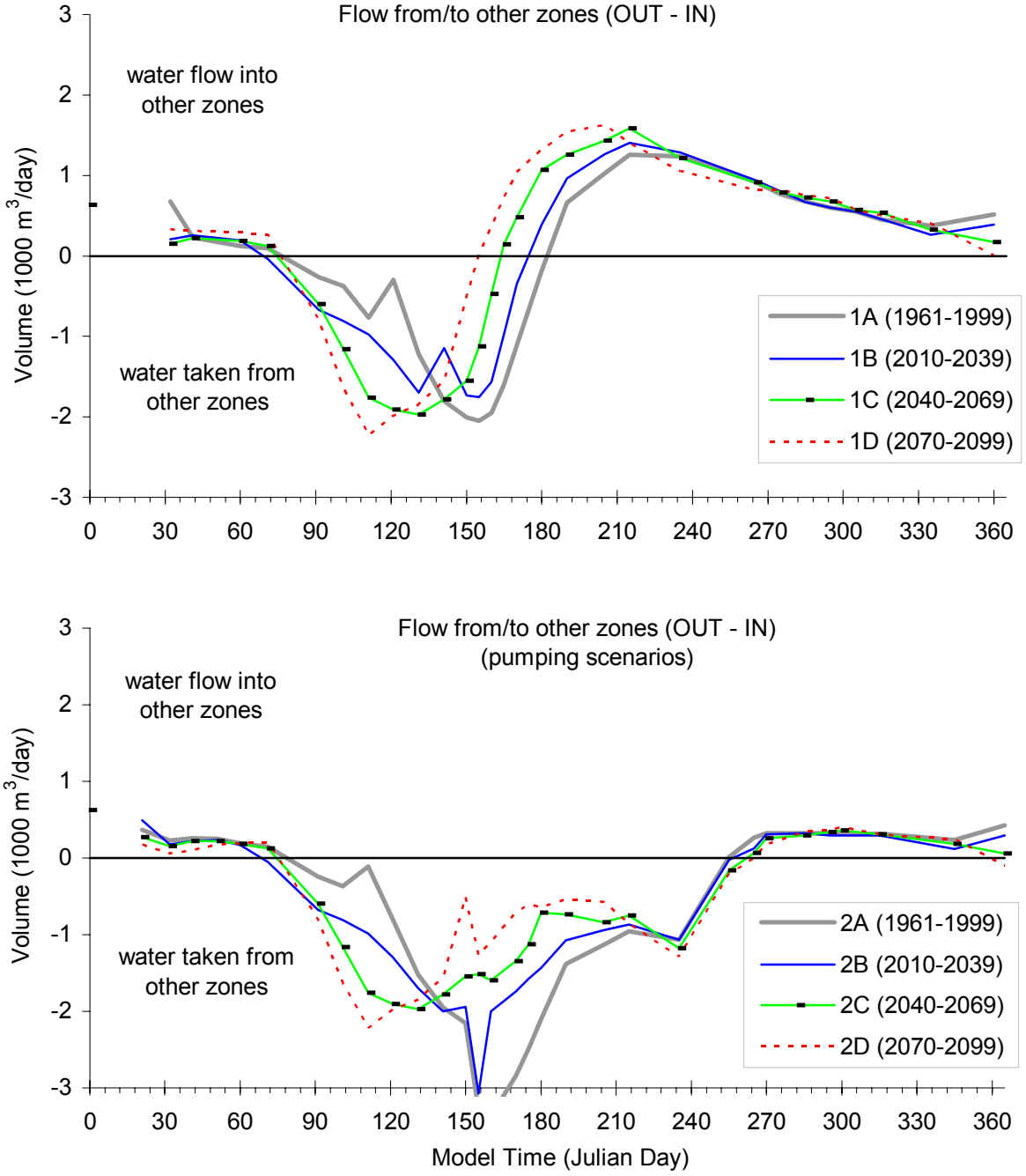

Figure C34 Transient model water Storage component of ZBUD for Zone 7 (Nursery Irrigation District) in Grand Forks aquifer. Comparing non-pumping to pumping and all climate change scenarios.
Symbol legend applies to both graphs. Horizontal axis is time in days, vertical axis is flow volume in 1000's m^3/day. Same scales on both graphs.

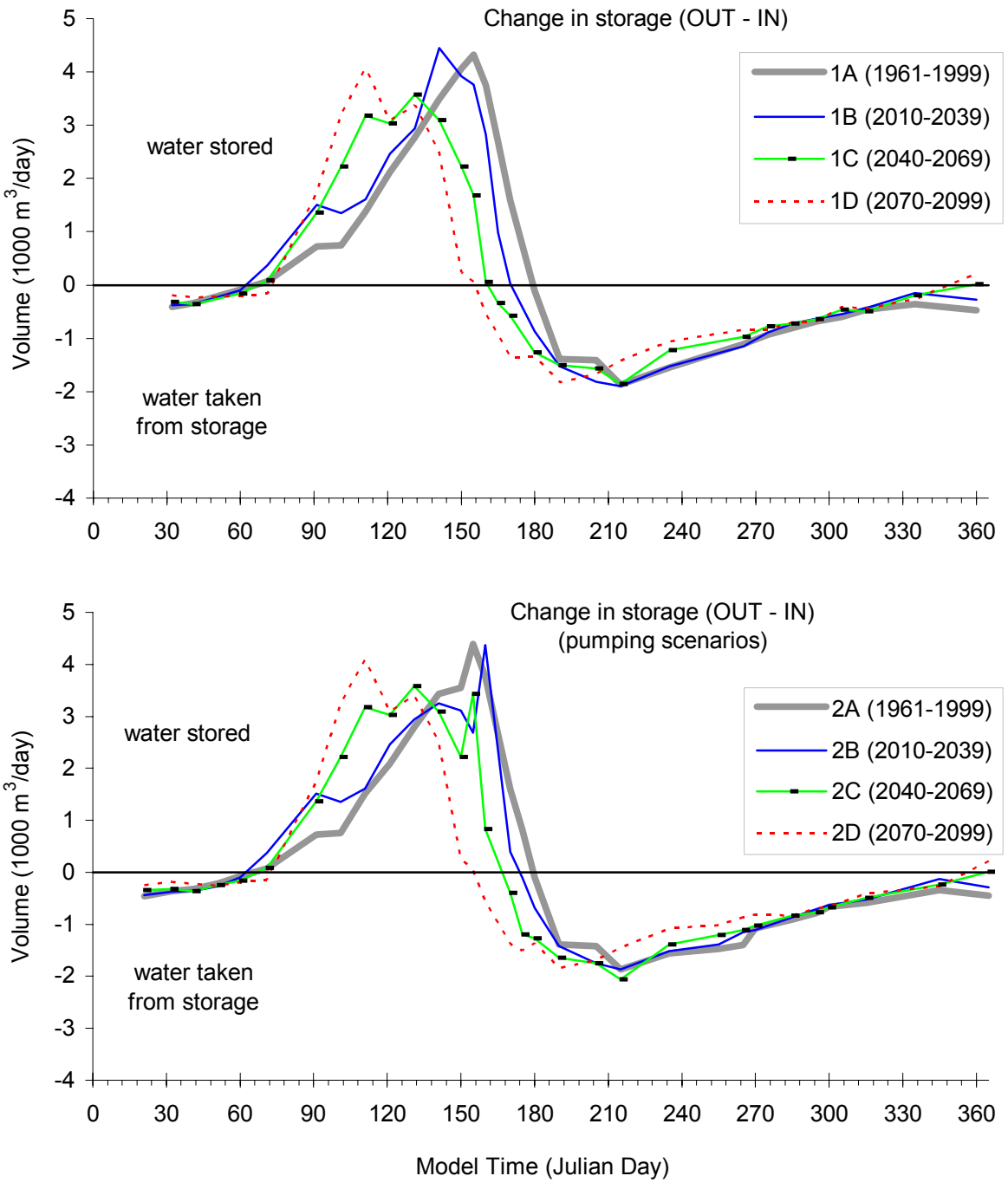

Figure C35 Transient model water flow to/from other zones for Zone 7 (Nursery Irrigation District) in Grand Forks aquifer. Comparing non-pumping to pumping and all climate change scenarios.
Symbol legend applies to both graphs. Horizontal axis is time in days, vertical axis is flow volume in 1000's m^3/day. Same scales on both graphs.

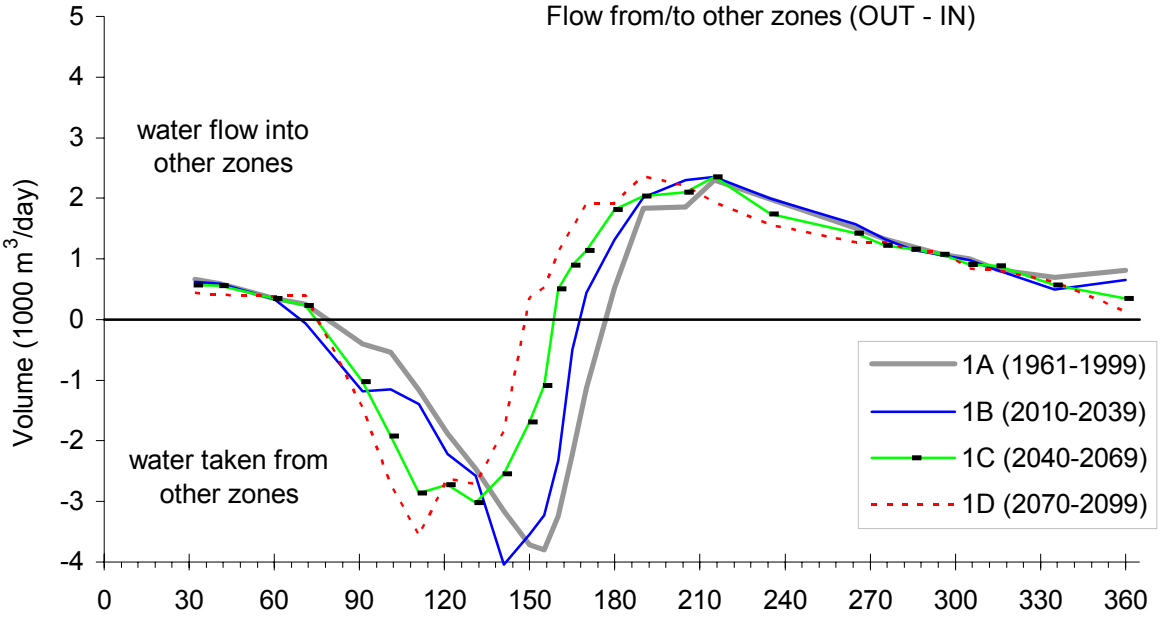

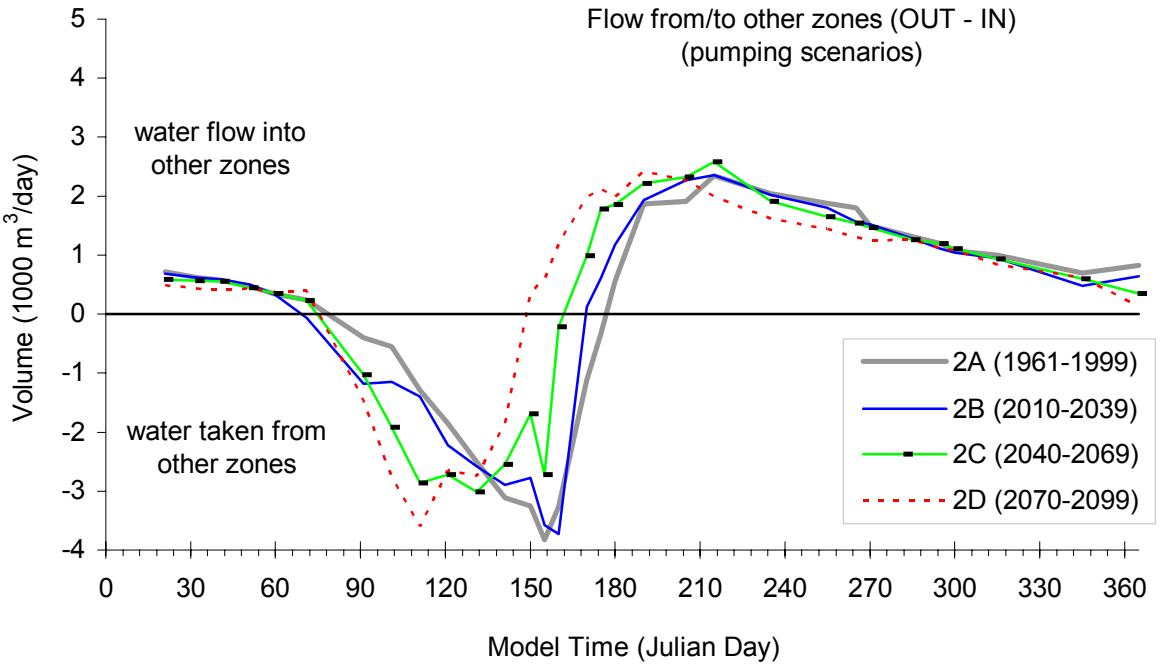

Figure C36 Transient model water Storage component of ZBUD for Zone 8 (Silty Layer) in Grand Forks aquifer. Comparing non-pumping to pumping and all climate change scenarios.
Symbol legend applies to both graphs. Horizontal axis is time in days, vertical axis is flow volume in 1000's m^3/day. Same scales on both graphs.

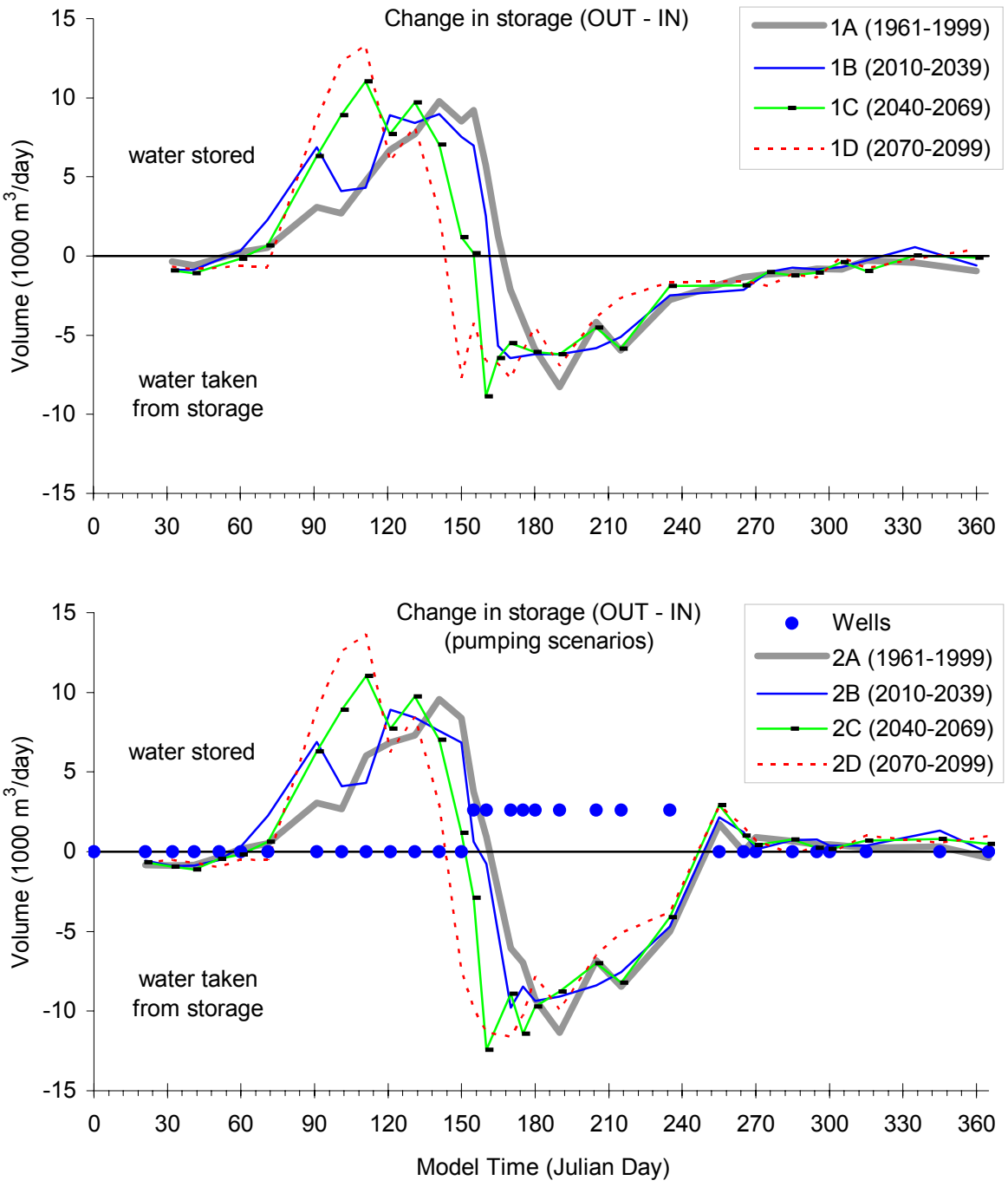

Figure CG37 Transient model water flow to/from other zones for Zone 8 (Silty Layer) in Grand Forks aquifer. Comparing non-pumping to pumping and all climate change scenarios.
Symbol legend applies to both graphs. Horizontal axis is time in days, vertical axis is flow volume in 1000's m^3/day. Same scales on both graphs.

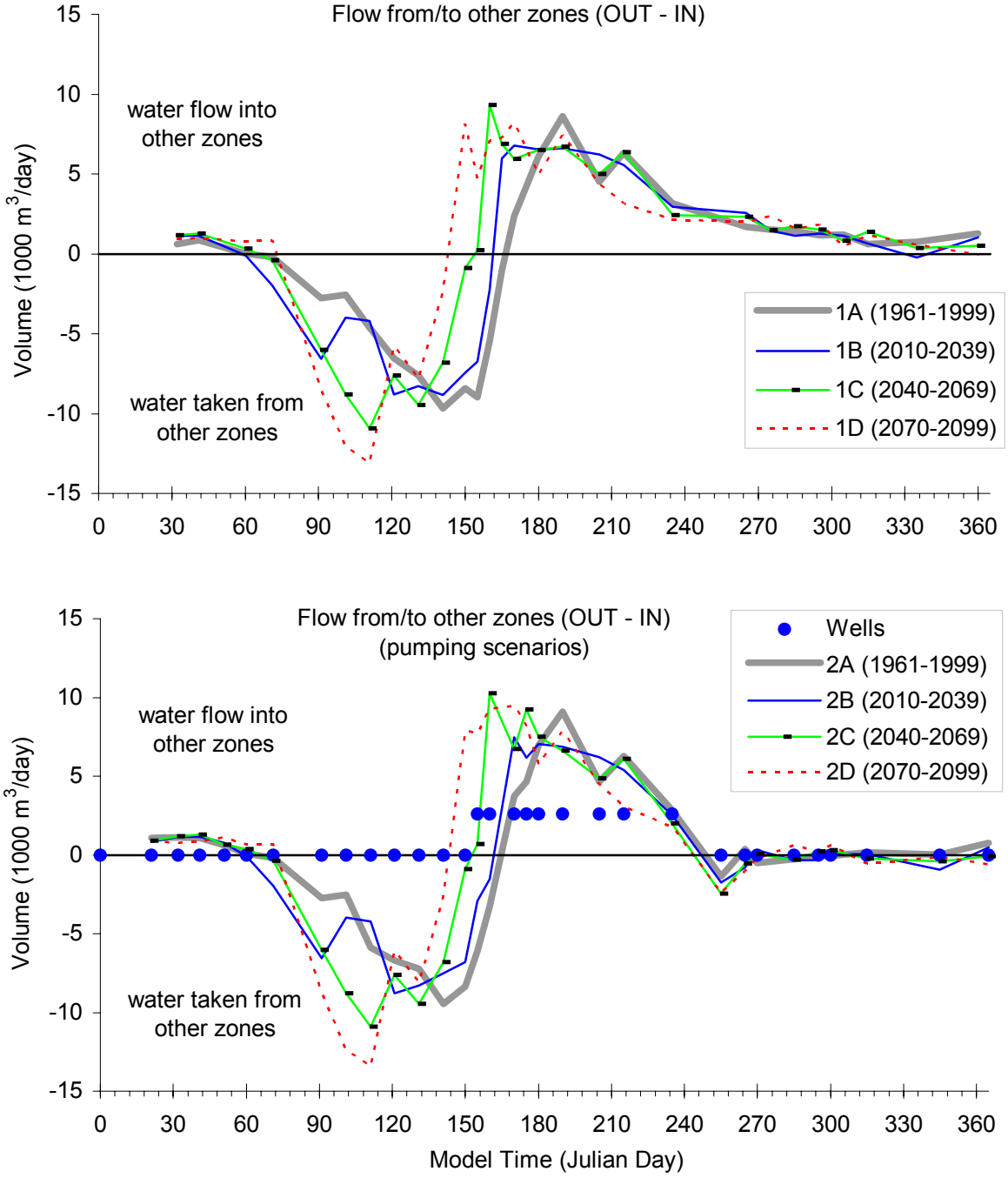

Figure C38 Transient model water Storage component of ZBUD for Zone 9 (Clay Layer) in Grand Forks aquifer. Comparing non-pumping to pumping and all climate change scenarios.
Symbol legend applies to both graphs. Horizontal axis is time in days, vertical axis is flow volume in 1000's m^3/day. Same scales on both graphs.

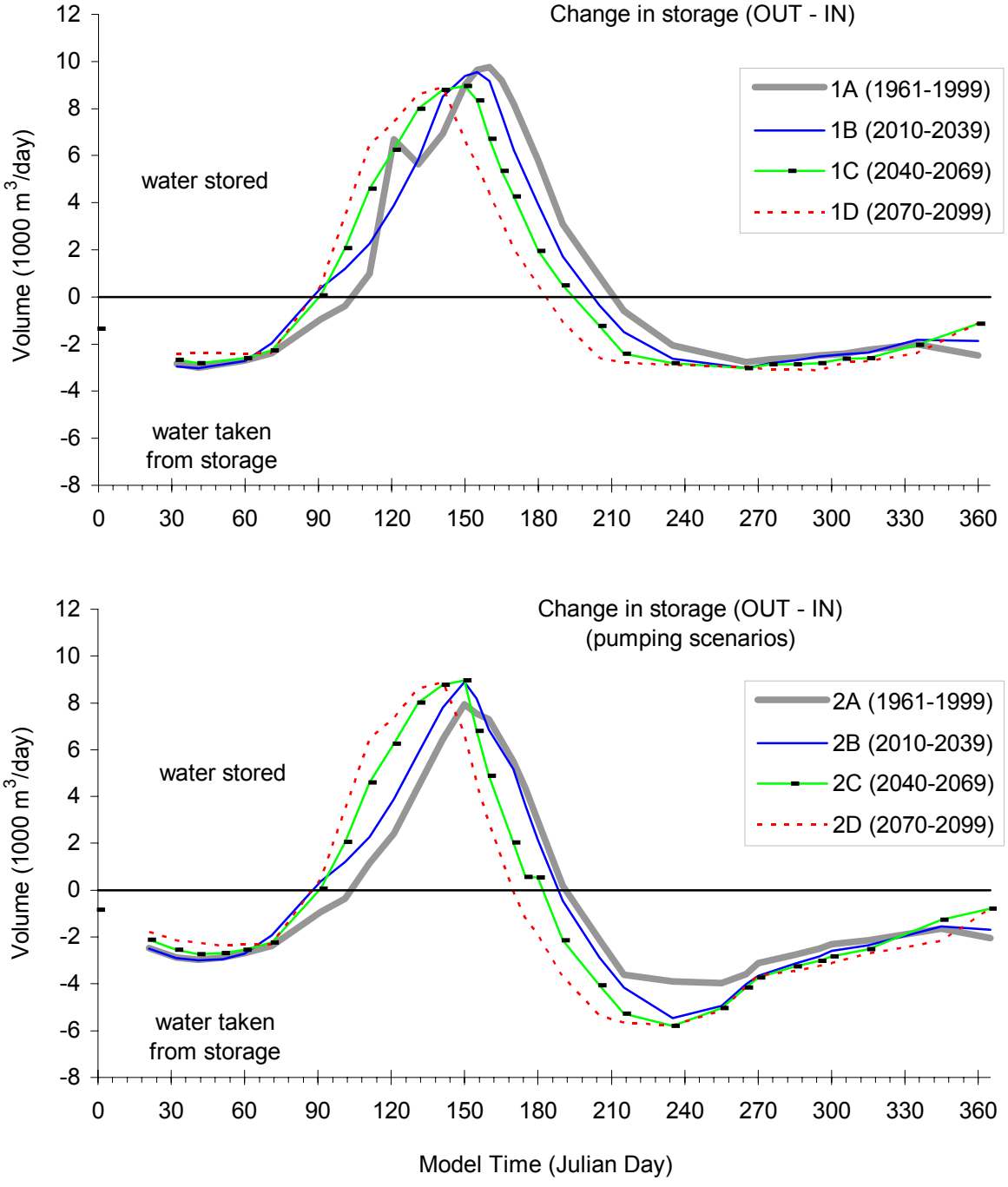

Figure C39 Transient model water flow to/from other zones for Zone 9 (Clay Layer) in Grand Forks aquifer. Comparing non-pumping to pumping and all climate change scenarios.
Symbol legend applies to both graphs. Horizontal axis is time in days, vertical axis is flow volume in 1000's m^3/day. Same scales on both graphs.

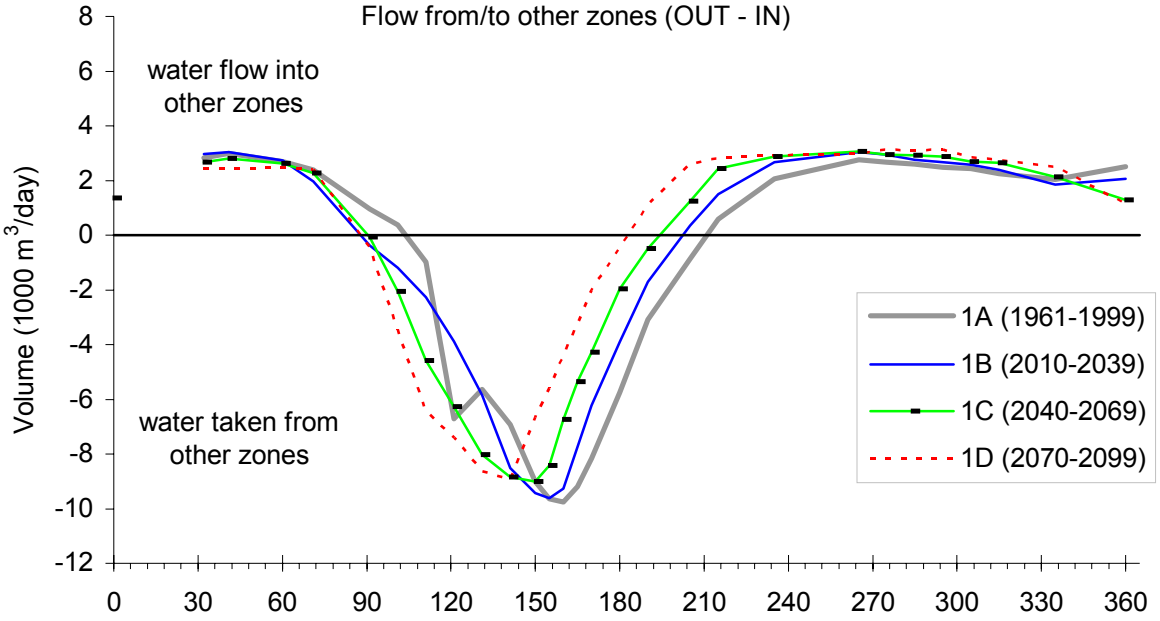

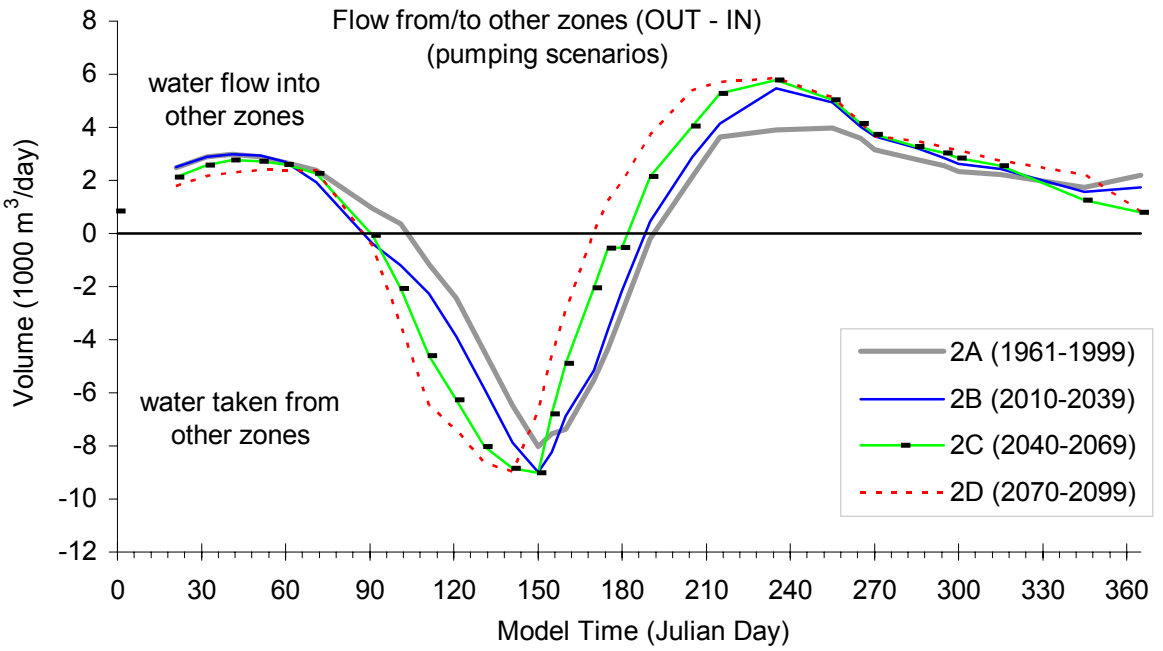

GRAPHS SHOWING THE EFFECT OF AQUIFER HETEROGENEITY ON GROUNDWATER STORAGE AND FLOW BETWEEN ZONES (PUMPING AND NON-PUMPING SCENARIOS AND CHANGES WITH CLIMATE)

Figure C40 Transient model Storage and Flow to Other Zones components of ZBUD for Zone 1 (GF Irrigation district and background) in Grand Forks aquifer. Comparing effect of aquifer heterogeneity on pumping model climate change predictions.
Horizontal axis is time in days, vertical axis is flow volume in 1000's m^3/day. Same scales on both graphs. Graphs show Difference between (OUT – IN) volume in scenario 4 (heterogeneous) model and scenario 2 model outputs. Storage and Flow from/to Other Zones has similar behaviours in heterogeneous model as in homogeneous model, except for the shown differences in these graphs.

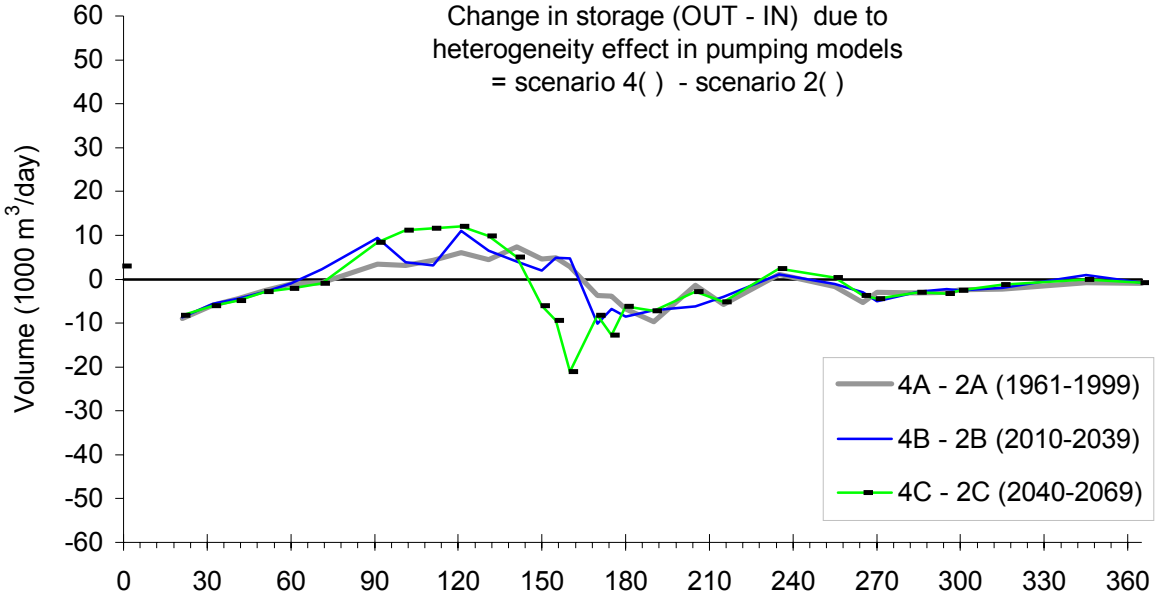

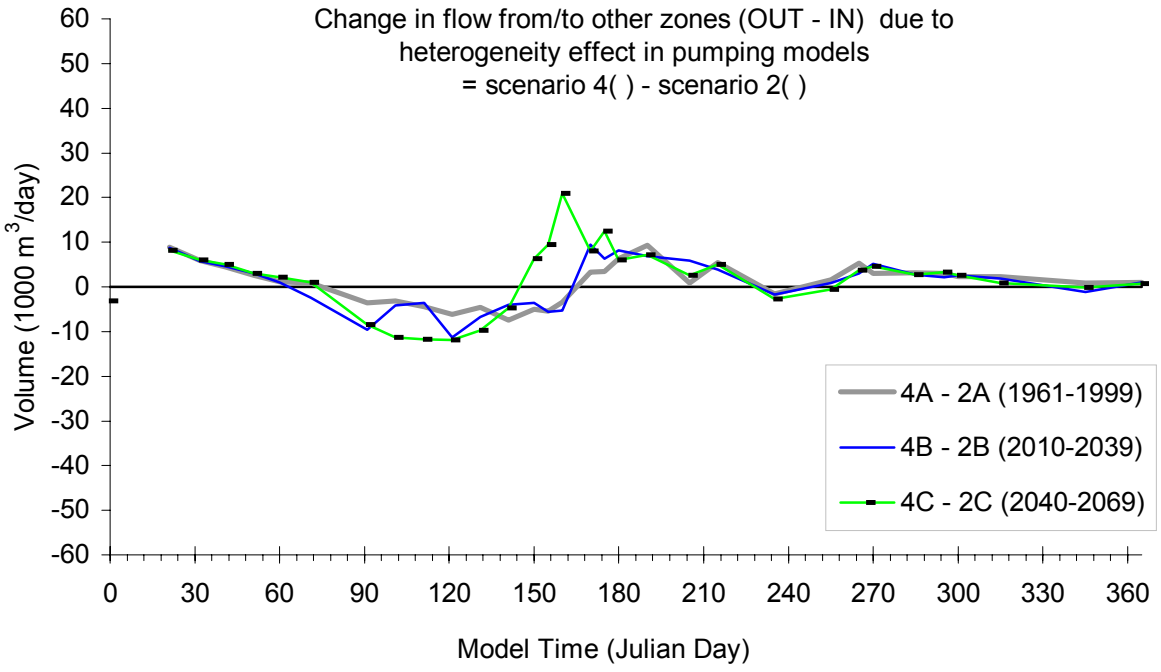

Figure C41 Transient model Storage and Flow to Other Zones components of ZBUD for Zone 1 (GF Irrigation District and background) in Grand Forks aquifer. Comparing effect of aquifer heterogeneity on pumping model climate change predictions as % difference.
Horizontal axis is time in days, vertical axis is % difference in flow rate. Same scales on both graphs. Graphs show Difference between (OUT – IN) rate in scenario 4 (heterogeneous) model and scenario 2 model outputs. Storage and Flow from/to Other Zones has similar behaviours in heterogeneous model as in homogeneous model, except for the shown differences in these graphs.

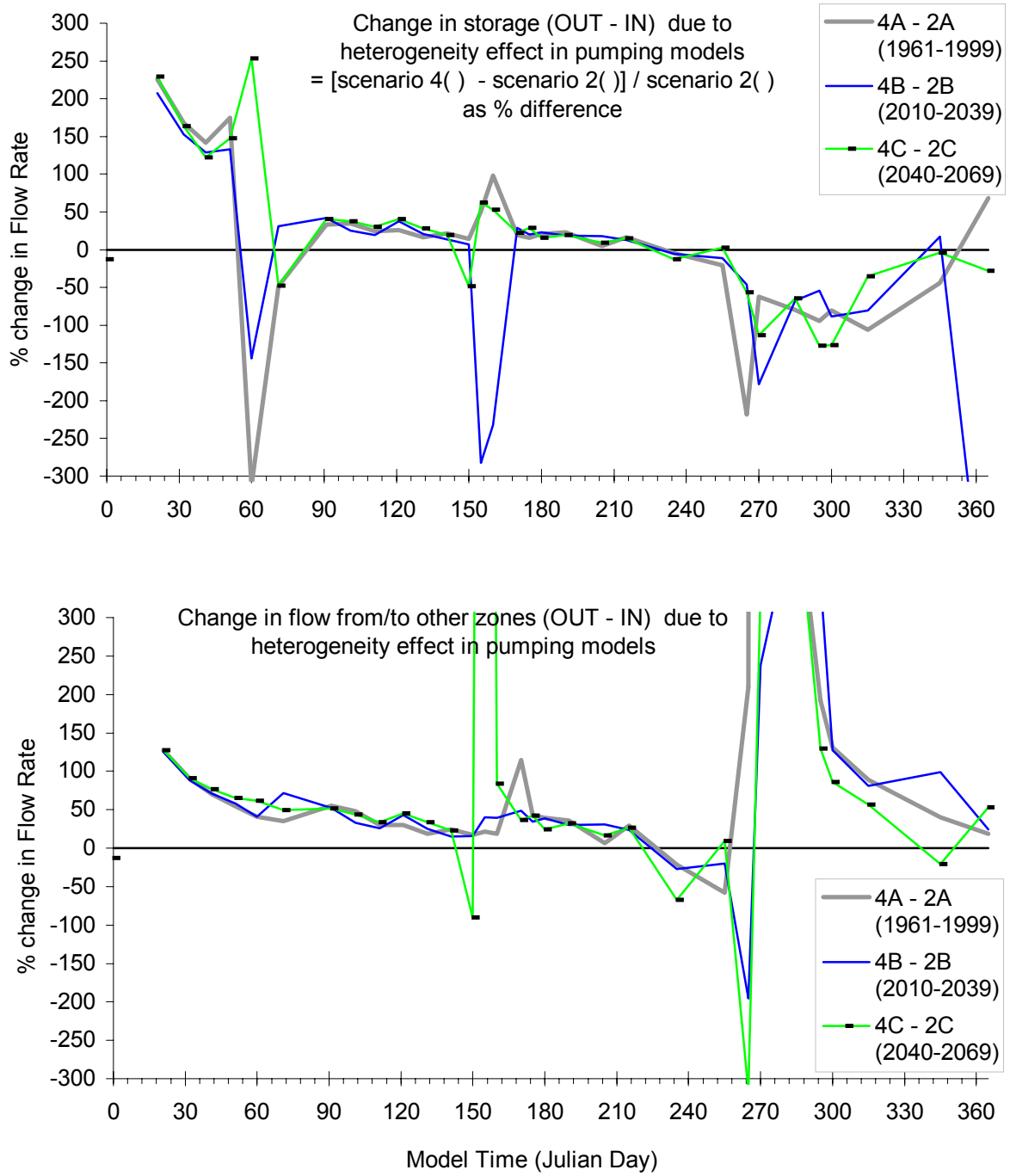

Figure C42 Transient model Storage and Flow to Other Zones components of ZBUD for Zone 2 (Floodplain) in Grand Forks aquifer. Comparing effect of aquifer heterogeneity on pumping model climate change predictions.
Horizontal axis is time in days, vertical axis is flow volume in 1000's m^3/day.
Same scales on both graphs. Graphs show Difference between (OUT – IN) volume in scenario 4 (heterogeneous) model and scenario 2 model outputs.
Storage and Flow from/to Other zones has similar behaviours in heterogeneous model as in homogeneous model, except for the shown differences in these graphs.

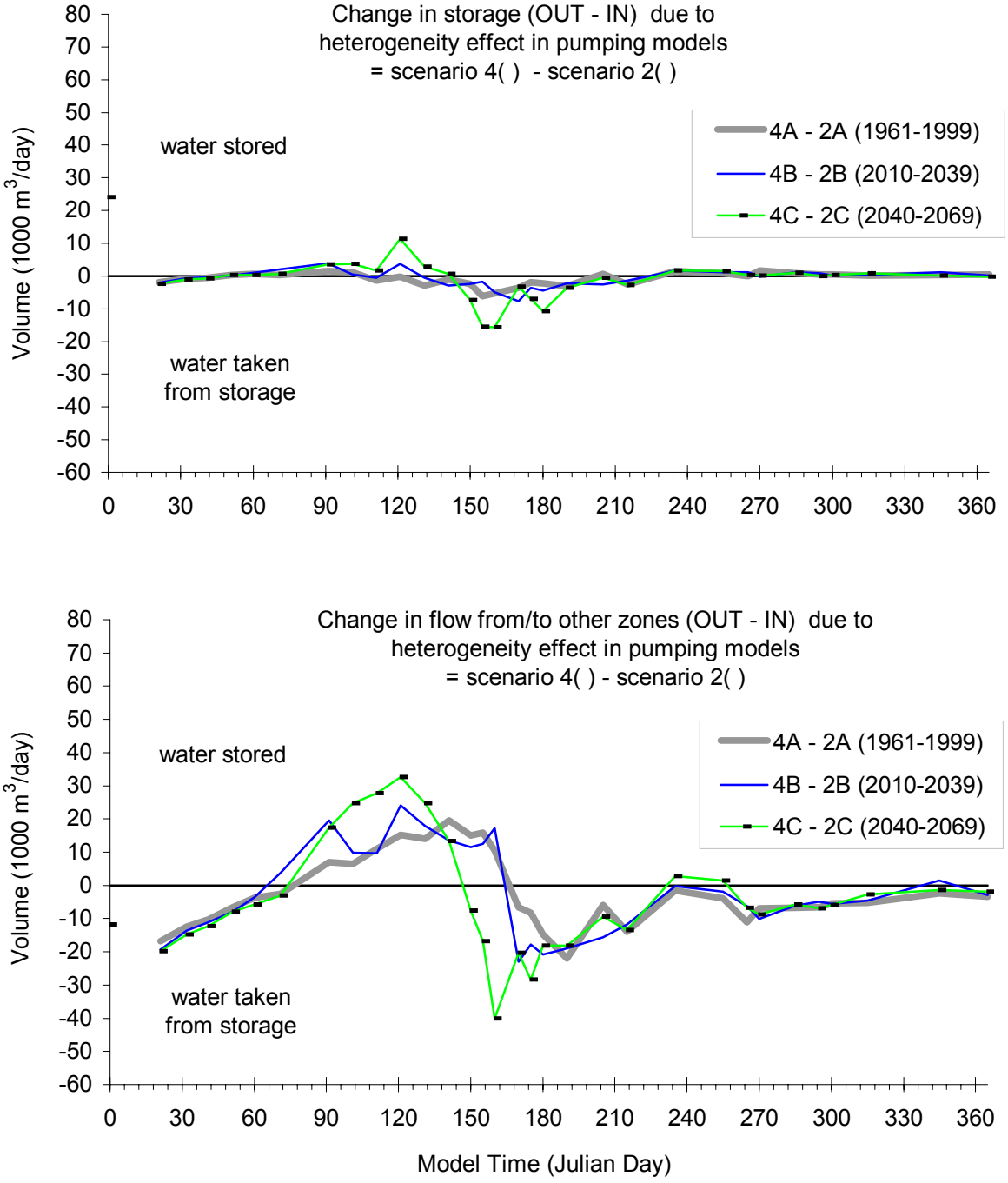

Figure C43 Transient model Storage and Flow to Other Zones components of ZBUD for Zone 3 (Sion 1) in Grand Forks aquifer. Comparing effect of aquifer heterogeneity on pumping model climate change predictions.
Horizontal axis is time in days, vertical axis is flow volume in m^3/day. Same scales on both graphs. Graphs show Difference between (OUT – IN) volume in scenario 4 (heterogeneous) model and scenario 2 model outputs. Storage and Flow from/to Other zones has similar behaviours in heterogeneous model as in homogeneous model, except for the shown differences in these graphs.

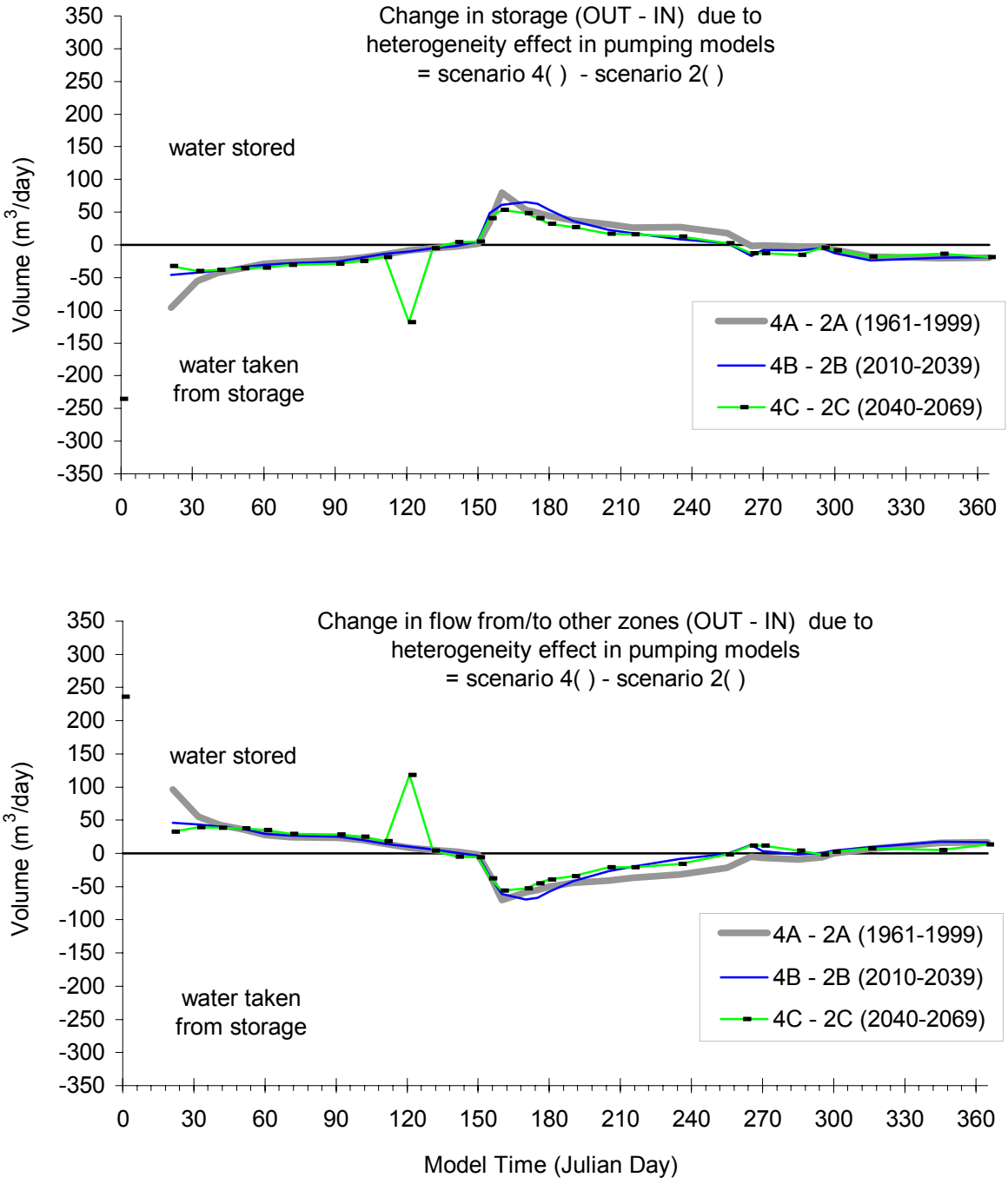

Figure C44 Transient model Storage and Flow to Other Zones components of ZBUD for Zone 4 (Sion 2 & 3) in Grand Forks aquifer. Comparing effect of aquifer heterogeneity on pumping model climate change predictions.
Horizontal axis is time in days, vertical axis is flow volume in 1000's m^3/day.
Same scales on both graphs. Graphs show Difference between (OUT – IN) volume in scenario 4 (heterogeneous) model and scenario 2 model outputs.
Storage and Flow from/to Other zones has similar behaviours in heterogeneous model as in homogeneous model, except for the shown differences in these graphs.

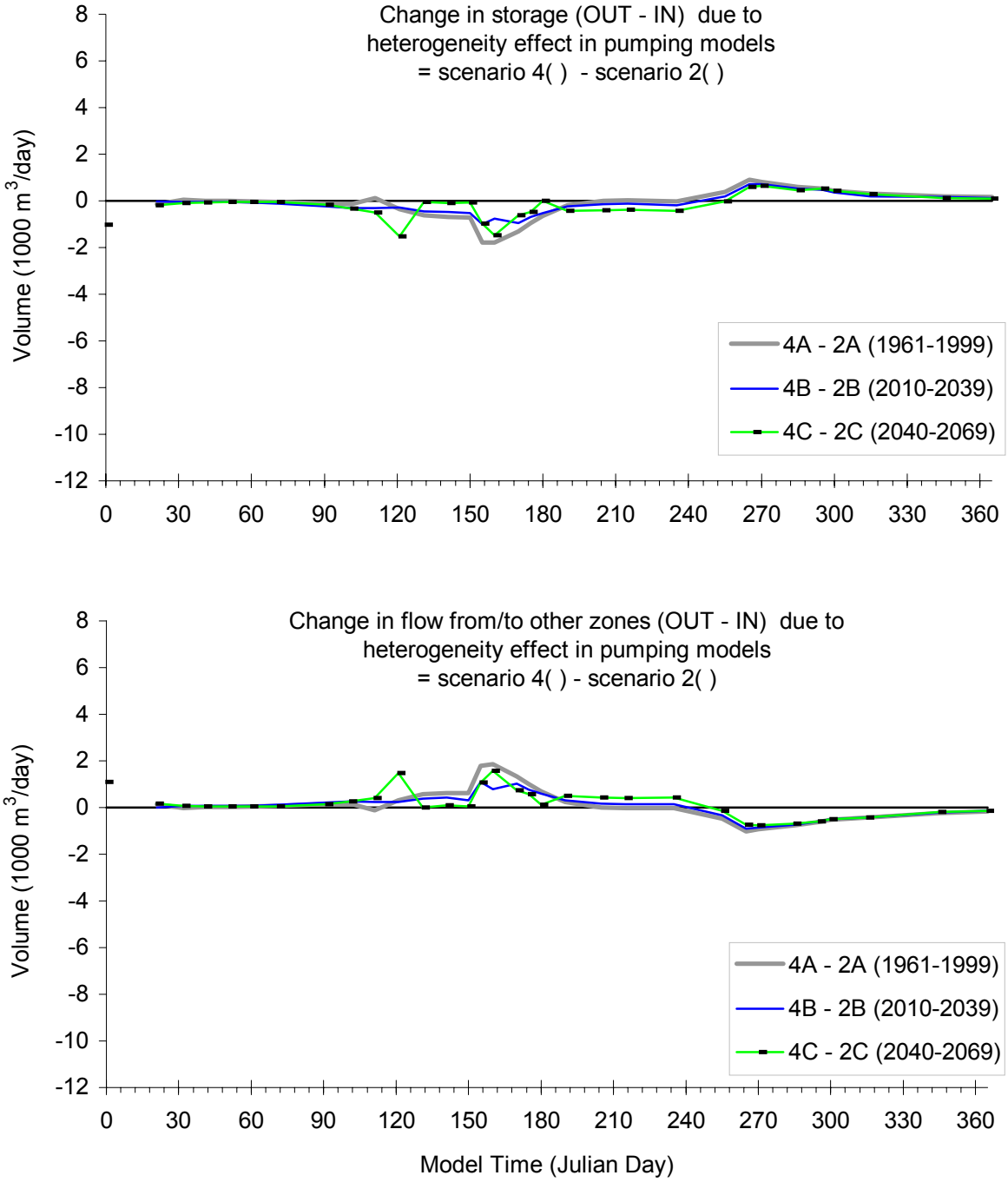

Figure C45 Transient model Storage and Flow to Other Zones components of ZBUD for Zone 5 (Big Y) in Grand Forks aquifer. Comparing effect of aquifer heterogeneity on pumping model climate change predictions.
Horizontal axis is time in days, vertical axis is flow volume in 1000's m^3/day. Same scales on both graphs. Graphs show Difference between (OUT – IN) volume in scenario 4 (heterogeneous) model and scenario 2 model outputs. Storage and Flow from/to Other zones has similar behaviours in heterogeneous model as in homogeneous model, except for the shown differences in these graphs.

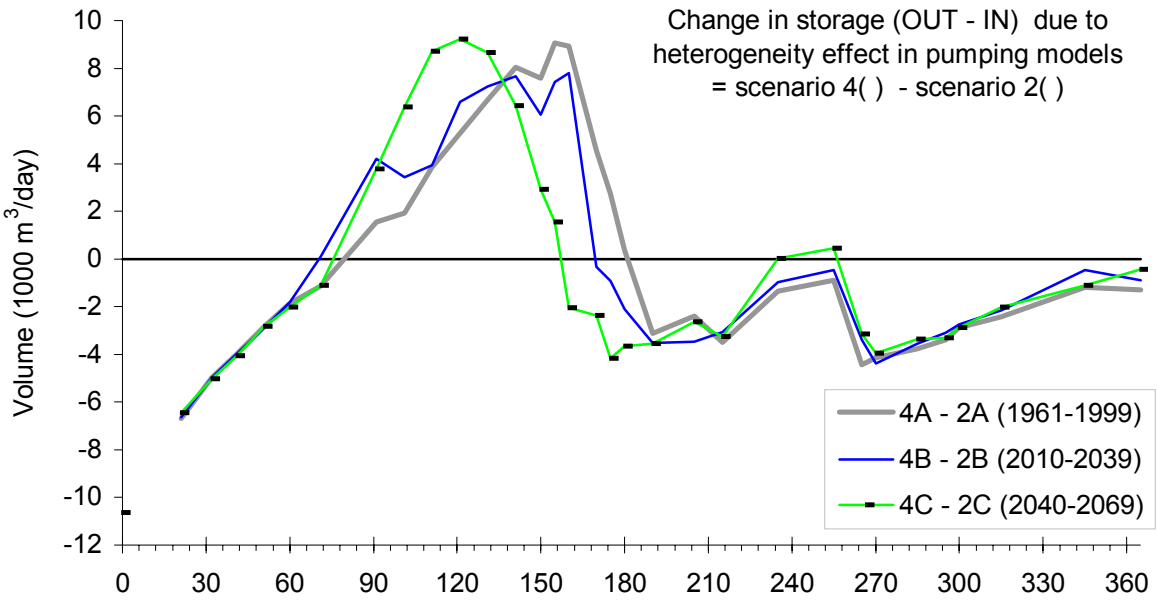

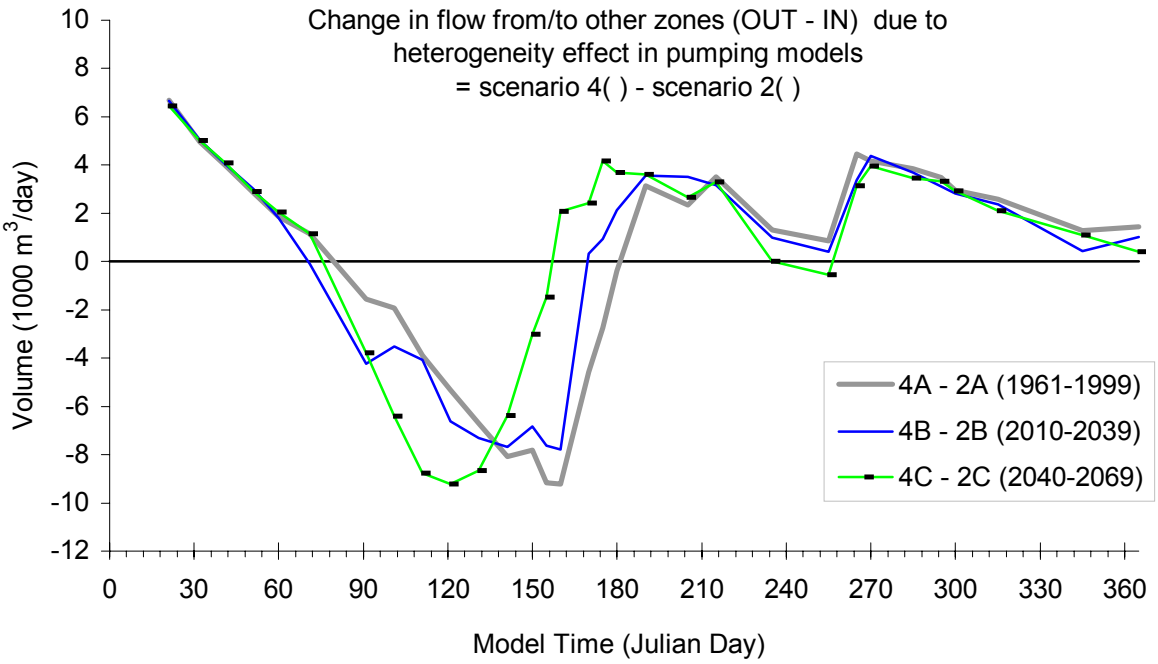

Figure C46 Transient model Storage and Flow to Other Zones components of ZBUD for Zone 6 (Covert) in Grand Forks aquifer. Comparing effect of aquifer heterogeneity on pumping model climate change predictions.
Horizontal axis is time in days, vertical axis is flow volume in 1000's m^3/day.
Same scales on both graphs. Graphs show Difference between (OUT – IN) volume in scenario 4 (heterogeneous) model and scenario 2 model outputs.
Storage and Flow from/to Other zones has similar behaviours in heterogeneous model as in homogeneous model, except for the shown differences in these graphs.

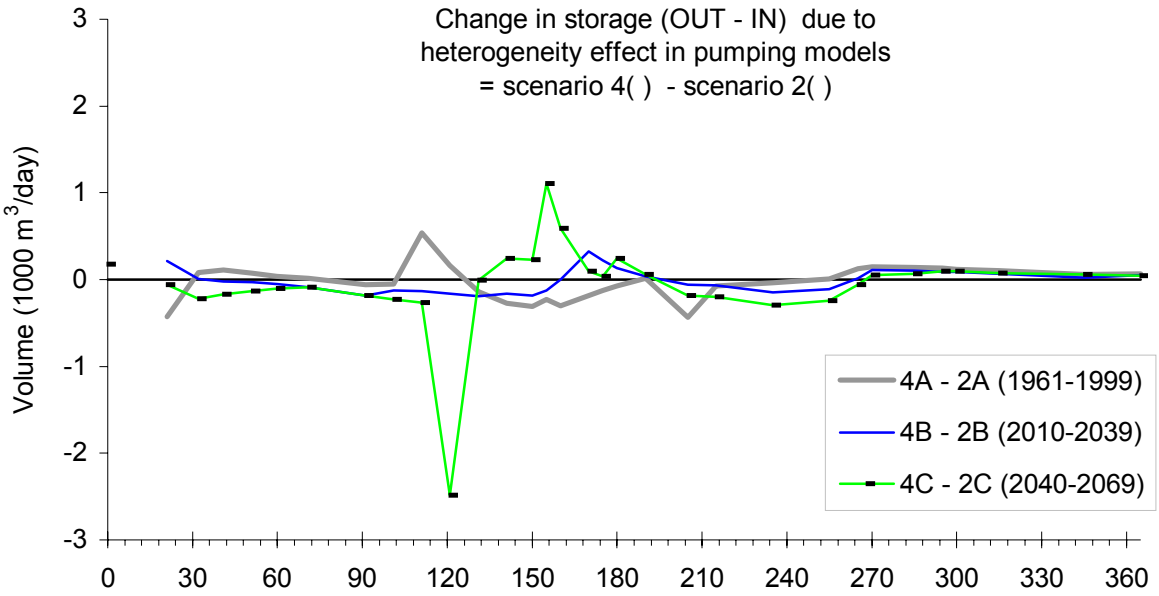

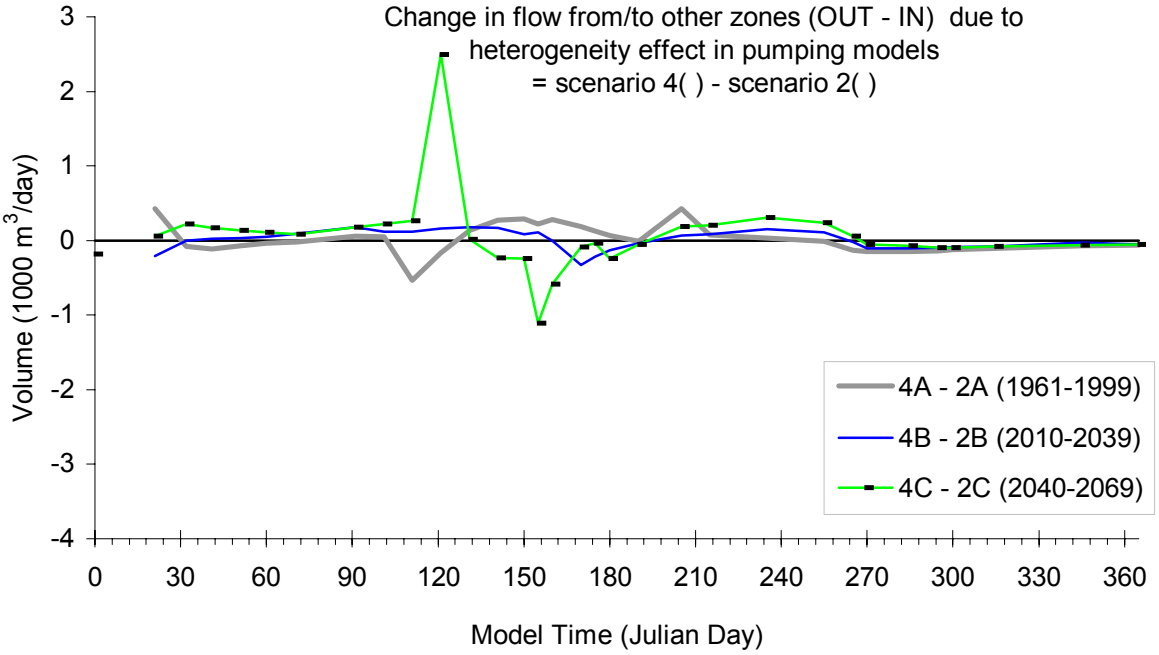

Figure C47 Transient model Storage and Flow to Other Zones components of ZBUD for Zone 7 (Nursery) in Grand Forks aquifer. Comparing effect of aquifer heterogeneity on pumping model climate change predictions.
Horizontal axis is time in days, vertical axis is flow volume in 1000's m^3/day.
Same scales on both graphs. Graphs show Difference between (OUT – IN) volume in scenario 4 (heterogeneous) model and scenario 2 model outputs.
Storage and Flow from/to Other zones has similar behaviours in heterogeneous model as in homogeneous model, except for the shown differences in these graphs.

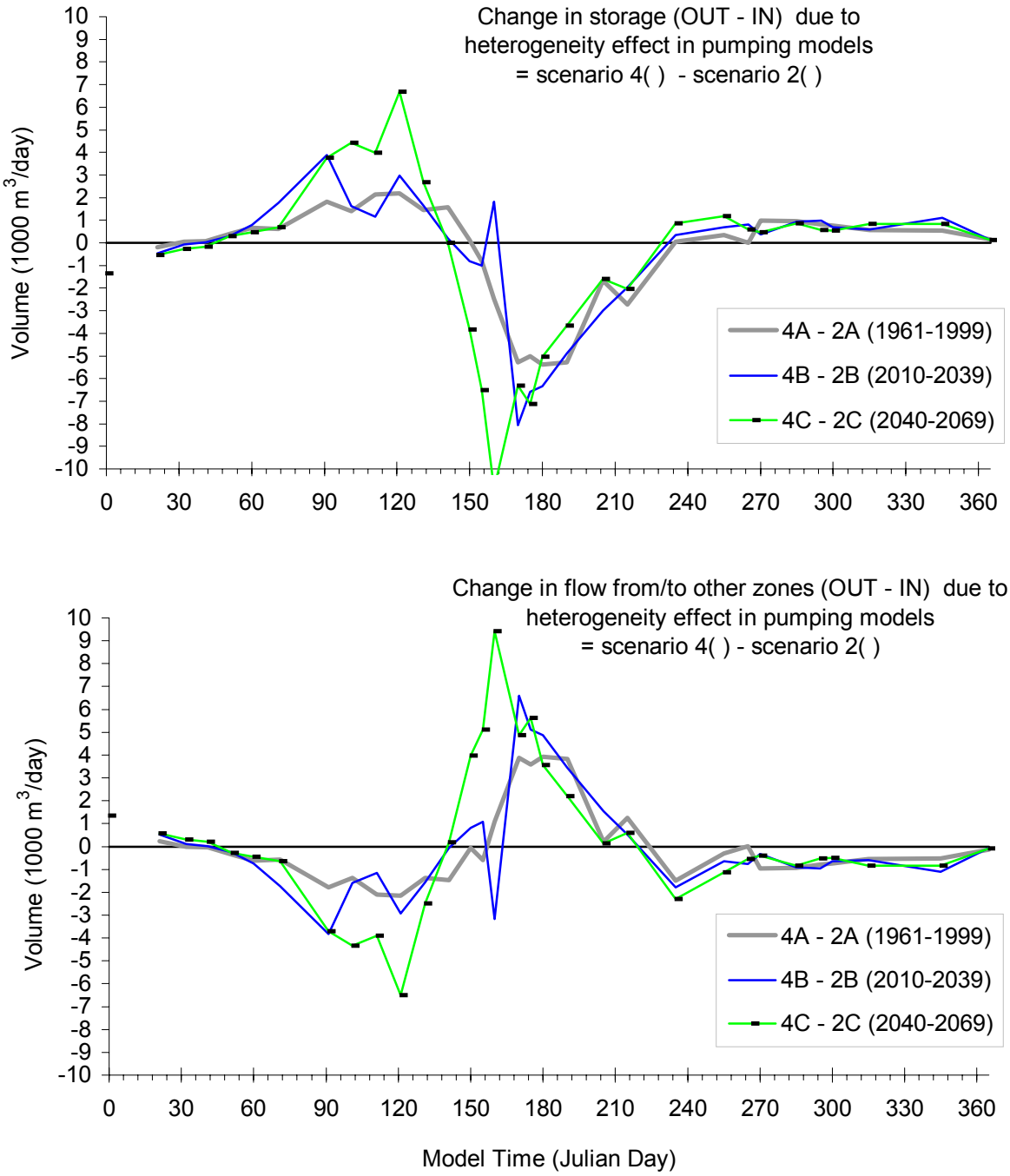

Figure C48 Transient model Storage and Flow to Other Zones components of ZBUD for Zone 8 (Silt Layer) in Grand Forks aquifer. Comparing effect of aquifer heterogeneity on pumping model climate change predictions.
Horizontal axis is time in days, vertical axis is flow volume in 1000's m^3/day. Same scales on both graphs. Graphs show Difference between (OUT – IN) volume in scenario 4 (heterogeneous) model and scenario 2 model outputs. Storage and Flow from/to Other zones has similar behaviours in heterogeneous model as in homogeneous model, except for the shown differences in these graphs.

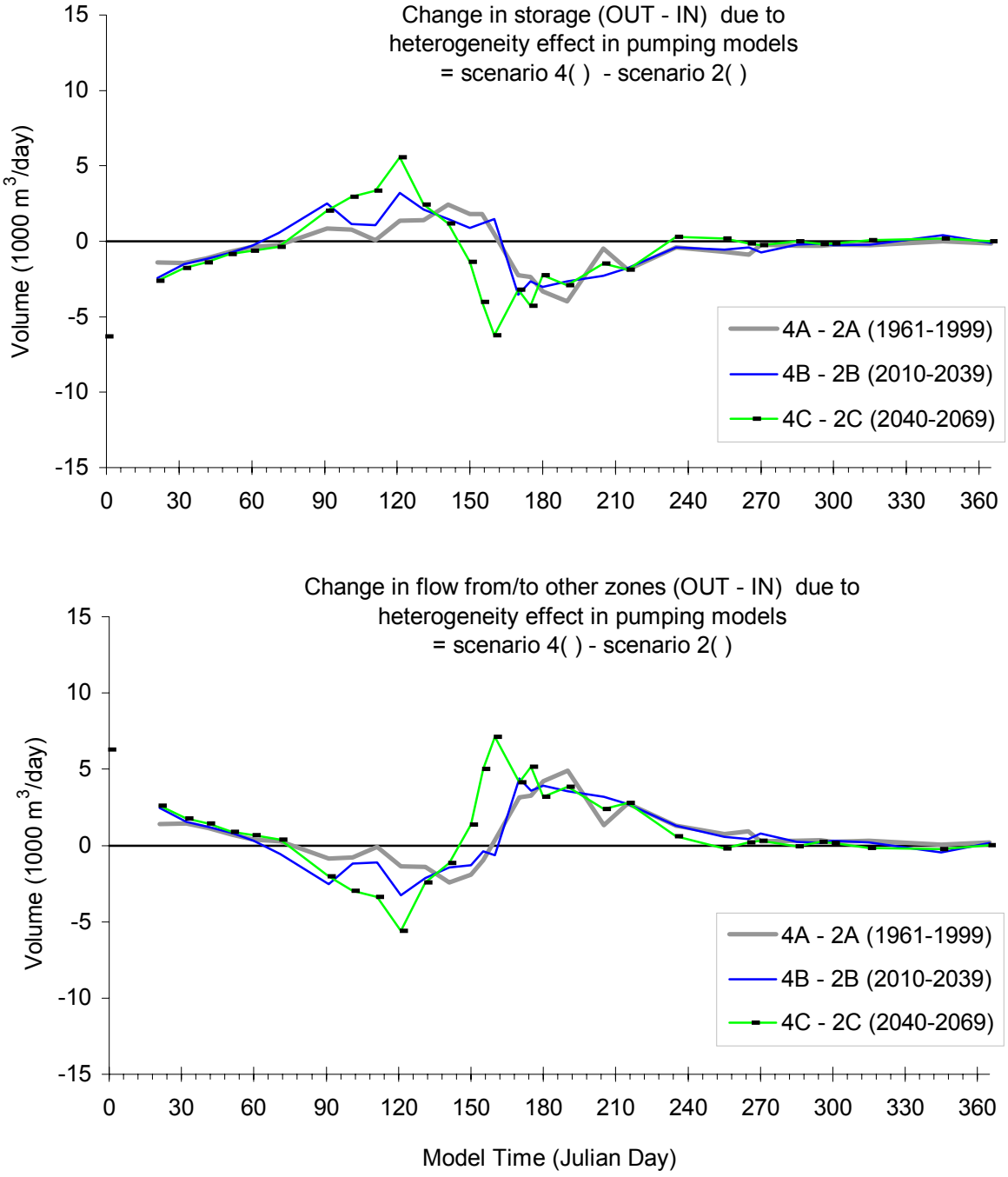

Figure C49 Transient model Storage and Flow to Other Zones components of ZBUD for Zone 9 (Clay Layer) in Grand Forks aquifer. Comparing effect of aquifer heterogeneity on pumping model climate change predictions.
Horizontal axis is time in days, vertical axis is flow volume in 1000's m^3/day.
Same scales on both graphs. Graphs show Difference between (OUT – IN) volume in scenario 4 (heterogeneous) model and scenario 2 model outputs.
Storage and Flow from/to Other zones has similar behaviours in heterogeneous model as in homogeneous model, except for the shown differences in these graphs.

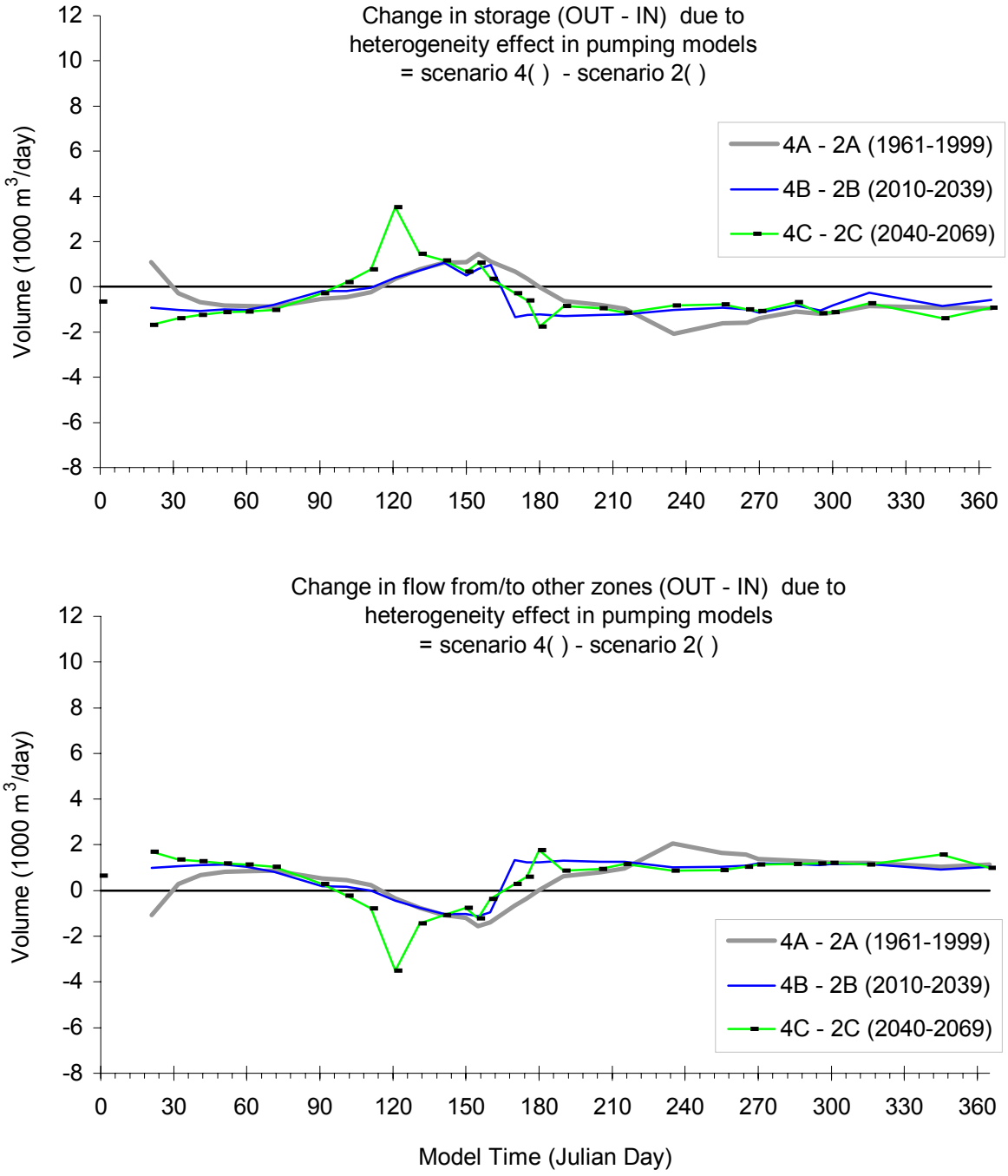

GRAPHS SHOWING THE EFFECT OF RECHARGE DISTRIBUTION AND TEMPORAL VARIATION ON GROUNDWATER STORAGE AND FLOW BETWEEN ZONES (NON-PUMPING SCENARIOS AND CHANGES WITH CLIMATE)

Figure C50 Transient model Storage and Flow to Other Zones components of ZBUD for Zone 1 (GF irrigation district and background) in Grand Forks aquifer. Comparing effect of recharge spatial and temporal distribution on non-pumping model climate change predictions.
Horizontal axis is time in days, vertical axis is flow volume in 1000's m^3/day. Same scales on both graphs. Graphs show Difference between (OUT – IN) volume in scenario 4 (heterogeneous) model and scenario 2 model outputs. Storage and Flow from/to Other Zones has similar behaviours in model 5(A or B) and 1(A), except for the shown differences in these graphs.

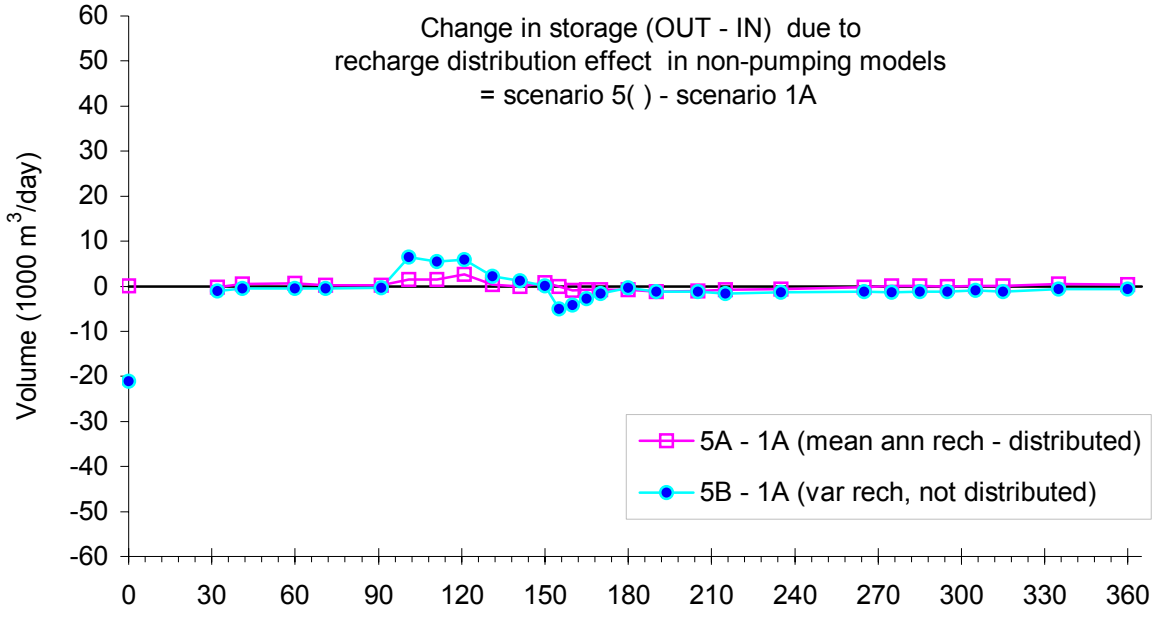

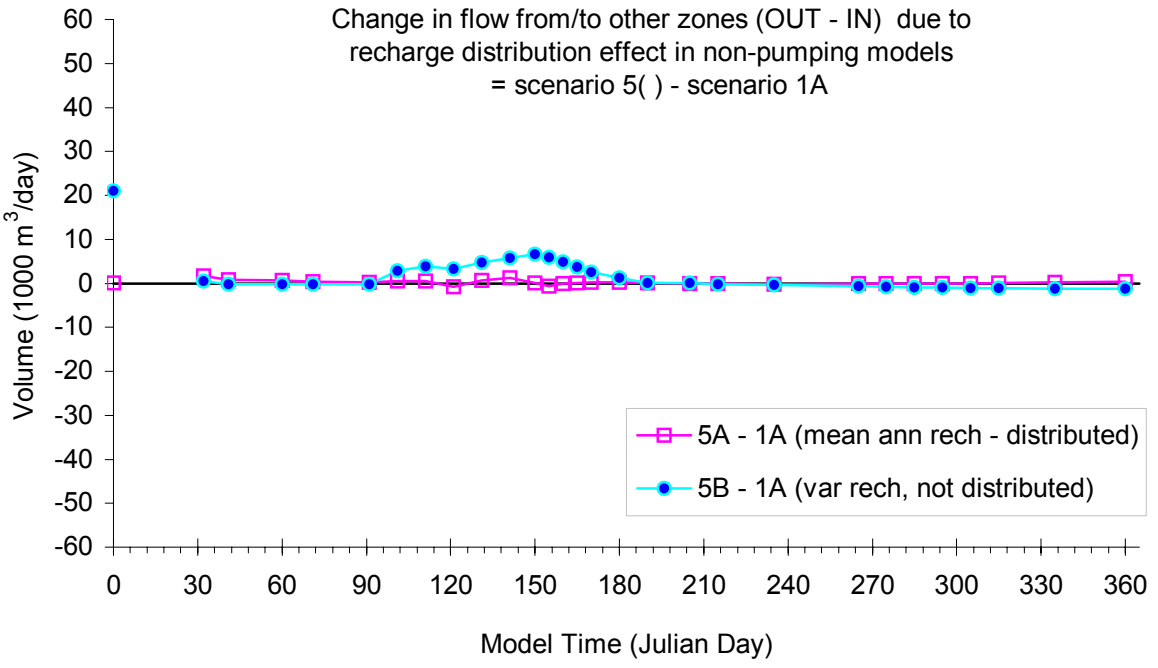

Figure C51 Transient model Storage and Flow to Other Zones components of ZBUD for Zone 2 (Floodplain) in Grand Forks aquifer. Comparing effect of recharge spatial and temporal distribution on non-pumping model climate change predictions. Horizontal axis is time in days, vertical axis is flow volume in 1000's m^3/day. Same scales on both graphs. Graphs show Difference between (OUT – IN) volume in scenario 4 (heterogeneous) model and scenario 2 model outputs. Storage and Flow from/to Other Zones has similar behaviours in model 5(A or B) and 1(A), except for the shown differences in these graphs.

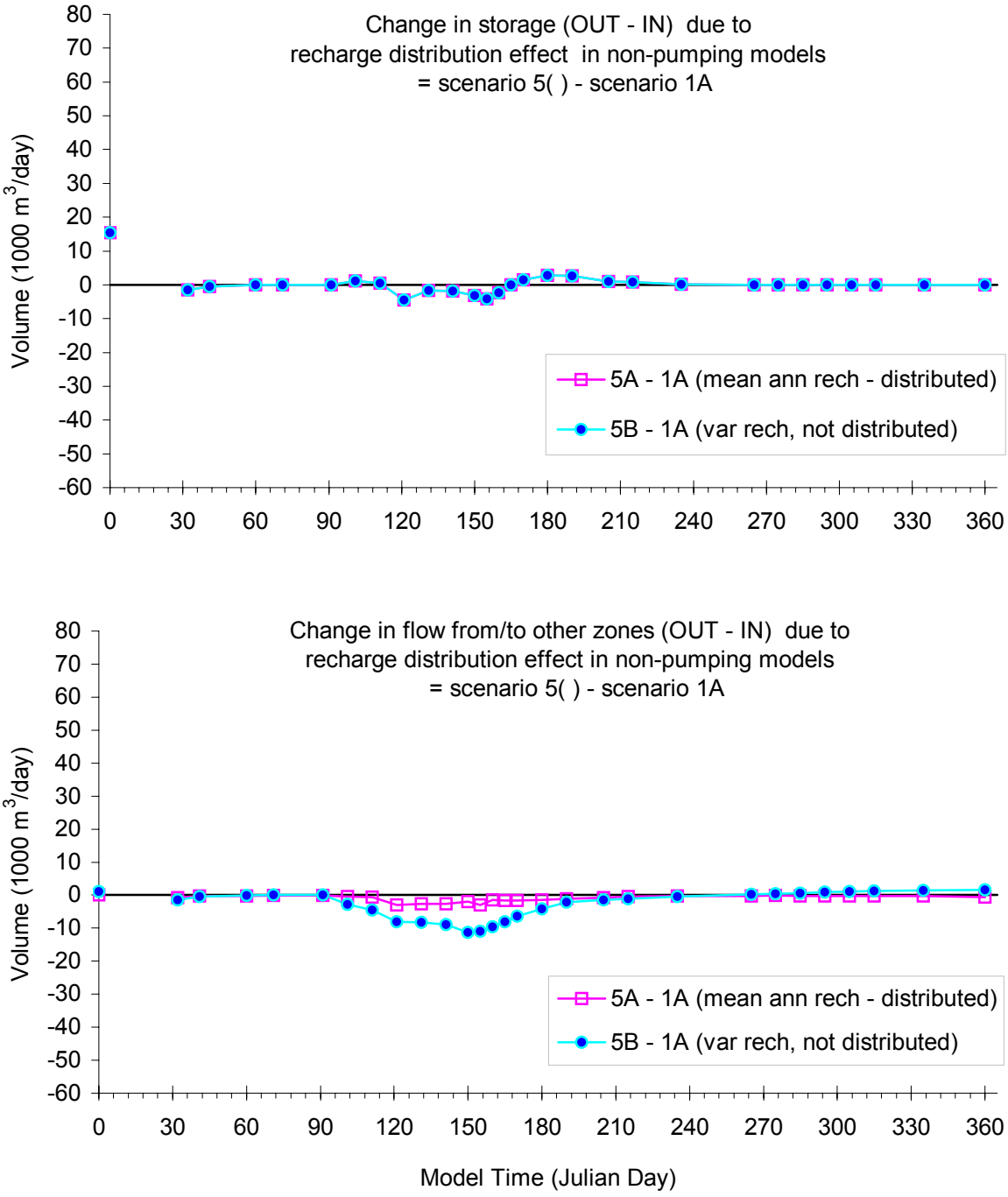

Figure C52 Transient model Storage and Flow to Other Zones components of ZBUD for Zone 3 (Sion 1) in Grand Forks aquifer. Comparing effect of recharge spatial and temporal distribution on non-pumping model climate change predictions. Horizontal axis is time in days, vertical axis is flow volume in 1000's m^3/day. Same scales on both graphs. Graphs show Difference between (OUT – IN) volume in scenario 4 (heterogeneous) model and scenario 2 model outputs. Storage and Flow from/to Other Zones has similar behaviours in model 5(A or B) and 1(A), except for the shown differences in these graphs.

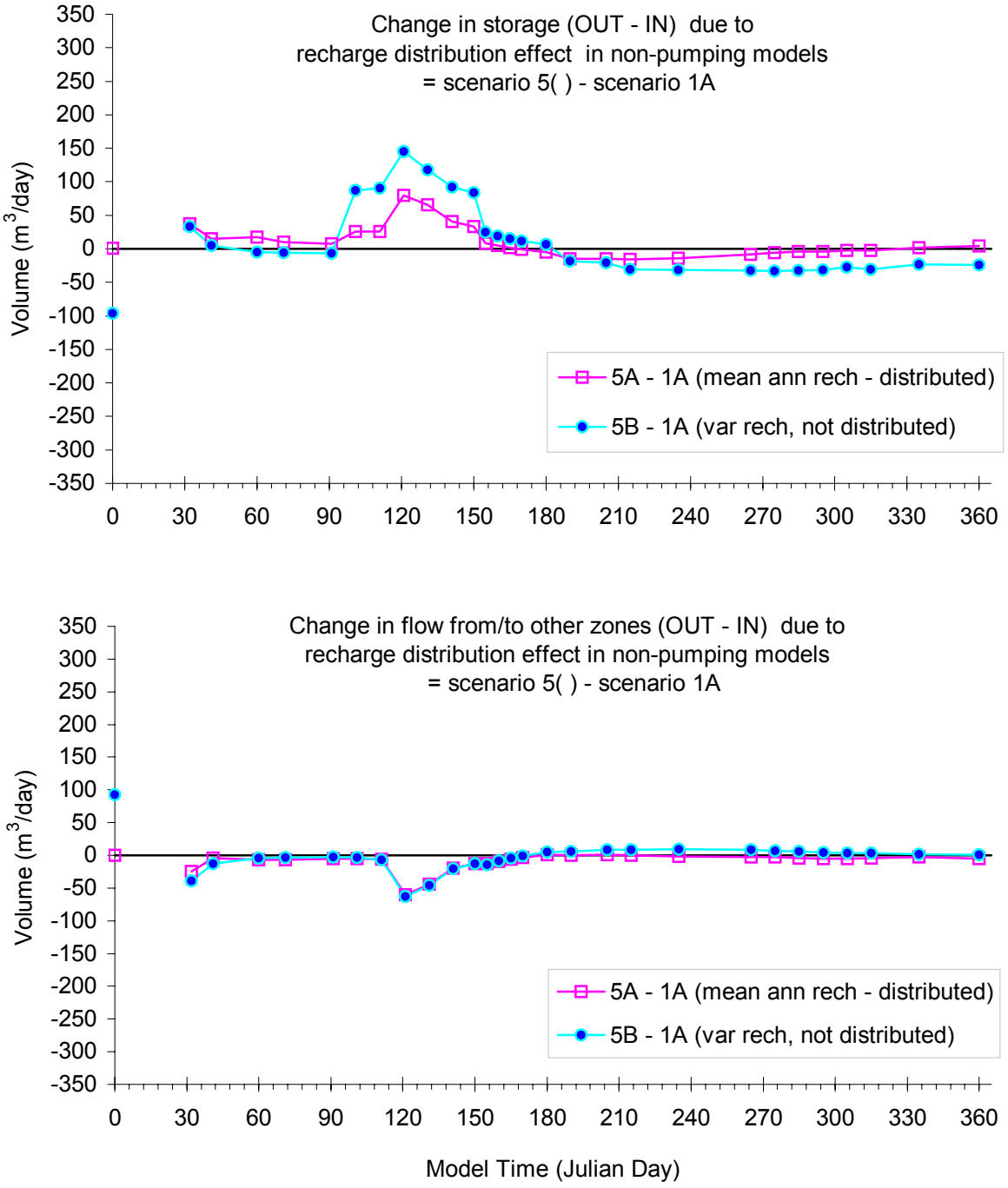

Figure C53 Transient model Storage and Flow to Other Zones components of ZBUD for Zone 4 (Sion 2 & 3) in Grand Forks aquifer. Comparing effect of recharge spatial and temporal distribution on non-pumping model climate change predictions. Horizontal axis is time in days, vertical axis is flow volume in 1000's m^3/day. Same scales on both graphs. Graphs show Difference between (OUT – IN) volume in scenario 4 (heterogeneous) model and scenario 2 model outputs. Storage and Flow from/to Other Zones has similar behaviours in model 5(A or B) and 1(A), except for the shown differences in these graphs.

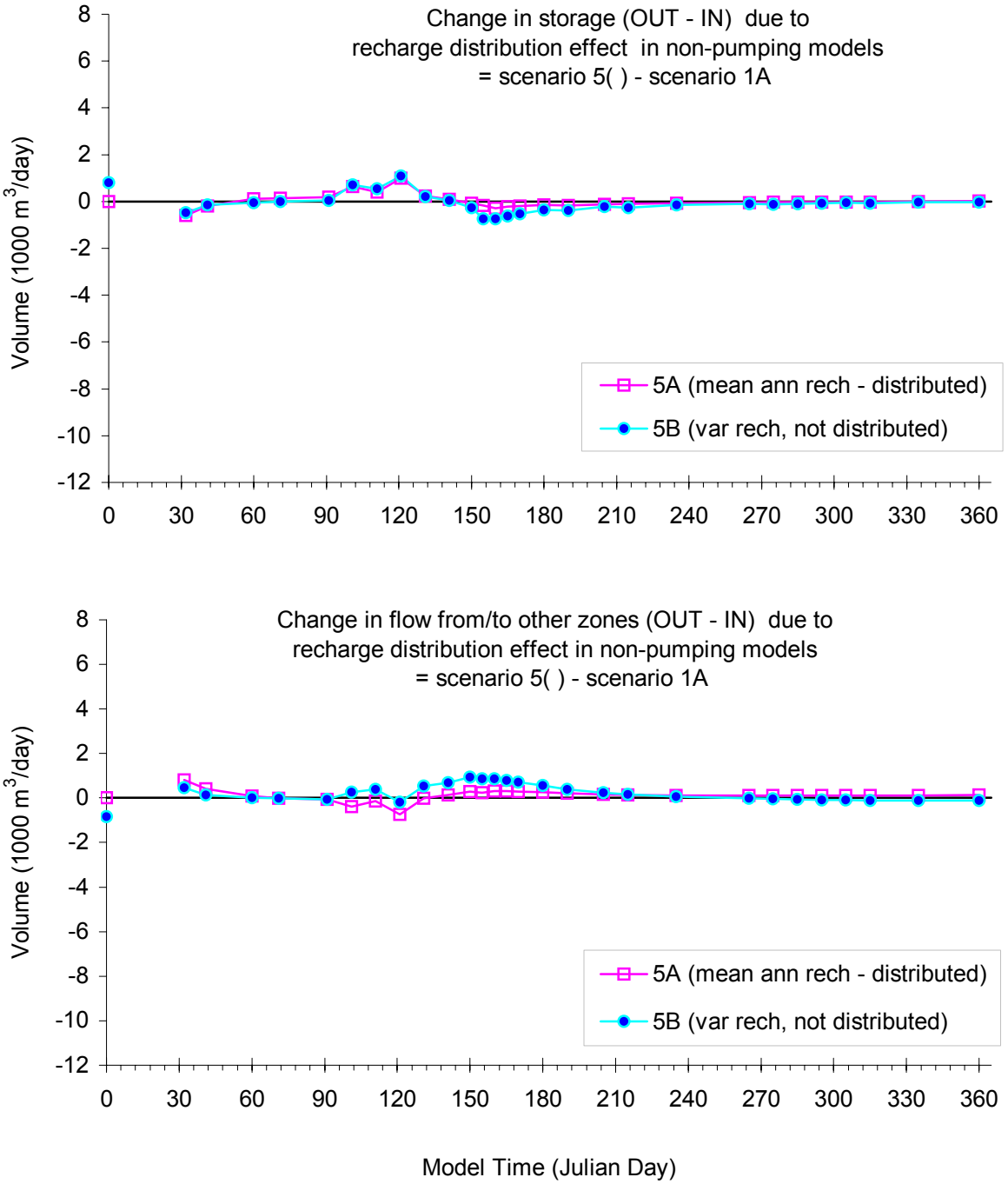

Figure C54 Transient model Storage and Flow to Other Zones components of ZBUD for Zone 5 (Big Y) in Grand Forks aquifer. Comparing effect of recharge spatial and temporal distribution on non-pumping model climate change predictions. Horizontal axis is time in days, vertical axis is flow volume in 1000's m^3/day. Same scales on both graphs. Graphs show Difference between (OUT – IN) volume in scenario 4 (heterogeneous) model and scenario 2 model outputs. Storage and Flow from/to Other Zones has similar behaviours in model 5(A or B) and 1(A), except for the shown differences in these graphs.

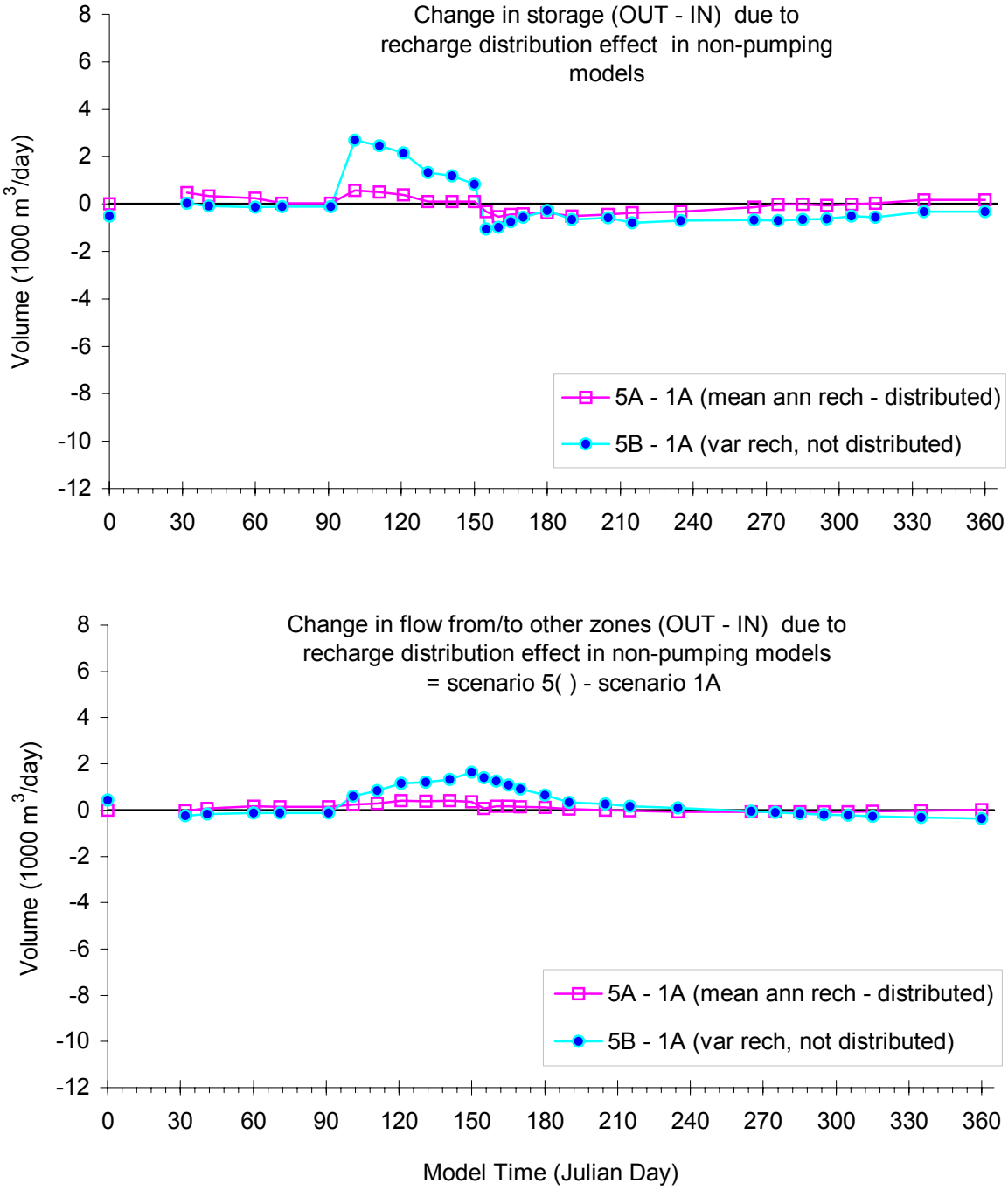

Figure C55 Transient model Storage and Flow to Other Zones components of ZBUD for Zone 6 (Covert) in Grand Forks aquifer. Comparing effect of recharge spatial and temporal distribution on non-pumping model climate change predictions. Horizontal axis is time in days, vertical axis is flow volume in 1000's m^3/day. Same scales on both graphs. Graphs show Difference between (OUT – IN) volume in scenario 4 (heterogeneous) model and scenario 2 model outputs. Storage and Flow from/to Other Zones has similar behaviours in model 5(A or B) and 1(A), except for the shown differences in these graphs.

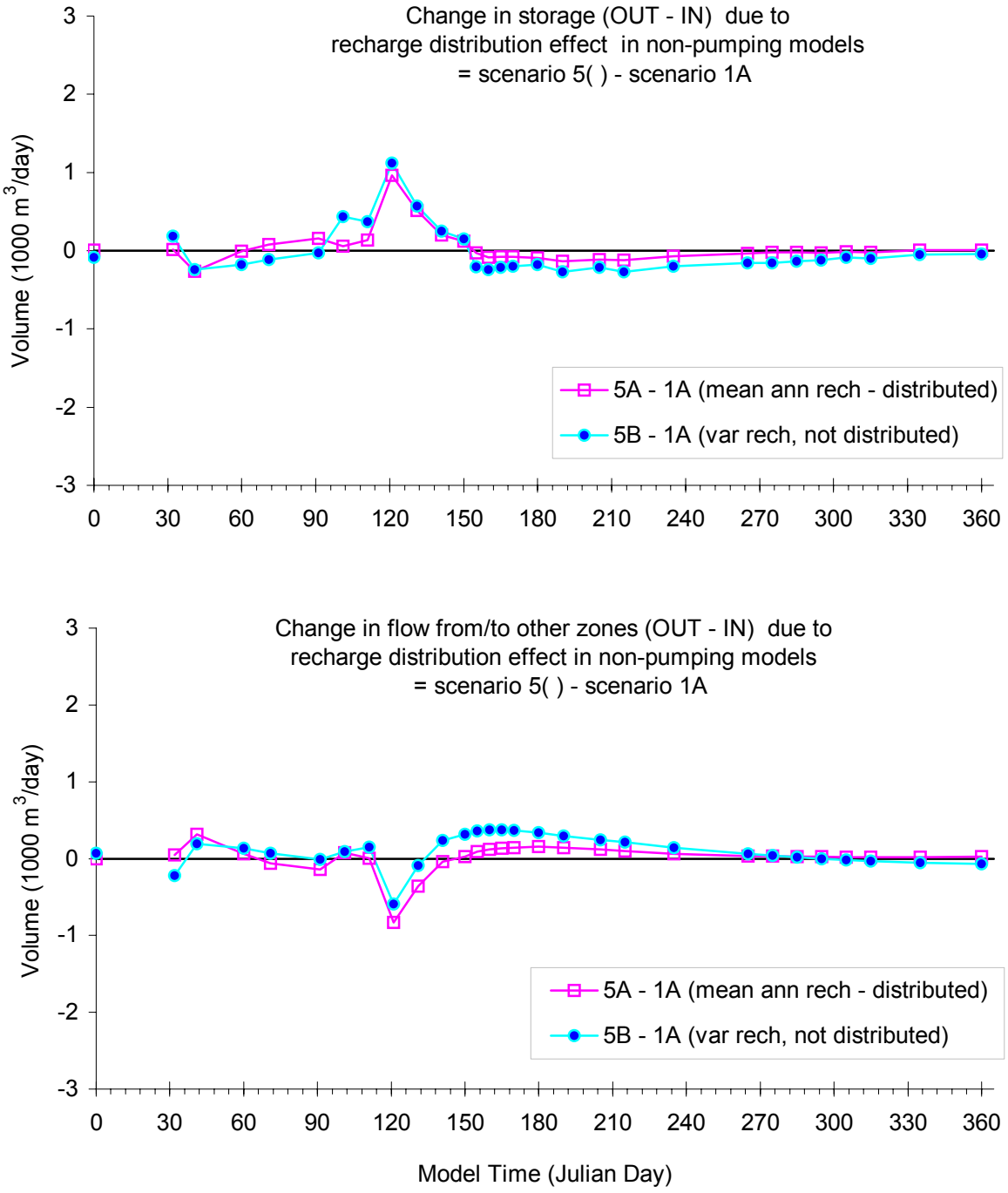

Figure C56 Transient model Storage and Flow to Other Zones components of ZBUD for Zone 7 (Nursery) in Grand Forks aquifer. Comparing effect of recharge spatial and temporal distribution on non-pumping model climate change predictions. Horizontal axis is time in days, vertical axis is flow volume in 1000's m^3/day. Same scales on both graphs. Graphs show Difference between (OUT – IN) volume in scenario 4 (heterogeneous) model and scenario 2 model outputs. Storage and Flow from/to Other Zones has similar behaviours in model 5(A or B) and 1(A), except for the shown differences in these graphs.

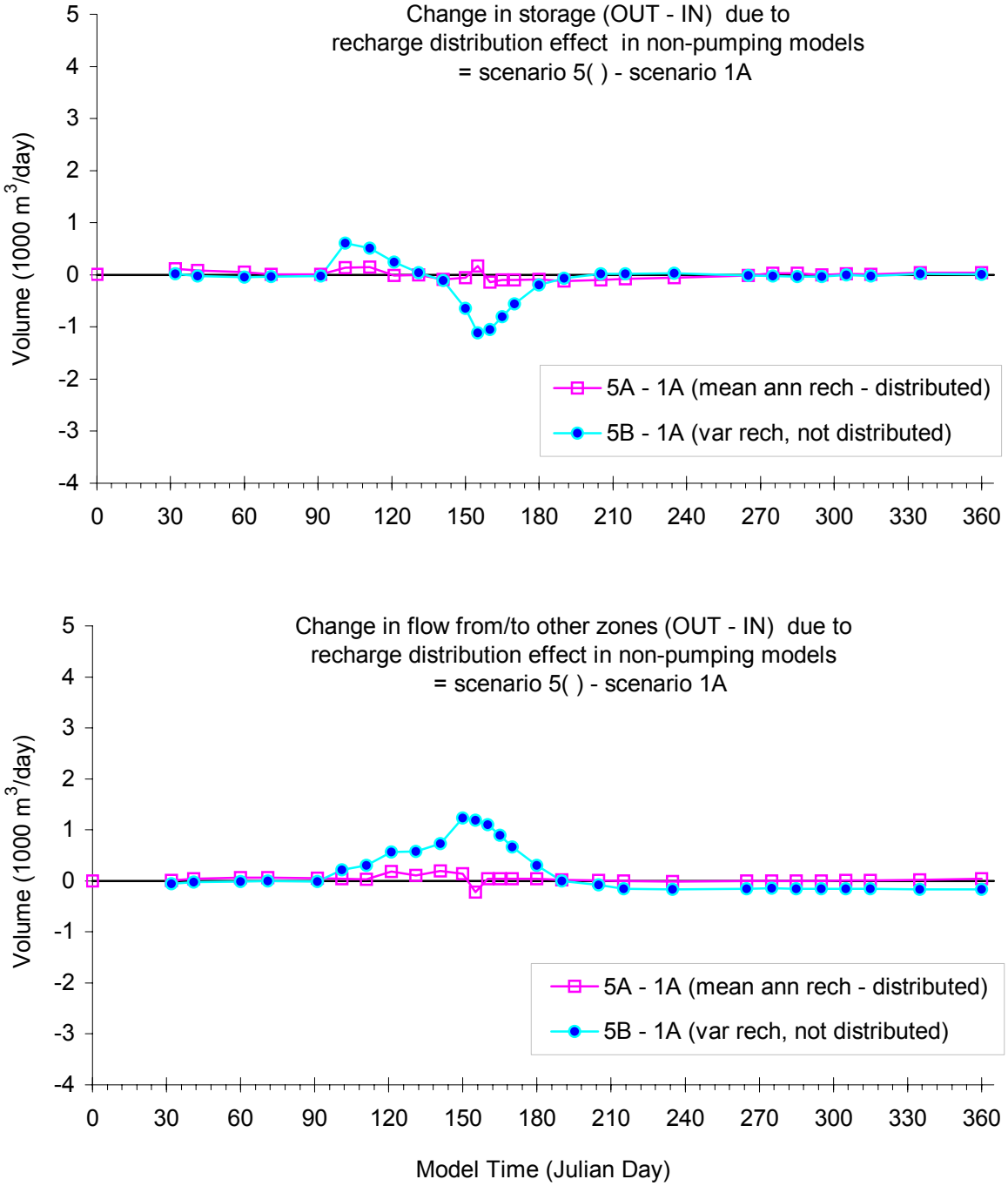

Figure C57 Transient model Storage and Flow to Other Zones components of ZBUD for Zone 8 (Silt Layer) in Grand Forks aquifer. Comparing effect of recharge spatial and temporal distribution on non-pumping model climate change predictions. Horizontal axis is time in days, vertical axis is flow volume in 1000's m^3/day. Same scales on both graphs. Graphs show Difference between (OUT – IN) volume in scenario 4 (heterogeneous) model and scenario 2 model outputs. Storage and Flow from/to Other Zones has similar behaviours in model 5(A or B) and 1(A), except for the shown differences in these graphs.

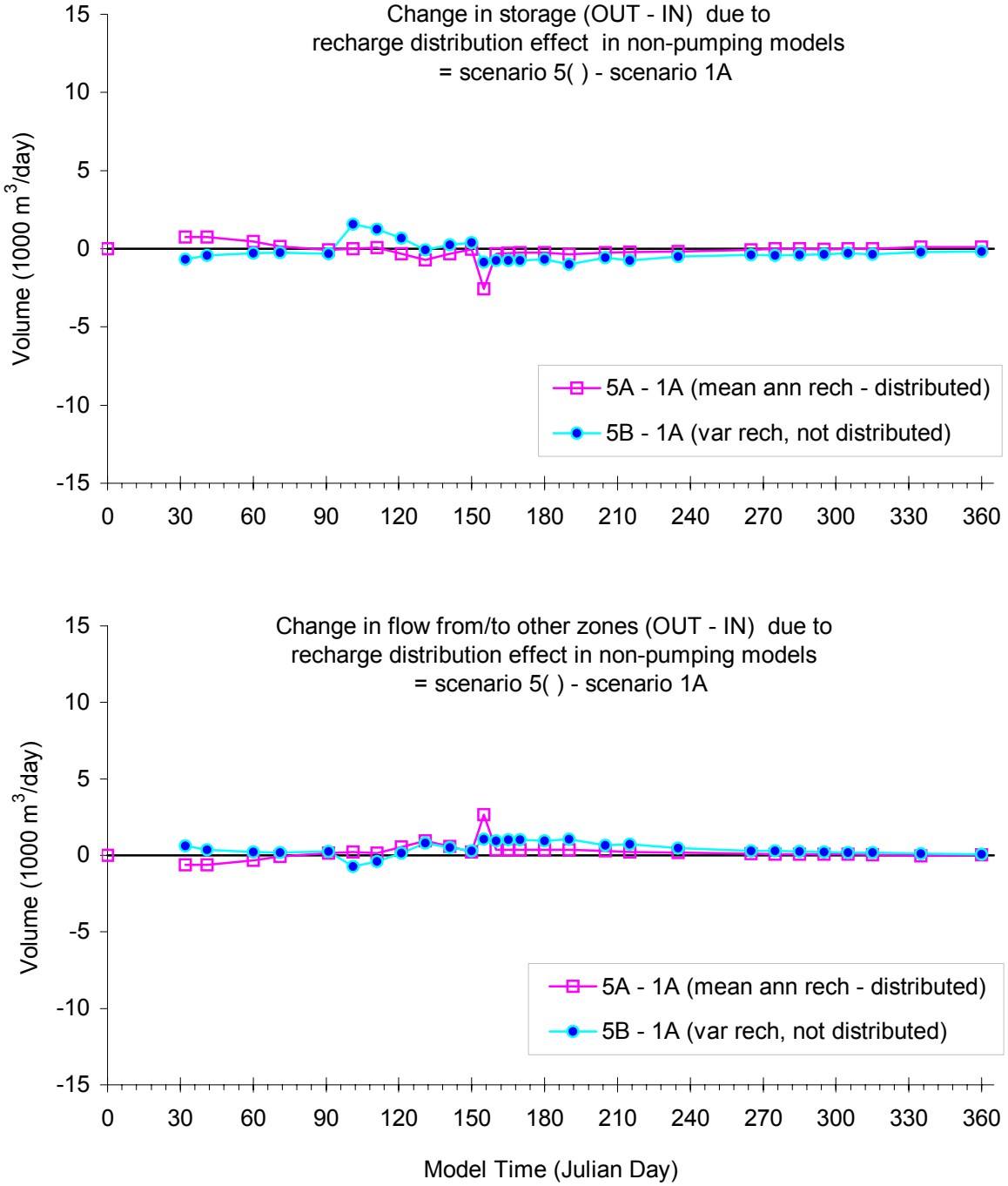

Figure C58 Transient model Storage and Flow to Other Zones components of ZBUD for Zone 9 (Clay Layer) in Grand Forks aquifer. Comparing effect of recharge spatial and temporal distribution on non-pumping model climate change predictions.
Horizontal axis is time in days, vertical axis is flow volume in 1000's m^3/day. Same scales on both graphs. Graphs show Difference between (OUT – IN) volume in scenario 4 (heterogeneous) model and scenario 2 model outputs. Storage and Flow from/to Other Zones has similar behaviours in model 5(A or B) and 1(A), except for the shown differences in these graphs.